# VACCINES, IMMUNOTHERAPY AND NEW ANTIFUNGAL THERAPY AGAINST FUNGI: UPDATES IN THE NEW FRONTIER

EDITED BY: Carlos P. Taborda and Joshua D. Nosanchuk
PUBLISHED IN: Frontiers in Microbiology

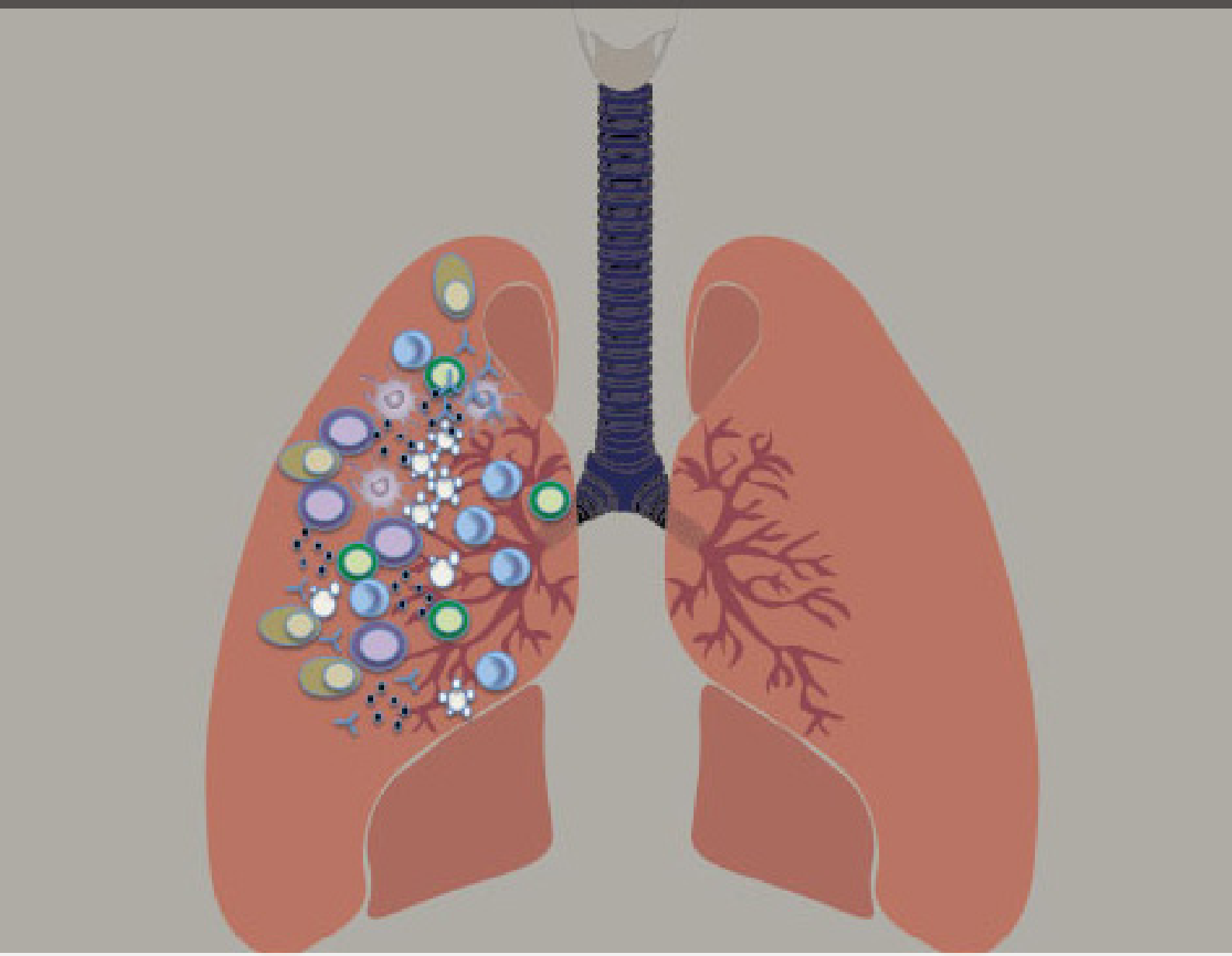

frontiers Research Topics

# frontiers



**ISSN 1664-8714**
**ISBN 978-2-88945-327-6**
**DOI 10.3389/978-2-88945-327-6**

## About Frontiers

Frontiers is more than just an open-access publisher of scholarly articles: it is a pioneering approach to the world of academia, radically improving the way scholarly research is managed. The grand vision of Frontiers is a world where all people have an equal opportunity to seek, share and generate knowledge. Frontiers provides immediate and permanent online open access to all its publications, but this alone is not enough to realize our grand goals.

## Frontiers Journal Series

The Frontiers Journal Series is a multi-tier and interdisciplinary set of open-access, online journals, promising a paradigm shift from the current review, selection and dissemination processes in academic publishing. All Frontiers journals are driven by researchers for researchers; therefore, they constitute a service to the scholarly community. At the same time, the Frontiers Journal Series operates on a revolutionary invention, the tiered publishing system, initially addressing specific communities of scholars, and gradually climbing up to broader public understanding, thus serving the interests of the lay society, too.

## Dedication to Quality

Each Frontiers article is a landmark of the highest quality, thanks to genuinely collaborative interactions between authors and review editors, who include some of the world's best academicians. Research must be certified by peers before entering a stream of knowledge that may eventually reach the public - and shape society; therefore, Frontiers only applies the most rigorous and unbiased reviews.
Frontiers revolutionizes research publishing by freely delivering the most outstanding research, evaluated with no bias from both the academic and social point of view.
By applying the most advanced information technologies, Frontiers is catapulting scholarly publishing into a new generation.

## What are Frontiers Research Topics?

Frontiers Research Topics are very popular trademarks of the Frontiers Journals Series: they are collections of at least ten articles, all centered on a particular subject. With their unique mix of varied contributions from Original Research to Review Articles, Frontiers Research Topics unify the most influential researchers, the latest key findings and historical advances in a hot research area! Find out more on how to host your own Frontiers Research Topic or contribute to one as an author by contacting the Frontiers Editorial Office: **researchtopics@frontiersin.org**

# VACCINES, IMMUNOTHERAPY AND NEW ANTIFUNGAL THERAPY AGAINST FUNGI: UPDATES IN THE NEW FRONTIER

Topic Editors:
**Carlos P. Taborda,** University of São Paulo, Brazil
**Joshua D. Nosanchuk,** Albert Einstein College of Medicine, United States

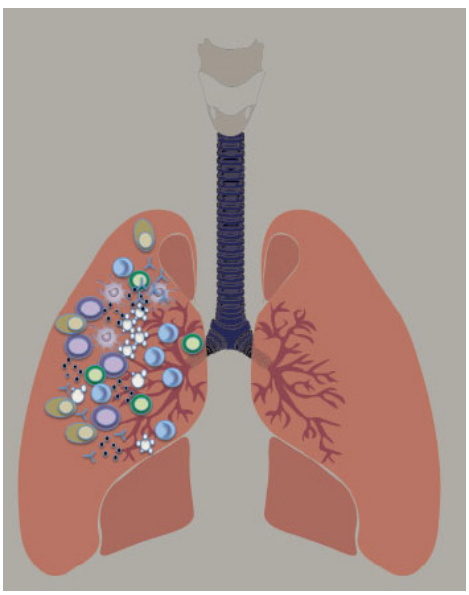

Vaccine, Immunotherapy and Antifungal Drugs: new tools against fungal infections.

Image by Carlos P. Taborda and Abigail Gouveia.

Invasive fungal diseases have increased many fold over the past 50 years. Current treatment regimens typically require prolonged administration of antifungal medications that can have significant toxicity. Moreover, our present potent antifungal armamentarium fails to eradicate fungal pathogens from certain compromised hosts. Additionally, invasive fungal diseases continue to have unacceptably high mortality rates. A growing body of work has focused on the utility of vaccines and/or immunotherapy as a powerful tool in combating mycoses, either for the active treatment, as an adjuvant, or in the prevention of specific fungal pathogens. Also, it is growing the interest over new drugs development as second choice for treatment when traditional chemotherapy fail. This Research Topic will detail the exciting progress in developing vaccines, immunotherapy and new drugs for fungi.

**Citation:** Taborda, C. P., Nosanchuk, J. D., eds. (2017). Vaccines, Immunotherapy and New Antifungal Therapy Against Fungi: Updates in the New Frontier. Lausanne: Frontiers Media.
doi: 10.3389/978-2-88945-327-6

# Table of Contents

## Pathogenicity and Cell Biology

frontiers in Microbiology

EDITORIAL
published: 08 September 2017
doi: 10.3389/fmicb.2017.01743

# Editorial: Vaccines, Immunotherapy and New Antifungal Therapy against Fungi: Updates in the New Frontier

*Carlos P. Taborda*[1,2]* *and Joshua D. Nosanchuk*[3]

[1] *Department of Microbiology, Institute of Biomedical Sciences, University of São Paulo, São Paulo, Brazil,* [2] *Laboratory of Medical Mycology, Institute of Tropical Medicine of São Paulo—LIM53/Medical School, University of São Paulo, São Paulo, Brazil,* [3] *Departments of Medicine and Microbiology and Immunology, Albert Einstein College of Medicine of Albert Einstein College of Medicine, Bronx, NY, United States*

**Keywords: vaccines, immunotherapy, antifungal agents, fungi, editorial**

## Editorial on the Research Topic

### Vaccines, Immunotherapy and New Antifungal Therapy against Fungi: Updates in the New Frontier

Systemic mycoses are caused by geographically delimitated thermally dimorphic fungi or by classical yeast or molds. Among the thermally dimorphic fungi group, we highlight the human diseases of paracoccidioidomycosis, coccidioidomycosis, blastomycosis, histoplasmosis, and sporotrichosis, the last as cause of subcutaneous mycosis. Although these diseases due to thermally dimorphic fungi are exacerbated by immune suppression, other invasive infections due to yeasts and mold are generally opportunistic. Patients with different degrees of immunodeficiency as a result of AIDS, diabetes, organ transplant, use of immunosuppressive drugs and etc, are at increased risks for developing candidiasis or cryptococcosis (reviewed by Travassos and Taborda, 2017). *Aspergillus fumigatus, Fusarium* spp., and *Penicillium* spp. are, for example, increased in patients undergoing hematopoietic stem cell transplantation for treatment of hematological malignancy (Reviewed by Travassos and Taborda, 2017). This editorial explores several different approaches for combating invasive mycoses and highlights exciting future avenues for study.

Fungi are a major cause of morbidity and mortality on the global stage, and while the pathogenesis of some, such as *Candida* spp. and *Aspergillus* spp. have been deeply investigated, others remain significantly understudied, such as *Paracoccidioides* spp. and *Penicillium* spp. Although the exact number of patients affected by invasive mycoses is unknown, it is estimated that there are over 1.5 million cases annually (Brown et al., 2012; Parente-Rocha et al., 2017; Travassos and Taborda, 2017). The most important tools for control of invasive fungal diseases are systemic antifungal drugs, and certain diseases require months to years of continuous administration. Despite this, there are frequent relapses of some diseases and there are numerous reports of increased drug resistance (Kneale et al., 2016; Parente-Rocha et al., 2017). The high costs of these medications limit their availability to some patients, especially in the developing world. There are four main types of antifungal drugs used for invasive infections: Amphotericin B, flucytosine, azoles, and echinocandins (Aguilar-Zapata et al., 2015; Kneale et al., 2016).

There are new and emerging fungal diseases that challenge the medical community. For example, *Candida auris*, first reported in 2009, is frequently multidrug-resistant (Sarma and Upadhyay, 2017). The mechanisms that lead to antifungal resistance in fungi are highly complex and may include mutation of drug targets, overexpression of the targeted protein, expression of an efflux pump, degradation of the drugs, and pleiotropic drug responses (Parente-Rocha et al., 2017; Scorzoni et al.). Besides multidrug-resistant isolates, the highly potent, broad-spectrum

OPEN ACCESS

***Edited by:***
*Hector Mora Montes, Universidad de Guanajuato, Mexico*

***Reviewed by:***
*Laura Bonifaz, Instituto Mexicano del Seguro Social (IMSS), Mexico*

***Correspondence:**
*Carlos P. Taborda*
*taborda@usp.br*

***Specialty section:***
*This article was submitted to Fungi and Their Interactions, a section of the journal Frontiers in Microbiology*

***Received:*** *31 July 2017*
***Accepted:*** *28 August 2017*
***Published:*** *08 September 2017*

***Citation:***
*Taborda CP and Nosanchuk JD (2017) Editorial: Vaccines, Immunotherapy and New Antifungal Therapy against Fungi: Updates in the New Frontier. Front. Microbiol. 8:1743. doi: 10.3389/fmicb.2017.01743*

amphotericin B is relatively restricted in use due to its side effects (Parente-Rocha et al., 2017). Due to issues such as drug resistance, toxicities, costs, and prolonged treatment regiments, there is an urgent need for the discovery of new drugs for the treatment of invasive mycoses. Screening of libraries of synthetic small molecules or natural products are exciting and promising methods to identify new drugs (Parente-Rocha et al., 2017). Nanotechnology is also being leveraged to improve the efficacy of traditional antifungal drugs with a particular focus on reducting toxicity, while improving biodistribution and drug targeting (Souza and Amaral). One promising option is the use of the natural polymer of alginate as drug delivery vehicle due to its non-toxicity, biodegradability, high biocompatibility, low cost, mucoadhesiveness, and non-immunogenic properties (de Castro Spadari et al.).

The concept of drug repurposing has led the screening of clinically available compounds for use as new antifungal drugs. The HIV aspartic peptidase inhibitors (indinavir, saquinavir, ritonavir, nelfinavir tipranavir, amprenavir, and lopinavir) also display activity against *Candida* spp. and *Cryptococcus* spp. (Cassone et al., 1999; Cenci et al., 2008). Aspartic-type peptidases participate in essential metabolic events of a fungal cell and help fungi during their interactions with the host (reviewed by Palmeira et al.). Palmeira et al. demonstrated the efficiency of aspartic peptidase inhibitors on the virulence by *Fonsecaea pedrosoi* conidial cells (the causative agent of a subcutaneous mycosis) conidial cells by blocking crucial biological process. The anti-helmithic compound mebendazole also has multiple antifungal effects on *Cryptococcus neoformans*, a neurotropic fungus (Joffe et al.). Notably, mebendazole achieves levels in the brain that have antifungal activity against phagocytized *C. neoformans* and the yeasts cells within cryptococcal biofilms as well as causes marked morphological alterations in the yeast cell (Joffe et al.).

Novel compounds have also been explored for their efficacy against fungi. For example, metal-based drugs are being studied due to their therapeutic potentials for diverse pharmacological applications (reviewed by Granato et al.). In this context investigators have analyzed the effect of 1,10-phenanthroline-5,6-dione (phendione) and its metal-based derivatives on *Phialophora verrucosa* conical cells (an agent of chromoblastomycosis, a subcutaneous mycosis) and *in vitro* tests have shown that phendione and its $Ag^{+}$ and $Cu^{2+}$ complexes represent a promising antifungal agent against *P. verrucosa* (Granato et al.).

A synthetic compound previously explored for its cancer chemotherapeutic activities, biphosphinic cyclopalladate C7a, has been tested against several microorganism and parasites, such as *Trypanosoma cruzi*, *Paracoccidioides brasiliensis*, *P. lutzii*, *C. neoformans,* and *C. albicans* (reviewed by Muñoz et al.). Here the authors have demonstrated that C7a is effective *in vitro* against different isolates of *Candida*, including azoles resistant strains (Muñoz et al.).

Genetic manipulation has also been explored as another option for controlling mycoses. For example, the inteins, invasive genetic elements that occur as intervening sequences in conserved coding host genes, are being explored as a new drug target against fungi as *Candida* ssp. (Fernandes et al.).

Antifungal drugs are the basis of systemic mycoses treatment of patients and, an in-depth understanding of the molecular mechanisms underlying their efficacy provides insights into fungal pathogenesis (Ding et al.). Immunosuppression may interfere with chemotherapy efficiency (Travassos and Taborda, 2017). Antifungal vaccines may boost the immune system and enhance the protective effect of antifungal drugs, which allows for a reduction in the time required for treatment and prevention of relapse (Travassos and Taborda, 2017). There is no licensed vaccine for the prevention or treatment of human mycoses. Albeit, there are some groups around the world involved with different strategies for vaccine development or immunotherapy using monoclonal antibodies against systemic mycosis.

Protection against most mycoses involves the activation of the cellular immune response through $CD4^{+}$ T helper cells. T-helper (Th) 1 or Th17 responses may be cytotoxic or involve the secretion of inflammatory cytokines such as IL-12, IL-17A, IFN-γ, GM-CSF, and TNF-α, which active different cell populations as neutrophils, macrophages, and dendritic cells (Parente-Rocha et al., 2017). The progression of fungal infection is related to a decrease in Th1-type response and an increase in the response mediated by $CD4^{+}$ T-helper cells type 2 (Th2), producing cytokines such as IL-4, IL-5, and IL-10. Although the Th2-type response is associated with aggravation of fungal infections, cytokines produced are essential for the control of exaggerated inflammatory responses (Cutler et al., 2007).

The production of vaccines from proteins (peptides) or polysaccharides is a standard approach to vaccination (Travassos and Taborda, 2017). The use of peptides as vaccines has many advantages: they are free of infectious material, can be produced in large scale; include multiple determinants or epitopes; can be modified by lipids, carbohydrates or phosphate, acetyl and terminal amide groups to increase their stability, immunogenicity and solubility; and may be covalently or non-covalently linked to macromolecules for increased immunogenicity (Purcell et al., 2007). Peptide delivery using different formulations is a challenge for the creation of an efficient vaccine. Dendritic cells are very important for both innate and adaptive immune response and play a significant role in the immune response to dimorphic fungi (Thind et al., 2015). Dendritic cells are up to 1,000-fold more efficient in activating T cells than traditional adjuvants. The use of dendritic cells primed with peptide 10 (P10), derived from the *P. brasiliensis* glycoprotein 43 (gp43), as prophylactic or therapeutic vaccine in experimental model using infected mice with yeast cells from *P. brasiliensis* reduces lung fungal burdens (Magalhães et al., 2012). Using a similar approach, Silva et al. utilized dendritic cells primed with P10 in combination with trimethoprim-sulfamethoxazole administration to treat immunocompromised mice infected with *P. brasiliensis*. The authors observed P10-pulsed dendritic cells with or without antifungal drugs are potently effective in combating invasive paracoccidiodomycosis.

During the infection, fungi induce the production of a heterogeneous population of polyclonal antibodies and, individually, these antibodies may increase or decrease

protection against fungal infections, as well as may have no effect at all. Since fungi can induce the production of protective antibodies, several studies have shown that these molecules can act as efficient vaccines in the fight against systemic infections caused by fungi such as aspergillosis (Chaturvedi et al., 2005), choroblastomycosis (Nimrichter et al., 2004), candidiasis (Coleman et al., 2009), cryptococcosis (Taborda et al., 2003), paracoccidioidomycosis (Buissa-Filho et al., 2008), and histoplasmosis (Nosanchuk et al., 2012) among others. The main advantage of administering humanized antibodies is that they may have fewer side effects compared to chimeric or non-human antibodies. As an example, a genetically engineered mAbP6E7 antibody against a 70-kDa *Sporothrix* antigen effectively decreased fungal burdens of *S. schenckii* in infected mice (de Almeida et al.).

The expansion of knowledge in mycology obviously is not phenomenon restricted to human or animal pathogens. For instance, the fungi play an extremely important function of the plantae kingdom. The identification of a new strain the can cause wheat stripe rust (Zheng et al.) and the hypovirulence of *Sclerotium rolfsii* caused by association of RNA mycoviurs (Zhong et al.) underscore their impact and the efforts underway to understand their biology.

In sum, the articles in this Frontier's topic broadly paint the spectrum of investigations on new antifungal drugs, host-pathogen interactions and provide a review of the state-of-the-art in vaccinology, immunotherapy, and chemotherapy against fungi. The information presented also underscores areas ripe for future study and details several promising improved therapeutics and therapeutic approaches against fungal invaders.

## AUTHOR CONTRIBUTIONS

All authors listed have made a substantial, direct and intellectual contribution to the work, and approved it for publication.

## ACKNOWLEDGMENTS

The authors sincerely acknowledge the efforts of all of the authors who contributed to this Research Topic. JN is supported in part by NIH AI52733 and AI124797. CT is supported by grants 2016/08730-6 from Fundação de Amparo à Pesquisa do Estado de São Paulo (FAPESP) and Conselho Nacional de Desenvolvimento Científico e Tecnológico (CNPq).

## REFERENCES

Aguilar-Zapata, D., Petraitiene, R., and Petraitis, V. (2015). Echinocandins: the expanding antifungal armamentarium. *Clin. Infect. Dis.* 61, S604–S611. doi: 10.1093/cid/civ814

Brown, G. D., Denning, D. W., Gow, N. A. R., Levitz, S. M., Netea, M. G., and White, T. C. (2012). Hidden killers: human fungal infections. *Sci. Transl. Med.* 4, 1–9. doi: 10.1126/scitranslmed.3004404

Buissa-Filho, R., Puccia, R., Marques, A. F. F., Pinto, F. A. A., Muñoz, J. E., Nosanchuk, J. D. D., et al. (2008). The monoclonal antibody against the major diagnostic antigen of *Paracoccidioides brasiliensis* mediates immune protection in infected BALB/c mice challenged intratracheally with the fungus. *Infect. Immun.* 76, 3321–3328. doi: 10.1128/IAI.00349-08

Cenci, E., Francisci, D., Belfiori, B., Pierucci, S., Baldelli, F., Bistoni, F., et al. (2008). Tipranavir exhibits different effects on opportunistic pathogenic fungi. *J. Infect.* 56, 58–64. doi: 10.1016/j.jinf.2007.08.004

Chaturvedi, A. K., Kavishwar, A., Shiva Keshava, G. B., and Shukla, P. K. (2005). Monoclonal immunoglobulin G1 directed against *Aspergillus fumigatus* cell wall glycoprotein protects against experimental murine aspergillosis. *Clin. Diagn. Lab. Immunol.* 12, 1063–1068. doi: 10.1128/CDLI.12.9.1063-1068.2005

Coleman, D. A., Oh, S. H., Zhao, X., Zhao, H., Hutchins, J. T., Vernachio, J. H., et al. (2009). Monoclonal antibodies specific for *Candida albicans* Als3 that immunolabel fungal cells *in vitro* and *in vivo* and block adhesion to host surfaces. *J. Microbiol. Methods* 78, 71–78. doi: 10.1016/j.mimet.2009.05.002

Cutler, J. E., Deepe, G. S., and Klein, B. S. (2007). Advances in combating fungal diseases: vaccines on the threshold. *Nat. Rev. Microbiol.* 5, 13–28. doi: 10.1038/nrmicro1537

Cassone, A., De Bernardis, F., Torosantucci, A., Tacconelli, E., Tumbarello, M., and Cauda, R. (1999). *In vitro* and *in vivo* anticandidal activity of human immunodeficiency virus protease inhibitors. *J. Infect. Dis.* 180, 448–453. doi: 10.1086/314871

Kneale, M., Bartholomew, J. S., Davies, E., and Denning, D. W. (2016). Global access to antifungal therapy and its variable cost. *J. Antimicrob. Chemother.* 71, 3599–3606. doi: 10.1093/jac/dkw325

Magalhães, A., Ferreira, K. S. S., Almeida, S. R. R., Nosanchuk, J. D. D., Travassos, L. R. R., and Taborda, C. P. P. (2012). Prophylactic and therapeutic vaccination using dendritic cells primed with peptide 10 derived from the 43-kilodalton glycoprotein of *Paracoccidioides brasiliensis*. *Clin. Vaccine Immunol.* 19, 23–29. doi: 10.1128/CVI.05414-11

Nimrichter, L., Barreto-Bergter, E., Mendonça-Filho, R. R., Kneipp, L. F., Mazzi, M. T., Salve, P., et al. (2004). A monoclonal antibody to glucosylceramide inhibits the growth of *Fonsecaea pedrosoi* and enhances the antifungal action of mouse macrophages. *Microbes Infect.* 6, 657–665. doi: 10.1016/j.micinf.2004.03.004

Nosanchuk, J. D., Zancopé-Oliveira, R. M., Hamilton, A. J., and Guimarães, A. J. (2012). Antibody therapy for histoplasmosis. *Front. Microbiol.* 3:21. doi: 10.3389/fmicb.2012.00021

Parente-Rocha, J. A., Bailão, A. M., Amaral, A. C., Taborda, C. P., Paccez, J. D., Borges, C. L., et al. (2017). Antifungal resistance, metabolic routes as drug targets, and new antifungal agents: an overview about endemic dimorphic fungi. *Mediators Inflamm.* 2017:9870679. doi: 10.1155/2017/9870679

Purcell, A. W., McCluskey, J., and Rossjohn, J. (2007). More than one reason to rethink the use of peptides in vaccine design. *Nat. Rev. Drug Discov.* 6, 404–414. doi: 10.1038/nrd2224

Sarma, S., and Upadhyay, S. (2017). Current perspective on emergence, diagnosis and drug resistance in Candida auris. *Infect. Drug Resist.* 10, 155–165. doi: 10.2147/IDR.S116229

Taborda, C. P. C. P., Rivera, J., Zaragoza, O., and Casadevall, A. (2003). More is not necessarily better: prozone-like effects in passive immunization with IgG. *J. Immunol.* 170, 3621–3630. doi: 10.4049/jimmunol.170.7.3621

Thind, S. K., Taborda, C. P., and Nosanchuk, J. D. (2015). Dendritic cell interactions with Histoplasma and Paracoccidioides. *Virulence* 6, 424–432. doi: 10.4161/21505594.2014.965586

Travassos, L. R., and Taborda, C. P. (2017). Linear epitopes of *Paracoccidioides brasiliensis* and other fungal agents of human systemic mycoses as vaccine candidates. *Front. Immunol.* 8:224. doi: 10.3389/fimmu.2017.00224

**Conflict of Interest Statement:** The authors declare that the research was conducted in the absence of any commercial or financial relationships that could be construed as a potential conflict of interest.

frontiers in Microbiology

REVIEW
published: 07 March 2017
doi: 10.3389/fmicb.2017.00336

# Antifungal Therapy for Systemic Mycosis and the Nanobiotechnology Era: Improving Efficacy, Biodistribution and Toxicity

*Ana C. O. Souza*[1]* *and Andre C. Amaral*[2]

[1] *Laboratory of Pathogenic Dimorphic Fungi, Institute of Biomedical Sciences, University of São Paulo, São Paulo, Brazil,*
[2] *Laboratory of Nano and Biotechnology, Institute of Tropical Pathology and Public Health, Federal University of Goiás, Goiânia, Brazil*

Fungal diseases have been emerging as an important public health problem worldwide with the increase in host predisposition factors due to immunological dysregulations, immunosuppressive and/or anticancer therapy. Antifungal therapy for systemic mycosis is limited, most of times expensive and causes important toxic effects. Nanotechnology has become an interesting strategy to improve efficacy of traditional antifungal drugs, which allows lower toxicity, better biodistribution, and drug targeting, with promising results *in vitro* and *in vivo*. In this review, we provide a discussion about conventional antifungal and nanoantifungal therapies for systemic mycosis.

**Keywords: antifungal therapy, fungal infection, mycosis, nanobiotechnology, drug delivery systems**

OPEN ACCESS

***Edited by:***
*Joshua D. Nosanchuk, Albert Einstein College of Medicine, USA*

***Reviewed by:***
*Akanksha Singh, Central Institute of Medicinal and Aromatic Plants, India*
*Maria Rapala-Kozik, Jagiellonian University, Poland*

***Correspondence:**
*Ana C. O. Souza*
*anacosouza@yahoo.com.br*

***Specialty section:***
*This article was submitted to Fungi and Their Interactions, a section of the journal Frontiers in Microbiology*

***Received:*** *24 November 2016*
***Accepted:*** *17 February 2017*
***Published:*** *07 March 2017*

***Citation:***
*Souza ACO and Amaral AC (2017) Antifungal Therapy for Systemic Mycosis and the Nanobiotechnology Era: Improving Efficacy, Biodistribution and Toxicity. Front. Microbiol. 8:336. doi: 10.3389/fmicb.2017.00336*

## INTRODUCTION

Fungal diseases have arisen as an important public health problem worldwide, having a great impact in human morbidity and mortality, specially among immunocompromised individuals (Denning and Hope, 2010; Shapiro et al., 2011; Caffrey and Obar, 2016; Prasad et al., 2016). Although superficial mycosis are the most common among fungal infections, affecting nearly 25% of the human population worldwide (Havlickova et al., 2008), invasive fungal infections are of greater concern, since they are life-threatening, difficult to diagnose and account with a limited number of therapeutic options (Brown et al., 2012a,b). It is estimated that systemic mycosis cause about 1.5 million deaths annually (Brown et al., 2012a; Caffrey and Obar, 2016).

Systemic fungal infections include both opportunistic and endemic mycosis, and are associated with high rates of mortality if not readily diagnosed and treated (Brown et al., 2012a; Caffrey and Obar, 2016). Opportunistic infections are caused by environmental or commensal fungi and affect immunocompromised or genetically predisposed hosts, accounting for about 2 million life-threatening reported cases each year worldwide (Brown et al., 2012a; Polvi et al., 2015; Caffrey and Obar, 2016). Species from genera *Aspergillus, Candida*, *Cryptococcus*, and *Pneumocystis* are responsible for more than 90% of all reported fungal-related deaths, although accurate incidence data is not officially available and may be underestimated (Brown et al., 2012a,b).

On the other hand, endemic mycoses are caused by thermal-dimorphic fungi and can affect especially immunocompetent hosts that live in particular geographic areas, although immunosuppression is a risk factor and contributes to the outcome of infection (Goughenour and Rappleye, 2017). Dimorphic fungi occur as saprophytic molds in the environment. After inhalation or trauma inoculation by the mammalian host, they transform into pathogenic

yeasts or spherules (Bonifaz et al., 2011; Sil and Andrianopoulos, 2015). Among the causative agents of endemic mycosis are *Histoplasma capsulatum*, *Coccidioides immitis* and *C. posadasii*, *Paracoccidioides brasiliensis,* and *P. lutzii*, *Blastomyces dermatitidis*, *Talaromyces marneffei,* and *Sporothrix schenckii*. Despite incidence data of infections by dimorphic fungi are usually inaccurate due to under-diagnosis and under-reporting, it is believed that endemic mycosis are responsible for approximately 65,000 life-threatening cases each year worldwide (Brown et al., 2012a; Goughenour and Rappleye, 2017).

The fact that fungi and animals are evolutionarily close makes the search for therapeutic targets a big challenge, since targets such as biomolecules synthesis have great potential for toxicity (Groll et al., 1998; Denning and Hope, 2010; Heitman, 2011; Shapiro et al., 2011; Polvi et al., 2015). Today, only a dozen of antifungal agents (**Table 1**) are approved for the treatment of invasive fungal infections (Seyedmousavi et al., 2017). Antifungal therapy for systemic mycosis is basically focused in three classes: polyenes, azoles, and echinocandins (Polvi et al., 2015). Therapies for invasive infection presents restrictions such as route of administration, toxicity, drug interactions and sometimes high costs, considering patients hospitalization (Denning and Hope, 2010; Brown et al., 2012b; Polvi et al., 2015). In some cases, prolonged treatment times are needed, together with clinical interventions due to side effects (Goughenour and Rappleye, 2017). Recently, drug resistance has also become a worrisome issue (Xie et al., 2014). Unfortunately, antifungal drug development does not follow the progressive increase of invasive infections resulted from modern medical interventions, primary, and acquired immunodeficiencies and immunosuppressive therapies. Besides, there are no approved human vaccines for fungal diseases at this moment (Brown et al., 2012b). To overcome these problems, it is interesting to develop cheaper and novel therapeutic strategies in the battle against fungal diseases.

In this review, we will discuss current antifungal therapies available for systemic infections and point out some of the strategies using nanobiotechnology to improve conventional therapy. We will give a brief introduction about nanoformulations, and provide an overview of current studies proposing nanostructuration as an approach to improve efficacy and bioavailability of conventional antifungal drugs.

## CONVENTIONAL THERAPY FOR INVASIVE FUNGAL DISEASES

In the late 1950s, polyenes emerged as the first class of antifungal agents. These molecules are produced by *Streptomyces nodosus* presenting high affinity for ergosterol, the major sterol in fungal cell membrane, which is responsible for membrane fluidity, asymmetry, and integrity (Odds et al., 2003; Carrillo-Muñoz et al., 2006; Mesa-Arango et al., 2012). By binding to ergosterol, polyene molecules complex forming pores that destabilize cell membrane, allowing leakage of cellular contents and resulting in fungal cell death (Finkelstein and Holz, 1973; Georgopapadakou, 1998; Mesa-Arango et al., 2012; Adler-Moore et al., 2016). Besides, induction of oxidative damage in the fungal cell also contributes to fungicidal activity (Georgopapadakou, 1998; Mesa-Arango et al., 2012). Unluckily, polyene agents can also interact with cholesterol, what confers potential toxicity for mammalian cells (Hsuchen and Feingold, 1973; Georgopapadakou, 1998; Mesa-Arango et al., 2012). Among Polyenes, Amphotericin B is the most used for the treatment of systemic fungal infections. Amphotericin B has fungicidal effects against a broad-spectrum of fungal pathogens and is approved for the treatment of numerous invasive mycosis, such as candidiasis, aspergillosis, cryptococcosis, blastomycosis, histoplasmosis, mucormycosis, and sporotrichosis (Georgopapadakou, 1998; Mesa-Arango et al., 2012; Adler-Moore et al., 2016; Nett and Andes, 2016).

Amphotericin B was first introduced in the market in 1958 as a sodium deoxycholate solution administrated by parenteral route (Bartner et al., 1958; Groll et al., 1998), and after almost 60 years, it is still considered the gold standard for the treatment of most life-threatening mycosis (Groll et al., 1998; Carrillo-Muñoz et al., 2006; Mesa-Arango et al., 2012). However, this formulation is associated with important acute and chronic side-effects, particularly nephrotoxicity (Carrillo-Muñoz et al., 2006; Laniado-Laborín and Cabrales-Vargas, 2009; Mesa-Arango et al., 2012; Nett and Andes, 2016). Amphotericin B has the ability to stimulate proinflammatory responses, enhancing antifungal activity, although this may also be associated with toxicity (Mesa-Arango et al., 2012). In order to circumvent toxicity problems, lipid formulations were developed, including liposomes (Ambisome®), lipid complexes (Abelcet®), and colloidal dispersions (Amphocil®/Amphotech®) (Georgopapadakou, 1998; Gulati et al., 1998; Dupont, 2002; Mesa-Arango et al., 2012; Nett and Andes, 2016). However, these alternatives can be up to 20-fold more expensive than sodium deoxycholate Amphotericin B (Georgopapadakou, 1998; Wong-Beringer et al., 1998; Dismukes, 2000; Falci et al., 2011), limiting its usage in public health systems with limited resources.

In the late 1960s, flucytosine (5-fluorocytosine), a synthetic pyrimidine analog originally designed for antitumor therapy, was first used in the treatment of invasive mycosis (Tassel and Madoff, 1968). After being imported to the fungal cell by cytosine permeases, 5-fluorocytosine is converted to fluorouracil, which gets incorporated into DNA and RNA molecules during their synthesis, inhibiting protein synthesis and DNA replication, thus impairing cell function (Groll et al., 1998; Nett and Andes, 2016; Prasad et al., 2016). These agents have activity against a limited spectrum of pathogenic yeasts, such as *C. albicans*, *C. glabrata*, *C. parapsilosis*, *C. tropicalis,* and *Cryptococcus* spp., and are poor effective against dimorphic or filamentous fungi (Nett and Andes, 2016; Prasad et al., 2016). Due to rapid occurrence of resistance during the therapy with flucytosine, specially among *Candida* species, its clinical use is preferable only in combination with other antifungal drugs, such as Amphotericin B in the treatment of cryptococcal meningitis and other life-threatening *Candida* infections (Tassel and Madoff, 1968; Francis and Walsh, 1992; Dismukes, 2000; Sanglard et al., 2009; Nett and Andes, 2016; Prasad et al., 2016). Besides, Flucytosine induces significant side-effects, like liver dysfunction and bone marrow suppression

**TABLE 1 | Current antifungal agents available for the therapy of systemic mycosis.**

| Antifungal spectrum | AMB | 5FC | FLU | ITR | VOR | POS | ISA | CAS | MIC | ANI |
|---|---|---|---|---|---|---|---|---|---|---|
| *Candida albicans* | ++ | ++ | ++ | ++ | ++ | ++ | ++ | ++ | ++ | ++ |
| *Candida glabrata* | ++ | ++ | + | + | ++ | ++ | ++ | + | + | + |
| *Candida parapsilosis* | ++ | ++ | ++ | ++ | ++ | ++ | ++ | ++ | ++ | ++ |
| *Candida tropicalis* | ++ | ++ | ++ | ++ | ++ | ++ | ++ | ++ | ++ | ++ |
| *Candida krusei* | ++ | + | – | + | ++ | ++ | ++ | ++ | ++ | ++ |
| *Candida lusitaniae* | – | ++ | ++ | ++ | ++ | ++ | ++ | ++ | ++ | ++ |
| *Aspergillus fumigatus* | ++ | – | – | + | ++ | ++ | ++ | + | + | + |
| *Cryptococcus neoformans* | ++ | ++ | ++ | ++ | ++ | ++ | ++ | – | – | – |
| Mucorales | ++ | – | – | – | – | ++ | ++ | – | – | – |
| *Fusarium* spp. | + | – | – | + | ++ | ++ | ++ | – | – | – |
| *Scedosporium* spp. | + | – | – | + | + | + | + | – | – | – |
| *Blastomyces dermatitidis* | ++ | – | + | ++ | ++ | ++ | ++ | – | – | – |
| *Coccidioides immitis* | ++ | – | ++ | ++ | ++ | ++ | ++ | – | – | – |
| *Histoplasma capsulatum* | ++ | – | + | ++ | ++ | ++ | ++ | – | – | – |

| | | | | |
|---|---|---|---|---|
| **Class** | Polyene | Pyrimidine | Azole | Echinocandins |
| **Target** | Ergosterol | Nucleic acid | Ergosterol | Cell wall |
| **Administration** | Intravenous | Oral | Oral/Intravenous | Intravenous |
| **Side Effects** | Infusion reactions, hepatotoxicity, nephrotoxicity | Bone marrow suppression, liver toxicity | Gastrointestinal upset, hepatotoxicity, liver failure | Infusion reactions, gastrointestinal upset, headache, liver toxicity |

*5FC, flucytosine; AMB, amphotericin B; ANI, anidulafungin; CAS, caspofungin; FLU, fluconazole; ISA, isavuconazole; ITR, itraconazole; MIC, micafungin; POS, posaconazole; VOR, voriconazole.*
*Adapted from Nett and Andes (2016).*

(Francis and Walsh, 1992; Groll et al., 1998; Dismukes, 2000; Nett and Andes, 2016; Prasad et al., 2016). In the United States, flucytosine is available in oral capsules (Groll et al., 1998; Nett and Andes, 2016).

Azoles are synthetic cyclic organic molecules introduced in the early 1970s in addition to antifungal arsenal. They are composed by a 5-member azole ring, which contains two (imidazoles) or three (triazoles) nitrogen atoms, attached to a complex side chain (Georgopapadakou, 1998; Groll et al., 2003). Azoles target is ergosterol biosynthesis, which is impaired due to inhibition of fungi cytochrome P-450 14-α sterol demethylase (Vanden Bossche et al., 1995; Georgopapadakou, 1998; Groll et al., 1998, 2003; Odds et al., 2003; Carrillo-Muñoz et al., 2006). As a consequence, cell membrane integrity is impaired, with sterol precursors accumulation inside fungal cell and depletion of ergosterol in cell membrane, altering normal permeability and fluidity (Georgopapadakou, 1998; Groll et al., 1998; Odds et al., 2003). In general, azoles have a fungistatic action, affecting cell growth and proliferation, and eventually, due to accumulation of toxic methylated sterols, fungal cell death may occur (Groll et al., 2003; Zonios and Bennett, 2008; Sanglard et al., 2009; Arnold et al., 2010; Shapiro et al., 2011; Prasad et al., 2016). Currently, azoles are the most diverse class of antifungal agents and they have been refined during the past 40 years (Odds et al., 2003). Imidazoles emerged first (Groll et al., 1998; Prasad et al., 2016), and among them, miconazole and ketoconazole were the only available for systemic use (Groll et al., 2003), with the last being the first orally absorbable antifungal and the first alternative to Amphotericin B (Groll et al., 1998; Seyedmousavi et al., 2017). Triazoles came next, Itraconazole in oral formulations, and Fluconazole, in both oral and i.v. formulations, both better tolerated and more effective than Ketoconazole (Dismukes, 2000), with increased potency, expanded antifungal spectrum and improved resistance to metabolic degradation (Como and Dismukes, 1994; Groll et al., 1998). Fluconazole has good activity against *Cryptococcus* spp., *Coccidioides* spp., and *Candida* spp. except for *C. krusei* and *C. glabrata* (Arnold et al., 2010; Denning and Hope, 2010; Nett and Andes, 2016; Seyedmousavi et al., 2017). Itraconazole has broader antifungal spectrum, being effective against *Candida* spp., *Cryptococcus neoformans*, *Aspergillus* spp., dimorphic fungi, and dermatophytes (Arnold et al., 2010; Denning and Hope, 2010; Nett and Andes, 2016).

Further modifications in the molecules gave rise to the second generation of triazoles, in which Voriconazole (structurally related to Fluconazole) and Posaconazole (related to Itraconazole) are available for systemic therapy with even better antifungal potency and specificity. Voriconazole spectrum of activity is improved in relation to first generation triazoles, also including *C. glabrata*, *Fusarium* spp., *Scedosporium* spp. (Arnold et al., 2010; Denning and Hope, 2010; Nett and Andes, 2016). Posaconazole exhibits the widest antifungal spectrum of the azoles, being active against both yeasts and molds, including several Mucorales species (Arnold et al., 2010; Denning and Hope, 2010; Nett and Andes, 2016). Isavuconazole is the newest triazole introduced in the market in 2015 and recently approved

for the treatment of invasive aspergillosis and mucormycosis in the USA and Europe (McCormack, 2015).

Although azole antifungals are generally well-tolerated (Odds et al., 2003; Carrillo-Muñoz et al., 2006), they are substrates and inhibitors of several cytochrome P-450 enzymes, what is the mainly cause of their adverse effects, specially hepatotoxicity (Carrillo-Muñoz et al., 2006). For this reason, azoles can also impair metabolism of coadministered drugs, what leads to decreased plasma concentration and unexpected toxicity (Groll et al., 1998; Dismukes, 2000; Shapiro et al., 2011; Nett and Andes, 2016; Prasad et al., 2016). Besides, due to teratogenic effects, azoles are contraindicated during pregnancy (Arnold et al., 2010; Nett and Andes, 2016). Lastly, the emergence of resistance among fungal isolates is another limitation and one of the motivations for the improvement of this class of antifungals (Dismukes, 2000; Shapiro et al., 2011; Prasad et al., 2016).

Echinocandins are the newest category of antifungals agents, consisting in fungi derived semisynthetic lipopeptides composed of a cyclic hexapeptide core and a variable lipid side chain responsible for their antifungal activity (Groll et al., 2003; Odds et al., 2003). Although they were discovered in the 1970s, only 30 years later their use was approved by the US Food and Drug Administration. Echinocandins inhibits the synthesis of 1,3-β-glucan, a structural fungal cell wall polysaccharide that is responsible for cell wall's shape and rigidity, osmotic integrity and is important in cell division and cell growth (Georgopapadakou, 2001; Groll et al., 2003; Odds et al., 2003). Echinocandins includes caspofungin, anidulafungin and micafungin, all of them only available for i.v. administration (Groll et al., 2003; Odds et al., 2003). Their effect is species-dependent, acting as fungicidal against *Candida* spp. and fungistatic against *Aspergillus* spp. (Nett and Andes, 2016), with variable activity against dematiaceous and endemic mold (Seyedmousavi et al., 2017). However, echinocandins have no activity against *Scedosporium* spp., *Fusarium* spp., and *C. neoformans* (Groll et al., 2003; Odds et al., 2003; Arnold et al., 2010; Nett and Andes, 2016). Since echinocandins target β-glucan, which is not present in the mammalian cell, they present minimal side effects in humans (Groll et al., 2003; Sanglard et al., 2009; Arnold et al., 2010; Shapiro et al., 2011; Prasad et al., 2016), which may include gastrointestinal upsets headache and increased liver aminotransferases. Few drug-drug interactions were reported since echinocandins are not metabolized through cytochrome P-450 enzymes (Arnold et al., 2010; Nett and Andes, 2016).

As stated above, although antifungal arsenal currently available for systemic mycoses is effective against the majority of fungal pathogens, they present limitations such as toxicity, drug-drug interactions, and emergence of clinical resistance. In order to overcome these problems, strategies like combination therapy (Mukherjee et al., 2005) and even repurposing of established medications (Butts and Krysan, 2012) are being exploited. The search for new compounds and new targets, together with the improvement of existing formulations are extremely needed. Nanostructuration of conventional antifungal agents may be an interesting alternative to achieve a better antifungal efficacy and safety (**Figure 1**).

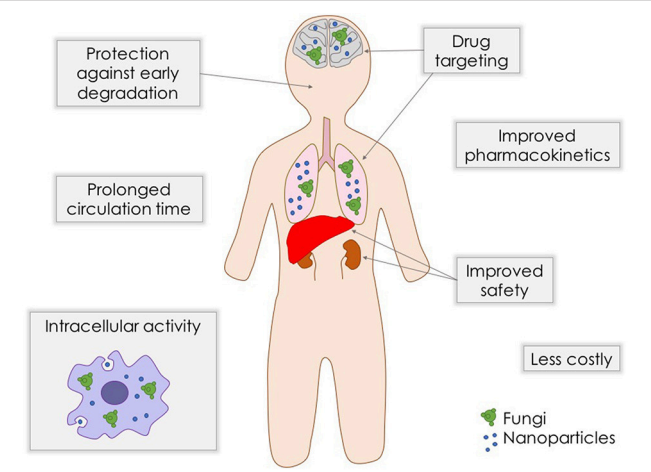


**FIGURE 1 | Benefits of nanobiotechnology approaches for delivery of antifungal drugs.**

## NANOBIOTECHNOLOGICAL APPROACHES FOR ANTIFUNGAL DELIVERY

Drug delivery systems containing nanoparticles have been object of intense investigation for the past decades, becoming an efficient strategy to increase drug bioavailability, reduce toxicity and enhance antifungal potency (Vyas and Gupta, 2006; Amaral and Felipe, 2013; de Sá et al., 2015; Stiufiuc et al., 2015). Among the advantages of this approach is the possibility to build formulations for a smart delivery, for example, targeting specific tissues and organs, such as the lungs, which are frequently the initial infection site during systemic fungal diseases (Amaral et al., 2009; Malathi and Balasubramanian, 2011; Moritz and Geszke-Moritz, 2015). In some cases, during intracellular infections, nanoparticles can penetrate the cells, leading the drug to act directly against the pathogen (Borborema et al., 2011; Dube et al., 2014). On the other hand, when coated with substances such as polyethylene glycol (PEG), they can evade recognition by the phagocytic system, preventing the attachment of opsonines, and promoting a longer circulation time (Stiufiuc et al., 2015). Studies have shown that nanoparticles also have desirable characteristics to be used as adjuvants in vaccines (Van Slooten et al., 2001; Agger et al., 2008; Bhowmick et al., 2008; Ribeiro et al., 2013). Currently, many types of nanostructures are under investigation for drug delivery of antifungal drugs, such as polymeric nanoparticles, solid lipid nanoparticles, liposomes, and magnetic nanoparticles (**Figure 2**).

Polymeric nanoparticles are prepared from various natural or synthetic polymers, both hydrophilic and hydrophobic (Pagels and Prud'homme, 2015). These polymers may be of natural origin, such as chitosan and alginate, or synthetics, such as poly (lactic acid, PLA) and poly (glycolic acid, PGA) or a combination of both forming the poly (lactide-*co*-glycolide acid, PLGA) (Bolhassani et al., 2014). When applied *in vivo*, polymeric

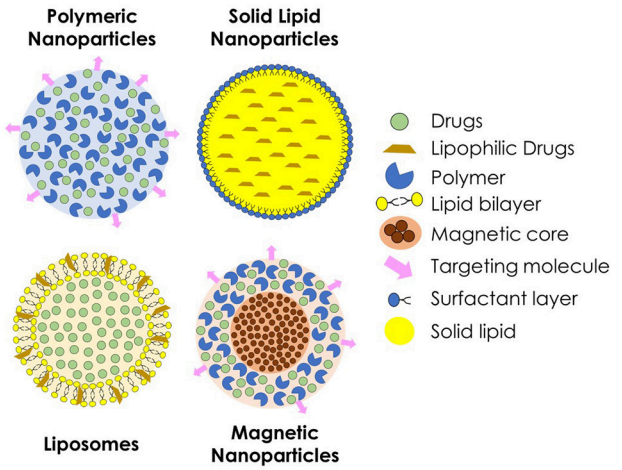


**FIGURE 2 | Schematic representation of different types of nanoparticles used for the delivery of antifungal agents.**

nanoparticles suffer biodegradation to be metabolized and excreted by the organism, what confers better biocompatibility (Amaral and Felipe, 2013). As the polymer is degraded, the drug incorporated within is released to the medium and can efficiently reach the site of action.

Liposomes are particles made by natural or synthetic phospholipids. Because of the nature of these molecules, when in contact with an aqueous medium, they form spherical structures containing an aqueous nucleus surrounded by a lipid bilayer (Bozzuto and Molinari, 2015), which can be suitable for delivery of both hydrophilic and hydrophobic substances (Stiufiuc et al., 2015). Because of their sensitivity to pH variations, liposomes permeability can be adjusted, releasing the drug into specific sites, such as macrophage compartments with altered pH during an infection (Wang et al., 2014; Jiang et al., 2015). A successful example of this class of nanoparticles is the commercially available liposomal Amphotericin B, brand name Ambisome® (Reis, 2015). In addition, solid lipid nanoparticles have been intensively investigated, specially for topical drug delivery (Kumar and Sinha, 2016; Trombino et al., 2016). They are spherical nanoparticles constituted of physiological and biodegradable lipids, such as stearic acid. Due to chemical composition, solid lipid nanoparticles allow the nanostructuration of insoluble drugs, and have low toxicity.

Magnetic nanoparticles have received special attention for biological applications, mainly because of their ability to be manipulated by a magnetic field, so that it can be directed and delivered to, theoretically, a specific site of the organism (Hussein et al., 2014). This type of nanoparticles can be prepared by different chemical and physical methodologies using ferrous compounds such as cobalt, manganese and zinc ferrites, magnetite, and maghemite. In the medical field, these magnetic nanoparticles are mainly used for clinical diagnosis through magnetic resonance imaging (MRI). This type of nanoparticle can also be associated with other nanostructures, such as polymeric nanoparticles or liposomes, to combine characteristics for both MRI and drug delivery (Jain et al., 2008). The superparamagnetic iron oxide nanoparticles, a specific kind of magnetic nanoparticle, respond more efficiently to an external magnetic field (Kumar et al., 2010) presenting a great potential to be used as drug carriers.

There are over a 100 publications proposing new nanoformulations for antifungal drugs (**Table 2**). In this review, we will summarize the major findings for nanoparticles that had proven *in vivo* and/ or *in vitro* antifungal activity.

## NANOPREPARATIONS FOR POLYENES

Among antifungal drugs, the investigation surrounding nanostructured delivery systems for polyenes are the most reported, the majority of them concerning Amphotericin B delivery. This is not surprising, since Amphotericin B is still the gold standard for antifungal therapy of severe systemic mycosis and the drug with the most potent antifungal capacity (Arnold et al., 2010). Amphotericin B nanoparticles have been investigated since 1980s, providing the opportunity to circumvent infusion-related side effects and nephrotoxicity, which are the main limiting factors concerning therapy with this drug. Further, because of the Amphotericin B poor solubility and oral bioavailability (Kang et al., 2010), such formulations are also intended to improve these characteristics, making it suitable for oral delivery.

Currently, lipid formulations for Amphotericin B are commercially available (Walsh et al., 1999; Kleinberg, 2006). The most successful is Ambisome®, which is considered a truly liposomal formulation, where Amphotericin B is embedded in the unilamellar liposome bilayer of about 45–80 nm (Adler-Moore, 1994). One of the advantages brought by this formulation is that it causes less toxicity and remains at high peaks in the circulation, presenting in a high biodistribution. A study using the murine model of pulmonary aspergillosis showed that Ambisome® was able to increase the survival of animals without toxicity, allowing the administration of a 10-fold higher dose than in animals receiving the conventional formulation in sodium deoxycholate (Takemoto, 2006). Liposomal formulations for topical applications have also been explored (Kang et al., 2010; Perez et al., 2016). Some of these preparations aim to increase the permanency of the formulation at the site of action, releasing the drug for longer time. Unfortunately, together with the higher biosafety, it was reported that antifungal effectiveness of Amphotericin B lipid formulations may be reduced in comparison to that of free drug (Andes et al., 2006; Burgess et al., 2013). In addition to that, the high costs are among the limitations to their widespread use (Dismukes, 2000; Falci et al., 2011; Italia et al., 2011; Van de Ven et al., 2012), encouraging the search for new options for Amphotericin B delivery.

In order to diminish costs of manufacturing, Nanosomal Amphotericin B was developed using phosphatidylcholine and sodium cholesteryl sulfate as excipients avoiding the use of organic solvents or detergents in the preparation (Sheikh et al., 2010). Nanosomal Amphotericin B induced less lysis of red blood cells than Amphotericin B sodium deoxycholate and

**TABLE 2 | Examples of studies reporting antifungal nanoparticles with *in vivo* and/or *in vitro* activity.**

| Antifungal agent | Type Of nanoparticle | Administration | *In vivo* | *In vitro* | References |
|---|---|---|---|---|---|
| Amphotericin B | Lipid nanoparticles | Inhalation | N/A | *Candida albicans, Cryptococcus neoformans* | Gangadhar et al., 2014 |
| | | Intravenous | *Aspergillus fumigatus* | *Candida albicans, Aspergillus fumigatus* | Jung et al., 2009 |
| | | Intravenous | *Aspergillus fumigatus* | N/A | Sheikh et al., 2010 |
| | | Intravenous | *Candida albicans* | N/A | Burgess et al., 2013 |
| | Liposomes | N/A | N/A | *Candida albicans, Candida tropicalis* | Albasarah et al., 2010 |
| | Magnetic nanoparticles | Nasal instilation | *Paracoccidioides brasiliensis* | N/A | Saldanha et al., 2016 |
| | Nanoemulsion | Topical | N/A | *Aspergillus fumigatus, Aspergilus niger, Candida albicans* | Hussain et al., 2016 |
| | Nanosuspension | Ocular | N/A | *Fusarium solani* | Das and Suresh, 2011 |
| | Polymeric nanoparticles | Inhalation | *Aspergillus fumigatus* | N/A | Shirkhani et al., 2015 |
| | | Intraperitoneal | *Aspergillus fumigatus* | N/A | Van de Ven et al., 2012 |
| | | Intraperitoneal | *Paracoccidioides brasiliensis* | N/A | Amaral et al., 2009; Souza et al., 2015 |
| | | Intravenous | *Candida albicans* | N/A | Tang et al., 2014, 2015a |
| | | Intravenous | *Candida glabrata* | N/A | Tang et al., 2015b |
| | | Intravenous | *Cryptococcus neoformans* | N/A | Xu et al., 2011 |
| | | Intravenous | N/A | *Candida albicans* | Han et al., 2007 |
| | | Intravenous | | *Candida albicans* | Zia et al., 2015 |
| | | N/A | *Candida glabrata* | N/A | Tang et al., 2015c |
| | | N/A | N/A | *Candida albicans* | Tiyaboonchai et al., 2001; Tang et al., 2014 |
| | | N/A | N/A | *Candida albicans, Candida tropicalis* | Casa et al., 2015 |
| | | Ocular | N/A | *Candida albicans* | Zhou et al., 2013 |
| | | Ocular | N/A | *Candida albicans, Aspergillus fumigatus* | Zhou et al., 2013 |
| | | Oral | *Candida albicans, Aspergillus fumigatus* | N/A | Serrano et al., 2015 |
| | Polymeric nanoparticles | Oral/intravenous | *Aspergillus fumigatus* | N/A | Italia et al., 2011 |
| | | Topical | *Candida albicans, Candida glabrata, Candida parapsilosis* | N/A | Sanchez et al., 2014 |
| | Solid Lipid Nanoparticles | N/A | N/A | *Candida albicans* | Vieira and Carmona-Ribeiro, 2008 |
| | | Oral | N/A | *Candida albicans* | Chaudhari et al., 2016 |
| Amphotericin B and Nystatin | Magnetic nanoparticles | N/A | N/A | *Candida albicans* | Niemirowicz et al., 2016 |
| Fluconazole | Polymeric nanoparticles | Ocular | *Candida albicans* | N/A | Rençber et al., 2016 |
| | Solid Lipid Nanoparticles | N/A | N/A | *Candida albicans, Candida glabrata, Candida parapsilosis* | Moazeni et al., 2016 |
| | | Topical | *Candida albicans* | N/A | Gupta and Vyas, 2012 |
| Itraconazole | Lipid nanoparticles | Inhalation | *Aspergillus fumigatus* | N/A | Pardeike et al., 2016 |
| | Polymeric nanoparticles | N/A | *Candida albicans* | N/A | Qiu et al., 2015 |

*(Continued)*

**TABLE 2 | Continued**

| Antifungal agent | Type Of nanoparticle | Administration | *In vivo* | *In vitro* | Reference |
|---|---|---|---|---|---|
| | | N/A | N/A | *Aspergillus flavus* | Patel et al., 2011 |
| | | N/A | N/A | *Candida albicans, Aspergillus fumigatus* | Essa et al., 2012 |
| | | N/A | N/A | *Paracoccidioides brasiliensis* | Cunha-Azevedo et al., 2011 |
| | | N/A | N/A | *Aspergillus flavus* | Patel et al., 2010 |
| | Solid Lipid Nanoparticles | Ocular | N/A | *Aspergillus flavus* | Mohanty et al., 2015 |
| Miconazole | Liposomes | Topical | *Candida albicans* | N/A | Pandit et al., 2014 |
| | Solid Lipid Nanoparticles | Topical | *Candida albicans* | N/A | Jain et al., 2010 |
| Nystatin | Polymeric nanoparticles | N/A | N/A | *Candida albicans* | Mohammadi et al., 2017 |
| Voriconazole | Polymeric nanoparticles | Oral | *Candida albicans* | N/A | Peng et al., 2008 |

was comparable to Ambisome®. No symptoms of toxicity, mortality or significant body weight reduction were observed in rabbits daily treated with this formulation for 28 days, with no hematological and gross pathological abnormalities. Besides, in mice disseminated *A. fumigatus* infection, intravenous administration of Nanosomal Amphotericin B resulted in 90% survival while only 30% survival with Ambisome®.

Anionic and PEG lipid nanoparticles were developed by Jung et al. (2009) for intravenous delivery of Amphotericin B (Jung et al., 2009). This formulation presented lower cytotoxicity against human kidney cells than Fungizone® and Ambisome®, and much lower hematotoxicity than that of Fungizone®. Antifungal activity *in vitro* of Amphotericin B lipid nanoparticles against *C. albicans* and *A. fumigatus* was better than the commercialized formulations and *in vivo* administration for the treatment of murine systemic aspergilloma was more effective than that of Ambisome®.

Burgess et al. (2013) developed a formulation consisting of a protein-phospholipid bioparticle (NanoDisk) containing a "super aggregate" form of amphotericin B (ND–AMB) (Burgess et al., 2013). ND–AMB presented lower *C. albicans* and *A. fumigatus* minimum inhibitory concentrations than those observed for Ambisome®. It also induced no kidney or liver toxicity in mice. In addition, in *C. albicans* infected immune-competent mice, ND-AMB treatment was as effective as sodium deoxycholate amphotericin B or Ambisome®, whereas in a leukopenic model of candidiasis, the 50% effective dose of ND-AMB was around threefold lower than Ambisome®.

In addition to the lipid formulations, polymeric systems for the delivery of Amphotericin B have been developed by several research groups (**Table 2**). The results proved this type of preparation to be satisfactory for the efficient delivery of this drug by several routes, such as intravenously (Amaral et al., 2009; Tang et al., 2014; Souza et al., 2015) and orally (Italia et al., 2009, 2011, 2012). The biological response may vary according to the type of polymer used or even by combining different polymer types. An example is the formulation developed by Tang et al. (2014), in which AMB was encapsulated within PLGA in association with ε-caprolactone. In this combination, the authors reported an AMB encapsulation efficiency of 84% and the same fungicidal effect on *C. albicans* as for the free drug (Tang et al., 2014). The proposed formulation was less toxic and caused lower mortality than free AMB, proving, as noted before, the potential of polymeric nanoparticles to protect against cytotoxicity but preserving the same fungicidal efficacy (Amaral et al., 2009).

Amaral et al. (2009) developed a nanostructured formulation for Amphotericin B within PLGA functionalized with dimercaptosuccinic acid (DMSA). This acid presents tropism to the lungs, being suitable to be incorporation in formulations for drug delivery to this organ (Amaral et al., 2009, 2010). In this study, authors noted that intraperitoneal administration of the formulation was able to cause the same therapeutic effect in murine model of paracoccidioidomycosis compared to sodium deoxycholate Amphotericin B. However, the great advantage of this polymeric formulation was that it was given to the animals every 3 days, considering the slow release of Amphotericin B from nanoparticles, in contrast to the conventional formulation, which was administrated daily. Complementary studies conducted by the same research group showed that amphotericin B PLGA nanoparticles were also comparable to Ambisome® in the therapy of murine paracoccidioidomycosis (Souza et al., 2015). In addition, both studies reported no undesirable side effects in animals at the dose used. High concentrations of Amphotericin B were found in lungs, liver and spleen of animals treated with this polymeric formulation (Souza et al., 2015).

Van de Ven et al. (2012) showed that both Amphotericin B PLGA nanoparticles and nanoemulsion had *in vitro*

antifungal capacity against *C. albicans*, *A. fumigatus,* and *Trichophyton rubrum* and were less hemolytic than sodium deoxycholate Amphotericin B (Van de Ven et al., 2012). In addition, both formulations were effective against murine disseminated aspergillosis after intraperitoneal administration, with similar or even better antifungal capacity than Fungizone® and Ambisome® at equivalent doses. Italia et al. (2011) proposed Amphotericin B PLGA nanoparticles for oral delivery, which significantly reduced fungal burden during invasive pulmonary and disseminated aspergillosis (Italia et al., 2011).

In a very interesting approach, Tang et al. (2015a) developed specialized pH-responsive Amphotericin B PLGA nanoparticles conjugated with poly(L-histidine) and PEG that had high affinity for fungal cell wall elements under acidic conditions and were further modified for increased targeting efficacy with anti-*C. albicans* antibody (Tang et al., 2015a). The formulation had reduced hemolytic activity and cytotoxicity on human renal tubular epithelial cells, and was effective against *C. albicans* both *in vivo* and *in vitro* after intravenous administration. Nystatin loaded PLGA nanoparticles functionalized with Glucosamine were formulated by Mohammadi et al. (2017) to enhance the adhesion of nanoparticles to *C. albicans* cell walls (Mohammadi et al., 2017). The nanoparticles exhibited higher antifungal activity than free Nystatin, suggesting an increase in Nystatin levels in fungal cell membrane by entrapment in the polymeric matrix.

Chitosan is a natural polysaccharide with cationic nature and mucoadhesive proprieties that has been frequently used to build biodegradable polymeric nanoparticles for drug delivery. Amphotericin B chitosan nanoparticles were developed by Serrano et al. (2015) intending to avoid drug gastrointestinal degradation, improve stability and enhance bioavailability in target organs such as lung, liver, and spleen, while diminishing kidney exposure (Serrano et al., 2015). They have demonstrated that oral administration of these nanoparticles was effective in the treatment of murine models of visceral leishmaniasis, candidiasis and aspergillosis, having comparable efficacy to parenteral Ambisome®. Chitosan nanoparticles were used by Sanchez et al. (2014) for topical delivery of Amphotericin B to burn wounds infected with *C. albicans,* with enhanced tissue healing and even better antifungal activity than sodium deoxycholate formulation (Sanchez et al., 2014). Amphotericin B loaded nanoparticles made of lecithin and chitosan were proposed by Chhonker et al. (2015) for prolonged ocular application such as during fungal keratitis (Chhonker et al., 2015). The formulation presented *in vitro* antifungal efficacy against *C. albicans* and *A. fumigatus*, pronounced mucoadhesive properties and improved bioavailablity as compared with Fungizone®.

Approaches to increase Amphotericin B delivery into central nervous system (CNS) are also under investigation. Amphotericin B polybutylcyanoacrylate nanoparticles modified with polysorbate 80 were used as therapy for cryptococcal meningitis murine model (Xu et al., 2011). Nanoparticles were detected in the brain 30 min after systemic administration into mice with a higher concentration than Amphotericin B liposomes. Survival rate of mice treated with nanoparticles was significantly higher than that of sodium deoxycholate and liposomal amphotericin B treated groups, with lower fungal burden in brain tissue. Another formulation based in transferrin transcytosis at the blood-brain barrier was proposed by Tang et al. (2015c). In this study, anti-transferrin receptor antibody-modified Amphotericin B-loaded PLA-PEG nanoparticles were developed and presented significant reduction of CNS fungal burden and increased mouse survival time when administered intravenously for the treatment of meningitis induced by *C. glabrata* inoculation (Tang et al., 2015c).

Shirkhani et al. (2015) developed Amphotericin B polymethacrylic acid nanoparticles for the prophylaxis of *A. fumigatus* infection in a transplant immunosuppression murine model with invasive aspergillosis. The formulation was given by nebulization and prevented fungal growth and lung inflammation (Shirkhani et al., 2015).

Amphotericin B magnetic nanoparticles were reported by Saldanha et al. (2016). In this study, authors developed Amphotericin B loaded lauric acid pre-coated magnetite nanoparticles and showed nanocomplex antifungal activity both *in vivo* and i*n vitro* against *P. brasiliensis* infection (Saldanha et al., 2016). The nanocomplex was more cytotoxic to fungal cells than to human urinary cells and murine peritoneal macrophages *in vitro*, while no biochemical and histopathological alterations were observed during intranasal therapy against murine paracoccidioidomycosis. The formulation exhibited similar antifungal activity to that of sodium deoxycholate Amphotericin B administrated intraperitonealy, with the advantage to allow a three-fold reduction in the number of applications and to be suitable for nasal delivery. Another Amphotericin B magnetic liposomal system were proposed by Zhao et al. (2014) aiming to enhance drug selectivity to CNS during fungal infections. The liposomal system was administered via carotid artery route in SD rats and could improve drug concentration and enhance magnetic targeting to brain tissue in the presence of a magnetic field. Amphotericin B and nystatin magnetic nanoparticles were also designed by Niemirowicz et al. (2016). Both nanosystems displayed stronger fungicidal activity than unbound drugs against *Candida* spp. (Niemirowicz et al., 2016). Nanosystems were more potent than free agents when tested against *Candida* strains and were able to prevent *Candida* biofilm formation more effectively with lower hemolytic capacity.

Some fungal pathogens have the ability to reside inside host cells, such as macrophages. Therefore, nanoparticles uptake by host cells is very desirable as a strategy to enhance antifungal abilities against intracellular fungi. Zia et al. (2015) showed that killing of intracellular *C. albicans* after treatment with amphotericin B polyglutamic acid nanoparticles was higher than with Ambisome® (Zia et al., 2015). Amphotericin B is also used for the treatment of infections caused by *Leishmania* spp., which is an intracellular parasite, so that intense investigation has been done in order to enhance drug antiparasitic effects throughout nanostruturation (Asthana et al., 2015; Jain et al., 2015; Bose et al., 2016).

## NANOPREPARATIONS FOR AZOLES

The increase of oral bioavailability of azoles is one of the advantages conferred by the use of nanotechnology for this class of drug. It is interesting to note that although preparing a formulation at the nanoscale may suggest similar results when using the same type of nanoparticle and material, this is not always true. For example, a study encapsulating econazole and clotrimazole in both PLGA and alginate (Pandey et al., 2005) demonstrated that the latter seems to be better at improving pharmacokinetic parameters. Though, both proved to be effective for the oral route.

Considering the severity of some fungal infections affecting the lungs, nanostructured delivery systems for drugs capable of reaching this organ are sought. Some studies showed the tropism for the lungs by PLGA nanoparticles. The PLGA-encapsulated voriconazole showed a higher accumulation in the lungs when compared with free voriconazole (Das et al., 2015). This characteristic was also observed by other researchers when they also encapsulated voriconazole in PLGA for nasal administration. The study demonstrated the system allows the early release of the drug in the lungs in the first 2 h, followed by a sustained release during 15 days (Sinha et al., 2013). Itraconazole PLGA nanoparticles conjugated with dimercaptosuccinic acid were developed for pulmonary delivery and induced antifungal inhibition against *P. brasiliensis* with lower *in vitro* cytotoxicity than free drug (Cunha-Azevedo et al., 2011).

Voriconazole loaded PLGA nanoparticles were developed by Peng et al. (2008) in order to improve drug bioavailability and stability for oral delivery (Peng et al., 2008). Nanoparticles had a more persistent and potent antifungal effect than free voriconazole both *in vitro* and *in vivo* in a systemic candidiasis murine model.

Other triazole loaded polymeric nanostructured formulations have been investigated and had *in vitro* antifungal activities against *A. flavus* (Patel et al., 2010, 2011), *A. fumigatus* (Essa et al., 2012), and *C. albicans* (Qiu et al., 2015). Some polymers have mucoadhesive properties, such as chitosan, and can be used to prepare drug delivery systems for mucosa from the eyes, mouth and vagina. Rençber et al. (2016) developed a buccal mucoadhesive nanoparticle containing fluconazole and EUDRAGIT®, a nonbiodegradable and cationic copolymer, for the local treatment of oral candidiasis. The formulation presented *in vitro* antifungal activity against *C. albicans* for an extended period, and no cytotoxic effect in chinese hamster ovary cells was observed. Rabbits with oral candidiasis were successfully treated with local administration of the nanoparticles once a day (Rençber et al., 2016). More sophisticated drug delivery systems formed by different types of nanoparticles can be prepared (Jøraholmen et al., 2014). For example, in one polymer the drug is encapsulated and this polymer is coated with another to present the proper *in vivo* application.

Ultraflexible liposomes carrying miconazole also showed to be more efficient and able to penetrate the cell barrier carrying the drug. As they are able to adapt their shape according to the characteristics of the near microenvironment, they are able to penetrate and release the drug more efficiently (Pandit et al., 2014). It is also possible to promote the release of miconazole only to the skin, without penetrating it or reaching the epidermis (Elmoslemany et al., 2012), which is important for reducing toxicity.

Solid lipid nanoparticles (SLN) have been intensively investigated for topical delivery of azole antifungals. Jain et al. (2010) developed a formulation of miconazole nitrate loaded SLN-bearing hydrogel for skin delivery (Jain et al., 2010). Studies indicated that miconazole SLN-bearing hydrogel resulted in considerably less skin irritation as compared to miconazole hydrogel and suspension after 24 h of application. In addition, micozanole SLN treatment of cutaneous candidiasis in albino rats presented greater efficiency and fast recovery. Mohanty et al. (2015) investigated SLNs for topical ocular delivery of itraconazole (Mohanty et al., 2015). Permeation of itraconazole in freshly excised goat corneas was observed, and SLN inhibited *Aspergillus flavus in vitro* growth, indicating antimicrobial efficacy of formulations.

Moazeni et al. (2016) tested fluconazole-loaded SLN efficacy against fluconazole-resistant *Candida* spp. strains. Fluconazole-resistant *C. albicans*, *C. parapsilosis,* and *C. glabrata* strains behaved as susceptible strains after treatment with fluconazole SLN, emphasizing the promising benefits of nanostructuration for the delivery of antifungal agents.

## CONCLUDING REMARKS

The high incidence of fungal infections is a problem that can be aggravated mainly by the increase of the elderly population and also by immunocompromised patients. In this way, it is important that new and more effective therapies are developed for the treatment of these mycoses. One strategy that has received importance for this purpose is the development of drugs applying the principles of nanotechnology. It is possible to use the same conventional drugs, but aiming to increase its therapeutic efficacy and also the reduction of its side effects. Thus, unlike the basic development of a novel antifungal molecule, which is also of relevant importance, conventional formulations may be improved in effectiveness by the resources of Nanobiotechnology.

## AUTHOR CONTRIBUTIONS

All authors listed, have made substantial, direct and intellectual contribution to the work, and approved it for publication.

## FUNDING

Ana Camila Oliveira Souza is funded by grant 2015/10390-6 from the Fundação de Amparo à Pesquisa de São Paulo (FAPESP).

## REFERENCES


Adler-Moore, J. (1994). AmBisome targeting to fungal infections. *Bone Marrow Transplant.* 14(Suppl. 5), S3–S7.

Adler-Moore, J. P., Gangneux, J. P., and Pappas, P. G. (2016). Comparison between liposomal formulations of amphotericin B. *Med. Mycol.* 54, 223–231. doi: 10.1093/mmy/myv111

Agger, E. M., Rosenkrands, I., Hansen, J., Brahimi, K., Vandahl, B. S., Aagaard, C., et al. (2008). Cationic liposomes formulated with synthetic mycobacterial cordfactor (CAF01): a versatile adjuvant for vaccines with different immunological requirements. *PLoS ONE* 3:e3116. doi: 10.1371/journal.pone.0003116

Albasarah, Y. Y., Somavarapu, S., Stapleton, P., and Taylor, K. M. (2010). Chitosan-coated antifungal formulations for nebulisation. *J. Pharm. Pharmacol.* 62, 821–828. doi: 10.1211/jpp.62.05.0002

Amaral, A. C., Bocca, A. L., Ribeiro, A. M., Nunes, J., Peixoto, D. L., Simioni, A. R., et al. (2009). Amphotericin B in poly(lactic-co-glycolic acid) (PLGA) and dimercaptosuccinic acid (DMSA) nanoparticles against paracoccidioidomycosis. *J. Antimicrob. Chemother.* 63, 526–533. doi: 10.1093/jac/dkn539

Amaral, A. C., and Felipe, M. S. S. (2013). Nanobiotechnology: an efficient approach to drug delivery of unstable biomolecules. *Curr. Protein Pept. Sci.* 14, 588–594. doi: 10.2174/1389203711209070632

Amaral, A. C., Marques, A. F., Muñoz, J. E., Bocca, A. L., Simioni, A. R., Tedesco, A. C., et al. (2010). Poly(lactic acid-glycolic acid) nanoparticles markedly improve immunological protection provided by peptide P10 against murine paracoccidioidomycosis. *Br. J. Pharmacol.* 159, 1126–1132. doi: 10.1111/j.1476-5381.2009.00617.x

Andes, D., Safdar, N., Marchillo, K., and Conklin, R. (2006). Pharmacokinetic-pharmacodynamic comparison of amphotericin B (AMB) and two lipid-associated AMB preparations, liposomal AMB and AMB lipid complex, in murine candidiasis models. *Antimicrob. Agents Chemother.* 50, 674–684. doi: 10.1128/AAC.50.2.674-684.2006

Arnold, T. M., Dotson, E., Sarosi, G. A., and Hage, C. A. (2010). Traditional and emerging antifungal therapies. *Proc. Am. Thorac. Soc.* 7, 222–228. doi: 10.1513/pats.200906-048AL

Asthana, S., Gupta, P. K., Jaiswal, A. K., Dube, A., and Chourasia, M. K. (2015). Overexpressed macrophage mannose receptor targeted nanocapsules-mediated cargo delivery approach for eradication of resident parasite: *in vitro* and *in vivo* studies. *Pharm. Res.* 32, 2663–2677. doi: 10.1007/s11095-015-1651-0

Bartner, E., Zinnes, H., Moe, R. A., and Kuleska, J. S. (1958). Studies on a new solubilized preparation of amphotericin B. *Antibiot. Annu.* 5, 53–58.

Bhowmick, S., Ravindran, R., and Ali, N. (2008). gp63 in stable cationic liposomes confers sustained vaccine immunity to susceptible BALB/c mice infected with *Leishmania donovani*. *Infect. Immun.* 76, 1003–1015. doi: 10.1128/IAI.00611-07

Bolhassani, A., Javanzad, S., Saleh, T., Hashemi, M., Aghasadeghi, M. R., and Sadat, S. M. (2014). Polymeric nanoparticles. *Hum. Vaccin. Immunother.* 10, 321–332. doi: 10.4161/hv.26796

Bonifaz, A., Vázquez-González, D., and Perusquía-Ortiz, A. M. (2011). Endemic systemic mycoses: coccidioidomycosis, histoplasmosis, paracoccidioidomycosis and blastomycosis. *J. Dtsch. Dermatol. Ges.* 9, 705–715. doi: 10.1111/j.1610-0387.2011.07731.x

Borborema, S. E., Schwendener, R. A., Osso, J. A., de Andrade, H. F. Jr., and do Nascimento, N. (2011). Uptake and antileishmanial activity of meglumine antimoniate-containing liposomes in Leishmania (Leishmania) major-infected macrophages. *Int. J. Antimicrob. Agents* 38, 341–347. doi: 10.1016/j.ijantimicag.2011.05.012

Bose, P. P., Kumar, P., and Dwivedi, M. K. (2016). Hemoglobin guided nanocarrier for specific delivery of amphotericin B to Leishmania infected macrophage. *Acta Trop.* 158, 148–159. doi: 10.1016/j.actatropica.2016.02.026

Bozzuto, G., and Molinari, A. (2015). Liposomes as nanomedical devices. *Int. J. Nanomedicine* 10, 975–999. doi: 10.2147/IJN.S68861

Brown, G. D., Denning, D. W., Gow, N. A., Levitz, S. M., Netea, M. G., and White, T. C. (2012a). Hidden killers: human fungal infections. *Sci. Transl. Med.* 4, 165rv13. doi: 10.1126/scitranslmed.3004404

Brown, G. D., Denning, D. W., and Levitz, S. M. (2012b). Tackling human fungal infections. *Science* 336, 647–647. doi: 10.1126/science.1222236

Burgess, B. L., He, Y., Baker, M. M., Luo, B., Carroll, S. F., Forte, T. M., et al. (2013). NanoDisk containing super aggregated amphotericin B: a high therapeutic index antifungal formulation with enhanced potency. *Int. J. Nanomedicine* 8, 4733–4743. doi: 10.2147/IJN.S50113

Butts, A., and Krysan, D. J. (2012). Antifungal drug discovery: something old and something new. *PLoS Pathog.* 8:e1002870. doi: 10.1371/journal.ppat.1002870

Caffrey, A. K., and Obar, J. J. (2016). Alarmin(g) the innate immune system to invasive fungal infections. *Curr. Opin. Microbiol.* 32, 135–143. doi: 10.1016/j.mib.2016.06.002

Carrillo-Muñoz, A. J., Giusiano, G., Ezkurra, P. A., and Quindós, G. (2006). Antifungal agents: mode of action in yeast cells. *Rev. Esp. Quimioter.* 19, 130–139.

Casa, D. M., Carraro, T. C., de Camargo, L. E., Dalmolin, L. F., Khalil, N. M., and Mainardes, R. M. (2015). Poly(L-lactide) nanoparticles reduce amphotericin B cytotoxicity and maintain its *in vitro* antifungal activity. *J. Nanosci. Nanotechnol.* 15, 848–854. doi: 10.1166/jnn.2015.9177

Chaudhari, M. B., Desai, P. P., Patel, P. A., and Patravale, V. B. (2016). Solid lipid nanoparticles of amphotericin B (AmbiOnp): *in vitro* and *in vivo* assessment towards safe and effective oral treatment module. *Drug Deliv. Transl. Res.* 6, 354–364. doi: 10.1007/s13346-015-0267-6

Chhonker, Y. S., Prasad, Y. D., Chandasana, H., Vishvkarma, A., Mitra, K., Shukla, P. K., et al. (2015). Amphotericin-B entrapped lecithin/chitosan nanoparticles for prolonged ocular application. *Int. J. Biol. Macromol.* 72, 1451–1458. doi: 10.1016/j.ijbiomac.2014.10.014

Como, J. A., and Dismukes, W. E. (1994). Oral azole drugs as systemic antifungal therapy. *N. Engl. J. Med.* 330, 263–272. doi: 10.1056/NEJM199401273300407

Cunha-Azevedo, E. P., Silva, J. R., Martins, O. P., Siqueira-Moura, M. P., Bocca, A. L., Felipe, M. S., et al. (2011). *In vitro* antifungal activity and toxicity of itraconazole in DMSA-PLGA nanoparticles. *J. Nanosci. Nanotechnol.* 11, 2308–2314. doi: 10.1166/jnn.2011.3576

Das, P. J., Paul, P., Mukherjee, B., Mazumder, B., Mondal, L., Baishya, R., et al. (2015). Pulmonary delivery of voriconazole loaded nanoparticles providing a prolonged drug level in lungs: a promise for treating fungal infection. *Mol. Pharm.* 12, 2651–2664. doi: 10.1021/acs.molpharmaceut.5b00064

Das, S., and Suresh, P. K. (2011). Nanosuspension: a new vehicle for the improvement of the delivery of drugs to the ocular surface. Application to amphotericin B. *Nanomedicine* 7, 242–247. doi: 10.1016/j.nano.2010.07.003

Denning, D. W., and Hope, W. W. (2010). Therapy for fungal diseases: opportunities and priorities. *Trends Microbiol.* 18, 195–204. doi: 10.1016/j.tim.2010.02.004

de Sá, F. A., Taveira, S. F., Gelfuso, G. M., Lima, E. M., and Gratieri, T. (2015). Liposomal voriconazole (VOR) formulation for improved ocular delivery. *Colloids Surf. B Biointerfaces* 133, 331–338. doi: 10.1016/j.colsurfb.2015.06.036

Dismukes, W. E. (2000). Introduction to antifungal drugs. *Clin. Infect. Dis.* 30, 653–657. doi: 10.1086/313748

Dube, A., Reynolds, J. L., Law, W.-C., Maponga, C. C., Prasad, P. N., and Morse, G. D. (2014). Multimodal nanoparticles that provide immunomodulation and intracellular drug delivery for infectious diseases. *Nanomedicine* 10, 831–838. doi: 10.1016/j.nano.2013.11.012

Dupont, B. (2002). Overview of the lipid formulations of amphotericin B. *J. Antimicrob. Chemother.* 49(Suppl. 1), 31–36. doi: 10.1093/jac/49.suppl_1.31

Elmoslemany, R. M., Abdallah, O. Y., El-Khordagui, L. K., and Khalafallah, N. M. (2012). Propylene glycol liposomes as a topical delivery system for miconazole nitrate: comparison with conventional liposomes. *AAPS PharmSciTech* 13, 723–731. doi: 10.1208/s12249-012-9783-6

Essa, S., Louhichi, F., Raymond, M., and Hildgen, P. (2012). Improved antifungal activity of itraconazole-loaded PEG/PLA nanoparticles. *J. Microencapsul.* 30, 1–13. doi: 10.3109/02652048.2012.714410

Falci, D. R., dos Santos, R. P., Wirth, F., and Goldani, L. Z. (2011). Continuous infusion of amphotericin B deoxycholate: an innovative, low-cost strategy in antifungal treatment. *Mycoses* 54, 91–98. doi: 10.1111/j.1439-0507.2009.01805.x

Finkelstein, A., and Holz, R. (1973). Aqueous pores created in thin lipid membranes by the polyene antibiotics nystatin and amphotericin B. *Membranes (Basel).* 2, 377–408.

Francis, P., and Walsh, T. J. (1992). Evolving role of flucytosine in immunocompromised patients: new insights into safety, pharmacokinetics, and antifungal therapy. *Clin. Infect. Dis.* 15, 1003–1018.

Gangadhar, K. N., Adhikari, K., and Srichana, T. (2014). Synthesis and evaluation of sodium deoxycholate sulfate as a lipid drug carrier to enhance the solubility, stability and safety of an amphotericin B inhalation formulation. *Int. J. Pharm.* 471, 430–438. doi: 10.1016/j.ijpharm.2014.05.066

Georgopapadakou, N. H. (1998). Antifungals: mechanism of action and resistance, established and novel drugs. *Curr. Opin. Microbiol.* 1, 547–557. doi: 10.1016/S1369-5274(98)80087-8

Georgopapadakou, N. H. (2001). Update on antifungals targeted to the cell wall: focus on β-1,3-glucan synthase inhibitors. *Expert Opin. Investig. Drugs* 10, 269–280. doi: 10.1517/13543784.10.2.269

Goughenour, K. D., and Rappleye, C. A. (2017). Antifungal therapeutics for dimorphic fungal pathogens. *Virulence* 8, 211–221. doi: 10.1080/21505594.2016.1235653

Groll, A. H., Gea-Banacloche, J. C., Glasmacher, A., Just-Nuebling, G., Maschmeyer, G., and Walsh, T. J. (2003). Clinical pharmacology of antifungal compounds. *Infect. Dis. Clin. North Am.* 17, 159–191. doi: 10.1016/S0891-5520(02)00068-5

Groll, A. H., Piscitelli, S. C., and Walsh, T. J. (1998). Clinical pharmacology of systemic antifungal agents: a comprehensive review of agents in clinical use, current investigational compounds, and putative targets for antifungal drug development. *Adv. Pharmacol.* 44, 343–500. doi: 10.1016/S1054-3589(08)60129-5

Gulati, M., Bajad, S., Singh, S., Ferdous, A. J., and Singh, M. (1998). Development of liposomal amphotericin B formulation. *J. Microencapsul.* 15, 137–151. doi: 10.3109/02652049809006844

Gupta, M., and Vyas, S. P. (2012). Development, characterization and *in vivo* assessment of effective lipidic nanoparticles for dermal delivery of fluconazole against cutaneous candidiasis. *Chem. Phys. Lipids* 165, 454–461. doi: 10.1016/j.chemphyslip.2012.01.006

Han, K., Miah, M. A. J., Shanmugam, S., Yong, C. S., Choi, H.-G., Kim, J. A., et al. (2007). Mixed micellar nanoparticle of amphotericin B and poly styrene-block-poly ethylene oxide reduces nephrotoxicity but retains antifungal activity. *Arch. Pharm. Res.* 30, 1344–1349. doi: 10.1007/BF02980276

Havlickova, B., Czaika, V. A., and Friedrich, M. (2008). Epidemiological trends in skin mycoses worldwide. *Mycoses* 51, 2–15. doi: 10.1111/j.1439-0507.2008.01606.x

Heitman, J. (2011). Microbial pathogens in the fungal kingdom. *Fungal Biol. Rev.* 25, 48–60. doi: 10.1016/j.fbr.2011.01.003

Hsuchen, C. C., and Feingold, D. S. (1973). Selective membrane toxicity of the polyene antibiotics: studies on natural membranes. *Antimicrob. Agents Chemother.* 4, 316–319.

Hussain, A., Samad, A., Singh, S. K., Ahsan, M. N., Haque, M. W., Faruk, A., et al. (2016). Nanoemulsion gel-based topical delivery of an antifungal drug: *in vitro* activity and *in vivo* evaluation. *Drug Deliv.* 23, 642–647. doi: 10.3109/10717544.2014.933284

Hussein, M. Z., Al Ali, S., Geilich, B. M., El Zowalaty, M. E., and Webster, T. J. (2014). Synthesis, characterization, and antimicrobial activity of an ampicillin-conjugated magnetic nanoantibiotic for medical applications. *Int. J. Nanomedicine* 9, 3801–3814. doi: 10.2147/IJN.S61143

Italia, J. L., Kumar, M. N. V. R., and Carter, K. C. (2012). Evaluating the potential of polyester nanoparticles for per oral delivery of amphotericin B in treating visceral leishmaniasis. *J. Biomed. Nanotechnol.* 8, 695–702. doi: 10.1166/jbn.2012.1414

Italia, J. L., Sharp, A., Carter, K. C., Warn, P., and Kumar, M. N. (2011). Peroral amphotericin B polymer nanoparticles lead to comparable or superior *in vivo* antifungal activity to that of intravenous Ambisome® or Fungizone™. *PLoS ONE* 6:e25744. doi: 10.1371/journal.pone.0025744

Italia, J. L., Yahya, M. M., Singh, D., and Ravi Kumar, M. N. (2009). Biodegradable nanoparticles improve oral bioavailability of amphotericin B and show reduced nephrotoxicity compared to intravenous fungizone®. *Pharm. Res.* 26, 1324–1331. doi: 10.1007/s11095-009-9841-2

Jain, K., Verma, A. K., Mishra, P. R., and Jain, N. K. (2015). Characterization and evaluation of amphotericin B loaded MDP conjugated poly(propylene imine) dendrimers. *Nanomedicine* 11, 705–713. doi: 10.1016/j.nano.2014.11.008

Jain, S. Jain, S., Khare, P., Gulbake, A., Bansal, D., and Jain, S. K. (2010). Design and development of solid lipid nanoparticles for topical delivery of an anti-fungal agent. *Drug Deliv.* 17, 443–451. doi: 10.3109/10717544.2010.483252

Jain, T. K., Richey, J., Strand, M., Leslie-Pelecky, D. L., Flask, C. A., and Labhasetwar, V. (2008). Magnetic nanoparticles with dual functional properties: drug delivery and magnetic resonance imaging. *Biomaterials* 29, 4012–4021. doi: 10.1016/j.biomaterials.2008.07.004

Jiang, L., Li, L., He, X., Yi, Q., He, B., Cao, J., et al. (2015). Overcoming drug-resistant lung cancer by paclitaxel loaded dual-functional liposomes with mitochondria targeting and pH-response. *Biomaterials* 52, 126–139. doi: 10.1016/j.biomaterials.2015.02.004

Jøraholmen, M. W., Vanić, Z., Tho, I., and Skalko-Basnet, N. (2014). Chitosan-coated liposomes for topical vaginal therapy: assuring localized drug effect. *Int. J. Pharm.* 472, 94–101. doi: 10.1016/j.ijpharm.2014.06.016

Jung, S. H., Lim, D. H., Jung, S. H., Lee, J. E., Jeong, K.-S., Seong, H., et al. (2009). Amphotericin B-entrapping lipid nanoparticles and their *in vitro* and *in vivo* characteristics. *Eur. J. Pharm. Sci.* 37, 313–320. doi: 10.1016/j.ejps.2009.02.021

Kang, J.-W., Davaa, E., Kim, Y.-T., and Park, J.-S. (2010). A new vaginal delivery system of amphotericin B: a dispersion of cationic liposomes in a thermosensitive gel. *J. Drug Target.* 18, 637–644. doi: 10.3109/10611861003649712

Kleinberg, M. (2006). What is the current and future status of conventional amphotericin B? *Int. J. Antimicrob. Agents* 27(Suppl. 1), 12–16. doi: 10.1016/j.ijantimicag.2006.03.013

Kumar, A., Jena, P. K., Behera, S., Lockey, R. F., Mohapatra, S., and Mohapatra, S. (2010). Multifunctional magnetic nanoparticles for targeted delivery. *Nanomedicine* 6, 64–69. doi: 10.1016/j.nano.2009.04.002

Kumar, R., and Sinha, V. R. (2016). Solid lipid nanoparticle: an efficient carrier for improved ocular permeation of voriconazole. *Drug Dev. Ind. Pharm.* 42, 1956–1967. doi: 10.1080/03639045.2016.1185437

Laniado-Laborín, R., and Cabrales-Vargas, M. N. (2009). Amphotericin B: side effects and toxicity. *Rev. Iberoam. Micol.* 26, 223–227. doi: 10.1016/j.riam.2009.06.003

Malathi, S., and Balasubramanian, S. (2011). Synthesis of biodegradable polymeric nanoparticles and their controlled drug delivery for tuberculosis. *J. Biomed. Nanotechnol.* 7, 150–151. doi: 10.1166/jbn.2011.1244

McCormack, P. L. (2015). Isavuconazonium: first global approval. *Drugs* 75, 817–822. doi: 10.1007/s40265-015-0398-6

Mesa-Arango, A. C., Scorzoni, L., and Zaragoza, O. (2012). It only takes one to do many jobs: amphotericin B as antifungal and immunomodulatory drug. *Front. Microbiol.* 3:286. doi: 10.3389/fmicb.2012.00286

Moazeni, M., Kelidari, H. R., Saeedi, M., Morteza-Semnani, K., Nabili, M., Gohar, A. A., et al. (2016). Time to overcome fluconazole resistant Candida isolates: solid lipid nanoparticles as a novel antifungal drug delivery system. *Colloids Surf. B Biointerfaces* 142, 400–407. doi: 10.1016/j.colsurfb.2016.03.013

Mohammadi, G., Shakeri, A., Fattahi, A., Mohammadi, P., Mikaeili, A., Aliabadi, A., et al. (2017). Preparation, physicochemical characterization and anti-fungal evaluation of nystatin-loaded PLGA-glucosamine nanoparticles. *Pharm. Res.* 34, 301–309. doi: 10.1007/s11095-016-2062-6

Mohanty, B., Majumdar, D. K., Mishra, S. K., Panda, A. K., and Patnaik, S. (2015). Development and characterization of itraconazole-loaded solid lipid nanoparticles for ocular delivery. *Pharm. Dev. Technol.* 20, 458–464. doi: 10.3109/10837450.2014.882935

Moritz, M., and Geszke-Moritz, M. (2015). Recent developments in application of polymeric nanoparticles as drug carriers. *Adv. Clin. Exp. Med.* 24, 749–758. doi: 10.17219/acem/31802

Mukherjee, P. K., Sheehan, D. J., Hitchcock, C. A., and Ghannoum, M. A. (2005). Combination treatment of invasive fungal infections. *Clin. Microbiol. Rev.* 18, 163–194. doi: 10.1128/CMR.18.1.163-194.2005

Nett, J. E., and Andes, D. R. (2016). Antifungal agents: spectrum of activity, pharmacology, and clinical indications. *Infect. Dis. Clin. North Am.* 30, 51–83. doi: 10.1016/j.idc.2015.10.012

Niemirowicz, K., Durnaś, B., Tokajuk, G., Głuszek, K., Wilczewska, A. Z., Misztalewska, I., et al. (2016). Magnetic nanoparticles as a drug delivery system that enhance fungicidal activity of polyene antibiotics. *Nanomedicine* 12, 2395–2404. doi: 10.1016/j.nano.2016.07.006

Odds, F. C., Brown, A. J., and Gow, N. A. R. (2003). Antifungal agents: mechanisms of action. *Trends Microbiol.* 11, 272–279. doi: 10.1016/S0966-842X(03)00117-3

Pagels, R. F., and Prud'homme, R. K. (2015). Polymeric nanoparticles and microparticles for the delivery of peptides, biologics, and soluble

therapeutics. *J. Control. Release* 219, 519–535. doi: 10.1016/j.jconrel.2015.09.001

Pandey, R., Ahmad, Z., Sharma, S., and Khuller, G. K. (2005). Nano-encapsulation of azole antifungals: potential applications to improve oral drug delivery. *Int. J. Pharm.* 301, 268–276. doi: 10.1016/j.ijpharm.2005.05.027

Pandit, J., Garg, M., and Jain, N. K. (2014). Miconazole nitrate bearing ultraflexible liposomes for the treatment of fungal infection. *J. Liposome Res.* 24, 163–169. doi: 10.3109/08982104.2013.871025

Pardeike, J., Weber, S., Zarfl, H. P., Pagitz, M., and Zimmer, A. (2016). Itraconazole-loaded nanostructured lipid carriers (NLC) for pulmonary treatment of aspergillosis in falcons. *Eur. J. Pharm. Biopharm.* 108, 269–276. doi: 10.1016/j.ejpb.2016.07.018

Patel, N. R., Damann, K., Leonardi, C., and Sabliov, C. M. (2010). Itraconazole-loaded poly(lactic-co-glycolic) acid nanoparticles for improved antifungal activity. *Nanomedicine (Lond).* 5, 1037–1050. doi: 10.2217/nnm.10.68

Patel, N. R., Damann, K., Leonardi, C., and Sabliov, C. M. (2011). Size dependency of PLGA-nanoparticle uptake and antifungal activity against *Aspergillus flavus*. *Nanomedicine (Lond).* 6, 1381–1395. doi: 10.2217/nnm.11.35

Peng, H. S., Liu, X. J., Lv, G. X., Sun, B., Kong, Q. F., Zhai, D. X., et al. (2008). Voriconazole into PLGA nanoparticles: improving agglomeration and antifungal efficacy. *Int. J. Pharm.* 352, 29–35. doi: 10.1016/j.ijpharm.2007.10.009

Perez, A. P., Altube, M. J., Schilrreff, P., Apezteguia, G., Celes, F. S., Zacchino, S., et al. (2016). Topical amphotericin B in ultradeformable liposomes: formulation, skin penetration study, antifungal and antileishmanial activity *in vitro*. *Colloids Surf. B Biointerfaces* 139, 190–198. doi: 10.1016/j.colsurfb.2015.12.003

Polvi, E. J., Li, X., O'Meara, T. R., Leach, M. D., and Cowen, L. E. (2015). Opportunistic yeast pathogens: reservoirs, virulence mechanisms, and therapeutic strategies. *Cell. Mol. Life Sci.* 72, 2261–2287. doi: 10.1007/s00018-015-1860-z

Prasad, R., Shah, A. H., and Rawal, M. K. (2016). "Antifungals: Mechanism of Action and Drug Resistance," in *Yeast Membrane Transporter Advances in Experimental Medicine and Biology*, eds J. Ramos, H. Sychrová, and M. Kschischo (Cham: Springer International Publishing), 327–349.

Qiu, L., Hu, B., Chen, H., Li, S., Hu, Y., Zheng, Y., et al. (2015). Antifungal efficacy of itraconazole-loaded TPGS-b-(PCL-ran-PGA) nanoparticles. *Int. J. Nanomedicine* 10, 1415–1423. doi: 10.2147/IJN.S71616

Reis, J. (2015). Liposomal formulations of amphotericin B : differences according to the scientific evidence. *Rev. Esp. Quimioter.* 28, 275–281.

Rençber, S., Karavana, S. Y., Yılmaz, F. F., Eraç, B., Nenni, M., Özbal, S., et al. (2016). Development, characterization, and *in vivo* assessment of mucoadhesive nanoparticles containing fluconazole for the local treatment of oral candidiasis. *Int. J. Nanomedicine* 11, 2641–2653. doi: 10.2147/IJN.S103762

Ribeiro, A. M., Souza, A. C. O., Amaral, A. C., Vasconcelos, N. M., Jeronimo, M. S., Carneiro, F. P., et al. (2013). Nanobiotechnological approaches to delivery of DNA vaccine against fungal infection. *J. Biomed. Nanotechnol.* 9, 221–230. doi: 10.1166/jbn.2013.1491

Saldanha, C. A., Garcia, M. P., Iocca, D. C., Rebelo, L. G., Souza, A. C. O., Bocca, A. L., et al. (2016). Antifungal activity of amphotericin B conjugated to nanosized magnetite in the treatment of paracoccidioidomycosis. *PLoS Negl. Trop. Dis.* 10:e0004754. doi: 10.1371/journal.pntd.0004754

Sanchez, D. A., Schairer, D., Tuckman-Vernon, C., Chouake, J., Kutner, A., Makdisi, J., et al. (2014). Amphotericin B releasing nanoparticle topical treatment of Candida spp. in the setting of a burn wound. *Nanomedicine* 10, 269–277. doi: 10.1016/j.nano.2013.06.002

Sanglard, D., Coste, A., and Ferrari, S. (2009). Antifungal drug resistance mechanisms in fungal pathogens from the perspective of transcriptional gene regulation. *FEMS Yeast Res.* 9, 1029–1050. doi: 10.1111/j.1567-1364.2009.00578.x

Serrano, D. R., Lalatsa, A., Dea-Ayuela, M. A., Bilbao-Ramos, P. E., Garrett, N. L., Moger, J., et al. (2015). Oral particle uptake and organ targeting drives the activity of amphotericin B nanoparticles. *Mol. Pharm.* 12, 420–431. doi: 10.1021/mp500527x

Seyedmousavi, S., Rafati, H., Ilkit, M., Tolooe, A., Hedayati, M. T., and Verweij, P. (2017). "Systemic Antifungal Agents: Current Status and Projected Future Developments," in *Methods in Molecular Biology*, ed T. Lion (New York, NY: Springer New York), 107–139.

Shapiro, R. S., Robbins, N., and Cowen, L. E. (2011). Regulatory circuitry governing fungal development, drug resistance, and disease. *Microbiol. Mol. Biol. Rev.* 75, 213–267. doi: 10.1128/MMBR.00045-10

Sheikh, S., Ali, S. M., Ahmad, M. U., Ahmad, A., Mushtaq, M., Paithankar, M., et al. (2010). Nanosomal amphotericin B is an efficacious alternative to ambisome for fungal therapy. *Int. J. Pharm.* 397, 103–108. doi: 10.1016/j.ijpharm.2010.07.003

Shirkhani, K., Teo, I., Armstrong-James, D., and Shaunak, S. (2015). Nebulised amphotericin B-polymethacrylic acid nanoparticle prophylaxis prevents invasive aspergillosis. *Nanomedicine* 11, 1217–1226. doi: 10.1016/j.nano.2015.02.012

Sil, A., and Andrianopoulos, A. (2015). Thermally dimorphic human fungal pathogens–polyphyletic pathogens with a convergent pathogenicity trait. *Cold Spring Harb. Perspect. Med.* 5:a019794. doi: 10.1101/cshperspect.a019794

Sinha, B., Mukherjee, B., and Pattnaik, G. (2013). Poly-lactide-co-glycolide nanoparticles containing voriconazole for pulmonary delivery: *in vitro* and *in vivo* study. *Nanomedicine* 9, 94–104. doi: 10.1016/j.nano.2012.04.005

Souza, A. C. O., Nascimento, A. L., de Vasconcelos, N. M., Jerônimo, M. S., Siqueira, I. M., Santos, R-L., et al. (2015). Activity and *in vivo* tracking of Amphotericin B loaded PLGA nanoparticles. *Eur. J. Med. Chem.* 95, 267–276. doi: 10.1016/j.ejmech.2015.03.022

Stiufiuc, R., Iacovita, C., Stiufiuc, G., Florea, A., Achim, M., and Lucaciu, C. M. (2015). A new class of pegylated plasmonic liposomes: synthesis and characterization. *J. Colloid Interface Sci.* 437, 17–23. doi: 10.1016/j.jcis.2014.09.023

Takemoto, K. (2006). Comparative study on the efficacy of AmBisome and Fungizone in a mouse model of pulmonary aspergillosis. *J. Antimicrob. Chemother.* 57, 724–731. doi: 10.1093/jac/dkl005

Tang, X., Dai, J., Xie, J., Zhu, Y., Zhu, M., Wang, Z., et al. (2015a). Enhanced Antifungal Activity by Ab-Modified Amphotericin B-Loaded Nanoparticles Using a pH-Responsive Block Copolymer. *Nanoscale Res. Lett.* 10:969. doi: 10.1186/s11671-015-0969-1

Tang, X., Jiao, R., Xie, C., Xu, L., Huo, Z., Dai, J., et al. (2015b). Improved antifungal activity of amphotericin B-loaded TPGS-b-(PCL-ran-PGA) nanoparticles. *Int. J. Clin. Exp. Med.* 8, 5150–5162. doi: 10.1016/j.ijbiomac.2014.10.014

Tang, X., Liang, Y., Zhu, Y., Xie, C., Yao, A., Chen, L., et al. (2015c). Anti-transferrin receptor-modified amphotericin B-loaded PLA-PEG nanoparticles cure Candidal meningitis and reduce drug toxicity. *Int. J. Nanomedicine* 10, 6227–6241. doi: 10.2147/IJN.S84656

Tang, X., Zhu, H., Sun, L., Hou, W., Cai, S., Zhang, R., et al. (2014). Enhanced antifungal effects of amphotericin B-TPGS-b-(PCL-ran-PGA) nanoparticles *in vitro* and *in vivo*. *Int. J. Nanomedicine* 9:5403. doi: 10.2147/IJN.S71623

Tassel, D., and Madoff, M. A. (1968). Treatment of Candida sepsis and Cryptococcus meningitis with 5-fluorocytosine. A new antifungal agent. *JAMA* 206, 830–832.

Tiyaboonchai, W., Woiszwillo, J., and Middaugh, C. R. (2001). Formulation and characterization of amphotericin B-polyethylenimine-dextran sulfate nanoparticles. *J. Pharm. Sci.* 90, 902–914. doi: 10.1002/jps.1042

Trombino, S., Mellace, S., and Cassano, R. (2016). Solid lipid nanoparticles for antifungal drugs delivery for topical applications. *Ther. Deliv.* 7, 639–647. doi: 10.4155/tde-2016-0040

Vanden Bossche, H., Koymans, L., and Moereels, H. (1995). P450 inhibitors of use in medical treatment: focus on mechanisms of action. *Pharmacol. Ther.* 67, 79–100.

Van de Ven, H., Paulussen, C., Feijens, P. B., Matheeussen, A., Rombaut, P., Kayaert, P., et al. (2012). PLGA nanoparticles and nanosuspensions with amphotericin B: potent *in vitro* and *in vivo* alternatives to Fungizone and AmBisome. *J. Control. Release* 161, 795–803. doi: 10.1016/j.jconrel.2012.05.037

Van Slooten, M. L., Boerman, O., Romøren, K., Kedar, E., Crommelin, D. J., and Storm, G. (2001). Liposomes as sustained release system for human interferon-gamma: biopharmaceutical aspects. *Biochim. Biophys. Acta* 1530, 134–145. doi: 10.1016/S1388-1981(00)00174-8

Vieira, D. B., and Carmona-Ribeiro, A. M. (2008). Cationic nanoparticles for delivery of amphotericin B: preparation, characterization and activity *in vitro*. *J. Nanobiotechnology* 6:6. doi: 10.1186/1477-3155-6-6.

Vyas, S. P., and Gupta, S. (2006). Optimizing efficacy of amphotericin B through nanomodification. *Int. J. Nanomedicine* 1, 417–432. doi: 10.2147/nano.2006.1.4.417

Walsh, T. J., Finberg, R. W., Arndt, C., Hiemenz, J., Schwartz, C., Bodensteiner, D., et al. (1999). Liposomal amphotericin B for empirical therapy in patients with persistent fever and neutropenia. National Institute of Allergy and Infectious Diseases Mycoses Study Group. *N. Engl. J. Med.* 340, 764–771. doi: 10.1056/NEJM199903113401004

Wang, L., Geng, D., and Su, H. (2014). Safe and efficient pH sensitive tumor targeting modified liposomes with minimal cytotoxicity. *Colloids Surf. B Biointerfaces* 123, 395–402. doi: 10.1016/j.colsurfb.2014.09.003

Wong-Beringer, A., Jacobs, R. A., and Guglielmo, B. J. (1998). Lipid formulations of amphotericin B: clinical efficacy and toxicities. *Clin. Infect. Dis.* 27, 603–618. doi: 10.1086/514704

Xie, J. L., Polvi, E. J., Shekhar-Guturja, T., and Cowen, L. E. (2014). Elucidating drug resistance in human fungal pathogens. *Future Microbiol.* 9, 523–542. doi: 10.2217/fmb.14.18

Xu, N., Gu, J., Zhu, Y., Wen, H., Ren, Q., and Chen, J. (2011). Efficacy of intravenous amphotericin B-polybutylcyanoacrylate nanoparticles against cryptococcal meningitis in mice. *Int. J. Nanomedicine* 6, 905–913. doi: 10.2147/IJN.S17503

Zhao, M., Hu, J., Zhang, L., Zhang, L., Sun, Y., Ma, N., et al. (2014). Study of amphotericin B magnetic liposomes for brain targeting. *Int. J. Pharm.* 475, 9–16. doi: 10.1016/j.ijpharm.2014.08.035

Zhou, W., Wang, Y., Jian, J., and Song, S. (2013). Self-aggregated nanoparticles based on amphiphilic poly(lactic acid)-grafted-chitosan copolymer for ocular delivery of amphotericin B. *Int. J. Nanomedicine* 8, 3715–3728. doi: 10.2147/IJN.S51186

Zia, Q., Khan, A. A., Swaleha, Z., and Owais, M. (2015). Self-assembled amphotericin B-loaded polyglutamic acid nanoparticles: preparation, characterization and *in vitro* potential against Candida albicans. *Int. J. Nanomedicine* 10, 1769–1790. doi: 10.2147/IJN.S63155

Zonios, D. I., and Bennett, J. E. (2008). Update on azole antifungals. *Semin. Respir. Crit. Care Med.* 29, 198–210. doi: 10.1055/s-2008-1063858

**Conflict of Interest Statement:** The authors declare that the research was conducted in the absence of any commercial or financial relationships that could be construed as a potential conflict of interest.

frontiers in Microbiology

ORIGINAL RESEARCH
published: 14 June 2017
doi: 10.3389/fmicb.2017.01057

# Dendritic Cells Primed with *Paracoccidioides brasiliensis* Peptide P10 Are Therapeutic in Immunosuppressed Mice with Paracoccidioidomycosis

*Leandro B. R. Silva[1], Lucas S. Dias[2], Glauce M. G. Rittner[2], Julián E. Muñoz[2], Ana C. O. Souza[2], Joshua D. Nosanchuk[3,4], Luiz R. Travassos[5] and Carlos P. Taborda[1,2]**

[1] Laboratory of Medical Mycology, Tropical Medicine Institute USP-LIM53, University of São Paulo, São Paulo, Brazil, [2] Department of Microbiology, Institute of Biomedical Sciences, University of São Paulo, São Paulo, Brazil, [3] Department of Medicine, Albert Einstein College of Medicine, Bronx, NY, United States, [4] Department of Microbiology and Immunology, Albert Einstein College of Medicine, Bronx, NY, United States, [5] Department of Microbiology, Immunology and Parasitology, Federal University of São Paulo, São Paulo, Brazil

Paracoccidioidomycosis (PCM) is an endemic systemic mycosis in Latin America, with the highest prevalence in Brazil, Colombia, and Venezuela. Fungi of the *Paracoccidioides* genus are etiologic agents of the disease. The 15 amino acid peptide P10 is derived from gp43, the main diagnostic antigen of *Paracoccidioides brasiliensis.* We previously reported that P10-pulsed dendritic cells (DCs) induce a protective response against *P. brasiliensis*. Presently, dexamethasone-treated BALB/c mice were intratracheally infected with *P. brasiliensis* Pb18 to establish the therapeutic efficacy of P10-pulsed DCs. Immunosuppressed and infected animals that received DCs had a reduction in their fungal burden, and this result was most pronounced in mice receiving DCs primed with P10. The efficacy of therapeutic DCs was significantly augmented by concomitant treatment with trimethoprim-sulfamethoxazole. Additionally, primed-DCs with or without the antifungal drug induced a beneficial $Th_1$-biased immune response and significantly reduced tissue damage. In conclusion, these studies with immunocompromised mice demonstrate that P10-pulsed DCs with or without concomitant antifungal drugs are potently effective in combating invasive PCM. These findings support further translational studies to validate the use of P10-primed DCs for PCM in immunocompetent and immunosuppressed hosts.

**Keywords:** ***Paracoccidioides brasiliensis,*** **paracoccidioidomycosis, P10, adjuvants, dendritic cells, vaccine**

OPEN ACCESS

***Edited by:***
*Hector Mora Montes, Universidad de Guanajuato, Mexico*

***Reviewed by:***
*Laura Bonifaz, Instituto Mexicano del Seguro Social (IMSS), Mexico*
*Guilherme Lanzi Sassaki, Federal University of Paraná, Brazil*

***Correspondence:**
*Carlos P. Taborda*
*taborda@usp.br*

***Specialty section:***
*This article was submitted to Fungi and Their Interactions, a section of the journal Frontiers in Microbiology*

***Received:*** *10 October 2016*
***Accepted:*** *26 May 2017*
***Published:*** *14 June 2017*

***Citation:***
*Silva LBR, Dias LS, Rittner GMG, Muñoz JE, Souza ACO, Nosanchuk JD, Travassos LR and Taborda CP (2017) Dendritic Cells Primed with Paracoccidioides brasiliensis Peptide P10 Are Therapeutic in Immunosuppressed Mice with Paracoccidioidomycosis. Front. Microbiol. 8:1057. doi: 10.3389/fmicb.2017.01057*

## INTRODUCTION

Paracoccidioidomycosis (PCM), caused by thermally dimorphic fungi of the *Paracoccidioides* genus, is one of the most important systemic granulomatous diseases in Latin America (Taborda et al., 2015). PCM is particularly prevalent in Brazil, affecting mainly rural workers (Restrepo, 1985; Travassos and Taborda, 2012b). In Brazil, approximately 1,853 (∼51.2%) of 3,583 confirmed deaths due to systemic mycoses from 1996 to 2006 were caused by PCM (Prado et al., 2009). Phylogenetic analyses have revealed that the clinically relevant *Paracoccidioides* species include *Paracoccidioides brasiliensis*, comprised of the three cryptic species S1, PS2, and PS3 (Theodoro et al., 2012), and *Paracoccidioides lutzii* (Teixeira et al., 2013).

Acquisition of *Paracoccidioides* spp. follows the inhalation of conidia, which are deposited into the lower respiratory tract. These propagules subsequently undergo morphogenic transformation into yeast forms, which constitute the pathogenic morphology in tissues (Taborda et al., 2015). PCM has two main clinical forms that are predicated upon the immunological status of the infected host. Within weeks to months after initial infection, young adults often develop the acute or subacute forms of disease, and these are typically aggressive and require immediate antifungal treatment (Bocca et al., 2013). The chronic form of PCM is manifested months or years after infection, and disease varies in severity, although this form can be as aggressive as the acute form (Bocca et al., 2013).

Although polyene and azoles as well as the combination of trimethoprim and sulfamethoxazole are the typical therapeutics administered to patients with PCM, antifungal treatment is prolonged, frequently over 2 years, and failures and/or relapses occur (Travassos et al., 2008b; Bocca et al., 2013).

An experimental vaccine against *P. brasiliensis* has been studied (Travassos and Taborda, 2012b) using a 15 mer peptide, known as peptide 10 or P10, with the sequence: QTLIAIHTLAIRYAN (Taborda et al., 1998). P10 is derived from the major diagnostic antigen of PCM, the 43,000 Daltons glycoprotein known as gp43 (Travassos et al., 1995). Over the past 10 years, the properties and several different forms of delivery of P10 have been studied, and have contributed to validating this peptide as a potential candidate for a human vaccine (Iwai et al., 2003; Travassos et al., 2008a; Travassos and Taborda, 2012b; Taborda et al., 2015). Using dexamethasone-treated mice, immunization with P10 has been shown to efficiently modulate the immune response in immunosuppressed hosts. Protection against pulmonary challenge with *P. brasiliensis* has been demonstrated by increased animal survival, reduced lung fungal burden and reduced pulmonary fibrosis in P10 immunized mice as compared to control animals (Muñoz et al., 2014).

We previously demonstrated protective immunity against murine *Paracoccidioides brasiliensis* infection after sub-cutaneous or intravenous injection of P10-primed dendritic cells (DCs). Mice receiving the P10-primed DCs had a mixed cytokine response pattern with a predominance of $Th_1$-type activation and a significant reduction of fungal burdens in comparison with control animals. This data supported our proposal that P10-primed DCs are promising therapeutics in the setting of established fungal infection (Magalhães et al., 2012; Thind et al., 2015). DCs are powerful inducers of T-lymphocyte immune responses against *Paracoccidioides* antigens (Magalhães et al., 2012; Thind et al., 2015). The administration of *in vitro* gp43-pulsed DCs into mice results in increased productions of IL-2 and IFN-$\gamma$ by $CD4^+$ T cells isolated from regional lymph nodes (Ferreira et al., 2003). There is significant interest in adoptive transfer of DCs as a means to harness T-cell mediated immunity as a therapy to combat pathogenic fungi, which is demonstrated by studies with DCs pulsed with fungal cells or with fungal RNA from *Candida albicans*, *Aspergillus fumigatus*, *Cryptococcus gattii,* and *Cryptococcus neoformans* (D'Ostiani et al., 2000; Bozza et al., 2003; Siegemund and Alber, 2008; Roy and Klein, 2012; Ueno et al., 2015, 2016).

However, there is yet limited information as to whether this modality of cell-induced therapy would be effective in the setting of immunocompromised patients, which is important since PCM is a frequent mycological cause of morbidity and mortality in patients with HIV in Brazil (Prado et al., 2009). In the present work, we simulated the acute/subacute form of PCM in immunocompromised mice by administering dexamethasone, which suppresses host immune responses through multiple mechanisms, including modulating inflammatory cytokines (Chung et al., 2011; Muñoz et al., 2014) prior to infection. Our findings show that the administration of P10-primed DCs to dexamethasone suppressed mice infected with *P. brasiliensis* are therapeutic in the setting of compromised immunity.

# MATERIALS AND METHODS

## Animal Use and Ethics Statement

BALB/c mice (6-to 8-week-old, males) used for infection and bone marrow harvesting were bred at the School of Medicine – University of São Paulo in pathogen-free conditions. All animal experiments were performed in strict accordance with the Brazilian Federal Law 11,794 establishing the Animal Protection Code for the State of São Paulo. This study was approved by the Ethics Committee on Animal Experiments at the School of Medicine, University of São Paulo (189/14).

## Fungus and Inoculum Preparation

The virulent isolate *P. brasiliensis* Pb18 was cultivated on solid Sabouraud medium at 37°C for 7 days. The fungus was collected and washed three times in phosphate buffered saline (PBS, pH 7.2). After decanting large and agglutinated cells, small isolated yeast cells were counted in a Neubauer chamber. The yeast cells used for experimentation displayed >95% viability as determined by staining with Trypan blue.

## Immunosuppressed Mice

The animals were immunosuppressed as previously described (Muñoz et al., 2014). Dexamethasone phosphate (Sigma, St Louis, MO, United States) was administrated daily in drinking water and the dose was calculated as 0.15 mg/kg considering an average water intake of 5 ml per day. Dexamethasone phosphate treatment was initiated 20 days before intratracheal (i.t.) infection and continued until the end of experiment. Immunosuppression was confirmed by the blood leukocyte levels in comparison with untreated mice. Animals were maintained in isolator cages. Cages were exchanged twice a week in a laminar flow hood and all bedding, food and water was autoclaved prior to use. Total leukocyte counts were determined using ∼200 μl of blood obtained via the ocular plexus. The blood was mixed with 20 μL of ACD (citric acid, sodium citrate, dextrose) to prevent clot formation and then Turk solution was used to hemolyze erythrocytes and stain leukocytes. Leukocyte counting was performed using blood smears on glass slides. Blood samples were also counted in a Neubauer chamber.

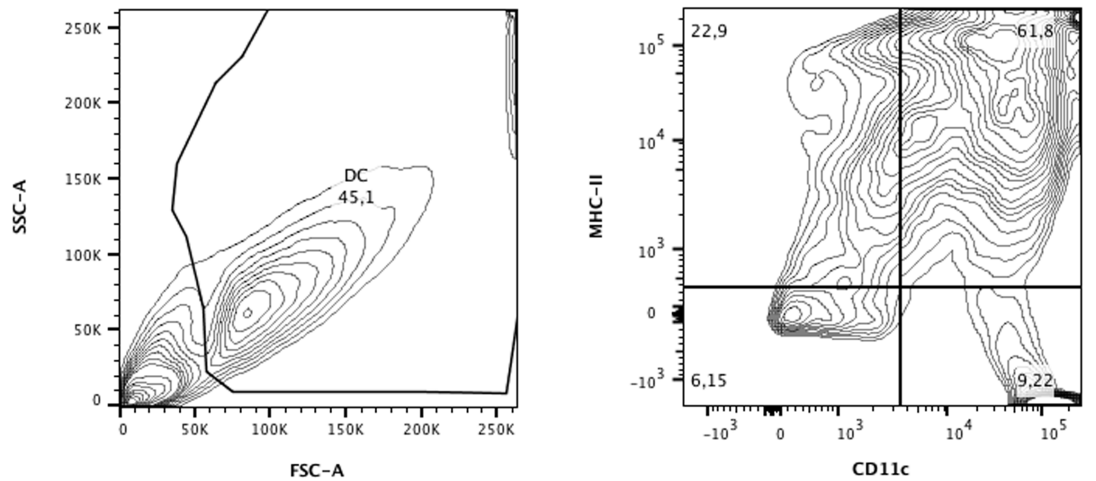


**FIGURE 1 |** Flow cytometric analysis of dendritic cells (DCs) from BALB/c differentiated for 9 days in medium containing GM-CSF and IL-4. Cells were separated according to granularity (SSC) and size (FSC) and double-labeling for CD11c and MHC-II was evaluated. In $CD11c^+/MHC\text{-}II^+$ populations (~60%), expression of CD80 and CD86 was also defined. Data were analyzed using FlowJo software (Tree Stars Inc.).

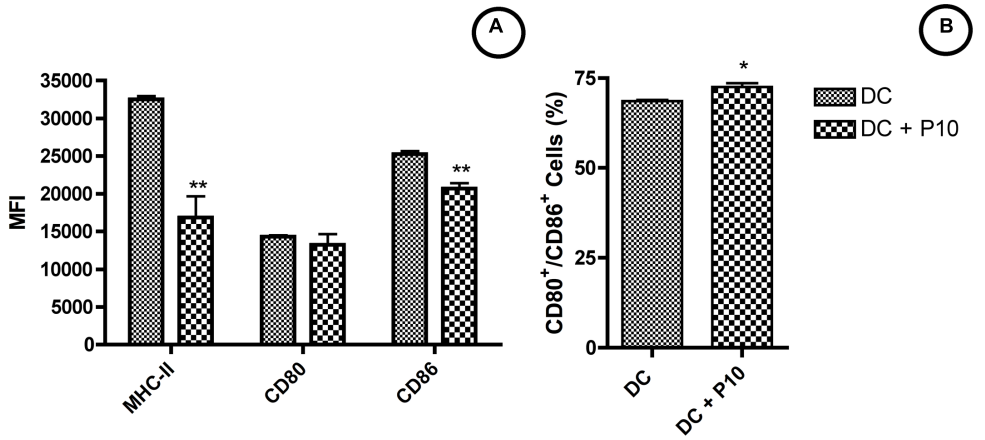


**FIGURE 2 |** Activation of DCs by peptide P10. DCs were analyzed for MHC-II, CD80 and CD86 expression **(A)** and frequency of $CD80^+/CD86^+$ cells **(B)**. Analysis by one-way ANOVA followed by Tukey's post-test, where $*p < 0.05$, $**p < 0.01$ in comparison with unstimulated group (DC).

## Intratracheal Infection

BALB/c mice were infected intratracheally (i.t.) with *P. brasiliensis* Pb18 20 days after immunosuppression was initiated. For the procedure, animals were anesthetized intraperitoneally using ~200 μl of a solution containing 80 mg/kg ketamine and 10 mg/kg xylazine (both from União Química Farmacêutica, Brazil). Five minutes after the injection of the anesthetics, a small longitudinal skin incision was made in the neck to expose the trachea and $3 \times 10^5$ yeast cells in 50 μl of PBS was injected. The incision was sutured with 5-0 silk.

## Peptide Synthesis and Purification

P10 peptide with amidated C-terminal was purchased from Peptide 2.0 (Chantilly, VA, United States). HPLC and MS analyses performed by the manufacturer showed that the synthetic P10 was 98% pure.

## Dendritic Cells Differentiation

Dendritic cells were obtained from bone marrow as described previously (Inaba et al., 1992). Briefly, femurs and tibias were collected from male BALB/c mice and flushed with RPMI (Vitrocell, Campinas, Brazil). Samples containing $10^7$ cells were cultivated in RPMI supplemented with 10% fetal calf serum (FCS; Vitrocell), 20 μg/ml gentamicin (Gibco BRL Life Technologies, Grand Island, NY, United States) and recombinant cytokines GM-CSF (30 ng/ml) and IL-4 (15 ng/ml) (both from Peprotech, Rocky Hill, NJ, United States) in 25 $cm^2$ cell culture flasks. On the second day, 80% of medium was removed and the same amount of fresh medium with growth factors was added. On the fourth, sixth, and eighth day, cell supernatants were centrifuged and pellets were plated in fresh medium containing growth factor. On the ninth day, cells were harvested and used in the experiments.

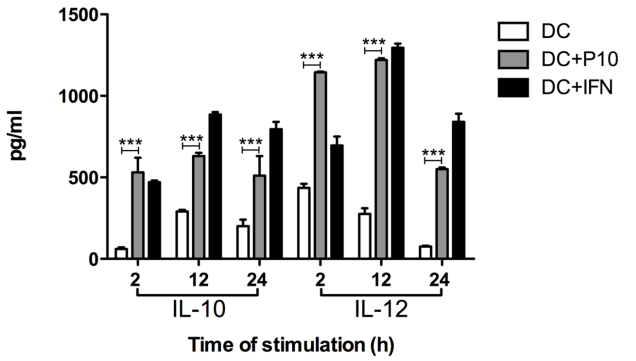


**FIGURE 3 |** Measurement of IL-10 and IL-12 cytokines in culture supernatants of differentiated DCs *ex vivo* pulsed or not with P10 or IFN-γ. Supernatants of DCs incubated in medium alone (DC; negative control) or with either P10 (DC + P10) or IFN-γ (DC + IFN; positive control) were tested for IL-10 and IL-12 production. Analysis by one-way ANOVA followed by Tukey's post-test, yielding $***p < 0.001$.

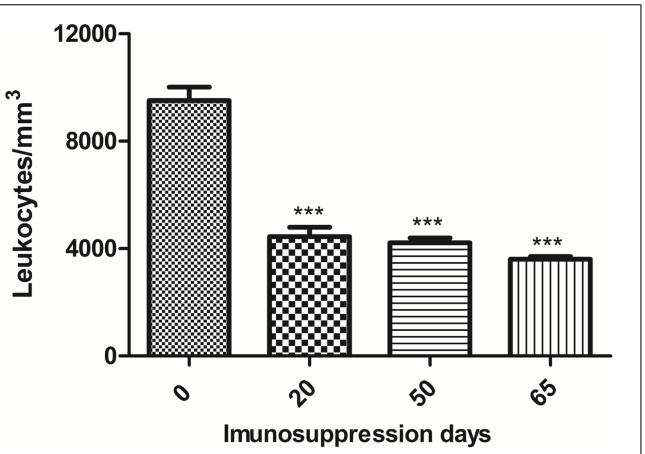


**FIGURE 4 |** Total leukocyte counts in peripheral blood of BALB/c mice treated with dexamethasone. Leukocyte counts of mice prior to the initiation of daily dexamethasone administration (Day 0), on the day of infection (Day 20), after randomization of mice into treatment groups (Day 50) and when mice were euthanized (Day 65). The results shown are only from uninfected mice that did not receive any DC preparations. Statistical analysis at day 20, 50, and 65 was done comparing the leukocyte levels to those measured before dexamethasone treatments $***p < 0.001$. Analyses were by one-way ANOVA followed by Tukey's post-test.

## Expression of Costimulatory Molecules and Kinetics of Cytokine Production on DCs Pulsed with P10 or IFN-γ

Dendritic cells were distributed into 24-well plates at a $10^6$/ml cell density and cultivated in medium alone or with P10 ($2.55 \times 10^{-1}$ mM) at 5% $CO_2$ and 37°C. After 2 h, cells were removed, washed in FACS buffer and incubated with antibodies to CD11c (BV711, Clone N418), MHC-II (APC-Cy7, Clone M5/114.15.2), CD86 (APC, Clone 16-10A1) and CD-80 (PE, GL1) for 30 min at 4°C. Cells were analyzed by flow cytometry (BD FACSCanto) to assess the expression of surface molecules. In addition, culture supernatants of DCs pulsed with or without P10 or IFN-γ (20 ng/ml) for 2, 12, and 24 h were assessed for IL-10 and IL-12 production using enzyme-linked immunosorbent assay (ELISA) kits (BD OpTeia, San Diego, CA, United States).

## *In Vitro* Activation of DCs and Treatment of Infected Mice

Dendritic cells ($10^6$/ml) were distributed into 24-well plates and cultivated in medium alone or with P10. After 2 h, cells were harvested and a total of $3 \times 10^5$ cells were injected subcutaneously in immunosuppressed mice 30 days post-infection. Mice were also randomized to receive either trimethoprim-sulfamethoxazole (TMP-SMX) 3–15 mg/kg every day for 15 days. Controls groups were treated with PBS.

## Fungal Burden in Organs of Infected Mice

Mice were euthanized 45 days after infection (day 65 of experiment) and lungs were removed. Portions of lung were weighed, homogenized in PBS and aliquots were plated on agar brain heart infusion (BHI) supplemented with 4% fetal bovine serum (Gibco, Grand Island, NY, United States), 5% supernatant of spent culture of *P. brasiliensis* Pb192, 10 IU/ml streptomycin-penicillin (Cultilab, Brazil) and 500 mg/ml cycloheximide (Sigma, St. Louis, MO, United States) (Moscardi-Bacchi et al., 1994). Plates were incubated at 37°C for 20 days, and the resulting Colony Forming Units (CFUs) were enumerated.

## Cytokine Detection

Lung sections were homogenized in PBS with protease inhibitors: benzamidine HCl (4 mM), EDTA disodium salt (1 mM), *N*-ethylmaleimide (1 mM), and pepstatin (1.5 mM) (Sigma, St. Louis, MO, United States). Supernatants were assayed for IL-4, IL-10, IL-12, and IFN-γ using ELISA kits (BD OpTeia, San Diego, CA, United States). The detection limits of the assays were as follow: 7.8 pg/ml for IL-4, 31.3 pg/ml for IFN-γ and IL-10, and 62.5 pg/ml for IL-12, as determined by the manufacturer.

## Histological Analyses

Additional lung sections were fixed in 10% buffered formalin and embedded in paraffin for cutting. Sections were stained by the Gomori-Grocott method and hematoxylin/eosin (HE).

## Statistical Analysis

Data shown are representative of at least two independent experiments. For *in vivo* experiments, a total of six animals per group were used. *In vitro* experiments were done in triplicates for each condition. Statistical analyses were performed using GraphPad Prism 5 software (San Diego, CA, United States). The results were expressed as mean values and standard deviations (SD) of the indicated values. Tukey's significant difference test was employed for non-parametric data. *p*-values of $\leq 0.05$ were used to indicate statistical significance.

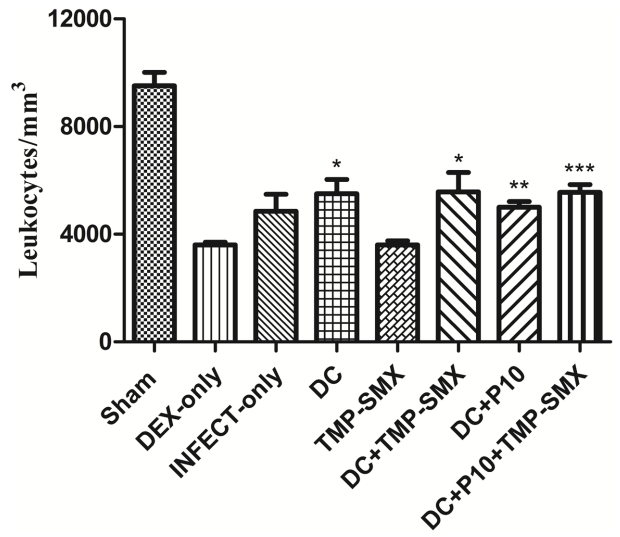


**FIGURE 5 |** Total leukocyte counts in peripheral blood of BALB/c mice treated with dexamethasone and infected with *P. brasiliensis*. Leukocyte counts were obtained after mice were euthanized (Day 65). Except for Sham, all groups were immunosuppressed with dexamethasone (DEX). Data show Sham (uninfected without immunosuppression or any treatments), DEX-only (uninfected and untreated), INFECT-only (infected and untreated), DC (infected and treated with non-pulsed DCs), TMP-SMX (infected and treated with sulfamethoxazole-trimethoprim), DC + TMP-SMX (infected and treated with DCs and trimethoprim-sulfamethoxazole), DC + P10 (infected and treated with P10-pulsed DCs) and DC + P10 + TMP-SMX (infected and treated with P10-pulsed DCs with trimethoprim-sulfamethoxazole). Data shown are representative of two independent experiments, analyzed by one-way ANOVA followed by Tukey's post-test, where $^{*}p < 0.05$, $^{**}p < 0.01$ or $^{***}p < 0.001$ in comparison to DEX-only.

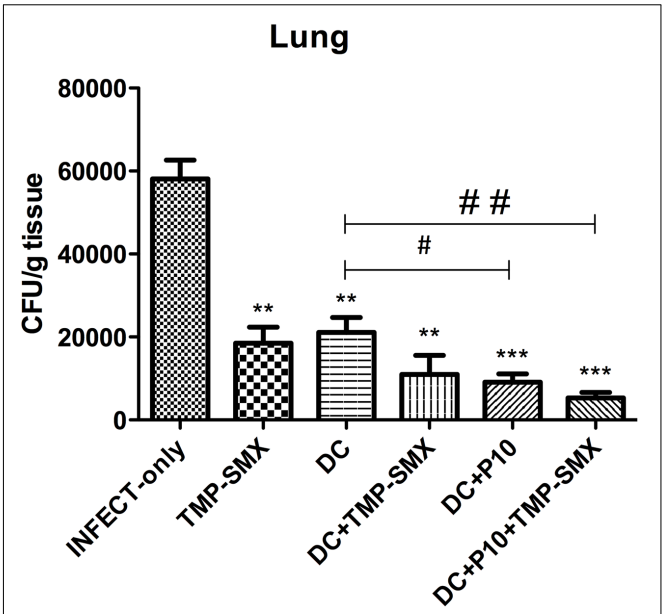


**FIGURE 6 |** Therapeutic delivery of P10-primed DCs significantly reduces pulmonary fungal burden. Immunosuppressed mice ($n = 6$) were randomized to different treatment groups 30 days after intratracheal infection with *P. brasiliensis*. The treatment groups were INFECT-only (infected and untreated), TMP-SMX (treated with sulfamethoxazole-trimethoprim); DC (treated with non-pulsed dendritic cells); DC + TMP-SMX (treated with non-pulsed DCs and TMP-SMX); DC + P10 (treated with P10-pulsed DCs); DC + P10 + TMP-SMX (treated with P10-pulsed DCs and TMP-SMX treated). Data shown are representative of two independent experiments, analyzed by one-way ANOVA followed by Tukey's post-test, where $^{**}p < 0.01$ or $^{***}p < 0.001$ in relation to INFECT-only and $^{\#}p < 0.05$ or $^{\#\#}p < 0.01$ in relation to DC.

# RESULTS

## *In Vitro* Characterization of DCs

Dendritic cells from BALB/c mice were analyzed by flow cytometry. Cell were first gated by granularity (SSC) and size (FSC) and then analyzed for CD11c and MHC-II expression. Double positive cells for CD11c and MHC-II were considered as differentiated DCs, reaching a frequency of appropriately 60% (**Figure 1**), as previously observed (Magalhães et al., 2012). Therefore, for *in vivo* experiments, each vaccine dose contained a total of $3 \times 10^5$ cells, of which $1.8 \times 10^5$ were DCs pulsed or not with P10.

## Activation Dendritic Cells by Peptide P10

We assessed the expression of MHC-II, CD80, and CD86 molecules within $MHCII^+/CD11c^+$ cell population after 2 h of stimulation with or without P10. According to the Median Fluorescence Intensity (MFI), we observed a decrease in MHC-II and increase of CD86 expression for P10-pulsed DCs and no significant changes for CD80 in comparison to control group (**Figure 2A**). However, the percentage of $CD80^+/CD86^+$ DCs showed a significant increase (**Figure 2B**), demonstrating that P10 might have a stimulatory effect for DCs activation.

## Measurements of IL-10 and IL-12 Cytokines in Culture Supernatants of *Ex Vivo* P10-Pulsed Dendritic Cells

Dendritic cells pulsed with P10 showed increased production of IL-10 and IL-12 compared with untreated DCs (**Figure 3**). P10 induced an increased production of these cytokines, which was even higher in DCs pulsed with IFN-γ, although these levels were higher in the setting of IFN-γ at 12 and 24 h.

## Immunosuppression of BALB/c Mice with Dexamethasone

Dexamethasone administered in water *"ad libitum"* to mice over a 65-day period significantly reduced the peripheral leukocyte counts in a sustained manner (**Figure 4**). **Figure 5** depicts leukocyte counts on day 65, demonstrating decreased leukocyte counts in all groups in comparison with non-immunosuppressed mice (Sham). Leukocyte levels of immunosuppressed animals (DEX-only) were statistically different from all groups treated with DCs (DC, DC + TMP-SMX, DC-P10, DC + P10 + TMP-SMX). All of the DC administration conditions increased leukocyte levels in comparison to dexamethasone treated mice (DEX only). However, treatment with DCs did not significantly increase leukocyte levels in comparison to INFECT-only group.

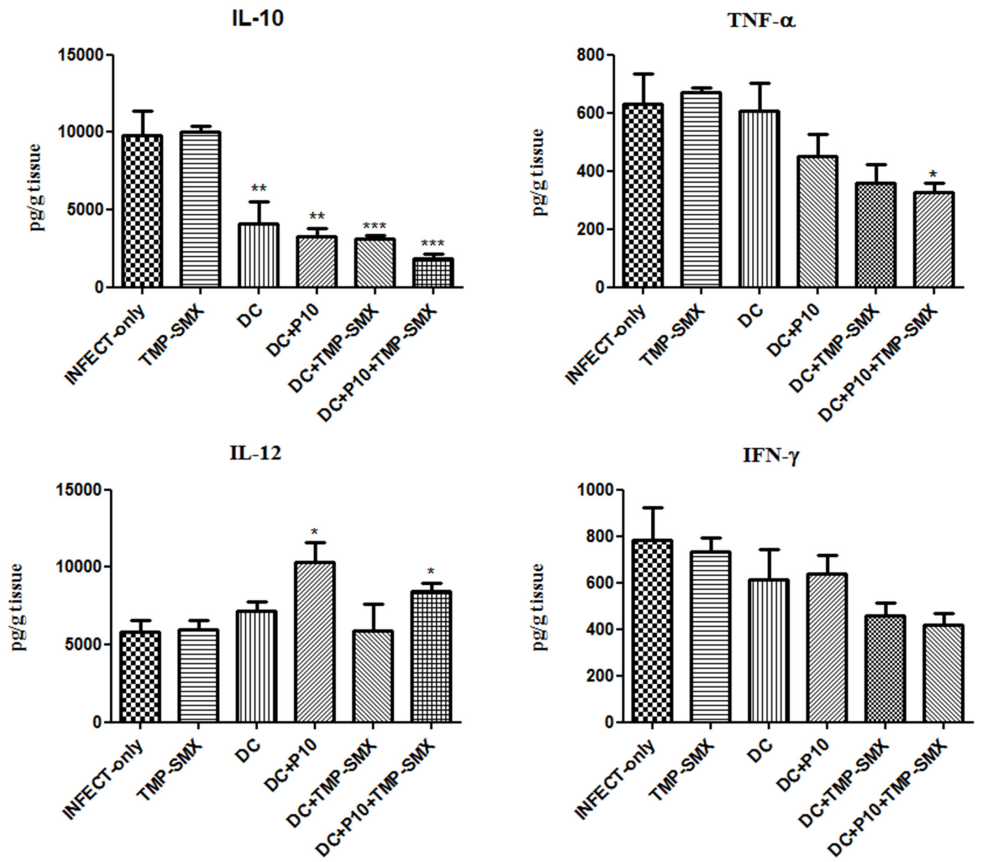


**FIGURE 7 |** Therapeutic administration of P10-primed DCs alters cytokine responses in the lungs of immunosuppressed mice infected with *P. brasiliensis*. IL-10, TNF-α, IL-12, and IFN-γ cytokines were assayed in the lungs of mice 45 days after intratracheal infection. Immunosuppressed animals ($n = 6$) were randomized into different groups: INFECT-only (infected and untreated), TMP-SMX (treated with sulfamethoxazole-trimethoprim); DC (treated with non-pulsed dendritic cells); DC + TMP-SMX (treated with non-pulsed DCs and TMP-SMX); DC + P10 (treated with P10-pulsed DCs); DC + P10 + TMP-SMX (treated with P10-pulsed DCs and TMP-SMX treated). Data shown are representative of two independent experiments, analyzed by one-way ANOVA followed by Tukey's post-test, where $^{*}p < 0.05$, $^{**}p < 0.01$, or $^{***}p < 0.001$ in comparison to INFECT-only.

## Immunization with P10-Primed DCs Reduces Fungal Burden

The pulmonary fungal burden of immunosuppressed mice infected with *P. brasiliensis* was significantly reduced by administration of either TMP-SMX or unprimed DCs (**Figure 6**). The combination of unprimed DCs and TMP-SMX further reduced CFUs. However, the greatest reduction occurred when DCs primed with P10 were administered and this effect was further augmented when TMP-SMX was added to therapy.

## Pattern of Cytokines Induced by *In Vivo* Treatment Using Dendritic Cells Pulsed with P10

IL-10, IL-12, IFN-γ, and TNF-α levels were measured by ELISA in the lungs of mice with different treatment regimens (**Figure 7**). A significant reduction of IL-10 was observed in all groups that received DCs with the greatest reduction occurring in mice that received P10-primed DCs together with TMP-SMX. Increased levels of IL-12 occurred in mice treated with P10-primed DCs with or without TMP-SMX treatment. Levels of TNF-α were reduced after the administration of DCs with TMP-SMX or primed DCs, but were only significantly reduced in the combination of primed DCs with TMP-SMX treatment. No significant differences were detected in IFN-γ levels, although there was a trend to lower levels in the groups treated with TMP-SMX combined with either P10-primed or unprimed DCs.

## Analysis of Histological Sections

Lung sections were subjected to Gomori-Grocott and HE staining. Gomori-Grocott stained micrographics (**Figure 8**) depict the fungal burden, showing the presence of fungal cells in lung tissue. **Figure 8A** demonstrates uninfected immunosuppressed mice with an absence of fungal cells. Abundant fungal cells were present in tissues of immunosuppressed mice in the following groups: infected and not treated (**Figure 8B**), infected and treated with (**Figure 8C**) and non-pulsed DCs treated groups (**Figure 8D**). In contrast, lung sections from immunosuppressed and infected animals treated with P10-pulsed DCs (**Figure 8E**), non-pulsed DCs and

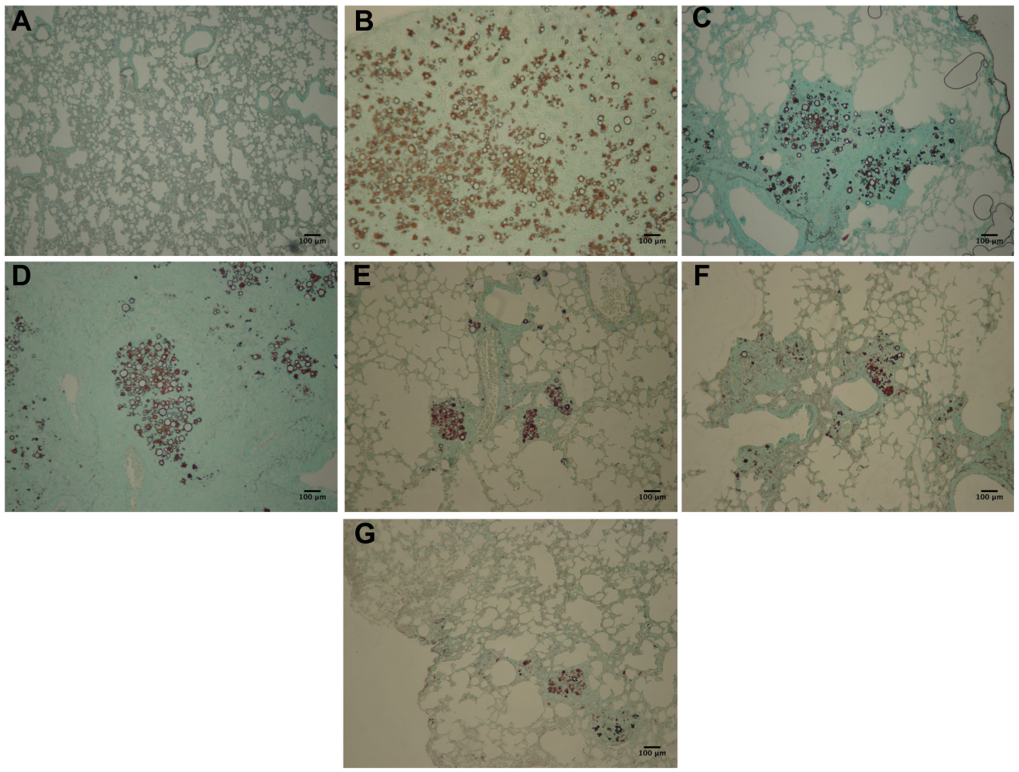


**FIGURE 8 |** Gomori-Grocott staining reveals that therapy with P10-primed DCs reduces pulmonary fungal load in *P. brasiliensis* infected mice. Representative Gomori-Grocott stained lung sections from immunosuppressed mice 45 days after intratracheal infection with *P. brasiliensis*. **(A)** uninfected and untreated animals; **(B)** infected and untreated; **(C)** infected and treated with TMP-SMX; **(D)** infected and treated with non-pulsed DCs; **(E)** infected and treated with P10-pulsed DCs; **(F)** infected and treated with non-pulsed DCs in combination with TMP-SMX; **(G)** infected and treated with P10-pulsed DCs in combination with TMP-SMX. Photographs were taken at 300× magnification. Bars denote 100 μm.

TMP-SMX (**Figure 8F**) and P10-pulsed DCs and TMP-SMX (**Figure 8G**) had a significantly lower fungal burden. Moreover, the animals that received P10-pulsed DCs (**Figures 8E,G**) presented the lowest burden of fungal cells in lung tissue.

Hematoxylin/eosin staining (**Figure 9**) revealed normal tissue architecture in non-infected mice (**Figure 9A**). It was observed the presence of granulomas with fungal cells and intense inflammatory infiltrates in lung parenchyma of immunosuppressed and infected-only (**Figure 9B**), infected and treated with TMP-SMX (**Figure 9C**) and infected and treated with P10-pulsed DCs (**Figure 9E**) groups. Granuloma-like structures were also observed in the other infected groups, but inflammatory infiltrates were reduced in the non-pulsed DCs (**Figure 9D**), non-pulsed DCs and TMP-SMX (**Figure 9F**) and P10-pulsed DCs and TMP-SMX treated (**Figure 9G**) groups. Lung parenchyma was significantly best preserved and less compromised in P10-pulsed DCs and TMP-SMX treated (**Figure 9G**) group.

## DISCUSSION

Acute and sub-acute forms of PCM are highly aggressive in the absence of early antifungal treatment immediately after the disease manifestation and death remains a relatively common outcome in this setting. Antifungal therapy requires a long and exhausting approach to prevent relapses. In addition, standard therapeutic regimens are associated with significant toxicities, such as nephrotoxicity and hepatotoxicity, and intense therapy does not prevent the development of disease sequelae, such as pulmonary fibrosis or scarring (Shikanai-Yasuda et al., 2006; Bocca et al., 2013; Buccheri et al., 2015). Hence, antifungal therapy alone does not inhibit the intense inflammatory responses in infected tissues that occur in response to the release of fungal antigens from dead or dying cells resulting in extensive tissue damage, which, in fact, can lead to death (Benard et al., 2012). To combat this adverse host response, we have been studying a therapeutic vaccine against *P. brasiliensis* based on a peptide known as P10, which induces a strong, protective immunological response that significantly reduces fungal burden, tissue injury and fibrosis in a murine experimental PCM model (Travassos et al., 2008a; Taborda et al., 2015).

Dendritic cells are potent stimulators of the immune response and are able to activate naïve T cells by presenting peptide antigens (Banchereau, 2000; Thind et al., 2015). Previously, we have demonstrated that intravenous or subcutaneous injection of P10-primed DCs into mice with established PCM led to a significant reduction in fungal burden and stimulated a

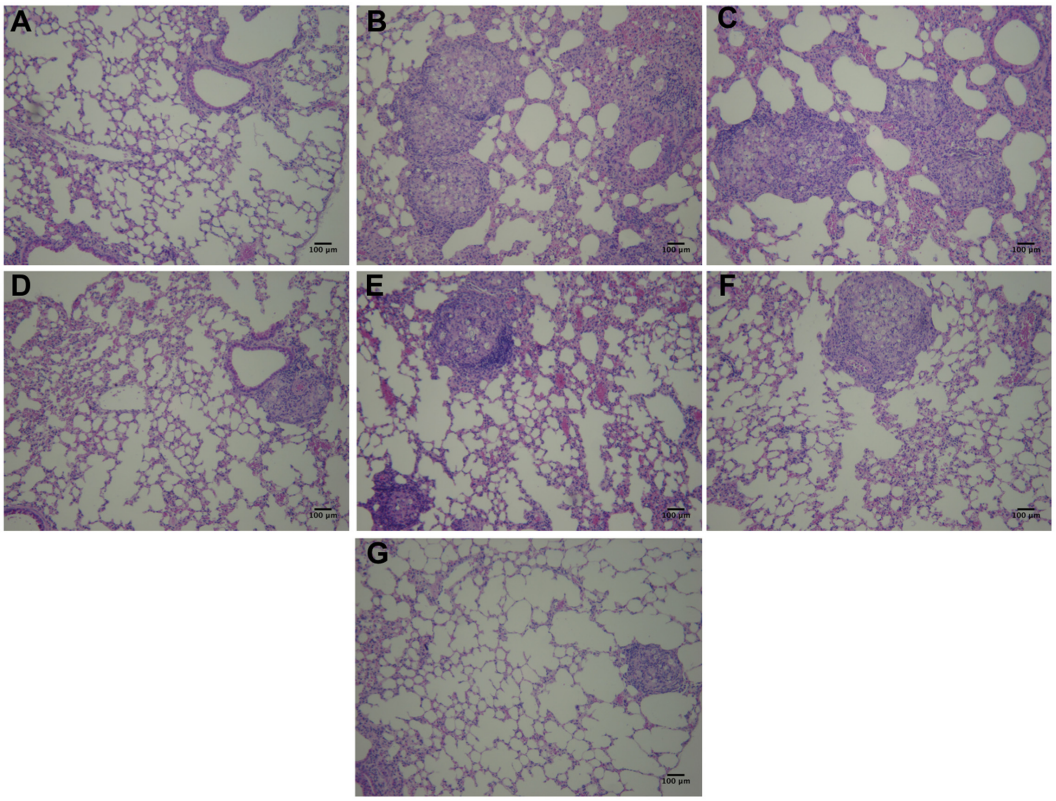


**FIGURE 9 |** Hematoxylin and Eosin staining reveals that therapy with P10-primed DCs reduces pulmonary damage in mice infected with *P. brasiliensis*. Representative Hematoxylin/Eosin stained lung sections from immunosuppressed mice 45 days after intratracheal infection with *P. brasiliensis*. **(A)** uninfected and untreated animals; **(B)** infected and untreated; **(C)** infected and treated with TMP-SMX; **(D)** infected and treated with non-pulsed DCs; **(E)** infected and treated with P10-pulsed DCs; **(F)** infected and treated with non-pulsed DCs in combination with TMP-SMX; **(G)** infected and treated with P10-pulsed DCs in combination with TMP-SMX. Photographs were taken at 300× magnification. Bars denote 100 μm.

$Th_1$-biased cytokine response (Magalhães et al., 2012). Here we demonstrated that *in vitro* DC stimulation with P10 increases the frequency of $CD80^+/CD86^+$ DCs, while also increasing the production of IL-12 by these cells. These data support our hypothesis that P10 stimulation activates DCs resulting in improved antigen presentation and T-cell responses that culminate in protection against *P. brasiliensis* infection.

In the present study, we also evaluated the therapeutic potential of P10-primed DCs in the setting of acute/subacute PCM in immunocompromised mice using dexamethasone, which effectively reduces airway inflammation through multiple mechanisms (Muñoz et al., 2014). Dexamethasone administered in drinking water for 20 days reduced the total number of leukocytes by ∼40%. Infecting these mice with *P. brasiliensis* Pb18 induced an aggressive disease that was similar to the acute/subacute form of PCM. In fact, dexamethasone immunosuppressed mice infected with $3 \times 10^5$ yeast cells of Pb18 have 100% mortality within 80 days (Muñoz et al., 2014). The administration of P10-primed DCs to dexamethasone treated, Pb18 infected mice significantly reduced the fungal burden, with the greatest reduction being achieved with or without concomitant antifungal treatment. These results were supported by the histological evaluations that revealed the dramatic protection of the lung architecture along with significant reductions in yeast cell numbers in mice treated with primed DCs, especially in the setting of antifungal combination therapy.

Protection against systemic fungal infection requires an effective cell immune response and the presence of IL-12 and IFN-γ appear to be essential to control the progression of PCM (Travassos and Taborda, 2012a). We have previously demonstrated that immunization with P10 can restore lymphoproliferation in immunosuppressed animals (Muñoz et al., 2014). In these prior experiments, murine DCs pulsed *in vitro* with P10 or IFN-γ (used as a control) induced significant IL-10, IL-12 production and enhanced MHC-II expression. In general, DCs stimulated with IFN-γ induces mature cells to preferentially produce IL-12, whereas DCs stimulated by IL-10 and prostaglandin E2 generate low amounts of IL-12 (Banchereau, 2000). In our present study, lung homogenates from immunosuppressed and Pb18 infected mice treated with DCs pulsed with P10, with or without antifungal drugs, contained significantly higher levels of IL-12 and significant reduction of IL-10 levels compared with the lungs of immunosuppressed and infected mice that did not receive DCs. The therapeutic use of P10-primed DCs in our non-immunosuppressed murine PCM

model also led to increased levels of IL-12 and reduced IL-10 levels in lung tissues, albeit high levels of IFN-γ were also present at the time the mice were euthanized in the prophylactic an therapeutic model (Magalhães et al., 2012). Similarly, we have found significant increased levels of IFN-γ and IL-12 and reduction of IL-10 level in the lungs of mice vaccinated with 20 μg of P10 in complete Freund's adjuvant that were subsequently infected with Pb18 (Muñoz et al., 2014). We believe that the peak of IFN-γ expression is likely occurring at different times in these different models, in which mice were also euthanized at different time points after infection. This hypothesis is supported by the present results, in which we found significant reductions of fungal cells when P10-pulsed DCs were administered with or without concomitant antifungal therapy.

## CONCLUSION

Out data indicate that P10-pulsed DCs, in the presence or not of antifungal drug, have the ability to induce specific immunity against *P. brasiliensis* in animals previously treated with corticosteroid in an experimental model that mimics the most aggressive form of PCM. These findings further support the active pursuit of P10 as a candidate for a human vaccine.

## AUTHOR CONTRIBUTIONS

LS performed experiments, analyzed data, and wrote the manuscript. AS, LD, GR, and JM performed experiments. JN, LT, and CT revised the manuscript. CT designed the experiments, wrote and revised the manuscript.

## ACKNOWLEDGMENTS

This work was supported by grants from FAPESP (2016/08730-6), CNPq, and CAPES. CT and LT are Research fellows of the CNPq. JN is supported in part by NIH AI52733, AI1033142-21S, and AI124797.

## REFERENCES

Banchereau, J. F. B. (2000). Immunobiology of dendritic cells. *Annu. Rev. Immunol.* 18, 767–811. doi: 10.1146/annurev.immunol.18.1.767

Benard, G., Campos, A. F., Netto, L. C., Gonçalves, L. G., Machado, L. R., Mimicos, E. V., et al. (2012). Treatment of severe forms of paracoccidioidomycosis: is there a role for corticosteroids? *Med. Mycol.* 50, 641–648. doi: 10.3109/13693786.2011.654135

Bocca, A. L., Amaral, A. C., Teixeira, M. M., Sato, P. K., Sato, P., Shikanai-Yasuda, M. A., et al. (2013). Paracoccidioidomycosis: eco-epidemiology, taxonomy and clinical and therapeutic issues. *Future Microbiol.* 8, 1177–1191. doi: 10.2217/fmb.13.68

Bozza, S., Perruccio, K., Montagnoli, C., Gaziano, R., Bellocchio, S., Burchielli, E., et al. (2003). A dendritic cell vaccine against invasive aspergillosis in allogeneic hematopoietic transplantation. *Blood* 102, 3807–3814. doi: 10.1182/blood-2003-03-0748

Buccheri, R., Khoury, Z., Barata, L. C. B., and Benard, G. (2015). Incubation period and early natural history events of the acute form of paracoccidioidomycosis: lessons from patients with a single *Paracoccidioides* spp. Exposure. *Mycopathologia* 181, 435–439. doi: 10.1007/s11046-015-9976-0

Chung, Y. J., Lee, J. I., Chong, S., Seok, J. W., Park, S. J., Jang, H. W., et al. (2011). Anti-proliferative effect and action mechanism of dexamethasone in human medullary thyroid cancer cell line. *Endocr. Res.* 36, 149–157. doi: 10.3109/07435800.2011.593012

D'Ostiani, C. F., Sero, G. D., Bacci, A., Montagnoli, C., Spreca, A., Mencacci, A., et al. (2000). Dendritic cells discriminate between yeasts and hyphae of the fungus *Candida albicans*: implications for initiation of t helper cell immunity in vitro and in vivo. *J. Exp. Med.* 191, 1661–1674. doi: 10.1084/jem.191.10.1661

Ferreira, K. S., Lopes, J. D., and Almeida, S. R. (2003). Regulation of T helper cell differentiation in vivo by GP43 from *Paracoccidioides brasiliensis* provided by different antigen-presenting cells. *Scand. J. Immunol.* 58, 290–297. doi: 10.1046/j.1365-3083.2003.01291.x

Inaba, K., Inaba, M., Romani, N., Aya, H., Deguchi, M., Ikehara, S., et al. (1992). Generation of large numbers of dendritic cells from mouse bone marrow cultures supplemented with granulocyte/macrophage colony-stimulating factor. *J. Exp. Med.* 176, 1693–1702. doi: 10.1084/jem.176.6.1693

Iwai, L. K., Yoshida, M., Sidney, J., Shikanai-Yasuda, M. A., Goldberg, A. C., Juliano, M. A., et al. (2003). In silico prediction of peptides binding to multiple HLA-DR molecules accurately identifies immunodominant epitopes from gp43 of *Paracoccidioides brasiliensis* frequently recognized in primary peripheral blood mononuclear cell responses from sensitized individuals. *Mol. Med.* 9, 209–219.

Magalhães, A., Ferreira, K. S., Almeida, S. R., Nosanchuk, J. D., Travassos, L. R., and Taborda, C. P. (2012). Prophylactic and therapeutic vaccination using dendritic cells primed with peptide 10 derived from the 43-kilodalton glycoprotein of *Paracoccidioides brasiliensis*. *Clin. Vaccine Immunol.* 19, 23–29. doi: 10.1128/CVI.05414-11

Moscardi-Bacchi, M., Brummer, E., and Stevens, D. A. (1994). Support of *Paracoccidioides brasiliensis* multiplication by human monocytes or macrophages: inhibition by activated phagocytes. *J. Med. Microbiol.* 40, 159–164. doi: 10.1099/00222615-40-3-159

Muñoz, J. E., Luft, V. D., Amorim, J., Magalhães, A., Thomaz, L., Nosanchuk, J. D., et al. (2014). Immunization with P10 peptide increases specific immunity and protects immunosuppressed BALB/c mice infected with virulent yeasts of *Paracoccidioides brasiliensis*. *Mycopathologia* 178, 177–188. doi: 10.1007/s11046-014-9801-1

Prado, M., da Silva, M. B., Laurenti, R., Travassos, L. R., and Taborda, C. P. (2009). Mortality due to systemic mycoses as a primary cause of death or in association with AIDS in Brazil: a review from 1996 to 2006. *Mem. Inst. Oswaldo Cruz* 104, 513–521. doi: 10.1590/S0074-02762009000300019

Restrepo, A. M. (1985). The ecology of *Paracoccidioides brasiliensis*: a puzzle still unsolved. *Sabouraudia* 23, 323–334. doi: 10.1080/00362178585380481

Roy, R. M., and Klein, B. S. (2012). Dendritic cells in antifungal immunity and vaccine design. *Cell Host Microbe* 11, 436–446. doi: 10.1016/j.chom.2012.04.005

Shikanai-Yasuda, M. A., Telles Filho, F. D. Q., Mendes, R. P., Colombo, A. L., Moretti, M. L., Kono, A., et al. (2006). Consenso em paracoccidioidomicose. *Rev. Soc. Bras. Med. Trop.* 39, 297–310. doi: 10.1590/S0037-86822006000300017

Siegemund, S., and Alber, G. (2008). Cryptococcus neoformans activates bone marrow-derived conventional dendritic cells rather than plasmacytoid dendritic cells and down-regulates macrophages. *FEMS Immunol. Med. Microbiol.* 52, 417–427. doi: 10.1111/j.1574-695X.2008.00391.x

Taborda, C. P., Juliano, M. A., Puccia, R., Franco, M., and Travassos, L. R. (1998). Mapping of the T-cell epitope in the major 43-kilodalton glycoprotein of *Paracoccidioides brasiliensis* which induces a Th-1 response protective against fungal infection in BALB/c mice. *Infect. Immun.* 66, 786–793.

Taborda, C. P., Urán, M. E., Nosanchuk, J. D., and Travassos, L. R. (2015). Paracoccidioidomycosis: challenges in the development of a vaccine against an endemic mycosis in the Americas. *Rev. Inst. Med. Trop. Saþo Paulo* 57(Suppl. 1), 21–24. doi: 10.1590/S0036-46652015000700005

Teixeira, M. D. M., Theodoro, R. C., Oliveira, F. F. M., De Machado, G. C., Hahn, R. C., Bagagli, E., et al. (2013). *Paracoccidioides lutzii* sp. nov.: biological

and clinical implications. *Med. Mycol.* 52, 19–28. doi: 10.3109/13693786.2013.794311

Theodoro, R. C., Teixeira, M. D. M., Felipe, M. S. S., Paduan, K. D. S., Ribolla, P. M., San-Blas, G., et al. (2012). Genus *Paracoccidioides*: species recognition and biogeographic aspects. *PLoS ONE* 7:e37694. doi: 10.1371/journal.pone.0037694

Thind, S. K., Taborda, C. P., and Nosanchuk, J. D. (2015). Dendritic cell interactions with *Histoplasma* and *Paracoccidioides*. *Virulence* 6, 424–432. doi: 10.4161/21505594.2014.965586

Travassos, L. R., Puccia, R., Cisalpino, P., Taborda, C., Rodrigues, E. G., Rodrigues, M., et al. (1995). Biochemistry and molecular biology of the main diagnostic antigen of *Paracoccidioides brasiliensis*. *Arch. Med. Res.* 26, 297–304.

Travassos, L. R., and Taborda, C. P. (2012a). New advances in the development of a vaccine against paracoccidioidomycosis. *Front. Microbiol.* 3:212. doi: 10.3389/fmicb.2012.00212

Travassos, L. R., and Taborda, C. P. (2012b). Paracoccidioidomycosis vaccine. *Hum. Vaccines Immunother.* 8, 1450–1453. doi: 10.4161/hv.21283

Travassos, L. R., Rodrigues, E. G., Iwai, L. K., and Taborda, C. P. (2008a). Attempts at a peptide vaccine against paracoccidioidomycosis, adjuvant to chemotherapy. *Mycopathologia* 165, 341–352. doi: 10.1007/s11046-007-9056-1

Travassos, L. R., Taborda, C. P., and Colombo, A. L. (2008b). Treatment options for paracoccidioidomycosis and new strategies investigated. *Expert Rev. Anti. Infect. Ther.* 6, 251–262. doi: 10.1586/14787210.6.2.251

Ueno, K., Kinjo, Y., Okubo, Y., Aki, K., Urai, M., Kaneko, Y., et al. (2015). Dendritic cell-based immunization ameliorates pulmonary infection with highly virulent *Cryptococcus gattii*. *Infect. Immun.* 83, 1577–1586. doi: 10.1128/IAI.02827-14

Ueno, K., Urai, M., Ohkouchi, K., Miyazaki, Y., and Kinjo, Y. (2016). Dendritic cell-based vaccine against fungal infection. *Methods Mol. Biol.* 1403, 537–549. doi: 10.1007/978-1-4939-3387-7_30

**Conflict of Interest Statement:** The authors declare that the research was conducted in the absence of any commercial or financial relationships that could be construed as a potential conflict of interest.

frontiers in Microbiology

ORIGINAL RESEARCH
published: 03 March 2017
doi: 10.3389/fmicb.2017.00345

# The Efficacy of Humanized Antibody against the *Sporothrix* Antigen, gp70, in Promoting Phagocytosis and Reducing Disease Burden

*José R. F. de Almeida[1†], Karla L. Santiago[1†], Gilberto H. Kaihami[2], Andrea Q. Maranhão[3], Marcelo de Macedo Brígido[3] and Sandro R. de Almeida[1]**

[1] Department of Clinical and Toxicological Analysis, Faculty of Pharmaceutical Sciences, University of São Paulo, São Paulo, Brazil, [2] Department of Biochemistry, Institute of Chemistry, University of São Paulo, São Paulo, Brazil, [3] Department of Cell Biology, Institute of Biological Sciences, University of Brasilia, Brasilia, Brazil

OPEN ACCESS

**Edited by:**
*Joshua D. Nosanchuk, Albert Einstein College of Medicine, USA*

**Reviewed by:**
*Joseph M. Bliss, Women & Infants Hospital of Rhode Island, USA*
*Marcos Sergio Toledo, Federal University of São Paulo, Brazil*

***Correspondence:**
*Sandro R. de Almeida*
*sandroal@usp.br*

*† These authors have contributed equally to this work.*

**Specialty section:**
*This article was submitted to Fungi and Their Interactions, a section of the journal Frontiers in Microbiology*

**Received:** *01 December 2016*
**Accepted:** *20 February 2017*
**Published:** *03 March 2017*

**Citation:**
*de Almeida JRF, Santiago KL, Kaihami GH, Maranhão AQ, de Macedo Brígido M and de Almeida SR (2017) The Efficacy of Humanized Antibody against the Sporothrix Antigen, gp70, in Promoting Phagocytosis and Reducing Disease Burden. Front. Microbiol. 8:345. doi: 10.3389/fmicb.2017.00345*

Sporotrichosis is a subcutaneous mycosis distributed worldwide and is frequently reported in countries with tropical climates, as Latin America countries. We previously demonstrated that mice with sporotrichosis produce specific antibodies against a 70-kDa fungal protein, indicating that specific antibodies against this molecule may help to control the sporotrichosis. IgG1 monoclonal antibody was generated, and called mAbP6E7, in mice against a 70-kDa glycoprotein (gp70) of *S. schenckii*. The mAbP6E7 showed prophylactic and therapeutic activity against sporotrichosis. However, this antibody has a murine origin, and this can generate an immune response when administered to humans, precluding its use for a prolonged time. For its possible use in the treatment of human sporotrichosis, we humanized the mAbP6E7 by genetic engineering. Once expressed, the humanized antibodies had good stability and were able to bind to the 70-kDa cell wall antigens of *Sporothrix schenckii* and *S. brasiliensis*. The humanized P6E7 were able to opsonize *S. schenckii* yeasts, thus increasing the phagocytic index in human monocyte-derived macrophages. The treatment with humanized P6E7 decreased fungal burden *in vivo*. These data suggest that humanized P6E7 may have a therapeutic role in sporotrichosis.

**Keywords: humanized antibody, *S. schenckii*, sporotrichosis**

## INTRODUCTION

Sporotrichosis is a subcutaneous mycosis, caused by *Sporothrix* sp., affecting animals and humans and frequently involves the lymphatic system. *Sporothrix* sp. include fungi with thermal dimorphism, in which the mycelial form, found in soil, is saprophytic, and the yeast form, which is found in the host tissue, is parasitic (Bonifaz and Vazquez-Gonzalez, 2010; Vasquez-del-Mercado et al., 2012). Sporotrichosis is distributed worldwide but is frequently reported in countries with subtropical and tropical climates, as the Latin America countries (Schechtman, 2010). The traumatic inoculation of the conidia and hyphae of this fungus results in the development of subcutaneous mycoses. Within the infected tissue, the fungus differentiates into its yeast form and may spread to other tissues (Barros et al., 2011). The largest epidemic of sporotrichosis because of zoonotic transmission was described in Rio de Janeiro between 1998 and 2004, in which 759

humans were diagnosed with sporotrichosis (Barros et al., 2008; Freitas et al., 2010). Marimon et al. (2007) described four new species, *S. globosa*, *S. brasiliensis*, *S. Mexicana*, and *S. luriei*. These new species have been found to have a worldwide distribution. However, *S. brasiliensis* is apparently restricted to Brazil, and *S. mexicana* is restricted to Mexico.

The fungus virulence and the host immune responses are essential for the development and severity of sporotrichosis. The recent sporotrichosis outbreaks in Rio de Janeiro city, demonstrates the emergence of feline zoonotic transmission and the prevalence of *S. brasiliensis* in the sporotrichosis, creating a new paradigm of this disease (Lopes-Bezerra and Mora-Montes, 2015).

Different drug protocols are used for the treatment of sporotrichosis and include terbinafine, potassium iodide, itraconazole, fluconazole, and the amphotericin B (Song et al., 2011). Adverse events, as vomiting and diarrhea, nausea, headache, hypersensitivity reactions, abdominal pain, and liver dysfunction, can occur (Lopez-Romero et al., 2011).

In a previous study, we demonstrated that sporotrichosis, caused by *Sporothrix schenckii* are able to produce specific IgG antibodies against a 70-kDa fungal protein (gp70), demonstrating that specific antibodies against the gp70 may help control the sporotrichosis (Nascimento et al., 2008). To understand the role of IgG mediated response in sporotrichosis, we produced an IgG1 monoclonal antibody against gp70 of *S. schenckii*, called mAbP6E7. To evaluate the protective effect of the mAbP6E7 *in vivo*, mice infected with *S. schenckii* were passively immunized. A significant reduction in fungal burden in the spleen and liver of mice treated with mAbP6E7 before and during experimental sporotrichosis caused by *S. schenckii* was observed (Nascimento et al., 2008). Recently, our group showed that mice treated with P6E7 and infected with a strain isolated from a case of feline sporotrichosis, strain 5110 (ATCC MYA – 4823) showed a decreased fungal burden in its organs (de Almeida et al., 2015).

The mAb P6E7 showed prophylactic and therapeutic activity against sporotrichosis. However, this antibody has a murine origin, and this can generate an immune response when administered to humans, precluding its use for a prolonged time. For its possible use in the treatment of human sporotrichosis, our proposal was the humanization of the mAb P6E7 through genetic engineering.

Here we humanized the mAbP6E7 and proved their binding ability to the fungus and effector function. We also demonstrated that the treatment with humanized P6E7 decreased the fungal burden in experimental sporotrichosis. Together, these data demonstrated the functionality of humanized P6E7 and their efficiency in the treatment of experimental sporotrichosis.

# MATERIALS AND METHODS

## Microorganism and Culture Conditions

The strains used were *Sporothrix schenckii* M-64 (ATCC MYA 4822) and *Sporothrix brasiliensis* 5110 (ATCC MYA 4823). The strains were maintained by regular passages on animals and were grown on Sabouraud dextrose agar at 25°C for 7 days. The yeast form was obtained by cultivation in BHI agar at 37°C for 7 days.

## Animals

Female BALB/c mice at 10 weeks of age (weighing approximately 24 g) were obtained from the Animal House Production and Experimentation Facility of the Faculty of Pharmaceutical Sciences and Institute of Chemistry of the University of São Paulo. The mice were maintained in a SPF environment (specific pathogen free) and housed in temperature controlled rooms at 23–25°C with free access to food and water throughout the experiments.

## Human Ethics Statement

This study was carried out in accordance with the recommendations of Ethical Committee of the Faculty of Pharmacy of the University of São Paulo with written informed consent from all subjects. All subjects gave written informed consent in accordance with the Declaration of Helsinki.

## Animal Ethics Statement

This study was carried out in accordance with the recommendations of Guide for the Care and Use of Laboratory Animals of the National Institutes of Health. The protocol was approved by the Brazilian Conselho Nacional de Controle da Experimentação Animal (CONCEA).

## Computational Analysis

For computational analysis, a standard protocol was used (Silva et al., 2009). Briefly, human VH and VL framework sequences were extracted from the Swiss-Prot or GenBank. (A sequence search was performed with FASTA (Pearson, 2000) or BLAST (Altschul et al., 1997). ClustalW (Higgins et al., 1996) was used for multisequence alignment, running in BioEdit[1]. Sterically constrained atoms were detected using similar tri-dimensional models from the Protein Data Bank[2]. Model visualization and atom-to-atom distance calculations were performed in RASMOL version 2.6 (Bernstein, 2000). Variable region numbering followed Kabat's convention (Kabat and Wu, 1991).

## Construction of Humanized FvFc Expression Vector

The plasmids were constructed using standard cloning methods (Sambrook and Russell, 2001). The VH and VL humanized P6E7 fragments were synthesized and confirmed by sequencing. The scFv (VH-linker-VL) region was cloned into a pMIRES vector using its *Xma*I and *Xho*I restriction sites to generate pHP6E7. This construction generated a VH-linker-VL fragment fused with the human IgG1 CH2CH3 domains. The nucleotide sequences were deposited in the GenBank with the accession numbers:

BankIt1984561 VL KY488459
BankIt1984561 VH KY488460

[1]http://www.mbio.ncsu.edu/bioedit/bioedit.html
[2]http://www.pdb.org

## hP6E7 Production and Purification

CHO-K1 cells were routinely cultured in Ham-F2 (HyClone) supplemented with 10% FBS. Approximately $9 \times 10^6$ cells were seeded in a 15-cm cell culture dish. Cells were transfected using the jetPEI reagent (Polyplus Transfection) according to the manufacturer's protocol and cultured in Ham-F2 with 1.25% ultra-low IgG FBS (Invitrogen). After 72 h, the culture supernatants were recovered. The supernatant containing the hP6E7 antibody were purified using a HiTrap Protein A column (GE Healthcare) equilibrated with 20 mM sodium phosphate at pH 7.0 and eluted with 0.1 M citric acid at pH 3.5. The eluted fractions were neutralized with 1 M Tris-HCl at pH 9.0. The buffer was exchanged using a PD-10 column (GE Healthcare) equilibrated with PBS. The proteins were concentrated with a Centriprep-Ultracel YM-10.000 MWCO (Millipore). The protein concentration was determined by BCA.

## Experimental Infection

Two groups of five mice each were inoculated through the intraperitoneal (i.p.) route with $5 \times 10^6$ yeast cells of *S. schenckii* M-64 suspended in 0.1 mL of sterile PBS. After 3 days of infection, the treated groups received 100 μg of hP6E7 in 0.2 mL of sterile PBS. The control group was inoculated with 0.2 mL of sterile PBS. After 10 days of infection, the five mice of each group were euthanized in a $CO_2$ chamber to measure the fungal burden. The spleen and liver were homogenized, and the supernatants were collected. The colony forming units (CFU) were assayed by serial dilution and plating on BHI agar plates. The plates were incubated up to seven days at 25°C. The CFU were counted, and the results are expressed as CFU per g of tissue.

## Human Monocyte-Derived Macrophages Isolation

Human monocyte-derived macrophages isolation was performed as previously described with a few modifications (Sousa et al., 2008). Briefly, the peripheral blood of healthy volunteers was collected in vacuum tubes containing heparin as an anticoagulant. The separation was performed by centrifugation for 40 min at 600 g on a density gradient using Ficoll–Hypaque (Sigma–Aldrich). The cells were aspirated and washed with sterile PBS. Positive selection using $CD14^+$ magnetic beads was performed according to the manufacturer's instructions (MiltenyiBiotec). The cells were centrifuged, washed and resuspended in sterile PBS. The monocytes were counted in a Neubauer chamber ($2 \times 10^5$) and plated on 24-well plates containing a round glass coverslip in the bottom in RPMI 1640 (Sigma–Aldrich) containing 10% FBS. The cell culture plates were incubated for seven days. Cells were left to adhere on culture plates for 2 days at 37°C, non-adherent cells were removed and the medium was exchanged for fresh RPMI 1640 containing 10% FBS.

## Phagocytosis Assay and Opsonization Condition

Prior to infection, *S. schenckii* M-64 yeast cells were opsonized with the hP6E7 antibody or not opsonized, as described previously, with some modifications (Nascimento et al., 2008). Briefly, $1 \times 10^6$ *S. schenckii* M-64 yeast cells were incubated with 25 μg of the hP6E7 antibody or without it (control) in PBS for 1 h at 37°C under constant agitation. After this incubation, the yeast cells were washed three times with PBS to remove the unbound antibodies. Human monocyte-derived macrophages were infected with the opsonized or non-opsonized *S. schenckii* M-64 yeast cells (at a proportion of three yeast cells to 1 macrophage) for 5 h. The coverslips were stained with the hematological staining kit InstantProv (NewProv), and the phagocytic index (PI) was calculated according to the following formula:

$$\mathrm{PI} = \left(\frac{\text{Number of internalized yeast}}{\text{Number of Monocytes in the same field}}\right) \times 100$$

## Immunofluorescence

An immunofluorescence assay was performed as previously described with a few modifications (Nascimento et al., 2008). Briefly, *S. schenckii* M-64 yeast cells from 10-day-old cultures grown in BHI agar were collected and resuspended in sterile PBS. The yeast cells ($5 \times 10^6$) were incubated for 1 h in sterile PBS containing 0.2% gelatin. The cell suspension was then incubated for 2 h with 20 μg of hP6E7 diluted in PBS containing 0.2% gelatin. In the negative control, the yeast cells were incubated only with sterile PBS. After this period, the opsonized and non-opsonized yeast cells were washed three times in sterile PBS and incubated with the anti-human IgG antibody conjugated with Alexa Fluor 488 (Life Technologies) (1:200) in sterile PBS containing 0.2% gelatin. All steps were performed under agitation (37°C). The yeast cells were washed with sterile PBS and mounted on glass slides in Gelvatol. Then, they were examined with a Nikon Microphot FX microscope.

## Western Blot

The hP6E7 antibody was evaluated for its binding capacity against gp70, which is present in the cell wall of *S. schenckii* and *S. brasiliensis*. The proteins from cell wall were obtained from yeast cells of *S. brasiliensis* 5110 and *S. schenckii* grown in Erlenmeyer flasks containing 400 mL of YCG medium (yeast nitrogen–glucose casamino acids) for 7 days with constant agitation at 9 *g* at 37°C. Then, the yeast cells were collected and incubated with an extraction solution (2 mM DTT, 1 mM PMSF, and 5 mM EDTA in 25 mM Tris/HCl at pH 8.5) at 4°C for 2 h with mild agitation. The supernatant containing the cell surface proteins was collected and concentrated. Five micrograms of cell wall proteins was separated by electrophoresis using a 12% SDS polyacrylamide gel, and subsequently, the proteins were electrotransferred to Hybond ECL nitrocellulose membranes (GE Healthcare). Finally, the membranes were washed and developed using the ECL Plus Kit (GE Healthcare).

## Statistical Analysis

GraphPad Prism 5 (GraphPad Software) was used for all statistical analyses. The data were compared using the unpaired

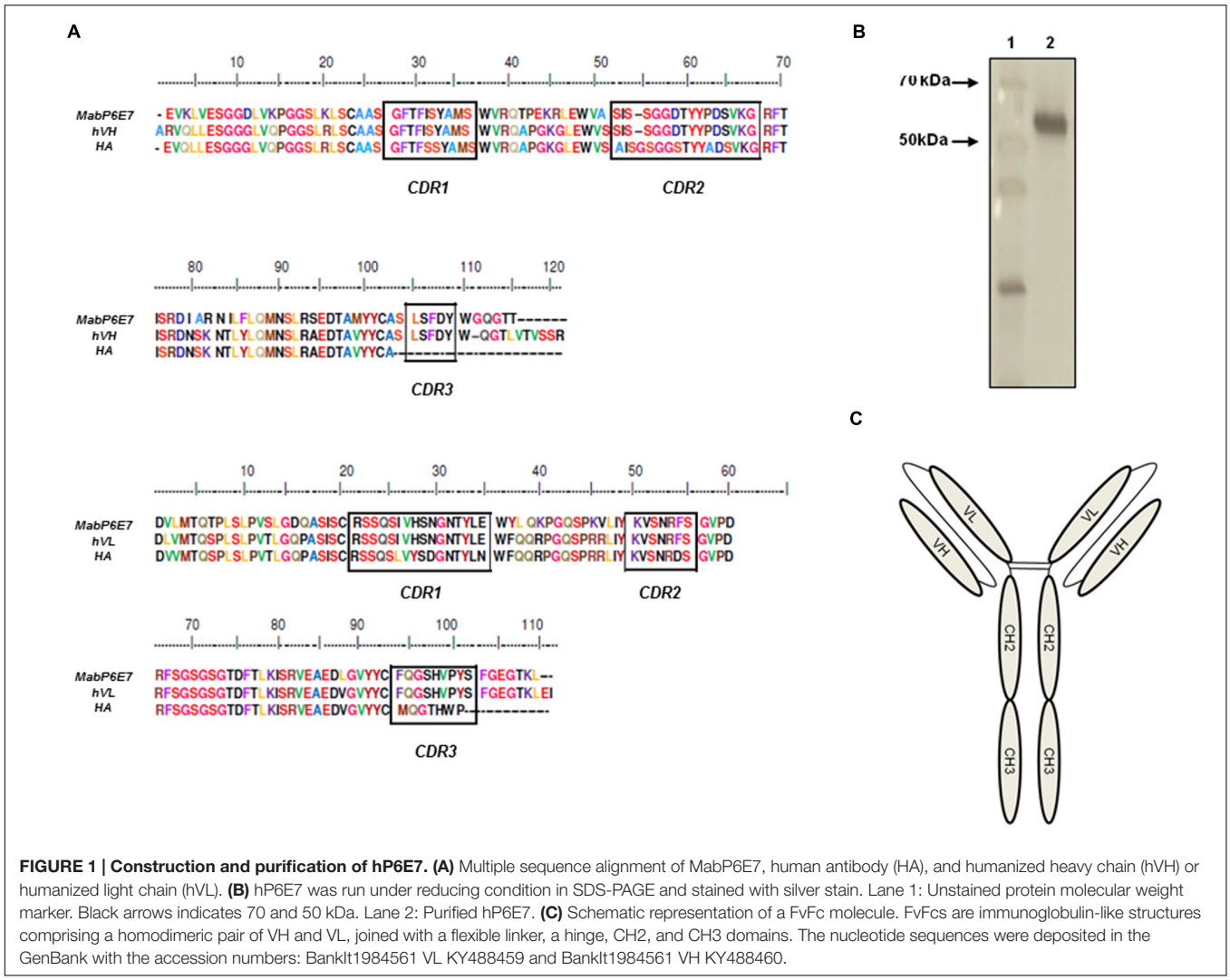


**FIGURE 1 | Construction and purification of hP6E7. (A)** Multiple sequence alignment of MabP6E7, human antibody (HA), and humanized heavy chain (hVH) or humanized light chain (hVL). **(B)** hP6E7 was run under reducing condition in SDS-PAGE and stained with silver stain. Lane 1: Unstained protein molecular weight marker. Black arrows indicates 70 and 50 kDa. Lane 2: Purified hP6E7. **(C)** Schematic representation of a FvFc molecule. FvFcs are immunoglobulin-like structures comprising a homodimeric pair of VH and VL, joined with a flexible linker, a hinge, CH2, and CH3 domains. The nucleotide sequences were deposited in the GenBank with the accession numbers: BankIt1984561 VL KY488459 and BankIt1984561 VH KY488460.

*t*-test. Differences were considered statistically significant at $^{*}p < 0.05$; $^{**}p < 0.01$; and $^{***}p < 0.001$.

# RESULTS

## Construction of the Humanized P6E7 Antibody as a scFc Molecule

Humanized antibodies are human-like antibodies in which only the complementarity determining regions (CDRs) are murine. This approach can be used to reduce the biggest issue with non-human antibody (HA) therapy, antibody immunogenicity (Clark, 2000). Therefore, to generate an effective antibody against the emerging mycosis sporotrichosis, the murine monoclonal antibody P6E7 was humanized. The P6E7 humanization was performed as described previously (Caldas et al., 2003). To reduce the mouse antibody immunogenicity, the VH and VL sequences of mAbP6E7 were compared to a HA database (GenBank, EMBL, PDB) to generate a similar human-like IgG polypeptide sequence.

These sequences were used as a framework for mAbP6E7 CDRs. Structural analyzes using the BioEdit Sequence Alignment Editor program were carried out to identify structural impediments in the human protein. The hP6E7 VH and VL were designed as scFc fragments (a single-chain Fv fused to a human IgG1 Fc) (**Figure 1C**) in the mammalian expression vector pMIRES. The sequences of heavy and light chain hP6E7 and MabP6E7 are similar (**Figure 1A**). The humanized antibody was expressed in the CHO-K1 cell line, and clones expressing the antibodies were obtained by positive selection. The humanized antibody was purified by affinity chromatography from cell culture supernatants. As expected, the hP6E7 preparation under reducing conditions is a 55-kDa homodimeric protein (**Figure 1B**), similar to other humanized scFc molecules (Silva et al., 2009).

## hP6E7 Recognizes the gp70 Protein

Our group characterized a 70-kDa antigen (gp70) in the exoantigen of *S. schenckii* and *S. brasiliensis* using mAbP6E7 (Nascimento et al., 2008; de Almeida et al., 2015). mAbP6E7

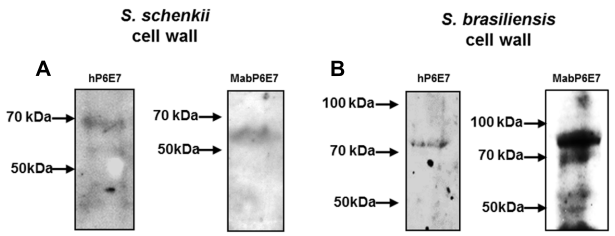


**FIGURE 2 | hP6E7 binds to *Sporothrix* sp. antigens.** Western blot analysis of the cell wall extracts of *Sporothrix schenckii* **(A)** or *S. brasiliensis* **(B)**. Membrane was incubated with hP6E7 or mAbP6E7.

recognizes the gp70 protein from *S. schenckii* and *S. brasiliensis* in the exoantigen preparation of these strains (Castro et al., 2013). To evaluate the capacity of hP6E7 to bind to gp70, the cell wall preparation proteins from *S. schenckii* and *S. brasiliensis* were resolved by SDS-PAGE for the immunodetection of gp70 by hP6E7 in Western blot assays. We showed that hP6E7 and the mAbP6E7 binds proteins with the same molecular weights in *S. schenckii* (**Figure 2A**) and *S. brasiliensis* (**Figure 2B**). In *S. schenckii* and *S. brasiliensis* the molecular weight of the gp70 protein recognized by both antibodies was closer to 70 kDa.

Our group showed that the molecular weight of gp70 may vary due to glycosylation sites present in gp70 in *S. brasiliensis*, while these sites are absent in *S. schenckii* (Castro et al., 2013). In conclusion, we suggest that hP6E7 could recognize the gp70 antigen in both *Sporothrix* sp. species.

## hP6E7 Binds to the gp70 Protein on the Surface of *S. schenckii* and *S. brasiliensis*

The next experiment was to analyze the binding activity of hP6E7 to gp70 on the surface of fungi. To probe this binding, we performed an immunofluorescence assay. Yeast cells of *S. schenckii* and *S. brasiliensis* were incubated with hP6E7 and then labeled with Alexa Fluor 488-conjugated anti-human IgG. As expected, we observed a strong signal on the surface of *S. schenckii* cells (**Figure 3A**). On the other hand, we observed a weak but reliable signal on the *S. brasiliensis* cell wall (**Figure 3B**). This weak fluorescence is due to the low amount of gp70 on the surface of *S. brasiliensis*, as previously demonstrated (Castro et al., 2013).

## hP6E7 Enhances the Phagocytosis of *S. schenckii* by Human Macrophages

As hP6E7 showed binding activity on the surface of fungus, we evaluated if human monocyte-derived macrophages were able to recognize the Fc human fraction from hP6E7 promoting yeast phagocytosis. Thus, we analyzed the interaction between

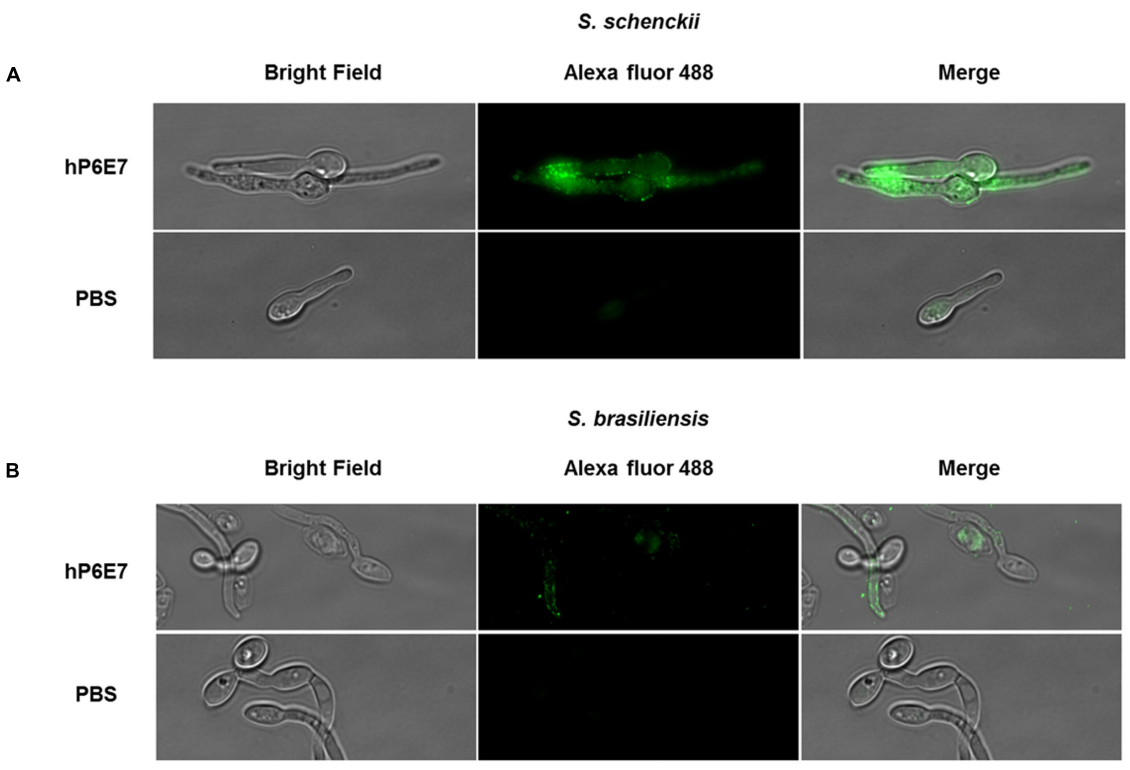


**FIGURE 3 | hP6E7 binds to *S. schenckii* and *S. brasiliensis* cell wall. (A)** *S. schenckii* and **(B)** *S. brasiliensis* cells were incubated for 2 h with or not 20 μg of hP6E7 diluted in PBS containing 0.2% of gelatin. Both groups, hP6E7 and control, were incubated with anti-human IgG conjugated with Alexa Fluor 488 in sterile PBS containing 0.2% gelatin, and visualized under a fluorescence microscopy.

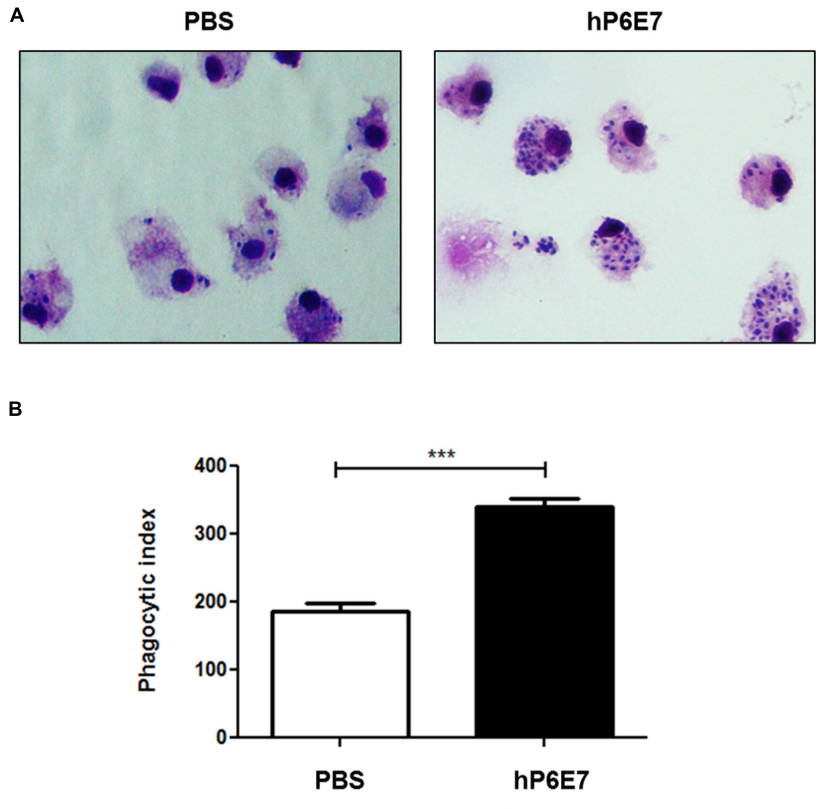


**FIGURE 4 | hP6E7 enhances the phagocytosis against *S. schenckii* by macrophages human cells. (A)** Monocyte-derived macrophages human cells were infected with *S. schenckii* yeast cells opsonized or not by hP6E7 for 5 h. Yeast internalization was counted by optical microscopy. **(B)** Phagocytosis index of yeast cells opsonized with 25 μg of hP6E7 and yeast cells treated with sterile PBS. Data are the means ± SD. ***$p < 0.001$.

*S. schenckii* and $CD14^+$ human monocyte-derived macrophages. As expected, human monocyte-derived macrophages were able to phagocytose the *S. schenckii* yeast, and opsonized yeast showed a higher phagocytosis ability compared to non-opsonized yeast (**Figure 4**). Our group has already shown that opsonization by mAbP6E7 was able to increase the phagocytosis index in murine macrophages in a concentration-dependent manner and increase NO production (Nascimento et al., 2008). These data demonstrate that hP6E7 is fully functional and is able to recognize the *Sporothrix* sp. antigen, leading to enhanced recognition by phagocytic cells.

## hP6E7 Treatment Decreases the Fungal Burden *In vivo*

We evaluated if the humanized antibody against gp70 could influence sporotrichosis infection (**Figure 5**). BALB/c mice were treated with hP6E7 after 3 days of *S. schenckii* infection and euthanized after 10 days of infection to evaluate the fungal burden in the spleen and liver (**Figure 5A**). Although hP6E7 has a human Fc fraction, it can be recognized by non-human cells, but with reduced effectivity. The treatment with hP6E7 decreased the fungal burden in the spleen after 10 days of infection compared with the control (**Figure 5B**).

## DISCUSSION

The treatment of sporotrichosis is not always easy, since the drugs of choice to combat sporotrichosis require long periods of treatment, and relapses occur, especially in immunocompromised patients. In some fungal diseases, such as paracoccidioidomycosis (Buissa-Filho et al., 2008) and candidiasis (Moragues et al., 2003) the use of mAbs confers protection. In some case, the use of mAbs modifies the course of infection as observed in experimental infection by *Cryptococcus neoformans* (Rivera et al., 2005). In addition, mAbs against *Cryptococcus neoformans* (Larsen et al., 2005) and *Candida albicans* (Pachl et al., 2006) have been approved for clinical evaluation by FDA. In systemic candidiasis, antifungal antibodies provide novel therapies for use in combination with antifungal drugs (Matthews and Burnie, 2001).

Our group demonstrated that the mAb against gp70 (P6E7) significantly decreased infections of *S. schenckii* and *S. brasiliensis in vivo* (Nascimento et al., 2008; de Almeida et al., 2015). However, the use of the murine monoclonal antibody in clinical practice could induce the production of anti-murine antibodies (HAMA) in patients (Chiu et al., 2011). Therefore, we developed a humanized anti-gp70 antibody as FvFc fragments. The antibody format was chosen for several advantages, as showed in the

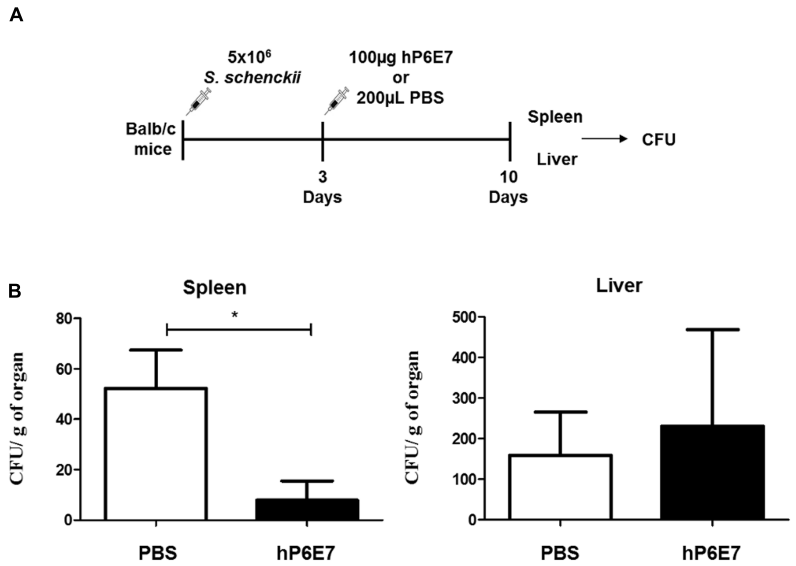


**FIGURE 5 | hP6E7 treatment decreases the fungal burden *in vivo*. (A)** Experimental approach for passive immunization with hP6E7 and fungal burden analysis. **(B)** Fungal burden in the spleen and the liver of infected mice after the treatment with hP6E7 or PBS. Data are the means ± SD. $^*p < 0.05$.

literature (Holliger and Hudson, 2005). The targeting specificity of the whole mAb is preserved in this fragment; it is poorly immunogenic and has an increased biodistribution and blood clearance properties (Hudson and Souriau, 2003; Holliger and Hudson, 2005).

The process used to complete the humanization of P6E7 replaced the murine components with the amino acid residues of human homologues to reduce the possibility of inducing immunogenicity in patients. Humanized antibodies have been used with success in alternative treatments for several disorders, including cancer, transplant rejection, and infectious diseases (Souriau and Hudson, 2003; Cai et al., 2015; DiGiandomenico and Sellman, 2015). A major problem after the humanization of an antibody is preserving the capacity of the antibody to bind the antigen. After the purification of hP6E7, we tested its capacity to bind gp70. We observed that the humanized antibody was able to bind to gp70, as demonstrated by immunoblotting and immunofluorescent assays. These results indicated that hP6E7 did not lose its affinity and capacity to bind the antigen.

An important mechanism in antibody-mediated protection is the opsonization of the microorganism by the Fc gamma receptor (FCR) (Alvarez et al., 2008). FCR mediates several macrophage functions, including phagocytosis, the stimulation of cytokine secretion, and the triggering of respiratory antibody-dependent cellular cytotoxicity (Clavel et al., 2008; Richards et al., 2008). The results obtained with murine P6E7 showed that the yeast cells with anti-gp70 increased the phagocytic index of murine macrophages. Our results showed that the FvFc fragments of human P6E7 have the ability to bind to gp70 and that the yeast cells of *S. schenckii* with FvFc increase the phagocytic index of monocyte-derived macrophages. Next, our group analyzed the efficiency of hP6E7 to control the disease *in vivo*. Our results showed that treatment with hP6E7 decreased the fungal burden only in the spleen during murine sporotrichosis. Recently, our group also observed the reduction of the fungal burden in spleen, but not in liver after the mAbP6E7 treatment in experimental sporotrichosis by *S. schenckii* and *S. brasiliensis* (de Almeida et al., 2015). As the hP6E7 is a humanized antibody, the Fc gamma receptor (FCR) of mice phagocytes cells can not have a full recognition of the humanized antibody, reducing the antibody efficiency. The spleen is an organ with enough phagocytes cells as macrophages and dendritic cells, being easier to recognize and clear the fungal load in this organ. While in the liver, maybe with more doses the fungal burden could reduce as well. These data show that hP6E7 is efficient in the treatment of sporotrichosis, showing similar results as mAbP6E7 *in vitro* and *in vivo*. Finally, our data suggest that humanized P6E7 could have a therapeutic role in sporotrichosis and may justify further development of the humanized antibody as a biopharmaceutical that could be used in the treatment of fungal infection.

## AUTHOR CONTRIBUTIONS

JdA, KS, and GK performed the experiments, AM, MdMB, and SdA designed the study and SdA wrote the paper. JdA and KS contributed equally to the work.

## ACKNOWLEDGMENTS

We thank Dr. Leila L. Bezzera from UERJ for providing the strain of *Sporothrix brasiliensis* 5110 (ATCC MYA 4823). This work was supported by FAPESP (São Paulo Research Foundation): Grant FAPESP 2012/18535-5.

## REFERENCES


Altschul, S. F., Madden, T. L., Schaffer, A. A., Zhang, J., Zhang, Z., Miller, W., et al. (1997). Gapped BLAST and PSI-BLAST: a new generation of protein database search programs. *Nucleic Acids Res.* 25, 3389–3402. doi: 10.1093/nar/25.17.3389

Alvarez, Y., Tang, X., Coligan, J. E., and Borrego, F. (2008). The CD300a (IRp60) inhibitory receptor is rapidly up-regulated on human neutrophils in response to inflammatory stimuli and modulates CD32a (FcgammaRIIa) mediated signaling. *Mol. Immunol.* 45, 253–258. doi: 10.1016/j.molimm.2007.05.006

Barros, M. B., De Almeida Paes, R., and Schubach, A. O. (2011). *Sporothrix schenckii* and Sporotrichosis. *Clin. Microbiol. Rev.* 24, 633–654. doi: 10.1128/CMR.00007-11

Barros, M. B., Schubach, A. O., Schubach, T. M., Wanke, B., and Lambert-Passos, S. R. (2008). An epidemic of sporotrichosis in Rio de Janeiro, Brazil: epidemiological aspects of a series of cases. *Epidemiol. Infect.* 136, 1192–1196. doi: 10.1017/S0950268807009727

Bernstein, H. J. (2000). Recent changes to RasMol, recombining the variants. *Trends Biochem. Sci.* 25, 453–455. doi: 10.1016/S0968-0004(00)01606-6

Bonifaz, A., and Vazquez-Gonzalez, D. (2010). Sporotrichosis: an update. *G. Ital. Dermatol. Venereol.* 145, 659–673.

Buissa-Filho, R., Puccia, R., Marques, A. F., Pinto, F. A., Munoz, J. E., Nosanchuk, J. D., et al. (2008). The monoclonal antibody against the major diagnostic antigen of *Paracoccidioides brasiliensis* mediates immune protection in infected BALB/c mice challenged intratracheally with the fungus. *Infect. Immun.* 76, 3321–3328. doi: 10.1128/IAI.00349-08

Cai, B., Wang, M., Zhu, X., Xu, J., Zheng, W., Zhang, Y., et al. (2015). The fab fragment of a humanized anti-toll like receptor 4 (TLR4) monoclonal antibody reduces the lipopolysaccharide response via TLR4 in mouse macrophage. *Int. J. Mol. Sci.* 16, 25502–25515. doi: 10.3390/ijms161025502

Caldas, C., Coelho, V., Kalil, J., Moro, A. M., Maranhao, A. Q., and Brigido, M. M. (2003). Humanization of the anti-CD18 antibody 6.7: an unexpected effect of a framework residue in binding to antigen. *Mol. Immunol.* 39, 941–952. doi: 10.1016/S0161-5890(03)00022-1

Castro, R. A., Kubitschek-Barreira, P. H., Teixeira, P. A., Sanches, G. F., Teixeira, M. M., Quintella, L. P., et al. (2013). Differences in cell morphometry, cell wall topography and gp70 expression correlate with the virulence of *Sporothrix brasiliensis* clinical isolates. *PLoS ONE* 8:e75656. doi: 10.1371/journal.pone.0075656

Chiu, W.-C., Lai, Y.-P., and Chou, M.-Y. (2011). Humanization and characterization of an anti-human TNF-α murine monoclonal antibody. *PLoS ONE* 6:e16373. doi: 10.1371/journal.pone.0016373

Clark, M. (2000). Chimeric and humanised–misunderstood. *Lancet* 355, 1557. doi: 10.1016/s0140-6736(05)74611-0

Clavel, C., Nogueira, L., Laurent, L., Iobagiu, C., Vincent, C., Sebbag, M., et al. (2008). Induction of macrophage secretion of tumor necrosis factor alpha through Fcgamma receptor IIa engagement by rheumatoid arthritis-specific autoantibodies to citrullinated proteins complexed with fibrinogen. *Arthritis Rheum.* 58, 678–688. doi: 10.1002/art.23284

de Almeida, J. R., Kaihami, G. H., Jannuzzi, G. P., and De Almeida, S. R. (2015). Therapeutic vaccine using a monoclonal antibody against a 70-kDa glycoprotein in mice infected with highly virulent *Sporothrix schenckii* and *Sporothrix brasiliensis*. *Med. Mycol.* 53, 42–50. doi: 10.1093/mmy/myu049

DiGiandomenico, A., and Sellman, B. R. (2015). Antibacterial monoclonal antibodies: the next generation? *Curr. Opin. Microbiol.* 27, 78–85. doi: 10.1016/j.mib.2015.07.014

Freitas, D. F., Do Valle, A. C., De Almeida Paes, R., Bastos, F. I., and Galhardo, M. C. (2010). Zoonotic Sporotrichosis in Rio de Janeiro, Brazil: a protracted epidemic yet to be curbed. *Clin. Infect. Dis.* 50, 453. doi: 10.1086/649891

Higgins, D. G., Thompson, J. D., and Gibson, T. J. (1996). Using CLUSTAL for multiple sequence alignments. *Methods Enzymol.* 266, 383–402. doi: 10.1016/S0076-6879(96)66024-8

Holliger, P., and Hudson, P. J. (2005). Engineered antibody fragments and the rise of single domains. *Nat. Biotechnol.* 23, 1126–1136. doi: 10.1038/nbt1142

Hudson, P. J., and Souriau, C. (2003). Engineered antibodies. *Nat. Med.* 9, 129–134. doi: 10.1038/nm0103-129

Kabat, E. A., and Wu, T. T. (1991). Identical V region amino acid sequences and segments of sequences in antibodies of different specificities. Relative contributions of VH and VL genes, minigenes, and complementarity-determining regions to binding of antibody-combining sites. *J. Immunol.* 147, 1709–1719.

Larsen, R. A., Pappas, P. G., Perfect, J., Aberg, J. A., Casadevall, A., Cloud, G. A., et al. (2005). Phase I evaluation of the safety and pharmacokinetics of murine-derived anticryptococcal antibody 18B7 in subjects with treated cryptococcal meningitis. *Antimicrob. Agents Chemother.* 49, 952–958. doi: 10.1128/AAC.49.3.952-958.2005

Lopes-Bezerra, L. M., and Mora-Montes, H. M. (2015). *Sporothrix* and sporotrichosis: contributions from the first international meeting sponsored by the Working Group on *Sporothrix* and sporotrichosis of the International Society for Human and Animal Mycology, Rio de Janeiro, Brazil. *Med. Mycol.* 53, 1–2. doi: 10.1093/mmy/myu096

Lopez-Romero, E., Reyes-Montes Mdel, R., Perez-Torres, A., Ruiz-Baca, E., Villagomez-Castro, J. C., Mora-Montes, H. M., et al. (2011). *Sporothrix schenckii* complex and sporotrichosis, an emerging health problem. *Future Microbiol.* 6, 85–102. doi: 10.2217/fmb.10.157

Marimon, R., Cano, J., Gene, J., Sutton, D. A., Kawasaki, M., and Guarro, J. (2007). *Sporothrix brasiliensis*, *S. globosa*, and *S. mexicana*, three new *Sporothrix* species of clinical interest. *J. Clin. Microbiol.* 45, 3198–3206. doi: 10.1128/JCM.00808-07

Matthews, R., and Burnie, J. (2001). Antifungal antibodies: a new approach to the treatment of systemic candidiasis. *Curr. Opin. Investig. Drugs* 2, 472–476.

Moragues, M. D., Omaetxebarria, M. J., Elguezabal, N., Sevilla, M. J., Conti, S., Polonelli, L., et al. (2003). A monoclonal antibody directed against a *Candida albicans* cell wall mannoprotein exerts three anti-*C. albicans* activities. *Infect. Immun.* 71, 5273–5279. doi: 10.1128/IAI.71.9.5273-5279.2003

Nascimento, R. C., Espindola, N. M., Castro, R. A., Teixeira, P. A., Loureiro, Y., Penha, C. V., et al. (2008). Passive immunization with monoclonal antibody against a 70-kDa putative adhesin of *Sporothrix schenckii* induces protection in murine sporotrichosis. *Eur. J. Immunol.* 38, 3080–3089. doi: 10.1002/eji.200838513

Pachl, J., Svoboda, P., Jacobs, F., Vandewoude, K., Van Der Hoven, B., and Spronk, P. (2006). A randomized, blinded, multicenter trial of lipid-associated amphotericin B alone versus in combination with an antibody-based inhibitor of heat shock protein 90 in patients with invasive candidiasis. *Clin. Infect. Dis.* 42, 1404–1413. doi: 10.1086/503428

Pearson, W. R. (2000). Flexible sequence similarity searching with the FASTA3 program package. *Methods Mol. Biol.* 132, 185–219.

Richards, J. O., Karki, S., Lazar, G. A., Chen, H., Dang, W., and Desjarlais, J. R. (2008). Optimization of antibody binding to FcgammaRIIa enhances macrophage phagocytosis of tumor cells. *Mol. Cancer Ther.* 7, 2517–2527. doi: 10.1158/1535-7163.MCT-08-0201

Rivera, J., Zaragoza, O., and Casadevall, A. (2005). Antibody-mediated protection against *Cryptococcus neoformans* pulmonary infection is dependent on B cells. *Infect. Immun.* 73, 1141–1150. doi: 10.1128/IAI.73.2.1141-1150.2005

Sambrook, J., and Russell, D. W. (2001). *Molecular Cloning: A Laboratory Manual*. Cold Spring Harbor, NY: Cold Spring Harbor Laboratory Press.

Schechtman, R. C. (2010). Sporotrichosis: part I. *Skinmed* 8, 216–220.

Silva, H. M., Vieira, P. M., Costa, P. L., Pimentel, B. M., Moro, A. M., Kalil, J., et al. (2009). Novel humanized anti-CD3 antibodies induce a predominantly immunoregulatory profile in human peripheral blood mononuclear cells. *Immunol. Lett.* 125, 129–136. doi: 10.1016/j.imlet.2009.06.009

Song, Y., Zhong, S. X., Yao, L., Cai, Q., Zhou, J. F., Liu, Y. Y., et al. (2011). Efficacy and safety of itraconazole pulses vs. continuous regimen in cutaneous sporotrichosis. *J. Eur. Acad. Dermatol. Venereol.* 25, 302–305. doi: 10.1111/j.1468-3083.2010.03785.x

Souriau, C., and Hudson, P. J. (2003). Recombinant antibodies for cancer diagnosis and therapy. *Expert Opin. Biol. Ther.* 3, 305–318. doi: 10.1517/14712598.3.2.305

Sousa, M. G., De Maria Pedrozo, E., Silva Azevedo, C., Nascimento, R. C., Ghosn, E. E., Santiago, K. L., et al. (2008). *Fonsecaea pedrosoi* infection induces differential modulation of costimulatory molecules and cytokines in monocytes from patients with severe and mild forms of chromoblastomycosis. *J. Leukoc. Biol.* 84, 864–870. doi: 10.1189/jlb.0308211

Vasquez-del-Mercado, E., Arenas, R., and Padilla-Desgarenes, C. (2012). Sporotrichosis. *Clin. Dermatol.* 30, 437–443. doi: 10.1016/j.clindermatol.2011.09.017

**Conflict of Interest Statement:** The authors declare that the research was conducted in the absence of any commercial or financial relationships that could be construed as a potential conflict of interest.

frontiers in Microbiology

ORIGINAL RESEARCH
published: 30 January 2017
doi: 10.3389/fmicb.2017.00076

# 1,10-Phenanthroline-5,6-Dione–Based Compounds Are Effective in Disturbing Crucial Physiological Events of *Phialophora verrucosa*

*Marcela Queiroz Granato[1], Diego de Souza Gonçalves[2,3], Sergio Henrique Seabra[4], Malachy McCann[5], Michael Devereux[6], André Luis Souza dos Santos[2,3] and Lucimar Ferreira Kneipp[1]**

[1] Laboratório de Taxonomia, Bioquímica e Bioprospecção de Fungos, Instituto Oswaldo Cruz, Fundação Oswaldo Cruz, Rio de Janeiro, Brazil, [2] Laboratório de Investigação de Peptidases, Departamento de Microbiologia Geral, Instituto de Microbiologia Paulo de Góes, Universidade Federal do Rio de Janeiro, Rio de Janeiro, Brazil, [3] Programa de Pós-Graduação em Bioquímica, Instituto de Química, Universidade Federal do Rio de Janeiro, Rio de Janeiro, Brazil, [4] Laboratório de Tecnologia em Cultura de Células, Centro Universitário Estadual da Zona Oeste (UEZO), Duque de Caxias, Brazil, [5] Chemistry Department, Maynooth University, National University of Ireland, Maynooth, Ireland, [6] Centre for Biomimetic and Therapeutic Research, Focas Research Institute, Dublin Institute of Technology, Dublin, Ireland

OPEN ACCESS

**Edited by:**
*Carlos Pelleschi Taborda, University of São Paulo, Brazil*

**Reviewed by:**
*Johanna Rivera, Albert Einstein College of Medicine, USA*
*Birinchi Kumar Sarma, Banaras Hindu University, India*

***Correspondence:**
*Lucimar F. Kneipp*
*lucimar@ioc.fiocruz.br*

**Specialty section:**
*This article was submitted to Fungi and Their Interactions, a section of the journal Frontiers in Microbiology*

**Received:** *17 October 2016*
**Accepted:** *11 January 2017*
**Published:** *30 January 2017*

**Citation:**
*Granato MQ, Gonçalves DdS, Seabra SH, McCann M, Devereux M, dos Santos ALS and Kneipp LF (2017) 1,10-Phenanthroline-5,6-Dione–Based Compounds Are Effective in Disturbing Crucial Physiological Events of Phialophora verrucosa. Front. Microbiol. 8:76. doi: 10.3389/fmicb.2017.00076*

*Phialophora verrucosa* is a dematiaceous fungus able to cause chromoblastomycosis, phaeohyphomycosis and mycetoma. All these fungal diseases are extremely difficult to treat and often refractory to the current therapeutic approaches. Therefore, there is an urgent necessity to develop new antifungal agents to combat these mycoses. In this context, the aim of the present work was to investigate the effect of 1,10-phenanthroline-5,6-dione (phendione) and its metal-based derivatives $[Ag(phendione)_2]ClO_4$ = ($[Ag(phendione)_2]^+$) and $[Cu(phendione)_3](ClO_4)_2.4H_2O$ = ($[Cu(phendione)_3]^{2+}$) on crucial physiological events of *P. verrucosa* conidial cells. Using the CLSI protocol, we have shown that phendione, $[Ag(phendione)_2]^+$ and $[Cu(phendione)_3]^{2+}$ were able to inhibit fungal proliferation, presenting MIC/$IC_{50}$ values of 12.0/7.0, 4.0/2.4, and 5.0/1.8 μM, respectively. $[Cu(phendione)_3]^{2+}$ had fungicidal action and when combined with amphotericin B, both at sub-MIC (½ × MIC) concentrations, significantly reduced (∼40%) the fungal growth. Cell morphology changes inflicted by phendione and its metal-based derivatives was corroborated by scanning electron microscopy, which revealed irreversible ultrastructural changes like surface invaginations, cell disruption and shrinkages. Furthermore, $[Cu(phendione)_3]^{2+}$ and $[Ag(phendione)_2]^+$ were able to inhibit metallopeptidase activity secreted by *P. verrucosa* conidia by approximately 85 and 40%, respectively. Ergosterol content was reduced (∼50%) after the treatment of *P. verrucosa* conidial cells with both phendione and $[Ag(phendione)_2]^+$. To different degrees, all of the test compounds were able to disturb the *P. verrucosa* conidia-into-mycelia transformation. Phendione and its $Ag^+$ and $Cu^{2+}$ complexes may represent a promising new group of antimicrobial agents effective at inhibiting *P. verrucosa* growth and morphogenesis.

**Keywords: *Phialophora verrucosa*, 1,10-phenanthroline-5,6-dione, metal-based drugs, antifungal activity, chromoblastomycosis**

## INTRODUCTION

*Phialophora verrucosa* is a melanized pathogenic fungus associated with a wide range of neglected diseases including phaeohyphomycosis, mycetoma, keratitis, endophthalmitis, osteomyelitis and endocarditis (Turiansky et al., 1995; Revankar and Sutton, 2010; Sun et al., 2010; Tong et al., 2013). However, this fungus is especially known to cause chromoblastomycosis (CBM), which is a chronic, progressive disease affecting the cutaneous and subcutaneous tissues (Torres-Guerrero et al., 2012; Krzyściak et al., 2014). Clinically, CBM is characterized by pseudoepitheliomatous hyperplasia with epidermal microabscesses and dermal granuloma. Chronic CBM lesions may undergo neoplastic transformation leading to skin cancer (Queiroz-Telles and Santos, 2012). This disease is most prevalent among individuals with outdoor occupations, such as farmers, gardeners and agricultural laborers. This risk group is usually exposed to soil, wood and rotting vegetation, which are the ubiquitous natural habitats of the fungal etiologic agents of CBM (Torres-Guerrero et al., 2012; Vicente et al., 2014). CBM usually occurs through trauma or skin penetration of fungal propagules in individuals lacking adequate protective footwear and clothing (Torres-Guerrero et al., 2012). This widespread mycosis is mostly common in tropical and subtropical regions of Africa, Asia, Australia and Latin America, with particular foci in Brazil, Madagascar, Mexico, Dominican Republic, Venezuela and India (Ameen, 2010; Krzyściak et al., 2014). Due to the chronic nature and the well-known multidrug-resistance profile, it is very difficult to treat patients with CBM using currently available therapies (Queiroz-Telles and Santos, 2012). Prolonged treatment and disease relapsed are huge concerns, and antifungal therapies especially for *Phialophora* infections have generally been disappointing (Gao et al., 2013). For these reasons, new antifungal agents should be studied in order to find out alternative therapeutic ways to treat CBM and other infections caused by *P. verrucosa*.

In the last years, metal-based drugs have been a subject of great interest due to their therapeutic values and pharmacological applications (Zhang and Lippard, 2003; Warra, 2011; Viganor et al., 2015). 1,10-Phenanthroline-5,6-dione (phendione) is a phenanthrene-based ligand and a derivative of the classical chelating agent 1,10-phenanthroline (Calderazzo et al., 2002; McCann et al., 2012a). Phendione has a structure similar to 1,10-phenanthroline with the addition of two carbonyl groups attached at positions 5 and 6. The bifunctional character of phendione made it an extremely versatile ligand, with special reactivity arising from its quinonoid and diiminic sites (Calderazzo et al., 2002; Calucci et al., 2006). The quinonoid functionality of phendione confers redox capability, whilst the juxtaposition is two *N* atoms make it ideally suited to chelating transition metal ions (Calderazzo et al., 2002; Calucci et al., 2006; McCann et al., 2012b). Phendione, both in its metal-free state and when coordinated to metal ions, is considered to have many interesting biological properties, such as anticancer and antimicrobial actions (McCann et al., 2004, 2012a; Deegan et al., 2006; Roy et al., 2008; Pivetta et al., 2014; Viganor et al., 2016). In recent years, researchers have synthesized several phendione-based compounds, including $[Ag(phendione)_2]ClO_4$ = $[Ag(phendione)_2]^+$ and $[Cu(phendione)_3](ClO_4)_2.4H_2O$ = $[Cu(phendione)_3]^{2+}$ (McCann et al., 2004), in an attempt to generate new complexes with improved antimicrobial activity and reduced toxicity to different cell lineages, *Galleria mellonella* larvae and mice (McCann et al., 2012a). $[Cu(phendione)_3]^{2+}$ was found to be active against the multi-resistant, filamentous fungus, *Scedosporium apiospermum*, while $[Ag(phendione)_2]^+$ exhibited better activity against the yeast, *Candida albicans* (McCann et al., 2012a). Moreover, $[Ag(phendione)_2]^+$ caused extensive and non-specific DNA cleavage, disrupted cell division and caused severe morphological alterations in *C. albicans* yeast cells (Eshwika et al., 2004; McCann et al., 2012a). Metal-free phendione exerts its antimicrobial effect in several ways, such as disturbing the microorganism's crucial metal metabolism as well as interfering in its metal ion acquisition and its bioavailability for essential reactions (e.g., inhibiting the activity of metalloproteins), affecting the microbial cell homeostasis and culminating in the blockage of primordial biological events (e.g., nutrition, proliferation, differentiation, adhesion, invasion, dissemination and infection) (Santos et al., 2012). Protease inhibition is also a prime cellular target of this class of ligand and its associated metal complexes (Kellett et al., 2013). In this context, the aim of the present work was to investigate the effect of phendione and its $Ag^+$ and $Cu^{2+}$ complexes on *P. verrucosa* proliferation, ultrastructure, metallopeptidase activity, sterol content and morphogenesis.

## MATERIALS AND METHODS

### Chemicals

All reagents used in electrophoresis and buffers components were purchased from Bio-Rad (Hercules, CA, USA) and Merck (Darmstaldt, Germany). Human serum albumin (HSA), 1,10-phenanthroline, resazurin, $AgClO_4$, $Cu(ClO_4)_2{\cdot}6H_2O$, dimethyl sulfoxide (DMSO), 3-(N-morpholino) propanesulfonic acid (MOPS), itraconazole (ITC), amphotericin B (AMB) ketoconazole (KTC), ergosterol, lanosterol, silica gel 60 plates, Czapek-Dox and Sabouraud-dextrose agar (SDA) components were obtained from Sigma-Aldrich Chemical Co (St Louis, MO, USA). Roswell Park Memorial Institute (RPMI) 1640 medium was purchased from Invitrogen (Camarillo, CA, USA). 1,10-Phenanthroline-5,6-dione (phendione), $[Cu(phendione)_3](ClO_4)_2{\cdot}4H_2O$ ($[Cu(phendione)_3]^{2+}$) and $[Ag(phendione)_2]ClO_4$ ($[Ag(phendione)_2]^+$) were prepared in accordance with published procedures (McCann et al., 2004).

### Microorganism and Growth Condition

*Phialophora verrucosa* (FMC.2214 strain) isolated from a human patient with CBM was grown on SDA medium. Fungal cells were cultivated for 7 days under constant agitation (130 rpm) at 26°C in 100 ml of Czapek-Dox, a chemically defined medium containing: 3 g sucrose; 0.3 g $NaNO_3$; 0.05 g $MgSO_4.7H_2O$; 0.05 g KCl; 0.1 g $KH_2PO_4$; 0.001 g $FeSO_4.7H_2O$, pH 5.5. Conidia were obtained after gauze filtration followed by centrifugation (4.000 × g/10

min). Then, conidia were washed three times in 0.85% NaCl and cell density estimated by counting in a Neubauer chamber (Granato et al., 2015). All the experiments with *P. verrucosa* were conducted under Biosafety Level 2 (BSL-2) conditions.

## Effects of Test Compounds on *P. verrucosa* Growth

Antifungal susceptibility testing was performed using the M38-A2 document for filamentous fungi as described by Clinical and Laboratory Standards Institute (CLSI, 2008) with some modifications (Granato et al., 2015). Briefly, the broth microdilution method was carried out using 96-well microtiter assay plates containing RPMI 1640 medium at pH 7.0 buffered with 0.16 M MOPS. All the test compounds were dissolved in DMSO and the maximum concentration of organic solvent was 2.0%. Serial dilution was made following CLSI guidelines in order to obtain final concentrations ranging from 0.01 to 20 mg/L of phendione and its derivatives, as well as the simple salts, $AgClO_4$ and $Cu(ClO_4)_2{\cdot}6H_2O$. The minimum inhibitory concentration (MIC) for each test compound was determined after 5 days of incubation by visual inspection and resazurin staining assay (Liu et al., 2007). The lowest concentration capable in inhibiting 100% of fungal growth was recorded as the MIC. ITC (0.01 to 100 mg/L) was used as reference antifungal drug. In addition, the minimum fungicidal concentration (MFC) was established before microtiter plate (MIC assay) spectrophotometric reading, in which the contents of the plate wells were homogenized and an aliquot from each well was transferred onto SDA drug-free plates. The plates were incubated at 30°C for 10 days and MFC was determined as the lowest concentration without visual fungal growth. A fungicidal effect was defined as the MFC value equal or up to four times the MIC value, as proposed by Pfaller et al. (2004). The $IC_{50}$ value, defined as the drug concentration (μM) able to cause a 50% reduction in fungal viability, was also calculated by using logarithmic regression after MIC determination, as detailed by Granato et al. (2015).

## Effects of Test Compounds on *P. verrucosa* Ultrastructure

The fungal ultrastructure was evaluated using scanning electron microscopy (SEM). Briefly, conidia ($5 \times 10^7$ cells) were incubated for 20 h at 26°C in the absence (control) or in the presence of phendione, $[Ag(phendione)_2]^+$ or $[Cu(phendione)_3]^{2+}$ at concentrations corresponding to MIC and 2 × MIC. Subsequently, the conidia were washed and fixed with 4% paraformaldehyde and 2.5% glutaraldehyde in 0.15 M sodium cacodylate buffer (pH 7.2) at 26°C for 2 h. Cells were washed and then post-fixed for 1 h at 26°C with 1% $OsO_4$ in the same buffer. Next, samples were dehydrated using a graded series of ethanol (50–100%), and dried by the critical point method. Finally, the samples were mounted on stubs, coated with gold and observed using a Jeol JSM 6490LV scanning electron microscope (Abi-chacra et al., 2013).

## Effects of Combinations of $[Cu(phendione)_3]^{2+}$ with Classical Antifungals on *P. verrucosa* Growth

All the test compounds were dissolved in DMSO. *P. verrucosa* conidia ($1 \times 10^3$/ml) were exposed to individual clinically used antifungal drugs [AMB (3.12 mg/L), KTC (1.56 mg/L) and ITC (0.78 mg/L) at concentration values corresponding to ½ × MIC of each drug] and also to $[Cu(phendione)_3]^{2+}$ (½ × MIC). In addition, combinations of separate samples of AMB, KTC and ITC with $[Cu(phendione)_3]^{2+}$ at these concentrations were also screened for 1 h at 26°C. After exposure, 0.1 ml of each system was plated onto solid Czapek-Dox medium without drugs and incubated for 5 days at 26°C. Fungal growth was estimated by counting colony-forming units (CFU) (Palmeira et al., 2008) and the results were compared to the untreated control.

## Effects of Test Compounds on the Metallopeptidase Activity of *P. verrucosa*

*P. verrucosa* conidial cells ($5 \times 10^9$) were resuspended in 0.2 ml of sterile phosphate-buffered saline (PBS, pH 7.2) supplemented with 2% glucose and incubated with constant agitation (130 rpm). After 2 h, conidia were removed by centrifugation (4000 × g/10 min) and the cell-free PBS-glucose supernatant was subjected to a peptidase activity assay as described by Granato et al. (2015). Briefly, 15 μl of cell-free PBS-glucose supernatant (10 μg of protein) and 1.5 μl HSA (1 mg/ml) were incubated for 20 h at 37°C in the absence (control) or in the presence of the classical metallopeptidase inhibitor, 1,10-phenanthroline (10 mM), and 8 × MIC of the test compounds, phendione, $[Ag(phendione)_2]^+$ and $[Cu(phendione)_3]^{2+}$. The reaction mixtures were then added to 15 μl sample buffer (125 mM Tris, pH 6.8, 4% SDS, 20% glycerol, 0.002% bromophenol blue and 10% β-mercaptoethanol), boiled at 100°C for 5 min, and subjected to sodium dodecyl sulfate-polyacrylamide gel electrophoresis (SDS-PAGE). Electrophoresis was carried out at 4°C, 120 V for 1.5 h. The degradation protein profiles were detected by silver staining (Granato et al., 2015). Densitometric quantification was performed using the free ImageJ software.

## Effects of Test Compounds on Sterol Content

Conidia ($1 \times 10^7$/ml) were incubated in Czapek-Dox medium in the absence (control) or in the presence of sub-inhibitory concentrations (½ × MIC and ¼ × MIC) of phendione, $[Ag(phendione)_2]^+$ or $[Cu(phendione)_3]^{2+}$. After 48 h, conidia were washed in PBS and total lipids were extracted with chloroform:methanol (2:1, 1:1 and 1:2). The combined extracts were mixed, dried and Folch partition was then performed (Folch et al., 1957). The lower phase containing the neutral lipids was recovered, evaporated and subjected to high performance thin layer chromatography (HPTLC). Chromatography was carried out on silica gel 60 plates, which were developed with a solvent system containing hexane:ether:acetic acid (60:30:1.5). The spots (violet-red color) were visualized after spraying the plate with

a reagent (comprising 50 mg iron chloride, 5 ml sulfuric acid, 5 ml acetic acid and 90 ml distilled water) and subsequent heating (Larsen et al., 2004). The sterol standards, ergosterol (4 μg) and lanosterol (1 μg) were used. Sterol quantitative determination was performed using ImageJ software.

## Effects of Test Compounds on *P. verrucosa* Morphogenesis

Conidia ($1 \times 10^6$/ml) were incubated at 26°C in the absence (control) or in the presence of sub-inhibitory concentrations (½ × MIC and ¼ × MIC) of phendione, $[Ag(phendione)_2]^+$ or $[Cu(phendione)_3]^{2+}$ in RPMI medium, pH 7.0 (without agitation), in order to induce the filamentation in *P. verrucosa*. The fungal cells were then observed using a Carl Zeiss MicroImaging GmbH optical microscope and images obtained every 24 h (Granato et al., 2015). Conidial viability after the treatment with the test compounds was performed using the resazurin assay (Liu et al., 2007).

## Statistical Analysis

All experiments were performed in triplicate in three independent experimental sets. The graphics and data were constructed and analyzed statistically by means of Student's *t*-test using GraphPad Prism 5.01 software. *P* values of 0.05 or less were assumed as significant.

# RESULTS AND DISCUSSION

## Anti-*P. verrucosa* Action of Phendione and Its Metal Complexes

The *in vitro* antifungal activities of phendione and its $Ag^+$ and $Cu^{2+}$ complexes were evaluated against *P. verrucosa*. All of the test compounds inhibited conidial cell growth with the following activity order based on the $IC_{50}$ values (μM): $[Cu(phendione)_3]^{2+} > [Ag(phendione)_2]^+ >$ phendione (**Figure 1**). Only $[Cu(phendione)_3]^{2+}$ showed a fungicidal effect. These data corroborate previously published results, which revealed that phendione-based metal complexes had higher antimicrobial activity than metal-free phendione toward different classes of microorganisms (McCann et al., 2012a; Viganor et al., 2016).

In order to confirm that the cytotoxic effect observed was due to the complexes, rather than the free $Ag^+$ and $Cu^{2+}$ ions, the antifungal activities of the simple perchlorate salts, $Cu(ClO_4)_2{\cdot}6H_2O$ and $AgClO_4$, were also assessed (**Figure 1**). While $AgClO_4$ showed moderate anti-*P. verrucosa* activity (MIC 24.0 μM), $Cu(ClO_4)_2{\cdot}6H_2O$ did not affect fungal growth, even at the maximum test concentration (MIC > 54.0 μM). The results showed that $Ag^+$ coordinated to phendione ($[Ag(phendione)_2]^+$) was about 6 times more effective (MIC 4.0 μM) than simple $AgClO_4$ (MIC 24.0 μM). Although, $Cu(ClO_4)_2{\cdot}6H_2O$ was essentially inactive (MFC > 54.0 μM),

**A**

| Compounds | MIC mg/L (μM) | $IC_{50}$ mg/L (μM) | MFC mg/L (μM) |
|---|---|---|---|
| Phendione | 2.5 (12.0) | 1.5 (7.0) | >20.0 (>96.0) |
| $[Ag(phendione)_2]^+$ | 2.5 (4.0) | 1.5 (2.4) | >20.0 (>32.0) |
| $[Cu(phendione)_3]^{2+}$ | 5.0 (5.0) | 1.7 (1.8) | 20.0* (20.0)* |
| $AgClO_4$ | 5.0 (24.0) | ND | ND |
| $Cu(ClO_4)_2{\cdot}6H_2O$ | >20.0 (>54.0) | ND | ND |

**B**

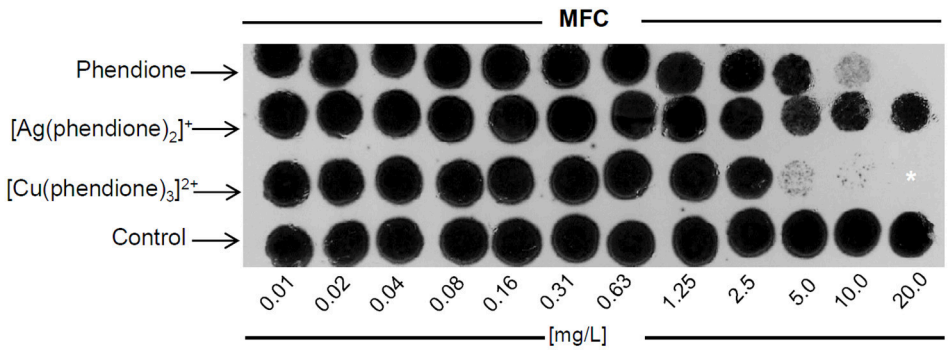


**FIGURE 1 | Effect of test compounds on *P. verrucosa* viability. (A)** Antifungal effects of phendione, $[Ag(phendione)_2]^+$, $[Cu(phendione)_3]^{2+}$ and the simple salts, $AgClO_4$ and $Cu(ClO_4)_2{\cdot}6H_2O$. **(B)** MFC representative images of phendione and its $Ag^+$ and $Cu^{2+}$ complexes on *P. verrucosa* growth. **(A,B)** Fungicidal effect was considered when the MFC value was either equal to or up to 4 × MIC value for a compound (Pfaller et al., 2004), which was indicated by asterisk (*). ND, Not determined.

$Cu^{2+}$ coordinated to phendione ($[Cu(phendione)_3]^{2+}$) was able to inhibit 100% *P. verrucosa* proliferation at 5.0 μM. It is believed that the phendione metal complexes have a higher lipophilicity than the simple metal salts (Viganor et al., 2016). This property is due to the total electron density reduction on the free ligand upon complexation to the metal ion, and also to the sharing of the positive charge of the metal cation with N-donor atoms of the phendione ligand, which promotes an electron delocalization all over the chelate ring (Raman et al., 2014; Viganor et al., 2016). Aqueous DMSO, which was used as the solvent for all of the test compounds, was inactive against *P. verrucosa* conidial proliferation (data not shown). Altogether, the present *P. verrucosa* growth inhibition results suggest that the activity of the metal complexes as a whole is superior to that of either the free metal ion or metal-free phendione ligand. $Ag^+$ ($d^{10}$ outer electron configuration) complexes have zero ligand field stabilization energy (LFSE) whilst octahedral $Cu^{2+}$ ($d^9$) has only a small amount of LFSE. As such, $Ag^+$ and $Cu^{2+}$ complexes are expected to be labile and the original chelating phendione ligands are expected to be rapidly exchanged for biological ligands present within the fungal cells and also in the growth medium (amino acids, proteins, ammonia, chloride etc.). It is thus likely that cell growth inhibition arises due to the destructive interference of cellular processes by the metal ion coupled with inactivation of other cell events by the phendione ligand. It also appears that it is the phendione ligand component of the administered metal complex that plays the dominant role in the demise of the conidia.

Our previous results described that *P. verrucosa* was also sensitive to 1,10-phenanthroline treatment, showing MIC equal to 4.4 μM (0.8 μg/ml) (Granato et al., 2015). Thus, the antifungal activity of 1,10-phenanthroline was superior to metal-free phendione, but similar to its $Ag^+$ and $Cu^{2+}$ complexes. However, neither 1,10-phenanthroline nor phendione presented fungicidal effect against *P. verrucosa* (Granato et al., 2015).

## Ultrastructural Alterations Induced by Phendione and Its Metal Derivatives

The effect of phendione, $[Ag(phendione)_2]^+$ and $[Cu(phendione)_3]^{2+}$ on *P. verrucosa* ultrastructure was probed using SEM. In contrast to control cells, which had typical spherical-to-oval morphology (**Figures 2A,B**), cells exposed

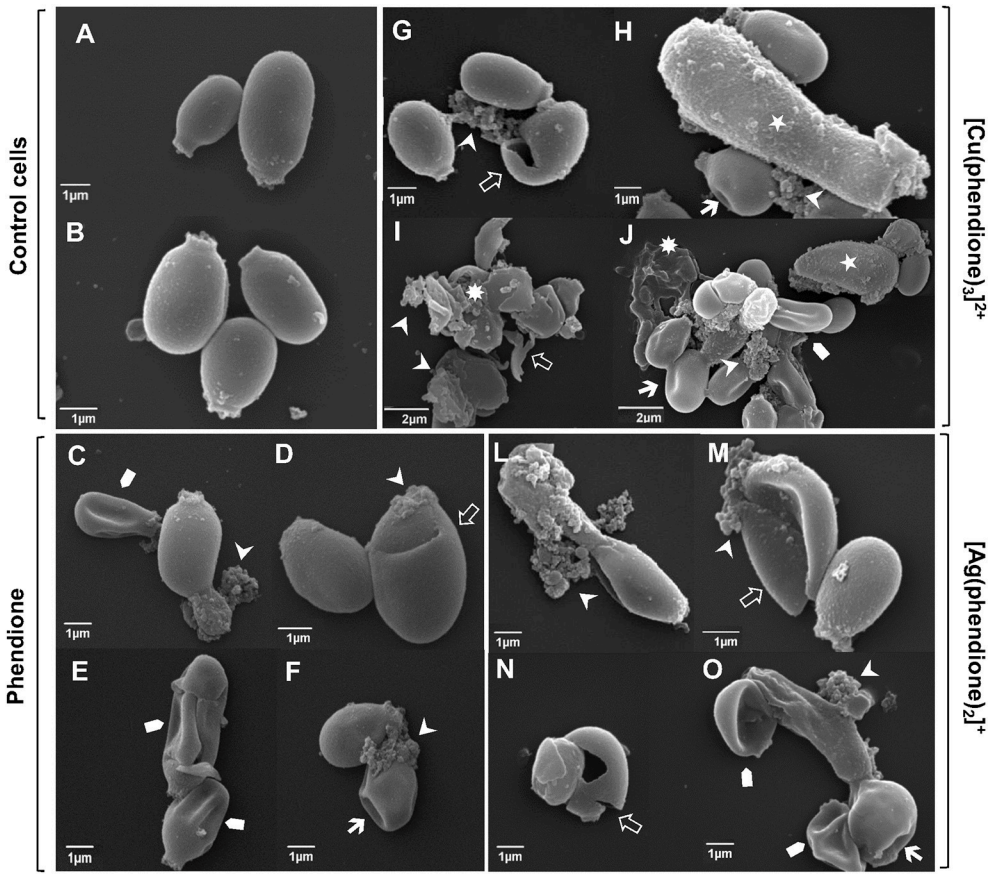


**FIGURE 2 | Effect of test compounds on *P. verrucosa* ultrastructure.** Representative SEM images showing untreated cells (control systems, **A,B**) and conidial cells treated with phendione **(C–F)**, $[Cu(phendione)_3]^{2+}$ **(G–J)** and $[Ag(phendione)_2]^+$ **(L–O)** at both MIC **(C,D,G,H,L,M)** and 2 × MIC **(E,F,I,J,N,O)**. In contrast to untreated conidial cells, treatment with the test compounds induced several ultrastructural alterations, including cell size increase (⋆), surface invaginations (➔), cell disruption (⇨), surface detachment (➤), cellular debris (✸) and cell shrinkage (➡).

to the test compounds exhibited several surface alterations, such as detachment of cell wall components, invaginations, cellular disruptions and shrinkages (**Figures 2C–O**), which are indicative of cell death. $[Cu(phendione)_3]^{2+}$ was the most aggressive in promoting changes on both conidial architecture and morphology, for example, inducing cell size increases when treated at the MIC concentration (**Figure 2H**) and cellular debris following incubation with 2 × MIC (**Figures 2I,J**).

Our previous study showed that 1,10-phenanthroline (25 μM) also caused irreversible ultrastructure alterations on *P. verrucosa* conidia, including cell wall detachment, intense intracellular vacuolization and reduction in the cytoplasm electron density (Granato et al., 2015). Similarly, phendione and $[Ag(phendione)_2]+$, both at 10 μg/ml, promoted changes in the internal structure of *C. albicans*, as observed by transmission electron microscopy (McCann et al., 2004). In that work, phendione promoted an increase in size as well as a reduction in the budding process of *C. albicans* yeast cells. Furthermore, *C. albicans* exhibited a diffuse cell wall, rupture of internal organelles and nucleus enlargement following treatment with phendione. *C. albicans* yeast cells treated with $[Ag(phendione)_2]^+$ had a distended cell wall, rupture of membranous organelles and, in some cases, a fragmented nucleus. Phendione and its $Ag^+$ complex were both able to cause a withdrawal of the cytoplasmic membrane from within the cell wall in *C. albicans* (McCann et al., 2004).

## Combination of $[Cu(phendione)_3]^{2+}$ with AMB Induces a Decrease in the Viability of *P. verrucosa*

In this set of experiments, the most potent test compound, $[Cu(phendione)_3]^{2+}$, was chosen to be combined with a selection of classical antifungal agents in an attempt to check their ability to control *P. verrucosa* growth. In this context, the combination of $[Cu(phendione)_3]^{2+}$ with AMB, both of which were deployed at (½ × MIC) concentrations, was able to significantly inhibit the fungal proliferation by around 40% (**Figure 3**). However, at the concentrations used, $[Cu(phendione)_3]^{2+}$ did not positively compliment the activities of either KTC or ITC, since *P. verrucosa* growth was not affected by these combinations (**Figure 3**).

Eshwika and coworkers [22] showed that pre-growth of *C. albicans* with sub-inhibitory concentrations (¼ × $MIC_{90}$) of $[Ag(phendione)_2]^+$ affected the subsequent susceptibility of this yeast to miconazole and AMB, reducing the concentrations of these clinical antifungal agents required to achieve $MIC_{90}$. Benefits of combination therapy are well-known and include broad spectrum efficacy, greater potency compared to monotherapy, improvements in both safety and tolerability as well as a reduction in the emergence of resistance (Cuenca-Estrella, 2004; Spitzer et al., 2016). Metal-based drugs can have modes of action distinct from classical antifungal agents, allowing their use in cases where there is resistance to conventional therapies. Furthermore, different mode(s) of action can be used by employing such metal-containing drugs in combination with existing antifungals in order to target two (or more) sites in the fungal cells. Thus, there is the potential of achieving the same therapeutic effect by reducing the concentration of clinical drugs used (Eshwika et al., 2004).

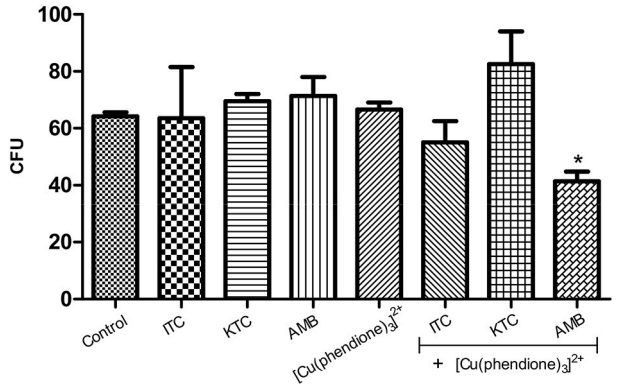


**FIGURE 3 | Effect of a combination of $[Cu(phendione)_3]^{2+}$ with classical antifungal agents on *P. verrucosa* development.** Conidia were untreated (control) or treated with a sub-inhibitory concentration (½ × MIC) of $[Cu(phendione)_3]^{2+}$ and classical antifungal drugs (AMB, ITC and KTC), alone or in combination. After 1 h, conidia were inoculated in a fresh solid Czapek-Dox medium to measure the CFU. Conidia treated only with DMSO (compound diluent) did not alter the cell growth. The values represent the mean ± standard deviation of three independent experiments performed in triplicate. Symbol (*) denotes the system that had a growth rate significantly different from the control ($P < 0.05$, Student's *t* test).

## Phendione-Based Compounds Modulate the Metallopeptidase Activity of *P. verrucosa*

$[Cu(phendione)_3]^{2+}$ and $[Ag(phendione)_2]^+$ were capable of inhibiting *P. verrucosa* extracellular metallopeptidase activity by around 85 and 40%, respectively (**Figure 4**). However, the metal-free ligand, phendione, did not affect this enzymatic activity (**Figure 4**). The presence of metallopeptidase in *P. verrucosa* PBS-glucose supernatant was confirmed by its inhibition by 10 mM of 1,10-phenanthroline (**Figure 4**).

Metal-chelating-type compounds may affect typical functions of several eukaryotic proteins, such as various metallo-type enzymes, including metallopeptidases (McCann et al., 2012b; Santos et al., 2012; Granato et al., 2015). In fact, the inhibition of metallopeptidases by 1,10-phenanthroline occurs mainly due to its ability of promoting $Zn^{2+}$ chelation, which is required for catalytic activity and which leaves an inactive apoenzyme (Santos et al., 2012). Our research group showed previously that $Zn^{2+}$ ions were able to stimulate the enzymatic activity of *P. verrucosa* extracellular peptidase in a typical dose-dependent manner, suggesting the presence of $Zn^{2+}$-metallopeptidase in this fungus (Granato et al., 2015). It is well-known that metallopeptidase inhibition can prevent fungal cells to obtain necessary peptides and amino acids for nutrition, leading to reduction or complete inhibition of cell growth (Santos et al., 2012).

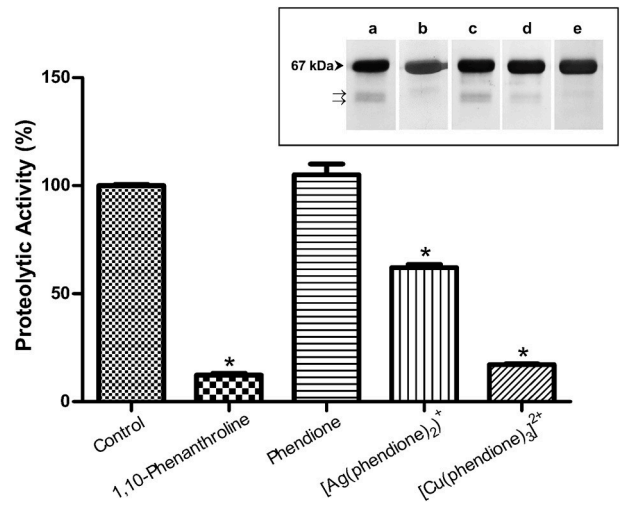


**FIGURE 4 | Effects of phendione and its derivatives on *P. verrucosa* metallopeptidase activity.** PBS-glucose supernatant was incubated at 37°C in 20 mM sodium acetate buffer, pH 3.0, and HSA in the absence (control) or in the presence of phendione and its metal complexes at concentrations corresponding to 8 × MIC value. After 20 h, the supernatant was subjected to the proteolytic activity assay, as detailed in Material and Methods. The graphic shows densitometric quantification of the bands observed in the SDS-PAGE (*inset*), which was performed using the software ImageJ. The HSA fragment of the control system was taken as 100%. Symbols (*) indicate the experimental systems considered statistically significant from the control ($P < 0.05$, Student's *t*-test). *Inset*: representative images of SDS-PAGE, in which *P. verrucosa* supernatant was treated with 1,10-phenantroline at 10 mM **(b)** and 8 × MIC of all other compounds, such as: phendione **(c)**, $[Ag(phendione)_2]^+$ **(d)** and $[Cu(phendione)_3]^{2+}$ **(e)**. Control system contained only HSA and PBS-glucose supernatant **(a)**. The number on the left represents the HSA molecular mass, expressed in kDa. The arrows (→) show fragmentation of the proteinaceous substrate after proteolysis.

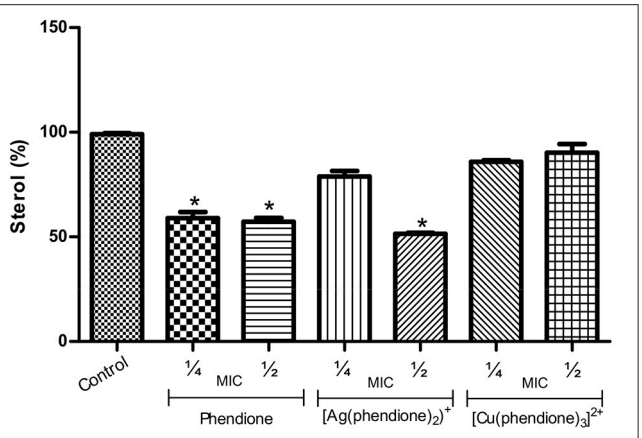


**FIGURE 5 | Effects of phendione and its metal complexes on *P. verrucosa* sterol content.** Conidia ($1 \times 10^7$ cells/ml) were either untreated (control) or treated for 48 h in the presence of sub-inhibitory concentrations (¼ × MIC and ½ × MIC) of each test compound. Afterwards, lipids were extracted, and neutral lipids were applied onto HPTLC plates. Graphics represent densitometric quantifications of results obtained by HPTLC using the software ImageJ. The sterol content of the control system was taken as 100%. Asterisk (*) denotes significant differences ($P < 0.05$, Student's *t* test) between treated systems and untreated cells (control).

## Phendione and Its Metal Complexes Inhibit Sterol Content of *P. verrucosa* Conidia

The treatment of conidial cells with phendione (¼ × MIC and ½ × MIC) and also with $[Ag(phendione)_2]^+$ (½ × MIC) promoted a reduction in ergosterol content by approximately 50% in relation to the control (untreated) cells (**Figure 5**). On the contrary, $[Cu(phendione)_3]^{2+}$ did not affect the sterol content of *P. verrucosa* (**Figure 5**).

Previous studies showed that sterol synthesis in *C. albicans* was also disturbed by phendione and its metal complexes (Eshwika et al., 2004). Interestingly, and in contrast to our results, $[Cu(phendione)_3]^{2+}$ diminished the ergosterol content in *C. albicans* yeast cells, while $[Ag(phendione)_2]^+$ enhanced the amount of this lipid level (Eshwika et al., 2004). It is well-known that sterol deficiency disturbs crucial cell membrane properties, leading to an increased fluidity and permeability, which may cause severe structural aberrations that contributes to cell death (Kathiravan et al., 2012).

## Phendione and Its Metal Complexes Affect Fungal Morphological Transition

The present studies demonstrated that all the test compounds were able to effectively block to a large extent the morphological transition (conidia-into-mycelial transformation) when compared to untreated fungal cells (**Figure 6**). It is important to notice that hyphal formation was mostly inhibited by phendione, followed by $[Ag(phendione)_2]^+$ and then by $[Cu(phendione)_3]^{2+}$ (**Figure 6**). In fact, several conidia (instead of hyphae form) were observed after the treatment with phendione and $[Ag(phendione)_2]^+$, both used at a sub-inhibitory concentration (¼ × MIC). It was also possible to observe some conidial cells in the $[Cu(phendione)_3]^{2+}$ system (¼ × MIC); however, the highest effect of this compound was its considerable ability to reduce hyphal branch growth (**Figure 6**).

Morphological transition is one of the strategies used by several fungi to survive in environment and in vertebrate hosts (Wang and Lin, 2012). In this context, several studies have shown that cell differentiation is an essential step in the establishment and success of fungal infection (Jacobsen et al., 2012; Wang and Lin, 2012). We have previously demonstrated that chelating compounds, such as 1,10-phenanthroline, were able to inhibit the conidia-into-hyphae transformation in *P. verrucosa* (Granato et al., 2015). Other studies also reported the same capacity of 1,10-phenanthroline to affect cell differentiation in *C. albicans*, *Pseudallescheria boydii*, and *Fonsecaea pedrosoi* (Santos et al., 2012). The mechanisms involved in the morphological transition of *P. verrucosa* have not been established. It is well-known that several factors are associated with fungal morphogenesis, including nutritional elements, temperature and aerobic conditions (Wang and Lin, 2012). Mendoza et al. (1993) showed that CBM fungi, including *P. verrucosa* produced large numbers of sclerotic bodies after inoculation into a defined pH 2.5 medium containing the metal ion $Ca^{2+}$ at 0.1 mM concentration. While higher concentrations of $Ca^{2+}$ (1 mM) reversed this pattern and promoted maintenance of *P. verrucosa* hyphal growth. Addition of the $Ca^{2+}$ chelator, ethylene glycol tetraacetic acid (EGTA, 8 mM) to the culture

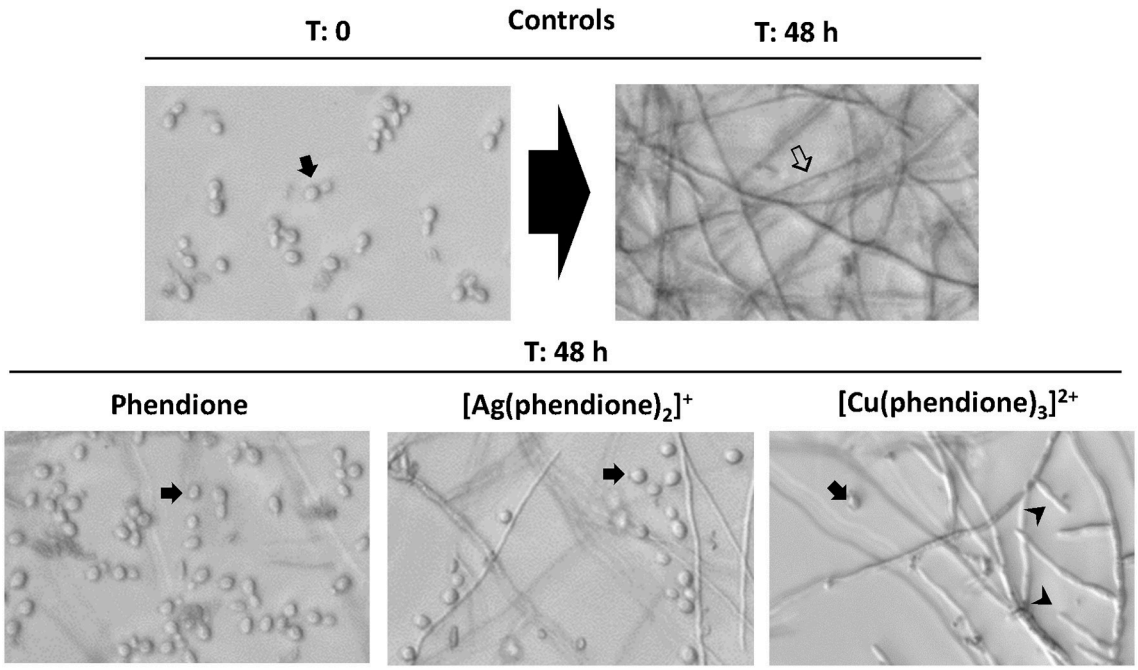


**FIGURE 6 | Effects of phendione and its metal complexes on *P. verrucosa* filamentation.** Conidia ($1 \times 10^6$ cells/ml) were grown in RPMI medium in either the absence (control) or the presence of sub-inhibitory concentration (¼ × MIC) of phendione, $[Ag(phendione)_2]^+$ and $[Cu(phendione)_3]^{2+}$. Conidia were observed before ($T = 0$: zero time) and after 48 h of incubation ($T = 48$ h) by optical microscopy, when the fungal filamentous form (⇨) was produced. The inhibition of *P. verrucosa* mycelial development by compounds was shown by conidia (➡) observation and hyphal branch (➤) growth reduction.

medium induced *P. verrucosa* sclerotic bodies, demonstrating the importance of metal ion $Ca^{2+}$ in this fungal essential process (Mendoza et al., 1993). In this context, these results revealed that metal ion chelating agents can modulate morphological transitions in CBM fungi.

## CONCLUSIONS

Metal-free phendione and its $Ag^+$ and $Cu^{2+}$ complexes are able to arrest the growth of *P. verrucosa*, especially $[Cu(phendione)_3]^{2+}$, which also presented a fungicidal action. In addition, these compounds blocked some vital fungal events, such as filamentation, as well as reducing both sterol production and the activity of metallo-type peptidase. Previous studies reported that metal-based drugs showed tolerable toxicity *in vivo*, confirming that they represent a novel group of antifungal agents. Moreover, these compounds could be used alone or in combination with classical antifungal agents, since *P. verrucosa* had its growth inhibited after the combined treatment with $[Cu(phendione)_3]^{2+}$ and AMB, as suggested in this study. In conclusion, our data point out that metallo-drugs have potential applications for the control and treatment of *P. verrucosa* infections.

## AUTHOR CONTRIBUTIONS

MG, MM, MD, AS, and LK conceived and designed the study. MG, DG, and SS performed the experiments. All authors analyzed the data. MM, MD, AS, and LK contributed reagents, materials and/or analysis tools. MG, MM, MD, AS, and LK wrote and revised the paper. All authors contributed to the research and approved the final version of the manuscript. All authors agree to be accountable for all aspects of the work.

## FUNDING

This study was supported by grants from the Brazilian agencies: Conselho Nacional de Desenvolvimento Científico e Tecnológico (CNPq), Fundação de Amparo à Pesquisa no Estado do Rio de Janeiro (FAPERJ), Coordenação de Aperfeiçoamento de Pessoal de Nível Superior (CAPES) and Fundação Oswaldo Cruz (FIOCRUZ).

## REFERENCES

Abi-chacra, É. A., Souza, L. O., Cruz, L. P., Braga-Silva, L. A., Gonçalves, D. S., Sodré, C. L., et al. (2013). Phenotypical properties associated with virulence from clinical isolates belonging to the *Candida parapsilosis* complex. *FEMS Yeast Res.* 13, 831–848. doi: 10.1111/1567-1364.12092

Ameen, M. (2010). Managing chromoblastomycosis. *Trop. Doct.* 40, 65–67. doi: 10.1258/td.2009.090264

Calderazzo, F., Pampaloni, G., and Passarelli, V. (2002). 1,10-phenanthroline-5,6-dione as a building block for the synthesis of homo- and heterometallic complexes. *Inorg. Chim. Acta* 330, 136–142. doi: 10.1016/S0020-1693(01)00711-3

Calucci, L., Pampaloni, G., Pinzino, C., and Prescimone, A. (2006). Transition metal derivatives of 1,10-phenanthroline-5,6-dione: controlled growth of coordination polynuclear derivatives. *Inorg. Chim. Acta* 359, 3911–3920. doi: 10.1016/j.ica.2006.04.040

CLSI (2008). *Clinical Laboratory Standards Institute. Reference Method for Broth Dilution Antifungal Susceptibility Testing of Filamentous Fungi, 2nd Edn*, Approved Standard M38-A2. Wayne, PA: CLSI.

Cuenca-Estrella, M. (2004). Combinations of antifungal agents in therapy–what value are they? *J. Antimicrob. Chemother.* 54, 854–869. doi: 10.1093/jac/dkh434

Deegan, C., Coyle, B., McCann, M., Devereux, M., and Egan, D. A. (2006). *In vitro* anti-tumour effect of 1,10-phenanthroline-5,6-dione (phendione), $[Cu(phendione)_3](ClO_4)_2.4H_2O$ and $[Ag(phendione)_2]ClO_4$ using human epithelial cell lines. *Chem. Biol. Interact.* 164, 115–125. doi: 10.1016/j.cbi.2006.08.025

Eshwika, A., Coyle, B., Devereux, M., McCann, M., and Kavanagh, K. (2004). Metal complexes of 1,10-phenanthroline-5,6-dione alter the susceptibility of the yeast *Candida albicans* to amphotericin B and miconazole. *Biometals* 17, 415–422. doi: 10.1023/B:BIOM.0000029438.97990.c6

Folch, A. J., Lees, M., and Stanley, G. H. S. (1957). A simple method for the isolation and purification of total lipids from animal tissues. *J. Biol. Chem.* 226, 497–509.

Gao, L. J., Yu, J., Wang, D. L., and Li, R. Y. (2013). Recalcitrant primary subcutaneous phaeohyphomycosis due to *Phialophora verrucosa*. *Mycopathologia* 175, 165–170. doi: 10.1007/s11046-012-9602-3

Granato, M. Q., Massapust, P. A., Rozental, S., Alviano, C. S., Santos, A. L. S., and Kneipp, L. F. (2015). 1,10-phenanthroline inhibits the metallopeptidase secreted by *Phialophora verrucosa* and modulates its growth, morphology and differentiation. *Mycopathologia* 179, 231–242. doi: 10.1007/s11046-014-9832-7

Jacobsen, I. D., Wilson, D., Wächtler, B., Brunke, S., Naglik, J. R., and Hube, B. (2012). *Candida albicans* dimorphism as a therapeutic target. *Expert Rev. Anti. Infect. Ther.* 10, 85–93. doi: 10.1586/eri.11.152

Kathiravan, M. K., Salake, A. B., Chothe, A. S., Dudhe, P. B., Watode, R. P., Mukta, M. S., et al. (2012). The biology and chemistry of antifungal agents: a review. *Bioorg. Med. Chem.* 20, 5678–5698. doi: 10.1016/j.bmc.2012.04.045

Kellett, A., Prisecaru, A., Slator, C., Molphy, Z., and McCann, M. (2013). Metal-based antimicrobial protease inhibitors. *Curr. Med. Chem.* 20, 3134–3151. doi: 10.2174/09298671311320250008

Krzyściak, P. M., Pindycka-Piaszczyńska, M., and Piaszczyński, M. (2014). Chromoblastomycosis. *Dermatol. Alergol.* 31, 310–321. doi: 10.5114/pdia.2014.40949

Larsen, T., Axelsen, J., and Ravn, H. W. (2004). Simplified and rapid method for extraction of ergosterol from natural samples and detection with quantitative and semi-quantitative methods using thin-layer chromatography. *J. Chromatogr. A.* 1026, 301–304. doi: 10.1016/j.chroma.2003.10.128

Liu, M., Seidel, V., Katerere, D. R., and Gray, A. I. (2007). Colorimetric broth microdilution method for the antifungal screening of plant extracts against yeasts. *Methods* 42, 325–329. doi: 10.1016/j.ymeth.2007.02.013

McCann, M., Coyle, B., Mckay, S., McCormack, P., Kavanagh, K., Devereux, M., et al. (2004). Synthesis and X-ray crystal structure of $[Ag(phendio)_2]ClO_4$(phendio = 1,10-phenanthroline-5,6-dione) and its effects on fungal and mammalian cells. *Biometals* 17, 635–645. doi: 10.1007/s10534-004-1229-5

McCann, M., Kellett, A. M., Kavanagh, K., Devereux, M., and Santos, A. L. (2012b). Deciphering the antimicrobial activity of phenanthroline chelators. *Curr. Med. Chem.* 19, 2703–2714. doi: 10.2174/092986712800609733

McCann, M., Santos, A. L. S., Silva, B. A., Romanos, M. T. V., Pyrrho, A. S., Devereux, M., et al. (2012a). *In vitro* and *in vivo* studies into the biological activities of 1,10-phenanthroline, 1,10-phenanthroline-5, 6-dione and its copper(II) and silver(I) complexes. *Toxicol. Res.* 1, 47–54. doi: 10.1039/c2tx00010e

Mendoza, L., Karuppayil, S. M., and Szaniszlo, P. J. (1993). Calcium regulates *in vitro* dimorphism in chromoblastomycotic fungi. *Mycoses* 36, 157–164. doi: 10.1111/j.1439-0507.1993.tb00744.x

Palmeira, V. F., Kneipp, L. F., Rozental, S., Alviano, C. S., and Santos, A. L. (2008). Beneficial effects of HIV peptidase inhibitors on *Fonsecaea pedrosoi*: promising compounds to arrest key fungal biological processes and virulence. *PLoS ONE* 3:e3382. doi: 10.1371/journal.pone.0003382

Pfaller, M. A., Sheehnan, D. J., and Rex, J. H. (2004). Determination of fungicidal activities against yeasts and molds: lessons learned from bactericidal testing and the need for standardization. *Clin. Microbiol.* 17, 268–280. doi: 10.1128/CMR.17.2.268-280.2004

Pivetta, T., Trudu, F., Valletta, E., Isaia, F., Castellano, C., Demartin, F., et al. (2014). Novel copper(II) complexes as new promising antitumour agents. A crystal structure of $[Cu(1,10\text{-phenanthroline-}5,6\text{-dione})_2(OH_2)(OClO_3)]ClO_4$. *J. Inorg. Biochem.* 141, 103–113. doi: 10.1016/j.jinorgbio.2014.08.011

Queiroz-Telles, F., and Santos, D. W. (2012). Chromoblastomycosis in the clinical practice. *Curr. Fungal Infect. Rep.* 6, 312–319. doi: 10.1007/s12281-012-0116-8

Raman, N., Mahalakshmi, R., and Mitu, L. (2014). Bio-sensitive activities of coordination compounds containing 1,10-phenanthroline as co-ligand: synthesis, structural elucidation and DNA binding properties of metal(II) complexes. *Spectrochim. Acta Mol. Biomol. Spectrosc.* 131, 355–364. doi: 10.1016/j.saa.2014.04.114

Revankar, S. G., and Sutton, D. A. (2010). Melanized fungi in human disease. *Clin. Microbiol. Rev.* 23, 884–928. doi: 10.1128/CMR.00019-10

Roy, S., Hagen, K. D., Maheswari, P. U., Lutz, M., Spek, A. L., Reedijk, J., et al. (2008). Phenanthroline derivatives with improved selectivity as DNA-targeting anticancer or antimicrobial drugs. *Chem. Med. Chem.* 3, 1427–1434. doi: 10.1002/cmdc.200800097

Santos, A. L., Sodré, C. L., Valle, R. S., Silva, B. A., Abi-chacra, E. A., Silva, L. V., et al. (2012). Antimicrobial action of chelating agents: repercussions on the microorganism development, virulence and pathogenesis. *Curr. Med. Chem.* 19, 2715–2737. doi: 10.2174/092986712800609788

Spitzer, M., Robbins, N., and Wright, G. D. (2016). Combinatorial strategies for combating invasive fungal infections. *Virulence* 7, 1–17. doi: 10.1080/21505594.2016.1196300

Sun, S., Yuan, G., Zhao, G., Chen, H., and Yu, B. (2010). Endophthalmitis caused by *Phialophora verrucosa* and *Streptococcus intermedius*: a case report. *Med. Mycol.* 48, 1108–1111. doi: 10.3109/13693786.2010.511283

Tong, Z., Chen, S. C., Chen, L., Dong, B., Li, R., Hu, Z., et al. (2013). Generalized subcutaneous phaeohyphomycosis caused by *Phialophora verrucosa*: report of a case and review of literature. *Mycopathologia* 175, 301–306. doi: 10.1007/s11046-013-9626-3

Torres-Guerrero, E., Isa-Isa, R., Isa, M., and Arenas, R. (2012). Chromoblastomycosis. *Clin. Dermatol.* 30, 403–408. doi: 10.1016/j.clindermatol.2011.09.011

Turiansky, G. W., Benson, P. M., Sperling, L. C., Sau, P., Salkin, I. F., McGinnis, M. R., et al. (1995). *Phialophora verrucosa*: a new cause of mycetoma. *J. Am. Acad. Dermatol.* 32, 311–315. doi: 10.1016/0190-9622(95)90393-3

Vicente, V. A., Najafzadeh, M. J., Sun, J., Gomes, R. R., Robl, D., Marques, S. G., et al. (2014). Environmental siblings of black agents of human chromoblastomycosis. *Fungal Divers.* 65, 47–63. doi: 10.1007/s13225-013-0246-5

Viganor, L., Galdino, A. C., Nunes, A. P., Santos, K. R., Branquinha, M. H., Devereux, M., et al. (2016). Anti-*Pseudomonas aeruginosa* activity of 1,10-phenanthroline-based drugs against both planktonic- and biofilm-growing cells. *J. Antimicrob. Chemother.* 71, 128–134. doi: 10.1093/jac/dkv292

Viganor, L., Skerry, C., McCann, M., and Devereux, M. (2015). Tuberculosis: an inorganic medicinal chemistry perspective. *Curr. Med. Chem.* 22, 2199–2224. doi: 10.2174/0929867322666150408112357

Wang, L., and Lin, X. (2012). Morphogenesis in fungal pathogenicity: shape, size, and surface. *PLoS Pathog.* 8:1003027. doi: 10.1371/journal.ppat.1003027

Warra, A. A. (2011). Transition metal complexes and their application in drugs and cosmetics - A Review. *J. Chem. Pharm. Res.* 3, 951–958.

Zhang, C. X., and Lippard, S. J. (2003). New metal complexes as potential therapeutics. *Curr. Opin. Chem. Biol.* 7, 481–489. doi: 10.1016/S1367-5931(03)00081-4

**Conflict of Interest Statement:** The authors declare that the research was conducted in the absence of any commercial or financial relationships that could be construed as a potential conflict of interest.

frontiers in Microbiology

ORIGINAL RESEARCH
published: 03 May 2017
doi: 10.3389/fmicb.2017.00771

# Antifungal Activity of the Biphosphinic Cyclopalladate C7a against *Candida albicans* Yeast Forms *In Vitro* and *In Vivo*

*Julian E. Muñoz[1,2†], Diego C. P. Rossi[1†], Kelly Ishida[1], Cristina C. Spadari[1], Marcia S. C. Melhem[3], Daniel M. Garcia[4], Antonio C. F. Caires[5‡], Carlos P. Taborda[1,6] and Elaine G. Rodrigues[7]**

[1] Department of Microbiology, Biomedical Sciences Institute, University of São Paulo, São Paulo, Brazil, [2] Faculty of Health Sciences, Colegio Mayor de Cundinamarca University, Bogotá, Colombia, [3] Parasitology Section, Technical Division of Medical Biology, Instituto Adolfo Lutz, São Paulo, Brazil, [4] Department of Pharmacology, Federal University of São Paulo, São Paulo, Brazil, [5] Interdisciplinary Center for Biochemical Investigation, University of Mogi das Cruzes, Mogi das Cruzes, Brazil, [6] Laboratory of Medical Mycology-LIM53/IMTSP, University of São Paulo, São Paulo, Brazil, [7] Department of Microbiology, Immunology and Parasitology, Paulista School of Medicine, Federal University of São Paulo (EPM-UNIFESP), São Paulo, Brazil

OPEN ACCESS

**Edited by:**
*Luis R. Martinez,*
*New York Institute of Technology, USA*

**Reviewed by:**
*Derek Thomas,*
*Grand Valley State University, USA*
*Ian A. Cleary,*
*Grand Valley State University, USA*

***Correspondence:**
*Elaine G. Rodrigues*
*rodrigues.elaine@unifesp.br*

*† These authors have contributed equally to this work.*

*‡ In memorian*

**Specialty section:**
*This article was submitted to Fungi and Their Interactions, a section of the journal Frontiers in Microbiology*

**Received:** *20 January 2017*
**Accepted:** *13 April 2017*
**Published:** *03 May 2017*

**Citation:**
*Muñoz JE, Rossi DCP, Ishida K, Spadari CC, Melhem MSC, Garcia DM, Caires ACF, Taborda CP and Rodrigues EG (2017) Antifungal Activity of the Biphosphinic Cyclopalladate C7a against Candida albicans Yeast Forms In Vitro and In Vivo. Front. Microbiol. 8:771. doi: 10.3389/fmicb.2017.00771*

Vulvovaginal and invasive candidiasis are frequent conditions in immunosuppressed individuals caused by *Candida albicans* and non-*albicans Candida* spp. Fluconazole and Amphotericin B are the main drugs used to fight the infection. However, resistance to fluconazole and other azole antifungal drugs is an important clinical problem that encourages the search for new therapeutic alternatives. In this work, we evaluate the antifungal activity of the biphosphinic cyclopalladate C7a in the *in vitro* and *in vivo* model. Our results showed fungicidal activity, with low values of minimal inhibitory concentrations and minimum fungicidal concentrations, even for fluconazole and/or miconazole resistant *Candida* isolates. Fluorescence microscopy and transmission electron microscopy revealed that the compound was able to inhibit the formation of hyphae/pseudohyphae and, moreover, promoted morphological alterations in cellular organelles and structures, such as disruption of cell wall, apparent mitochondrial swelling, chromatin marginalization into the nuclei and increased numbers of electron-lucent vacuoles. C7a significantly decreased the biofilm formation and reduced the viability of yeast cells in mature biofilms when tested against a virulent *C. albicans* strain. *In vivo* assays demonstrated a significant decrease of fungal burden in local (vaginal canal) and disseminated (kidneys) infection. In addition, we observed a significant increase in the survival of the systemically infected animals treated with C7a. Our results suggest C7a as a novel therapeutic agent for vaginal and disseminated candidiasis, and an alternative for conventional drug-resistant *Candida*.

**Keywords: *Candida* spp., clinical isolates, antifungal chemotherapy, cyclopalladated C7a, vaginal candidiasis, disseminated candidiasis, drug-resistant yeast**

## INTRODUCTION

Invasive candidiasis is a disease caused by the fungal genus *Candida*. It is a serious infection that can affect the blood, heart, brain, eyes, bones, and other tissues (Antinori et al., 2016). Moreover, it is the most common fungal disease among hospitalized, oncologic and immunosuppressed patients in the developed world (Antinori et al., 2016). The mortality among patients with invasive candidiasis is as high as 40%, even when patients receive treatment (Hassan et al., 2009). Mucosal infections are also very common, with vulvovaginal candidiasis (VVC) being the second most frequent gynecological condition after bacterial vaginosis (Anderson et al., 2004). VVC is a disease that significantly impacts the quality of life of affected women worldwide, particularly those with chronic and recurrent infections (Sobel, 2016).

Common therapies for invasive candidiasis and mucocutaneous infections, such as VVC, include treatment with polyenes (nystatin, amphotericin B and its lipid formulations), azoles (fluconazole and voriconazole) and echinocandins (caspofungin) (Pappas et al., 2016). Although the efficacy of currently used anticandidal drugs is satisfactory, there are reports of infections by multidrug-resistant *Candida albicans* (Pappas et al., 2016). Moreover, these antifungals have various drawbacks regarding their spectrum of activity, pharmacokinetic properties and host toxicity, suggesting that the discovery of new antifungal compounds is urgently needed (Campoy and Adrio, 2016).

Cancer chemotherapeutic agents based on transition metals, especially those of the platinum group, are effective against tumors, however, come with the cost of an extremely high toxicity to the patient (Harper et al., 2008). In the search for alternative drugs containing a transition metal of the same group but with reduced toxicity and a broader spectrum of activity for cancer treatment, palladium (II) complexes were found to be promising candidates *in vitro*. Due to their extremely high lability under physiological conditions, cyclopalladated compounds complexed with a biphosphinic group were synthetized. Given the increased stability of the complexes, the effective dose was able to be lowered, thereby significantly reducing the toxicity of the drug (reviewed in Caires, 2007). One of these complexes, the biphosphinic cyclopalladated C7a, $\{Pd_2\ [S_{(-)}C^2, N\text{-dmpa}]_2\ (\mu\text{-dppe})Cl_2\}$, showed strong activity *in vitro* and *in vivo* against murine melanoma, several human tumor cells (Rodrigues et al., 2003; Serrano et al., 2011) and in a patient-derived xenograft model of Adult T Cell Leukemia/Lymphoma (Guimaraes-Correa et al., 2011). Interestingly, low doses of C7a were also effective *in vitro* and *in vivo* against *Trypanosoma cruzi* (Matsuo et al., 2010) and the fungi *Paracoccidioides brasiliensis* and *Paracoccidioides lutzii* (Arruda et al., 2015). *In vitro*, C7a reduced colony forming units (CFU) of *Cryptococcus neoformans* and *Candida albicans* (Arruda et al., 2015).

In tumor cells, C7a induced apoptosis by dissipating the mitochondrial membrane potential, thereby activating effector caspases, causing chromatin condensation and DNA degradation (Rodrigues et al., 2003; Guimaraes-Correa et al., 2011; Serrano et al., 2011). In *Trypanosoma cruzi,* the compound evokes an apoptosis-like cell death through mitochondrial disruption (Matsuo et al., 2010). Likewise, in *Paracoccidioides lutzii* and *Paracoccidioides brasiliensis* isolates, C7a promotes apoptosis and autophagy-like cell death *in vitro* (Arruda et al., 2015).

In this study, we demonstrate that C7a is effective *in vitro* against several strains of *Candida*, including azoles resistant strains. Besides inhibiting the pseudohyphae/hyphae formation by *Candida* yeast cells, the compound induced morphological alterations suggestive of cell death. C7a also decreased the biofilm formation by *Candida albicans* and reduced the viability of yeast cells forming mature biofilms. Furthermore, C7a proved to be effective at controlling vaginal and systemic *Candida* infections in experimental models. It is therefore a novel and promising candidate for candidiasis treatment and an alternative compound for use in the treatment of the multi-drug resistant isolates.

## MATERIALS AND METHODS

### Microorganisms

The clinical isolates of fluconazole-susceptible and resistant *Candida* were obtained from Instituto Adolfo Lutz (São Paulo, Brazil): *Candida albicans* ($n = 14$), *Candida parapsilosis* ($n = 9$), *Candida tropicalis* ($n = 10$), *Candida glabrata* ($n = 10$), and *Candida krusei* ($n = 10$). Standard strains of *C. albicans* (SC5314, ATCC 10231 and ATCC 24433), *C. parapsilosis* (ATCC 22019), *C. tropicalis* (ATCC 200956 and ATCC 28707), *C. glabrata* (ATCC 2001) and *C. krusei* (ATCC 6258) were also included. All strains were maintained at −80°C. To perform the experiments, the fungi were subcultured in Sabouraud dextrose broth (Becton, Dickinson and Company; Sparks, NV, USA) at 37°C for 24 h at 150 rpm before each assay.

### Cyclopalladated Compound

The biphosphinic cyclopalladated complex C7a was synthesized from N,N-dimethyl-1-phenethylamide (dmpa) and complexed to 1,2 ethanebis (diphenylphosphine, dppe) ligand, as previously described (Rodrigues et al., 2003). The compound was diluted to a final concentration of 10 mM in DMSO (cell culture tested, Sigma–Aldrich, St. Louis, MO, USA), and for *in vitro* and *in vivo* assays, diluted to the final concentration in culture media or PBS, respectively. For use in the vaginal candidiasis model, C7a (2.5 and 5% w/w) was incorporated into a vaginal cream (10% wax self-nonionic emulsifier, 2% mineral oil, 5% propylene glycol and 84% distilled water, pH 4.5) and applied topically (Rossi et al., 2012).

### Standard Antifungal Agents

Three antifungal agents were used as references: amphotericin B (AMB; Sigma–Aldrich) diluted in DMSO to obtain the concentration of 1,600 μg/mL; miconazole (MCZ; Sigma–Aldrich) diluted in DMSO to obtain the concentration of 1,600 μg/mL; and fluconazole (FCZ; Pfizer, São Paulo, Brazil) diluted in sterile water to obtain the concentration of 2,560 μg/mL. The stock solutions were stored at −20°C. For *in vitro* and *in vivo* assays, antifungals were diluted to the final concentration in culture media or PBS, respectively. For use in

the vaginal candidiasis model, MCZ (2% w/w) was incorporated into the vaginal cream described above.

## Antifungal Susceptibility Assay on Planktonic Cells of *Candida*

The antifungal susceptibility of planktonic cells of *Candida* spp. clinical isolates and standard strains was assessed by broth microdilution assay as described in the protocols M27-A3 (Clinical, and Laboratory Standards Institute [CLSI], 2008) and M27-S4 (Clinical, and Laboratory Standards Institute [CLSI], 2012), according to the Clinical and Laboratory Standards Institute.

The $IC_{50}$ and $IC_{90}$ values were determined by spectrophotometric reading at 492 nm in a microtiter plate reader (Epoch, Biotek Instruments, USA). The minimum inhibitory concentration (MIC, Supplementary Table S1) was defined as the lowest concentration inhibiting 90% ($IC_{90}$, for polyene agents) and 50% ($IC_{50}$, for azole agents) of fungal growth (Clinical, and Laboratory Standards Institute [CLSI], 2008). For C7a compound, MIC values were defined as the $IC_{90}$. As fungal populations were higher than 10 strains, $MIC_{50}$ and $MIC_{90}$ could be determined and are defined as the concentrations that inhibit 50 and 90% of population, respectively (**Table 1**).

**TABLE 1 | Values of minimum inhibitory concentration (MIC, expressed in μg/ml) of the C7a, AMB and MCZ and FCZ determined in clinical isolates of *Candida* spp.**

| Strains | Antifungal drugs | Concentrations (μg/mL) | | |
|---|---|---|---|---|
| | | MIC Range | $MIC_{50}$ | $MIC_{90}$ |
| All species | **C7a** | 0.25–4 | 1 | 4 |
| | **AMB** | 0.125–16 | 1 | 1 |
| | **MCZ** | 0.03–>16 | 0.25 | 4 |
| | **FCZ** | 0.03–>64 | 1 | >64 |
| *Candida albicans* | **C7a** | 0.25–1 | 0.5 | 1 |
| | **AMB** | 0.5–1 | 1 | 1 |
| | **MCZ** | 0.03–4 | 0.03 | 0.5 |
| | **FCZ** | 0.03–>64 | 0.25 | 64 |
| *Candida tropicalis* | **C7a** | 0.5–2 | 1 | 2 |
| | **AMB** | 0.5–2 | 1 | 2 |
| | **MCZ** | 0.06–8 | 0.5 | 8 |
| | **FCZ** | 0.25–>64 | 1 | 64 |
| *Candida parapsilosis* | **C7a** | 1–4 | 2 | 4 |
| | **AMB** | 0.5–1 | 1 | 1 |
| | **MCZ** | 0.06–4 | 0.25 | 4 |
| | **FCZ** | 0.06–>64 | 1 | 16 |
| *Candida glabrata* | **C7a** | 0.25–4 | 1 | 2 |
| | **AMB** | 0.125–2 | 0.5 | 1 |
| | **MCZ** | 0.03–16 | 0.03 | 0.5 |
| | **FCZ** | 0.25–>64 | 2 | 8 |
| *Candida krusei* | **C7a** | 1 | 1 | 1 |
| | **AMB** | 0.5–1 | 0.5 | 1 |
| | **MCZ** | 2–8 | 4 | 8 |
| | **FCZ** | 64–>64 | 64 | >64 |

***All species,*** *represents the combination of all clinical isolates in this study.*

To evaluate the minimum fungicidal concentration (MFC), aliquots (10 μL) were taken from each well of the broth microdilution assay, plated in drug-free media (Sabouraud dextrose agar) and incubated at 37°C for 48 h. The MFC was defined as the lowest concentration that completely inhibited the formation of colonies. The cumulative percentage of isolates inhibited by C7a or AMB, the most effective compounds, for each dilution is presented in **Table 2**. For MIC and MFC determinations, each point was performed in triplicate. MIC and MFC results shown in Supplementary Table S1 represent the median value of 3 experiments executed.

## Fluorescence Microscopy

*Candida albicans* ATCC 10231 yeasts ($10^3$ CFU/mL) were treated with 0.5 μg/mL of C7a for 24 h at 37°C in RPMI 1640 media buffered with MOPS 0.16 M. After this period, C7a-treated and untreated cells were washed with PBS pH 7.2, fixed with 4% paraformaldehyde in PBS for 30 min, adhered to glass coverslips previously covered with poly-L-lysine and stained with Calcofluor-White 1 mg/mL (Sigma–Aldrich) for 5 min. The coverslips were washed and mounted in n-propyl gallate solution (1%) and observed under EVOS FL microscope (AMG, WA, EUA). For quantification, about 300 cells were counted in random fields in the untreated and C7a-treated groups. Result shows representative images of two independent experiments.

## Transmission Electron Microscopy

*Candida albicans* ATCC 10231 treated 24 h with 0.5 μg/mL C7a were fixed with 2.5% glutaraldehyde in 0.1 M cacodylate buffer (pH 7.2) for 2 h at room temperature. Post-fixation was carried out in 1% osmium tetroxide in cacodylate buffer containing 1.25% potassium ferrocyanide and 5 mM $CaCl_2$ for 2 h. Thereafter, the cells were dehydrated with increasing ethanol concentrations, 100% propylene and embedded in Spurr's resin. Ultrathin sections were stained with uranyl acetate and lead citrate, and observed in a transmission electron microscope (model Jeol 100CX, JEOL, Japan).

## Biofilm Minimal Inhibitory Concentration (BMICs)

The minimum concentration of C7a and AMB that inhibited the biofilm formation and preformed biofilm cell viability was verified as previously described (Pierce et al., 2008). To evaluate the effect of C7a and AMB in preventing the biofilm formation, 50 μL of each compound serially diluted in RPMI 1640 media (Sigma–Aldrich) buffered with 0.16 M MOPS pH 7.0, were added to plates containing 50 μL of *C. albicans* ATCC 10231 $2 \times 10^6$ CFU/mL in a 96-well plate. To evaluate the efficacy of the compounds against preformed biofilms, biofilms grown for 24 h were gently washed and 100 μL of serially diluted compounds was added. After the addition of C7a or AMB, the plates were sealed with parafilm and incubated at 37°C for 24 h. Plates were washed twice with PBS to remove non-adherent cells and the XTT viability test was performed to determine the metabolic activity of the biofilm. The positive control was the viability of untreated yeast cells and the negative

control was the absorbance of the medium alone. BMIC was defined as the first concentration of C7a that reduced the metabolism of yeast cells in the biofilm compared to the positive control. Results show one representative experiment out of three independent experiments executed, samples in quadruplicates.

## *In Vivo* Infections and Treatments

Isogenic BALB/c mice (6–8 weeks old females) were bred at the University of São Paulo, Brazil, in an animal facility under specific pathogen-free conditions. The procedures involving animals and their care were conducted according to the local ethics committee and international rules and all experiments were approved by the Institutional Animal Care and Use Committee of Institute of Biomedical Sciences (ICB), University of São Paulo (USP).

Disseminated candidiasis in immunocompetent animals was induced by intravenous inoculation (tail vein) of $3 \times 10^6$ *C. albicans* ATCC 10231 yeast cells suspended in 100 μL of PBS on day 0. Mice were treated intraperitoneally (i.p.) with PBS (control), C7a (0.3 mg/kg) or FCZ (20 mg/kg) every day for 7 days, starting on day 1. Animals were sacrificed 8 days after infection and kidneys were collected for fungal burden determination. Results show one representative experiment out of three independent experiments executed.

For disseminated candidiasis in immunosuppressed animals, two doses of 100 mg/kg cyclophosphamide (Sigma–Aldrich) were administered i.p. 4 days and 1 day before infection with *C. albicans*, then again on day 3 post infection and every 4 days thereafter (Rossi et al., 2012). The animals were kept in cages lined with wood shavings and closed with an autoclaved filter, and served autoclaved food and water in order to maintain a sterile environment. Cages were exchanged twice a week in laminar flow hoods. The animals were considered anergic when the number of blood leukocytes was found to be fewer than 100 cells/$mm^3$ (Andes et al., 2008). On day 0, animals were intravenously (i.v.) infected with $1 \times 10^4$ *C. albicans* ATCC 10231 yeast cells suspended in 100 μL of PBS. Mice were treated i.p. with PBS (control), C7a (0.3 mg/kg) or FCZ (20 mg/kg), every day for 7 days, starting on day 1. The survival of the animals was evaluated for 30 days after infection. Results show one representative experiment out of three independent experiments executed.

For vaginal candidiasis, the pseudo-oestrus phase was induced by subcutaneous administration of 0.5 mg of 17 beta-estradiol valerate (Sigma–Aldrich) dissolved in sesame oil (Sigma–Aldrich) 3 days before vaginal infection (Hamad et al., 2004). Mice were infected intravaginally with $3 \times 10^6$ *C. albicans* ATCC 10231 yeast cells suspended in 10 μL of PBS, on day 0. Topical treatment was performed with C7a and AMB incorporated in a vaginal cream, as described above, every day for 7 days, starting on day 1. The vaginas were collected on day 8 for fungal burden determination and histopathological analysis. Results show one representative experiment out of three independent experiments executed.

## Fungal Burden in Organs of Infected Mice

Mice were sacrificed 8 days after intravenous or vaginal infection and kidneys and vaginas, respectively, were removed and weighed. Tissues were individually homogenized by mechanical disruption in 1 mL of PBS and 100 μL of these suspensions were inoculated in plates containing brain-heart infusion (BHI) agar media. Colonies were counted visually after 24 h of incubation at 37°C.

## Histopathology

The vaginal canal was excised 8 days after infection, fixed in 10% buffered formalin, and embedded in paraffin for sectioning. Sections were stained with Periodic acid–Schiff (PAS) and examined microscopically at 100× magnification (Optiphot-2, Nikon, Tokyo, Japan).

**TABLE 2 | Cumulative percentage of the minimum fungicidal concentration (MFC) of C7a and AMB determined in clinical isolates of *Candida* spp.**

| | | Cumulative Percentage of MFC (%) | | | | | | | | |
|---|---|---|---|---|---|---|---|---|---|---|
| **MFC (μg/mL)** | | **0.12** | **0.25** | **0.5** | **1** | **2** | **4** | **8** | **16** | **>16** |
| All species | **C7a** | | 11.5 | 31.2 | 72.2 | 78.7 | 86.9 | 90.2 | 93.5 | 100 |
| | **AMB** | | | 13.1 | 67.1 | 83.5 | 86.8 | 86.8 | 86.8 | 100 |
| *C. albicans* | **C7a** | | 41.2 | 88.1 | 100 | | | | | |
| | **AMB** | | | 11.7 | 58.7 | 64.5 | 64.5 | 64.5 | 64.5 | 100 |
| *C. parapsilosis* | **C7a** | | | | 10 | 10 | 50 | 70 | 90 | 100 |
| | **AMB** | | | 10 | 40 | 90 | 100 | | | |
| *C. tropicalis* | **C7a** | | | 16.6 | 66.6 | 91.6 | 91.6 | 91.6 | 91.6 | 100 |
| | **AMB** | | | | 83.3 | 83.3 | 83.3 | 83.3 | 83.3 | 100 |
| *C. glabrata* | **C7a** | | | 18.1 | 81.7 | 81.7 | 90.7 | 90.7 | 90.7 | 100 |
| | **AMB** | | | 9 | 72.6 | 90.7 | 100 | | | |
| *C. krusei* | **C7a** | | | 0 | 81.8 | 90.8 | 90.8 | 90.8 | 90.8 | 100 |
| | **AMB** | | | 36.3 | 81.7 | 100 | | | | |

*Results represent the percentage of isolates showing total growth inhibition at each compound concentration.* ***All species,*** *represents the combination of all clinical isolates in this study.*

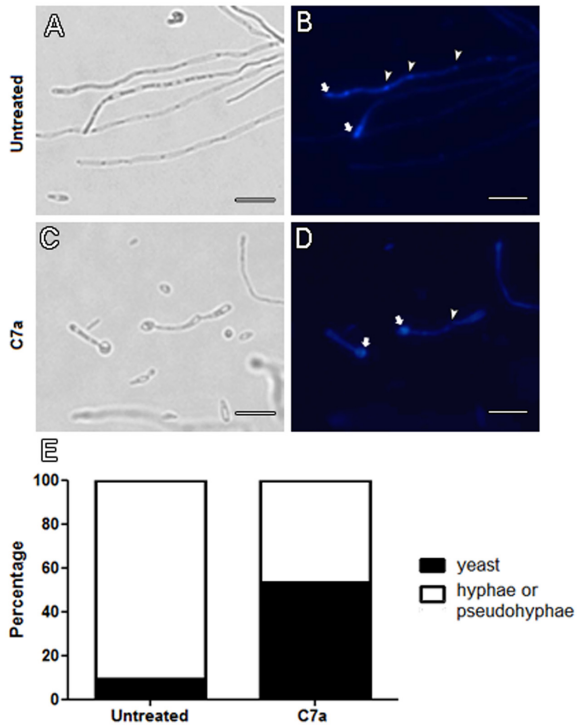


**FIGURE 1 | Hyphae/pseudohyphae formation is impaired in C7a-treated cells.** Yeast cells of *Candida albicans* ATCC 10231 were treated with 0.5 μg/mL of C7a for 24 h at 37°C in RPMI 1640 buffered with MOPS 0.16 M. Thereafter, untreated cells **(A,B)** and cells treated with C7a **(C,D)** were stained with Calcofluor White. Arrows in **(B,D)** show Calcofluor White staining at the end of hyphae and yeast-mother cell, respectively. Arrowheads in **(B)** show chitin-rich septa stained by Calcofluor White and in **(D)** absence of this structure. Yeasts and hyphae/psedohyphae were quantified as described in section "Material and Methods" **(E)**. Bars = 20 micrometers.

## Statistical Analysis

Statistical analyses were performed using GraphPad Prism version 6.0 (GraphPad Software, San Diego, CA, USA). Statistical comparisons were made by analysis of variance (one-way ANOVA) followed by a Tukey-Kramer post-test. *P*-values of $<0.05$ indicated statistical significance. Survival curves were analyzed by the Log-rank (Mantel–Cox) test and *p*-values of $\leq 0.05$ were used to indicate statistical significance. A 95% confidence interval was determined in all experiments.

# RESULTS

## Anticandidal Activity of Compound C7a *In Vitro*

Susceptibility of the clinical isolates and ATCC standard strains of *C. albicans*, *C. tropicalis*, *C. parapsilosis*, *C. glabrata,* and *C. krusei* to C7a *in vitro* is compiled in Supplementary Table S1 and **Tables 1**, **2**.

Supplementary Table S1 shows the MIC and MFC values for each isolate individually. Amongst clinical isolates and ATCC standard strains of all *Candida* species there are two multidrug-resistant strains (*C. tropicalis* ATCC 200956 and ATCC 28707) and one resistant isolate only to AMB (*C. glabrata* IAL-23); however, there are several isolates resistant to FCZ, including all *C. krusei* isolates (Supplementary Table S1).

Also of note is that FCZ- and MCZ-susceptible isolates (low MIC values) showed elevated MFC values for at least one of these drugs (>16 or >64), suggesting a fungistatic effect (Supplementary Table S1). Most of *Candida* strains were susceptible to low concentrations of C7a as well as AMB (MFC values are close to MIC values) suggesting a fungicidal action (Supplementary Table S1).

When all individual values of clinical isolates are grouped (*All species*, **Table 1**) and MIC values are evaluated, it is of notice that C7a and AMB showed a short MIC range, 0.25–4 μg/mL and 0.125–16 μg/mL, respectively. MCZ and FCZ showed a wider range of MIC values, 0.03–>16 μg/mL and 0.03−>64 μg/mL, respectively, suggesting that the susceptibility/resistance response of clinical isolates to these azole compounds are highly variable (*All species*, **Table 1**). Individual *Candida* species showed similar results (**Table 1**). The fungicidal effect of the most active compounds, C7a and AMB, is shown as the cumulative percentage of MFC in **Table 2**. Considering grouped values of clinical isolates (*all species*, **Table 2**), C7a was more efficacious than AMB at low concentrations (0.25 and 0.5 μg/mL), however, at higher concentrations both compounds demonstrated similar effect killing most of isolates (≥80%). It is important to note that C7a was more efficacious against *C. albicans* than AMB: at concentrations of 0.25 and 1 μg/mL C7a killed 41.2 and 100% of isolates, respectively, whereas AMB at the concentration of 0.5 μg/mL eliminated only 11.7% of isolates and 100% of isolates were killed only in concentrations higher than 16 μg/mL (**Table 2**). However, AMB was more efficacious against isolates of *C. parapsilosis* (**Table 2**). For the other *Candida* species, the two compounds showed similar fungicidal efficacy (**Table 2**). When MFC values of compounds were compared, there was no significant difference between C7a and AMB ($P = 0.8399$, Supplementary Table S1). Significant differences were found when C7a was compared to FCZ or MCZ ($P < 0.0001$, Supplementary Table S1).

## Morphological Alterations of *C. albicans* Treated with C7a

Treatment of *C. albicans* with 0.5 μg/mL C7a induced morphological modifications on yeast cells *in vitro*. Fluorescence microscopy with Calcofluor White of C7a-treated cells revealed that the compound was able to decrease (40%) the formation of hyphae/pseudohyphae compared to untreated cells (**Figure 1E**). This is supported by the observation of an intense staining of Calcofluor White in the yeast-mother cell in treated cultures (arrows, **Figure 1D**), while staining of untreated cells occurred at the end of hyphae corresponding to the cell apical growth region (arrows, **Figure 1B**). In addition, septa are formed in the untreated cells in contrast to the absence of septa in the C7a-treated cells (arrowheads in the **Figures 2B,D**,

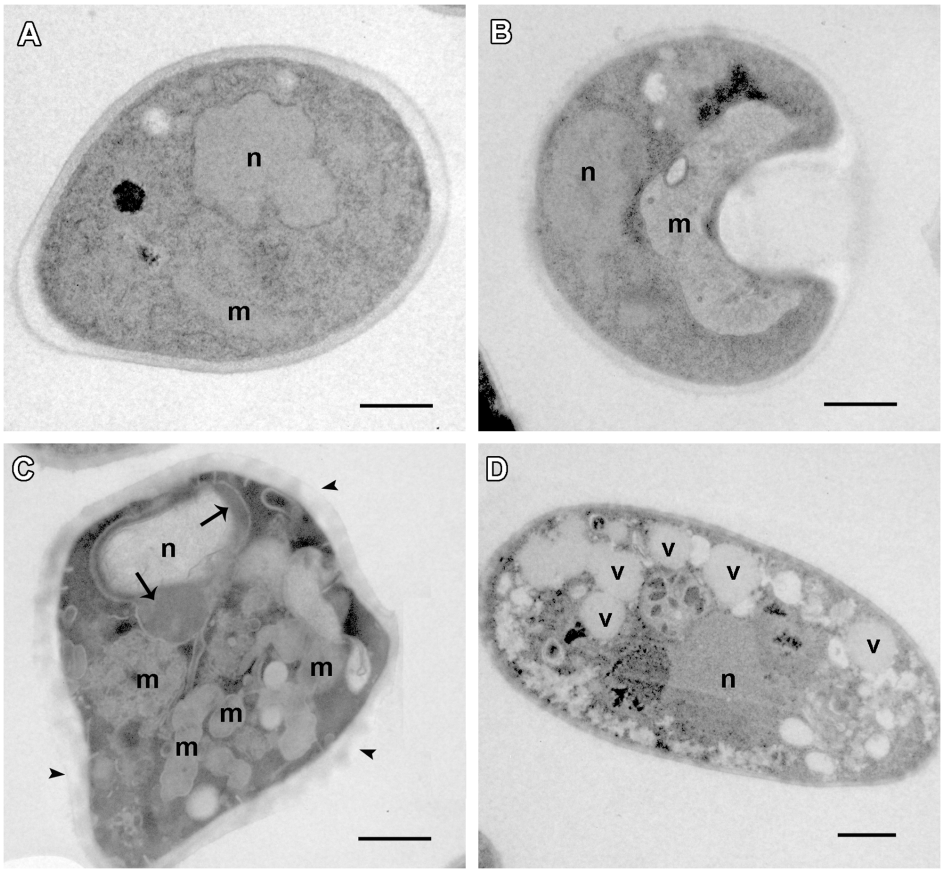


**FIGURE 2 | Morphological alterations were observed in C7a-treated cells.** Transmission electron microscopy of *Candida albicans* ATCC 10231 yeast cells untreated **(A)** and treated with 0.5 μg/ml of C7a **(B–D)** for 24 h at 37°C in RPMI 1640 buffered with MOPS 0.16 M. n, nucleus; m, mitochondria; v, vacuole. Bars = 1 micrometer. DNA marginalization is pointed with arrows and damage at cell wall with arrowheads in **(C).**

respectively). These results suggest that C7a affects the formation of hyphae/pseudohyphae by yeast cells in culture.

The morphological effects induced in *C. albicans* by the treatment with C7a were also evaluated using transmission electron microscopy which showed important alterations in some organelles and structures that may be potential targets for C7a. Untreated cells of *Candida albicans* ATCC 10231 presented a normal cell ultrastructure, such as compact and electron-dense cell wall, cytoplasmic membrane, homogeneous and electron-dense cytoplasm, nucleus and mitochondria (**Figure 2A**). Cells treated with 0.5 μg/mL of C7a for 24 h at 37°C exhibited a damaged cell wall (arrowheads in the **Figure 2C**). In addition, increased numbers of electron-lucent vacuoles (**Figure 2D**), DNA alterations as marginalization of genetic material in the nucleus (arrow in the **Figure 2C**) and apparent mitochondrial swelling were observed in C7a-treated cells (**Figures 2B,C**). Additional images are shown in **Supplementary Figure S1**.

## Effect of C7a on *C. albicans* Biofilm Formation and Mature Biofilms *In Vitro*

The BMIC, minimum concentration of C7a that significantly reduced the metabolism of yeasts in a mature biofilm (**Figure 3A**) and reduced the biofilm formation (**Figure 3B**), was 1 μg/mL. Although effective, C7a was less effective than AMB which interfered with the mature biofilm and biofilm formation of *C. albicans* ATCC 10231 yeast cells in concentrations 8 and 4 times lower, respectively.

## Evaluation of the Antifungal Activity of C7a *In Vivo*

Previously immunosuppressed female BALB/c mice were injected in the tail vein with $1 \times 10^4$ *Candida albicans* ATCC 10231 yeast cells, and were treated i.p. with 0.3 mg/kg of C7a or 20 mg/kg of FCZ every 24 h for 7 days. On day 8, the fungal load of treated and untreated animals was evaluated by quantifying the CFUs from recovered kidneys. The treatment with C7a or FCZ showed a significant reduction ($P < 0.05$) in the fungal burden when compared with untreated mice (**Figure 4**). Although a dose 66 folder high of FCZ was used (Rossi et al., 2012) the fungal burden reduction induced by both compounds was similar (**Figure 4**).

The effect of C7a treatment on survival of immunosuppressed animals infected systemically with *Candida albicans* was assessed.

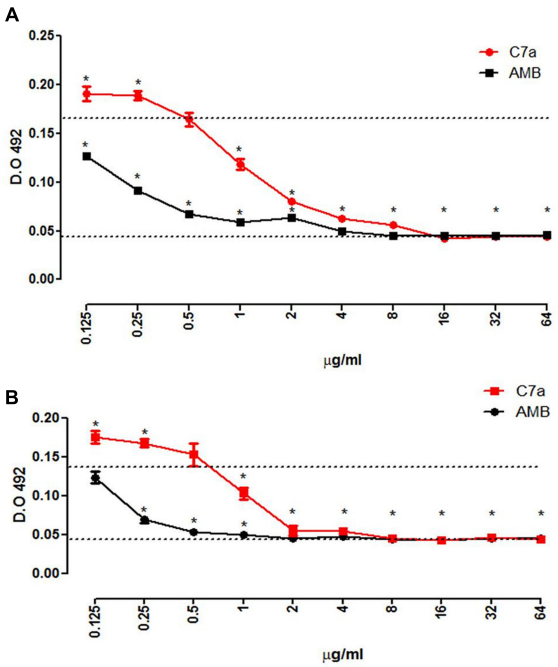


**FIGURE 3 | C7a affects the maturation process and the mature biofilm.** Effect of C7a or AMB in the mature biofilm **(A)** and in the maturation of the biofilm **(B)** of *C. albicans* ATCC 10231 was determined by XTT reduction assay. Upper dotted line represents the untreated positive control, and the lower dotted line represents the negative control. Mean and standard deviation of each point is shown. *$P < 0.05$, determined by analysis of *t*-test two-tailed compared to the positive control.

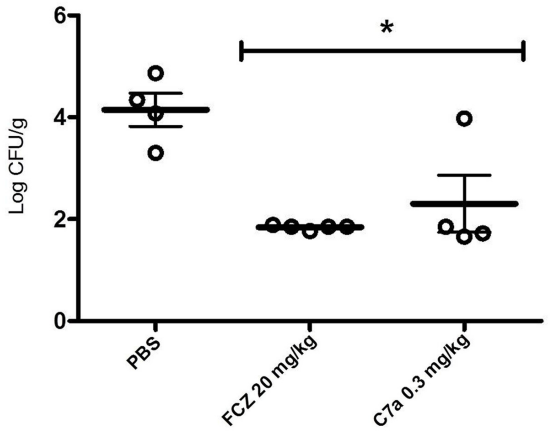


**FIGURE 4 | Cyclopalladated C7a treatment of disseminated candidiasis.** The disseminated candidiasis was induced by intravenous injection of $3 \times 10^6$ *C. albicans* ATCC 10231 yeasts in female BALB/c mice. Intraperitoneal treatment was carried out every 24 h for 7 days after infection, and animals were inoculated with PBS, 0.3 mg/kg of C7a, or 20 mg/kg of FCZ. Treatment was evaluated by determination of the number of colony forming units (CFU) per gram of tissue of the kidneys, 8 days after infection. Animals are represented individually, and 1 representative experiment out of 3 is showed. *Indicates statistical significance (ANOVA with post-Tukey test, $P < 0.05$) compared to PBS-inoculated group.

The group of infected animals treated with PBS reached 100% mortality 21 days post infection. Treatment of infected animals with 0.3 mg/kg of C7a produced a survival rate of 78% and treatment with 20 mg/kg of FCZ produced a survival rate of 100% within 30 days post infection (**Figure 5**).

Treatment of vaginal candidiasis with a topical cream containing 5% (but not 2.5%) of C7a or 2% of MCZ led to a significant ($P < 0.05$) decrease in vaginal CFU when compared to untreated mice (**Figure 6**). Histopathological analyses of vaginal canal tissue samples collected from BALB/c mice

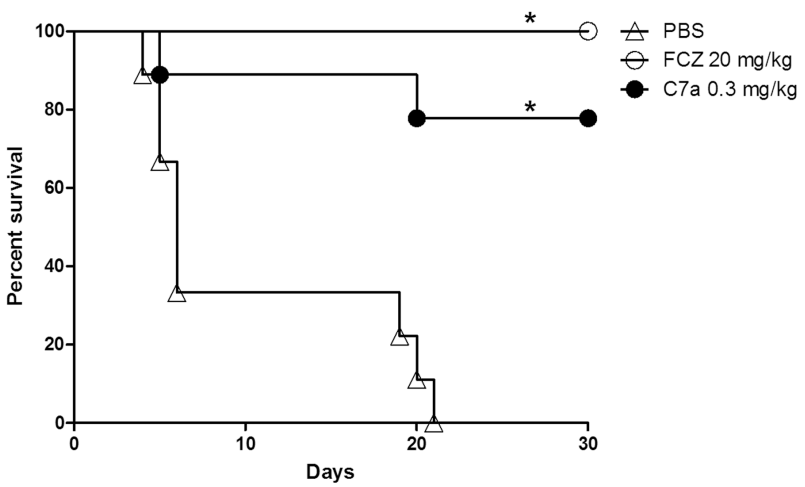


**FIGURE 5 | Survival of immunosuppressed mice with disseminated candidiasis treated with C7a or FCZ.** Previously immunosuppressed animals were intravenously infected with $10^4$ yeasts of *C. albicans* ATCC 10231. The animals ($n = 10$/group) were intraperitoneally treated with PBS, 0.3 mg/kg of C7a or 20 mg/kg of FCZ every 24 h for 7 days. Animal survival was observed for 30 days after infection. *Indicates statistical significance compared to PBS-inoculated group (Long-rank test, $P < 0.05$). One representative experiment out of 3 is showed.

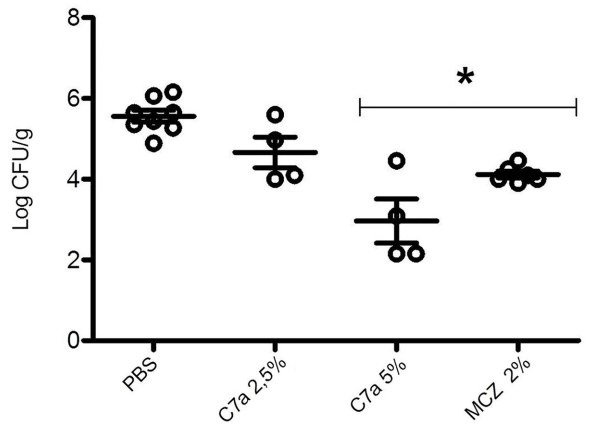


**FIGURE 6 | Cyclopalladated C7a treatment of vaginal candidiasis.** The vaginal candidiasis was induced by local inoculation of $3 \times 10^6$ *C. albicans* ATCC 10231 yeasts suspended in 10 μL of PBS in BALB/c mice. Animals were treated every 24 h for 7 days with a vaginal cream containing PBS, 2.5% or 5% of C7a, or 2% of MCZ. Treatment was evaluated by determination of the number of colony forming units (CFU) per gram of tissue of the vaginas, 8 days after infection. Animals are represented individually, and 1 representative experiment out of 3 is showed. *Indicates statistical significance (ANOVA with post-Tukey test, $P < 0.05$) compared to PBS-inoculated group.

in which vaginal candidiasis was induced but not treated showed an established infection by *Candida albicans,* with several yeasts and the formation of pseudohyphae/hyphae (**Figure 7A**). A clear reduction in the vaginal fungal burden was observed in the group of animals treated with the topical cream containing MCZ 2% (**Figure 7B**). Mice submitted to treatment with a topical cream containing 5% of C7a also showed a robust decrease in the vaginal fungal burden when compared to the untreated group (**Figure 7C**).

## DISCUSSION

In the present study, we evaluated the antifungal activity of the biphosphinic cyclopalladated compound C7a against *Candida* spp. *in vitro* and *in vivo*. C7a was tested *in vitro* against 56 clinical and ATCC standard isolates of *C. albicans*, *C. tropicalis*, *C. parapsilosis*, *C. krusei,* and *C. glabrata* (susceptible- and resistant-azoles strains) and *in vivo* against the systemic and vaginal experimental infections induced by *C. albicans.*

We observed that C7a has an antifungal effect on different strains of *Candida* spp., even on those that are FCZ resistant. The MIC range of C7a on clinical isolates was of 0.25–4.0 μg/mL for *C. tropicalis*, *C. glabrata*, *C. krusei*, *C. parapsilosis,* and *C. albicans*, and similar MIC range was obtained with AMB, with no statistical difference between them ($p = 0.056$) (**Table 1**). MIC values obtained with MCZ and FCZ were broader, suggesting variability on the isolates' response to these antifungals (**Table 1**). Although there was not a statistical difference between MIC values of C7a and MCZ ($p = 0.9383$), the difference between FCZ and C7a MIC values was significant, demonstrating that C7a was more efficacious, mainly against FCZ-resistant isolates. Previous work has also demonstrated the efficacy of C7a against *P. brasiliensis* and *P. lutzii* isolates *in vitro* at low concentrations ($IC_{50}$ from 0.04 to 0.43 μg/mL and $IC_{90}$ from 0.1 to 0.76 μg/mL) (Arruda et al., 2015).

The fungicidal activity of C7a and AMB, the most efficacious compounds against these isolates, was evaluated. On **Table 2**, we observed that the activity of both compounds on *C. tropicalis*, *C. glabrata,* and *C. krusei* was similar ($p = 0.8399$); however, while C7a was much more efficacious against clinical isolates of *C. albicans*, AMB showed stronger activity on *C. parapsilosis* clinical isolates.

The ability of *C. albicans* to infect diverse host niches is supported by a wide range of virulence factors and fitness attributes, as the morphological transition between yeast and filamentous forms, the expression of adhesins and invasins on the cell surface, the formation of biofilms, the secretion of hydrolytic enzymes, metabolic flexibility, amongst others (Mayer et al., 2013).

We evaluated the effect of C7a on the production of hyphae/pseudohyphae by *C. albicans*. Through calcofluor white staining, we observed that C7a decreased the *in vitro* formation of hyphae and pseudohyphae of *C. albicans* by 40% (**Figure 1E**). Microscopic analysis showed that the untreated control group presented an intense staining by calcofluor white on the hyphae tips, meaning that these regions are rich in chitin and are in growing phase (Gil et al., 1990). On the other hand, calcofluor white staining was present only in the mother yeast cell and not in the hyphae tips in the C7a-treated group. Moreover, yeast cells synthesize a chitin-rich septum during cell division (Cabib, 2004), and this structure was not observed in C7a-treated *C. albicans* (**Figure 1D**). This indicates that the compound inhibited the formation of hyphae and/or pseudohyphae, and even when these structures were formed they were not actively growing (**Figures 1A–D**).

Another important virulence factor of *Candida* species is biofilm formation which can confer resistance to some antifungal drugs such as FCZ (Mukherjee et al., 2003). To evaluate the effect of C7a on this virulence factor of *C. albicans*, we used a dual approach by employing two stages of biofilm development in order to correlate the effect of C7a on the initial and mature biofilm phases compared to AMB. We demonstrated that C7a inhibited the formation of the biofilm within 24 h at a BMIC of 1 μg/mL. The same concentration reduced the viability of *C. albicans* yeast cells already established in a mature biofilm (**Figure 3**). These results indicate that C7a is efficacious against *C. albicans* planktonic cells, inhibiting the biofilm formation, as well as against biofilm organisms, which present increased resistance to antifungals compared to their planktonic counterpart.

Cellular and molecular alterations have been shown after C7a-treatment of tumor cells and microorganisms. In C7a-treated *P. brasiliensis* yeast cells, the induction of

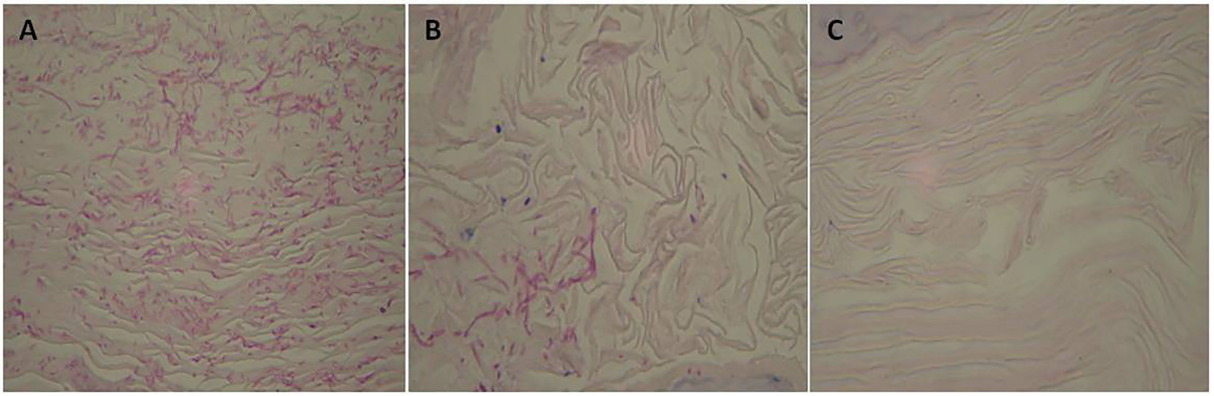


**FIGURE 7 | Histological sections of vaginal canal from BALB/c female mice infected intravaginally with 3 × $10^5$ *C. albicans* ATCC 10231 yeast cells and treated with a topical cream containing MCZ (2%) or C7a (5%).** Animals were treated every 24 h for 7 days, vaginal canals were removed after 8 days of infection. **(A)** control group, infected animals and treated with vehicle alone, **(B)** mice infected and treated with MCZ, **(C)** mice infected and treated with C7a. PAS staining of the tissue sections and 100× magnification. Representative images of 10 animals per group.

chromatin condensation, DNA degradation, superoxide anion production and increased metacaspase activity were observed, as well as increased autophagic vacuole numbers and acidification, suggestive of apoptosis and autophagy, respectively (Arruda et al., 2015). Alterations like mitochondrial swelling, formation of abnormal membrane structures and atypical vacuoles were also observed in the trypomastigote form of *T. cruzi* parasites when treated with C7a (Matsuo et al., 2010). C7a-treated tumor cells showed similar alterations, as well as dissipation of the mitochondrial membrane potential, leading to Bax translocation, increased cytosolic calcium concentration, decreased ATP levels, activation of effector caspases, chromatin condensation and DNA degradation (Serrano et al., 2011).

TEM results showed that C7a induces morphological changes in *C. albicans* cells, similar to that observed previously in other microorganisms and tumor cells. Using 0.5 μg/mL of C7a, we observed a damage to the cell wall, mitochondrial apparent swelling, DNA alterations such as chromatin marginalization inside the nucleus, and a significant increase of electro-lucent vacuoles (**Figure 2** and **Supplementary Figure S1**).

Animals intravenously infected with *C. albicans* (ATCC 10231) yeast cells and intraperitoneally treated with C7a (0.3 mg/kg) showed a significant increase in survival compared to control animals (78% survival 30 days after infection vs. 0% survival 21 days after infection, respectively; **Figure 5**). C7a also significantly reduced the fungal burden in kidneys of systemically infected animals (**Figure 4**). When compared to FCZ, no statistical difference was observed for fungal burden and survival of the systemic candidiasis.

C7a was also efficacious in an experimental model of vaginal candidiasis and topical treatment with a vaginal cream, showing a significant decrease in colony forming units when compared with vehicle treatment (control group) (**Figure 6**). Histopathological analysis of infected tissue confirmed the therapeutic effect of C7a, leading to fungal elimination in the vaginal canal (**Figure 7**). When compared to MCZ, there was not statistical difference between this drug and C7a for treatment of vaginal candidiasis.

In addition, C7a has demonstrated low toxicity *in vivo*. Arruda et al. (2015) described that the compound was not toxic to animals when 600 μg/kg was administered i.p. sequentially for 5 days, with no morphological alterations in the kidney, liver, heart, lung, or spleen tissue. Moreover, Rodrigues et al. (2003) described a dose-escalating experiment, where mice showed no histological alterations in liver, lungs, kidney, heart, and spleen, after being inoculated three times per week with increasing doses of C7a, starting at 5 and ending at 60 μM.

In summary, the biphosphinic cyclopalladated C7a can be an alternative to treat candidiasis by *Candida* species, including *Candida* non-*albicans* and azoles-resistant isolates, mainly due to the low MIC values, fungicidal effect and low toxicity. The C7a mechanism of action on *Candida* spp. cell death remains to be completely determined, however, C7a is able to cause important morphological alterations, mainly inhibiting hyphae/pseudohyphae and biofilms. Thus, C7a can be a promising antifungal candidate for the treatment of fungal infections associated to the biofilms, such as systemic and vaginal candidiasis.

## AUTHOR CONTRIBUTIONS

JM and DR designed and performed experiments, analyzed data and wrote the manuscript. KI and MM designed and supervised experiments, analyzed data. CS performed experiments, analyzed data. DG synthesized and purified compound C7a. AC designed and supervised synthesis of C7a. CT designed and supervised experiments, analyzed data. ER conceived the study, participated in its design and coordination, wrote the manuscript.

## ACKNOWLEDGMENTS

This work was supported by CAPES 88881.062125/2014-01, FAPESP 2013/18655-3, 2012/08760-1 and CNPq. We are grateful to Dulcinéia de Matos Castro, curator of the Mycology Collection in the Adolfo Lutz Institute. We also thank Amy K. Poupore, ScM at W. Harry Feinstone Department of Molecular Microbiology and Immunology, Bloomberg School of Public Health, Johns Hopkins University, Baltimore, Maryland, USA, for reviewing the manuscript.

## SUPPLEMENTARY MATERIAL

The Supplementary Material for this article can be found online at: http://journal.frontiersin.org/article/10.3389/fmicb.2017.00771/full#supplementary-material

**FIGURE S1 | Additional images showing morphological alterations in C7a-treated cells.** Transmission electron microscopy of *Candida albicans* ATCC 10231 yeast cells untreated **(A–C)** and treated with 0.5 μg/ml of C7a **(D–F)** for 24 h at 37°C in RPMI 1640 buffered with MOPS 0.16 M. n, nucleus; m, mitochondria; v, vacuole. Arrowheads, damage at cell wall. Bars = 1 micrometers.

## REFERENCES

Anderson, M. R., Klink, K., and Cohrssen, A. (2004). Evaluation of vaginal complaints. *JAMA* 291, 1368–1379. doi: 10.1001/jama.291.11.1368

Andes, D., Diekema, D. J., Pfaller, M. A., Prince, R. A., Marchillo, K., Ashbeck, J., et al. (2008). *In vivo* pharmacodynamic characterization of anidulafungin in a neutropenic murine candidiasis model. *Antimicrob. Agents Chemother.* 52, 539–550. doi: 10.1128/AAC.01061-07

Antinori, S., Milazzo, L., Sollima, S., Galli, M., and Corbellino, M. (2016). Candidemia and invasive candidiasis in adults: a narrative review. *Eur. J. Intern. Med.* 34, 21–28. doi: 10.1016/j.ejim.2016.06.029

Arruda, D. C., Matsuo, A. L., Silva, L. S., Real, F., Leitão, N. P., Pires, J. H. S., et al. (2015). Cyclopalladated compound 7a induces apoptosis-and autophagy-like mechanisms in *Paracoccidioides* and is a candidate for paracoccidioidomycosis treatment. *Antimicrob. Agents Chemother.* 59, 7214–7223. doi: 10.1128/AAC.00512-15

Cabib, E. (2004). The septation apparatus, a chitin-requiring machine in budding yeast. *Arch. Biochem. Biophys.* 426, 201–207. doi: 10.1016/j.abb.2004.02.030

Caires, A. C. F. (2007). Recent advances involving palladium (II) complexes for the cancer therapy. *Anticancer Agents Med. Chem.* 7, 484–491. doi: 10.2174/187152007781668661

Campoy, S., and Adrio, J. L. (2016). Antifungals. *Biochem. Pharmacol.* doi: 10.1016/j.bcp.2016.11.019 [Epub ahead of print].

Clinical, and Laboratory Standards Institute [CLSI] (2008). *Reference Method for Broth Dilution Antifungal Susceptibility Testing of Yeasts. Approved Standard CLSI Document M27-A3*. Wayne, PA: Clinical and Laboratory Standards Institute.

Clinical, and Laboratory Standards Institute [CLSI] (2012). *Reference Method for Broth Dilution Antifungal Susceptibility Testing of Yeasts: Fourth Informational Supplement M27-S4*. Wayne, PA: Clinical and Laboratory Standards Institute.

Gil, C., Pomes, R., and Nombela, C. (1990). Isolation and characterization of *Candida albicans* morphological mutants derepressed for the formation of filamentous hypha-type structures. *J. Bacteriol.* 172, 2384–2391. doi: 10.1128/jb.172.5.2384-2391.1990

Guimaraes-Correa, A. B., Crawford, L. B., Figueiredo, C. R., Gimenes, K. P., Pinto, L. A., Grassi, M. F. R., et al. (2011). C7a, a biphosphinic cyclopalladated compound, efficiently controls the development of a patient-derived xenograft model of adult T cell leukemia/lymphoma. *Viruses* 3, 1041–1058. doi: 10.3390/v3071041

Hamad, M., Abu-Elteen, K. H., and Ghaleb, M. (2004). Estrogen-dependent induction of persistent vaginal candidosis in naïve mice. *Mycoses* 47, 304–309. doi: 10.1111/j.1439-0507.2004.00994.x

Harper, B. W., Krause-Heuer, A. M., Grant, M. P., Manohar, M., Garbutcheon-Singh, K. B., and Aldrich-Wright, J. R. (2008). Advances in platinum chemotherapeutics. *Chemistry* 16, 7064–7077. doi: 10.1002/chem.201000148

Hassan, I., Powell, G., Sidhu, M., Hart, W. M., and Denning, D. W. (2009). Excess mortality, length of stay and cost attributable to candidaemia. *J. Infect.* 59, 360–365. doi: 10.1016/j.jinf.2009.08.020

Matsuo, A. L., Silva, L. S., Torrecilhas, A. C., Pascoalino, B. S., Ramos, T. C., Rodrigues, E. G., et al. (2010). *In vitro* and *in vivo* trypanocidal effects of the cyclopalladated compound 7a, a drug candidate for treatment of Chagas' disease. *Antimicrob. Agents Chemother.* 54, 3318–3325. doi: 10.1128/AAC.00323-10

Mayer, F. L., Wilson, D., and Hube, B. (2013). *Candida albicans* pathogenicity mechanisms. *Virulence* 4, 119–128. doi: 10.4161/viru.22913

Mukherjee, P. K., Chandra, J., Kuhn, D. M., and Ghannoum, M. A. (2003). Mechanism of fluconazole resistance in *Candida albicans* biofilms: phase-specific role of efflux pumps and membrane sterols. *Infect. Immun.* 71, 4333–4340. doi: 10.1128/IAI.71.8.4333-4340.2003

Pappas, P. G., Kauffman, C. A., Andes, D. R., Clancy, C. J., Marr, K. A., Ostrosky-Zeichner, L., et al. (2016). Clinical practice guideline for the management of candidiasis: 2016 update by the infectious diseases society of America. *Clin. Infect. Dis.* 62, e1–e50. doi: 10.1093/cid/civ933

Pierce, C. G., Uppuluri, P., Tristan, A. R., Wormley, F. L., Mowat, E., Ramage, G., et al. (2008). A simple and reproducible 96-well plate-based method for the formation of fungal biofilms and its application to antifungal susceptibility testing. *Nat. Protoc.* 3, 1494–1500. doi: 10.1038/nport.2008.141

Rodrigues, E. G., Silva, L. S., Fausto, D. M., Hayashi, M. S., Dreher, S., Santos, E. L., et al. (2003). Cyclopalladated compounds as chemotherapeutic agents: antitumor activity against a murine melanoma cell line. *Int. J. Cancer* 107, 498–504. doi: 10.1002/ijc.11434

Rossi, D. C., Muñoz, J. E., Carvalho, D. D., Belmonte, R., Faintuch, B., Borelli, P., et al. (2012). Therapeutic use of a cationic antimicrobial peptide from the spider *Acanthoscurria gomesiana* in the control of experimental candidiasis. *BMC Microbiol.* 12:28. doi: 10.1186/1471-2180-12-28

Serrano, F. A., Matsuo, A. L., Monteforte, P. T., Bechara, A., Smaili, S. S., Santana, D. P., et al. (2011). A cyclopalladated complex interacts with mitochondrial membrane thiol-groups and induces the apoptotic intrinsic pathway in murine and cisplatin-resistant human tumor cells. *BMC Cancer* 11:296. doi: 10.1186/1471-2407-11-296

Sobel, J. D. (2016). Recurrent vulvovaginal candidiasis. *Am. J. Obstet. Gynecol.* 214, 15–21. doi: 10.1016/j.ajog.2015.06.067

**Conflict of Interest Statement:** The authors declare that the research was conducted in the absence of any commercial or financial relationships that could be construed as a potential conflict of interest.

frontiers in Microbiology

REVIEW
published: 23 January 2017
doi: 10.3389/fmicb.2017.00036

# Antifungal Therapy: New Advances in the Understanding and Treatment of Mycosis

*Liliana Scorzoni, Ana C. A. de Paula e Silva, Caroline M. Marcos, Patrícia A. Assato, Wanessa C. M. A. de Melo, Haroldo C. de Oliveira, Caroline B. Costa-Orlandi, Maria J. S. Mendes-Giannini and Ana M. Fusco-Almeida**

*Laboratório de Micologia Clínica, Departamento de Análises Clínicas, Universidade Estadual Paulista (UNESP), Faculdade de Ciências Farmacêuticas, Araraquara, Brasil*

The high rates of morbidity and mortality caused by fungal infections are associated with the current limited antifungal arsenal and the high toxicity of the compounds. Additionally, identifying novel drug targets is challenging because there are many similarities between fungal and human cells. The most common antifungal targets include fungal RNA synthesis and cell wall and membrane components, though new antifungal targets are being investigated. Nonetheless, fungi have developed resistance mechanisms, such as overexpression of efflux pump proteins and biofilm formation, emphasizing the importance of understanding these mechanisms. To address these problems, different approaches to preventing and treating fungal diseases are described in this review, with a focus on the resistance mechanisms of fungi, with the goal of developing efficient strategies to overcoming and preventing resistance as well as new advances in antifungal therapy. Due to the limited antifungal arsenal, researchers have sought to improve treatment via different approaches, and the synergistic effect obtained by the combination of antifungals contributes to reducing toxicity and could be an alternative for treatment. Another important issue is the development of new formulations for antifungal agents, and interest in nanoparticles as new types of carriers of antifungal drugs has increased. In addition, modifications to the chemical structures of traditional antifungals have improved their activity and pharmacokinetic parameters. Moreover, a different approach to preventing and treating fungal diseases is immunotherapy, which involves different mechanisms, such as vaccines, activation of the immune response and inducing the production of host antimicrobial molecules. Finally, the use of a mini-host has been encouraging for *in vivo* testing because these animal models demonstrate a good correlation with the mammalian model; they also increase the speediness of as well as facilitate the preliminary testing of new antifungal agents. In general, many years are required from discovery of a new antifungal to clinical use. However, the development of new antifungal strategies will reduce the therapeutic time and/or increase the quality of life of patients.

**Keywords: antifungal drugs, antifungal resistance, biofilms, fungal vaccine, new antifungal therapy, alternative animal models, nanoparticles**

OPEN ACCESS

***Edited by:***
*Carlos Pelleschi Taborda, University of São Paulo, Brazil*

***Reviewed by:***
*Susana Frases, Federal University of Rio de Janeiro, Brazil*
*Praveen Rao Juvvadi, Duke University, USA*

****Correspondence:***
*Ana M. Fusco-Almeida*
*ana.marisa@uol.com.br*

***Specialty section:***
*This article was submitted to Fungi and Their Interactions, a section of the journal Frontiers in Microbiology*

***Received:*** *11 November 2016*
***Accepted:*** *06 January 2017*
***Published:*** *23 January 2017*

***Citation:***
*Scorzoni L, de Paula e Silva ACA, Marcos CM, Assato PA, de Melo WCMA, de Oliveira HC, Costa-Orlandi CB, Mendes-Giannini MJS and Fusco-Almeida AM (2017) Antifungal Therapy: New Advances in the Understanding and Treatment of Mycosis. Front. Microbiol. 8:36. doi: 10.3389/fmicb.2017.00036*

## INTRODUCTION

When compared with antibacterial research, little progress has been made in the development of new antifungal agents, which has been justified by the low occurrence of fungal infections. However, the current increase in incidence of fungal infections has led to aggressive research on new antifungal agents as evidenced by the rise in the number of publications since the 1960s (Maertens, 2004; Ngo et al., 2016). Another reason for the slow development of antifungal agents is the fact that fungi are eukaryotic, with a close evolutionary relationship with human hosts, which complicates the search for antifungal targets. Nonetheless, detailed knowledge regarding the structure, composition and biochemistry of fungal cells, in addition to various facets of fungal infections, has contributed to our understanding about the mechanism of action of many antifungal agents (Borgers, 1980; Kanafani and Perfect, 2008). Typically a long period of 8 to 10 years is required for an antifungal to be approved for clinical use. Reducing toxicity, enhancing bioavailability, improving the antifungal spectrum and combating resistance are efforts that are expected to increase the efficacy of the available antifungals. Indeed, elucidation of the mode of action of a potential antifungal compound can shorten the time from lead to candidate drug. Small antifungal molecules from natural products could represent structural templates for structure-activity relationship studies, thus providing more information to optimize potential new antifungal agents (Sheng and Zhang, 2011). Overall, new strategies regarding antifungal therapy, target identification and rational drug design technologies can significantly accelerate the process of new antifungal development, reducing the time to cure or providing better quality of life to patients.

## ANTIFUNGAL MECHANISM OF ACTION: OLD AND NEW TARGETS OF ANTIFUNGAL CANDIDATES

Although the commercially available antifungal agents to date have targets that are restricted to the plasma membrane and the cell wall (Odds et al., 2003; Sundriyal et al., 2006; Ngo et al., 2016), a certain diversity of targets has been discovered. To develop new therapies, recent studies have focused on the inhibition of fungal virulence factors. Some mechanisms of action are described below, and an overview is presented in **Figure 1**.

### Ergosterol

Ergosterol is a lipid responsible for membrane fluidity and permeability and for the function of fungal integral membrane proteins; accordingly, this sterol is essential for cell viability (Leber et al., 2003; Tatsumi et al., 2013; Song et al., 2016). Several antifungals primarily target ergosterol, either by inhibiting its biosynthesis or by binding to it, causing formation of pores in the membrane.

Azole antifungals act by inhibiting ergosterol biosynthesis via the cytochrome P450 enzyme 14-α demethylase, which catalyzes the conversion of lanosterol to ergosterol (Kathiravan et al., 2012). Azoles affect the integrity of fungal membranes, altering their morphology and inhibiting growth (Kathiravan et al., 2012; Tatsumi et al., 2013).

The allylamine class, represented by terbinafine and naftifine, function by inhibiting the early steps of fungal ergosterol biosynthesis (Kathiravan et al., 2012) by targeting the enzyme squalene epoxidase, encoded by ERG1. This inhibition leads to accumulation of squalene and the absence of other

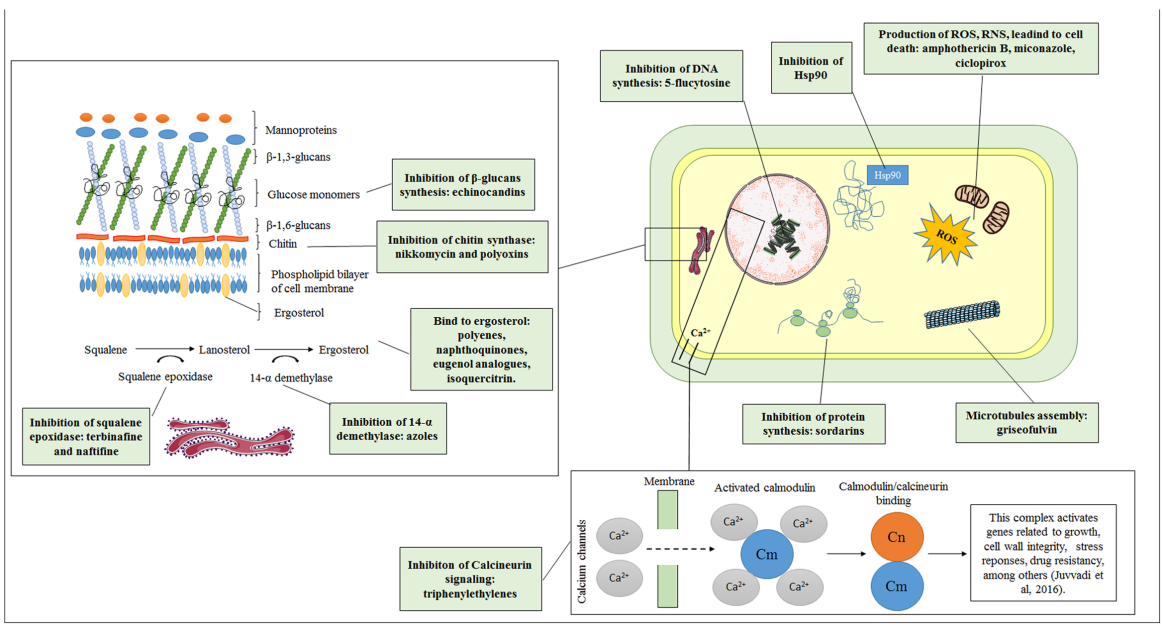


**FIGURE 1 | Old and new targets as antifungal candidates.**

sterol derivatives. Allylamines are highly effective against dermatophytes because they have been shown to accumulate more in the skin and nail beds relative to the blood, possibly due to their lipophilicity (Ngo et al., 2016).

Polyenes, such as nystatin and amphotericin B, exhibit fungicidal activity primarily by binding to ergosterol to form a complex capable of disrupting the membrane and leading to leakage of monovalent ions as well as other cytoplasmic contents (Odds et al., 2003; Walsh et al., 2008; Baginski and Czub, 2009). A second mechanism of polyene action involves a cascade of oxidation reactions and interactions with lipoproteins that impair membrane permeability through the release of free radicals (Sangalli-Leite et al., 2011; Mesa-Arango et al., 2012, 2014).

## Cell Wall

The fungal cell wall, which is primarily composed of chitin, glucans, mannans, and glycoproteins, is essential for adhesion and fungal pathogenesis and also serves as a protective barrier, limiting the access of molecules to the plasma membrane (Bowman and Free, 2006; van der Weerden et al., 2013). The two main mechanisms of action of antifungals targeting the cell wall are related to the inhibition of chitin and β-glucan synthesis.

In the period between 2001 and 2006, the echinocandin class of drugs, represented by caspofungin, micafungin, and anidulafungin, was developed. This class has different mechanisms of action that are specific for the fungal cell wall. Echinocandins target the protein complex responsible for the synthesis of β-1,3 glucans by blocking the enzyme glucan synthase (Odds et al., 2003). This blockage causes a decrease in the incorporation of glucose monomers linking β-1,3 and β-1,6 glucans, thereby weakening the cell wall and leading to fungal cell lysis (Kathiravan et al., 2012; Song and Stevens, 2016).

Chitin, a β-1-4-linked *N*-acetylglucosamine polymer, is an essential component of the fungal cell wall, though it is only present in very small amounts in yeasts (1–2%) but in considerable quantities in filamentous fungi (10–20%) (Bowman and Free, 2006; Morozov and Likhoshway, 2016). Nikkomycin and polyoxins are antifungal agents that target chitin synthase, which is responsible for elongation of the chitin chain and, therefore, is considered an attractive target (Kathiravan et al., 2012).

## Inhibition of Nucleic Acid, Protein, and Microtubule Syntheses

Inhibition of nucleic acid synthesis is related to the action of 5-flucytosine, which is converted primarily to 5-fluorouracil by the enzyme cytosine deaminase and then to 5-fluorouridylic acid by UMP pyrophosphorylase (Odds et al., 2003). Although 5-flucytosine was synthesized in 1957, its antifungal property was not discovered until 1964, 7 years later (Shukla et al., 2016). This acid can be incorporated into RNA, resulting in premature chain termination, thereby inhibiting DNA synthesis through effects on the enzyme thymidylate synthase (Polak and Scholer, 1975; Odds et al., 2003; Kathiravan et al., 2012).

With respect to the synthesis of microtubules, it is known that griseofulvin interferes with intracellular production, thus inhibiting fungal mitosis (Kathiravan et al., 2012).

Finally, sordarins suppress protein synthesis, which retards cell growth. Essentially, two fungal proteins have been described as target of sordarins: translation elongation factor 2 (eEF2) and the large ribosomal subunit protein rpP0 (Botet et al., 2008). Attempting to elucidate the mechanism of action, Justice et al. (1998) performed genetic assays using *Saccharomyces cerevisiae* mutants to demonstrate the fungal specificity of sordarins and proved that eEF2 is a target.

## Reactive Oxygen Species (ROS)

It is known that treatment with some antifungals such as AmB and itraconazole can cause more than one effect on fungal cells (Ferreira et al., 2013; Mesa-Arango et al., 2014). According to Mesa-Arango et al. (2014), mitochondria naturally produce free radicals. However, under adverse conditions, such as in the presence of oxidants and UV light, these free radicals are produced in abundance, causing damage to proteins, lipids and DNA and leading to cell death. Accordingly, ROS production is also associated with apoptosis. Treatment with AmB is able to induce oxidative and nitrosative bursts in *Candida*, *Cryptococcus*, and *Trichosporon*, enhancing its fungicidal effect (Ferreira et al., 2013; Mesa-Arango et al., 2014).

## Inhibition of Heat Shock Protein 90 (Hsp90)

Heat shock protein 90 (Hsp90) is a molecular chaperone of the heat shock protein (Hsp) family. Synthesized as an adaptive response to noxious conditions, these proteins contribute to the survival of pathogenic microorganisms in the host (Jacob et al., 2015). Hsp90 has been related to fungal pathogenicity, phase transition in dimorphic fungi and antifungal drug resistance, making it a potential target for antifungal therapy (Burnie et al., 2006; Brown et al., 2010; Jacob et al., 2015). Jacob et al. (2015) examined the transcription profiles of *Trichophyton rubrum* under different stress conditions, such as interaction with nail and skin cells and molecules, nutrients and treatment with antifungal drugs. In addition to suggesting the role of Hsp90 in the pathogenesis and susceptibility to dermatophytosis antifungal agents, the authors also related this protein to the regulation of other heat shock proteins.

## Inhibition of Calcineurin Signaling

Calcineurin is defined as a conserved $Ca^{2+}$-calmodulin (CaM)-activated protein phosphatase 2B that belongs to the phosphor-protein phosphatase family (Juvvadi et al., 2016). This protein is involved in calcium-dependent signaling and regulation of several important cellular processes in yeasts (*Candida* spp., *Cryptococcus* spp.) and filamentous fungi (*Aspergillus fumigatus*), including growth, cell wall integrity, transition between morphological states, cation homeostasis, stress responses, and drug resistance (Blankenship et al., 2003; Steinbach et al., 2006; Chen et al., 2013; Juvvadi et al., 2016). More important is the role of calcineurin in maintaining the integrity

of the fungal cell wall by regulating downstream effectors and influencing the biosynthesis of ergosterol, chitin and β-glucans. Odom (2014) suggested that triphenylethylenes, described by Butts et al. (2014), are a novel class of antifungal drugs that act on calcium homeostasis in *Cryptococcus neoformans* via direct inhibition of the calcineurin activator calmodulin.

## MOLECULAR MECHANISMS OF ANTIFUNGAL RESISTANCE

The widespread use of antifungal agents and the limited arsenal associated with the increased number of opportunistic infections have resulted in the progression of resistance to available drugs. The antifungal resistance mechanism may occur through different conditions such as a decrease in the effective drug concentration, changes or overexpression of the drug targets, and metabolic bypasses (Sanglard, 2016). **Figure 2** depicts an overview of several antifungal resistance mechanisms described for *Candida* spp.

## Molecular Mechanisms of Resistance to Azoles

Azole resistance includes the following mechanisms: (1) activation of efflux pumps, (2) qualitative changes in the target enzyme, (3) quantitative changes caused by overexpression of ERG11, and (4) alterations in cell wall composition.

### Activation of Efflux Pumps

Reduction in intracellular antifungal accumulation in *Candida* spp. is a consequence of the overexpression of membrane-associated transporters acting as multidrug efflux pumps (Prasad and Rawal, 2014). Two main classes of transporters are described as being involved in this resistance mechanism. The superfamily of ATP-binding cassette (ABC) proteins comprises the primary activity, hydrolyzing ATP to provide energy to drive the efflux of drugs. Transporters belonging to the major facilitator superfamily (MFS) constitute the secondary activity; these pumps utilize a proton electrochemical gradient across the plasma membrane to extrude substrates (Cannon et al.,

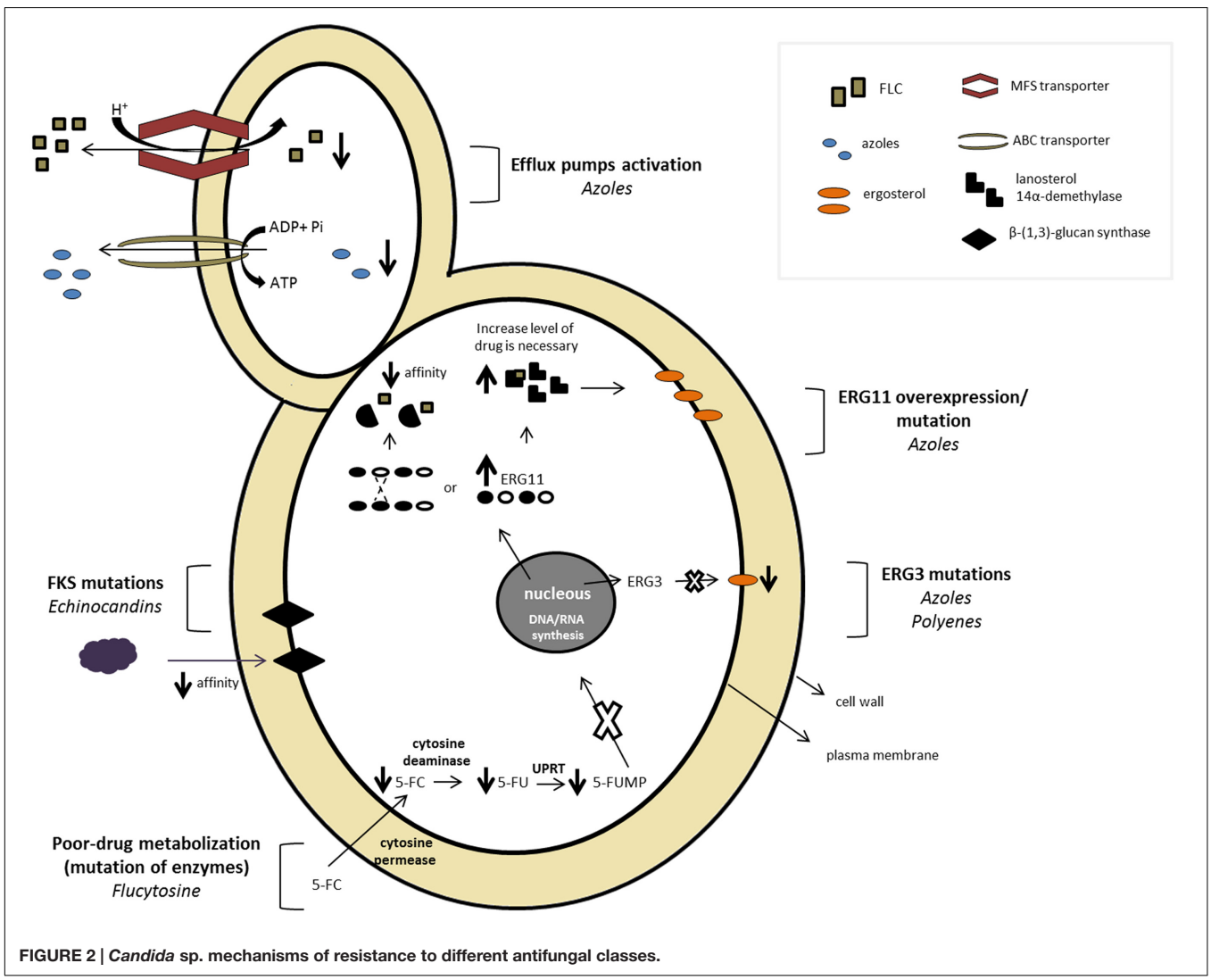


**FIGURE 2 | *Candida* sp. mechanisms of resistance to different antifungal classes.**

**TABLE 1 | Burch and Russell: The three R's concept and the action required for its application.**

| 3 R rule | Action required |
|---|---|
| Reduction | Careful experimental design<br>Consult the literature<br>Organize a pilot experiment before using a bigger amount of animals<br>Realize an appropriate statistical test<br>Get the great amount of data from each animal |
| Refinement | Eliminate the pain and search for better alternatives for animal welfare<br>Be trained before execute the procedures<br>Use adequate doses of analgesics and anesthetic for the painful procedures<br>Perform post chirurgical procedures like (e.g., thermoregulation) |
| Replacement | use *in silico* methods (e.g., computer software)<br>use *in vitro* methods (e.g., cell culture and cell tissue) |

2009). Although most *Candida* species are naturally susceptible to azoles, an increasing number of cases of acquired resistance have been reported in clinical isolates of patients exposed to prolonged treatment, especially to FLZ (White et al., 1998; Pfaller and Diekema, 2007; Arendrup, 2014; Espinel-Ingroff et al., 2014).

*Candida albicans* azole-resistant isolates can overexpress one or more efflux pumps (White, 1997; Franz et al., 1998; Lopez-Ribot et al., 1998). *C. albicans* possesses 28 putative types of ABC transporters, two of which, CDR1 and CDR2, are well characterized and overexpressed in resistant-isolates. Cdr1 has a greater contribution to FLZ resistance than Cdr2 (Sanglard et al., 1997; Sanglard et al., 2009; Prasad and Goffeau, 2012). Additionally, gain-of-function mutation of TAC1 (transcriptional activator of CDR genes) is related to increased levels of CDR1 and CRD2 (Coste et al., 2007). Regarding MFS transporters, *C. albicans* has 96 potential MFS transporters, though only one has been described with respect to azole resistance, the MDR1 member of the DHA1 family (Gaur et al., 2008).

It has been postulated that CDR genes in *C. albicans* are involved in the removal of different azoles. CDR1 efflux is associated with a wide range of substrates, whereas MDR1 appears to be specific for FLZ, as its overexpression results in moderate resistance to FLZ (Sanglard et al., 1995; White et al., 1998; Hiller et al., 2006; Cheng et al., 2007). The ABC and MFS pumps differ in relation to their structures and mechanisms, and differences in substrate specificity are expected (Keniya et al., 2015).

The exact mechanism underlying FLZ resistance in *C. glabrata* is not well defined; however, different studies indicate an essential role for ABC transporters (Abbes et al., 2013). FLZ-resistant *C. glabrata* clinical isolates present CDR1 and CDR2 upregulation (Sanglard et al., 1999; Bennett et al., 2004). Sanguinetti et al. (2005) observed increased expression of SQN2 (another ABC transporter) in two isolates (among 29) expressing normal levels of CRD1 and CRD2; SQN2 is possibly involved in the resistance of this species.

Studies have demonstrated that the primary mechanisms of azole resistance in clinical isolates of *C. dubliniensis* is upregulation of Mdr1 (Moran et al., 1998). Mdr1 is invariably overexpressed in *C. dubliniensis* strains with reduced susceptibility to FLZ (Perea et al., 2001). Moreover, among clinical isolates obtained from HIV-infected individuals with oropharyngeal candidiasis, Perea et al. (2002) reported upregulation of Mdr1 in all isolates with a high FLZ-resistance level, whereas less than half of the isolates presented CDR upregulation. Despite the 92% identity of the *C. dubliniensis* CDR1 gene with *C. albicans*, this may occur because *C. dubliniensis* genotype 1, previously described by Gee et al. (2002), possesses a non-sense mutation in CDR1 that converts a normal codon to a stop codon (TAG), resulting in expression of a truncated protein of 85 kDa instead of the wild-type 170 kDa (Perea et al., 2002).

*Candida krusei* carries two homologous genes for ABC transporters previously described for *C. albicans*: ABC1 and ABC2. The ABC1 gene is upregulated in cultures exposed to imidazole and cycloheximide. However, cycloheximide exhibits antagonist activity against FLZ, and this correlation between antagonism and upregulation suggests that FLZ and other azoles may be substrates for the ABC1 transporter (Katiyar and Edlind, 2001). Thereafter, Lamping et al. (2009) showed the involvement of ABC1 in the innate azole resistance of *C. krusei*, and Guinea et al. (2006) found that MDR proteins have a role in *C. krusei* resistance. However, expression of MFS transporters was not reported determined in FLZ-resistant *C. krusei*.

The FLZ resistance of *C. parapsilosis* has been linked to overexpression of MRR1 in high association with a mutation (Zhang et al., 2015) that concomitantly results in overexpression of MDR1 and overexpression of CRD1 (Souza et al., 2015; Zhang et al., 2015). The involvement of efflux pumps in *C. tropicalis* clinical isolate antifungal resistance has not yet been observed, but there is an *in vitro* study demonstrating the development of FLZ-resistance associated with the up-regulation of MDR1 and CDR1 (Barchiesi et al., 2000).

The involvement of efflux pumps has also been described in other pathogenic fungi. In *C. neoformans*, overexpression of the AFR1 gene, of the ABC transporter family, is associated with FLZ resistance (Posteraro et al., 2003; Sanguinetti et al., 2006). In addition, afr2p and Mdr1p, members of the ABC and MFS families, respectively, from *C. neoformans* and *C. gattii* can also promote resistance to FLZ and other azoles (Basso et al., 2015).

The ABC transporter Afr1 also acts in azole resistance in *Aspergillus* because overexpression of the AFR1 gene from *A. fumigatus* can confer itraconazole resistance (Slaven et al., 2002). Although *Aspergillus fumigatus* has four Mdr-like efflux pumps, itraconazole-resistant isolates or strains under itraconazole treatment only present overexpression of *mdr3* and *mdr4* (da Silva Ferreira et al., 2004).

Efflux appears to be the most prevalent mechanism of resistance in dermatophytes. Increased expression of the ABC transporters genes TruMDR1 and TruMDR2 from *T. rubrum* is observed in the presence of azoles (Cervelatti et al., 2006; Fachin et al., 2006). The use of efflux pumps by dermatophytes is also

implicated in resistance to other antifungals, such as terbinafine, amphotericin B and griseofulvin (Cervelatti et al., 2006; Paião et al., 2007; Yu et al., 2007; Ghannoum, 2016; Martins et al., 2016).

## ERG11: Overexpression and Changes in Drug Targets

In the presence of FLZ, *C. albicans* increases ERG11 expression, most likely via compensatory mechanisms, to deplete ergosterol (Albertson et al., 1996). However, Franz et al. (1998) showed that even in the absence of FLZ, resistant isolates express ERG11 at higher levels compared to susceptible isolates exposed to the drug. Overexpression of ERG11 results in increased concentrations of lanosterol 14α-demethylase; consequently, larger amounts of the antifungal are required to inhibit the enzyme (Morschhäuser, 2002). This mechanism has been described for many *C. albicans* FLZ-resistant isolates (White et al., 2002; Chau et al., 2004; Goldman et al., 2004). ERG11 overexpression in azole-resistant isolates can occur via two mechanisms of ERG11 amplification. One is formation of an isochromosome containing two copies of the left arm of chromosome 5, where ERG11 resides, and duplication of the entire chromosome (Selmecki et al., 2006). The second mechanism is mutation in the zinc cluster finger transcription factor Upc2, which results in overexpression of ERG11 in *C. albicans* (Dunkel et al., 2008). Overexpression of ERG11 has also been reported for other azole-resistant *Candida* species; however, the mechanisms remain unknown (Barchiesi et al., 2000; Redding et al., 2002; Vandeputte et al., 2005; Rogers, 2006; Jiang et al., 2013; Cowen et al., 2014).

Another mechanism of azole resistance among *Candida* strains involves non-synonymous point mutations in the ERG11 gene, which encodes the target enzyme lanosterol 14α-demethylase. Mutations in ERG11 can result in post-translational modifications in the amino acid sequence and consequently in the three dimensional structure of Erg11p, causing decreased binding affinity for azole components and also reducing ergosterol biosynthesis without impeding enzyme function but generating yeast with an altered phenotype resistant to azole (Xiang et al., 2013). Among 160 different amino acid substitutions, only 10 have been confirmed in FLZ resistance; four were obtained in the laboratory but not yet detected in clinical isolates (Chen et al., 2007). The substitutions R467K, I471T, G464S, S405F, and K143R were only related to azole-resistant *C. albicans* isolates (Sanglard et al., 1998; Lamb et al., 2000; Morio et al., 2010), with the most common being R467K and G464S (Morio et al., 2010). ERG11 mutations have been described for other azole-resistant clinical *Candida* isolates, including *C. dubliniensis* (Perea et al., 2002), *C. krusei* (Ricardo et al., 2014), *C. tropicalis* (Vandeputte et al., 2005; Jiang et al., 2013) and more recently *C. parapsilosis* (Grossman et al., 2015). However, the same finding has not yet described for *C. glabrata* (Gonçalves et al., 2016).

In non-*Candida* species, the most common mechanism of azole resistance is alteration of the target protein. Several studies describe point mutations in the ERG11 (CYP51) gene, encoding 14-α-demethylase, leading to amino acid substitution that decreases the affinity for azole (Xie et al., 2014).

In *Cryptococcus* spp., three point mutations in ERG11 have been described in association with azole resistance: point mutation G1855T leading to amino acid substitution of glycine 484 with a serine (G484S) (Rodero et al., 2003); substitution of tyrosine 132 by phenylalanine occurring in the catalytic domain (Sionov et al., 2012); and point mutation G1855A, also resulting in the amino acid substitution G484S (Bosco-Borgeat et al., 2016). *Cryptococcus neoformans* under FLZ stress is also able to adapt via duplication of chromosome 1, on which the genes ERG11 and AFR1 and that encoding the FLZ transporter protein are found (Sionov et al., 2010).

*Aspergillus* spp. have two genes encoding 14-α-demethylase: CYP51A and CYP51B. However, azole resistance is more associated with mutation in *CYP51A* (Gonçalves et al., 2016). Different point mutations and non-synonymous mutations have been described in *CYP51A*, and the different patterns of azole resistance depend on these mutations (Diaz-Guerra et al., 2003; Mann et al., 2003; Chowdhary et al., 2014a; Leonardelli et al., 2016). For example, non-synonymous mutations in codons 98,138, 220, 431, 434, and 448 may confer resistance to all azoles in *Aspergillus* spp. (Howard et al., 2009).

In drug-resistant *Aspergillus*, tandem repeat mutation associated with amino acid substitution in the *CYP51A* promoter have been described, such as $TR_{34}$/L98H and TR46/Y121F/T289A (Verweij et al., 2007; Vermeulen et al., 2013). The most prevalent is $TR_{34}$/L98H, which is found in different resistant *Aspergillus* isolates worldwide and seems to be the major mutation associated with azole resistance (Lockhart et al., 2011; Chowdhary et al., 2012, 2014b; Badali et al., 2013; Seyedmousavi et al., 2013; Chen et al., 2016).

In *Histoplasma capsulatum*, a Y136F substitution in CYP51Ap has also been implicated in decreased susceptibility to FLZ and voriconazole (Wheat et al., 2006).

## Erg3 Mutations: Alteration of Ergosterol Biosynthesis

Fungi exposed to azoles suffer from ergosterol depletion and accumulation of toxic sterols, resulting in growth arrest (Kanafani and Perfect, 2008). Another less frequent mechanism of azole resistance is inactivation of the enzyme sterol $\Delta^{5,6}$-desaturase encoded by the gene ERG3, which is essential for ergosterol biosynthesis (Sanglard and Odds, 2002). Therefore, ERG3 protects yeast against toxic sterols; in contrast, deletions or mutations in ERG3 result in high levels of azole resistance once the production of toxic sterols is bypassed (Watson et al., 1989; Kelly et al., 1997). ERG3 mutants have been well studied in *C. albicans* and *C. dubliniensis* (Morio et al., 2012). Nonetheless, few of these mutations result in amino acid changes in Erg3 (Pinjon et al., 2003; Chau et al., 2005; Martel et al., 2010; Vale-Silva et al., 2012). Indeed, the exact mechanism by which a single substitution results in azole resistance needs to be investigated. Studies to date have demonstrated that cross-resistance between azoles and polyenes may occur because of ERG3 loss of function, which results in low ergosterol contents, protecting yeast against the toxic effects of AmB (Anderson et al., 2014; Sanglard, 2016). Some studies point to other mutations in genes of ergosterol biosynthesis suspected to be related to azole resistance, such as ERG6, ERG24, and ERG2

(Jensen-Pergakes et al., 1998; Jia et al., 2002; Vincent et al., 2013).

## Molecular Mechanisms of Resistance to Flucytosine

In relation to 5-FC, approximately 10% of *C. albicans* isolates present primary resistance, even in the absence of drug exposure (Arikan and Rex, 2005). Different studies have shown that resistance to 5-FC is related to its metabolism. In *C. glabrata* and *C. albicans,* mutation in cytosine deaminase confers primary resistance to 5-FC, and deficiencies in cytosine permease activity have also been associated with resistance in *Candida* species (Hope et al., 2004; Vandeputte et al., 2011). Cytosine permease is involved in the uptake of 5-FC, after which cytosine deaminase produces 5-fluorouracil using cytosine; thus, 5-FC resistance is associated with deficiency in enzymes related to uptake, transport and transformation of 5-FC that result in failure to metabolize to the active drug (Bondaryk et al., 2013). A *C. lusitaniae* mutant lacking the enzyme uracil phosphoribosyl transferase, encoded by the gene FUR1 (Papon et al., 2007), exhibits secondary resistance to 5-FC. The enzyme UPRT converts 5-fluorouracil to 5-fluorouridine monophosphate and inhibits thymidylate synthetase by disrupting DNA synthesis.

The molecular mechanism of the resistance of *Cryptococcus neoformans* to 5-FC is not well established but is often related to mutation in pyrimidine salvage enzymes, as occurs in *C. albicans* (Whelan, 1987).

Song et al. (2012) demonstrated that *C. neoformans* might possess different mechanism of resistance against 5-FC that are based on sensor histidine kinases. *C. neoformans* possesses a two-component system, Tco2 and Tco1, to regulate 5-FC response; deletion of *TCO2* leads to strong 5-FC resistance, and mutation in *TCO1* increases susceptibility. In addition, through transcriptomic analysis, it was found that 5-FC-regulated genes in *C. neoformans* differ from those of *S. cerevisiae*. As most of these genes are of unknown function in other fungi, *C. neoformans* appears to have a unique mechanism of resistance against 5-FC.

## Molecular Mechanisms of Resistance to Echinocandins

Mutations in the FKS1 gene lead to alterations in the conformation of the encoded enzyme, resulting in lower affinity between Fks1 and echinocandins and consequently resistance to these drugs (Gonçalves et al., 2016). Mutations in two hot spot regions of FKS1 are conserved in clinical isolates of *C. albicans*: the region between 641 and 648 (comprising a cytoplasmic domain/binding site of echinocandins) and 1345–1365 are hot spot 1 and hot spot 2 (HS2), respectively. These sites are responsible for the majority of mutations conferring resistance to echinocandins, including the most described: substitution of serine at position 645 (Balashov et al., 2006). Different studies have demonstrated alterations in FKS1 in other *Candida* species (Park et al., 2005; Desnos-Ollivier et al., 2008; Garcia-Effron et al., 2008, 2010), whereas mutations in Fks1 and its paralog Fks2 have been associated with resistance in *C. glabrata* (Garcia-Effron et al., 2009; Pham et al., 2014; Perlin, 2015).

*Candida parapsilosis* and *C. guilliermondii* show reduced susceptibility to echinocandins, most likely due to a natural polymorphism in the Fks1p hot spot region corresponding to mutations acquired in resistant isolates of other species: substitution of proline to alanine at positions 660 and 642 (Perlin, 2007; Garcia-Effron et al., 2008). Studies have shown that activation of cell wall recovery or compensatory pathways increases chitin production and that mutations that increase the chitin level result in reduced caspofungin susceptibility in *C. albicans* (Plaine et al., 2008).

Alterations in the Fks subunit have also been associated with echinocandin resistance in other fungi. A mutant with an amino acid substitution S678P in Fks1p resulted in resistance of *A. fumigatus* to echinocandins (Rocha et al., 2007). Alterations in FKS are also involved in *Fusarium* intrinsic resistance to echinocandin (Katiyar and Edlind, 2009).

*Cryptococcus neoformans* is intrinsically resistant to echinocandins without Fks alteration (Maligie and Selitrennikoff, 2005). Recently, Huang et al. (2016) investigated the molecular basis of *C. neoformans* resistance to echinocandins through a high-throughput genetic screen and found that the *CDC50* gene may be involved in echinocandin resistance. *CDC50* encodes the β-unit of membrane lipid flippase, which mediates the lipid trafficking pathway.

## Molecular Mechanisms of Resistance to Polyenes

Although the development of acquired resistance to AmB rarely occurs in *Candida*, there are some reports to date (Favel et al., 2003; da Matta et al., 2007). Resistance to AmB generated a common phenotype with alterations in the membrane lipid composition and consequently a change in fluidly and permeability. A greater number of cases of therapy failure of AmB have been associated with *C. lusitaniae* (Minari et al., 2001; Favel et al., 2003; Atkinson et al., 2008). The main alterations involved in polyene resistance are in enzymes participating in ergosterol biosynthesis. Defects in ERG2 and ERG3, encoding C-8 sterol isomerase (converting fecosterol to episterol with low affinity for AmB) and $\Delta^{5,6}$-desaturase, respectively, result in quantitative and qualitative modifications in the membrane sterol content, influencing the amount of ergosterol or its availability for the action of polyenes (Arikan and Rex, 2005; Sheikh et al., 2013). A defective ERG3 gene resulted in low ergosterol levels in the fungal membrane of fungal, conferring azole/polyene cross-resistance to *Candida* isolates. Another likely AmB-resistance mechanism is via enhanced activity of catalases, which reduce oxidative damage (Sokol-Anderson et al., 1986; Kanafani and Perfect, 2008).

Although the mechanisms of resistance to AmB in *Candida* spp. are well described, these mechanisms in non-*Candida* species remain unclear. Resistance to AmB in *C. neoformans* isolated from AIDS patients was linked to alterations in sterol delta 8-7 isomerase (Kelly et al., 1994). *Aspergillus* strains are commonly resistant to AmB, though this varies among species, without alteration in ergosterol content. One of the mechanisms

proposed for *A. terreus* AmB resistance is blockage of the Ras signaling pathway by Hsp90 and Hsp70, inhibiting the formation of aqueous pores (Blum et al., 2013; Blatzer et al., 2015).

## BIOFILM AND ANTIFUNGAL RESISTANCE

The ability of many fungi to form biofilms is one of the reasons for antifungal drug resistance. Many medically important fungi are described as biofilm-forming organisms, such as *Candida* spp. (Chandra et al., 2005; Hinrichsen et al., 2008; Finkel and Mitchell, 2011; Pires et al., 2011), *Pneumocystis* spp. (Cushion et al., 2009), *Coccidioides* spp. (Davis et al., 2002), *Aspergillus* spp. (Mowat et al., 2009; Kaur and Singh, 2014), Zygomycetes (Singh et al., 2011), *Malassezia* spp. (Cannizzo et al., 2007; Figueredo et al., 2012), *Trichosporon* spp. (Di Bonaventura et al., 2006; Colombo et al., 2011), *Cryptococcus* (Walsh et al., 1986; Martinez and Casadevall, 2007), *Histoplasma capsulatum* (Pitangui et al., 2012), *Trichophyton* spp. (Costa-Orlandi et al., 2014) and *Paracoccidioides* spp. (Sardi et al., 2015).

Biofilms are highly structured and complex microbial communities embedded in a self-produced extracellular matrix (ECM) that attach to a wide range of surfaces and (Fanning and Mitchell, 2012). Several factors contribute to initial surface attachment, such as pH, temperature, osmolarity, flow of the surrounding biologic medium, host immune factors and even the presence of antimicrobial agents (Baillie and Douglas, 2000; Chandra et al., 2001; Ramage et al., 2008).

Fungal biofilm formation occurs through a sequential process including planktonic cell adhesion to an appropriate substratum, colonization, ECM production, biofilm maturation, and dispersion (Fanning and Mitchell, 2012). Despite these specific characteristics, all types of fungal biofilms have distinct properties from planktonic yeast cells and increase antifungal drug resistance up to 1000-fold (Ramage et al., 2001; Uppuluri et al., 2010). Indeed, several studies have shown the inefficacy of antifungal therapy against different fungal biofilms.

Multiple other biofilm-specific factors contribute simultaneously to the resistance of yeasts to antifungal drugs, including cell density, quorum sensing, efflux pump activity, persister cells, ECM presence, stress responses and overexpression of drug targets.

The cell density is an important factor that contributes to the antifungal resistance of biofilms. However, some studies show that this is not a biofilm-specific resistance mechanism because a similar trend was observed for planktonic cells. Perumal et al. (2007) studied the efficacy of different azoles, AmB and caspofungin on planktonic cells at densities similar to those found in biofilms. The susceptibility of dissociated biofilm cells was similar to that of planktonic cells at the same cell density, and this susceptibility decreased as the density of the cells increased (Perumal et al., 2007). This phenomenon was also demonstrated by Seneviratne et al. (2008), who noted the density-dependent susceptibility of planktonic or biofilm for ketoconazole and 5-FC. Lass-Florl et al. (2003) showed similar drug resistance results by increasing the inoculum sizes of *Aspergillus* species, supporting the idea that the physical density of the cells influences antifungal agent activity.

By providing microorganisms with the ability to communicate and coordinate population growth/morphology via the secretion of signaling molecules, cell density can be considered a key aspect of the quorum-sensing process (Ramage et al., 2009, 2012). QS for fungi was first described in *C. albicans* by Hornby et al. (2001), who identified farnesol as a molecule that inhibits the hyphal transitional stage of *C. albicans* and increases adhesion (Saville et al., 2003; Ramage et al., 2009). Exposing *C. albicans* to farnesol also resulted in alterations in gene expression involving hyphal developmental genes (*TUP1* and *CRK1*), cell surface hydrophobicity genes and those involved in drug resistance (*FCR1* and *PDR16*) (Cao et al., 2005; Enjalbert and Whiteway, 2005). In addition, farnesol induces apoptosis in both *A. nidulans* and *Fusarium graminearum* (Semighini et al., 2006, 2008). Tyrosol, the second QS molecule identified in *C. albicans,* promotes germ tube formation. According to Alem et al. (2006), tyrosol enhances the early phase of biofilm formation and may also inhibit farnesol activity, thereby controlling cell population morphology.

Khot et al. (2006) for the first time studied the mRNA levels of genes involved in ergosterol biosynthesis (ERG genes) and in β-1,6-glucan biosynthesis (SKN1 and KRE genes) in comparison between planktonic and biofilm-associated cells. The authors described the appearance of a unique transcript profile in a subpopulation of AmB-resistant blastospores with significant upregulation of ERG25, SKN1, and KRE1 and downregulation of ERG1. Mukherjee et al. (2003) reported that ergosterol levels were significantly decreased in intermediate and mature phases when compared to early-phase biofilms, suggesting that the biofilm resistance to azole might be explained by ergosterol alterations in biofilm membranes. Subsequent studies (Borecká-Melkusová et al., 2009; Nett et al., 2009; Nailis et al., 2010) compared the exposure of young and mature biofilms to fluconazole, concluding that both induce downregulation of genes encoding enzymes involved in ergosterol biosynthesis (Ca*ERG1*, Ca*ERG3*, Ca*ERG11,* and Ca*ERG25*). In addition, treatment of both young and mature biofilms with AmB predominantly resulted in overexpression of Ca*SKN1*, with only modest upregulation of Ca*KRE1* (Nailis et al., 2010).

Induction of ergosterol pathway genes has been described in different biofilms of *Candida* species. For example, incubation with fluconazole caused upregulation of Cd*ERG3* and Cd*ERG25* in *C. dubliniensis* (Borecká-Melkusová et al., 2009) and of genes involved in ergosterol biosynthesis in *C. parapsilosis*, resulting in antifungal resistance (Rossignol et al., 2009).

Moreover, drug efflux pumps also participate in drug resistance of biofilms. Ramage et al. (2002) investigated the role of efflux pumps, ABC and MFS transporters, of *C. albicans* biofilm. Expression of CDR genes predominated at the beginning of biofilm formation (24 h), whereas MDR1 was solely overexpressed after 24 h. Expression of CDR1, CDR2, and MDR1 showed that *C. albicans* was susceptible to azoles when grown planktonically but exhibiting resistance when grown in a biofilm. Several subsequent studies confirmed these results, suggesting that the expression of these genes is necessary for biofilm

resistance (Mukherjee et al., 2003; Perumal et al., 2007). Gao et al. (2014) showed that fluconazole increased the expression of CDR1, CDR2 and MDR1 and that the combination with doxycycline downregulated the gene overexpression induced by FLZ.

Later, Nett et al. (2009) performed an *in vivo* study of *C. albicans* biofilm formation on implanted catheters and showed upregulation of genes during biofilm development: CDR2 at 12 h and MDR1 at both 12 and 24 h. Similar results were reported for other *Candida* species, including *C. glabrata,* in which the expression of *CDR1* and *CDR2* was found at early (6 h) and intermediate (15 h) biofilm stages, even though neither gene was upregulated at the mature phase (48 h) (Song et al., 2009). *C. tropicalis* showed increased expression of MDR1 after 24 h of biofilm formation (Bizerra et al., 2008). In *A. fumigatus*, the initial phase of biofilm formation was associated with increased activity of the efflux pump MDR and gene upregulation at 8 h when treated with voriconazole (Rajendran et al., 2011). Thus, all reports support the idea that efflux pump expression is a mechanism of biofilm resistance, especially in the early phase of biofilm growth until ECM production.

The ECM is considered one of the essential mechanisms of biofilms resistance, conferring enhanced antimicrobial resistance and protection from host immune responses (Sutherland, 2001; Davies, 2003). The ECM may act as an adsorbent, reducing the amount of antimicrobial available to interact with the biofilm, and the structure physically reduces the penetration of antimicrobial agents by walling off access to regions of the biofilm (Taraszkiewicz et al., 2013). The matrix is composed of a variety of proteins, nucleic acids, phospholipids, lipids, amyloid fibers, humid substances, and in some cases, surprising amounts of extracellular DNA (e-DNA) (Estrela et al., 2009; Dogsa et al., 2013). The ECM confers important characteristics to biofilm, such as providing for mechanical stability, an external digestive system, and intense cell interactions, including cell–cell communication and synergistic microconsortia, and serving as a nutrient, energy, and recycling source (Flemming and Wingender, 2010).

During biofilm formation, β-1,3 glucan is one of the principle carbohydrate components of the ECM (Ramage et al., 2012). It is responsible for sequestering azoles, echinocandins, pyrimidines, and polyenes, acting as a "drug sponge," and confers resistance to *C. albicans* biofilms (Nett et al., 2010a,b). In addition, the ECM of non-*albicans Candida* strains also contains β-1,3 glucan, which contributes to azole resistance via specific binding (Mitchell et al., 2013). FKS1 was the first gene described as encoding β-1,3 glucan synthase of *C. albicans* (Nett et al., 2010a). Other genes essential for the *C. albicans* ECM are SMI1 and RLM1, which are involved in the protein kinase C cell-wall integrity pathway, controlling the cell wall glucan content in response to stress. Recently, Taff et al. (2012) showed that glucan transferases and exoglucanase are crucial for the accumulation and delivery of β-1,3 glucan to the matrix.

Biofilm presents persister cells, which are directly correlated with accumulating high concentrations of antimicrobial agents. In essence, a persister is a dormant cell that with little or no cell wall synthesis; drugs bind to their target molecules but are unable to promote cell death (Lewis, 2007). The simplest route to form a dormant persister cell might be through the overproduction of proteins that are toxic to the cell and inhibit growth (Lewis, 2010). Different from bacteria, these cells have only been detected in yeast biofilms and not in planktonic populations (LaFleur et al., 2006). Due to the ECM, the persisters present in the biofilm can withstand both antifungal treatment and the immune system (Lewis, 2007). Persisters may be mainly responsible for re-infection once when the concentration of antimicrobial decreases, and they can repopulate the biofilm (Lewis, 2001). Recently, a dose-dependent study involving AmB and chlorhexidine against *C. albicans* in planktonic and biofilm forms reported complete elimination of planktonic cells in both exponential and stationary stages. However, biphasic killing occurred in the mature biofilm, suggesting the presence of persisters. After AmB treatment, surviving *C. albicans* in the biofilm capable of producing a new biofilm with a new subpopulation of persisters, suggesting that yeast persisters are not mutants but phenotypic variants of the wild-type population (LaFleur et al., 2006). In addition, Sun et al. (2016) showed that *C. albicans* AMB-tolerant persisters were produced mainly during the adhesion phase and that the maintenance of these cells was dependent of surface adhesion. Further studies showed the presence of persister cells after the treatment of *C. krusei* and *C. parapsilosis* biofilms with AmB. However, the biofilm of *C. albicans* SC5314 under the same treatment condition did not reveal surviving cells, indicating a lack of persister cells (Al-Dhaheri and Douglas, 2008).

Based on the above, it is possible to affirm that biofilm confers antifungal resistance and that this occurs through various mechanisms. Accordingly, the discovery of new strategies to overcome these microbial communities has been deeply researched.

The development of new drug formulations is one of the main options of studies, including echinocandins and AmB lipid forms that are inhibit fungal biofilm both *in vitro* (Kuhn et al., 2002; Ramage et al., 2013) and *in vivo* (Mukherjee et al., 2009; Kucharikova et al., 2013).

The association of drugs is another example of a strategy against fungal biofilms. Some studies have reported the efficacy of a combination of AmB and aspirin (Zhou et al., 2012), FLZ and doxycycline (Gao et al., 2013), and caspofungin and diclofenac (Bink et al., 2012). The sensitization of *C. albicans* biofilms to different antifungals by the immunosuppressant drug cyclosporine A also resulted in enhanced biofilm inhibition (Shinde et al., 2012).

The presence of e-DNA, which is an important component of the ECM, has prompted some strategies using DNase to decrease biofilm biomass and to enhance the activity of antifungal agents (Martins et al., 2010). Lactonases and α-amylases are also used to control fungal biofilms (Taraszkiewicz et al., 2013). Moreover, an interesting therapeutic option is to block *persister* survival. Bink et al. (2011) discovered that superoxide dismutase (SOD) may be an inhibitor of *N,N*'-diethyldithiocarbamate (DDC) in *C. albicans* biofilms, reducing the miconazole-resistant *persister* fraction by 18-fold (Bink et al., 2011).

The application of antimicrobial photodynamic therapy has been investigated for anti-fungal biofilm properties with regard to the efficiency of inhibiting several microorganisms, with minimal damage to the host cell (Biel, 2010). This therapy involves the combination of photosensitizer (PS), light and molecular oxygen (de Melo et al., 2013). In addition, strategies involving nanoparticles (Allaker, 2010; Ramasamy et al., 2016), plant extracts (Wojnicz et al., 2012), and chitosan (Carlson et al., 2008) have been applied against microbial biofilm, with significant results. Further studies are necessary for identifying means to overcome fungal biofilm resistance.

## DRUG COMBINATIONS

Based on the problems discussed above with regard to antifungal treatment, one of the options is the combination of drugs. Using more than one drug can increase efficacy due to the possibility of action on more than one target; in addition, toxicity is reduced because less of the drug is used (Chen et al., 2014). Drug combinations can lead to improved activity, such as synergist activity, or decrease antagonist action. Evaluation of the effect of a drug combination *in vitro* can be realized by the checkerboard method (Johnson et al., 2004).

Most studies on the *in vitro* and *in vivo* combination of azoles with AmB do not show synergistic activity, though previous treatment with azole can influence the action of polyenes. This can be explained by the fact that both drugs have the same target: ergosterol. However, because azoles inhibit ergosterol biosynthesis, less ergosterol is available for polyene to bind (Louie et al., 2001; Sanglard, 2002). Nonetheless, invasive mucormycosis has been successfully treat with an antifungal combination of AmB and posaconazole (Pagano et al., 2013).

There are numerous *in vitro* studies of antifungal combinations using triazole with echinocandin or triazole with AmB (Elefanti et al., 2013; Katragkou et al., 2014). Regardless, the clinical results of combinatory treatment remain unclear and are generally described for infections caused by fungi, which present difficulty in treatment, such as in aspergillosis and mucormycosis (Belanger et al., 2015). The combination of caspofungin and voriconazole showed *in vitro* synergistic activity against *Aspergillus* spp. (Walsh et al., 2008). Moreover, this combination showed efficacy in a mammalian model (Kirkpatrick et al., 2002). Treatment of patients with invasive aspergillosis with a combination of voriconazole and anidulafungin improved survival in comparison with treatment with voriconazole monotherapy (Marr et al., 2015). However, in another study, triazole and echinocandin combination showed the same effect as triazole alone (Raad et al., 2015).

The antifungal 5-FC in combination with AmB or with azole did not show synergistic activity for *Candida* sp. (Scheid et al., 2012). However, this was efficient for the treatment of cryptococcal meningitis. It should be noted that the lack of availability of 5-FC results in the use of less effective combinations in many countries (Perfect et al., 2010). Moreover, this compound is associated with rapid development of resistance (Vandeputte et al., 2011).

Interaction with non-antifungal agents has also been described as potentiating antifungal activity. Triclosan, a compound exhibiting antimicrobial activity, is widely used in soap, toothpaste, and other personal care products. This molecule showed *in vitro* synergistic activity with FLZ against *C. albicans* (Yu et al., 2011). Triclosan is also active against *C. neoformans* by activating the apoptosis pathway and also shows synergic activity with AmB and FLZ (Movahed et al., 2016). As ion homeostasis is a fundamental factor in the development of fungal disease, ion chelators have been used in the treatment of fungal infections. However, synergistic activity with antifungal drugs did not result in favorable responses *in vitro* (Lai et al., 2016). Treatment of cardio-vascular disorders has been realized with calcium channel blockers, which also demonstrate antifungal activity (Yu et al., 2014). Recent work shows that the calcium channel blockers amlodipine, nifedipine, benidipine, and flunarizine present synergistic activity with FLZ in *C. albicans* isolates resistant to FLZ via a mechanism not related to efflux pump inactivation (Liu S. et al., 2016).

Natural source molecules with antifungal activity are also described as having *in vitro* synergistic activity with traditional antifungal drugs, reducing the concentration of both substances (Soares et al., 2014; Sardi et al., 2016; Wang et al., 2016). Use of the natural substance beauvericin with traditional antifungals was able to inhibit efflux pumps and morphogenesis in FLZ-resistant *C. albicans* and potentiate the action of this azole (Shekhar-Guturja et al., 2016).

## NEW ANTIFUNGAL FORMULATIONS AND NEW ANTIFUNGAL DRUG STRUCTURE MODIFICATION

Two different strategies have been developed to increase the therapeutic index of antifungal agents: chemical modifications and/or elaboration of new formulations of antifungal agents to obtain less toxic derivatives (Sheng and Zhang, 2011).

Theoretical and experimental studies on the mechanism of action of AmB and its derivatives were performed by Borowski (2000). Two generations of derivatives were developed. First-generation compounds are modified at the carboxyl group, which improves selective toxicity based on disturbance of the hydrogen bond network in complex with sterols. Second-generation compounds have introduction of a bulky substituent, resulting in an appropriate steric hindrance effect that disturbs interaction with cholesterol but not with ergosterol, leading to improved selective toxicity (Borowski, 2000). Among second-generation derivatives, *N*-methyl-*N*-D-fructosyl AMB methyl ester (MFAME) is considered the most interesting compound because it is able to form water-soluble salts, has a broad antifungal spectrum, and lower toxicity than AMB toward animal cells in *in vitro* and *in vivo* experiments (Szlinder-Richert et al., 2001).

Despite the huge effort made to decrease fungal resistance and the toxicity of AmB, the development of rational chemical modification of known antifungal agents was insufficient to solve

these problems. Thus, new delivery systems have been evaluated to reach this goal (Borowski, 2000; Sheng and Zhang, 2011).

Since 1990, nanostructured systems have been studied as carriers of antifungal agents. Clinically, the intravenous dosage form of AmB-deoxycholate has adverse effects, mainly nephrotoxicity. The synthesis of AmB analogs such as AmB esters or a preparation including an AmB lipid complex, AmB colloidal dispersion, liposomal AmB and intralipid AmB have been generated to improve the therapeutic index and lower toxicity (Gupta and Tomas, 2003; Vyas and Gupta, 2006; Voltan et al., 2016).

In addition, other delivery systems, such as carriers based on solid and nanostructure lipids, synthetic and natural polymers, inorganic and metal nanostructure lipids, dendrimers, silica, and carbon materials (magnetic nanoparticles), have been pursued. These delivery systems are able to improve bioavailability and reduce toxicity and present specificity for target tissues; however, there is an associated high cost of production (Vyas and Gupta, 2006; Sato et al., 2015; Voltan et al., 2016).

Recent work shows that the composition of nanoparticles used as delivery vehicles is fundamental for increasing antifungal activity. Ahmad et al. (2016) produced a conjugate system with AmB and metal nanoparticles that displayed synergistic antifungal activity due to the antimicrobial property of silver against *C. albicans* and *C. tropicalis*. Niemirowicz et al. (2016) reported synergistic activity for the combination of polyenes and magnetic nanoparticles. This bio-active nano-sized formulation exhibited enhanced efficiency against two clinical isolates of *Candida* species in planktonic and biofilm states.

For many years, the only available antifungal for invasive fungal infections was AmB, which has been incorporated into three lipid formulations. However, the imidazole class offers new treatment options because it is proven to be less toxic and in some cases more effective than AmB (Shalini et al., 2011). Although the imidazole class has been available for a decade, improvements in safety were necessary. Accordingly, this class was also subjected to rational chemical modifications. The triazole class was generated by the addition of a nitrogen atom to a cyclic ring. This modification provided a broad spectrum of activity as well as improved safety and pharmacokinetic profile (Allen et al., 2015). In this sense, the introduction of triazoles accelerated the pace of drug development.

New azoles have been developed to combat resistant pathogens to improve the tolerability and administration. Voriconazole is structurally similar to FLZ, with the exception of a fluoropyrimidine group in place of a triazole moiety, which leads to better bioavailability. Alternatively, posaconazole has a spectrum of antifungal activity comparable to that of voriconazole, but the molecular structure with a hydroxylated analog is similar to that of itraconazole. Currently, isavuconazole, ravuconazole, albaconazole, and efinaconazole are the four best studied agents in research aiming to identify an ideal antifungal with a wide spectrum and reliable pharmacokinetics, parenteral and oral dosage forms, and a favorable adverse effect profile (Shalini et al., 2011; Allen et al., 2015).

In addition, Moazeni et al. (2016) reported that the combination of solid lipid nanoparticles with FLZ was able to avoid recognition by efflux pump proteins, preventing extrusion when tested against FLZ-resistant *Candida* isolates. In another study, an aqueous nano-suspension of itraconazole for the treatment of bronchopulmonary aspergillosis solved pharmacokinetic problem of adequate concentration (Rundfeldt et al., 2013).

In addition to all azole agents, echinocandins are among the newest class of antifungal agents and act by inhibiting glucan synthesis in the fungal cell wall. Echinocandins are composed of a complex hexapeptide core with an *N*-terminus acylated by a long hydrophobic chain. Although echinocandins are fungicidal with good selectivity, they cannot be orally administered because of their complex lipopeptide structure. To address the limitation, several small molecule glucan synthesis inhibitors have been discovered. However, none is under clinical evaluation thus far (Sheng and Zhang, 2011; Liu N. et al., 2016).

## ANTIFUNGAL IMMUNOTHERAPY: VACCINES

Given their increasing frequency and unacceptably high morbidity and mortality rates, prevention of invasive fungal infections has become of vital importance (Spellberg, 2011; Medici and Del Poeta, 2015). Vaccination of high-risk groups is a particularly promising strategy to prevent invasive fungal infections because easily identifiable risk factors are clearly defined for many such infections (Perlroth et al., 2007; Spellberg, 2011).

Advances in our understanding of the host defense and pathogenic mechanisms underlying fungal infections has supported the development of effective vaccines to combat these diseases. Accordingly, researchers have dedicated studies to developing robust, durable and safe fungal vaccines, especially those that may be useful for endemic infections or in chronic or superimposed infections in intensive care patients (Santos and Levitz, 2014; Shahid, 2016).

Although very few clinical trials have been performed in humans, a growing number of antifungal vaccine candidates are being evaluated in pre-clinical studies. This may be due to the renewed interest in the potential use of vaccines, replacing or associated with chemotherapy, to reduce antifungal drug use and consequently limit drug resistance and toxicity.

For most active vaccines studied against invasive fungal infections, the key to protection has been the induction of cell-mediated, pro-inflammatory, Th1 or Th17 responses, which improve phagocytic killing of the fungus. It is also clear that antigens targeted for vaccination need not be restricted to virulence factors, markedly increasing the antigen repertoire available for testing. Additionally, the concept of niche vaccination of acutely at-risk patients or patients in restricted geographical areas is a new idea that opens doors in vaccinology (Spellberg, 2011).

The greatest advances in fungal vaccines are with regard to studies of invasive candidiasis, and two promising vaccines are

presently in the clinical trial phase. The first, containing the rAls3p-N antigen, is in Phase IIa and prevents fungal adhesion and invasion in immunized hosts. Protection with this vaccine has been found to largely be mediated by T cells via neutrophil recruitment and a specific antibody in vaccinated hosts (Edwards, 2012; Shahid, 2016).

The second candidal vaccine in clinical trial phase is a virosome-based vaccine containing a Sap2 antigen/truncated recombinant Sap2 antigen. The truncated form is stable, immunogenic and harmless. The Sap2 vaccine administered intra-muscularly or intra-vaginally induces systemic and 100% mucosal protective immunity (Vecchiarelli et al., 2012; Shahid, 2016).

Another important molecule that has been studied in candidiasis vaccination is heat shock protein 90 (Hsp90-CA). Raska et al. (2005) tested an Hsp90-CA DNA vaccine and found that vaccinated mice exhibited survival times prolonged by 64% compared with the untreated control. In addition, vaccination with the recombinant protein r-hsp90-CA significantly increased survival compared to the control groups.

A monoclonal antibody that binds to the immunodominant epitope of *C. albicans* Hsp90p was tested pre-clinically. A synergistic action with AMB against FLZ-sensitive and -resistant *C. albicans* strains was demonstrated in *in vivo* and *in vitro* experiments. The same antibody was used in a multicenter double-blind placebo-controlled trial of patients with invasive candidiasis, and complete mycological resolution reached 84% in the combination therapy group compared to 48% in the AMB monotherapy group. Moreover, clearance of infections in the combination therapy group was twice that of AMB therapy alone, resulting in 4 and 18% mortality, respectively (Matthews et al., 2003; Bugli et al., 2013; Wang et al., 2015).

In a different approach, *S. cerevisiae* cells were genetically engineered to display Enolase 1 (Eno1p) antigens of *C. albicans* on their surface. Oral administration of these cells could elicit an immune response and aid the survival of mice challenged with *C. albicans* (Vecchiarelli et al., 2012; Shibasaki et al., 2013; Shahid, 2016). Interestingly, by sharing some elements with *Aspergillus* species, *Candida* enolase also exerts a protective function against aspergillosis.

Studies on vaccines protective against other fungi are still in the early pre-clinical phase (Fernandes et al., 2011; Hsieh et al., 2011; Edwards, 2012; Hole and Wormley, 2012; Shahid, 2016).

For protection against aspergillosis, studies have shown that the type 1, cell-mediated immune response, which is efficient in protecting against this disease, can be induced by recombinant protein antigens from *Aspergillus*, as observed by Bozza et al. (2002). Administration of recombinant allergen Asp 16 f in conjunction with CpG oligonucleotides improved the survival of mice infected by inhaled *A. fumigatus*. Vaccination with crude antigen preparations from *A. fumigatus* was also tested, and it was observed that such vaccination improved the survival of mice infected by inhaled and intravenously administered fungi, even in those that were subsequently immunocompromised (Cenci et al., 2000; Ito and Lyons, 2002).

In the case of *Cryptococcus*, Devi et al. (1991) proposed the use of an anti-phagocytic antigen from the capsule of *C. neoformans*, glucuronoxylomannan (GMX), as a vaccine to elicit antibody-mediated protection. In a different approach, Wozniak et al. (2011) administered T-cell depleted mice, mimicking a T-cell-deficient host, with an engineered strain of *C. neoformans* that could express IFN-g. After the immunization, a secondary pulmonary infection using a pathogenic strain was produced, and the mice were protected against the infection. The results demonstrate that it is possible to generate a protective immune response to *Cryptococcus* even after becoming immunocompromised, such as in cases of HIV.

Recently, Rella et al. (2015) proposed the use of a live attenuated mutant strain lacking sterol glucosidase enzyme (Δsgl1) as a vaccine. In this study, immunization of mice with Δsgl1 cells led to strong protection against challenge with *C. neoformans* and *C. gattii* and could also elicit protective immunity in mice deficient for T CD4+ cells, a frequent condition in cryptococcosis patients.

Another possible therapeutic agent in the prophylaxis of *Cryptococcus* is glycosphingolipid glucosylceramide (GlcCer), a *C. neoformans* virulence factor. In a recently study, Mor et al. (2016) demonstrated that administration of GlcCer prior to infection with *C. neoformans* in a murine model prevented dissemination of the fungi from the lungs to the brain and led to 60% mouse survival while preventing side effects such as hepatic injury, a common and great problem in the use of the antifungal therapy currently available.

A peptide derived from the gp43 adhesin of *P. brasiliensis*, named p10, protects mice from paracoccidioidomycosis (PCM), and combination of immunization with this peptide and different antifungal drugs showed an additive protective effect. The finding suggests that this is an important molecule to be tested in clinical trials against PCM (Taborda et al., 1998; Marques et al., 2006; Marques et al., 2008; Rittner et al., 2012).

To date, few vaccines have reached the clinical stage. However, the importance of mycosis to public health around the world indicates that efforts should be given to the discovery of new molecules and compounds that can be used in the prophylaxis and treatment of these diseases. The challenges are numerous, but the efforts offer hope for controlling these diseases that tend to increase in incidence over time.

## ALTERNATIVE ANIMAL MODELS TO STUDY FUNGAL VIRULENCE AND ANTIFUNGAL DRUGS

Classically, mammalian models are considered the gold standard for drug discovery, virulence and immune response studies. However, in 1959, the concept of the "alternative animal model" was described by Burch and Russell with "the three R's: Refinement, Reduction, and Replacement" (Russell and Burch, 1959). In **Table 1** are described the three R concept and the actions required for its application. In recent decades, the use of alternative animals, also called "mini hosts" or "non-conventional animal models" have been encouraging for *in vivo* testing. Amoeba, insects, nematodes, fish and chicken embryos are used for the following reasons: (1) because the neural systems of these

animals are poorly developed, they are almost painless; (2) a large number of animals can be used for each experiment; (3) maintenance is cheaper than for traditional animals; (4) there is a good correlation between alternative animals and mammalian animals (Trevijano-Contador and Zaragoza, 2014).

Chicken embryos have been used since 1971 for fungal virulence studies (Partridge et al., 1971), and many studies have been published using this model to evaluate virulence of different fungi such as *Candida* spp., *Rhizopus,* and *A. fumigatus* (Jacobsen et al., 2010, 2011; Kaerger et al., 2015). Moreover, with this model, it is possible to evaluate the role of genes using mutants and to study the immune response of the host during infection (Jacobsen et al., 2010). Despite the importance of this model to date, experiments of antifungal efficacy have not been validated. Although chicken embryos are not consider worldwide to be living organisms and the ethical issues for this type of experimentation are less complicated, it is important to highlight that the euthanasia performed after experiments should be administered properly using anesthesia (Aleksandrowicz and Herr, 2015).

Another non-conventional model widely used for *in vivo* testing is zebrafish embryos, larvae, and adults. The main advantage is that it is possible to analyze different biological processes due to the presence of organs and systems, providing complete raw data analysis for different fields of science (MacRae and Peterson, 2015). This model was useful for studying of the *C. albicans* virulence (Chao et al., 2010; Brothers et al., 2011; Chen et al., 2015) and C. *neoformans* pathogenesis (Tenor et al., 2015). Similar to chicken embryos, there is no description thus far of the evaluation of antifungal efficacy using zebrafish. However, toxicity assays and teratogenic testing have provided important information. It is essential to highlight that after 120 h post-fertilization (hpf), ethical regulations are required for zebrafish experiments (Strähle et al., 2012).

Insects can also be used as an alternative animal model. The fruit fly *Drosophila melanogaster* is described as a model for investigating the virulence of human pathogens, due to similarities between its immune system and that of mammals, and for verifying the efficacy of novel antifungal compounds. Infection can be achieved by injection, rolling contact or ingestion (Lionakis and Kontoyiannis, 2012). Different *Candida* species have been evaluated using this model; the virulence of *C. parapsilosis* was found to be lower than that of *C. albicans*, similar to observations in humans; FLZ also increased the survival of susceptible strains (Chamilos et al., 2006). This model is also suitable for virulence evaluation of *C. neoformans* mutants (Apidianakis et al., 2004). The virulence of clinical and environmental isolates of *A. flavus* have been evaluated, as well as different mating types (Ramírez-Camejo et al., 2014). In *Drosophila melanogaster*, antifungal treatment is realized by ingestion, mixed with food. This model showed a correlation with mammalian models with regard to synergism of tacrolimus with posaconazole for the treatment of *Rhizopus oryzae* (Lewis et al., 2013). *Fusarium moniliforme* and *Scedosporium apiospermum* are able to infect *D. melanogaster*, and ingestion of food containing voriconazole increased the survival of infected flies (Lamaris et al., 2007).

*Galleria mellonella* has been described in different fields of science for numerous purposes, and the number of studies is increasing every year. Concerning virulence fungal assays, studies have been reported using *G. mellonella* as an infection model for different *Candida* species (Scorzoni et al., 2013; Frenkel et al., 2016; Moralez et al., 2016), *Cryptococcus* spp. (Benaducci et al., 2016), *Sporothrix schenckii* (Clavijo-Giraldo et al., 2016), *Paracoccidioides* spp. (Thomaz et al., 2013; Scorzoni et al., 2015), *Histoplasma capsulatum* (Thomaz et al., 2013), and *Fusarium* sp. (Coleman et al., 2011) and also for biofilm formation and behavior studies (Fuchs et al., 2010a; Benaducci et al., 2016).

The advances of this model are due to the ease of manipulation, low cost, and large range of larval incubation temperatures (25–37°C) with the possibility of mimicking the human body temperature. However, one disadvantage is that the genome is not fully sequenced, resulting in a lack of mutant strains to study host responses. Most of the work related to infection and treatment of *G. mellonella* has been via injection through one of the prolegs (Fuchs et al., 2010b). The benefit of this is that the inoculum and the treatment are controlled. *G. mellonella* is useful for *in vivo* treatment with conventional antifungal drugs (Coleman et al., 2011; de Lacorte Singulani et al., 2016), for assessing antifungal synergistic activity (Gu et al., 2016; Sangalli-Leite et al., 2016) and for evaluating the *in vivo* efficacy of new drug candidates (Browne et al., 2014).

The nematode *Caenorhabditis elegans* is been used for decades in different fields of biology. This organism has a short life cycle, produces a large number of progeny, and is transparent; moreover, the genome is fully sequenced with the possibility of studying host pathways through RNA interference (RNAi) techniques or constructing transgenic strains. *C. elegans* is maintained on agar medium and fed non-pathogenic *E. coli* (Muhammed et al., 2016). *C. elegans* is susceptible to infection by human pathogenic yeasts and filamentous fungi (Johnson et al., 2009; Pukkila-Worley et al., 2009; Desalermos et al., 2015). For this reason, this organism can be used for high-throughput screening of antifungal drugs candidates. The *C. elegans* model of infection is well described in antifungal drug discovery. A study with 1,266 compounds identified 15 anti-candidal substances that prolonged the survival of infected larvae and inhibited *in vivo* filamentation of the yeast (Breger et al., 2007). In another screen with 3,228 candidate substances, nine compounds with potential antifungal activity were identified (Okoli et al., 2009). Synergistic antifungal activity of tyrocidines and caspofungin was successfully evaluated *in vitro* and *in vivo* using *C. elegans* (Troskie et al., 2014). Moreover, *C. elegans* is a suitable model for studying the immune response because it is able to produce different antimicrobial peptides that are regulated upon infection; these peptides can also serve as new antimicrobial candidates (Ewbank and Zugasti, 2011).

Although different types of animal models are discussed here, it is important to evaluate which is the best system for each study. Regardless, although alternative models have benefits, mammalian models are still considered the gold standard, and many additional studies are necessary before the complete substitution of mammalian models for alternative animals.

At present, alternative animals are suitable for screening prior to further studies in mammals.

## CONCLUSION

Despite the increasing number of reports regarding advances in antifungal therapy, the number of cases of infection and antifungal resistance are still alarmingly high, and control of antifungal disease is far from being achieved. Important new advances have been made in the discovery of antimicrobial fungal targets; however, many years are necessary from discovery to clinical use. Because of this, improving existing molecules and developing new formulations and alternative therapy for prevention and treatment are important for treating fungal infections and increasing treatment options and quality of life.

## AUTHOR CONTRIBUTIONS

All the authors contributed selecting the topics, reviewing the literature, selecting important and atual informations. Moreover the authors read and approved the final manuscript.

## FUNDING

This work was supported by Fundação de Amparo à Pesquisa do Estado de São Paulo-FAPESP [2013/10917-9 (LS), 2015/03700-9 (MM-G), 2015/14023-8 (HdO), 2016/17048-4 (CM)], Coordenação de Aperfeiçoamento de Pessoal de Nível Superior and Programa de Apoio ao Desenvolvimento Científico da Faculdade de Ciências Farmacêuticas da UNESP and Conselho Nacional de Desenvolvimento Científico e Tecnológico 150261/2016-0 (CC-O).

## REFERENCES

Abbes, S., Mary, C., Sellami, H., Michel-Nguyen, A., Ayadi, A., and Ranque, S. (2013). Interactions between copy number and expression level of genes involved in fluconazole resistance in *Candida glabrata*. *Front. Cell Infect. Microbiol.* 3:74. doi: 10.3389/fcimb.2013.00074

Ahmad, A., Wei, Y., Syed, F., Tahir, K., Taj, R., Khan, A. U., et al. (2016). Amphotericin B-conjugated biogenic silver nanoparticles as an innovative strategy for fungal infections. *Microb. Pathog.* 99, 271–281. doi: 10.1016/j.micpath.2016.08.031

Albertson, G. D., Niimi, M., Cannon, R. D., and Jenkinson, H. F. (1996). Multiple efflux mechanisms are involved in *Candida albicans* fluconazole resistance. *Antimicrob. Agents Chemother.* 40, 2835–2841.

Al-Dhaheri, R. S., and Douglas, L. J. (2008). Absence of amphotericin B-tolerant persister cells in biofilms of some *Candida* species. *Antimicrob. Agents Chemother.* 52, 1884–1887. doi: 10.1128/AAC.01473-07AAC.01473-07

Aleksandrowicz, E., and Herr, I. (2015). Ethical euthanasia and short-term anesthesia of the chick embryo. *ALTEX* 32, 143–147.

Alem, M. A., Oteef, M. D., Flowers, T. H., and Douglas, L. J. (2006). Production of tyrosol by *Candida albicans* biofilms and its role in quorum sensing and biofilm development. *Eukaryot. Cell* 5, 1770–1779. doi: 10.1128/EC.00219-06

Allaker, R. P. (2010). The use of nanoparticles to control oral biofilm formation. *J. Dent. Res.* 89, 1175–1186. doi: 10.1177/0022034510377794002203451037779400220345103777940

Allen, D., Wilson, D., Drew, R., and Perfect, J. (2015). Azole antifungals: 35 years of invasive fungal infection management. *Expert Rev. Anti. Infect. Ther.* 13, 787–798. doi: 10.1586/14787210.2015.1032939

Anderson, T. M., Clay, M. C., Cioffi, A. G., Diaz, K. A., Hisao, G. S., Tuttle, M. D., et al. (2014). Amphotericin forms an extramembranous and fungicidal sterol sponge. *Nat. Chem. Biol.* 10, 400–406. doi: 10.1038/nchembio.1496

Apidianakis, Y., Rahme, L. G., Heitman, J., Ausubel, F. M., Calderwood, S. B., and Mylonakis, E. (2004). Challenge of *Drosophila melanogaster* with *Cryptococcus neoformans* and role of the innate immune response. *Eukaryot. Cell* 3, 413–419. doi: 10.1128/EC.3.2.413-419.2004

Arendrup, M. C. (2014). Update on antifungal resistance in *Aspergillus* and *Candida*. *Clin. Microbiol. Infect* 20(Suppl. 6), 42–48. doi: 10.1111/1469-0691.12513

Arikan, S., and Rex, J. H. (2005). "Resistance to antifungal agents," in *Topley and Wilson's Microbiology and Microbial Infec- tions: Medical Mycology,* 10th Edn, eds W.G. Merz and R. J.Hay (London: Hodder Arnold), 168–181.

Atkinson, B. J., Lewis, R. E., and Kontoyiannis, D. P. (2008). Candida lusitaniae fungemia in cancer patients: risk factors for amphotericin B failure and outcome. *Med. Mycol.* 46, 541–546. doi: 10.1080/13693780801968571

Badali, H., Vaezi, A., Haghani, I., Yazdanparast, S. A., Hedayati, M. T., Mousavi, B., et al. (2013). Environmental study of azole-resistant *Aspergillus fumigatus* with TR34/L98H mutations in the cyp51A gene in Iran. *Mycoses* 56, 659–663. doi: 10.1111/myc.12089

Baginski, M., and Czub, J. (2009). Amphotericin B and its new derivatives – mode of action. *Curr. Drug Metab.* 10, 459–469. doi: 10.2174/138920009788898019

Baillie, G. S., and Douglas, L. J. (2000). Matrix polymers of Candida biofilms and their possible role in biofilm resistance to antifungal agents. *J. Antimicrob. Chemother.* 46, 397–403. doi: 10.1093/jac/46.3.397

Balashov, S. V., Park, S., and Perlin, D. S. (2006). Assessing resistance to the echinocandin antifungal drug caspofungin in *Candida albicans* by profiling mutations in FKS1. *Antimicrob. Agents Chemother.* 50, 2058–2063. doi: 10.1128/AAC.01653-05

Barchiesi, F., Schimizzi, A. M., Caselli, F., Novelli, A., Fallani, S., Giannini, D., et al. (2000). Interactions between triazoles and amphotericin B against *Cryptococcus neoformans*. *Antimicrob. Agents Chemother.* 44, 2435–2441. doi: 10.1128/AAC.44.9.2435-2441.2000

Basso, L. R., Gast, C. E., Bruzual, I., and Wong, B. (2015). Identification and properties of plasma membrane azole efflux pumps from the pathogenic fungi *Cryptococcus gattii* and *Cryptococcus neoformans*. *J. Antimicrob. Chemother.* 70, 1396–1407. doi: 10.1093/jac/dku554

Belanger, E. S., Yang, E., and Forrest, G. N. (2015). Combination antifungal therapy: when, where, and why. *Curr. Clin. Microbiol. Rep.* 2, 67–75. doi: 10.1007/s40588-015-0017-z

Benaducci, T., Sardi, J. E. C., Lourencetti, N. M., Scorzoni, L., Gullo, F. P., Rossi, S. A., et al. (2016). Virulence of *Cryptococcus* sp. Biofilms *In Vitro* and *In Vivo* using galleria mellonella as an alternative model. *Front. Microbiol.* 7:290. doi: 10.3389/fmicb.2016.00290

Bennett, J. E., Izumikawa, K., and Marr, K. A. (2004). Mechanism of increased fluconazole resistance in *Candida glabrata* during prophylaxis. *Antimicrob. Agents Chemother.* 48, 1773–1777. doi: 10.1128/AAC.48.5.1773-1777.2004

Biel, M. A. (2010). Photodynamic therapy of bacterial and fungal biofilm infections. *Methods Mol. Biol.* 635, 175–194. doi: 10.1007/978-1-60761-697-9_13

Bink, A., Kucharikova, S., Neirinck, B., Vleugels, J., Van Dijck, P., Cammue, B. P., et al. (2012). The nonsteroidal antiinflammatory drug diclofenac potentiates the in vivo activity of caspofungin against *Candida albicans* biofilms. *J. Infect. Dis.* 206, 1790–1797. doi: 10.1093/infdis/jis594jis594

Bink, A., Vandenbosch, D., Coenye, T., Nelis, H., Cammue, B. P., and Thevissen, K. (2011). Superoxide dismutases are involved in *Candida albicans* biofilm persistence against miconazole. *Antimicrob. Agents Chemother.* 55, 4033–4037. doi: 10.1128/AAC.00280-11AAC.00280-11

Bizerra, F. C., Nakamura, C. V., de Poersch, C., Estivalet Svidzinski, T. I., Borsato Quesada, R. M., Goldenberg, S., et al. (2008). Characteristics of biofilm formation by *Candida tropicalis* and antifungal resistance. *FEMS Yeast Res.* 8, 442–450. doi: 10.1111/j.1567-1364.2007.00347.xFYR347

Blankenship, J. R., Wormley, F. L., Boyce, M. K., Schell, W. A., Filler, S. G., Perfect, J. R., et al. (2003). Calcineurin is essential for *Candida albicans* survival in serum and virulence. *Eukaryot. Cell* 2, 422–430. doi: 10.1128/EC.2.3.422-430.2003

Blatzer, M., Blum, G., Jukic, E., Posch, W., Gruber, P., Nagl, M., et al. (2015). Blocking Hsp70 enhances the efficiency of amphotericin B treatment

against resistant *Aspergillus terreus* strains. *Antimicrob. Agents Chemother.* 59, 3778–3788. doi: 10.1128/AAC.05164-14

Blum, G., Kainzner, B., Grif, K., Dietrich, H., Zelger, B., Sonnweber, T., et al. (2013). In vitro and in vivo role of heat shock protein 90 in Amphotericin B resistance of *Aspergillus terreus*. *Clin. Microbiol. Infect.* 19, 50–55. doi: 10.1111/j.1469-0691.2012.03848.x

Bondaryk, M., Kurzątkowski, W., and Staniszewska, M. (2013). Antifungal agents commonly used in the superficial and mucosal candidiasis treatment: mode of action and resistance development. *Postepy Dermatol. Alergol.* 30, 293–301. doi: 10.5114/pdia.2013.38358

Borecká-Melkusová, S., Moran, G. P., Sullivan, D. J., Kucharíková, S., Chorvát, D., and Bujdáková, H. (2009). The expression of genes involved in the ergosterol biosynthesis pathway in *Candida albicans* and *Candida dubliniensis* biofilms exposed to fluconazole. *Mycoses* 52, 118–128. doi: 10.1111/j.1439-0507.2008.01550.x

Borgers, M. (1980). Mechanism of action of antifungal drugs, with special reference to the imidazole derivatives. *Rev. Infect. Dis.* 2, 520–534. doi: 10.1093/clinids/2.4.520

Borowski, E. (2000). Novel approaches in the rational design of antifungal agents of low toxicity. *Farmaco* 55, 206–208. doi: 10.1016/S0014-827X(00)00024-0

Bosco-Borgeat, M. E., Mazza, M., Taverna, C. G., Córdoba, S., Murisengo, O. A., Vivot, W., et al. (2016). Amino acid substitution in *Cryptococcus neoformans* lanosterol 14-α-demethylase involved in fluconazole resistance in clinical isolates. *Rev. Argent Microbiol.* 48, 137–142. doi: 10.1016/j.ram.2016.03.003

Botet, J., Rodríguez-Mateos, M., Ballesta, J. P., Revuelta, J. L., and Remacha, M. (2008). A chemical genomic screen in *Saccharomyces cerevisiae* reveals a role for diphthamidation of translation elongation factor 2 in inhibition of protein synthesis by sordarin. *Antimicrob. Agents Chemother.* 52, 1623–1629. doi: 10.1128/AAC.01603-07

Bowman, S. M., and Free, S. J. (2006). The structure and synthesis of the fungal cell wall. *Bioessays* 28, 799–808. doi: 10.1002/bies.20441

Bozza, S., Gaziano, R., Lipford, G. B., Montagnoli, C., Bacci, A., Di Francesco, P., et al. (2002). Vaccination of mice against invasive aspergillosis with recombinant *Aspergillus* proteins and CpG oligodeoxynucleotides as adjuvants. *Microbes Infect.* 4, 1281–1290. doi: 10.1016/S1286-4579(02)00007-2

Breger, J., Fuchs, B. B., Aperis, G., Moy, T. I., Ausubel, F. M., and Mylonakis, E. (2007). Antifungal chemical compounds identified using a *C. elegans* pathogenicity assay. *PLoS Pathog.* 3:e18. doi: 10.1371/journal.ppat.0030018

Brothers, K. M., Newman, Z. R., and Wheeler, R. T. (2011). Live imaging of disseminated candidiasis in zebrafish reveals role of phagocyte oxidase in limiting filamentous growth. *Eukaryot. Cell* 10, 932–944. doi: 10.1128/EC.05005-11

Brown, A. J., Leach, M. D., and Nicholls, S. (2010). The relevance of heat shock regulation in fungal pathogens of humans. *Virulence* 1, 330–332. doi: 10.4161/viru.1.4.12364

Browne, N., Hackenberg, F., Streciwilk, W., Tacke, M., and Kavanagh, K. (2014). Assessment of in vivo antimicrobial activity of the carbene silver(I) acetate derivative SBC3 using *Galleria mellonella* larvae. *Biometals* 27, 745–752. doi: 10.1007/s10534-014-9766-z

Bugli, F., Cacaci, M., Martini, C., Torelli, R., Posteraro, B., Sanguinetti, M., et al. (2013). Human monoclonal antibody-based therapy in the treatment of invasive candidiasis. *Clin. Dev. Immunol.* 2013:403121. doi: 10.1155/2013/403121

Burnie, J. P., Carter, T. L., Hodgetts, S. J., and Matthews, R. C. (2006). Fungal heat-shock proteins in human disease. *FEMS Microbiol. Rev.* 30, 53–88. doi: 10.1111/j.1574-6976.2005.00001.x

Butts, A., Koselny, K., Chabrier-Roselló, Y., Semighini, C. P., Brown, J. C., Wang, X., et al. (2014). Estrogen receptor antagonists are anti-cryptococcal agents that directly bind EF hand proteins and synergize with fluconazole in vivo. *MBio* 5:e00765-13. doi: 10.1128/mBio.00765-13

Cannizzo, F. T., Eraso, E., Ezkurra, P. A., Villar-Vidal, M., Bollo, E., Castellá, G., et al. (2007). Biofilm development by clinical isolates of *Malassezia pachydermatis*. *Med. Mycol.* 45, 357–361. doi: 10.1080/13693780701225767

Cannon, R. D., Lamping, E., Holmes, A. R., Niimi, K., Baret, P. V., Keniya, M. V., et al. (2009). Efflux-mediated antifungal drug resistance. *Clin. Microbiol. Rev.* 22, 291–321. doi: 10.1128/CMR.00051-08

Cao, Y. Y., Cao, Y. B., Xu, Z., Ying, K., Li, Y., Xie, Y., et al. (2005). cDNA microarray analysis of differential gene expression in *Candida albicans* biofilm exposed to farnesol. *Antimicrob. Agents Chemother.* 49, 584–589. doi: 10.1128/AAC.49.2.584-589.2005

Carlson, R. P., Taffs, R., Davison, W. M., and Stewart, P. S. (2008). Anti-biofilm properties of chitosan-coated surfaces. *J. Biomater. Sci. Polym. Ed.* 19, 1035–1046. doi: 10.1163/156856208784909372

Cenci, E., Mencacci, A., Bacci, A., Bistoni, F., Kurup, V. P., and Romani, L. (2000). T cell vaccination in mice with invasive pulmonary aspergillosis. *J. Immunol.* 165, 381–388. doi: 10.4049/jimmunol.165.1.381

Cervelatti, E. P., Fachin, A. L., Ferreira-Nozawa, M. S., and Martinez-Rossi, N. M. (2006). Molecular cloning and characterization of a novel ABC transporter gene in the human pathogen *Trichophyton rubrum*. *Med. Mycol.* 44, 141–147. doi: 10.1080/13693780500220449

Chamilos, G., Lionakis, M. S., Lewis, R. E., Lopez-Ribot, J. L., Saville, S. P., Albert, N. D., et al. (2006). *Drosophila melanogaster* as a facile model for large-scale studies of virulence mechanisms and antifungal drug efficacy in *Candida* species. *J. Infect. Dis.* 193, 1014–1022. doi: 10.1086/500950

Chandra, J., Mukherjee, P. K., Leidich, S. D., Faddoul, F. F., Hoyer, L. L., Douglas, L. J., et al. (2001). Antifungal resistance of candidal biofilms formed on denture acrylic in vitro. *J. Dent. Res.* 80, 903–908. doi: 10.1177/00220345010800031101

Chandra, J., Patel, J. D., Li, J., Zhou, G., Mukherjee, P. K., McCormick, T. S., et al. (2005). Modification of surface properties of biomaterials influences the ability of *Candida albicans* to form biofilms. *Appl. Environ. Microbiol.* 71, 8795–8801. doi: 10.1128/AEM.71.12.8795-8801.2005

Chao, C. C., Hsu, P. C., Jen, C. F., Chen, I. H., Wang, C. H., Chan, H. C., et al. (2010). Zebrafish as a model host for *Candida albicans* infection. *Infect. Immun.* 78, 2512–2521. doi: 10.1128/IAI.01293-09

Chau, A. S., Gurnani, M., Hawkinson, R., Laverdiere, M., Cacciapuoti, A., and McNicholas, P. M. (2005). Inactivation of sterol Delta5,6-desaturase attenuates virulence in *Candida albicans*. *Antimicrob. Agents Chemother.* 49, 3646–3651. doi: 10.1128/AAC.49.9.3646-3651.2005

Chau, A. S., Mendrick, C. A., Sabatelli, F. J., Loebenberg, D., and McNicholas, P. M. (2004). Application of real-time quantitative PCR to molecular analysis of *Candida albicans* strains exhibiting reduced susceptibility to azoles. *Antimicrob. Agents Chemother.* 48, 2124–2131. doi: 10.1128/AAC.48.6.2124-2131.2004

Chen, S. H., Sheng, C. Q., Xu, X. H., Jiang, Y. Y., Zhang, W. N., and He, C. (2007). Identification of Y118 amino acid residue in *Candida albicans* sterol 14alpha-demethylase associated with the enzyme activity and selective antifungal activity of azole analogues. *Biol. Pharm. Bull.* 30, 1246–1253. doi: 10.1248/bpb.30.1246

Chen, X., Ren, B., Chen, M., Liu, M. X., Ren, W., Wang, Q. X., et al. (2014). ASDCD: antifungal synergistic drug combination database. *PLoS ONE* 9:e86499. doi: 10.1371/journal.pone.0086499

Chen, Y., Lu, Z., Zhao, J., Zou, Z., Gong, Y., Qu, F., et al. (2016). Epidemiology and molecular characterizations of azole resistance in clinical and environmental *Aspergillus fumigatus* isolates from China. *Antimicrob. Agents Chemother.* 60, 5878–5884. doi: 10.1128/AAC.01005-16

Chen, Y. L., Lehman, V. N., Lewit, Y., Averette, A. F., and Heitman, J. (2013). Calcineurin governs thermotolerance and virulence of *Cryptococcus gattii*. *G3 (Bethesda)* 3, 527–539. doi: 10.1534/g3.112.004242

Chen, Y. Z., Yang, Y. L., Chu, W. L., You, M. S., and Lo, H. J. (2015). Zebrafish egg infection model for studying *Candida albicans* adhesion factors. *PLoS ONE* 10:e0143048. doi: 10.1371/journal.pone.0143048

Cheng, S., Clancy, C. J., Nguyen, K. T., Clapp, W., and Nguyen, M. H. (2007). A *Candida albicans* petite mutant strain with uncoupled oxidative phosphorylation overexpresses MDR1 and has diminished susceptibility to fluconazole and voriconazole. *Antimicrob. Agents Chemother.* 51, 1855–1858. doi: 10.1128/AAC.00182-07

Chowdhary, A., Kathuria, S., Xu, J., Sharma, C., Sundar, G., Singh, P. K., et al. (2012). Clonal expansion and emergence of environmental multiple-triazole-resistant *Aspergillus fumigatus* strains carrying the TR34/L98H mutations in the cyp51A gene in India. *PLoS ONE* 7:e52871. doi: 10.1371/journal.pone.0052871

Chowdhary, A., Sharma, C., Hagen, F., and Meis, J. F. (2014a). Exploring azole antifungal drug resistance in *Aspergillus fumigatus* with special reference to resistance mechanisms. *Future Microbiol.* 9, 697–711. doi: 10.2217/fmb.14.27

Chowdhary, A., Sharma, C., van den Boom, M., Yntema, J. B., Hagen, F., Verweij, P. E., et al. (2014b). Multi-azole-resistant *Aspergillus fumigatus* in the environment in Tanzania. *J. Antimicrob. Chemother.* 69, 2979–2983. doi: 10.1093/jac/dku259

Clavijo-Giraldo, D. M., Matínez-Alvarez, J. A., Lopes-Bezerra, L. M., Ponce-Noyola, P., Franco, B., Almeida, R. S., et al. (2016). Analysis of *Sporothrix schenckii* sensu stricto and *Sporothrix brasiliensis* virulence in *Galleria mellonella*. *J. Microbiol. Methods* 122, 73–77. doi: 10.1016/j.mimet.2016.01.014

Coleman, J. J., Muhammed, M., Kasperkovitz, P. V., Vyas, J. M., and Mylonakis, E. (2011). *Fusarium* pathogenesis investigated using *Galleria mellonella* as a heterologous host. *Fungal Biol.* 115, 1279–1289. doi: 10.1016/j.funbio.2011.09.005

Colombo, A. L., Padovan, A. C., and Chaves, G. M. (2011). Current knowledge of *Trichosporon* spp. and Trichosporonosis. *Clin. Microbiol. Rev.* 24, 682–700. doi: 10.1128/CMR.00003-1124/4/682

Costa-Orlandi, C. B., Sardi, J. C., Santos, C. T., Fusco-Almeida, A. M., and Mendes-Giannini, M. J. (2014). in vitro characterization of *Trichophyton rubrum* and *T. mentagrophytes* biofilms. *Biofouling* 30, 719–727. doi: 10.1080/08927014.2014.919282

Coste, A., Selmecki, A., Forche, A., Diogo, D., Bougnoux, M. E., d'Enfert, C., et al. (2007). Genotypic evolution of azole resistance mechanisms in sequential *Candida albicans* isolates. *Eukaryot. Cell* 6, 1889–1904. doi: 10.1128/EC.00151-07

Cowen, L. E., Sanglard, D., Howard, S. J., Rogers, P. D., and Perlin, D. S. (2014). Mechanisms of antifungal drug resistance. *Cold Spring Harb. Perspect. Med.* 5:a019752. doi: 10.1101/cshperspect.a019752

Cushion, M. T., Collins, M. S., and Linke, M. J. (2009). Biofilm formation by *Pneumocystis* spp. *Eukaryot. Cell* 8, 197–206. doi: 10.1128/EC.00202-08EC.00202-08

da Matta, D. A., de Almeida, L. P., Machado, A. M., Azevedo, A. C., Kusano, E. J., Travassos, N. F., et al. (2007). Antifungal susceptibility of 1000 *Candida* bloodstream isolates to 5 antifungal drugs: results of a multicenter study conducted in São Paulo, Brazil, 1995-2003. *Diagn. Microbiol. Infect. Dis.* 57, 399–404. doi: 10.1016/j.diagmicrobio.2006.10.011

da Silva Ferreira, M. E., Capellaro, J. L., dos Reis Marques, E., Malavazi, I., Perlin, D., Park, S., et al. (2004). in vitro evolution of itraconazole resistance in *Aspergillus fumigatus* involves multiple mechanisms of resistance. *Antimicrob. Agents Chemother.* 48, 4405–4413. doi: 10.1128/AAC.48.11.4405-4413.2004

Davies, D. (2003). Understanding biofilm resistance to antibacterial agents. *Nat. Rev. Drug Discov.* 2, 114–122. doi: 10.1038/nrd1008nrd1008

Davis, L. E., Cook, G., and Costerton, J. W. (2002). Biofilm on ventriculo-peritoneal shunt tubing as a cause of treatment failure in coccidioidal meningitis. *Emerg. Infect. Dis.* 8, 376–379. doi: 10.3201/eid0804.010103

de Lacorte Singulani, J., Scorzoni, L., de Paula, E., Silva, A. C., Fusco-Almeida, A. M., and Mendes-Giannini, M. J. (2016). Evaluation of the efficacy of antifungal drugs against *Paracoccidioides brasiliensis* and *Paracoccidioides lutzii* in a *Galleria mellonella* model. *Int. J. Antimicrob. Agents* 48, 292–297. doi: 10.1016/j.ijantimicag.2016.05.012

de Melo, W. C., Avci, P., de Oliveira, M. N., Gupta, A., Vecchio, D., Sadasivam, M., et al. (2013). Photodynamic inactivation of biofilm: taking a lightly colored approach to stubborn infection. *Expert Rev. Anti Infect. Ther.* 11, 669–693. doi: 10.1586/14787210.2013.811861

Desalermos, A., Tan, X., Rajamuthiah, R., Arvanitis, M., Wang, Y., Li, D., et al. (2015). A multi-host approach for the systematic analysis of virulence factors in *Cryptococcus neoformans*. *J. Infect. Dis.* 211, 298–305. doi: 10.1093/infdis/jiu441

Desnos-Ollivier, M., Bretagne, S., Raoux, D., Hoinard, D., Dromer, F., Dannaoui, E., et al. (2008). Mutations in the fks1 gene in *Candida albicans*, *C. tropicalis*, and *C. krusei* correlate with elevated caspofungin MICs uncovered in AM3 medium using the method of the European Committee on Antibiotic Susceptibility Testing. *Antimicrob. Agents Chemother.* 52, 3092–3098. doi: 10.1128/AAC.00088-08

Devi, S. J., Schneerson, R., Egan, W., Ulrich, T. J., Bryla, D., Robbins, J. B., et al. (1991). *Cryptococcus neoformans* serotype A glucuronoxylomannan-protein conjugate vaccines: synthesis, characterization, and immunogenicity. *Infect. Immun.* 59, 3700–3707.

Di Bonaventura, G., Pompilio, A., Picciani, C., Iezzi, M., D'Antonio, D., and Piccolomini, R. (2006). Biofilm formation by the emerging fungal pathogen *Trichosporon asahii*: development, architecture, and antifungal resistance. *Antimicrob. Agents Chemother.* 50, 3269–3276. doi: 10.1128/AAC.00556-06

Diaz-Guerra, T. M., Mellado, E., Cuenca-Estrella, M., and Rodriguez-Tudela, J. L. (2003). A point mutation in the 14alpha-sterol demethylase gene cyp51A contributes to itraconazole resistance in *Aspergillus fumigatus*. *Antimicrob. Agents Chemother.* 47, 1120–1124. doi: 10.1128/AAC.47.3.1120-1124.2003

Dogsa, I., Brloznik, M., Stopar, D., and Mandic-Mulec, I. (2013). Exopolymer diversity and the role of levan in Bacillus subtilis biofilms. *PLoS ONE* 8:e62044. doi: 10.1371/journal.pone.0062044

Dunkel, N., Liu, T. T., Barker, K. S., Homayouni, R., Morschhäuser, J., and Rogers, P. D. (2008). A gain-of-function mutation in the transcription factor Upc2p causes upregulation of ergosterol biosynthesis genes and increased fluconazole resistance in a clinical *Candida albicans* isolate. *Eukaryot. Cell* 7, 1180–1190. doi: 10.1128/EC.00103-08

Edwards, J. E. (2012). Fungal cell wall vaccines: an update. *J. Med. Microbiol.* 61(Pt. 7), 895–903. doi: 10.1099/jmm.0.041665-0

Elefanti, A., Mouton, J. W., Verweij, P. E., Tsakris, A., Zerva, L., and Meletiadis, J. (2013). Amphotericin B- and voriconazole-echinocandin combinations against *Aspergillus* spp.: effect of serum on inhibitory and fungicidal interactions. *Antimicrob. Agents Chemother.* 57, 4656–4663. doi: 10.1128/AAC.00597-13

Enjalbert, B., and Whiteway, M. (2005). Release from quorum-sensing molecules triggers hyphal formation during *Candida albicans* resumption of growth. *Eukaryot. Cell* 4, 1203–1210. doi: 10.1128/EC.4.7.1203-1210.2005

Espinel-Ingroff, A., Pfaller, M. A., Bustamante, B., Canton, E., Fothergill, A., Fuller, J., et al. (2014). Multilaboratory study of epidemiological cutoff values for detection of resistance in eight *Candida* species to fluconazole, posaconazole, and voriconazole. *Antimicrob. Agents Chemother.* 58, 2006–2012. doi: 10.1128/AAC.02615-13

Estrela, A. B., Heck, M. G., and Abraham, W. R. (2009). Novel approaches to control biofilm infections. *Curr. Med. Chem.* 16, 1512–1530. doi: 10.2174/092986709787909640

Ewbank, J. J., and Zugasti, O. (2011). *C. elegans*: model host and tool for antimicrobial drug discovery. *Dis. Model. Mech.* 4, 300–304. doi: 10.1242/dmm.006684

Fachin, A. L., Ferreira-Nozawa, M. S., Maccheroni, W., and Martinez-Rossi, N. M. (2006). Role of the ABC transporter TruMDR2 in terbinafine, 4-nitroquinoline N-oxide and ethidium bromide susceptibility in *Trichophyton rubrum*. *J. Med. Microbiol.* 55(Pt 8), 1093–1099. doi: 10.1099/jmm.0.46522-0

Fanning, S., and Mitchell, A. P. (2012). Fungal biofilms. *PLoS Pathog.* 8:e1002585. doi: 10.1371/journal.ppat.1002585PPATHOGENS-D-11-02842

Favel, A., Michel-Nguyen, A., Peyron, F., Martin, C., Thomachot, L., Datry, A., et al. (2003). Colony morphology switching of *Candida lusitaniae* and acquisition of multidrug resistance during treatment of a renal infection in a newborn: case report and review of the literature. *Diagn. Microbiol. Infect. Dis.* 47, 331–339. doi: 10.1016/S0732-8893(03)00094-4

Fernandes, V. C., Coitinho, J. B., Veloso, J. M., Araújo, S. A., Pedroso, E. P., and Goes, A. M. (2011). Combined use of *Paracoccidioides brasiliensis* recombinant rPb27 and rPb40 antigens in an enzyme-linked immunosorbent assay for immunodiagnosis of paracoccidioidomycosis. *J. Immunol. Methods* 367, 78–84. doi: 10.1016/j.jim.2011.02.006

Ferreira, G. F., Baltazar, L. E. M., Santos, J. R., Monteiro, A. S., Fraga, L. A., Resende-Stoianoff, M. A., et al. (2013). The role of oxidative and nitrosative bursts caused by azoles and amphotericin B against the fungal pathogen *Cryptococcus gattii*. *J. Antimicrob. Chemother.* 68, 1801–1811. doi: 10.1093/jac/dkt114

Figueredo, L. A., Cafarchia, C., Desantis, S., and Otranto, D. (2012). Biofilm formation of *Malassezia pachydermatis* from dogs. *Vet. Microbiol.* 160, 126–131. doi: 10.1016/j.vetmic.2012.05.012

Finkel, J. S., and Mitchell, A. P. (2011). Genetic control of *Candida albicans* biofilm development. *Nat. Rev. Microbiol.* 9, 109–118. doi: 10.1038/nrmicro2475nrmicro2475

Flemming, H. C., and Wingender, J. (2010). The biofilm matrix. *Nat. Rev. Microbiol.* 8, 623–633. doi: 10.1038/nrmicro2415nrmicro2415

Franz, R., Kelly, S. L., Lamb, D. C., Kelly, D. E., Ruhnke, M., and Morschhäuser, J. (1998). Multiple molecular mechanisms contribute to a stepwise development of fluconazole resistance in clinical *Candida albicans* strains. *Antimicrob. Agents Chemother.* 42, 3065–3072.

Frenkel, M., Mandelblat, M., Alastruey-Izquierdo, A., Mendlovic, S., Semis, R., and Segal, E. (2016). Pathogenicity of *Candida albicans* isolates from bloodstream and mucosal candidiasis assessed in mice and *Galleria mellonella*. *J. Mycol. Med.* 26, 1–8. doi: 10.1016/j.mycmed.2015.12.006

Fuchs, B. B., Eby, J., Nobile, C. J., El Khoury, J. B., Mitchell, A. P., and Mylonakis, E. (2010a). Role of filamentation in *Galleria mellonella* killing by *Candida albicans*. *Microbes Infect.* 12, 488–496. doi: 10.1016/j.micinf.2010.03.001

Fuchs, B. B., O'Brien, E., Khoury, J. B., and Mylonakis, E. (2010b). Methods for using *Galleria mellonella* as a model host to study fungal pathogenesis. *Virulence* 1, 475–482. doi: 10.4161/viru.1.6.12985

Gao, Y., Li, H., Liu, S., Zhang, X., and Sun, S. (2014). Synergistic effect of fluconazole and doxycycline against *Candida albicans* biofilms resulting from calcium fluctuation and downregulation of fluconazole-inducible efflux pump gene overexpression. *J. Med. Microbiol.* 63(Pt. 7), 956–961. doi: 10.1099/jmm.0.072421-0jmm.0.072421-0

Gao, Y., Zhang, C., Lu, C., Liu, P., Li, Y., Li, H., et al. (2013). Synergistic effect of doxycycline and fluconazole against *Candida albicans* biofilms and the impact of calcium channel blockers. *FEMS Yeast Res.* 13, 453–462. doi: 10.1111/1567-1364.12048

Garcia-Effron, G., Chua, D. J., Tomada, J. R., DiPersio, J., Perlin, D. S., Ghannoum, M., et al. (2010). Novel FKS mutations associated with echinocandin resistance in *Candida* species. *Antimicrob. Agents Chemother.* 54, 2225–2227. doi: 10.1128/AAC.00998-09

Garcia-Effron, G., Katiyar, S. K., Park, S., Edlind, T. D., and Perlin, D. S. (2008). A naturally occurring proline-to-alanine amino acid change in Fks1p in *Candida parapsilosis*, *Candida orthopsilosis*, and *Candida metapsilosis* accounts for reduced echinocandin susceptibility. *Antimicrob. Agents Chemother.* 52, 2305–2312. doi: 10.1128/AAC.00262-08

Garcia-Effron, G., Lee, S., Park, S., Cleary, J. D., and Perlin, D. S. (2009). Effect of *Candida glabrata* FKS1 and FKS2 mutations on echinocandin sensitivity and kinetics of 1,3-beta-D-glucan synthase: implication for the existing susceptibility breakpoint. *Antimicrob. Agents Chemother.* 53, 3690–3699. doi: 10.1128/AAC.00443-09

Gaur, M., Puri, N., Manoharlal, R., Rai, V., Mukhopadhayay, G., Choudhury, D., et al. (2008). MFS transportome of the human pathogenic yeast *Candida albicans*. *BMC Genomics* 9:579. doi: 10.1186/1471-2164-9-579

Gee, S. F., Joly, S., Soll, D. R., Meis, J. F., Verweij, P. E., Polacheck, I., et al. (2002). Identification of four distinct genotypes of *Candida dubliniensis* and detection of microevolution in vitro and in vivo. *J. Clin. Microbiol.* 40, 556–574. doi: 10.1128/JCM.40.2.556-574.2002

Ghannoum, M. (2016). Azole resistance in dermatophytes: prevalence and mechanism of action. *J. Am. Podiatr. Med. Assoc.* 106, 79–86. doi: 10.7547/14-109

Goldman, G. H., da Silva, Ferreira, M. E., dos Reis, Marques, E., Savoldi, M., et al. (2004). Evaluation of fluconazole resistance mechanisms in *Candida albicans* clinical isolates from HIV-infected patients in Brazil. *Diagn. Microbiol. Infect. Dis.* 50, 25–32. doi: 10.1016/j.diagmicrobio.2004.04.009

Gonçalves, S. S., Souza, A. C., Chowdhary, A., Meis, J. F., and Colombo, A. L. (2016). Epidemiology and molecular mechanisms of antifungal resistance in *Candida* and *Aspergillus*. *Mycoses* doi: 10.1111/myc.12469 [Epub ahead of print].

Grossman, N. T., Pham, C. D., Cleveland, A. A., and Lockhart, S. R. (2015). Molecular mechanisms of fluconazole resistance in *Candida parapsilosis* isolates from a U.S. surveillance system. *Antimicrob. Agents Chemother.* 59, 1030–1037. doi: 10.1128/AAC.04613-14

Gu, W., Guo, D., Zhang, L., Xu, D., and Sun, S. (2016). Synergistic effect of azoles and fluoxetine against resistant *Candida albicans* attributed to attenuating fungal virulence. *Antimicrob. Agents Chemother.* 60, 6179–6188. doi: 10.1128/AAC.03046-15

Guinea, J., Sánchez-Somolinos, M., Cuevas, O., Peláez, T., and Bouza, E. (2006). Fluconazole resistance mechanisms in *Candida krusei*: the contribution of efflux-pumps. *Med. Mycol.* 44, 575–578. doi: 10.1080/13693780600561544

Gupta, A. K., and Tomas, E. (2003). New antifungal agents. *Dermatol. Clin.* 21, 565–576. doi: 10.1016/S0733-8635(03)00024-X

Hiller, D., Sanglard, D., and Morschhäuser, J. (2006). Overexpression of the MDR1 gene is sufficient to confer increased resistance to toxic compounds in *Candida albicans*. *Antimicrob. Agents Chemother.* 50, 1365–1371. doi: 10.1128/AAC.50.4.1365-1371.2006

Hinrichsen, S. L., Falcão, E., Vilella, T. A., Colombo, A. L., Nucci, M., Moura, L., et al. (2008). Candidemia in a tertiary hospital in northeastern Brazil. *Rev. Soc. Bras. Med. Trop.* 41, 394–398. doi: 10.1590/S0037-86822008000400014

Hole, C. R., and Wormley, F. L. (2012). Vaccine and immunotherapeutic approaches for the prevention of cryptococcosis: lessons learned from animal models. *Front. Microbiol.* 3:291. doi: 10.3389/fmicb.2012.00291

Hope, W. W., Tabernero, L., Denning, D. W., and Anderson, M. J. (2004). Molecular mechanisms of primary resistance to flucytosine in *Candida albicans*. *Antimicrob. Agents Chemother.* 48, 4377–4386. doi: 10.1128/AAC.48.11.4377-4386.2004

Hornby, J. M., Jensen, E. C., Lisec, A. D., Tasto, J. J., Jahnke, B., Shoemaker, R., et al. (2001). Quorum sensing in the dimorphic fungus *Candida albicans* is mediated by farnesol. *Appl. Environ. Microbiol.* 67, 2982–2992. doi: 10.1128/AEM.67.7.2982-2992.2001

Howard, S. J., Cerar, D., Anderson, M. J., Albarrag, A., Fisher, M. C., Pasqualotto, A. C., et al. (2009). Frequency and evolution of Azole resistance in *Aspergillus fumigatus* associated with treatment failure. *Emerg. Infect. Dis.* 15, 1068–1076. doi: 10.3201/eid1507.090043

Hsieh, S. H., Lin, J. S., Huang, J. H., Wu, S. Y., Chu, C. L., Kung, J. T., et al. (2011). Immunization with apoptotic phagocytes containing *Histoplasma capsulatum* activates functional CD8(+) T cells to protect against histoplasmosis. *Infect. Immun.* 79, 4493–4502. doi: 10.1128/IAI.05350-11

Huang, W., Liao, G., Baker, G. M., Wang, Y., Lau, R., Paderu, P., et al. (2016). Lipid flippase subunit Cdc50 mediates drug resistance and virulence in *Cryptococcus neoformans*. *MBio* 7:e00478-16. doi: 10.1128/mBio.00478-16

Ito, J. I., and Lyons, J. M. (2002). Vaccination of corticosteroid immunosuppressed mice against invasive pulmonary aspergillosis. *J. Infect. Dis.* 186, 869–871. doi: 10.1086/342509

Jacob, T. R., Peres, N. T., Martins, M. P., Lang, E. A., Sanches, P. R., Rossi, A., et al. (2015). Heat shock protein 90 (Hsp90) as a molecular target for the development of novel drugs against the dermatophyte *Trichophyton rubrum*. *Front. Microbiol.* 6:1241. doi: 10.3389/fmicb.2015.01241

Jacobsen, I. D., Grosse, K., Berndt, A., and Hube, B. (2011). Pathogenesis of *Candida albicans* infections in the alternative chorio-allantoic membrane chicken embryo model resembles systemic murine infections. *PLoS ONE* 6:e19741. doi: 10.1371/journal.pone.0019741

Jacobsen, I. D., Grosse, K., Slesiona, S., Hube, B., Berndt, A., and Brock, M. (2010). Embryonated eggs as an alternative infection model to investigate *Aspergillus fumigatus* virulence. *Infect. Immun.* 78, 2995–3006. doi: 10.1128/IAI.00268-10

Jensen-Pergakes, K. L., Kennedy, M. A., Lees, N. D., Barbuch, R., Koegel, C., and Bard, M. (1998). Sequencing, disruption, and characterization of the *Candida albicans* sterol methyltransferase (ERG6) gene: drug susceptibility studies in erg6 mutants. *Antimicrob. Agents Chemother.* 42, 1160–1167.

Jia, N., Arthington-Skaggs, B., Lee, W., Pierson, C. A., Lees, N. D., Eckstein, J., et al. (2002). *Candida albicans* sterol C-14 reductase, encoded by the ERG24 gene, as a potential antifungal target site. *Antimicrob. Agents Chemother.* 46, 947–957. doi: 10.1128/AAC.46.4.947-957.2002

Jiang, C., Dong, D., Yu, B., Cai, G., Wang, X., Ji, Y., et al. (2013). Mechanisms of azole resistance in 52 clinical isolates of *Candida tropicalis* in China. *J. Antimicrob. Chemother.* 68, 778–785. doi: 10.1093/jac/dks481

Johnson, C. H., Ayyadevara, S., McEwen, J. E., and Shmookler Reis, R. J. (2009). *Histoplasma capsulatum* and *Caenorhabditis elegans*: a simple nematode model for an innate immune response to fungal infection. *Med. Mycol.* 47, 808–813. doi: 10.3109/13693780802660532

Johnson, M. D., MacDougall, C., Ostrosky-Zeichner, L., Perfect, J. R., and Rex, J. H. (2004). Combination antifungal therapy. *Antimicrob. Agents Chemother.* 48, 693–715. doi: 10.1128/AAC.48.3.693-715.2004

Justice, M. C., Hsu, M. J., Tse, B., Ku, T., Balkovec, J., Schmatz, D., et al. (1998). Elongation factor 2 as a novel target for selective inhibition of fungal protein synthesis. *J. Biol. Chem.* 273, 3148–3151. doi: 10.1074/jbc.273.6.3148

Juvvadi, P. R., Lee, S. C., Heitman, J., and Steinbach, W. J. (2016). Calcineurin in fungal virulence and drug resistance: prospects for harnessing targeted inhibition of calcineurin for an antifungal therapeutic approach. *Virulence* doi: 10.1080/21505594.2016.1201250 [Epub ahead of print].

Kaerger, K., Schwartze, V. U., Dolatabadi, S., Nyilasi, I., Kovács, S. A., Binder, U., et al. (2015). Adaptation to thermotolerance in *Rhizopus* coincides with virulence as revealed by avian and invertebrate infection models, phylogeny, physiological and metabolic flexibility. *Virulence* 6, 395–403. doi: 10.1080/21505594.2015.1029219

Kanafani, Z. A., and Perfect, J. R. (2008). Antimicrobial resistance: resistance to antifungal agents: mechanisms and clinical impact. *Clin. Infect. Dis.* 46, 120–128. doi: 10.1086/524071

Kathiravan, M. K., Salake, A. B., Chothe, A. S., Dudhe, P. B., Watode, R. P., Mukta, M. S., et al. (2012). The biology and chemistry of antifungal agents: a review. *Bioorg. Med. Chem.* 20, 5678–5698. doi: 10.1016/j.bmc.2012.04.045S0968-0896(12)00329-X

Katiyar, S. K., and Edlind, T. D. (2001). Identification and expression of multidrug resistance-related ABC transporter genes in *Candida krusei*. *Med. Mycol.* 39, 109–116. doi: 10.1080/mmy.39.1.109.116

Katiyar, S. K., and Edlind, T. D. (2009). Role for Fks1 in the intrinsic echinocandin resistance of *Fusarium solani* as evidenced by hybrid expression in *Saccharomyces cerevisiae*. *Antimicrob. Agents Chemother.* 53, 1772–1778. doi: 10.1128/AAC.00020-09

Katragkou, A., McCarthy, M., Meletiadis, J., Petraitis, V., Moradi, P. W., Strauss, G. E., et al. (2014). In vitro combination of isavuconazole with micafungin or amphotericin B deoxycholate against medically important molds. *Antimicrob. Agents Chemother.* 58, 6934–6937. doi: 10.1128/AAC.03261-14

Kaur, S., and Singh, S. (2014). Biofilm formation by *Aspergillus fumigatus*. *Med. Mycol.* 52, 2–9. doi: 10.3109/13693786.2013.81959213693786.2013.819592

Kelly, S. L., Lamb, D. C., Kelly, D. E., Manning, N. J., Loeffler, J., Hebart, H., et al. (1997). Resistance to fluconazole and cross-resistance to amphotericin B in *Candida albicans* from AIDS patients caused by defective sterol delta5,6-desaturation. *FEBS Lett.* 400, 80–82. doi: 10.1016/S0014-5793(96)01360-9

Kelly, S. L., Lamb, D. C., Taylor, M., Corran, A. J., Baldwin, B. C., and Powderly, W. G. (1994). Resistance to amphotericin B associated with defective sterol delta 8–>7 isomerase in a *Cryptococcus neoformans* strain from an AIDS patient. *FEMS Microbiol. Lett.* 122, 39–42. doi: 10.1111/j.1574-6968.1994.tb07140.x

Keniya, M. V., Fleischer, E., Klinger, A., Cannon, R. D., and Monk, B. C. (2015). Inhibitors of the *Candida albicans* major facilitator superfamily transporter Mdr1p responsible for fluconazole resistance. *PLoS ONE* 10:e0126350. doi: 10.1371/journal.pone.0126350

Khot, P. D., Suci, P. A., Miller, R. L., Nelson, R. D., and Tyler, B. J. (2006). A small subpopulation of blastospores in *Candida albicans* biofilms exhibit resistance to amphotericin B associated with differential regulation of ergosterol and beta-1,6-glucan pathway genes. *Antimicrob. Agents Chemother.* 50, 3708–3716. doi: 10.1128/AAC.00997-06

Kirkpatrick, W. R., Perea, S., Coco, B. J., and Patterson, T. F. (2002). Efficacy of caspofungin alone and in combination with voriconazole in a Guinea pig model of invasive aspergillosis. *Antimicrob. Agents Chemother.* 46, 2564–2568. doi: 10.1128/AAC.46.8.2564-2568.2002

Kucharikova, S., Sharma, N., Spriet, I., Maertens, J., Van Dijck, P., and Lagrou, K. (2013). Activities of systemically administered echinocandins against in vivo mature *Candida albicans* biofilms developed in a rat subcutaneous model. *Antimicrob. Agents Chemother.* 57, 2365–2368. doi: 10.1128/AAC.02288-12AAC.02288-12

Kuhn, D. M., George, T., Chandra, J., Mukherjee, P. K., and Ghannoum, M. A. (2002). Antifungal susceptibility of *Candida* biofilms: unique efficacy of amphotericin B lipid formulations and echinocandins. *Antimicrob. Agents Chemother.* 46, 1773–1780. doi: 10.1128/AAC.46.6.1773-1780.2002

LaFleur, M. D., Kumamoto, C. A., and Lewis, K. (2006). *Candida albicans* biofilms produce antifungal-tolerant persister cells. *Antimicrob. Agents Chemother.* 50, 3839–3846. doi: 10.1128/AAC.00684-06

Lai, Y. W., Campbell, L. T., Wilkins, M. R., Pang, C. N., Chen, S., and Carter, D. A. (2016). Synergy and antagonism between iron chelators and antifungal drugs in *Cryptococcus*. *Int. J. Antimicrob. Agents* 48, 388–394. doi: 10.1016/j.ijantimicag.2016.06.012

Lamaris, G. A., Chamilos, G., Lewis, R. E., and Kontoyiannis, D. P. (2007). Virulence studies of *Scedosporium* and *Fusarium* species in *Drosophila* melanogaster. *J. Infect. Dis.* 196, 1860–1864. doi: 10.1086/523765

Lamb, D. C., Kelly, D. E., White, T. C., and Kelly, S. L. (2000). The R467K amino acid substitution in *Candida albicans* sterol 14alpha-demethylase causes drug resistance through reduced affinity. *Antimicrob. Agents Chemother.* 44, 63–67. doi: 10.1128/AAC.44.1.63-67.2000

Lamping, E., Ranchod, A., Nakamura, K., Tyndall, J. D., Niimi, K., Holmes, A. R., et al. (2009). Abc1p is a multidrug efflux transporter that tips the balance in favor of innate azole resistance in *Candida krusei*. *Antimicrob. Agents Chemother.* 53, 354–369. doi: 10.1128/AAC.01095-08

Lass-Florl, C., Speth, C., Kofler, G., Dierich, M. P., Gunsilius, E., and Wurzner, R. (2003). Effect of increasing inoculum sizes of *Aspergillus* hyphae on MICs and MFCs of antifungal agents by broth microdilution method. *Int. J. Antimicrob. Agents* 21, 229–233. doi: 10.1016/S0924-8579(02)00189-9

Leber, R., Fuchsbichler, S., Klobucníková, V., Schweighofer, N., Pitters, E., Wohlfarter, K., et al. (2003). Molecular mechanism of terbinafine resistance in *Saccharomyces cerevisiae*. *Antimicrob. Agents Chemother.* 47, 3890–3900. doi: 10.1128/AAC.47.12.3890-3900.2003

Leonardelli, F., Macedo, D., Dudiuk, C., Cabeza, M. S., Gamarra, S., and Garcia-Effron, G. (2016). *Aspergillus fumigatus* intrinsic fluconazole resistance is due to the naturally occurring T301I substitution in Cyp51Ap. *Antimicrob. Agents Chemother.* 60, 5420–5426. doi: 10.1128/AAC.00905-16

Lewis, K. (2001). Riddle of biofilm resistance. *Antimicrob. Agents Chemother.* 45, 999–1007. doi: 10.1128/AAC.45.4.999-1007.2001

Lewis, K. (2007). Persister cells, dormancy and infectious disease. *Nat. Rev. Microbiol.* 5, 48–56. doi: 10.1038/nrmicro1557

Lewis, K. (2010). Persister cells. *Annu. Rev. Microbiol.* 64, 357–372. doi: 10.1146/annurev.micro.112408.134306

Lewis, R. E., Ben-Ami, R., Best, L., Albert, N., Walsh, T. J., and Kontoyiannis, D. P. (2013). Tacrolimus enhances the potency of posaconazole against *Rhizopus oryzae* in vitro and in an experimental model of mucormycosis. *J. Infect. Dis.* 207, 834–841. doi: 10.1093/infdis/jis767

Lionakis, M. S., and Kontoyiannis, D. P. (2012). Drosophila melanogaster as a model organism for invasive aspergillosis. *Methods Mol. Biol.* 845, 455–468. doi: 10.1007/978-1-61779-539-8_32

Liu, N., Wang, C., Su, H., Zhang, W., and Sheng, C. (2016). Strategies in the discovery of novel antifungal scaffolds. *Future Med Chem* 8, 1435–1454. doi: 10.4155/fmc-2016-0020

Liu, S., Yue, L., Gu, W., Li, X., Zhang, L., and Sun, S. (2016). Synergistic Effect of Fluconazole and Calcium Channel Blockers against Resistant *Candida albicans*. *PLoS ONE* 11:e0150859. doi: 10.1371/journal.pone.0150859

Lockhart, S. R., Frade, J. P., Etienne, K. A., Pfaller, M. A., Diekema, D. J., and Balajee, S. A. (2011). Azole resistance in *Aspergillus fumigatus* isolates from the ARTEMIS global surveillance study is primarily due to the TR/L98H mutation in the cyp51A gene. *Antimicrob. Agents Chemother.* 55, 4465–4468. doi: 10.1128/AAC.00185-11

Lopez-Ribot, J. L., McAtee, R. K., Lee, L. N., Kirkpatrick, W. R., White, T. C., Sanglard, D., et al. (1998). Distinct patterns of gene expression associated with development of fluconazole resistance in serial *candida albicans* isolates from human immunodeficiency virus-infected patients with oropharyngeal candidiasis. *Antimicrob. Agents Chemother.* 42, 2932–2937.

Louie, A., Kaw, P., Banerjee, P., Liu, W., Chen, G., and Miller, M. H. (2001). Impact of the order of initiation of fluconazole and amphotericin B in sequential or combination therapy on killing of *Candida albicans In Vitro* and in a rabbit model of endocarditis and pyelonephritis. *Antimicrob. Agents Chemother.* 45, 485–494. doi: 10.1128/AAC.45.2.485-494.2001

MacRae, C. A., and Peterson, R. T. (2015). Zebrafish as tools for drug discovery. *Nat. Rev. Drug Discov.* 14, 721–731. doi: 10.1038/nrd4627

Maertens, J. A. (2004). History of the development of azole derivatives. *Clin. Microbiol. Infect.* 10(Suppl. 1), 1–10. doi: 10.1111/j.1470-9465.2004.00841.x

Maligie, M. A., and Selitrennikoff, C. P. (2005). *Cryptococcus neoformans* resistance to echinocandins: (1,3)beta-glucan synthase activity is sensitive to echinocandins. *Antimicrob. Agents Chemother.* 49, 2851–2856. doi: 10.1128/AAC.49.7.2851-2856.2005

Mann, P. A., Parmegiani, R. M., Wei, S. Q., Mendrick, C. A., Li, X., Loebenberg, D., et al. (2003). Mutations in *Aspergillus fumigatus* resulting in reduced susceptibility to posaconazole appear to be restricted to a single amino acid in the cytochrome P450 14alpha-demethylase. *Antimicrob. Agents Chemother.* 47, 577–581. doi: 10.1128/AAC.47.2.577-581.2003

Marques, A. F., da Silva, M. B., Juliano, M. A., Munhõz, J. E., Travassos, L. R., and Taborda, C. P. (2008). Additive effect of P10 immunization and chemotherapy in anergic mice challenged intratracheally with virulent yeasts of *Paracoccidioides brasiliensis*. *Microbes Infect.* 10, 1251–1258. doi: 10.1016/j.micinf.2008.07.027

Marques, A. F., da Silva, M. B., Juliano, M. A., Travassos, L. R., and Taborda, C. P. (2006). Peptide immunization as an adjuvant to chemotherapy in

mice challenged intratracheally with virulent yeast cells of *Paracoccidioides brasiliensis*. *Antimicrob. Agents Chemother.* 50, 2814–2819. doi: 10.1128/AAC.00220-06

Marr, K. A., Schlamm, H. T., Herbrecht, R., Rottinghaus, S. T., Bow, E. J., Cornely, O. A., et al. (2015). Combination antifungal therapy for invasive aspergillosis: a randomized trial. *Ann. Intern. Med.* 162, 81–89. doi: 10.7326/M13-2508

Martel, C. M., Parker, J. E., Bader, O., Weig, M., Gross, U., Warrilow, A. G., et al. (2010). Identification and characterization of four azole-resistant erg3 mutants of *Candida albicans*. *Antimicrob. Agents Chemother.* 54, 4527–4533. doi: 10.1128/AAC.00348-10

Martinez, L. R., and Casadevall, A. (2007). *Cryptococcus neoformans* biofilm formation depends on surface support and carbon source and reduces fungal cell susceptibility to heat, cold, and UV light. *Appl. Environ. Microbiol.* 73, 4592–4601. doi: 10.1128/AEM.02506-06

Martins, M., Uppuluri, P., Thomas, D. P., Cleary, I. A., Henriques, M., Lopez-Ribot, J. L., et al. (2010). Presence of extracellular DNA in the *Candida albicans* biofilm matrix and its contribution to biofilms. *Mycopathologia* 169, 323–331. doi: 10.1007/s11046-009-9264-y

Martins, M. P., Franceschini, A. C., Jacob, T. R., Rossi, A., and Martinez-Rossi, N. M. (2016). Compensatory expression of multidrug-resistance genes encoding ABC transporters in dermatophytes. *J. Med. Microbiol.* 65, 605–610. doi: 10.1099/jmm.0.000268

Matthews, R. C., Rigg, G., Hodgetts, S., Carter, T., Chapman, C., Gregory, C., et al. (2003). Preclinical assessment of the efficacy of mycograb, a human recombinant antibody against fungal HSP90. *Antimicrob. Agents Chemother.* 47, 2208–2216. doi: 10.1128/AAC.47.7.2208-2216.2003

Medici, N. P., and Del Poeta, M. (2015). New insights on the development of fungal vaccines: from immunity to recent challenges. *Mem. Inst. Oswaldo Cruz* 110, 966–973. doi: 10.1590/0074-02760150335

Mesa-Arango, A. C., Scorzoni, L., and Zaragoza, O. (2012). It only takes one to do many jobs: amphotericin B as antifungal and immunomodulatory drug. *Front. Microbiol.* 3:286. doi: 10.3389/fmicb.2012.00286

Mesa-Arango, A. C., Trevijano-Contador, N., Román, E., Sánchez-Fresneda, R., Casas, C., Herrero, E., et al. (2014). The production of reactive oxygen species is a universal action mechanism of Amphotericin B against pathogenic yeasts and contributes to the fungicidal effect of this drug. *Antimicrob. Agents Chemother.* 58, 6627–6638. doi: 10.1128/AAC.03570-14

Minari, A., Hachem, R., and Raad, I. (2001). *Candida lusitaniae*: a cause of breakthrough fungemia in cancer patients. *Clin. Infect. Dis.* 32, 186–190. doi: 10.1086/318473

Mitchell, K. F., Taff, H. T., Cuevas, M. A., Reinicke, E. L., Sanchez, H., and Andes, D. R. (2013). Role of matrix β-1,3 glucan in antifungal resistance of non-albicans *Candida* biofilms. *Antimicrob. Agents Chemother.* 57, 1918–1920. doi: 10.1128/AAC.02378-12Sz

Moazeni, M., Kelidari, H. R., Saeedi, M., Morteza-Semnani, K., Nabili, M., Gohar, A. A., et al. (2016). Time to overcome fluconazole resistant *Candida* isolates: solid lipid nanoparticles as a novel antifungal drug delivery system. *Colloids Surf. B Biointerfaces* 142, 400–407. doi: 10.1016/j.colsurfb.2016.03.013

Mor, V., Farnoud, A. M., Singh, A., Rella, A., Tanno, H., Ishii, K., et al. (2016). Glucosylceramide administration as a vaccination strategy in mouse models of Cryptococcosis. *PLoS ONE* 11:e0153853. doi: 10.1371/journal.pone.0153853

Moralez, A. T., Perini, H. F., Furlaneto-Maia, L., Almeida, R. S., Panagio, L. A., and Furlaneto, M. C. (2016). Phenotypic switching of *Candida tropicalis* is associated with cell damage in epithelial cells and virulence in *Galleria mellonella* model. *Virulence* 7, 379–386. doi: 10.1080/21505594.2016.1140297

Moran, G. P., Sanglard, D., Donnelly, S. M., Shanley, D. B., Sullivan, D. J., and Coleman, D. C. (1998). Identification and expression of multidrug transporters responsible for fluconazole resistance in *Candida dubliniensis*. *Antimicrob. Agents Chemother.* 42, 1819–1830.

Morio, F., Loge, C., Besse, B., Hennequin, C., and Le Pape, P. (2010). Screening for amino acid substitutions in the *Candida albicans* Erg11 protein of azole-susceptible and azole-resistant clinical isolates: new substitutions and a review of the literature. *Diagn. Microbiol. Infect. Dis.* 66, 373–384. doi: 10.1016/j.diagmicrobio.2009.11.006

Morio, F., Pagniez, F., Lacroix, C., Miegeville, M., and Le Pape, P. (2012). Amino acid substitutions in the *Candida albicans* sterol Δ5,6-desaturase (Erg3p) confer azole resistance: characterization of two novel mutants with impaired virulence. *J. Antimicrob. Chemother.* 67, 2131–2138. doi: 10.1093/jac/dks186

Morozov, A. A., and Likhoshway, Y. V. (2016). Evolutionary history of the chitin synthases of eukaryotes. *Glycobiology* 26, 635–639. doi: 10.1093/glycob/cww018

Morschhäuser, J. (2002). The genetic basis of fluconazole resistance development in *Candida albicans*. *Biochim. Biophys. Acta* 1587, 240–248. doi: 10.1016/S0925-4439(02)00087-X

Movahed, E., Tan, G. M., Munusamy, K., Yeow, T. C., Tay, S. T., Wong, W. F., et al. (2016). Triclosan demonstrates synergic effect with amphotericin B and fluconazole and Induces apoptosis-like cell death in *Cryptococcus neoformans*. *Front. Microbiol.* 7:360. doi: 10.3389/fmicb.2016.00360

Mowat, E., Williams, C., Jones, B., McChlery, S., and Ramage, G. (2009). The characteristics of *Aspergillus fumigatus* mycetoma development: is this a biofilm? *Med. Mycol.* 47(Suppl. 1), S120–S126. doi: 10.1080/13693780802238834

Muhammed, M., Arvanitis, M., and Mylonakis, E. (2016). Whole animal HTS of small molecules for antifungal compounds. *Expert Opin. Drug Discov.* 11, 177–184. doi: 10.1517/17460441.2016.1122591

Mukherjee, P. K., Chandra, J., Kuhn, D. M., and Ghannoum, M. A. (2003). Mechanism of fluconazole resistance in *Candida albicans* biofilms: phase-specific role of efflux pumps and membrane sterols. *Infect. Immun.* 71, 4333–4340. doi: 10.1128/IAI.71.8.4333-4340.2003

Mukherjee, P. K., Long, L., Kim, H. G., and Ghannoum, M. A. (2009). Amphotericin B lipid complex is efficacious in the treatment of *Candida albicans* biofilms using a model of catheter-associated *Candida* biofilms. *Int. J. Antimicrob. Agents* 33, 149–153. doi: 10.1016/j.ijantimicag.2008.07.030S0924-8579(08)00367-1

Nailis, H., Vandenbosch, D., Deforce, D., Nelis, H. J., and Coenye, T. (2010). Transcriptional response to fluconazole and amphotericin B in *Candida albicans* biofilms. *Res. Microbiol.* 161, 284–292. doi: 10.1016/j.resmic.2010.02.004

Nett, J. E., Crawford, K., Marchillo, K., and Andes, D. R. (2010a). Role of Fks1p and matrix glucan in *Candida albicans* biofilm resistance to an echinocandin, pyrimidine, and polyene. *Antimicrob. Agents Chemother.* 54, 3505–3508. doi: 10.1128/AAC.00227-10AAC.00227-10

Nett, J. E., Lepak, A. J., Marchillo, K., and Andes, D. R. (2009). Time course global gene expression analysis of an in vivo *Candida* biofilm. *J. Infect. Dis.* 200, 307–313. doi: 10.1086/599838

Nett, J. E., Sanchez, H., Cain, M. T., and Andes, D. R. (2010b). Genetic basis of *Candida* biofilm resistance due to drug-sequestering matrix glucan. *J. Infect. Dis.* 202, 171–175. doi: 10.1086/651200

Ngo, H. X., Garneau-Tsodikova, S., and Green, K. D. (2016). A complex game of hide and seek: the search for new antifungals. *Medchemcomm* 7, 1285–1306. doi: 10.1039/C6MD00222F

Niemirowicz, K., Durnaś, B., Tokajuk, G., Głuszek, K., Wilczewska, A. Z., Misztalewska, I., et al. (2016). Magnetic nanoparticles as a drug delivery system that enhance fungicidal activity of polyene antibiotics. *Nanomedicine* 12, 2395–2404. doi: 10.1016/j.nano.2016.07.006

Odds, F. C., Brown, A. J., and Gow, N. A. (2003). Antifungal agents: mechanisms of action. *Trends Microbiol.* 11, 272–279. doi: 10.1016/S0966-842X(03)00117-3

Odom, A. R. (2014). The triphenylethylenes, a novel class of antifungals. *MBio* 5, e1126–e1114. doi: 10.1128/mBio.01126-14

Okoli, I., Coleman, J. J., Tampakakis, E., Tempakakis, E., An, W. F., Holson, E., et al. (2009). Identification of antifungal compounds active against *Candida albicans* using an improved high-throughput *Caenorhabditis elegans* assay. *PLoS ONE* 4:e7025. doi: 10.1371/journal.pone.0007025

Pagano, L., Cornely, O. A., Busca, A., Caira, M., Cesaro, S., Gasbarrino, C., et al. (2013). Combined antifungal approach for the treatment of invasive mucormycosis in patients with hematologic diseases: a report from the SEIFEM and FUNGISCOPE registries. *Haematologica* 98, e127–e130. doi: 10.3324/haematol.2012.083063

Paião, F. G., Segato, F., Cursino-Santos, J. R., Peres, N. T., and Martinez-Rossi, N. M. (2007). Analysis of *Trichophyton rubrum* gene expression in response to cytotoxic drugs. *FEMS Microbiol. Lett.* 271, 180–186. doi: 10.1111/j.1574-6968.2007.00710.x

Papon, N., Noël, T., Florent, M., Gibot-Leclerc, S., Jean, D., Chastin, C., et al. (2007). Molecular mechanism of flucytosine resistance in *Candida lusitaniae*: contribution of the FCY2, FCY1, and FUR1 genes to 5-fluorouracil and fluconazole cross-resistance. *Antimicrob. Agents Chemother.* 51, 369–371. doi: 10.1128/AAC.00824-06

Park, S., Kelly, R., Kahn, J. N., Robles, J., Hsu, M. J., Register, E., et al. (2005). Specific substitutions in the echinocandin target Fks1p account for reduced susceptibility of rare laboratory and clinical *Candida* sp. isolates. *Antimicrob. Agents Chemother.* 49, 3264–3273. doi: 10.1128/AAC.49.8.3264-3273.2005

Partridge, B. M., Athar, M. A., and Winner, H. I. (1971). Chick embryo inoculation as a pathogenicity test for *Candida* species. *J. Clin. Pathol.* 24, 645–648. doi: 10.1136/jcp.24.7.645

Perea, S., López-Ribot, J. L., Kirkpatrick, W. R., McAtee, R. K., Santillán, R. A., Martínez, M., et al. (2001). Prevalence of molecular mechanisms of resistance to azole antifungal agents in *Candida albicans* strains displaying high-level fluconazole resistance isolated from human immunodeficiency virus-infected patients. *Antimicrob. Agents Chemother.* 45, 2676–2684. doi: 10.1128/AAC.45.10.2676-2684.2001

Perea, S., López-Ribot, J. L., Wickes, B. L., Kirkpatrick, W. R., Dib, O. P., Bachmann, S. P., et al. (2002). Molecular mechanisms of fluconazole resistance in *Candida dubliniensis* isolates from human immunodeficiency virus-infected patients with oropharyngeal candidiasis. *Antimicrob. Agents Chemother.* 46, 1695–1703. doi: 10.1128/AAC.46.6.1695-1703.2002

Perfect, J. R., Dismukes, W. E., Dromer, F., Goldman, D. L., Graybill, J. R., Hamill, R. J., et al. (2010). Clinical practice guidelines for the management of cryptococcal disease: 2010 update by the infectious diseases society of america. *Clin. Infect. Dis.* 50, 291–322. doi: 10.1086/649858

Perlin, D. S. (2007). Resistance to echinocandin-class antifungal drugs. *Drug Resist. Updat.* 10, 121–130. doi: 10.1016/j.drup.2007.04.002

Perlin, D. S. (2015). Echinocandin resistance in *Candida*. *Clin. Infect. Dis.* 61(Suppl. 6), S612–S617. doi: 10.1093/cid/civ791

Perlroth, J., Choi, B., and Spellberg, B. (2007). Nosocomial fungal infections: epidemiology, diagnosis, and treatment. *Med. Mycol.* 45, 321–346. doi: 10.1080/13693780701218689

Perumal, P., Mekala, S., and Chaffin, W. L. (2007). Role for cell density in antifungal drug resistance in *Candida albicans* biofilms. *Antimicrob. Agents Chemother.* 51, 2454–2463. doi: 10.1128/AAC.01237-06

Pfaller, M. A., and Diekema, D. J. (2007). Epidemiology of invasive candidiasis: a persistent public health problem. *Clin. Microbiol. Rev.* 20, 133–163. doi: 10.1128/CMR.00029-06

Pham, C. D., Bolden, C. B., Kuykendall, R. J., and Lockhart, S. R. (2014). Development of a Luminex-based multiplex assay for detection of mutations conferring resistance to Echinocandins in *Candida glabrata*. *J. Clin. Microbiol.* 52, 790–795. doi: 10.1128/JCM.03378-13

Pinjon, E., Moran, G. P., Jackson, C. J., Kelly, S. L., Sanglard, D., Coleman, D. C., et al. (2003). Molecular mechanisms of itraconazole resistance in *Candida dubliniensis*. *Antimicrob. Agents Chemother.* 47, 2424–2437. doi: 10.1128/AAC.47.8.2424-2437.2003

Pires, R. H., Santos, J. M., Zaia, J. E., Martins, C. H., and Mendes-Giannini, M. J. (2011). *Candida parapsilosis* complex water isolates from a haemodialysis unit: biofilm production and *in vitro* evaluation of the use of clinical antifungals. *Mem. Inst. Oswaldo Cruz* 106, 646–654. doi: 10.1590/S0074-02762011000600002

Pitangui, N. S., Sardi, J. C., Silva, J. F., Benaducci, T., Moraes da Silva, R. A., Rodríguez-Arellanes, G., et al. (2012). Adhesion of *Histoplasma capsulatum* to pneumocytes and biofilm formation on an abiotic surface. *Biofouling* 28, 711–718. doi: 10.1080/08927014.2012.703659

Plaine, A., Walker, L., Da Costa, G., Mora-Montes, H. M., McKinnon, A., Gow, N. A., et al. (2008). Functional analysis of *Candida albicans* GPI-anchored proteins: roles in cell wall integrity and caspofungin sensitivity. *Fungal Genet. Biol.* 45, 1404–1414. doi: 10.1016/j.fgb.2008.08.003

Polak, A., and Scholer, H. J. (1975). Mode of action of 5-fluorocytosine and mechanisms of resistance. *Chemotherapy* 21, 113–130. doi: 10.1159/000221854

Posteraro, B., Sanguinetti, M., Sanglard, D., La Sorda, M., Boccia, S., Romano, L., et al. (2003). Identification and characterization of a *Cryptococcus neoformans* ATP binding cassette (ABC) transporter-encoding gene, CnAFR1, involved in the resistance to fluconazole. *Mol. Microbiol.* 47, 357–371.

Prasad, R., and Goffeau, A. (2012). Yeast ATP-binding cassette transporters conferring multidrug resistance. *Annu. Rev. Microbiol.* 66, 39–63. doi: 10.1146/annurev-micro-092611-150111

Prasad, R., and Rawal, M. K. (2014). Efflux pump proteins in antifungal resistance. *Front. Pharmacol.* 5:202. doi: 10.3389/fphar.2014.00202

Pukkila-Worley, R., Peleg, A. Y., Tampakakis, E., and Mylonakis, E. (2009). *Candida albicans* hyphal formation and virulence assessed using a *Caenorhabditis elegans* infection model. *Eukaryot. Cell* 8, 1750–1758. doi: 10.1128/EC.00163-09

Raad, I. I., Zakhem, A. E., Helou, G. E., Jiang, Y., Kontoyiannis, D. P., and Hachem, R. (2015). Clinical experience of the use of voriconazole, caspofungin or the combination in primary and salvage therapy of invasive aspergillosis in haematological malignancies. *Int. J. Antimicrob. Agents* 45, 283–288. doi: 10.1016/j.ijantimicag.2014.08.012

Rajendran, R., Mowat, E., McCulloch, E., Lappin, D. F., Jones, B., Lang, S., et al. (2011). Azole resistance of *Aspergillus fumigatus* biofilms is partly associated with efflux pump activity. *Antimicrob. Agents Chemother.* 55, 2092–2097. doi: 10.1128/AAC.01189-10AAC.01189-10

Ramage, G., Bachmann, S., Patterson, T. F., Wickes, B. L., and Lopez-Ribot, J. L. (2002). Investigation of multidrug efflux pumps in relation to fluconazole resistance in *Candida albicans* biofilms. *J. Antimicrob. Chemother.* 49, 973–980. doi: 10.1093/jac/dkf049

Ramage, G., Jose, A., Sherry, L., Lappin, D. F., Jones, B., and Williams, C. (2013). Liposomal amphotericin B displays rapid dose-dependent activity against *Candida albicans* biofilms. *Antimicrob. Agents Chemother.* 57, 2369–2371. doi: 10.1128/AAC.02344-12AAC.02344-12

Ramage, G., Mowat, E., Jones, B., Williams, C., and Lopez-Ribot, J. (2009). Our current understanding of fungal biofilms. *Crit. Rev. Microbiol.* 35, 340–355. doi: 10.3109/10408410903241436

Ramage, G., Rajendran, R., Sherry, L., and Williams, C. (2012). Fungal biofilm resistance. *Int. J. Microbiol.* 2012:528521. doi: 10.1155/2012/528521

Ramage, G., Vande Walle, K., Wickes, B. L., and Lopez-Ribot, J. L. (2001). Standardized method for in vitro antifungal susceptibility testing of *Candida albicans* biofilms. *Antimicrob. Agents Chemother.* 45, 2475–2479. doi: 10.1128/AAC.45.9.2475-2479.2001

Ramage, G., Wickes, B. L., and Lopez-Ribot, J. L. (2008). A seed and feed model for the formation of *Candida albicans* biofilms under flow conditions using an improved modified Robbins device. *Rev. Iberoam. Micol.* 25, 37–40. doi: 10.1016/S1130-1406(08)70009-3

Ramasamy, M., Lee, J. H., and Lee, J. (2016). Potent antimicrobial and antibiofilm activities of bacteriogenically synthesized gold-silver nanoparticles against pathogenic bacteria and their physiochemical characterizations. *J. Biomater. Appl.* 31, 366–378. doi: 10.1177/0885328216646910085328216646910

Ramírez-Camejo, L. A., Torres-Ocampo, A. P., Agosto-Rivera, J. L., and Bayman, P. (2014). An opportunistic human pathogen on the fly: strains of *Aspergillus flavus* vary in virulence in *Drosophila melanogaster*. *Med. Mycol.* 52, 211–219. doi: 10.1093/mmy/myt008

Raska, M., Beláková, J., Wudattu, N. K., Kafková, L., Rùzicková, K., Sebestová, M., et al. (2005). Comparison of protective effect of protein and DNA vaccines hsp90 in murine model of systemic candidiasis. *Folia Microbiol. (Praha)* 50, 77–82. doi: 10.1007/BF02931297

Redding, S. W., Kirkpatrick, W. R., Coco, B. J., Sadkowski, L., Fothergill, A. W., Rinaldi, M. G., et al. (2002). *Candida glabrata* oropharyngeal candidiasis in patients receiving radiation treatment for head and neck cancer. *J. Clin. Microbiol.* 40, 1879–1881. doi: 10.1128/JCM.40.5.1879-1881.2002

Rella, A., Mor, V., Farnoud, A. M., Singh, A., Shamseddine, A. A., Ivanova, E., et al. (2015). Role of Sterylglucosidase 1 (Sgl1) on the pathogenicity of *Cryptococcus neoformans*: potential applications for vaccine development. *Front. Microbiol.* 6:836. doi: 10.3389/fmicb.2015.00836

Ricardo, E., Miranda, I. M., Faria-Ramos, I., Silva, R. M., Rodrigues, A. G., and Pina-Vaz, C. (2014). In vivo and in vitro acquisition of resistance to voriconazole by *Candida krusei*. *Antimicrob. Agents Chemother.* 58, 4604–4611. doi: 10.1128/AAC.02603-14

Rittner, G. M., Muñoz, J. E., Marques, A. F., Nosanchuk, J. D., Taborda, C. P., and Travassos, L. R. (2012). Therapeutic DNA vaccine encoding peptide P10 against experimental paracoccidioidomycosis. *PLoS Negl. Trop. Dis.* 6:e1519. doi: 10.1371/journal.pntd.0001519

Rocha, E. M., Garcia-Effron, G., Park, S., and Perlin, D. S. (2007). A Ser678Pro substitution in Fks1p confers resistance to echinocandin drugs in *Aspergillus fumigatus*. *Antimicrob. Agents Chemother.* 51, 4174–4176. doi: 10.1128/AAC.00917-07

Rodero, L., Mellado, E., Rodriguez, A. C., Salve, A., Guelfand, L., Cahn, P., et al. (2003). G484S amino acid substitution in lanosterol 14-alpha demethylase

(ERG11) is related to fluconazole resistance in a recurrent *Cryptococcus neoformans* clinical isolate. *Antimicrob. Agents Chemother.* 47, 3653–3656. doi: 10.1128/AAC.47.11.3653-3656.2003

Rogers, T. R. (2006). Antifungal drug resistance: limited data, dramatic impact? *Int. J. Antimicrob. Agents* 27(Suppl. 1), 7–11. doi: 10.1016/j.ijantimicag.2006.03.012

Rossignol, T., Ding, C., Guida, A., d'Enfert, C., Higgins, D. G., and Butler, G. (2009). Correlation between biofilm formation and the hypoxic response in *Candida parapsilosis*. *Eukaryot. Cell* 8, 550–559. doi: 10.1128/EC.00350-08EC.00350-08

Rundfeldt, C., Steckel, H., Scherliess, H., Wyska, E., and Wlaź, P. (2013). Inhalable highly concentrated itraconazole nanosuspension for the treatment of bronchopulmonary aspergillosis. *Eur. J. Pharm. Biopharm.* 83, 44–53. doi: 10.1016/j.ejpb.2012.09.018

Russell, W., and Burch, R. (1959). *The Principles of Humane Experimental Technique*. London: Methuen Publishing.

Sangalli-Leite, F., Scorzoni, L., Alves de Paula, E., Silva, A. C., da Silva, J. F., de Oliveira, H. C., et al. (2016). Synergistic effect of pedalitin and amphotericin B against *Cryptococcus neoformans* by in vitro and in vivo evaluation. *Int. J. Antimicrob. Agents* 48, 504–511. doi: 10.1016/j.ijantimicag.2016.07.025

Sangalli-Leite, F., Scorzoni, L., Cecilia Mesa-Arango, A., Casas, C., Herrero, E., Mendes Gianinni, M. J. S., et al. (2011). Amphotericin B mediates killing in *Cryptococcus neoformans* through the induction of a strong oxidative burst. *Microbes Infect.* 13, 457–467. doi: 10.1016/j.micinf.2011.01.015

Sanglard, D. (2002). Resistance of human fungal pathogens to antifungal drugs. *Curr. Opin. Microbiol.* 5, 379–385. doi: 10.1016/S1369-5274(02)00344-2

Sanglard, D. (2016). Emerging threats in antifungal-resistant fungal pathogens. *Front. Med. (Lausanne)* 3:11. doi: 10.3389/fmed.2016.00011

Sanglard, D., Coste, A., and Ferrari, S. (2009). Antifungal drug resistance mechanisms in fungal pathogens from the perspective of transcriptional gene regulation. *FEMS Yeast Res.* 9, 1029–1050. doi: 10.1111/j.1567-1364.2009.00578.x

Sanglard, D., Ischer, F., Calabrese, D., Majcherczyk, P. A., and Bille, J. (1999). The ATP binding cassette transporter gene CgCDR1 from *Candida glabrata* is involved in the resistance of clinical isolates to azole antifungal agents. *Antimicrob. Agents Chemother.* 43, 2753–2765.

Sanglard, D., Ischer, F., Koymans, L., and Bille, J. (1998). Amino acid substitutions in the cytochrome P-450 lanosterol 14alpha-demethylase (CYP51A1) from azole-resistant *Candida albicans* clinical isolates contribute to resistance to azole antifungal agents. *Antimicrob. Agents Chemother.* 42, 241–253.

Sanglard, D., Ischer, F., Monod, M., and Bille, J. (1997). Cloning of *Candida albicans* genes conferring resistance to azole antifungal agents: characterization of CDR2, a new multidrug ABC transporter gene. *Microbiology* 143(Pt 2), 405–416. doi: 10.1099/00221287-143-2-405

Sanglard, D., Kuchler, K., Ischer, F., Pagani, J. L., Monod, M., and Bille, J. (1995). Mechanisms of resistance to azole antifungal agents in *Candida albicans* isolates from AIDS patients involve specific multidrug transporters. *Antimicrob. Agents Chemother.* 39, 2378–2386. doi: 10.1128/AAC.39.11.2378

Sanglard, D., and Odds, F. C. (2002). Resistance of *Candida* species to antifungal agents: molecular mechanisms and clinical consequences. *Lancet Infect. Dis.* 2, 73–85. doi: 10.1016/S1473-3099(02)00181-0

Sanguinetti, M., Posteraro, B., Fiori, B., Ranno, S., Torelli, R., and Fadda, G. (2005). Mechanisms of azole resistance in clinical isolates of *Candida glabrata* collected during a hospital survey of antifungal resistance. *Antimicrob. Agents Chemother.* 49, 668–679. doi: 10.1128/AAC.49.2.668-679.2005

Sanguinetti, M., Posteraro, B., La Sorda, M., Torelli, R., Fiori, B., Santangelo, R., et al. (2006). Role of AFR1, an ABC transporter-encoding gene, in the in vivo response to fluconazole and virulence of *Cryptococcus neoformans*. *Infect. Immun.* 74, 1352–1359. doi: 10.1128/IAI.74.2.1352-1359.2006

Santos, E., and Levitz, S. M. (2014). Fungal vaccines and immunotherapeutics. *Cold Spring Harb. Perspect. Med.* 4:a019711. doi: 10.1101/cshperspect.a019711

Sardi, J. C., Gullo, F. P., Freires, I. A., Pitangui, N. S., Segalla, M. P., Fusco-Almeida, A. M., et al. (2016). Synthesis, antifungal activity of caffeic acid derivative esters, and their synergism with fluconazole and nystatin against *Candida* spp. *Diagn. Microbiol. Infect. Dis.* 86, 387–391. doi: 10.1016/j.diagmicrobio.2016.08.002

Sardi, J. E. C., Pitangui, N. E. S., Voltan, A. R., Braz, J. D., Machado, M. P., Fusco Almeida, A. M., et al. (2015). In vitro *Paracoccidioides brasiliensis* biofilm and gene expression of adhesins and hydrolytic enzymes. *Virulence* 6, 642–651. doi: 10.1080/21505594.2015.1031437

Sato, M. R., da Silva, P. B., de Souza, R. A., dos Santos, K. C., and Chorilli, M. (2015). Recent advances in nanoparticle carriers for coordination complexes. *Curr. Top. Med. Chem* 15, 287–297. doi: 10.2174/1568026615666150108145614

Saville, S. P., Lazzell, A. L., Monteagudo, C., and Lopez-Ribot, J. L. (2003). Engineered control of cell morphology in vivo reveals distinct roles for yeast and filamentous forms of *Candida albicans* during infection. *Eukaryot. Cell* 2, 1053–1060. doi: 10.1128/EC.2.5.1053-1060.2003

Scheid, L. A., Mario, D. A., Kubiça, T. F., Santurio, J. M., and Alves, S. H. (2012). In vitro activities of antifungal agents alone and in combination against fluconazole-susceptible and -resistant strains of *Candida dubliniensis*. *Braz. J. Infect. Dis.* 16, 78–81. doi: 10.1016/S1413-8670(12)70279-9

Scorzoni, L., de Lucas, M. P., Mesa-Arango, A. C., Fusco-Almeida, A. M., Lozano, E., Cuenca-Estrella, M., et al. (2013). Antifungal efficacy during *Candida krusei* infection in non-conventional models correlates with the yeast in vitro susceptibility profile. *PLoS ONE* 8:e60047. doi: 10.1371/journal.pone.0060047

Scorzoni, L., de Paula, E., Silva, A. C., Singulani, J. L., Leite, F. S., de Oliveira, H. C., et al. (2015). Comparison of virulence between *Paracoccidioides brasiliensis* and *Paracoccidioides lutzi*i using *Galleria mellonella* as a host model. *Virulence* 6, 766–776. doi: 10.1080/21505594.2015.1085277

Selmecki, A., Forche, A., and Berman, J. (2006). Aneuploidy and isochromosome formation in drug-resistant *Candida albicans*. *Science* 313, 367–370. doi: 10.1126/science.1128242

Semighini, C. P., Hornby, J. M., Dumitru, R., Nickerson, K. W., and Harris, S. D. (2006). Farnesol-induced apoptosis in *Aspergillus nidulans* reveals a possible mechanism for antagonistic interactions between fungi. *Mol. Microbiol.* 59, 753–764. doi: 10.1111/j.1365-2958.2005.04976.x

Semighini, C. P., Murray, N., and Harris, S. D. (2008). Inhibition of *Fusarium graminearum* growth and development by farnesol. *FEMS Microbiol. Lett.* 279, 259–264. doi: 10.1111/j.1574-6968.2007.01042.xFML1042

Seneviratne, C. J., Jin, L., and Samaranayake, L. P. (2008). Biofilm lifestyle of *Candida*: a mini review. *Oral Dis.* 14, 582–590. doi: 10.1111/j.1601-0825.2007.01424.xODI1424

Seyedmousavi, S., Hashemi, S. J., Zibafar, E., Zoll, J., Hedayati, M. T., Mouton, J. W., et al. (2013). Azole-resistant *Aspergillus fumigatus*. *Iran. Emerg. Infect. Dis.* 19, 832–834. doi: 10.3201/eid1905.130075

Shahid, S. K. (2016). Newer patents in antimycotic therapy. *Pharm. Pat. Anal.* 5, 115–134. doi: 10.4155/ppa-2015-0001

Shalini, K., Kumar, N., Drabu, S., and Sharma, P. K. (2011). Advances in synthetic approach to and antifungal activity of triazoles. *Beilstein J. Org. Chem.* 7, 668–677. doi: 10.3762/bjoc.7.79

Sheikh, N., Jahagirdar, V., Kothadia, S., and Nagoba, B. (2013). Antifungal drug resistance in *Candida* species. *Eur. J. Gen. Med.* 10, 254–258.

Shekhar-Guturja, T., Tebung, W. A., Mount, H., Liu, N., Köhler, J. R., Whiteway, M., et al. (2016). Beauvericin potentiates azole activity via inhibition of multidrug efflux, blocks *C. albicans* morphogenesis, and is effluxed via Yor1 and circuitry controlled by Zcf29. *Antimicrob. Agents Chemother.* 60, 7468–7480. doi: 10.1128/AAC.01959-16

Sheng, C., and Zhang, W. (2011). New lead structures in antifungal drug discovery. *Curr. Med. Chem.* 18, 733–766. doi: 10.2174/092986711794480113

Shibasaki, S., Aoki, W., Nomura, T., Miyoshi, A., Tafuku, S., Sewaki, T., et al. (2013). An oral vaccine against candidiasis generated by a yeast molecular display system. *Pathog. Dis.* 69, 262–268. doi: 10.1111/2049-632X.12068

Shinde, R. B., Chauhan, N. M., Raut, J. S., and Karuppayil, S. M. (2012). Sensitization of *Candida albicans* biofilms to various antifungal drugs by cyclosporine A. *Ann. Clin. Microbiol. Antimicrob.* 11:27. doi: 10.1186/1476-0711-11-271476-0711-11-27

Shukla, P. K., Singh, P., Yadav, R. K., Pandey, S., and Bhunia, S. S. (2016). *Past, Present, and Future of Antifungal Drug Development*. Berlin: Springer.

Singh, R., Shivaprakash, M. R., and Chakrabarti, A. (2011). Biofilm formation by zygomycetes: quantification, structure and matrix composition. *Microbiology* 157(Pt 9), 2611–2618. doi: 10.1099/mic.0.048504-0

Sionov, E., Chang, Y. C., Garraffo, H. M., Dolan, M. A., Ghannoum, M. A., and Kwon-Chung, K. J. (2012). Identification of a *Cryptococcus neoformans* cytochrome P450 lanosterol 14α-demethylase (Erg11) residue critical for differential susceptibility between fluconazole/voriconazole and itraconazole/posaconazole. *Antimicrob. Agents Chemother.* 56, 1162–1169. doi: 10.1128/AAC.05502-11

Sionov, E., Lee, H., Chang, Y. C., and Kwon-Chung, K. J. (2010). *Cryptococcus neoformans* overcomes stress of azole drugs by formation of disomy in specific multiple chromosomes. *PLoS Pathog.* 6:e1000848. doi: 10.1371/journal.ppat.1000848

Slaven, J. W., Anderson, M. J., Sanglard, D., Dixon, G. K., Bille, J., Roberts, I. S., et al. (2002). Increased expression of a novel *Aspergillus fumigatus* ABC transporter gene, atrF, in the presence of itraconazole in an itraconazole resistant clinical isolate. *Fungal Genet. Biol.* 36, 199–206. doi: 10.1016/S1087-1845(02)00016-6

Soares, L. A., Gullo, F. P., Sardi, J. E. C., Pitangui, N. E. S., Costa-Orlandi, C. B., Sangalli-Leite, F., et al. (2014). Anti-trichophyton activity of protocatechuates and their synergism with fluconazole. *Evid. Based Complement. Alternat. Med.* 2014:957860. doi: 10.1155/2014/957860

Sokol-Anderson, M. L., Brajtburg, J., and Medoff, G. (1986). Amphotericin B-induced oxidative damage and killing of *Candida albicans*. *J. Infect. Dis.* 154, 76–83. doi: 10.1093/infdis/154.1.76

Song, J., Zhai, P., Zhang, Y., Zhang, C., Sang, H., Han, G., et al. (2016). The *Aspergillus fumigatus* damage resistance protein family coordinately regulates ergosterol biosynthesis and azole susceptibility. *MBio* 7:e01919-15. doi: 10.1128/mBio.01919-15

Song, J. C., and Stevens, D. A. (2016). Caspofungin: pharmacodynamics, pharmacokinetics, clinical uses and treatment outcomes. *Crit. Rev. Microbiol.* 42, 813–846. doi: 10.3109/1040841X.2015.1068271

Song, J. W., Shin, J. H., Kee, S. J., Kim, S. H., Shin, M. G., Suh, S. P., et al. (2009). Expression of CgCDR1, CgCDR2, and CgERG11 in *Candida glabrata* biofilms formed by bloodstream isolates. *Med. Mycol.* 47, 545–548. doi: 10.1080/13693780802210726795279371

Song, M. H., Lee, J. W., Kim, M. S., Yoon, J. K., White, T. C., Floyd, A., et al. (2012). A flucytosine-responsive Mbp1/Swi4-like protein, Mbs1, plays pleiotropic roles in antifungal drug resistance, stress response, and virulence of *Cryptococcus neoformans*. *Eukaryot. Cell* 11, 53–67. doi: 10.1128/EC.05236-11

Souza, A. C., Fuchs, B. B., Pinhati, H. M., Siqueira, R. A., Hagen, F., Meis, J. F., et al. (2015). *Candida parapsilosis* resistance to fluconazole: molecular mechanisms and in vivo impact in infected *Galleria mellonella* larvae. *Antimicrob. Agents Chemother.* 59, 6581–6587. doi: 10.1128/AAC.01177-15

Spellberg, B. (2011). Vaccines for invasive fungal infections. *F1000 Med. Rep.* 3:13. doi: 10.3410/M3-13

Steinbach, W. J., Cramer, R. A., Perfect, B. Z., Asfaw, Y. G., Sauer, T. C., Najvar, L. K., et al. (2006). Calcineurin controls growth, morphology, and pathogenicity in *Aspergillus fumigatus*. *Eukaryot. Cell* 5, 1091–1103. doi: 10.1128/EC.00139-06

Strähle, U., Scholz, S., Geisler, R., Greiner, P., Hollert, H., Rastegar, S., et al. (2012). Zebrafish embryos as an alternative to animal experiments–a commentary on the definition of the onset of protected life stages in animal welfare regulations. *Reprod. Toxicol.* 33, 128–132. doi: 10.1016/j.reprotox.2011.06.121

Sun, J., Li, Z., Chu, H., Guo, J., Jiang, G., and Qi, Q. (2016). *Candida albicans* amphotericin B-tolerant persister formation is closely related to surface adhesion. *Mycopathologia* 181, 41–49. doi: 10.1007/s11046-015-9894-110.1007/s11046-015-9894-1

Sundriyal, S., Sharma, R. K., and Jain, R. (2006). Current advances in antifungal targets and drug development. *Curr. Med. Chem.* 13, 1321–1335. doi: 10.2174/092986706776873023

Sutherland, I. (2001). Biofilm exopolysaccharides: a strong and sticky framework. *Microbiology* 147(Pt 1), 3–9. doi: 10.1099/00221287-147-1-3

Szlinder-Richert, J., Mazerski, J., Cybulska, B., Grzybowska, J., and Borowski, E. (2001). MFAME, N-methyl-N-D-fructosyl amphotericin B methyl ester, a new amphotericin B derivative of low toxicity: relationship between self-association and effects on red blood cells. *Biochim. Biophys. Acta* 1528, 15–24. doi: 10.1016/S0304-4165(01)00166-0

Taborda, C. P., Juliano, M. A., Puccia, R., Franco, M., and Travassos, L. R. (1998). Mapping of the T-cell epitope in the major 43-kilodalton glycoprotein of *Paracoccidioides brasiliensis* which induces a Th-1 response protective against fungal infection in BALB/c mice. *Infect. Immun.* 66, 786–793.

Taff, H. T., Nett, J. E., Zarnowski, R., Ross, K. M., Sanchez, H., Cain, M. T., et al. (2012). A *Candida* biofilm-induced pathway for matrix glucan delivery: implications for drug resistance. *PLoS Pathog.* 8:e1002848. doi: 10.1371/journal.ppat.1002848

Taraszkiewicz, A., Fila, G., Grinholc, M., and Nakonieczna, J. (2013). Innovative strategies to overcome biofilm resistance. *Biomed. Res. Int.* 2013:150653. doi: 10.1155/2013/150653

Tatsumi, Y., Nagashima, M., Shibanushi, T., Iwata, A., Kangawa, Y., Inui, F., et al. (2013). Mechanism of action of efinaconazole, a novel triazole antifungal agent. *Antimicrob. Agents Chemother.* 57, 2405–2409. doi: 10.1128/AAC.02063-12

Tenor, J. L., Oehlers, S. H., Yang, J. L., Tobin, D. M., and Perfect, J. R. (2015). Live imaging of host-parasite interactions in a zebrafish infection model reveals cryptococcal determinants of virulence and central nervous system invasion. *MBio* 6:e01425-15. doi: 10.1128/mBio.01425-15

Thomaz, L., García-Rodas, R., Guimarães, A. J., Taborda, C. P., Zaragoza, O., and Nosanchuk, J. D. (2013). *Galleria mellonella* as a model host to study *Paracoccidioides lutzii* and *Histoplasma capsulatum*. *Virulence* 4, 139–146. doi: 10.4161/viru.23047

Trevijano-Contador, N., and Zaragoza, O. (2014). Expanding the use of alternative models to investigate novel aspects of immunity to microbial pathogens. *Virulence* 5, 454–456. doi: 10.4161/viru.28775

Troskie, A. M., Rautenbach, M., Delattin, N., Vosloo, J. A., Dathe, M., Cammue, B. P., et al. (2014). Synergistic activity of the tyrocidines, antimicrobial cyclodecapeptides from *Bacillus* aneurinolyticus, with amphotericin B and caspofungin against *Candida albicans* biofilms. *Antimicrob. Agents Chemother.* 58, 3697–3707. doi: 10.1128/AAC.02381-14

Uppuluri, P., Chaturvedi, A. K., Srinivasan, A., Banerjee, M., Ramasubramaniam, A. K., Kohler, J. R., et al. (2010). Dispersion as an important step in the *Candida albicans* biofilm developmental cycle. *PLoS Pathog.* 6:e1000828. doi: 10.1371/journal.ppat.1000828

Vale-Silva, L. A., Coste, A. T., Ischer, F., Parker, J. E., Kelly, S. L., Pinto, E., et al. (2012). Azole resistance by loss of function of the sterol Δ5,6-desaturase gene (ERG3) in *Candida albicans* does not necessarily decrease virulence. *Antimicrob. Agents Chemother.* 56, 1960–1968. doi: 10.1128/AAC.05720-11

van der Weerden, N. L., Bleackley, M. R., and Anderson, M. A. (2013). Properties and mechanisms of action of naturally occurring antifungal peptides. *Cell. Mol. Life Sci.* 70, 3545–3570. doi: 10.1007/s00018-013-1260-1

Vandeputte, P., Larcher, G., Bergès, T., Renier, G., Chabasse, D., and Bouchara, J. P. (2005). Mechanisms of azole resistance in a clinical isolate of *Candida tropicalis*. *Antimicrob. Agents Chemother.* 49, 4608–4615. doi: 10.1128/AAC.49.11.4608-4615.2005

Vandeputte, P., Pineau, L., Larcher, G., Noel, T., Brèthes, D., Chabasse, D., et al. (2011). Molecular mechanisms of resistance to 5-fluorocytosine in laboratory mutants of *Candida glabrata*. *Mycopathologia* 171, 11–21. doi: 10.1007/s11046-010-9342-1

Vecchiarelli, A., Pericolini, E., Gabrielli, E., and Pietrella, D. (2012). New approaches in the development of a vaccine for mucosal candidiasis: progress and challenges. *Front. Microbiol.* 3:294. doi: 10.3389/fmicb.2012.00294

Vermeulen, E., Lagrou, K., and Verweij, P. E. (2013). Azole resistance in *Aspergillus fumigatus*: a growing public health concern. *Curr. Opin. Infect. Dis.* 26, 493–500. doi: 10.1097/QCO.0000000000000005

Verweij, P. E., Mellado, E., and Melchers, W. J. (2007). Multiple-triazole-resistant aspergillosis. *N. Engl. J. Med.* 356, 1481–1483. doi: 10.1056/NEJMc061720

Vincent, B. M., Lancaster, A. K., Scherz-Shouval, R., Whitesell, L., and Lindquist, S. (2013). Fitness trade-offs restrict the evolution of resistance to amphotericin B. *PLoS Biol.* 11:e1001692. doi: 10.1371/journal.pbio.1001692

Voltan, A. R., Quindós, G., Alarcón, K. P., Fusco-Almeida, A. M., Mendes-Giannini, M. J., and Chorilli, M. (2016). Fungal diseases: could nanostructured drug delivery systems be a novel paradigm for therapy? *Int. J. Nanomedicine* 11, 3715–3730. doi: 10.2147/IJN.S93105

Vyas, S. P., and Gupta, S. (2006). Optimizing efficacy of amphotericin B through nanomodification. *Int. J. Nanomedicine* 1, 417–432. doi: 10.2147/nano.2006.1.4.417

Walsh, T. J., Anaissie, E. J., Denning, D. W., Herbrecht, R., Kontoyiannis, D. P., Marr, K. A., et al. (2008). Treatment of aspergillosis: clinical practice guidelines of the infectious diseases society of America. *Clin. Infect. Dis.* 46, 327–360. doi: 10.1086/525258

Walsh, T. J., Schlegel, R., Moody, M. M., Costerton, J. W., and Salcman, M. (1986). Ventriculoatrial shunt infection due to *Cryptococcus neoformans*: an ultrastructural and quantitative microbiological study. *Neurosurgery* 18, 373–375. doi: 10.1097/00006123-198603000-00025

Wang, X. J., Sui, X., Yan, L., Wang, Y., Cao, Y. B., and Jiang, Y. Y. (2015). Vaccines in the treatment of invasive candidiasis. *Virulence* 6, 309–315. doi: 10.4161/21505594.2014.983015

Wang, Y. H., Dong, H. H., Zhao, F., Wang, J., Yan, F., Jiang, Y. Y., et al. (2016). The synthesis and synergistic antifungal effects of chalcones against drug resistant *Candida albicans*. *Bioorg. Med. Chem. Lett.* 26, 3098–3102. doi: 10.1016/j.bmcl.2016.05.013

Watson, P. F., Rose, M. E., Ellis, S. W., England, H., and Kelly, S. L. (1989). Defective sterol C5-6 desaturation and azole resistance: a new hypothesis for the mode of action of azole antifungals. *Biochem. Biophys. Res. Commun.* 164, 1170–1175. doi: 10.1016/0006-291X(89)91792-0

Wheat, L. J., Connolly, P., Smedema, M., Durkin, M., Brizendine, E., Mann, P., et al. (2006). Activity of newer triazoles against *Histoplasma capsulatum* from patients with AIDS who failed fluconazole. *J. Antimicrob. Chemother.* 57, 1235–1239. doi: 10.1093/jac/dkl133

Whelan, W. L. (1987). The genetic basis of resistance to 5-fluorocytosine in *Candida* species and *Cryptococcus neoformans*. *Crit. Rev. Microbiol.* 15, 45–56. doi: 10.3109/10408418709104447

White, T. C. (1997). Increased mRNA levels of ERG16, CDR, and MDR1 correlate with increases in azole resistance in *Candida albicans* isolates from a patient infected with human immunodeficiency virus. *Antimicrob. Agents Chemother.* 41, 1482–1487.

White, T. C., Holleman, S., Dy, F., Mirels, L. F., and Stevens, D. A. (2002). Resistance mechanisms in clinical isolates of *Candida albicans*. *Antimicrob. Agents Chemother.* 46, 1704–1713. doi: 10.1128/AAC.46.6.1704-1713.2002

White, T. C., Marr, K. A., and Bowden, R. A. (1998). Clinical, cellular, and molecular factors that contribute to antifungal drug resistance. *Clin. Microbiol. Rev.* 11, 382–402.

Wojnicz, D., Kucharska, A. Z., Sokół-Łêtowska, A., Kicia, M., and Tichaczek-Goska, D. (2012). Medicinal plants extracts affect virulence factors expression and biofilm formation by the uropathogenic *Escherichia coli*. *Urol. Res.* 40, 683–697. doi: 10.1007/s00240-012-0499-6

Wozniak, K. L., Young, M. L., and Wormley, F. L. (2011). Protective immunity against experimental pulmonary cryptococcosis in T cell-depleted mice. *Clin Vaccine Immunol.* 18, 717–723. doi: 10.1128/CVI.00036-11

Xiang, M. J., Liu, J. Y., Ni, P. H., Wang, S., Shi, C., Wei, B., et al. (2013). Erg11 mutations associated with azole resistance in clinical isolates of *Candida albicans*. *FEMS Yeast Res.* 13, 386–393. doi: 10.1111/1567-1364.12042

Xie, J. L., Polvi, E. J., Shekhar-Guturja, T., and Cowen, L. E. (2014). Elucidating drug resistance in human fungal pathogens. *Future Microbiol.* 9, 523–542. doi: 10.2217/fmb.14.18

Yu, L., Ling, G., Deng, X., Jin, J., Jin, Q., and Guo, N. (2011). *In vitro* interaction between fluconazole and triclosan against clinical isolates of fluconazole-resistant *Candida albicans* determined by different methods. *Antimicrob. Agents Chemother.* 55, 3609–3612. doi: 10.1128/AAC.01313-10

Yu, L., Zhang, W., Wang, L., Yang, J., Liu, T., Peng, J., et al. (2007). Transcriptional profiles of the response to ketoconazole and amphotericin B in *Trichophyton rubrum*. *Antimicrob. Agents Chemother.* 51, 144–153. doi: 10.1128/AAC.00755-06

Yu, Q., Ding, X., Zhang, B., Xu, N., Jia, C., Mao, J., et al. (2014). Inhibitory effect of verapamil on *Candida albicans* hyphal development, adhesion and gastrointestinal colonization. *FEMS Yeast Res.* 14, 633–641. doi: 10.1111/1567-1364.12150

Zhang, L., Xiao, M., Watts, M. R., Wang, H., Fan, X., Kong, F., et al. (2015). Development of fluconazole resistance in a series of *Candida parapsilosis* isolates from a persistent candidemia patient with prolonged antifungal therapy. *BMC Infect. Dis.* 15:340. doi: 10.1186/s12879-015-1086-6

Zhou, Y., Wang, G., Li, Y., Liu, Y., Song, Y., Zheng, W., et al. (2012). *In vitro* interactions between aspirin and amphotericin B against planktonic cells and biofilm cells of *Candida albicans* and *C. parapsilosis*. *Antimicrob. Agents Chemother.* 56, 3250–3260. doi: 10.1128/AAC.06082-11AAC.06082-11

**Conflict of Interest Statement:** The authors declare that the research was conducted in the absence of any commercial or financial relationships that could be construed as a potential conflict of interest.

frontiers in Microbiology

REVIEW
published: 10 October 2016
doi: 10.3389/fmicb.2016.01585

# Evolution and Application of Inteins in *Candida* species: A Review

*José A. L. Fernandes[1†], Tâmara H. R. Prandini[2†], Maria da Conceição A. Castro[1], Thales D. Arantes[1,3], Juliana Giacobino[2], Eduardo Bagagli[2] and Raquel C. Theodoro[1]**

[1] Institute of Tropical Medicine of Rio Grande do Norte, Universidade Federal do Rio Grande do Norte, Natal, Brazil, [2] Department of Microbiology and Immunology, Institute of Biosciences, Universidade Estadual Paulista Julio de Mesquita Filho, Botucatu, Brazil, [3] Post-graduation Program in Biochemistry, Universidade Federal do Rio Grande do Norte, Natal, Brazil

Inteins are invasive intervening sequences that perform an autocatalytic splicing from their host proteins. Among eukaryotes, these elements are present in many fungal species, including those considered opportunistic or primary pathogens, such as *Candida* spp. Here we reviewed and updated the list of *Candida* species containing inteins in the genes *VMA, THRRS* and *GLT1* and pointed out the importance of these elements as molecular markers for molecular epidemiological researches and species-specific diagnosis, since the presence, as well as the size of these inteins, is polymorphic among the different species. Although absent in *Candida albicans*, these elements are present in different sizes, in some environmental *Candida* spp. and also in most of the non-albicans *Candida* spp. considered emergent opportunistic pathogens. Besides, the possible role of these inteins in yeast physiology was also discussed in the light of the recent findings on the importance of these elements as post-translational modulators of gene expression, reinforcing their relevance as alternative therapeutic targets for the treatment of non-albicans *Candida* infections, because, once the splicing of an intein is inhibited, its host protein, which is usually a housekeeping protein, becomes non-functional.

**Keywords: *Candida* spp., intein, vacuolar ATPase, threonyl-tRNA synthetase, glutamate syntethase, molecular identification, new therapeutic targets**

OPEN ACCESS

***Edited by:***
*Joshua D. Nosanchuk, Albert Einstein College of Medicine, USA*

***Reviewed by:***
*Arianna Tavanti, University of Pisa, Italy*
*Margi Butler, University of Otago, New Zealand*

***Correspondence:**
*Raquel C. Theodoro*
*raquel.ctheodoro@gmail.com*

*† These authors have contributed equally to this work.*

***Specialty section:***
*This article was submitted to Fungi and Their Interactions, a section of the journal Frontiers in Microbiology*

***Received:*** *16 August 2016*
***Accepted:*** *21 September 2016*
***Published:*** *10 October 2016*

***Citation:***
*Fernandes JAL, Prandini THR, Castro MdCA, Arantes TD, Giacobino J, Bagagli E and Theodoro RC (2016) Evolution and Application of Inteins in Candida species: A Review. Front. Microbiol. 7:1585. doi: 10.3389/fmicb.2016.01585*

## INTRODUCTION

Inteins are invasive genetic elements that occur as intervening sequences in conserved coding host genes. They are transcribed and translated with the flanking host protein sequences and then self-excised by protein splicing. The flanking protein sequences (exteins) are joined by a peptide bond, constituting the functional protein (Chong et al., 1996; Perler, 2005).

Over the past three decades, inteins have been detected mainly in unicellular microorganisms in the three domains of life and in viruses (Perler, 2002). Among the Eukarya domain, inteins are found mostly in fungi, some green algae and other basal eukaryotes (Liu, 2000; Butler et al., 2001, 2006). In a recent review, 2729 genomes of bacteria, 345 of archaea and 6648 of eukarya were analyzed (Topilina et al., 2015b) and 24, 47, and 1.1% of these genomes, respectively, presented at least one intein.

Inteins are usually found at conserved sites of housekeeping proteins that have vital functions in the cell, such as DNA and RNA polymerases, aminoacyl tRNA synthetases, recombinases, topoisomerases, helicases and essential components of the spliceosome (Novikova et al., 2014).

Some hypothesis for this distribution already exist and are in part supported by some evolutionary scenarios, including probable horizontal transfer, as well as genetic mobility of inteins by homing endonuclease, which means that the spread and increase of this element in populations is due to a gene conversion process by homologous recombination, rather than any selective advantage (Nagasaki et al., 2005; Gogarten and Hilario, 2006; Swithers et al., 2009). This idea rendered to inteins the title of "parasitic" genetic elements during the past 25 years, although some domesticated inteins, such as HO gene of *Saccharomyces cerevisiae* showed to have "gained" a function in the cell biology. In this specific case, the HO gene encodes for an endonuclease responsible for mating type conversion in yeast and its splicing domain is not active anymore (Koufopanou and Burt, 2005).

Nevertheless, recent works have evidenced a possible function for inteins in the post-translational regulation of gene expression. For instance, the splicing of SufB intein of *Mycobacterium tuberculosis* showed to be inhibited by reactive oxygen and nitrogen species (ROS and RNS) when expressed in *Escherichia coli*. These stressful conditions are also experimented by *M. tuberculosis* inside the macrophage (Topilina et al., 2015a). Other evidence came from the splicing modulation of RadA intein from the hyperthermophilic archaeon *Pyrococcus horikoshii* according to the temperature, solution conditions and remote extein point mutations. So, RadA intein might function as an environmental sensor, releasing the intein for full activity only at optimal growth conditions for the native organism (high temperatures), while sparing ATP consumption under cold-shock. The authors observed intein splicing at low temperature only after adding a combination of the detergent SDS and the ionic liquid 1-butyl-3-methylimidazolium chloride, showing that, besides temperature, other factors may also interfere in RadA intein splicing (Topilina et al., 2015b).

Although the experimental evidence for the intein's role in modulation of gene expression is based on a non-native context (different extein and different host cell), it is an important clue for the actual functionality of these elements in nature. Their presence in particular conserved motifs might be explained by an adaptive process (Novikova et al., 2014). Novikova et al. (2015) observed that inteins have a certain "preference" for specific functional domains of related housekeeping proteins, like ATPase domains for example, and this does not entirely fit to the models describing inteins as merely mobile parasitic elements. The authors argue that this intein distribution might be a result of a selective retention of these elements, which might be beneficial under certain environmental stresses. So, the sporadic nature of intein in closely related species could be explained by different environmental stresses. If there is no strong selective pressure for intein maintenance in a certain subpopulation and its presence reduces the adaptive value of the host microorganism, the intein-free alleles will increase in this population by means of natural selection (Gogarten and Hilario, 2006).

Nevertheless, we are far from a global understanding about the reason for intein persistence in different housekeeping host proteins, only in unicellular organisms, over millions of years. It seems consensual that their maintenance may be due to either their parasitic nature, since they are invasive elements, as well as to a possible role in specific physiological conditions of the host cell. Yet, among the mobile elements, inteins are the least studied, so that few inteins have already had their activity tested under different conditions; and therefore their real function is still a puzzle. Regarding that most of the produced knowledge on genome organization during the last years has been changing the status of many mobile genes, mainly retrotransposable elements, which are intensively studied, from parasitic entities to dynamic elements involved in genome evolution and gene expression (Mita and Boeke, 2016), it seems plausible that intein's function in cell deserves more scientific investigation. The more we understand about inteins, the better we can explore their biotechnological applicability.

Few fungal inteins have been described, most of them are located in *PRP8* (precursor mRNA protein) and *VMA* (vacuolar ATPase) coding genes, others can be observed in some RNA Polymerase subunits, *GLT1* (glutamate synthase), *CHS2* (chitin synthase) and *THRRS* (threonyl-tRNA synthetase) coding genes (Poulter et al., 2007). Most fungal inteins are present in the *PRP8* and *VMA* genes. The PRP8 intein is widely dispersed in Fungi Kingdom (fungi containing this intein are found in different phyla), being present in many important human pathogens, such as *Cryptococcus neoformans, Cryptococcus gattii, Histoplasma capsulatum, Emmonsia* spp., *Paracoccidioides* spp., *Blastomyces dermatitidis, Aspergillus nidulans, Aspergillus fumigatus* (Liu and Yang, 2004; Butler and Poulter, 2005; Butler et al., 2006; Theodoro et al., 2010). The VMA intein, on the other hand, is specifically distributed among Saccharomycetes, such as *Saccharomyces*, *Zygosacchromyces* and some *Candida*.

Here we updated the information on the intein distribution among *Candida* species and explored their potential as a source of phylogenetic information and, therefore, as species-specific diagnostic tool. Besides, the possible impact of the presence of these elements in housekeeping genes in *Candida* species life style was discussed raising their promising application as drug targets for most of the medically relevant non-albicans emergent *Candida* species.

## TYPES OF INTEINS AND HOW THEY OPERATE

Inteins come in three configurations: full-length, mini and split (**Figure 1A**). The full-length inteins have a homing endonuclease domain (HE) splitting the splicing domain in N and C-Spl terminals. When active, the HE recognizes a cognate allele, without the intein, performs a double strand break (DSB) and, by homologous recombination, copies the intein using the intein-containing allele as template for DNA repair. Mini-inteins lack the HE domain and have a continuous splicing domain, while split-inteins are mini-inteins, whose N and C-Spl terminals are transcribed and translated with different exteins. When the N and C-Spl terminals are assembled, the intein suffers a *trans*-splicing reaction, ligating the different exteins (Wood et al., 1999; Volkmann and Iwaı, 2010).

Intein mobility is triggered by its HE domain which recognizes long, and therefore specific, DNA sequences (14–40 bp) lacking

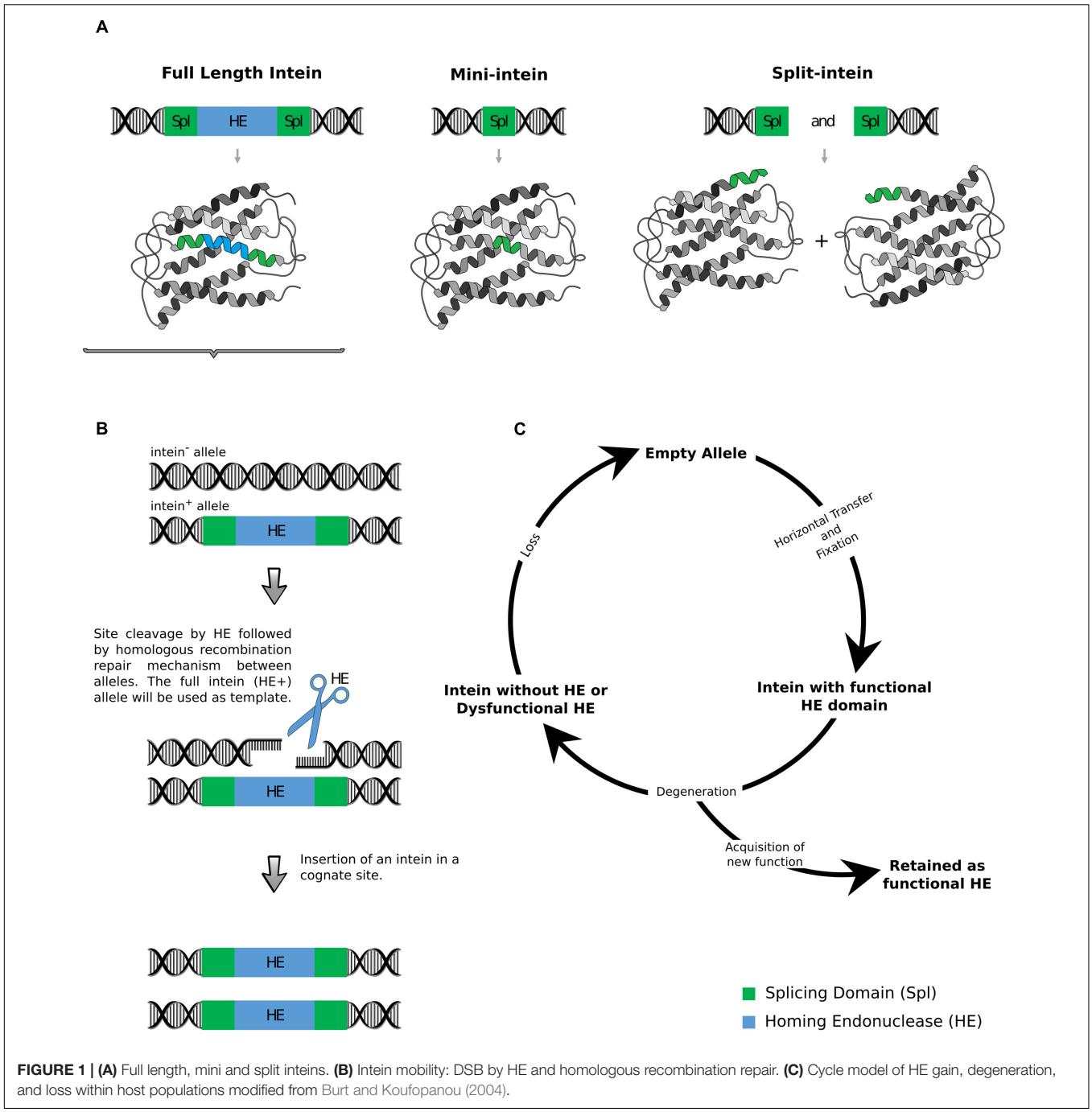


**FIGURE 1 | (A)** Full length, mini and split inteins. **(B)** Intein mobility: DSB by HE and homologous recombination repair. **(C)** Cycle model of HE gain, degeneration, and loss within host populations modified from Burt and Koufopanou (2004).

the intein, producing a DSB. The host repair system is then activated and the template containing the intein is "copied" to the recipient chromosome by a gene conversion event (**Figure 1B**), distorting the Mendelian segregation, causing a Super-Mendelian inheritance or a rapid dissemination and fixation of the intein in population. When all alleles of a certain population are occupied by the intein there is no selection pressure for functional HE, because both, functional and non-functional HEs will be equally maintained in population simply by cellular propagation and the HE domain is "free" to degenerate (**Figure 1C**). That is why the HE domain is expected to have more sequence variation, including its complete degeneration and/or deletion, than the splicing domain (Burt and Koufopanou, 2004; Koufopanou and Burt, 2005; Gogarten and Hilario, 2006).

Inteins are particularly interesting as a source of phylogenetic information because they present the well-preserved splicing domain (N and C terminals), with the conserved motifs A, B (for the N-splicing) and F, G (for the C-splicing), flanking the central and more variable HE domain, in the full-length inteins. The presence of the motifs C, D, E, and H, as well as the two aspartic

acid residues, one in C and other in E, in HEs from LAGLIDADG family (the most common in fungal inteins), indicate that the HE domain is probably active (Gimble and Thorner, 1992; Liu, 2000; Posey et al., 2004). In mini-inteins, HE domains are supposed to be completely deleted. In addition, their location in highly conserved genes facilitates the design of primers for their amplification (Butler and Poulter, 2005; Theodoro and Bagagli, 2009; Prandini et al., 2013).

Besides its potential as molecular markers, inteins have been largely used for biotechnological purposes, accordingly to their functional mechanisms. The splicing domain, for example, is explored for purification of recombinant proteins, cyclization of proteins, protein labeling, production of selenoproteins (Miraula et al., 2015) and, for pathogenic microorganisms, it has been studied as a drug target (Paulus, 2007; Zhang et al., 2010). The HE domain has also been intensively studied as a biotechnological tool, in this case for genome editing, since these enzymes can be reprogrammed to specifically cut a genome site and deliver a gene of interest by homologous recombination. The applications of this technology are numerous for different social-economic fields, such as gene therapy for monogenic diseases, insect vector control (already developed for malaria mosquitoes) and gene delivery for transgenic plants, such as maize (Belfort and Bonocora, 2014).

## INTEINS IN *Candida* SPECIES

*Candida* species belong to Ascomycota phylum, Hemiascomycetes class and Saccharomycetales order. These species are distributed in three different clades making *Candida* a non-monophyletic group (Diezmann et al., 2004). With the exception of *C. glabrata*, which is in clade 3, together with *C. castelli*, *C. norvegica, Saccharomyces cerevisiae* and other biotechnologically important yeast species, the most relevant clinical species of *Candida* are clustered in clade 1, which includes *C. albicans, C. parapsilosis, C. orthopsilosis, C. metapsilosis, C. tropicalis,* and *C. viswanathii*, as well as two non-pathogenic species, *Candida maltosa* and *Lodderomyces elongisporus*. *C. guilliermondii, C. intermedia, C. famata,* and *C. zeylanoides* are clustered in clade 2. The clades 1 and 2 are also referred as CUG group by distinctly translate this codon as serine instead of the standard leucine. Whether this attribute may play a hole in pathogenicity is still unknown (Diezmann et al., 2004).

*Candida* spp. can colonize human tissues in different ways, varying from a normal microbiota in the intestinal mucosa, contiguously to the vaginal mucosa, to a true pathogen. The transition to pathogenicity in *Candida* species, mainly in *C. albicans,* occurs generally due to the host immunological condition, leading to a microbiota unbalance, which associated with important virulence factors, such as biofilm formation and hydrolytic enzymes production, promotes fungal dissemination to other sites and organs. The clinical manifestations vary from a localized mucosa or skin infection to disseminated disease (Lagunes and Rello, 2016).

Although less common, disseminated candidiasis has significantly increased over the last 15 years, affecting mainly patients under debilitating and immunosuppressive conditions. Data from Centers for Disease Control and Prevention (CDC) and the National Healthcare Safety Network, show that *Candida* species are the fifth pathogen related to nosocomial diseases and fourth pathogen among bloodstream infections – BSI (Wisplinghoff et al., 2004; Pfaller and Diekema, 2007). These nosocomial *Candida* infections are related to increment of invasive procedures and also to the intensive use of broad-spectrum antimicrobials, particularly in patients admitted in Intensive Care Units – ICU (Colombo et al., 2013).

About 95% of diagnosed fungal infections are related to *Candida* spp., mainly involving the species *C. albicans, C. glabrata, C. tropicalis, C. parapsilosis, C. krusei, C. guilliermondii, C. lusitaniae, C. dubliniensis, C. pelliculosa, C. kefyr, C. lipolytica, C. famata, C. inconspicua, C. rugosa, and C. norvegensis*, but *C. albicans* is still the most frequent species causing infection (Yapar, 2014). However, *Candida* infections caused by non-albicans *Candida* spp. have been increasing in the last few years (Richardson and Lass-Flörl, 2008). In a recent epidemiological analysis, non-albicans species accounted for more than 50% of all cases of invasive candidiasis in patients enrolled in the Prospective Antifungal Therapy Alliance, a sentinel surveillance network comprising 23 medical centers in the US and two in Canada. The non-albicans species identified were *C. glabrata* (46.4%), *C. parapsilosis* (24.7%), *C. tropicalis* (13.9%), *C. krusei* (5.5%), *C. lusitaniae* (1.6%), *C. dubliniensis* (1.5%) and *C. guilliermondii* (0.4%) (Pfaller et al., 2014). While *C. albicans* infections have been progressively replaced by *C. glabrata* infections in North America and in many European countries, *C. parapsilosis* or *C. tropicalis* are the most frequent non-albicans species in Latin America (Nucci et al., 2010; Cleveland et al., 2012; Lockhart et al., 2012). The central factor for the emergence of these non-albicans *Candida* spp. seems to be the undiscriminating use of antifungal drugs (Yapar, 2014).

The treatment of *Candida* infections, mainly candidemias, is based on antifungal agents that interfere on different metabolic pathways being fungicide, such as polyenes, azoles and equinocandis, or fungistatic, such as nucleoside analogs (Lopez-Martinez, 2010; Maubon et al., 2014). The polyenes act on the ergosterol, increasing the permeability of cell membrane by producing aqueous pores; the azoles inhibit the ergosterol biosynthesis and the echinocandins inhibit the synthesis of 1,3 β-glucan, a polysaccharide responsible for the cell wall integrity; and the nucleoside analogs inhibit DNA synthesis being used in combination with amphotericin B or fluconazole (Spampinato and Leonardi, 2013; Paramythiotou et al., 2014), which are the usual chosen drugs for treatment of *Candida* infections (Paramythiotou et al., 2014). The antifungal susceptibility can be easily accessed by Clinical and Laboratory Standards Institute (CLSI) reference microdilution method and also by commercially available antifungal susceptibility testing systems, such as the Sensititre YeastOne colorimetric panel (TREK Diagnostic Systems, Cleveland, OH, USA) (Pfaller et al., 2012).

Monitoring changes in antifungal drug resistance is as important as determining the incidence of candidemia by different *Candida* species. A recent report of surveillance for candidemia in Atlanta, GA, USA and Baltimore, MD, USA over

a 5-year period, showed a shift in the species distribution among causative organisms, with a significant increase in *C. glabrata*, as well as in its resistance to echinocandin and fluconazole (Wang et al., 2012; Cleveland et al., 2015). This emergence of antifungal resistance, due to inappropriate prescriptions (Sardi et al., 2013), and the usual toxic side effects of some of these drugs strengthen the demand for new therapeutic targets.

The fungal systemic disease caused by *Candida* is an important cause of mortality, mainly in nosocomial infections and, since the antifungal susceptibility may vary among the different species (Bassetti et al., 2015), the correct diagnosis at species level is necessary. This can be accomplished by classical phenotypic methods, biochemical and physiological tests, which have automated versions, such as Vitek 2 ID – YST (bioMerieux), (Higashi et al., 2015). However, molecular epidemiological studies using different molecular markers (25S group I intron, rDNA D1/D2 region and ITS1-5.8S-ITS2) have revealed intraspecific variation in *C. albicans* and non-albicans *Candida* species and its correlation to antifungal susceptibility (Miletti and Leibowitz, 2000; Karahan et al., 2004; Steuer et al., 2004; Fahami et al., 2010; Gurbuz and Kaleli, 2010; Merseguel et al., 2015).

Besides intraspecific variation, molecular markers have also pointed out the existence of cryptic species in *C. parapsilosis,* actually composed by three species: *C. parapsilosis, C. metapsilosis* and *C. orthopsilosis* (Tavanti et al., 2005), which present differences in virulence and antifungal response. *C. parapsilosis* and *C. orthopsilosis* are more virulent in reconstituted human tissues models and the minimal inhibitory concentration values (MIC) of amphotericin B, caspofungin, anidulafungin and micafungin for *C. orthopsilosis* and *C. metapsilosis* isolates were significantly lower than those for *C. parapsilosis* (Gacser et al., 2007; Lockhart et al., 2008).

The correct recognition of close fungal genotypes or cryptic species would improve the treatment; however, this is not achieved by the usual biochemical methods available in most routine laboratories, mainly in developing countries. The distinction of these very close *Candida* species requires molecular techniques such as PCR- RFLP of *SADH* gene (Tavanti et al., 2005), quantitative PCR (qPCR) (Hays et al., 2011; Souza et al., 2012), pyrosequencing (Borman et al., 2009), microsatellite analysis (Lasker et al., 2006) or matrix-assisted laser desorption ionization–time (MALDI-TOF MS analysis) (Quiles-Melero et al., 2012). This last technique is based on the mass spectrum analysis of crude protein cell extract and requires validated databases for the achievement of rapid and reliable pathogen identification. Recent researches have created databases for the identification of bloodstream yeasts and showed practically 100% accuracy in distinguishing medically important species, such as *C. tropicalis, C. parapsilosis, C. pelliculosa, C. orthopsilosis, C. albicans, C. rugosa, C. guilliermondii, C. lipolytica, C. metapsilosis, C. nivariensis* (De Carolis et al., 2014; Ghosh et al., 2015). The main apparent disadvantage of this technology is the up-front cost of purchasing a MALDI-TOF MS instrument; however, it is offset in about 3 years, providing a noteworthy long-term cost saving for the laboratory (Tran et al., 2015). Some authors have also pointed out the relatively low analytical sensitivity of the method, as well as the few advances for distinguishing filamentous fungi, when compared to the yeast databases (Bailey et al., 2013).

In this scenario, intein research is particularly interesting because they might be a valuable additional or alternative molecular markers for species identification, such as observed for *Cryptococcus* spp., *Paracoccidioides* spp., *Histoplasma capsulatum,* and *Candida* spp. (Butler and Poulter, 2005; Theodoro et al., 2008; Prandini et al., 2013; Theodoro et al., 2013; Satish Kumar and Ramesh, 2014) and also, since they are usually present in housekeeping genes and absent in multicellular eukaryotes, they can be explored as drug targets, because protein splicing inhibition would make the host protein non-functional (Paulus, 2003; Liu and Yang, 2004). However, drug screening for the inhibition of intein splicing has only been carried out for bacterial pathogens, such as *M. tuberculosis.* The intein MtuRecA was inserted in the GFP (green fluorescent protein) coding sequence and its splicing efficiency was evaluated according to the fluorescence emission. More than 85 thousand compounds were tested. Some electrophilic compounds, such as cisplatin inhibited the intein MtuRecA splicing by blocking the intein's first *N*-Spl cystein residue (Paulus, 2007; Zhang et al., 2010).

Three host proteins, considered essential for cell physiology, have been observed containing inteins in Saccharomycetales species: vacuolar ATPase (VMA), threonyl-tRNAsynthetase (ThrRS) and glutamate synthase (GLT1) (Poulter et al., 2007).

In order to update the distribution of these inteins in *Candida*, we carried out a search for inteins sequences in 81 sequenced genomes of 30 *Candida* species (Supplementary Table 1). Public Contigs deposited into MycoCosmosDB and NCBI WGS Databases were downloaded. By using GetORF program, all genomes were converted into six frames amino-acids sequences, for their ORFs deduction. Using those sequences, a local database was created, using NCBI Local BLAST+ (v.3.1.4) program in a UNIX system. Finally, sequences of VMA, ThrRS, GLT1 inteins were blasted to this database. This analysis revealed inteins in VMA, ThrRS and GLT1 proteins in *Candida* species, in which they have not been described before.

The VMA, ThrRS and GLT1 inteins are present in 14, 6, and 3 *Candida* species, respectively. The differences among *Candida* species concerning intein presence and/or size polymorphism (**Table 1**) can be easily accessed as molecular markers for species differentiation.

Some *Candida* species have more than one intein in their genome. The species *C. maltosa, C. metapsilosis* and *C. orthopsilosis* present both VMA and ThrRS inteins and *C. famata* presents both VMA and GLT1 inteins (**Table 1**). No inteins were found in *C. albicans, C. arabinofermentans, C. auris, C. boidinii, C. dubliniensis, C. succiphila, C. tanzawaensis, C. tenuis, C. infanticola*, *C. krusei, C. lusitaniae,* and *C. ciferri*.

Inteins are not exclusively found in clinically relevant *Candida* species, some of the intein containing species listed on **Table 1** are frequently isolated from environmental sources. For instance, *C. apicola* is found in wine and cachaça fermentation processes (Vega-Alvarado et al., 2015), *C. homilentoma* is commonly associated to insects (Yun et al., 2015), *C. sorboxylosa* was originally found in fruits and described as close related to

**TABLE 1 | Inteins encoded by *Candida* spp.**

| Host protein | Candida species | Intein nomenclature | Size(aa residues) | Essential aspartate residue* | |
|---|---|---|---|---|---|
| | | | | Block C | Block E |
| VMA1, vacuolar ATPase | *C. castellii*** | CcaVMA | 367 | D | I |
| | *C. apicola*** | CapVMA | 389 | T | K |
| | *C. glabrata* | CglVMA | 415 | S | Q |
| | *C. nivariensis*** | CniVMA | 424 | S | K |
| | *C. bracarensis*** | CbrVMA | 420 | S | K |
| | *C. homilentoma*** | ChoVMA | 491 | D | D |
| | *C. sorboxylosa*** | CsorVMA | 374 | T | V |
| | *C. tropicalis* | CtrVMA | 471 | I | A |
| | *C. sojae*** | CsoVMA | 501 | D | N |
| | *C. metapsilosis* | CmeVMA | 454 | N | D |
| | *C. orthopsilosis* | CorVMA | 530 | D | D |
| | *C. intermedia*** | CinVMA | 455 | T | D |
| | *C. maltosa*** | CmaVMA | 451 | N | D |
| | *C. famata* | CfaVMA (DhaVMA) | 395 | N | D |
| ThrRS, threonyl-tRNA synthetase | *C. tropicalis* | CtrThrRS | 345 | N | S |
| | *C. sojae*** | CsoThrRS | 338 | T | S |
| | *C. maltosa*** | CmaThrRS | 444 | D | D |
| | *C. orthopsilosis* | CorThrRS-A | 180 | – | – |
| | *C. orthopsilosis* | CorThrRS-B | 439 | D | D |
| | *C. parapsilosis* | CpaThrRS | 183 | – | – |
| | *C. metapsilosis* | CmeThrRS | 172 | – | – |
| GLT1, glutamate synthase | *C. famata* | CfaGLT1 | 607 | D | D |
| | *C. carpophila*** | Ccar GLT1 | 557 | D | D |
| | *C. guilliermondii* | Cgu GLT1 | 553 | E | D |

**Aspartic acids residues from block C and E considered essential for HE domain function. ***Inteins found in new available Candida genomes.*

*C. krusei* (Nakase, 1971) and *C. sojae* can be isolated from water-soluble substances of defatted soybean flakes (Nakase et al., 1994).

Some environmental species presenting inteins, listed on **Table 1**, have been rarely reported in invasive candidemia in human. This is the case of *C. intermedia,* isolated from soil, beer, grapes and also present on skin, throat, or animal feces (Ruan et al., 2010), as well as *C. famata* (*Debaryomyces hansenii*), which is commonly found in natural substrates and in various types of cheese and accounts for 0.08–0.5% of isolates recovered during invasive candidiasis. *C. famata* is sometimes misidentified as *C. guilliermondii,* which has a variety of environmental sources and is a common constituent of the normal human microbiota, being associated with only 1–2% of candidemias (Desnos-Ollivier et al., 2008). The species *C. castellii, C. nivariensis* and *C. bracarensis* belong to *Nakaseomyces* genus (Kurtzman, 2003), being closely related to *C. glabrata.* The high genetic proximity between *C. nivariensis* or *C. bracarensis* and *C. glabrata* may have caused their misidentification as *C. glabrata* (Alcoba-flórez et al., 2005; Correia et al., 2006; Bishop et al., 2008), so that their emergent character may have been due to recent advances in molecular epidemiology tools. The ecological niches of these species are still poorly understood. *C. nivariensis* has been isolated from flowering plants in Australia, indicating a possible environmental source for human infections (Lachance et al., 2001). Despite their environmental aspect, *C. nivariensis* and *C. bracarensis* show an expansion in EPA genes, a family of glycosylphosphatydylinositol (GPI)-anchored cell-wall protein, considered an important virulence factor for emergent pathogens, such as *C. glabrata* (Gabaldón et al., 2013).

## VMA Inteins

The first evidence of an intein arose from structural studies and expression analysis of the vacuolar ATPase gene and its encoded protein (VMA) in *S. cerevisiae* (Hirata et al., 1990). Since then, VMA inteins have been described in several species of Saccharomycetales order, including yeasts of biotechnological and medical interests, and seem to follow a model of invasion, fixation, degeneration, loss and reinvasion (Okuda et al., 2003; Burt and Koufopanou, 2004; Butler et al., 2006), leading to its sporadic distribution. For this reason two very close sister species might differ concerning the presence of the intein in the *VMA* gene. Most of the VMA inteins have a degenerated HE domain (from LAGLIDADG family). Some of the few active HE may also recognize allelic sites in other yeast species. Actually, the HE domain of the VMA intein (also called VDE) from *S. cariocanus* is more effective in cutting the *VMA* recognition site of *S. cerevisiae* than its own *VMA* (Posey et al., 2004), which would allow horizontal transfer. Notwithstanding, once the intein is acquired, it tends to be transmitted vertically, reflecting the group phylogeny (Butler et al., 2006; Goodwin et al., 2006). Comparing the VMA intein patterns in related *Saccharomyces*

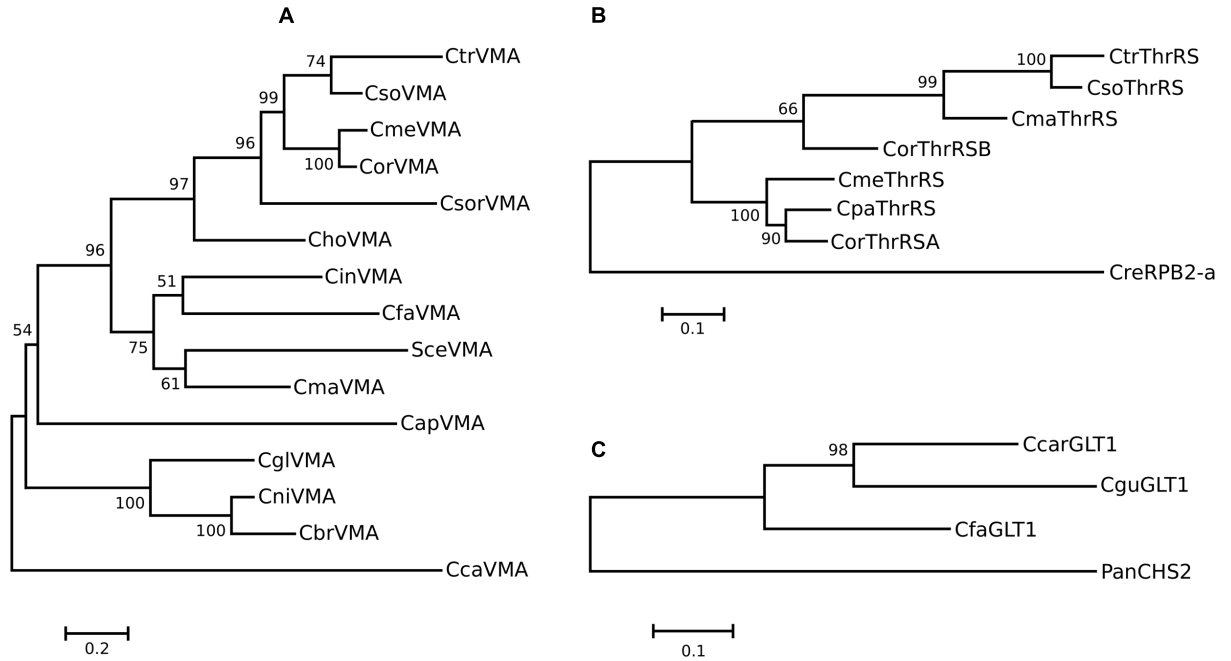


**FIGURE 2 | Molecular Phylogenetic analysis by Maximum Likelihood method conducted in Mega v.6.0 (Tamura et al., 2013) for the amino acids aligned sequences of the inteins VMA, ThrRS and GLT1 from *Candida* and their close relative inteins.** The trees with the highest log likelihood are shown. The trees are drawn to scale, with branch lengths measured in the number of substitutions per site. All sites containing alignment gaps were removed (Complete deletion). **(A)** VMA intein phylogeny inferred based on the Le_Gascuel_2008 model (Le and Gascuel, 2008). A discrete Gamma distribution was used to model evolutionary rate differences among sites [5 categories (+*G*, parameter = 2.0642)] and the rate variation model allowed for some sites to be evolutionarily invariable ([+*I*], 8.7480% sites). **(B)** ThrRS intein phylogeny inferred based on the Whelan And Goldman model (Whelan and Goldman, 2001). The rate variation model allowed for some sites to be evolutionarily invariable. **(C)** GLT1 intein phylogeny inferred based on the Whelan And Goldman model (Whelan and Goldman, 2001). The rate variation model allowed for some sites to be evolutionarily invariable.

species, it was also possible to document hybridization process, such as in a diploid strain of *S. carslbergensis* that contain two distinct alleles, one with the VMA intein, supposedly received from *S. cerevisiae*, and the other with only the intein-less *VMA* sequence, probably received from *S. pastorianus* (Okuda et al., 2003).

The amino acid sequence alignment of VMA inteins in *Candida* species shows large degeneration process in the HE domain, mainly in those species lacking both aspartate residues, one in block C and the other in E (Supplementary Figure S1).

The phylogenetic relationships among these elements revealed a non-vertically inheritance pattern, since the intein from *C. maltosa* was clustered apart from *C. tropicalis, C. metapsilosis* and *C. orthopsilosis* inteins (**Figure 2A**). According to a combined maximum likelihood analysis of six genes (*ACT1, EF2, RPB1, RPB2, 18S* rDNA, and *26S* rDNA) (Diezmann et al., 2004) these four species belong to a unique clade, named clade 1. Besides, although *C. glabrata, C. castellii, C. nivariensis* and *C. bracarensis* share a common ancestor with *S. cerevisiae*, belonging to clade 3 (Diezmann et al., 2004), their inteins were not clustered together in our analysis. Actually, the intein SceVMA showed to be closer to CmaVMA, than to the inteins of other species from clade 3. These observations corroborate the hypothesis of VDE adaptation for horizontal transfer. This hypothesis is supported by the high conservation of its 31 bp long recognition site and also by the incongruence between host and inteins phylogenies. This horizontal transfer seems to occur preferentially between closely related species, probably by eventual hybridization events (Goddard and Burt, 1999; Koufopanou et al., 2002).

Horizontal transfer has also been proposed as an explanation to the peculiar distribution of other inteins. For instance, the PRP8 intein, which occurs, sporadically, in many ascomycetes is also found in only four basidiomycetes from Tremellales order (*Cryptococcus neoformans, Cryptococcus gattii, Cryptococcus laurentii* and *Cryptococcus bacillisporus*) (Butler and Poulter, 2005; Butler et al., 2006). It was speculated that a co-phagocytosis event by a metazoan macrophage could be a possible scenario for PRP8 intein transfer from an ascomycete to a basidiomycete (Poulter et al., 2007).

It seems plausible that, for sharing part of their ecological niches, such as metazoan tissues, as well as some environmental sources, and being closely related, *Candida* species could hybridize creating suitable conditions for HE invasion in new and empty alleles, carrying the VMA intein. In fact, there are some researches that point out the occurrence of hybridization events in *Candida*. For instance, hybrid lineages between the two subspecies of *C. orthopsilosis* have been described in distant continents (Pryszcz et al., 2014). The same authors also found genomic evidence that some *C. metapsilosis* strains worldwide

distributed are heterozygous hybrids resulting from the same past hybridization event involving two non-pathogenic parental lineages. This observation corroborates the idea of hybridization as a source for the emergence of virulence attributes (Pryszcz et al., 2015).

The vacuolar H+-ATPase is a fundamental and therefore highly conserved enzyme in almost every eukaryotic cell. It functions as ATP-dependent proton pumps energizing various organelles and membranes, making numerous secondary transport processes possible. Yeast genetics researches identified the properties of individual subunits of V-ATPase and discovered the factors involved in its biogenesis and assembly. Null mutations in genes encoding V-ATPase subunits of *S. cerevisiae* result in a phenotype that is unable to grow at high pH and is sensitive to high and low metal-ion concentrations (Nelson et al., 2000).

The VMA intein is inserted in a P-loop containing the Nucleoside Triphosphate Hydrolase domain of VMA protein, the most prevalent domain of the several distinct nucleotide-binding protein folds. The most common reaction catalyzed by enzymes of the P-loop NTPase fold is the hydrolysis of the beta-gamma phosphate bond of a bound nucleoside triphosphate (NTP). The energy from NTP hydrolysis is typically utilized to induce conformational changes in other molecules, which constitutes the basis of the biological functions of most P-loop NTPases (Leipe et al., 2004).

The VMA intein is sporadically distributed among *Candida* species, with very close related species differing in its presence. For instance, this intein is absent in *C. parapsilosis*, while it is present, in different sizes, in *C. orthopsilosis* and *C. metapsilosis* (as described on **Table 1**), although *C. orthopsilosis* and *C. parapsilosis* share a most recent common ancestor, being closer to each other than either of them to *C. metapsilosis* (Pryszcz et al., 2015). It is possible that the clonal nature of *C. parapsilosis* lineage (Tavanti et al., 2005), in contrast to the possible mating occurrence in *C. orthopsilosis* and *C. metapsilosis* (Sai et al., 2011; Pryszcz et al., 2015), could have contributed to the loss of VMA intein. On the other hand, the sexual reproductive mode, as well as the occurrence of hybridization events, combined to a certain adaptation for lateral transfer of VDE, would prevent the intein loss in *C. orthopsilosis* and *C. metapsilosis*. The presence/absence and size polymorphisms make the VMA intein an easy strategy to differentiate these cryptic species (Prandini et al., 2013), constituting the most practical DNA-based method proposed so far for the correct identification of the species from the complex, since it does not requires PCR digestion or sequencing. However, additional retrospective analysis of more isolates known to belong to *C. parapsilosis* complex should be carried out in order to better explore the VMA intein as a phylogenetic tool.

Zhang and Rao (2010) discussed the contributions of V-ATPase function to pathogenicity and reviewed the functional link between V-ATPase and the lipid components of the membrane, showing that ergosterol removing or inhibition (performed by azoles, morpholines and allylamines) alters the V-ATPase conformation. Also, *erg* mutants showed the same phenotype of *vma* mutants, which is the inability to grow in alkaline medium. Besides, the authors also pointed out that fluconazole treatment, as well as *ERG3* deletion or *vma7-/-* mutation cause inhibition of filamentation, which, for *Candida* pathogenic species, is an important virulence treat for tissue invasion (Lo et al., 1997; Saville et al., 2006; Bastidas and Heitman, 2009). Furthermore, *C. albicans vma7-/-* mutant cells are eliminated by macrophages and fail to colonize epithelial cells. These observations show that azole drugs may have an effect on V-ATPase function, disrupting the pH homeostasis in fungal pathogens (Zhang and Rao, 2010). Despite no data is available for *vma* mutants in non-albicans *Candida* species, the conservative aspect of the VMA protein makes plausible the assumption that this protein is actually essential for the survival of all yeast species, mainly in alkaline medium, and it may also play an important role for fungal maintenance during infection in other *Candida* species. For this reason, we suppose this data reinforce the importance of the intein in V-ATPase protein as a potential drug target for the inhibition of the normal function of this protein in those *Candida* species that present this genetic element.

It is interesting to note that the most prevalent *Candida* species in hospital infections is *C. albicans*, which does not have any intein, while non-albicans *Candida* spp. predominated in samples collected from environment (Ferreira et al., 2013). If we consider that some physiological conditions may decrease the intein splicing efficiency, the existence of an intein in an important protein can modulate its post-translational expression. Regarding the importance of the V-ATPase for cell homeostasis and even for filamentation, it seems reasonable that the loss of this intein in *C. albicans* lineage might have contributed, together with many virulence factors, for its maintenance in vertebrate tissue as a member of the normal microbiota and eventual pathogen. The absence of the intein in VMA protein could have contributed, for example, for the highly efficient filamentation of *C. albicans* when compared to other *Candida* species, that have the VMA intein, such as *C. glabrata* and *C. tropicalis*, whose pathogenicity might be associated with many other virulence factors rather than to filamentation capacity (Sudbery, 2011). Among the non-albicans *Candida* spp., whose incidence is becoming more expressive, are the species *C. parapsilosis* and *C. krusei,* which also lack the VMA intein. In these species, the *VMA* gene expression is not under post-translational regulation controlled by intein splicing, so that it could be more efficiently expressed in a larger variety of physiological conditions when compared to the intein containing species. However, no experiment has been conducted to assess the splicing of the VMA intein in *Candida* species in different physiological and stressing conditions.

## ThrRS Intein

The ThrRS intein is inserted in the threonyl-tRNAsynthetase gene (*THRRS*) which encodes an aminoacyl-tRNAsynthetase (aaRS), responsible for engaging the amino acid threonine with the corresponding tRNA (anticodon). The ThrRS intein is located in the Class II tRNA aaRS catalytic core domain. Class II amino acyl-tRNA synthetases (aaRSs) share a common fold and generally attach an amino acid to the 3′ OH of the tRNA ribose. This domain is primarily responsible for

ATP-dependent formation of the enzyme bound aminoacyl-adenylate (O'Donoghue and Luthey-Schulten, 2003).

The ThrRS intein has already been described as full-length intein in *C. tropicalis* and as mini-intein in *C. parapsilosis*, as well as in *C. orthopsilosis* (CorThrRS-A) and *C. metapsilosis.* Nevertheless, some isolates of *C. orthopsilosis* present a full-length intein (CorThrRS-B) in the same insertion site. This was the first report of two types of intein in the same insertion site in the same species (Prandini et al., 2013), though in distinct strains. The finding of both inteins (CorThrRS-A and CorThrRS-B in the same *C. orthopsilosis* strain is also possible, since they are diploids. Here we also described a full-length intein in *C. maltosa* (CmaThrRS), which, like the CorThrRS-B, presents both aspartic acids residues (D), and in *C. sojae* (CsoThrRS), whose aspartic acid residues were replaced by the amino acids T and S (**Table 1**; Supplementary Figure S2).

Phylogeny of the ThrRS inteins clearly distinguished the *Candida* species from the *C. parapsilosis* complex (**Figure 2B**), but it does not corroborate the species phylogeny initially proposed, in which *C. metapsilosis* and *C. orthopsilosis* share a most recent common ancestor and are the sister clade of *C. parapsilosis* (Tavanti et al., 2005; Wolfe et al., 2012). However, a more recent phylogenetic analysis using 396 conserved, as well as a super-tree derived from the whole phylome using a gene tree parsimony approach, supported a basal position of *C. metapsilosis* to the exclusion of *C. orthopsilosis* and *C. parapsilosis* (Pryszcz et al., 2015).

The splicing domain of the intein CorThrRS-B (a full-length intein) does not group with the other intein of *C. orthopsilosis*, the CorThrRS-A (a mini intein), since it is more closely related to ThrRS inteins from *C. tropicalis, C. maltosa* and *C. sojae* (**Figure 2B**). This might reflect the occurrence of independent intein invasions. The ancestor of *C. orthopsilosis* species might have its *THRRS* gene invaded by an intein (ThrRS-A), which, following the homing cycle "rules," might have been fixed in most of population, leading to its HE degeneration (explaining its current mini-intein structure). Since the homing endonuclease is no longer functional, empty sites could have arisen being occupied again by another intein, the ThrRS-B, which also invaded the *THRRS* gene from *C. tropicalis, C. sojae,* and *C. maltosa.*

The ThrRS intein has 29.33% of similarity with one of the four inteins located in the RNA polymerase II of *Chlamydomonas reinhardtii* (the CreRPB2-a intein), a green unicellular algae. Indeed, the RPB2-a intein was discovered because of its similarity to the threonyl-tRNA synthetase intein from *C. tropicalis*, which suggest the occurrence of horizontal transfer (Goodwin et al., 2006; Poulter et al., 2007). This horizontal transfer, if recent, can be evidenced by the sequence similarity between the exteins and between the inteins and also by differences in codon usage between intein and extein, as demonstrated for the DnaB intein and its extein in *Rhodothermus marinus* (Liu and Hu, 1997). If two homologous inteins are not related through recent lateral transfer, the sequence divergence between them is larger than between their extein sequences, in a similar way that happens to introns, whose sequences usually diverge faster than exon sequences. Accordingly, in the well-known case of lateral transfer of DnaB intein from *Synechocystis* sp. to *R. marinus*, the intein aminoacid sequences share a 54% sequence identity that is noticeably higher than the 37% sequence identity shared by the DnaB extein sequences (Liu and Hu, 1997). In the case of the CtrThrRS and CreRPB2 inteins: their identity is 29.33%, which is higher than the 17.77% sequence identity shared by the extein sequences. But, of course, this low identity is already expected since these exteins are not homologous genes. However, no pronounced deviation in relative synonymous codon usage (RSCU) (Sharp et al., 1986) is observed between the ThrRS intein and its extein or between the RPB2-a intein and its extein, suggesting that the possible lateral transfer was not a recent event (**Figures 3A,B**). The same is not observed between both inteins and also between both exteins, which present a great codon usage deviation (Supplementary Figures S4A,B).

The aaRSs are considered important therapeutic target for antibiotics, antifungals and antiprotozoal drugs. Most inhibitors of aaRSs act by competitive binding at the active site where normally the cognate amino acid would bind (Vondenhoff and Van Aerschot, 2011; Kalidas et al., 2014). Most of these compounds are not commercial and few have reached the stage of clinical development. Icofungipen, for example is an antifungal that inhibits IleRS, presenting satisfactory clinical efficacy and safety, although low mycological eradication rates were observed in HIV-positive patients (Ochsner et al., 2007). Cispentacin, a cyclic β-amino acid that has been isolated from *Bacillus cereus* and *Streptomyces setonii* inhibits IleRS and proved to be effective against *C. albicans* infection in mice (Konishi et al., 1989; Ochsner et al., 2007).

The presence of an intein in the ThrRS protein would represent an additional approach for its inhibition, as well as it would assure a specific and therefore safer antifungal mechanism, because, despite the functional evolutionary convergence, as all the aaRS carry out the same basic biochemical function (O'Donoghue and Luthey-Schulten, 2003), only the ThrRS protein of the fungal pathogen has an intervening intein.

## GLT1 Intein

The *GLT1* gene codifies an oligomeric enzyme named glutamate synthase (GOGAT), which is composed by three identical subunits. This enzyme, together with glutamine synthase, encoded by *GLN1* gene, is involved in one of the three pathways for the synthesis of glutamate, in yeast cells. GOGAT catalyzes the reductive synthesis of L-glutamate from 2-oxoglutarate and L-glutamine via intramolecular channeling of ammonia. It is a multifunctional enzyme that functions through three distinct active centers, carrying out L-glutamine hydrolysis, conversion of 2-oxoglutarate into L-glutamate and electron uptake from an electron donor (Filetici et al., 1996).

In this review we described, for the first time the GLT1 intein in *C. carpophila,* a distinct species that is closely related to both *P. guilliermondii* and *C. fermentati*. Before being described as a different species, *C. carpophila,* previously named as *C. guilliermondii* var. *carpophila*, was considered as a member of a genetically heterogeneous complex comprising several

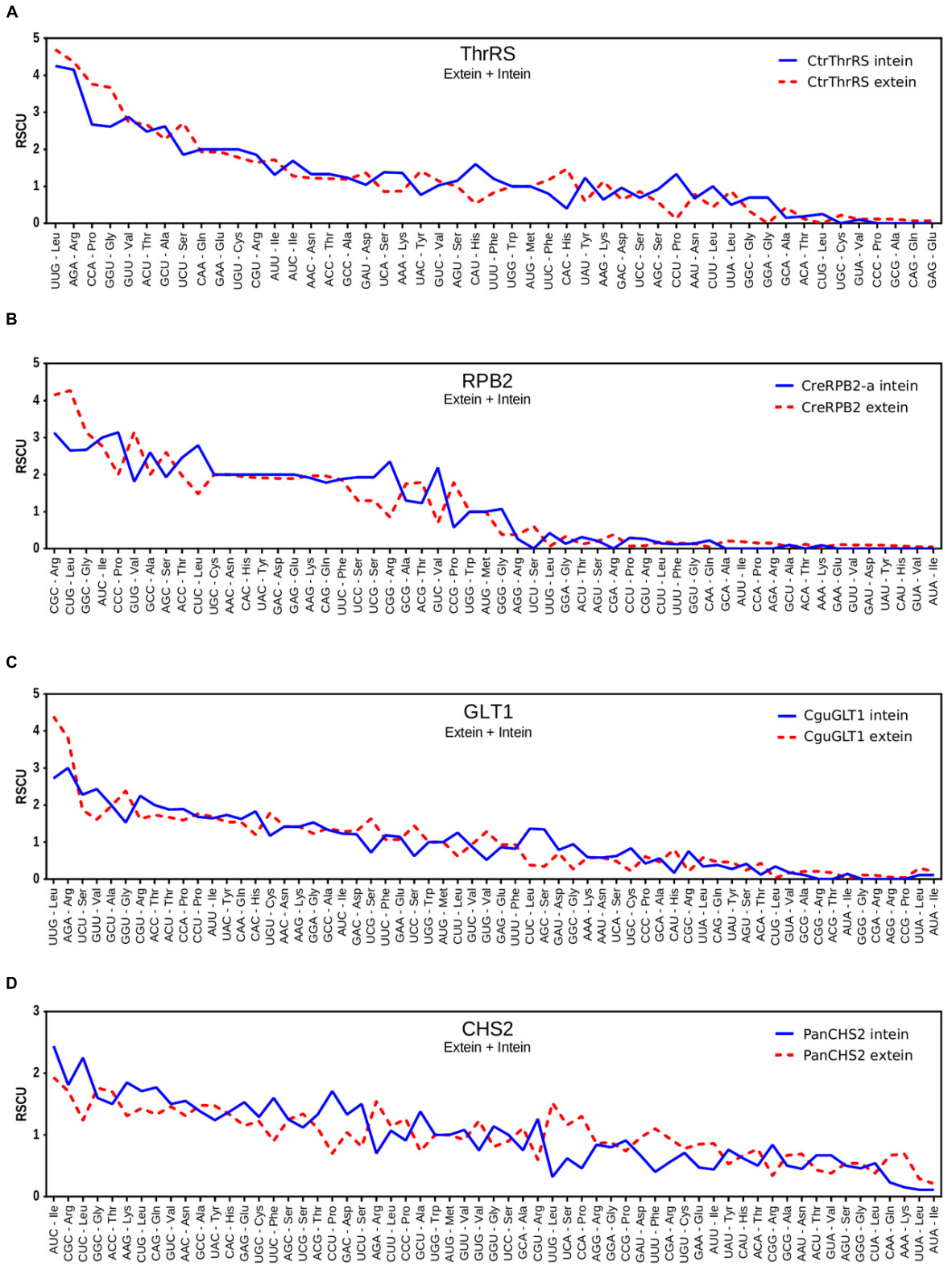


**FIGURE 3 | Graphic view of RSCU values for codon usage in ThrRS, GLT1, RBP2 and CHS2 inteins and their respective exteins.** Comparison between: **(A)** RSCU values for CtrThrRS intein and *THRRS* gene of *C. tropicalis* without intein; **(B)** RSCU values for CreRBP2-a intein and *RPB2* gene of *C. reinhardtii* without intein; **(C)** RSCU values for CguGLT1 intein and *GLT1* gene of *C. tropicalis* without intein and **(D)** RSCU values for PanCHS2 intein and *CHS2* gene of *P. anserina* without intein.

phenotypically indistinguishable taxa inside *C. guilliermondii* (Vaughan-Martini et al., 2005).

Both CfaGLT1 and CcarGLT1 inteins present the two aspartic acid residues, known to be essential for HE function, while CguGLT1 presented a substitution to E residue in the first aspartate (**Table 1**; Supplementary Figure S3). Phylogenetic analysis previously indicated that these inteins were very closely related to a non-allelic intein, the PanCHS2 (the intein in chitin synthase 2, from *Podospora anserina*) (Poulter et al., 2007). Similarly to that observed for the ThrRS intein, the RSCU between the GLT1 intein and its extein is concordant for most codons, also indicating that the possible lateral transfer of this intein from CHS2 to GLT1 is ancient (**Figures 3C,D**). The same is not observed between both inteins and also between both exteins, which present a great codon usage deviation (Supplementary Figures S4C,D).

As we can infer from **Figure 2C**, the GLT1 intein probably invaded the *GLT1* gene before the divergence of *Candida* species from the clade 2 proposed by Diezmann et al. (2004), which includes *C. guilliermondii, C. intermedia, C. famata* and *C. zeylanoides*. Evidently this intein was lost in *C. intermedia* and *C. zeylanoides,* probably due to HE degeneration and genetic drift.

According to KEEG Orthology (entry: YDL171C), the host protein for this intein, the GOGAT protein, is involved in cryptic pathways such as (i) alanine, aspartate and glutamate metabolism; (ii) nitrogen metabolism; (iii) biosynthesis of secondary metabolites; (iv) biosynthesis of antibiotics; and (v) biosynthesis of amino-acids. Connecting all these pathways, there is high nitrogen dependency. Nitrogen is a very important component, which is present in the chemical structure of almost every single molecule in cell's constituents. Yeasts cannot make their own nitrogen by taking it from the air, so it is necessary external sources of this macronutrient to keep it constantly available. So, the cell needs to adapt their metabolism to obtain or catabolize the available nitrogen sources, such as ammonia, glutamine, asparagine, glutamate, and proteins.

As the life style of *Candida* ssp. ranges from environmental to commensal and/or parasitic, the nutrient availability varies as well. During infection, *Candida* ssp. needs to obtain nitrogen from a broad range of different sources, which may change dramatically depending on the anatomical site of infection. The changing from commensal to pathogenic growth depends on a differential gene expression, which allows the establishment of infection (Ramachandra et al., 2014).

*Candida* spp. are constantly exposed to stressful agents, such as nitrogen deprivation in their microenvironment changing. Also, it is known that nitrogen source utilization modulates some morphological and physiological changes, sexual and asexual sporulation and virulence factors expression (Marzluf, 1997; Biswas et al., 2007). Therefore, the presence of the intein in this protein, by a post-translational expression modulation, could allow fine adjustments in nitrogen pathway during infection.

GLT1 expression is highly modulated in *S. cerevisiae*, being repressed in the presence of glutamate rich nitrogen sources, which suggests that GOGAT may have an important role in glutamate biosynthesis under conditions where this amino acid becomes limiting. It seems that GOGAT constitute an ancillary pathway, supplying low but continuous glutamate production, even in the presence of other glutamate pathways, suggesting that a high intracellular glutamate concentration may be needed for optimal growth, mainly under conditions in which carbon and nitrogen are limiting (Valenzuela et al., 1998). *GLT1* knockout evaluation showed that GOGAT does not significantly influence cellular physiology, corroborating its auxiliary characteristic in glutamate synthesis (Brambilla et al., 2016), though GOGAT non-expression yeasts accumulated more ROS, when treated with hydrogen peroxide.

The use of different glutamate pathways in *Candida* was compared to Saccharomyces (Holmes et al., 1989). The authors compared the NADP+-dependent GDH and GOGAT pathways activities in four *Candida* species (*C. albicans, Candida pseudotropicalis, C. parapsilosis* and *C. tropicalis*) and *S. cerevisiae*. The relative contribution of GOGAT in *S. cerevisiae* is around 1.6%, while among *Candida* species it ranges from 13 to 70%, being most expressive in *C. albicans*. This observation may indicate that, in *Candida*, GOGAT pathway may have a greater impact in nitrogen metabolism than in *S. cerevisiae*, so a post-translational regulatory role of the intein in this gene would be noteworthy in *Candida.* Thus, if the relative contribution of GOGAT is as expressive in non-albicans *Candida* species containing GLT1 intein as it is in *C. albicans,* the GLT1 intein could also be considered an additional drug target.

## CONCLUSION

In this review, the list of intein containing *Candida* species was updated, as well as their sequence features and phylogenetic relationships. The horizontally transferred nature of VMA inteins was corroborated by our phylogeny. The possible lateral transfer of inteins from *C. reinhardtii* (*RPB2* gene) and *P. anserina* (*CHS2* gene) to *THRRS* and *GLT1* genes, respectively, of *Candida* species, might be very ancient, since no significant deviation of RSCU was observed between these inteins and their respective exteins. Besides the peculiar evolutionary history of the inteins, their presence or absence, as well as their polymorphic sizes, should also be explored as molecular markers for species or cryptic species recognition, assisting the diagnosis and the therapeutic choices, since different species diverge in their clinical and antifungal susceptibility aspects.

The recent discussions about whether inteins are parasitic genetic elements or post-translational expression modulators gives rise to important questions: Can the splicing efficiency of an intein be altered under different life-style conditions of opportunistic or pathogenic fungal species? Can inteins regulate gene expression in different ways during infection? Here we reviewed the importance of the *VMA, ThrRS* and *GLT1* genes in the yeast cell physiology. Besides acidifying vacuoles, the VMA protein can also be important for fungal filamentation, an important virulence feature in *C. albicans*. Can the presence of an intein in the VMA protein modulate its function in the

intein-containing *Candida* species, interfering in their filamentation capacity? The ThrRS protein is essential for protein synthesis in cell; the splicing inefficiency of its intein would prevent cell proliferation and maintenance. This protein is inhibited by some drugs and the presence of an intein in some species would add another way to target it, by inhibiting its intein splicing. The GOGAT protein, coding by *GLT1* gene, on the other hand, is not considered so essential because it is part of one out of three possible pathways to synthetize glutamate, however, since this pathway seems to be largely used in some *Candida* species, the GLT1 intein could also constitute an important therapeutic target for those non-albicans *Candida* species that contain it.

In order to address the aforementioned questions many experimental researches must be done, clarifying the actual role of inteins in fungal pathogens and possibly opening new prospects for antifungal drugs researches. The use of inteins as a new drug target is, clearly, limited to the species in which they are present in at least one protein, while their absence/presence should also be explored as a molecular marker. The merit of this discussion can be extended for other pathogenic fungi, besides *Candida* spp., that contain inteins in housekeeping genes, and may open a new study field in medical mycology concerning invasive genetic elements as tools for drug screening and diagnosis.

## AUTHOR CONTRIBUTIONS

JF, TP, and RT conceived, designed, did the literature review, provided and wrote the manuscript. JF carried out the search for inteins in *Candida* genomes and the RSCU analysis. TA, MC, and JG reviewed the taxonomy and epidemiology of *Candida* species. TA, MC, JG, and EB assisted in the preparation, final review, and co-wrote the manuscript.

## ACKNOWLEDGMENTS

This work was supported by fellowships and grants provided by Conselho Nacional de Desenvolvimento Científico e Tecnológico (CNPq/Universal 475525/2013-2), Universidade Federal do Rio Grande do Norte (PROPESQ-NUPLAM) and Fundação de Amparo a Pesquisa do Estado de São Paulo (FAPESP Grants 2012/04003-1, 2012/07741-3).

## SUPPLEMENTARY MATERIAL

The Supplementary Material for this article can be found online at: http://journal.frontiersin.org/article/10.3389/fmicb.2016.01585

## REFERENCES

Alcoba-flórez, J., Méndez-álvarez, S., Guarro, J., Pérez-roth, E., Arévalo, P., Cano, J., et al. (2005). Phenotypic and molecular characterization of *Candida nivariensis* sp. nov., a possible new opportunistic fungus. *J. Clin. Microbiol.* 43, 4107–4111. doi: 10.1128/JCM.43.8.4107

Bailey, D., Diamandis, E. P., Greub, G., Poutanen, S. M., Christensen, J. J., and Kostrzew, M. (2013). Use of MALDI-TOF for diagnosis of microbial infections. *Clin. Chem.* 59, 1435–1441. doi: 10.1373/clinchem.2013.204644

Bassetti, M., Merelli, M., Ansaldi, F., De Florentiis, D., Sartor, A., Scarparo, C., et al. (2015). Clinical and therapeutic aspects of candidemia: a five year single centre study. *PLoS ONE* 10:e0127534. doi: 10.1371/journal.pone.0127534

Bastidas, R. J., and Heitman, J. (2009). Trimorphic stepping stones pave the way to fungal virulence. *Proc. Natl. Acad. Sci. U.S.A.* 106, 351–352. doi: 10.1073/pnas.0811994106

Belfort, M., and Bonocora, R. P. (2014). Homing endonucleases: from genetic anomalies to programmable genomic clippers. *Methods Mol. Biol.* 1123, 1–26. doi: 10.1007/978-1-62703-968-0_1

Bishop, J. A., Chase, N., Magill, S. S., Kurtzman, C. P., Fiandaca, M. J., and Merz, W. G. (2008). *Candida* bracarensis detected among isolates of *Candida glabrata* by peptide nucleic acid fluorescence in situ hybridization: susceptibility data and documentation of presumed infection. *J. Clin. Microbiol.* 46, 443–446. doi: 10.1128/JCM.01986-07

Biswas, S., Van Dijck, P., and Datta, A. (2007). Environmental sensing and signal transduction pathways regulating morphopathogenic determinants of *Candida albicans*. *Microbiol. Mol. Biol. Rev.* 71, 348–376. doi: 10.1128/MMBR.00009-06

Borman, A. M., Linton, C. J., Oliver, D., Palmer, M. D., Szekely, A., Odds, F. C., et al. (2009). Pyrosequencing analysis of 20 nucleotides of internal transcribed spacer 2 discriminates *Candida parapsilosis*, *Candida metapsilosis*, and *Candida orthopsilosis*. *J. Clin. Microbiol.* 47, 2307–2310. doi: 10.1128/JCM.00240-09

Brambilla, M., Adamo, G. M., Frascotti, G., Porro, D., and Branduardi, P. (2016). Physiological effects of GLT1 modulation in *Saccharomyces cerevisiae* strains growing on different nitrogen sources. *J. Microbiol. Biotechnol.* 26, 326–336. doi: 10.4014/jmb.1508.08002

Burt, A., and Koufopanou, V. (2004). Homing endonuclease genes: the rise and fall and rise again of a selfish element. *Curr. Opin. Genet. Dev.* 14, 609–615. doi: 10.1016/j.gde.2004.09.010

Butler, M. I., Goodwin, T. J. D., and Poulter, R. T. M. (2001). A nuclear-encoded intein in the fungal pathogen *Cryptococcus neoformans*. *Yeast* 18, 1365–1370. doi: 10.1002/yea.781

Butler, M. I., Gray, J., Goodwin, T. J. D., and Poulter, R. T. M. (2006). The distribution and evolutionary history of the PRP8 intein. *BMC Evol. Biol.* 6:42. doi: 10.1186/1471-2148-6-42

Butler, M. I., and Poulter, R. T. M. (2005). The PRP8 inteins in *Cryptococcus* are a source of phylogenetic and epidemiological information. *Fungal Genet. Biol.* 42, 452–463. doi: 10.1016/j.fgb.2005.01.011

Chong, S., Shao, Y., Paulus, H., Benner, J., Perler, F. B., and Xu, M. (1996). Protein splicing involving the *Saccharomyces cerevisiae* VMA intein. *J. Biol. Chem.* 271, 22159–22168. doi: 10.1074/jbc.271.36.22159

Cleveland, A. A., Farley, M. M., Harrison, L. H., Stein, B., Hollick, R., Lockhart, S. R., et al. (2012). Changes in incidence and antifungal drug resistance in candidemia: results from population-based laboratory surveillance in Atlanta and Baltimore, 2008-2011. *Clin. Infect. Dis.* 55, 1352–1361. doi: 10.1093/cid/cis697

Cleveland, A. A., Harrison, L. H., Farley, M. M., Hollick, R., Stein, B., Chiller, T. M., et al. (2015). Declining incidence of candidemia and the shifting epidemiology of *Candida* resistance in two US metropolitan areas, 2008–2013: results from population-based surveillance. *PLoS ONE* 10:e0120452. doi: 10.1371/journal.pone.0120452

Colombo, A. L., Guimarães, T., Camargo, L. F. A., Richtmann, R., de Queiroz-Telles, F., Salles, M. J. C., et al. (2013). Brazilian guidelines for the management of candidiasis – a joint meeting report of three medical societies: Sociedade Brasileira de Infectologia, Sociedade Paulista de Infectologia and Sociedade Brasileira de Medicina Tropical. *Braz. J. Infect. Dis.* 17, 283–312. doi: 10.1016/j.bjid.2013.02.001

Correia, A., Sampaio, P., James, S., and Pais, C. (2006). *Candida* bracarensis sp. nov., a novel anamorphic yeast species phenotypically similar to *Candida glabrata*. *Int. J. Syst. Evol. Microbiol.* 56, 313–317. doi: 10.1099/ijs.0.64076-0

De Carolis, E., Vella, A., Vaccaro, L., Torelli, R., Posteraro, P., Ricciardi, W., et al. (2014). Development and validation of an in-house database for matrix

assisted laser desorption ionization–time of flight mass spectrometry-based yeast Identification using a fast protein extraction procedure. *J. Clin. Microbiol.* 52, 1453–1458. doi: 10.1128/JCM.03355-13

Desnos-Ollivier, M., Ragon, M., Robert, V., Raoux, D., Gantier, J. C., and Dromer, F. (2008). *Debaryomyces hansenii* (*Candida* famata), a rare human fungal pathogen often misidentified as *Pichia guilliermondii* (*Candida guilliermondii*). *J. Clin. Microbiol.* 46, 3237–3242. doi: 10.1128/JCM.01451-08

Diezmann, S., Cox, C. J., Scho, G., Vilgalys, R. J., and Mitchell, T. G. (2004). Phylogeny and evolution of medical species of *Candida* and related taxa: a multigenic analysis. *J. Clin. Microbiol.* 42, 5624–5635. doi: 10.1128/JCM.42.12.5624

Fahami, S., Kordbacheh, P., Moazeni, M., Mahmoodi, M., and Mirhendi, H. (2010). Species identification and strain typing of *Candida* isolates by PCR-RFLP and RAPD-PCR analysis for determining the probable sources of nosocomial infections. *Iranian Red Crescent Med. J.* 12, 539–547.

Ferreira, A. V., Prado, C. G., Carvalho, R. R., Dias, K. S. T., and Dias, A. L. T. (2013). *Candida albicans* and Non-*C. albicans Candida* species: comparison of biofilm production and metabolic activity in biofilms, and putative virulence properties of isolates from hospital environments and infections. *Mycopathologia* 175, 265–272. doi: 10.1007/s11046-013-9638-z

Filetici, P., Martegani, M. P., Valenzuela, L., González, A., and Ballario, P. (1996). Sequence of the GLT1 gene from *Saccharomyces cerevisiae* reveals the domain structure of yeast glutamate synthase. *Yeast* 12, 1359–1366. doi: 10.1002/(SICI)1097-0061(199610)12:13<1359::AID-YEA3>3.0.CO;2-5

Gabaldón, T., Martin, T., Marcet-Houben, M., Durrens, P., Bolotin-Fukuhara, M., Lespinet, O., et al. (2013). Comparative genomics of emerging pathogens in the *Candida glabrata* clade. *BMC Genomics* 14:623. doi: 10.1186/1471-2164-14-623

Gacser, A., Schafer, W., Nosanchuk, J. S., Salomon, S., and Nosanchuk, J. D. (2007). Virulence of *Candida parapsilosis*, *Candida orthopsilosis* and *Candida metapsilosis* in reconstituted human tissue models. *Fungal Genet. Biol.* 44, 1336–1341. doi: 10.1016/j.fgb.2007.02.002

Ghosh, A. K., Paul, S., Sood, P., Rudramurthy, S. M., Rajbanshi, A., Jillwin, T. J., et al. (2015). Matrix-assisted laser desorption ionization time-of-fight mass spectrometry for the rapid identification of yeasts causing bloodstream infections. *Clin. Microbiol. Infect.* 21, 372–378. doi: 10.1016/j.cmi.2014.11.009

Gimble, F. S., and Thorner, J. (1992). Homing of a DNA endonuclease gene by meiotic gene conversion in *Saccharomyces cerevisiae*. *Nature* 357, 301–306. doi: 10.1038/357301a0

Goddard, M. R., and Burt, A. (1999). Recurrent invasion and extinction of a selfish gene. *Proc. Natl. Acad. Sci. U.S.A.* 96, 13880–13885. doi: 10.1073/pnas.96.24.13880

Gogarten, J. P., and Hilario, E. (2006). Inteins, introns, and homing endonucleases: recent revelations about the life cycle of parasitic genetic elements. *BMC Evol. Biol.* 6:94. doi: 10.1186/1471-2148-6-94

Goodwin, T. J. D., Butler, M. I., and Poulter, R. T. M. (2006). Multiple, non-allelic, intein-coding sequences in eukaryotic RNA polymerase genes. *BMC Biol.* 4:38. doi: 10.1186/1741-7007-4-38

Gurbuz, M., and Kaleli, I. (2010). Molecular analysis of *Candida albicans* isolates from clinical specimens. *Mycopathologia* 169, 261–267. doi: 10.1007/s11046-009-9263-z

Hays, C., Duhamel, C., Cattoir, V., and Bonhomme, J. (2011). Rapid and accurate identification of species belonging to the *Candida parapsilosis* complex by real-time PCR and melting curve analysis. *J. Med. Microbiol.* 60, 477–480. doi: 10.1099/jmm.0.026633-0

Higashi, C. M., Takashina, F. H., Zendrini, D., Stipp-abe, A. T., Vespero, E. C., and Mariuza, R. (2015). Comparison of Vitek-2 automated identification system and PCR-ITS for species characterization of clinical isolates. *Semina* 36, 233–242. doi: 10.5433/1679-0367.2015v36n1Suplp233

Hirata, R., Ohsumi, Y., Nakano, A., Kawasaki, H., Suzuki, K., and Anraku, Y. (1990). Molecular structure of a gene, VMA1, encoding the catalytic subunit of H(+)-translocating adenosine triphosphatase from vacuolar membranes of *Saccharomyces cerevisiae*. *J. Biol. Chem.* 265, 6726–6733.

Holmes, A. R., Collings, A., Farnden, K. J., and Shepherd, M. G. (1989). Ammonium assimilation by *Candida albicans* and other yeasts: evidence for activity of glutamate synthase. *J. Gen. Microbiol.* 135, 1423–1430.

Kalidas, S., Cestari, I., Monnerat, S., Li, Q., Regmi, S., Hasle, N., et al. (2014). Genetic validation of aminoacyl-tRNA synthetases as drug targets in *Trypanosoma brucei*. *Eukaryot. Cell* 13, 504–516. doi: 10.1128/EC.00017-14

Karahan, Z., Güriz, H., Agirbasli, H., Balaban, N., Gocmen, J. S., Aysev, D., et al. (2004). Genotype distribution of *Candida albicans* isolates by 25S intron analysis with regard to invasiveness. *Mycoses* 47, 465–469. doi: 10.1111/j.1439-0507.2004.01022.x

Konishi, M., Nishio, M., Saitoh, K., Miyaki, T., Oki, T., and Kawaguchi, H. (1989). Cispentacin, A new antifungal antibiotic I. Production, isolation, physico-chemical properties and structure. *J. Antibiot. (Tokyo)* 42, 1749–1755. doi: 10.7164/antibiotics.42.1749

Koufopanou, V., and Burt, A. (2005). Degeneration and domestication of a selfish gene in yeast: molecular evolution versus site-directed mutagenesis. *Mol. Biol. Evol.* 22, 1535–1538. doi: 10.1093/molbev/msi149

Koufopanou, V., Goddard, M. R., and Burt, A. (2002). Adaptation for horizontal transfer in a homing endonuclease. *Mol. Biol. Evol.* 19, 239–246. doi: 10.1093/oxfordjournals.molbev.a004077

Kurtzman, C. P. (2003). Phylogenetic circumscription of *Saccharomyces*, *Kluyveromyces* and other members of the Saccharomycetaceae, and the proposal of the new genera *Lachancea*, *Nakaseomyces*, *Naumovia*, *Vanderwaltozyma* and *Zygotorulaspora*. *FEMS Yeast Res.* 4, 233–245. doi: 10.1016/S1567-1356(03)00175-2

Lachance, M. A., Starmer, W. T., Rosa, C. A., Bowles, J. M., Barker, J. S., and Janzen, D. H. (2001). Biogeography of the yeasts of ephemeral flowers and their insects. *FEMS Yeast Res.* 1, 1–8. doi: 10.1016/S1567-1356(00)00003-9

Lagunes, L., and Rello, J. (2016). Invasive candidiasis: from mycobiome to infection, therapy, and prevention. *Eur. J. Clin. Microbiol. Infect. Dis.* 35, 1221–1226. doi: 10.1007/s10096-016-2658-0

Lasker, B. A., Butler, G., and Lott, T. J. (2006). Molecular genotyping of *Candida parapsilosis* group I clinical isolates by analysis of polymorphic microsatellite markers. *J. Clin. Microbiol.* 44, 750–759. doi: 10.1128/JCM.44.3.750

Le, S. Q., and Gascuel, O. (2008). An improved general amino acid replacement matrix. *Mol. Biol. Evol.* 25, 1307–1320. doi: 10.1093/molbev/msn067

Leipe, D. D., Koonin, E. V., and Aravind, L. (2004). STAND, a class of P-Loop NTPases including animal and plant regulators of programmed cell death: multiple, complex domain architectures, unusual phyletic patterns, and evolution by horizontal gene transfer. *J. Mol. Biol.* 343, 1–28. doi: 10.1016/j.jmb.2004.08.023

Liu, X. Q. (2000). Protein-splicing intein: genetic mobility, origin, and evolution. *Annu. Rev. Genet.* 34, 61–76. doi: 10.1146/annurev.genet.34.1.61

Liu, X. Q., and Hu, Z. (1997). A DnaB intein in *Rhodothermus marinus*: indication of recent intein homing across remotely related organisms. *Proc. Natl. Acad. Sci. U.S.A.* 94, 7851–7856. doi: 10.1073/pnas.94.15.7851

Liu, X. Q., and Yang, J. (2004). Prp8 intein in fungal pathogens: target for potential antifungal drugs. *FEBS Lett.* 572, 46–50. doi: 10.1016/j.febslet.2004.07.016

Lo, H. J., Köhler, J. R., Didomenico, B., Loebenberg, D., Cacciapuoti, A., and Fink, G. R. (1997). Nonfilamentous *C. albicans* mutants are avirulent. *Cell* 90, 939–949. doi: 10.1016/S0092-8674(00)80358-X

Lockhart, S. R., Iqbal, N., Cleveland, A. A., Farley, M. M., Harrison, L. H., Bolden, C. B., et al. (2012). Species identification and antifungal susceptibility testing of *Candida* bloodstream isolates from population-based surveillance studies in two U.S. cities from 2008 to 2011. *J. Clin. Microbiol.* 50, 3435–3442. doi: 10.1128/JCM.01283-12

Lockhart, S. R., Messer, S. A., Pfaller, M. A., and Diekema, D. J. (2008). Geographic distribution and antifungal susceptibility of the newly described species *Candida orthopsilosis* and *Candida metapsilosis* in comparison to the closely related species *Candida parapsilosis*. *J. Clin. Microbiol.* 46, 2659–2664. doi: 10.1128/JCM.00803-08

Lopez-Martinez, R. (2010). Candidosis, a new challenge. *Clin. Dermatol.* 28, 178–184. doi: 10.1016/j.clindermatol.2009.12.014

Marzluf, G. A. (1997). Genetic regulation of nitrogen metabolism in the fungi. *Microbiol. Mol. Biol. Rev.* 61, 17–32.

Maubon, D., Garnaud, C., Calandra, T., Sanglard, D., and Cornet, M. (2014). Resistance of *Candida* spp. to antifungal drugs in the ICU: where are we now? *Intensive Care Med.* 40, 1241–1255. doi: 10.1007/s00134-014-3404-7

Merseguel, K., Nishikaku, A., Rodrigues, A., Padovan, A., Ferreira, R., de Azevedo Melo, A. S., et al. (2015). Genetic diversity of medically important and

emerging *Candida* species causing invasive infection. *BMC Infect. Dis.* 15:57. doi: 10.1186/s12879-015-0793-3

Miletti, K. E., and Leibowitz, M. J. (2000). Pentamidine inhibition of group I intron splicing in *Candida albicans* correlates with growth inhibition. *Antimicrob. Agents Chem.* 44, 958–966. doi: 10.1128/AAC.44.4.958-966.2000

Miraula, M., Enculescu, C., Schenk, G., and Mitić, N. (2015). Applications of splicing-promoting proteins. *Am. J. Mol. Biol.* 5, 42–56. doi: 10.4236/ajmb.2015.52005

Mita, P., and Boeke, J. D. (2016). How retrotransposons shape genome regulation. *Curr. Opin. Genet. Dev.* 37, 90–100. doi: 10.1016/j.gde.2016.01.001

Nagasaki, K., Shirai, Y., Tomaru, Y., Nishida, K., and Pietrokovski, S. (2005). Algal viruses with distinct intraspecies host specificities include identical intein elements. *Appl. Environ. Microbiol.* 71, 3599–3607. doi: 10.1128/AEM.71.7.3599-3607.2005

Nakase, T. (1971). New species resembling of yeasts *Candida krusei* (cast.) Berkhout. *J. Gen. Appl. Microbiol.* 398, 383–398. doi: 10.2323/jgam.17.383

Nakase, T., Suzuki, M., Takashima, M., Miyakawa, Y., Kagaya, K., Fukazawa, Y., et al. (1994). *Candida sojae*, a new species of yeast isolated from an extraction process of water soluble substances of defatted soubean flakes. *J. Gen. Appl. Microbiol.* 40, 161–169. doi: 10.2323/jgam.40.161

Nelson, N., Perzov, N., Cohen, A., Hagai, K., Padler, V., and Nelson, H. (2000). The cellular biology of proton-motive force generation by V-ATPases. *J. Exp. Biol.* 203, 89–95.

Novikova, O., Jayachandran, P., Kelley, D. S., Morton, Z., Merwin, S., Topilina, N. I., et al. (2015). Intein clustering suggests functional importance in different domains of life. *Mol. Biol. Evol.* 33, 783–799. doi: 10.1093/molbev/msv271

Novikova, O., Topilina, N., and Belfort, M. (2014). Enigmatic distribution, evolution, and function of Inteins. *J. Biol. Chem.* 289, 14490–14497. doi: 10.1074/jbc.R114.548255

Nucci, M., Queiroz-Telles, F., Tobón, A. M., Restrepo, A., and Colombo, A. L. (2010). Epidemiology of opportunistic fungal infections in Latin America. *Clin. Infect. Dis.* 51, 561–570. doi: 10.1086/655683

Ochsner, U. A., Sun, X., Jarvis, T., Critchley, I., and Janjic, N. (2007). Aminoacyl-tRNA synthetases: essential and still promising targets for new anti-infective agents. *Expert. Opin. Investig. Drug* 16, 573–593. doi: 10.1517/13543784.16.5.573

O'Donoghue, P., and Luthey-Schulten, Z. (2003). On the evolution of structure in aminoacyl-tRNA synthetases. *Microbiol. Mol. Biol. Rev.* 67, 550–573. doi: 10.1128/MMBR.67.4.550

Okuda, Y., Sasaki, D., Nogami, S., Kaneko, Y., Ohya, Y., and Anraku, Y. (2003). Occurrence, horizontal transfer and degeneration of VDE intein family in Saccharomycete yeasts. *Yeast* 20, 563–573. doi: 10.1002/yea.984

Paramythiotou, E., Frantzeskaki, F., Flevari, A., Armaganidis, A., and Dimopoulos, G. (2014). Invasive fungal infections in the ICU: how to approach, how to treat. *Molecules* 19, 1085–1119. doi: 10.3390/molecules19011085

Paulus, H. (2003). Inteins as targets for potential antimycobacterial drugs. *Front. Biosci.* 1:1157–1165. doi: 10.2741/1195

Paulus, H. (2007). Protein splicing inhibitors as a new class of antimycobacterial agents. *Drugs Fut.* 32, 973–984. doi: 10.1358/dof.2007.032.11.1140690

Perler, F. B. (2002). InBase: the intein database. *Nucleic Acids Res.* 30, 383–384. doi: 10.1093/nar/30.1.383

Perler, F. B. (2005). Protein splicing mechanisms and applications. *IUBMB Life* 57, 469–476. doi: 10.1080/15216540500163343

Pfaller, M. A., Andes, D. R., Diekema, D. J., Horn, D. L., Reboli, A. C., Rotstein, C., et al. (2014). Epidemiology and outcomes of invasive candidiasis due to non-albicans species of *Candida* in 2,496 patients: data from the Prospective Antifungal Therapy (PATH) registry 2004–2008. *PLoS ONE* 9:e101510. doi: 10.1371/journal.pone.0101510

Pfaller, M. A., Chaturvedi, V., Diekema, D. J., Ghannoum, M. A., Holliday, N. M., Killian, S. B., et al. (2012). Comparison of the sensititre YeastOne colorimetric antifungal panel with CLSI microdilution for antifungal susceptibility testing of the echinocandins against *Candida* spp., using new clinical breakpoints and epidemiological cutoff values. *Diagn. Microbiol. Infect. Dis.* 73, 365–368. doi: 10.1016/j.diagmicrobio.2012.05.008

Pfaller, M. A., and Diekema, D. J. (2007). Epidemiology of invasive candidiasis: a persistent public health problem. *Clin. Microbiol. Rev.* 20, 133–163. doi: 10.1128/CMR.00029-06

Posey, K. L., Koufopanou, V., Burt, A., and Gimble, F. S. (2004). Evolution of divergent DNA recognition specificities in VDE homing endonucleases from two yeast species. *Nucleic Acids Res.* 32, 3947–3956. doi: 10.1093/nar/gkh734

Poulter, R. T. M., Goodwin, T. J. D., and Butler, M. I. (2007). The nuclear-encoded inteins of fungi. *Fungal Genet. Biol.* 44, 153–179. doi: 10.1016/j.fgb.2006.07.012

Prandini, T. H. R., Theodoro, R. C., Bruder-Nascimento, A. C. M. O., Scheel, C. M., and Bagagli, E. (2013). Analysis of inteins in the *Candida parapsilosis* complex for simple and accurate species identification. *J. Clin. Microbiol.* 51, 2830–2836. doi: 10.1128/JCM.00981-13

Pryszcz, L. P., Németh, T., Gácser, A., and Gabaldón, T. (2014). Genome comparison of *Candida orthopsilosis* clinical strains reveals the existence of hybrids between two distinct subspecies. *Genome Biol. Evol.* 6, 1069–1078. doi: 10.1093/gbe/evu082

Pryszcz, L. P., Németh, T., Saus, E., Ksiezopolska, E., Hegedűsová, E., Nosek, J., et al. (2015). The genomic aftermath of hybridization in the opportunistic pathogen *Candida metapsilosis*. *PLoS Genet.* 11:e1005626. doi: 10.1371/journal.pgen.1005626

Quiles-Melero, I., García-Rodríguez, J., Gómez-López, A., and Mingorance, J. (2012). Evaluation of matrix-assisted laser desorption/ionisation time-of-flight (MALDI-TOF) mass spectrometry for identification of *Candida parapsilosis*, *C. orthopsilosis* and *C. metapsilosis*. *Eur. J. Clin. Microbiol. Infect. Dis.* 31, 67–71. doi: 10.1007/s10096-011-1277-z

Ramachandra, S., Linde, J., Brock, M., Guthke, R., Hube, B., and Brunke, S. (2014). Regulatory networks controlling nitrogen sensing and uptake in *Candida albicans*. *PLoS ONE* 9:e92734. doi: 10.1371/journal.pone.0092734

Richardson, M., and Lass-Flörl, C. (2008). Changing epidemiology of systemic fungal infections. *Clin. Microbiol. Infect.* 14, 5–24. doi: 10.1111/j.1469-0691.2008.01978.x

Ruan, S.-Y., Chien, J.-Y., Hou, Y.-C., and Hsueh, P.-R. (2010). Catheter-related fungemia caused by *Candida* intermedia. *Int. J. Infect. Dis.* 14, 147–149. doi: 10.1016/j.ijid.2009.03.015

Sai, S., Holland, L. M., McGee, C. F., Lynch, D. B., and Butler, G. (2011). Evolution of mating within the *Candida parapsilosis* species group. *Eukaryot. Cell* 10, 578–587. doi: 10.1128/EC.00276-10

Sardi, J. C. O., Scorzoni, L., Bernardi, T., Fusco-Almeida, A. M., and Mendes Giannini, M. J. S. (2013). *Candida* species: current epidemiology, pathogenicity, biofilm formation, natural antifungal products and new therapeutic options. *J. Med. Microbiol.* 62, 10–24. doi: 10.1099/jmm.0.045054-0

Satish Kumar, R., and Ramesh, S. (2014). Novel intein-containing DNA specific primers for rapid identification of *Candida glabrata* using Real-Time PCR assays. *J. Med. Mycol.* 24, 337–340. doi: 10.1016/j.mycmed.2014.08.002

Saville, S. P., Lazzell, A. L., Bryant, A. P., Fretzen, A., Monreal, A., Solberg, E. O., et al. (2006). Inhibition of filamentation can be used to treat disseminated candidiasis. *Antimicrob. Agents Chemother.* 50, 3312–3316. doi: 10.1128/AAC.00628-06

Sharp, P. M., Tuohy, T. M. F., and Mosurski, K. R. (1986). Codon usage in yeast: cluster analysis clearly differentiates highly and lowly expressed genes. *Nucleic Acids Res.* 14, 5125–5143. doi: 10.1093/nar/14.13.5125

Souza, A. C. R., Ferreira, R. C., Gonçalves, S. S., Quindós, G., Eraso, E., Bizerra, F. C., et al. (2012). Accurate identification of *Candida parapsilosis* (sensu lato) by use of mitochondrial DNA and real-time PCR. *J. Clin. Microbiol.* 50, 2310–2314. doi: 10.1128/JCM.00303-12

Spampinato, C., and Leonardi, D. (2013). *Candida* infections, causes, targets, and resistance mechanisms: traditional and alternative antifungal agents. *Biomed Res. Int.* 2013:204237. doi: 10.1155/2013/204237

Steuer, S., Pingoud, V., Pingoud, A., and Wende, W. (2004). Chimeras of the homing endonuclease PI-Scel and the homologous *Candida tropicalis* intein: a study to explore the possibility of exchanging DNA-binding modules to obtain highly specific endonucleases with altered specificity. *Chembiochem* 5, 206–213. doi: 10.1002/cbic.200300718

Sudbery, P. E. (2011). Growth of *Candida albicans* hyphae. *Nat. Rev. Microbiol.* 9, 737–748. doi: 10.1038/nrmicro2636

Swithers, K., Senejani, A., Fournier, G., and Gogarten, J. P. (2009). Conservation of intron and intein insertion sites: implications for life histories of parasitic genetic elements. *BMC Evol. Biol.* 9:303. doi: 10.1186/1471-2148-9-303

Tamura, K., Stecher, G., Peterson, D., Filipski, A., and Kumar, S. (2013). MEGA6: molecular evolutionary genetics analysis version 6.0. *Mol. Biol. Evol.* 30, 2725–2729. doi: 10.1093/molbev/mst197

Tavanti, A., Davidson, A. D., Gow, N. A. R., Maiden, M. C. J., and Odds, F. C. (2005). *Candida parapsilosis* groups II and III. *J. Clin. Microbiol.* 43, 284–292. doi: 10.1128/JCM.43.1.284

Theodoro, R. C., and Bagagli, E. (2009). Inteins in pathogenic fungi: a phylogenetic tool and perspectives for therapeutic applications. *Mem. Inst. Oswaldo Cruz* 104, 497–504. doi: 10.1590/S0074-02762009000300017

Theodoro, R. C., Bagagli, E., and Oliveira, C. (2008). Phylogenetic analysis of PRP8 intein in *Paracoccidioides brasiliensis* species complex. *Fungal Genet. Biol.* 45, 1284–1291. doi: 10.1016/j.fgb.2008.07.003

Theodoro, R. C., Scheel, C. M., Brandt, M. E., Kasuga, T., and Bagagli, E. (2013). PRP8 intein in cryptic species of *Histoplasma capsulatum*: evolution and phylogeny. *Infect. Genet. Evol.* 18, 174–182. doi: 10.1016/j.meegid.2013.05.001

Theodoro, R. C., Volkmann, G., Liu, X. Q., and Bagagli, E. (2010). PRP8 intein in Ajellomycetaceae family pathogens: sequence analysis, splicing evaluation and homing endonuclease activity. *Fungal Genet. Biol.* 48, 80–91. doi: 10.1016/j.fgb.2010.07.010

Topilina, N. I., Green, C. M., Jayachandran, P., Kelley, D. S., Stanger, M. J., Lyn, C., et al. (2015a). SufB intein of *Mycobacterium tuberculosis* as a sensor for oxidative and nitrosative stresses. *Proc. Natl. Acad. Sci. U.S.A.* 112, 10348–10353. doi: 10.1073/pnas.1512777112

Topilina, N. I., Novikova, O., Stanger, M., Banavali, N. K., and Belfort, M. (2015b). Post-translational environmental switch of RadA activity by extein – intein interactions in protein splicing. *Nucleic Acids Res.* 43, 6631–6648. doi: 10.1093/nar/gkv612

Tran, A., Alby, K., Kerr, A., Jones, M., and Gilligan, P. H. (2015). Cost savings realized by implementation of routine microbiological Identification by matrix-assisted laser desorption ionization–time of flight mass spectrometry. *J. Clin. Microbiol.* 53, 2473–2479. doi: 10.1128/JCM.00833-15

Valenzuela, L., Ballario, P., Aranda, C., Filetici, P., and González, A. (1998). Regulation of expression of GLT1, the gene encoding glutamate synthase in *Saccharomyces cerevisiae*. *J. Bacteriol.* 180, 3533–3540.

Vaughan-Martini, A., Kurtzman, C. P., Meyer, S. A., and O'Neill, E. B. (2005). Two new species in the *Pichia guilliermondii* clade: *Pichia caribbica* sp. nov., the ascosporic state of *Candida fermentati*, and *Candida carpophila* comb. nov. *FEMS Yeast Res.* 5, 463–469. doi: 10.1016/j.femsyr.2004.10.008

Vega-Alvarado, L., Gómez-Angulo, J., Escalante-García, Z., Grande, R., Gschaedler-Mathis, A., Amaya-Delgado, L., et al. (2015). High-quality draft genome sequence of *Candida apicola* NRRL Y-50540. *Genome Announc.* 3, e00437-15. doi: 10.1128/genomeA.00437-15

Volkmann, G., and Iwaı, H. (2010). Protein trans -splicing and its use in structural biology?: opportunities and limitations. *Mol. Biosyst.* 6, 2110–2121. doi: 10.1039/c0mb00034e

Vondenhoff, G. H. M., and Van Aerschot, A. (2011). Aminoacyl-tRNA synthetase inhibitors as potential antibiotics. *Eur. J. Med. Chem.* 46, 5227–5236. doi: 10.1016/j.ejmech.2011.08.049

Wang, H., Xiao, M., Chen, S. C. A., Kong, F., Sun, Z. Y., Liao, K., et al. (2012). In Vitro susceptibilities of yeast species to fluconazole and voriconazole as determined by the 2010 National China Hospital invasive fungal surveillance net (CHIF-NET) study. *J. Clin. Microbiol.* 50, 3952–3959. doi: 10.1128/JCM.01130-12

Whelan, S., and Goldman, N. (2001). A general empirical model of protein evolution derived from multiple protein families using a maximum-likelihood approach. *Mol. Biol. Evol.* 18, 691–699. doi: 10.1093/oxfordjournals.molbev.a003851

Wisplinghoff, H., Bischoff, T., Tallent, S. M., Seifert, H., Wenzel, R. P., and Edmond, M. B. (2004). Nosocomial bloodstream infections in US hospitals: analysis of 24,179 cases from a prospective nationwide surveillance study. *Clin. Infect. Dis.* 39, 309–317. doi: 10.1086/421946

Wolfe, K. H., Riccombeni, A., Vidanes, G., Proux-we, E., and Butler, G. (2012). Sequence and analysis of the genome of the pathogenic yeast *Candida orthopsilosis*. *PLoS ONE* 7:e35750. doi: 10.1371/journal.pone.0035750

Wood, D. W., Wu, W., Belfort, G., Derbyshire, V., and Belfort, M. (1999). A genetic system yields self-cleaving inteins for bioseparations. *Nat. Biotechnol.* 17, 889–892. doi: 10.1038/12879

Yapar, N. (2014). Epidemiology and risk factors for invasive candidiasis. *Ther. Clin. Risk Manag.* 10, 95–105. doi: 10.2147/TCRM.S40160

Yun, Y. H., Suh, D. Y., Yoo, H. D., Oh, M. H., and Kim, S. H. (2015). Yeast associated with the ambrosia beetle, *Platypus* koryoensis, the pest of oak trees in Korea. *Mycobiology* 43, 458–466. doi: 10.5941/MYCO.2015.43.4.458

Zhang, L., Zheng, Y., Callahan, B., Belfort, M., and Liu, Y. (2010). Cisplatin inhibits protein splicing, suggesting inteins as therapeutic targets in mycobacteria. *J. Biol. Chem.* 286, 1277–1282. doi: 10.1074/jbc.M110.171124

Zhang, Y.-Q., and Rao, R. (2010). Beyond ergosterol: linking pH to antifungal mechanisms. *Virulence* 1, 551–554. doi: 10.4161/viru.1.6.13802

**Conflict of Interest Statement:** The authors declare that the research was conducted in the absence of any commercial or financial relationships that could be construed as a potential conflict of interest.

frontiers in Microbiology

ORIGINAL RESEARCH
published: 19 May 2017
doi: 10.3389/fmicb.2017.00918

# HIV Aspartic Peptidase Inhibitors Modulate Surface Molecules and Enzyme Activities Involved with Physiopathological Events in *Fonsecaea pedrosoi*

*Vanila F. Palmeira[1,2], Daniela S. Alviano[2], Lys A. Braga-Silva[1,3], Fátima R. V. Goulart[2], Marcela Q. Granato[4], Sonia Rozental[5], Celuta S. Alviano[2], André L. S. Santos[1,3]* and Lucimar F. Kneipp[4]**

[1] Laboratório de Investigação de Peptidases, Departamento de Microbiologia Geral, Instituto de Microbiologia Paulo de Góes, Universidade Federal do Rio de Janeiro, Rio de Janeiro, Brazil, [2] Laboratório de Estrutura de Microrganismos, Departamento de Microbiologia Geral, Universidade Federal do Rio de Janeiro, Rio de Janeiro, Brazil, [3] Programa de Pós-Graduação em Bioquímica, Instituto de Química, Universidade Federal do Rio de Janeiro, Rio de Janeiro, Brazil, [4] Laboratório de Taxonomia, Bioquímica e Bioprospecção de Fungos, Instituto Oswaldo Cruz, Fundação Oswaldo Cruz, Rio de Janeiro, Brazil, [5] Laboratório de Biologia Celular de Fungos, Instituto de Biofísica Carlos Chagas Filho, Universidade Federal do Rio de Janeiro, Rio de Janeiro, Brazil

OPEN ACCESS

**Edited by:**
*Carlos Pelleschi Taborda, University of São Paulo, Brazil*

**Reviewed by:**
*Guilherme Lanzi Sassaki, Federal University of Paraná, Brazil*
*Maria Rapala-Kozik, Jagiellonian University, Poland*

***Correspondence:**
*André L. S. Santos*
*andre@micro.ufrj.br*
*Lucimar F. Kneipp*
*lucimar@ioc.fiocruz.br*

**Specialty section:**
*This article was submitted to Fungi and Their Interactions, a section of the journal Frontiers in Microbiology*

**Received:** *20 February 2017*
**Accepted:** *04 May 2017*
**Published:** *19 May 2017*

**Citation:**
*Palmeira VF, Alviano DS, Braga-Silva LA, Goulart FRV, Granato MQ, Rozental S, Alviano CS, Santos ALS and Kneipp LF (2017) HIV Aspartic Peptidase Inhibitors Modulate Surface Molecules and Enzyme Activities Involved with Physiopathological Events in Fonsecaea pedrosoi. Front. Microbiol. 8:918. doi: 10.3389/fmicb.2017.00918*

*Fonsecaea pedrosoi* is the main etiological agent of chromoblastomycosis, a recalcitrant disease that is extremely difficult to treat. Therefore, new chemotherapeutics to combat this fungal infection are urgently needed. Although aspartic peptidase inhibitors (PIs) currently used in the treatment of human immunodeficiency virus (HIV) have shown anti-*F. pedrosoi* activity their exact mechanisms of action have not been elucidated. In the present study, we have investigated the effects of four HIV-PIs on crucial virulence attributes expressed by *F. pedrosoi* conidial cells, including surface molecules and secreted enzymes, both of which are directly involved in the disease development. In all the experiments, conidia were treated with indinavir, nelfinavir, ritonavir and saquinavir (100 μM) for 24 h, and then fungal cells were used to evaluate the effects of HIV-PIs on different virulence attributes expressed by *F. pedrosoi*. In comparison to untreated controls, exposure of *F. pedrosoi* cells to HIV-PIs caused (i) reduction on the conidial granularity; (ii) irreversible surface ultrastructural alterations, such as shedding of electron dense and amorphous material from the cell wall, undulations/invaginations of the plasma membrane with and withdrawal of this membrane from the cell wall; (iii) a decrease in both mannose-rich glycoconjugates and melanin molecules and an increase in glucosylceramides on the conidial surface; (iv) inhibition of ergosterol and lanosterol production; (v) reduction in the secretion of aspartic peptidase, esterase and phospholipase; (vi) significant reduction in the viability of non-pigmented conidia compared to pigmented ones. In summary, HIV-PIs are efficient drugs with an ability to block crucial biological processes of *F. pedrosoi* and can be seriously considered as potential compounds for the development of new chromoblastomycosis chemotherapeutics.

**Keywords: chromoblastomycosis, *Fonsecaea pedrosoi*, peptidases, HIV aspartic peptidase inhibitors, antifungal action**

## INTRODUCTION

*Fonsecaea pedrosoi* is a saprophyte black fungus that is the principal etiological agent of chromoblastomycosis in humans (Santos et al., 2007). This mycosis is a chronic granulomatous infection usually observed in the epidermis, dermis and subcutaneous tissue, which occurs in humid tropical and subtropical regions around the world and with high incidence in Brazil, Mexico, Venezuela, Madagascar and Japan (Rippon, 1988; Deng et al., 2015). The management of the diseases caused by *F. pedrosoi* continues to be an arduous challenge and treatment is quite dependent on an early diagnosis. However, this tends to be quite a difficult task since affected individuals are generally low-income workers engaged in agricultural or manual labor and who do not seek help before the infection becomes uncomfortable (Santos et al., 2007). The most common treatment strategy against chromoblastomycosis focuses on the use of systemic antifungal agents in conjunction with other therapies, such as the surgical removal of lesions and cryotherapy (Queiroz-Telles and Santos, 2013). The suggested drug interventions are expensive, involving high doses of itraconazole and/or terbinafine daily for over 1 year. Even under such treatment, relapses are very common (Santos et al., 2007; Queiroz-Telles and Santos, 2013). Although some antifungals are available for treating chromoblastomycosis they act on relatively few distinct molecular targets and the emergence of resistance is a frequent problem (Andrade et al., 2004). Thus, the search for new targets and novel therapeutic strategies are the primary challenges in the sustained effort to combat this debilitating mycosis.

Proteolytic enzymes are well-known virulence factors produced by numerous opportunistic/pathogenic human fungi (Santos, 2011a). Aspartic-type peptidases, in particular, participate in essential metabolic events of a fungal cell, including nutrition, growth, proliferation, differentiation, signaling and regulated death pathways. Aspartic peptidases also help fungi during distinct facets of the interaction with the host, including (i) degradation of extracellular matrix components for dissemination, (ii) adhesion to host structures, (iii) invasion and evasion of host cells, and (iv) immune escape by the cleavage of proteinaceous components from the host response arsenal which includes immunoglobulins, complement system proteins, interleukins and antimicrobial peptides (Monod et al., 2002; Naglik et al., 2003; Santos, 2011b). Therefore, aspartic peptidases have emerged as potential targets to the development of new antifungal chemotherapeutics. Corroborating these findings, several groups have reported that aspartic peptidase inhibitors (PIs) used in anti-human immunodeficiency virus (HIV) therapy (e.g., nelfinavir, indinavir, saquinavir, ritonavir, tipranavir, amprenavir, and lopinavir) delivered antifungal effects *in vitro* and *in vivo* (Borg-von Zepelin et al., 1999; Cassone et al., 1999; Monari et al., 2005; Cenci et al., 2008; Santos et al., 2013). For instance, the HIV-PIs ritonavir and indinavir demonstrated anti-*Candida albicans* activity in a rat vaginitis model (Cassone et al., 1999). In *Cryptococcus neoformans*, tipranavir showed a therapeutic effect in experimental systemic cryptococcosis, reducing fungal burden in the brain and the liver of both immunocompetent and immunodepressed mice (Cenci et al., 2008).

Our research group previously demonstrated that both the conidial and the mycelial forms of *F. pedrosoi* secreted aspartic peptidases into the extracellular environment and that these enzymes were able to degrade extracellular matrix-forming proteins (laminin, fibronectin and collagen) as well as serum proteins (albumin, IgG and fibrinogen) (Palmeira et al., 2006a,b). Interestingly, clinical strains of *F. pedrosoi*, freshly isolated from human lesions, produced higher levels of extracellular aspartic peptidase activity compared to a long time laboratory-adapted strain, suggesting that enzyme production may be stimulated by interaction with the host (Palmeira et al., 2006b). Furthermore, we demonstrated that nelfinavir, saquinavir, ritonavir and indinavir inhibited the secreted aspartic proteolytic activity of conidia and mycelia of *F. pedrosoi*, in a dose-dependent manner (Palmeira et al., 2006b, 2008). Drastic morphological alterations were also observed after treatment of *F. pedrosoi* with HIV-PIs, which culminated in conidial death. These morphological perturbations led to an inability of conidia to (i) adhere to and enter into animal cells, (ii) differentiate into mycelia, and (iii) resist macrophage killing mechanisms (Palmeira et al., 2008).

Herein, we report the alterations in the production of relevant and crucial biomolecules by *F. pedrosoi* conidia upon treatment with HIV-PIs. In this context, we have focused on surface molecules (mannose- and sialic acid-containing glycoconjugates, glucosylceramide, melanin and sterol) and extracellular hydrolytic enzymes (peptidase, esterase and phospholipase), which act as potential virulence attributes of this human opportunistic fungus (Soares et al., 1995; Limongi et al., 1997; Alviano et al., 2004a,b; Nimrichter et al., 2005; Palmeira et al., 2010).

## MATERIALS AND METHODS

### Chemicals

Indinavir, saquinavir, ritonavir and nelfinavir were obtained from the National Institutes of Health (NIH), and were dissolved in methanol to obtain a final concentration of 20 mM. Bovine serum albumin (BSA), pepstatin A, Tween 80, ergosterol, lanosterol, fluorescein isothiocyanate (FITC)-labeled secondary antibodies, and FITC-Concanavalin A (Con A) and FITC-*Sambucus nigra* (SNA) agglutinins were purchased from Sigma-Aldrich (St. Louis, MO, United States). Media constituents, reagents used in microscopy and buffer components were purchased from Amersham (Little Chalfont, United Kingdom). All other reagents were of analytical grade.

### Microorganism and Growth Conditions

A pathogenic strain of *F. pedrosoi* (ATCC 46428, formerly 5VLP), isolated from a human patient with chromoblastomycosis (Oliveira et al., 1973), was used throughout the experimental work. For conidium formation, cultures were incubated for 5 days under constant agitation (200 rpm) at room temperature in 250-ml Erlenmeyer flasks containing 100 ml of Czapek-Dox

chemically defined medium (Palmeira et al., 2008). The fungal cultures were centrifuged (4000 × *g*, 10 min, 4°C) and the conidia were washed three times in phosphate-buffered saline (PBS; 150 mM NaCl, 20 mM phosphate buffer, pH 7.2). Growth was estimated by counting the conidia in a Neubauer chamber.

## Fungal Treatment with HIV-PIs

*Fonsecaea pedrosoi* conidia ($10^3$ or $10^6$ cells) were incubated with each HIV-PI (indinavir, saquinavir, ritonavir and nelfinavir) at 100 μM concentration for 24 h at room temperature. Afterward, conidia were washed three times in PBS and viability was assessed by colony-forming unit (CFU) measurements (Palmeira et al., 2008). The untreated and methanol-treated conidia were used in all the experimental sets. For all the subsequent experiments (except when discriminated), $10^6$ conidia were treated (or not) with each HIV-PI at 100 μM for 24 h in order to detect (i) morphological changes, (ii) expression of surface molecules, and (iii) extracellular enzymes.

## Morphological Parameters

Conidia were processed for flow cytometry in order to measure two morphological parameters: size and granularity. Briefly, conidia were centrifuged (4000 × *g*, 10 min, 4°C), washed with PBS and fixed in 4% paraformaldehyde at 4°C for 30 min. Then, fungal cells were analyzed in a flow cytometer (FACSCalibur; BD Bioscience) equipped with a 15-mW argon laser emitting at 488 nm. Each experimental population was mapped ($n = 10{,}000$ events) using a two parameter histogram of forward-angle light scatter (FSC) versus side scatter (SSC), respectively, to evaluate cellular size and granularity (Braga-Silva and Santos, 2011).

## Ultrastructural Analysis

Conidia were fixed with a solution containing 2.5% glutaraldehyde, 4% paraformaldehyde, 10 mM $CaCl_2$ in 0.1 M cacodylate buffer (pH 7.2) for 1 h at 25°C. Then, conidia were washed with the same buffer and post-fixed for 1 h in a solution containing 1% $OsO_4$ and 0.8% potassium ferricyanide in cacodylate buffer. Subsequently, the cells were rinsed, dehydrated in a graded series of acetone and embedded in Spurr resin. Ultrathin sections were obtained, stained with uranyl acetate and lead citrate, and examined using a JEOL 1200 EX transmission electron microscope (Palmeira et al., 2008).

## Sterol Content

Conidia were subjected to successive extractions with a chloroform:methanol (2:1) mixture in order to remove lipids from the fungal cells (Soares et al., 1995). Precipitated material was removed by centrifugation and the solution was then reduced to dryness under nitrogen. Following Folch partition (Folch et al., 1957) sterol content of the lipid extract was analyzed by high-performance thin-layer chromatography (HPTLC) using as solvent mixture of hexane-ether-acetic acid (80:40:2) and revealed with a solution comprising 50 mg of $FeCl_3$, 90 ml of water, 5 ml of acetic acid and 5 ml of $H_2SO_4$. The plate was heated to 100°C for 5 min and the bands of sterol were then visualized and compared to sterol standards, ergosterol and lanosterol (Larsen et al., 2004). Sterol quantitative determinations were performed using ImageJ software (Granato et al., 2017).

## Surface Molecules

For fluorocytometric analysis, conidia were fixed in 4% paraformaldehyde for 1 h, rinsed in PBS and then incubated for 1 h at room temperature in the presence of fluorescent probes, FITC-Con A (5 μg/ml) and FITC-SNA (40 μg/ml) agglutinins, in order to detect mannose- and sialic acid-containing glycoconjugates, respectively (Limongi et al., 1997; Alviano et al., 2004b). In addition, both anti-CMH and anti-melanin antibodies, at 1:100 dilution, were also incubated to detect glucosylceramide and melanin pigment, respectively (Alviano et al., 2004a; Nimrichter et al., 2005). Cells were washed and the conidia were then treated with primary antibodies followed by a 1 h incubation period with FITC-secondary antibody. In parallel, conidial cells that had not been incubated with agglutinins or antibodies were also prepared in order to run as autofluorescence control systems. Finally, fungal cells were washed in PBS and analyzed by flow cytometry. Control cells were analyzed first in order to determine their autofluorescence and relative size. Each experimental population was mapped using a two-parameter histogram of FSC versus SSC. The mapped population ($n = 10{,}000$ events) was analyzed for log green fluorescence by using a single-parameter histogram. The results were expressed by means of two parameters: percentage of fluorescent cells and mean of fluorescence intensity (MFI).

## Phospholipase and Esterase Assays

Determination of phospholipase production was performed by using egg-yolk agar plates (Price et al., 1982). The esterase production was assayed using Tween 80 agar medium. Briefly, conidia (10 μl containing $10^6$ cells) were placed in the center of agar plates and incubated at 37°C up to 10 days (Palmeira et al., 2010). The colony diameter (*a*) and the diameter of colony plus precipitation zone (*b*) were measured by a digital paquimeter. Phospholipase and esterase activities were expressed as P*z* value (*a*/*b*) (Price et al., 1982), in which low P*z* values mean high enzymatic production and, inversely, high P*z* values indicate low enzymatic production.

## Extracellular Proteolytic Activity

Following treatment with HIV-PIs, conidia were washed three times in PBS and re-suspended in Czapek-Dox medium for 2 h at room temperature. Subsequently, the fungal cells were harvested (4000 × *g*/10 min/4°C) and the cell-free culture supernatants were used to measure proteolytic activity (Buroker-Kilgore and Wang, 1993). Sample normalization was performed by protein concentration. The protein content was measured using the method described by Lowry et al. (1951), using BSA as standard. Briefly, 50 μl of supernatant (equivalent to 1 μg of protein), BSA (0.5 mg/ml) and 10 mM sodium citrate (pH 4.0) were added to a microcentrifuge tube (350 μl) and incubated for 1 h at 37°C. Afterward, three aliquots (100 μl each) of the reaction mixture were transferred to wells on a microtiter plate containing 50 μl of water and 100 μl of a Coomassie solution (0.025% Coomassie brilliant blue G-250, 11.75% ethanol and 21.25% phosphoric

acid). A control, in which the substrate was added just after the reactions were stopped, was used as a blank. After 10 min (to allow for dye binding) the plate was read on a Molecular Devices Thermomax microplate reader at 595 nm. One unit of enzyme activity was defined as the amount of enzyme that caused an increase of 0.01 absorbance unit, under standard assay conditions (Palmeira et al., 2006b, 2008). Alternatively, the supernatant fluids were pre-incubated for 15 min at 37°C in the absence or presence of pepstatin A (1 and 10 μM) and then their ability to cleave BSA was measured.

## Aspartic Peptidase Production and Susceptibility to HIV-PIs in Pigmented and Non-pigmented Conidia

In order to obtain non-pigmented cells, conidia were grown in flasks filled with Czapek-Dox medium almost to the top (to decrease aeration) and incubated in the dark for 5 days at room temperature under constant agitation (200 rpm) (Alviano et al., 1991). Subsequently, both pigmented and non-pigmented conidia were evaluated for the production of aspartic peptidase and their susceptibility to HIV-PIs (in this last test, $10^3$ cells were used).

## Statistical Analysis

All the experiments were repeated at least three times and all the systems were performed in triplicate. Data were analyzed statistically using Student's *t*-test using EPI-INFO 6.04 (Database and Statistics Program for Public Health) computer software. *P* values of 0.05 or less were considered statistically significant.

# RESULTS AND DISCUSSION

## Anti-*Fonsecaea pedrosoi* Action of HIV-PIs

Aspartic peptidases produced by *F. pedrosoi* cells are apparently key regulators of growth, development, morphogenesis and interaction with host cells/tissues (Palmeira et al., 2006b, 2008; Santos et al., 2007). For instance, the classical aspartic PI,

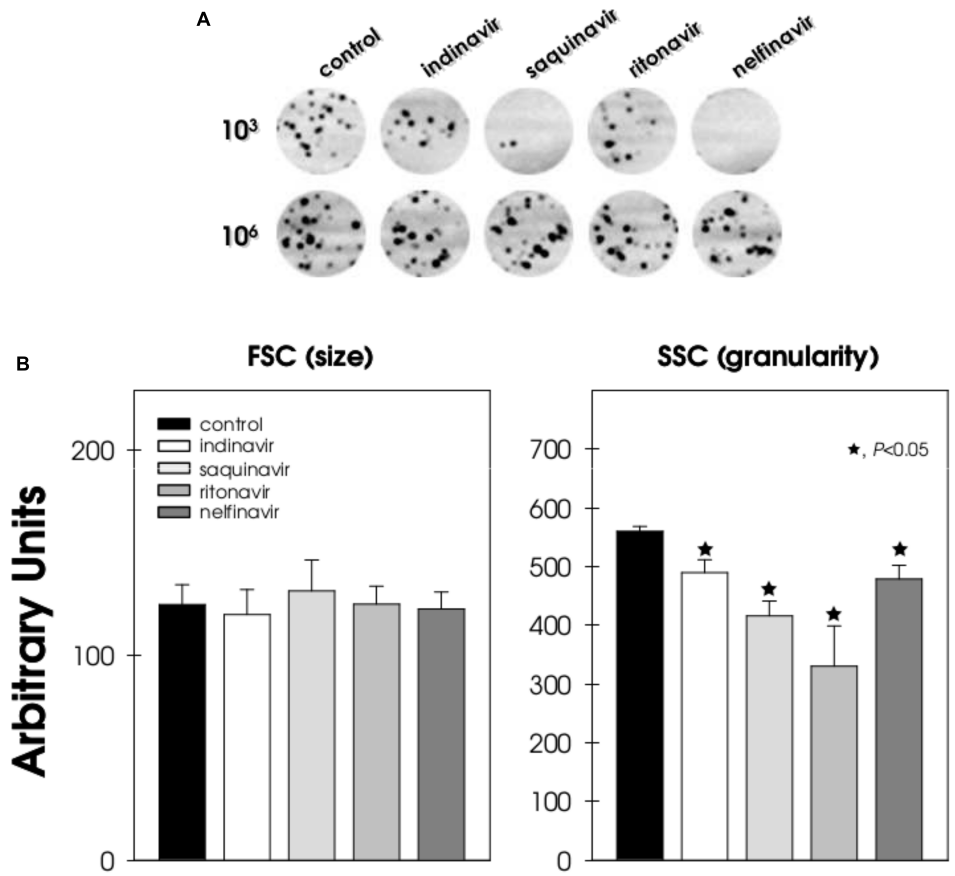


**FIGURE 1 | Effect of HIV-PIs on the growth behavior and morphology of *F. pedrosoi* conidial cells. (A)** Different conidial cell densities ($10^3$ and $10^6$ cells/ml) were incubated in the absence (control) or in the presence of indinavir, nelfinavir, ritonavir and saquinavir at 100 μM for 24 h. Subsequently, the mixtures were plated onto fresh solid medium without drugs. Image digitalization of the plates is shown. **(B)** In parallel, $10^6$ conidial cells/ml were treated (or not) with the HIV-PIs (100 μM) for 24 h and then analyzed by flow cytometry in order to measure cell size and granularity. Forward scatter (FSC) measurement is related to cell size and side scatter (SSC) measurement is related to the internal granularity and/or complexity of a cell. The values represent the mean ± standard deviation of three independent experiments performed in triplicate. Symbols (★) indicate the experimental systems considered statistically significant from the control ($P < 0.05$, Student's *t*-test).

pepstatin A, was able to reduce the viability of *F. pedrosoi* conidia in a manner which was dependent upon both cell number and drug concentration (Palmeira et al., 2008). Based on this observation, we initially investigated the effect of HIV-PIs on the cellular viability of *F. pedrosoi*. In this way, two conidial cell densities ($10^3$ and $10^6$ cells/ml) were each treated for 24 h with 100 μM HIV-PIs, and then plated onto drug-free solid medium in order to quantify the CFU. As previously shown by our group (Palmeira et al., 2008), drug treatment of $10^3$ conidia significantly reduced the cell viability, especially nelfinavir

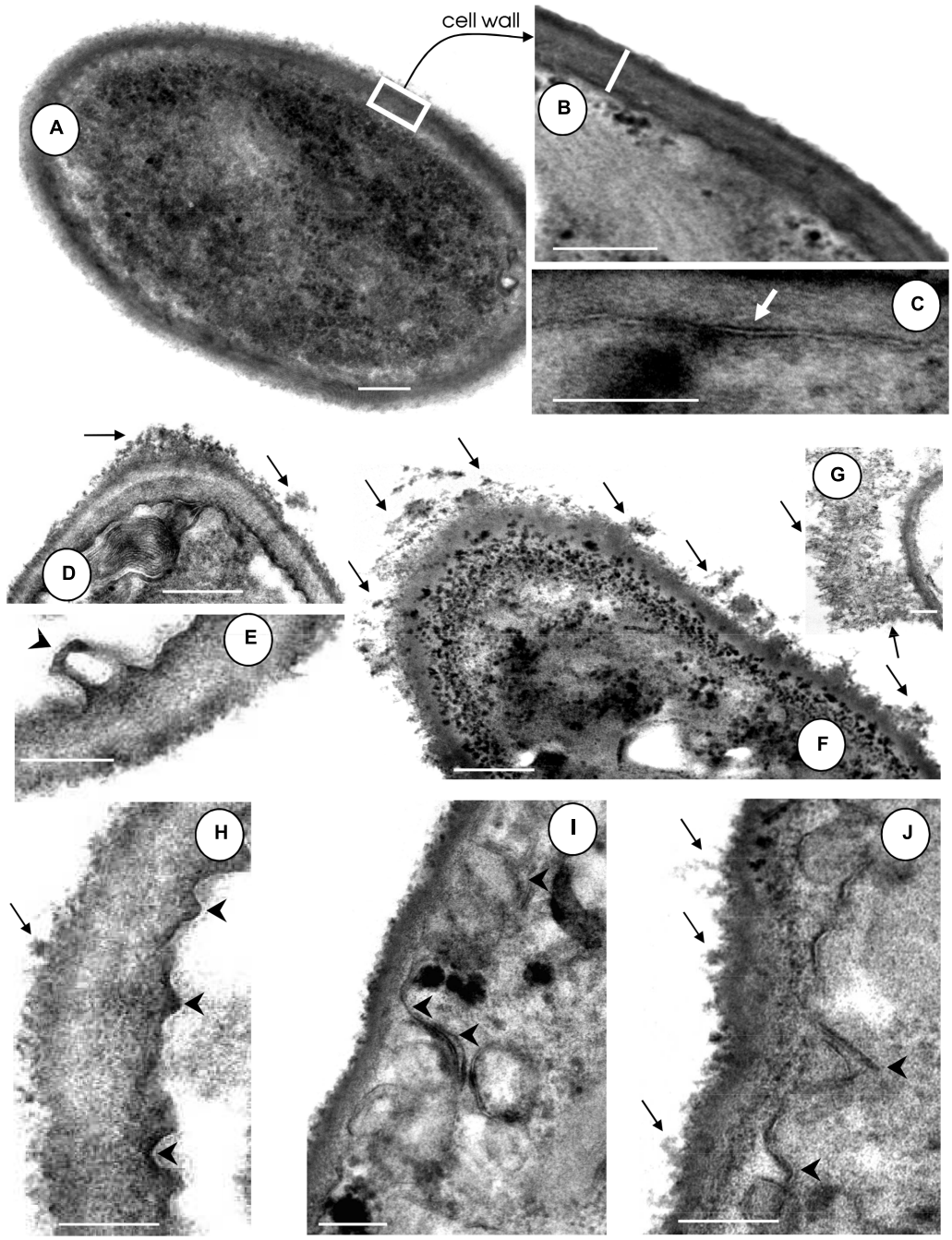


**FIGURE 2 | Effect of HIV-PIs on the ultrastructure of *F. pedrosoi* conidial cells. (A–C)** Untreated and **(D–J)** HIV-PI-treated (100 μM for 24 h) conidial cells were processed and analyzed by transmission electron microscopy. Control conidial cells present a dense cytoplasm **(A)** with a distinct and compact cell wall (**B**, *white bar* shows the wall thickness) and well-delineated plasma membrane (**C**, *white arrow*). Black arrows show the releasing of electron dense and amorphous material from the cell surface and black arrowheads indicate the invaginations of the plasma membrane with consequent withdrawal from the cell wall following treatment of conidia with indinavir **(D,E)**, nelfinavir **(F,G)**, ritonavir **(H)** and saquinavir **(I,J)**. Scale bars: **(A,D,F)**, 0.4 μm; **(B–J)**, 0.25 μm.

(≈100%) and saquinavir (≈90%), compared to the non-treated cells (**Figure 1A**). In contrast, the treatment of $10^6$ conidia with the HIV-PIs did not alter the growth behavior, resulting in comparable CFU numbers (**Figure 1A**). Similarly, exposing different densities of *C. albicans* yeast cells to amprenavir at a concentration of 100 μM gave the same antifungal profile (Braga-Silva and Santos, 2011). It is well-known that the antimicrobial action of a given compound depends on the microbial inoculum, drug concentration and time of treatment (Gehrt et al., 1995). In this context, for example, increasing the number of microbial targets may exceed the capability of a given drug amount to inhibit growth of the test organism. Inoculum concentration may particularly affect antifungal drugs whose antimicrobial activity is based on an enzymatic mechanism (Gehrt et al., 1995; Palmeira et al., 2006a,b, 2008).

The direct antifungal action of HIV-PIs against other opportunistic fungi, especially *C. albicans*, *C. parapsilosis*, *C. neoformans*, and *Pneumocystis jiroveci*, has been reported previously (Atzori et al., 2000; Asencio et al., 2005; Monari et al., 2005; Santos and Braga-Silva, 2013). In parallel with these earlier studies, no alteration in cell size was observed when $10^6$ *F. pedrosoi* conidia cells were treated with HIV-PIs in comparison to untreated cells. However, a significant reduction on the granularity parameter was seen in HIV-PI-treated conidia, as revealed by flow cytometry (**Figure 1B**). In contrast, amprenavir (100 μM concentration) was previously

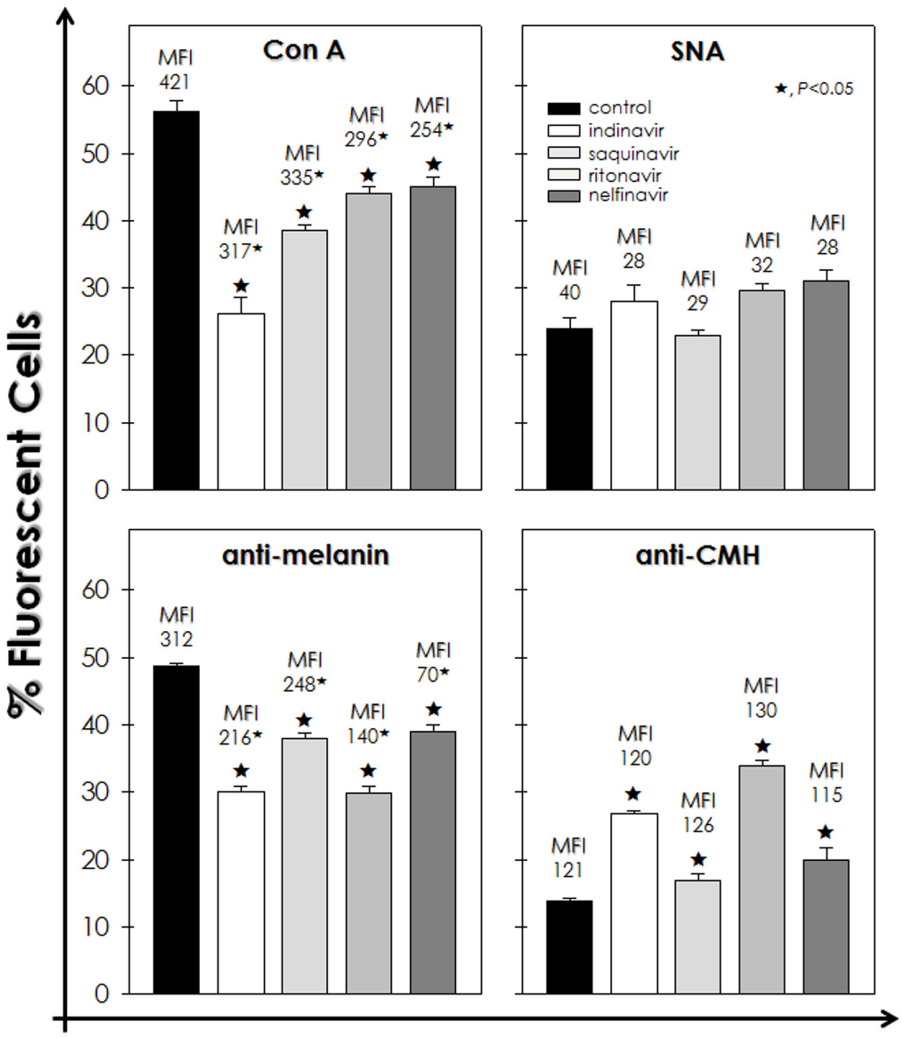


**FIGURE 3 | Effect of HIV-PIs on the expression of surface molecules of *F. pedrosoi* conidial cells.** Untreated (control) and HIV-PI-treated (100 μM for 24 h) conidial cells were processed to detect mannose- and sialic acid-containing glycoconjugates by using FITC-Con A and FITC-SNA agglutinins, respectively, as well as melanin and glucosylceramide by means of anti-melanin and anti-CMH antibodies, respectively. Afterward, conidial cells were analyzed by flow cytometry and the percentages of positive-labeled cells were shown. Moreover, in each analysis, the values of mean fluorescence intensity (MFI) are shown above the bars. The autofluorescence value of conidial cells not treated with either FITC-agglutinins or antibodies was discounted from the treated ones. The values represent the mean ± standard deviation of three independent experiments performed in triplicate. Symbols (★) indicate the experimental systems considered statistically significant from the control ($P < 0.05$, Student's *t*-test).

shown to cause a significant reduction (≈30%) on the size of *C. albicans* cells compared to the non-treated yeast cells, although no differences in granularity occurred (Santos and Braga-Silva, 2013).

## Ultrastructural Alterations by HIV-PIs: Focus at the Surface of *F. pedrosoi* Conidia

In this set of experiments, the effects of HIV-PIs (indinavir, ritonavir and also saquinavir and nelfinavir) on the fungal cell surface were evaluated. In comparison to untreated control conidia, which had normal morphology with typical dark and dense cytoplasm (**Figure 2A**), classical cell wall (**Figure 2B**) and a well-delineated cytoplasmic membrane (**Figure 2C**), cells exposed to HIV-PIs showed significant changes in surface topography, including (i) shedding of a great amount of electron dense and amorphous material on the outer side of the cell wall (**Figures 2D,F–H,J** black arrows) and (ii) a cytoplasmic membrane presenting numerous undulations and/or invaginations as well as withdrawal of the cytoplasmic membrane from the cell wall (**Figures 2E,H,I**, arrowheads). Although all of these morphological alterations were clearly evident following treatment with the four HIV-PIs, saquinavir and nelfinavir induced the greatest effects, a result which corroborates their anti-proliferative properties and also our previous findings (Palmeira et al., 2008). Likewise, images obtained using scanning electron microscopy revealed drastic changes on the morphology of *C. albicans* yeasts treated with amprenavir (Braga-Silva et al., 2010). Surface invaginations and detachment of the external fibril layer were clearly observed, giving rise to fungal cells with a smooth surface. Additionally, the release of surface materials from the cell wall culminated in an inability of *C. albicans* to adhere and, consequently, to form a robust and mature biofilm on polystyrene (Braga-Silva et al., 2010; Braga-Silva and Santos, 2011).

## HIV-PIs Modulate the Surface Molecules Produced by *F. pedrosoi* Conidia

Considering the observed fungal surface alterations, the effects of HIV-PIs on the expression of surface molecules (e.g., mannose- and sialic acid-containing glycoconjugates, sterol, melanin and glucosylceramide), usually expressed by *F. pedrosoi* and associated with virulence, was evaluated (**Figure 3**). In this set of experiments, $10^6$ fungal cells/ml was the cellular density selected for treatment with HIV-PIs, since at this density the conidia maintained their viability post-treatment (**Figure 1**).

Flow cytometry analyses demonstrated that indinavir, saquinavir, ritonavir and nelfinavir significantly diminished the percentage of fluorescently Con A-labeled cells by approximately 54, 32, 22, and 20%, respectively, when compared to untreated cells. In addition, it was evidenced a considerable dropped in the MFI values after the treatment with the HIV-PIs, which indicates a reduction in the surface amount of mannose-rich glycoconjugates in *F. pedrosoi* conidial cells (**Figure 3**). In contrast, the sialic acid expression was not significantly altered, since similar percentage of SNA-labeled cells and MFI values were observed in untreated and HIV-PIs-treated fungal cells (**Figure 3**). Indinavir and ritonavir diminished the number of melanin-positive cells by around 40%, while saquinavir and nelfinavir by approximately 20%. However, all the four HIV-PIs significantly reduced the MFI parameter, especially nelfinavir, suggesting a reduction on the

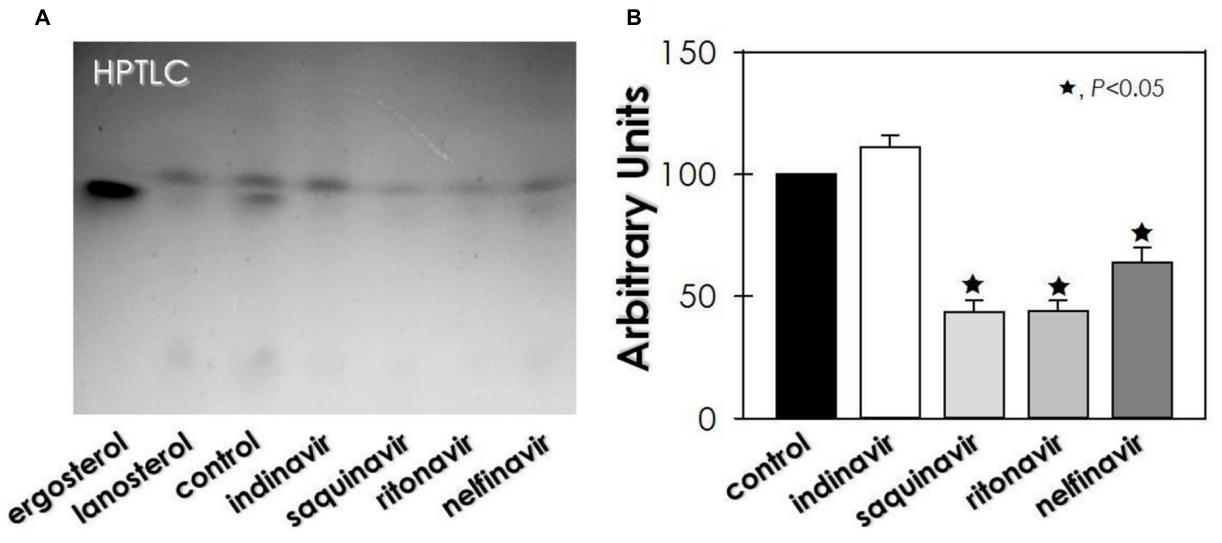


**FIGURE 4 | Effect of HIV-PIs on the sterol synthesis of *F. pedrosoi* conidial cells. (A)** Representative image of untreated (control) and HIV-PI-treated (100 μM for 24 h) conidial cells. For sterol analysis, the lipid extracts were loaded into HPTLC silica plates, separated using a mixture of solvents (hexane-ether-acetic, 80:40:2) and revealed by spraying a solution containing ferric chloride, water, acetic acid and sulfuric acid, which revealed the sterol as red-violet color spots. **(B)** Densitometric analyses of the lanosterol bands, expressed in arbitrary units. Symbols (★) indicate the experimental systems considered statistically significant from the control ($P < 0.05$, Student's *t*-test).

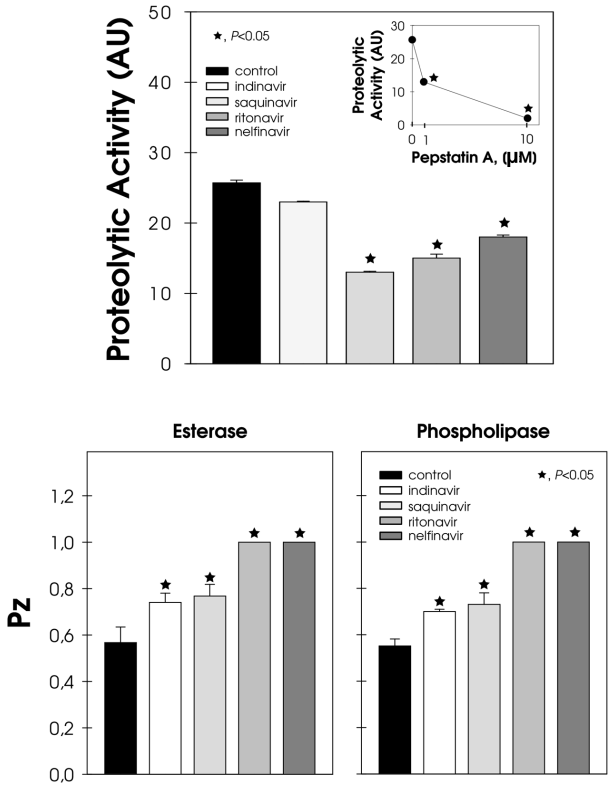


**FIGURE 5 | Effect of HIV-PIs on the secretion of hydrolytic enzymes by *F. pedrosoi* conidial cells.** Untreated (control) and HIV-PI-treated (100 μM for 24 h) conidial cells were washed and re-suspended in Czapek-Dox medium for an additional 2 h. After this period, the cell-free culture supernatants were submitted to a proteolytic activity assay. In addition, the supernatant obtained from the control cells was pre-incubated in either the absence or presence of pepstatin A (1 and 10 μM) and then checked for their ability to cleave BSA (*inset graphic*). The proteolytic activities were expressed as arbitrary units (AU). In parallel, conidia treated (or not) with HIV-PI were placed in the center of either Tween 80 or egg-yolk agar plates to detect esterase and phospholipase activities, respectively. The lipase activities were expressed as Pz and the values represent the mean ± standard deviation of three independent experiments performed in triplicate. Symbols (★) indicate the experimental systems considered statistically significant from the control ($P < 0.05$, Student's *t*-test).

melanin production (**Figure 3**). Interestingly, a considerable augmentation in the number of glucosylceramide-positive cells was observed after incubation with HIV-PIs as follows: ritonavir > indinavir > nelfinavir > saquinavir; however, no changes were detected in MFI values (**Figure 3**).

Regarding sterol content, untreated conidia of *F. pedrosoi* showed an equal proportion of lanosterol (a precursor in ergosterol biosynthesis) and ergosterol (the final product) (**Figure 4**). On the other hand, no ergosterol was detected in HIV-PIs-treated conidia, whereas lanosterol production was inhibited (≈56%) by saquinavir and ritonavir, as well as by nelfinavir (≈36%) (**Figure 4**).

Adherence is one of the most important determinants of microbial pathogenesis. This step is normally followed by microbial internalization, which can be used by the pathogen to replicate inside the host cells and evade immune responses (Tronchin et al., 2008). In this way, surface-located molecules act as adhesive structures, and thus the inhibition of their synthesis and/or expression can diminish the ability of fungal cells to interact with both abiotic and biotic surfaces (Santos and Braga-Silva, 2013). Fungal mannose-containing glycoconjugates are directly involved in the initial adhesion step to host cell surface (Kohatsu et al., 2006), including in *F. pedrosoi* (Limongi et al., 1997). Our group previously demonstrated that HIV-PIs were able to diminish the adhesion and invasion capabilities of *F. pedrosoi* conidia during the interaction with epithelial cells, fibroblasts and macrophages (Palmeira et al., 2008), an effect which can now be explained, at least in part, as being due to the significant reduction in the surface level of mannose-rich glycoconjugates observed in the present study.

In several microbial species, including fungi, sialic acids are considered as anti-recognition molecules that elude the host immune system by, for example, protecting against phagocytosis (Alviano et al., 2004b). Our current study showed that the HIV-PIs treatment did not considerably alter the expression of sialic acid on surface glycoconjugates of *F. pedrosoi* conidia. Similarly, *C. albicans* cells treated with the HIV-PI, amprenavir, at the same concentration used herein (100 μM), did not modulate the expression of surface sialic acid molecules (Braga-Silva et al., 2010).

It is well-known that *F. pedrosoi* constitutively produces the pigment, melanin, which is a complex polymer that is deposited on the cell wall and in cytoplasmic structures (melanosomes) as well as being released into the extracellular environment (Alviano et al., 1991, 2004a; Rozental et al., 1994; Cunha et al., 2010). Melanin is a classical virulence factor due to its ability to protect fungal cells against oxidative stressors, to inhibit cell-mediated host immune responses, to interfere with complement cascade activation and to reduce the susceptibility to antifungal agents (Bocca et al., 2006; Nosanchuk and Casadevall, 2006; Santos et al., 2007). Moreover, melanin is able to block the access of several molecules through the cell wall (Nimrichter et al., 2005; Nosanchuk and Casadevall, 2006). For example, high melanized conidia of *F. pedrosoi* blocked the access of antibodies against glucosylceramide, an antigenic sphingolipid involved in fungal growth and differentiation (Nimrichter et al., 2005; Del Poeta et al., 2014). In contrast, anti-glucosylceramide antibody was able to efficiently penetrate the cell wall and bind to its target in melanin-depleted *F. pedrosoi* cells, culminating in fungal death (Nimrichter et al., 2005). Interestingly, indinavir and ritonavir were the most effective HIV-PIs for reducing the production of melanin, concomitantly to the increased recognition of anti-glucosylceramide antibody to the surface of *F. pedrosoi* conidial cells. Also, the reduced melanin-producing capability of HIV-PIs-treated conidia, as observed herein, helps explain the previously reported enhanced killing capacity of macrophages (Palmeira et al., 2008). Corroborating our hypothesis, the inhibition of the melanin synthesis pathway by tricyclazole also increased the susceptibility of *F. pedrosoi* conidia to mouse macrophages (Cunha et al., 2005). Furthermore, a very interesting, previously published study revealed a positive correlation between human melanogenesis and aspartic peptidase activity (Rochin et al.,

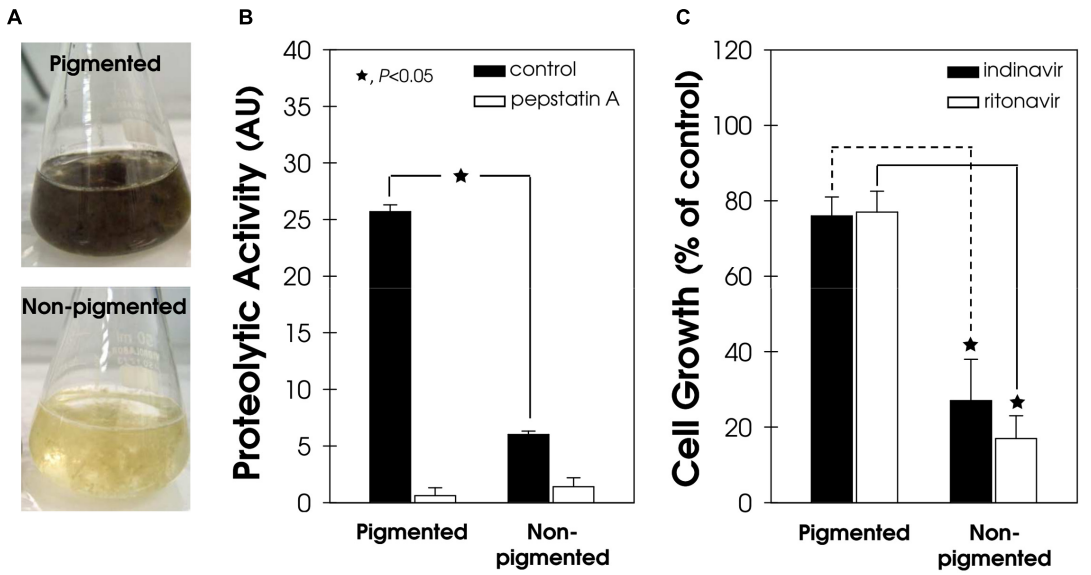


**FIGURE 6 | Secretion of aspartic peptidase and susceptibility to HIV-PIs in pigmented and non-pigmented *F. pedrosoi* conidial cells. (A)** Representative image of pigmented (melanized) and non-pigmented (non-melanized) *in vitro* conidial growth. **(B)** The cell-free culture supernatants from both pigmented and non-pigmented conidia were used to quantify the acidic proteolytic activity, using BSA as the soluble protein substrate, in the absence/presence (10 μM) of pepstatin A. The proteolytic activities were expressed as arbitrary units (AU). **(C)** Conidia ($10^3$ cells/ml) were incubated in the absence (control) or in the presence of indinavir and ritonavir (100 μM) for 24 h. Subsequently, the mixtures were plated on fresh solid medium without drugs. In all graphics, the values represent the mean ± standard deviation of three independent experiments performed in triplicate. Symbols (★) indicate the experimental systems considered statistically significant from the control ($P < 0.05$, Student's *t*-test).

2013). Briefly, the β-secretase BACE2 (beta-site cleaving enzyme), which is an aspartic-type peptidase, is able to process the pigment cell-specific protein melanocyte (PMEL) to form the melanosome amyloid matrix in pigment cells. The pharmacological inhibition of BACE2, or its RNA silencing, interfered in the melanosome morphogenesis and, consequently, in pigmentation defect as shown in *in vitro* studies using the human melanocytic MNT1 cell line as well as in *in vivo* studies using Bace2$^{-/-}$ mice.

Almost all of the current test HIV-PIs were also able to decrease the sterol content in *F. pedrosoi* conidia. The disturbance of sterol synthesis, a bioregulator of membrane fluidity, asymmetry and integrity, may lead the fungal cells to death (Kathiravan et al., 2012). In this sense, the ultrastructural changes observed in HIV-PI-treated *F. pedrosoi* conidia [also reported by Palmeira et al. (2008)], including invaginations in the cytoplasmic membrane and detachment of this structure from the cell wall, culminated in abnormal cellular division, the disfiguring of regular conidia morphology and irreversible injuries that ultimately led to conidia death.

## Effect of HIV-PIs on the Secretion of Hydrolytic Enzymes in *F. pedrosoi* Conidia

Conidia cells were able to extracellularly release aspartic-type peptidase, whose hydrolytic activity was inhibited by pepstatin A, in a typical dose-dependent manner (**Figure 5**, inset). Conversely, the pre-treatment of conidia with HIV-PIs, particularly saquinavir, ritonavir and nelfinavir, notably arrested the secretion of pepstatin A-sensitive aspartic peptidase, inhibiting this activity by around 50, 40, and 30%, respectively (**Figure 5**). HIV-PIs also interfered with the production of esterase and phospholipase, which are two unrelated enzymes belonging to the lipase class (**Figure 5**). Ritonavir and nelfinavir inhibited lipolytic activities by around 70%, while indinavir and saquinavir affected substrate hydrolysis by approximately 30% (**Figure 5**).

Peptidases and lipases are ubiquitous enzymes involved in diverse processes, which includes homeostasis, nutrient acquisition and fungal virulence (Santos, 2011a; Park et al., 2013). As fungal enzymes play roles in several crucial pathophysiological events, the inhibition of at least one of the many stages controlled by them will probably contribute to the containment of the pathogen and thus should help to control disease development (Santos, 2011a; Park et al., 2013). In this sense, HIV-PIs were able to directly inhibit the enzymatic activity of aspartic peptidase secreted by *F. pedrosoi* (Palmeira et al., 2008) and also, as demonstrated herein, its secretion into the extracellular milieu. *F. pedrosoi* is also renowned as an excellent producer of esterase and phospholipase (Palmeira et al., 2010). Interestingly, HIV-PIs have previously been shown to significantly reduce the secretion of both of the latter lipases by *C. albicans* (Cenci et al., 2008; Braga-Silva et al., 2010). The inhibitory capability of non-proteolytic enzymes by HIV-PIs was also observed during the treatment of *C. neoformans* with indinavir, with the drugs prompting a significant reduction in the production of urease, which is an essential virulence factor of this opportunistic fungus (Monari et al., 2005). Indinavir also

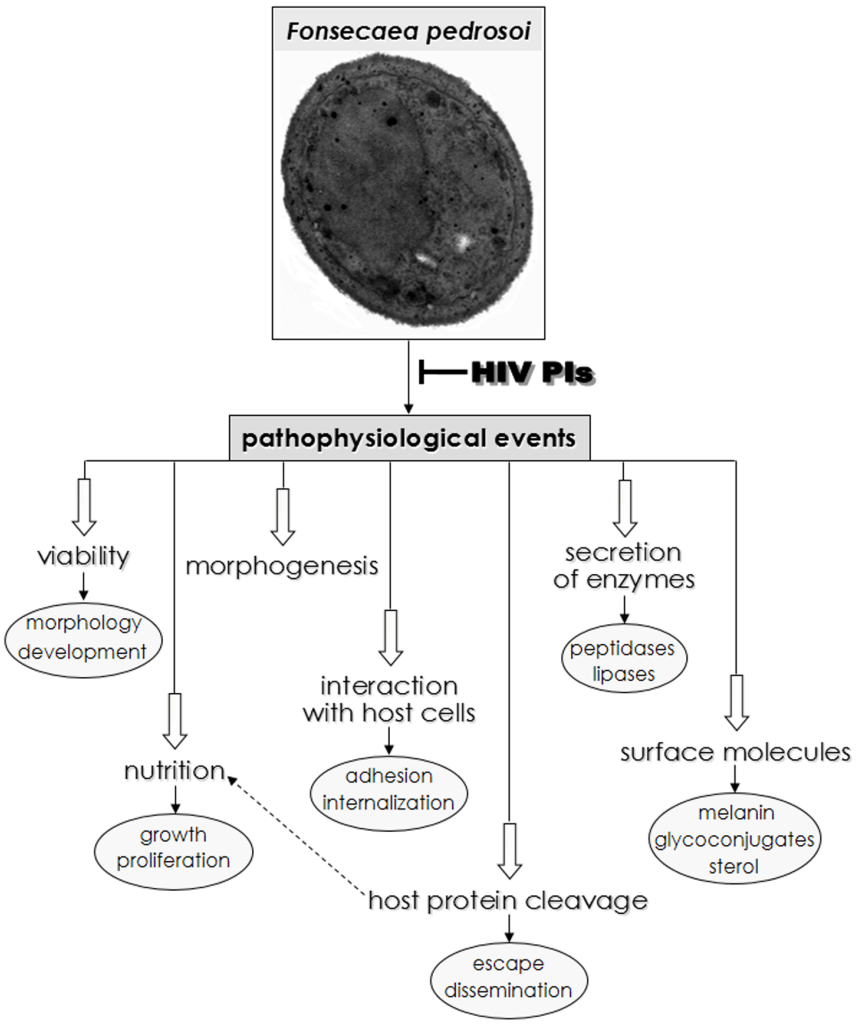


**FIGURE 7 | Overview of possible HIV-PIs action on *F. pedrosoi* conidial cells in central metabolic processes as well as in distinct phases of interaction with host cell structures.** Both physiological and pathological events that occur in some species of yeast and filamentous fungi, including *F. pedrosoi* are inhibited, in different extensions, by the HIV-PIs (for review see Santos et al., 2013).

powerfully inhibited capsule formation, another major virulence factor of *C. neoformans*, whilst both melanin and phospholipase productions were unaffected by this HIV-PI (Monari et al., 2005). Moreover, HIV-PIs were active in blocking the morphological transition, which is recognized as an integral step in the establishment of a successful fungal infection by *C. albicans* (Braga-Silva and Santos, 2011) and *F. pedrosoi* (Palmeira et al., 2008).

## Correlation among Melanin, Secretion of Aspartic Peptidase, and Susceptibility to HIV-PIs

The secretion of aspartic peptidase in both pigmented and non-pigmented conidial cells of *F. pedrosoi* (**Figure 6A**) was also evaluated. The aspartic-type peptidase activity was four-fold higher in pigmented conidial cells compared to the non-pigmented ones (**Figure 6B**). In the same way, the process of melanization in phytopathogenic fungi directly affects the secretion of proteins, including lytic enzymes (Henson et al., 1999). For instance, the spot blotch caused by the fungus *Bipolaris sorokiniana* is one of the most important diseases of wheat and barley in South Asia and, recently, a positive correlation was found between high melanin production, elevated amounts of extracellular enzymes, including peptidase, and the aggressiveness of isolates from naturally infected barley (Chand et al., 2014).

Melanin can reduce the fungal susceptibility to different classes of antifungal agents (Cunha et al., 2005) because it forms a protecting shield around the fungal cell. In support of this finding, indinavir and ritonavir only slightly reduced the viability of pigmented *F. pedrosoi* cells by around 23%, while non-pigmented conidia were drastically affected by exposure to both of these HIV-PIs (**Figure 6C**).

## CONCLUSION

Chromoblastomycosis disease is often recalcitrant and difficult to treat using available pharmacotherapy. Taken together, our results clearly show that HIV-PIs, especially nelfinavir and saquinavir, dramatically affect *F. pedrosoi* conidia growth and ultrastructure. Moreover, HIV-PIs modulate *F. pedrosoi* sterol content and important surface molecules, including melanin and glucosylceramide, as well as secreted enzymes (aspartic peptidase, esterase and phospholipase). The results obtained in the current and previous studies (Palmeira et al., 2008) revealed that HIV-PIs are efficient drugs able to modulate vital pathophysiological processes in *F. pedrosoi*, as summarized in **Figure 7**. Thus, HIV-PIs may be candidates as lead compounds for the development of novel chromoblastomycosis treatments. Drugs with a distinct mechanism of action or a multitargeted combination therapy could be attractive to control *F. pedrosoi* infections. We previously showed that the combination of amphotericin B (3 μg/ml) and nelfinavir (25 μM), both at sub-inhibitory MIC values, caused significant killing (by around 70%) of *F. pedrosoi* conidial cells compared to the individual treatment with amphotericin B or nelfinavir. This finding indicated that both compounds acted synergistically to kill *F. pedrosoi* conidial cells (Palmeira et al., 2008). In this context, HIV-PIs could be used alone or in combination with current antifungal drugs leading to their use as alternative and topical therapeutic agents. It is important to emphasize that the creation of more-specific PIs possessing high, selective toxicity against *F. pedrosoi* and related fungi, would truly represent a therapeutic breakthrough in the fight against chromoblastomycosis.

## AUTHOR CONTRIBUTIONS

VP, DA, LB-S, CA, SR, AS, and LK conceived and designed the experiments. VP, DA, LB-S, FG, and MG performed the experiments. All authors analyzed the data. DA, CA, SR, AS, and LK contributed reagents/materials/analysis tools. VP, DA, CA, SR, AS, and LK wrote and revised the paper. All authors contributed to the research and approved the final version of the manuscript. All authors agree to be accountable for all aspects of the work.

## FUNDING

This study was supported by grants from the Brazilian agencies: Fundação de Amparo à Pesquisa no Estado do Rio de Janeiro (FAPERJ), Conselho Nacional de Desenvolvimento Científico e Tecnológico (CNPq), Coordenação de Aperfeiçoamento de Pessoal de Nível Superior (CAPES), and Fundação Oswaldo Cruz (FIOCRUZ).

## ACKNOWLEDGMENTS

We would like to thank Denise Rocha de Souza, who is supported by an FAPERJ scholarship, for technical assistance. The authors also wish thank Dr Malachy McCann (Chemistry Department, National University of Ireland Maynooth, Co. Kildare, Ireland) for the valuable critical English review.

## REFERENCES

Alviano, C. S., Farbiarz, S. R., De Souza, W., Angluster, J., and Travassos, L. R. (1991). Characterization of *Fonsecaea pedrosoi* melanin. *J. Gen. Microbiol.* 137, 837–844. doi: 10.1099/00221287-137-4-837

Alviano, D. S., Franzen, A. J., Travassos, L. R., Holandino, C., Rozental, S., Ejzemberg, R., et al. (2004a). Melanin from *Fonsecaea pedrosoi* induces production of human antifungal antibodies and enhances the antimicrobial efficacy of phagocytes. *Infect. Immun.* 72, 229–237. doi: 10.1128/IAI.72.1.229-237.2004

Alviano, D. S., Rodrigues, M. L., Almeida, C. A., Santos, A. L. S., Couceiro, J. N., Soares, R. M. A., et al. (2004b). Differential expression of sialylglycoconjugates and sialidase activity in distinct morphological stages of *Fonsecaea pedrosoi*. *Arch. Microbiol.* 181, 278–286. doi: 10.1007/s00203-004-0653-9

Andrade, T. S., Castro, L. G., Nunes, R. S., Gimenes, V. M., and Cury, A. E. (2004). Susceptibility of sequential *Fonsecaea pedrosoi* isolates from chromoblastomycosis patients to antifungal agents. *Mycoses* 47, 216–221. doi: 10.1111/j.1439-0507.2004.00984.x

Asencio, M. A., Garduño, E., Pérez-Giraldo, C., Blanco, M. T., Hurtado, C., and Gómez-García, A. C. (2005). Exposure to therapeutic concentrations of ritonavir, but not saquinavir, reduces secreted aspartyl proteinase of *Candida parapsilosis*. *Chemotherapy* 51, 252–255. doi: 10.1159/000087252

Atzori, C., Angeli, E., Mainini, A., Agostoni, F., Micheli, V., and Cargnel, A. (2000). *In vitro* activity of human immunodeficiency virus protease inhibitors against *Pneumocystis carinii*. *J. Infect. Dis.* 181, 1629–1634. doi: 10.1086/315437

Bocca, A. L., Brito, P. P., Figueiredo, F., and Tosta, C. E. (2006). Inhibition of nitric oxide production by macrophages in chromoblastomycosis: a role for *Fonsecaea pedrosoi* melanin. *Mycopathologia* 161, 195–203. doi: 10.1007/s11046-005-0228-6

Borg-von Zepelin, M., Meyer, I., Thomssen, R., Würzner, R., Sanglard, D., Telenti, A., et al. (1999). HIV-Protease inhibitors reduce cell adherence of *Candida albicans* strains by inhibition of yeast secreted aspartic proteases. *J. Invest. Dermatol.* 113, 747–751. doi: 10.1046/j.1523-1747.1999.00747.x

Braga-Silva, L. A., Mogami, S. S., Valle, R. S., Silva-Neto, I. D., and Santos, A. L. S. (2010). Multiple effects of amprenavir against *Candida albicans*. *FEMS Yeast Res.* 10, 221–224. doi: 10.1111/j.1567-1364.2009.00595.x

Braga-Silva, L. A., and Santos, A. L. S. (2011). Aspartic protease inhibitors as potential anti–*Candida albicans* drugs: impacts on fungal biology, virulence and pathogenesis. *Curr. Med. Chem.* 18, 2401–2419. doi: 10.2174/092986711795843182

Buroker-Kilgore, M., and Wang, K. K. W. (1993). A Coomassie brilliant blue G-250-based colorimetric assay for measuring activity of calpain and other proteases. *Anal. Biochem.* 208, 387–392. doi: 10.1006/abio.1993.1066

Cassone, A., De Bernardis, F., Torosantucci, A., Tacconelli, E., Tumbarello, M., and Cauda, R. (1999). *In vitro* and *in vivo* anticandidal activity of human immunodeficiency virus protease inhibitors. *J. Infect. Dis.* 180, 448–453. doi: 10.1086/314871

Cenci, E., Francisci, D., Belfiori, B., Pierucci, S., Baldelli, F., Bistoni, F., et al. (2008). Tipranavir exhibits different effects on opportunistic pathogenic fungi. *J. Infect.* 56, 58–64. doi: 10.1016/j.jinf.2007.08.004

Chand, R., Kumar, M., Kushwaha, C., Shah, K., and Joshi, A. K. (2014). Role of melanin in release of extracellular enzymes and selection of aggressive isolates of *Bipolaris sorokiniana* in barley. *Curr. Microbiol.* 69, 202–211. doi: 10.1007/s00284-014-0559-y

Cunha, M. M., Franzen, A. J., Alviano, D. S., Zanardi, E., Alviano, C. S., De Souza, W., et al. (2005). Inhibition of melanin synthesis pathway by tricyclazole increases susceptibility of *Fonsecaea pedrosoi* against mouse macrophages. *Microsc. Res. Tech.* 68, 377–384. doi: 10.1002/jemt.20260

Cunha, M. M., Franzen, A. J., Seabra, S. H., Herbst, M. H., Vugman, N. V., Borba, L. P., et al. (2010). Melanin in *Fonsecaea pedrosoi*: a trap for oxidative radicals. *BMC Microbiol.* 10:80. doi: 10.1186/1471-2180-10-80

Del Poeta, M., Nimrichter, L., Rodrigues, M. L., and Luberto, C. (2014). Synthesis and biological properties of fungal glucosylceramide. *PLoS Pathog.* 11:e1004886 doi: 10.1371/journal.ppat.1003832

Deng, S., Tsui, C. K. M., Gerrits van den Ende, A. H. G., Yang, L., Najafzadeh, M. J., Badali, H., et al. (2015). Global spread of human chromoblastomycosis is driven by recombinant *Cladophialophora carrionii* and predominantly clonal *Fonsecaea* species. *PLoS Negl. Trop. Dis.* 9:10. doi: 10.1371/journal.pntd.0004004

Folch, A. J., Lees, M., and Stanley, G. H. S. (1957). A simple method for the isolation and purification of total lipids from animal tissues. *J. Biol. Chem.* 226, 497–509.

Gehrt, A., Peter, J., Pizzo, P., and Walsh, T. (1995). Effect of increasing inoculum sizes of pathogenic filamentous fungi on MICs of antifungal agents by broth microdilution method. *J. Clin. Microbiol.* 33, 1302–1307.

Granato, M. Q., Gonçalves, D. S., Seabra, S. H., McCann, M., Devereux, M., Santos, A. L. S., et al. (2017). 1,10-Phenanthroline-5,6-dione-based compounds are effective in disturbing crucial physiological events of *Phialophora verrucosa*. *Front. Microbiol.* 8:76. doi: 10.3389/fmicb.2017.00076

Henson, J. M., Butler, M. J., and Day, A. W. (1999). The dark side of the mycelium: melanin of phytopathogenic fungi. *Annu. Rev. Phytopathol.* 37, 447–471. doi: 10.1146/annurev.phyto.37.1.447

Kathiravan, M. K., Salake, A. B., Chothe, A. S., Dudhe, P. B., Watode, R. P., Mukta, M. S., et al. (2012). The biology and chemistry of antifungal agents: a review. *Bioorg. Med. Chem.* 20, 5678–5698. doi: 10.1016/j.bmc.2012.04.045

Kohatsu, L., Hsu, D. K., Jegalian, A. G., Liu, F. T., and Baum, L. G. (2006). Galectin-3 induces death of *Candida* species expressing specific beta-1,2-linked mannans. *J. Immunol.* 177, 4718–4726. doi: 10.4049/jimmunol.177.7.4718

Larsen, T., Axelsen, J., and Ravn, H. W. (2004). Simplified and rapid method for extraction of ergosterol from natural samples and detection with quantitative and semi-quantitative methods using thin-layer chromatography. *J. Chromatogr. A* 1026, 301–304. doi: 10.1016/j.chroma.2003.10.128

Limongi, C. L., Rozental, S., Alviano, C. S., and de Souza, W. (1997). The influence of surface carbohydrates on the interaction of *Fonsecaea pedrosoi* with Chinese hamster ovary glycosylation mutant cells. *Mycopathologia* 138, 127–135. doi: 10.1023/A:1006841529438

Lowry, O. H., Rosebrough, N. J., Farr, A. L., and Randall, R. J. (1951). Protein measurement with the Folin phenol reagent. *J. Biol. Chem.* 193, 265–275.

Monari, C., Pericolini, E., Bistoni, G., Cenci, E., Bistoni, F., and Vecchiarelli, A. (2005). Influence of indinavir on virulence and growth of *Cryptococcus neoformans*. *J. Infect. Dis.* 191, 307–311. doi: 10.1086/426828

Monod, M., Capoccia, S., Léchenne, B., Zaugg, C., Holdom, M., and Jousson, O. (2002). Secreted proteases from pathogenic fungi. *Int. J. Med. Microbiol.* 292, 405–419. doi: 10.1078/1438-4221-00223

Naglik, J. R., Challacombe, S. J., and Hube, B. (2003). *Candida albicans* secreted aspartyl proteinases in virulence and pathogenesis. *Microbiol. Mol. Biol. Rev.* 67, 400–428. doi: 10.1128/MMBR.67.3.400-428.2003

Nimrichter, L., Cerqueira, M. D., Leitão, E. A., Miranda, K., Nakayasu, E. S., Almeida, S. R., et al. (2005). Structure, cellular distribution, antigenicity, and biological functions of *Fonsecaea pedrosoi* ceramide monohexosides. *Infect. Immun.* 73, 7860–7868. doi: 10.1128/IAI.73.12.7860-7868.2005

Nosanchuk, J. D., and Casadevall, A. (2006). Impact of melanin on microbial virulence and clinical resistance to antimicrobial compounds. *Antimicrob. Agents Chemother.* 50, 3519–3528. doi: 10.1128/AAC.00545-06

Oliveira, L. G., Resende, M. A., Lopes, C. F., and Cisalpino, E. O. (1973). Isolamento e identificação dos agentes da cromoblastomicose em Belo Horizonte. *Rev. Soc. Bras. Med. Trop.* 7, 7–10. doi: 10.1590/S0037-86821973000100002

Palmeira, V. F., Kneipp, L. F., Alviano, C. S., and Santos, A. L. S. (2006a). The major chromoblastomycosis fungal pathogen, *Fonsecaea pedrosoi*, extracellularly releases proteolytic enzymes whose expression is modulated by culture medium composition: implications on the fungal development and cleavage of key's host structures. *FEMS Immunol. Med. Microbiol.* 46, 21–29. doi: 10.1111/j.1574-695X.2005.00003.x

Palmeira, V. F., Kneipp, L. F., Alviano, C. S., and Santos, A. L. S. (2006b). Secretory aspartyl peptidase activity from mycelia of the human fungal pathogen *Fonsecaea pedrosoi*: effect of HIV aspartyl proteolytic inhibitors. *Res. Microbiol.* 157, 819–826. doi: 10.1016/j.resmic.2006.07.003

Palmeira, V. F., Kneipp, L. F., Alviano, C. S., and Santos, A. L. S. (2010). Phospholipase and esterase production by clinical strains of *Fonsecaea pedrosoi* and their interactions with epithelial cells. *Mycopathologia* 170, 31–37. doi: 10.1007/s11046-010-9293-6

Palmeira, V. F., Kneipp, L. F., Rozental, S., Alviano, C. S., and Santos, A. L. S. (2008). Beneficial effects of HIV peptidase inhibitors on *Fonsecaea pedrosoi*: promising compounds to arrest key fungal biological processes and virulence. *PLoS ONE* 3:10. doi: 10.1371/journal.pone.0003382

Park, M., Do, E., and Jung, W. H. (2013). Lipolytic enzymes involved in the virulence of human pathogenic fungi. *Mycobiology* 41, 67–72. doi: 10.5941/MYCO.2013.41.2.67

Price, M. F., Wilkinson, I. D., and Gentry, L. O. (1982). Plate method for detection of phospholipase activity in *Candida albicans*. *Sabouraudia* 15, 179–185. doi: 10.1080/00362177785190271

Queiroz-Telles, F., and Santos, D. W. (2013). Challenges in the therapy of chromoblastomycosis. *Mycopathologia* 175, 477–488. doi: 10.1007/s11046-013-9648-x

Rippon, J. W. (1988). "Chromoblastomycosis," in *Medical Mycology*, ed. W. B. Sauders (Philadelphia, PA: Harcourt Brace Jovanovich, Inc), 276–296.

Rochin, L., Hurbain, I., Serneels, L., Fort, C., Watt, B., Leblanc, P., et al. (2013). BACE2 processes PMEL to form the melanosome amyloid matrix in pigment cells. *Proc. Natl. Acad. Sci. U.S.A.* 110, 10658–10663. doi: 10.1073/pnas.1220748110

Rozental, S., Alviano, C. S., and de Souza, W. (1994). The in vitro susceptibility of *Fonsecaea pedrosoi* to activated macrophages. *Mycopathologia* 126, 85–91. doi: 10.1007/BF01146200

Santos, A. L. S. (2011a). Protease expression by microorganisms and its relevance to crucial physiological/pathological events. *World J. Biol. Chem.* 26, 48–58. doi: 10.4331/wjbc.v2.i3.48

Santos, A. L. S. (2011b). Aspartic proteases of human pathogenic fungi are prospective targets for the generation of novel and effective antifungal inhibitors. *Curr. Enzym. Inhib.* 7, 96–118. doi: 10.2174/157340811796575281

Santos, A. L. S., and Braga-Silva, L. A. (2013). Aspartic protease inhibitors: effective drugs against the human fungal pathogen *Candida albicans*. *Mini Rev. Med. Chem.* 13, 155–162. doi: 10.2174/138955713804484802

Santos, A. L. S., Braga-Silva, L. A., Silva, B. A., Palmeira, V. F., Valle, R. S., Abi-chacra, E. A., et al. (2013). "Aspartic proteolytic inhibitors induce cellular and biochemical alterations in fungal cells," in *Proteases in Health and Disease*, eds S. Chakraborti and N. S. Dhalla (New York, NY: Springer), 89–119.

Santos, A. L. S., Palmeira, V. F., Rozental, S., Kneipp, L. F., Nimrichter, L., Alviano, D. S., et al. (2007). Biology and pathogenesis of *Fonsecaea pedrosoi*, the major etiologic agent of chromoblastomycosis. *FEMS Microbiol. Rev.* 31, 570–591. doi: 10.1111/j.1574-6976.2007.00077.x

Soares, R. M. A., Angluster, J., de Souza, W., and Alviano, C. S. (1995). Carbohydrate and lipid components of hyphae and conidia of human pathogen *Fonsecaea pedrosoi*. *Mycopathologia* 32, 71–77. doi: 10.1007/BF01103778

Tronchin, G., Pihet, M., Lopes-Bezerra, L. M., and Bouchara, J. P. (2008). Adherence mechanisms in human pathogenic fungi. *Med. Mycol.* 46, 749–772. doi: 10.1080/13693780802206435

**Conflict of Interest Statement:** The authors declare that the research was conducted in the absence of any commercial or financial relationships that could be construed as a potential conflict of interest.

frontiers in Microbiology

REVIEW
published: 30 January 2017
doi: 10.3389/fmicb.2017.00097

# Potential Use of Alginate-Based Carriers As Antifungal Delivery System

*Cristina de Castro Spadari[1], Luciana B. Lopes[2] and Kelly Ishida[1]**

[1] Departamento de Microbiologia, Instituto de Ciências Biomédicas, Universidade de São Paulo, São Paulo, Brazil,
[2] Departamento de Farmacologia, Instituto de Ciências Biomédicas, Universidade de São Paulo, São Paulo, Brazil

Fungal infections have become a major public health problem, growing in number and severity in recent decades due to an increase of immunocompromised patients. The use of therapeutic agents available to treat these fungal infections is limited by their toxicity, low bioavailability, antifungal resistance, and high cost of treatment. Thus, it becomes extremely important to search for new therapeutic options. The use of polymeric systems as drug carriers has emerged as a promising alternative to conventional formulations for antifungals. Alginate is a natural polymer that has been explored in the last decade for development of drug delivery systems due to its non-toxicity, biodegradability, biocompatibility, low cost, mucoadhesive, and non-immunogenic properties. Several antifungal agents have been incorporated in alginate-based delivery systems, including micro and nanoparticles, with great success, displaying promising *in vitro* and *in vivo* results for antifungal activities, reduction in the toxicity and the total drug dose used in the treatment, and improved bioavailability. This review aims at discussing the potential use and benefits of alginate-based nanocarriers and other delivery systems containing antifungal agents in the therapy of fungal infections.

**Keywords: antifungal, alginate, drug delivery systems, nanoparticles, amphotericin B**

OPEN ACCESS

***Edited by:***
*Joshua D. Nosanchuk, Albert Einstein College of Medicine, USA*

***Reviewed by:***
*Erin E. McClelland, Middle Tennessee State University, USA*
*Rohitashw Kumar, University at Buffalo, USA*

****Correspondence:***
*Kelly Ishida*
*ishidakelly@usp.br*

***Specialty section:***
*This article was submitted to Fungi and Their Interactions, a section of the journal Frontiers in Microbiology*

***Received:*** *09 November 2016*
***Accepted:*** *13 January 2017*
***Published:*** *30 January 2017*

***Citation:***
*Spadari CC, Lopes LB and Ishida K (2017) Potential Use of Alginate-Based Carriers As Antifungal Delivery System. Front. Microbiol. 8:97. doi: 10.3389/fmicb.2017.00097*

## INTRODUCTION

Fungal infections have become a major public health problem and are growing in number and severity over the past three decades. The development of new medical treatments, including therapy with immunosuppressive agents and chemotherapy of cancer, led to a dramatic increase in the number of immunocompromised individuals who are vulnerable to infections which otherwise would have been easily resolved (Karkowska-Kuleta et al., 2009). More than 1.7 billion people worldwide are estimated to suffer from fungal diseases, ranging from superficial to invasive infections (Brown et al., 2012), and some of these infections cause more deaths per year than tuberculosis or malaria (Gaffi – Global Action Fund for Fungal Infections, 2016). However, deaths resulting from invasive or chronic fungal infections are often overlooked, and most public health agencies present little or no mycological surveillance programs (Brown et al., 2012). Preventive measures, premature diagnosis, and the availability of appropriate antifungal treatment could reduce death rates by fungal infections.

The current antifungal therapy is based on three major chemical classes: echinocandins, polyenes, and azoles. Echinocandins are β(1,3)-glucan synthase inhibitors, disrupting the synthesis of the cell wall β(1,3)-D-glucan polymer. Polyenes and azoles alter cytoplasm membrane

permeability; polyenes bind irreversibly to ergosterol whilst azoles inhibit ergosterol biosynthesis specifically inhibiting cytochrome P450 dependent enzyme lanosterol 14-α-demethylase. Other antifungals as allylamines and pyrimidine analogs find use against a few fungal infections, mainly to treat cutaneous mycosis (Ostrosky-Zeichner et al., 2010). It is important to emphasize that most antifungal compounds are approved for treatment of superficial mycoses, especially in topical formulations (Denning and Bromley, 2015). In contrast, the clinical repertoire for treatment of invasive fungal infections (IFIs) is much smaller, with only nine approved compounds: amphotericin B, fluconazole, voriconazole, itraconazole, posaconazole, caspofungin, anidulafungin, micafungin, and flucytosine (Denning and Bromley, 2015).

However, the use of these compounds for IFIs is complicated by their poor solubility and bioavailability due to problems in drug absorption and distribution. The situation is aggravated by difficulties to deliver the drug to its target, which leads to an increased incidence of adverse effects resultant from the lack of drug selectivity, which compromise efficacy and safety. An example is the polyene amphotericin B; the drug displays a broad spectrum of action and fungicidal effect, but the significant number of serious adverse effects (which include nephrotoxicity) limits its wider therapeutic use (Hamill, 2013). Triazole agents also exhibit adverse effects associated mainly to hepatic disorders, and their interaction with other drugs have been described due to their ability to modulate the activity of cytochrome P450 enzymes and the hepatic oxidative metabolism of many drugs (Peyton et al., 2015). Even the newest antifungal agents, the echinocandins, present low oral bioavailability and cause gastrointestinal effects after intravenous administration (Chen et al., 2011).

This scenario becomes more complicated if we take into consideration the challenges related to the development of new antifungal agents. The fact that fungi are evolutionarily close to their human host impairs the discovery of new compounds with selective action (Seneviratne and Rosa, 2016). These factors associated with increases in antifungal resistance (Pfaller, 2012), emergence of uncommon fungi (Davoudi et al., 2015; Roilides, 2016), and high mortality rates (Brown et al., 2012; Gaffi – Global Action Fund for Fungal Infections, 2016) have led the scientific community to search for other ways to improve drug targeting and efficacy while reducing adverse effects.

In this context, drug delivery systems emerge as promising alternatives to improve therapy and overcome the above-mentioned limitations (**Figure 1A**). They have been demonstrated to reduce toxicity caused by conventional drug treatments, improve drug efficacy and bioavailability, reduce dose and administration frequency, and might allow oral administration of compounds with unfavorable pharmacokinetic characteristics, formerly used in topical and/or intravenous forms (Kumar et al., 2013). Various nanocarriers, such as dendrimers, polymers, liposomes, nanoemulsions, and micelles have been investigated for drug delivery (Jeevanandam et al., 2016).

Amphotericin B lipid formulations are examples of the successful application of drug nanocarriers to improve therapeutic outcomes. Three lipid formulations of amphotericin B are available for medical use: liposomal (L-AMB); colloidal dispersion (ABCD); and a lipid complex (ABLC). All were developed to reduce nephrotoxicity without compromising the antifungal efficacy (Falci et al., 2015). The L-AMB formulation (Ambisome®) incorporates the drug into liposomes, lipid vesicles of 55–75 nm in diameter composed of soy lecithin, cholesterol, and distearoylphosphatidylglycerol. In the ABCD formulation (Amphocil®), amphotericin B is co-incorporated with cholesterol sulfate in microdiscs of an average diameter of 122 nm. The ABLC formulation (Abelcet®) is a macromolecular complex of amphotericin B with dimyristoylphosphatidylcholine and dimyristoylphosphatidylglycerol forming ribbon-like particles ranging in length from 1,600 to 6,000 nm (Tiphine et al., 1999; Martinez, 2006; Voltan et al., 2016).

Amphotericin B association with lipids improves drug dissolution, facilitates parenteral infusion, protects the drug from destruction by enzymatic degradation and/or host immune factor inactivation and changes the pharmacokinetic profile of amphotericin B by slow drug release resulting in the protection of potentially vulnerable tissues (most importantly, the kidneys) (Hamill, 2013). In a review, the lipid-based compounds were associated with less risk of changes in renal function, while the risk of a doubling in serum creatinine from baseline was 58% less likely with the lipid based formulations (Barrett et al., 2003). Moreover, the slow and continuous release of amphotericin B from lipid formulations allow the administration of higher doses and longer treatment (Hamill, 2013). However, although lipid-based amphotericin B formulations have shown equivalent efficacy and reduced toxicity compared with the conventional amphotericin B formulation, they are often reserved as a secondary treatment option, presumably because of the differences in costs (Wade et al., 2013).

Various other antifungal agents could benefit from the ability of delivery systems to modify pharmacokinetics and reduce adverse effects. In fact, several studies have been conducted on incorporation of other antifungal agents in various types of delivery systems in the past years, suggesting a demand for novel cost-effective and safe delivery platforms. In this review, we will discuss non-lipid drug carriers for antifungal agents, emphasizing the relevance of alginate-based carriers as an interesting approach for delivery of antifungal agents.

## POLYMERIC SYSTEMS

Among the many types of modified release systems developed, polymer-based systems have attracted attention as they offer significant advantages over other carrier platforms primarily due to the tremendous versatility of polymer matrices, which allows for tailoring of the carrier properties to meet the specific intended need. Other advantages of polymeric systems include ease of production, high encapsulation efficiency of the molecule of interest, protection of the drug against physicochemical degradation, flexibility of their physicochemical properties (such as size, surface charge, and hydrophobicity), slow or fast polymer degradation and

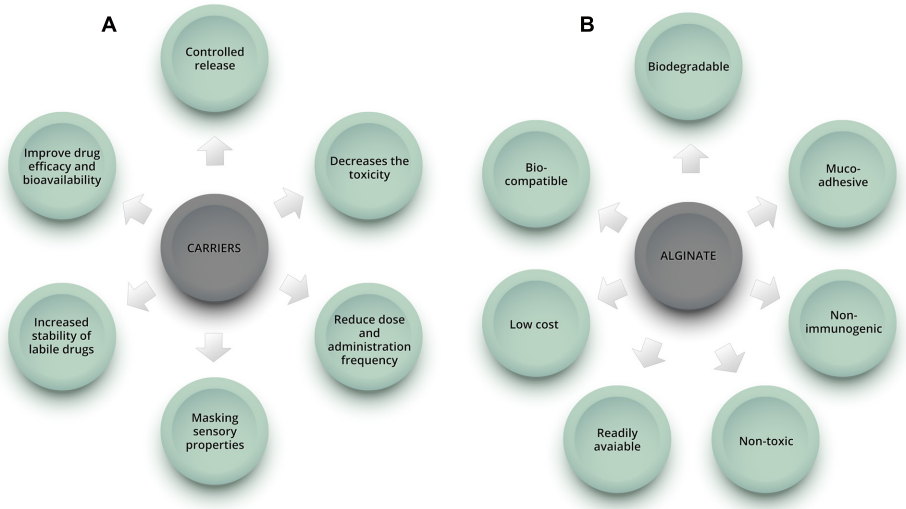


**FIGURE 1 | Schematic representation showing some of the benefits of using carriers in drug formulations (A)** and advantages of alginate natural polymer **(B)**.

stimuli-responsive polymer erosion for temporal control over the release of drugs (Van Vlerken et al., 2007; Voltan et al., 2016).

Bulk gels, films, micro and nanocarriers have been prepared using natural polymers, such as alginate (Liakos et al., 2013; Elsayed et al., 2015), chitosan (Al-Kassas et al., 2016; Islam and Ferro, 2016), gelatin (Mahor et al., 2016), dextran (Gallovic et al., 2016), or synthetic polymers, such as polylactic acid (PLA) (Tyler et al., 2016), poly(lactide-co-glycolide) (PLGA) (Han et al., 2016; Thomas et al., 2016) and others. Natural polysaccharides are advantageous compared to the synthetic polymers due to their abundance in nature, low processing cost, biocompatibility, biodegradability, water solubility, bioactivity, and environmental safety (Sundar et al., 2010; Debele et al., 2016). Among the biopolymers used, alginate represents an excellent alternative for obtainment of drug carriers and is the main focus of this review.

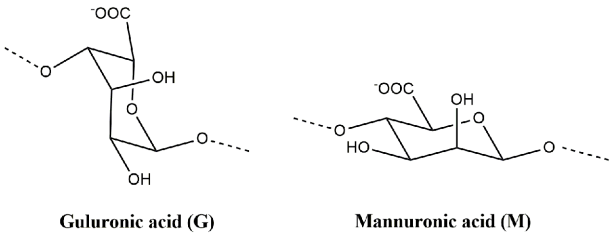


**FIGURE 2 | Molecular structures of α-L-guluronic acid (G) and β-D-mannuronic acid (M) from alginate polymer.**

## ALGINATE

Alginate is a generic name assigned to a series of natural unbranched polyanionic polysaccharides of β-D-mannuronic acid (M) and α-L-guluronic acid (G) (**Figure 2**) repeating units linked by a 1→4 linkage and displaying chain homosequences of MMM and GGG, interdispersed with MGM heterosequences (Lee and Mooney, 2012; Sosnik, 2014). Molecular weights in the range of 32–400 kg/mol together with different relative G/M compositions and variations in the proportion and chain arrangements of M and G blocks might be found depending on type of seaweed from which alginate was extracted (Sosnik, 2014; Cardoso et al., 2016).

This polysaccharide is frequently obtained from brown seaweeds, including *Laminaria hyperborea*, *Laminaria digitata*, *Laminaria japonica*, *Ascophyllum nodosum*, and *Macrocystis pyrifera* (Lee and Mooney, 2012). Alginate extraction is conducted by treatment with aqueous alkali solutions, typically sodium hydroxide, in which the natural alginate in various salt forms is converted into water-soluble sodium alginate; the extract is filtered, and either sodium or calcium chloride is added to the filtrate in order to precipitate alginate. After further purification and conversion, water-soluble sodium alginate powder is produced (Qin, 2008; Lee and Mooney, 2012). On a dry weight basis, the alginate contents are 22–30% for *A. nodosum*, 25–44% for *L. digitata,* and 17–33 and 25–30%, respectively, for the fronds and stems of *L. hyperborea* (Qin, 2008).

Another alginate source is bacteria from the *Azotobacter* and *Pseudomonas* species. The alginate biosynthesis pathway in bacteria can be divided into four different stages: (i) synthesis of precursor substrate, (ii) polymerization and cytoplasmic membrane transfer, (iii) periplasmic transfer and modification, and (iv) export through the outer membrane. However, even under optimized fermentation conditions, production yields are quite low (around 4 g/l) (Remminghorst and Rehm, 2006), and

the process is not considered economically viable for commercial applications (Goh et al., 2012).

Alginate has important characteristics that make it one of the most used polymers for drug delivery application: it is non-toxic, biocompatible, non-immunogenic, biodegradable, mucoadhesive, readily available and has low cost (**Figure 1B**) (Hosseini et al., 2013; Paques et al., 2014). Various modified drug delivery systems can be obtained using alginate, such as hydrogels (polymeric networks with three-dimensional configuration capable of imbibing high amounts of water or biological fluid), microparticles (diameter from 1 to 200 μm) and nanoparticles (diameter from 10 to 1000 nm) (Hamidi et al., 2008; Sosnik, 2014). Depending on the desired application and formulation characteristics, different techniques can be used to produce the carriers. The ionotropic gelation is the most common method used to obtain alginate-based nano and microparticles, beads and hydrogels, among other systems, due to its simplicity and non-toxic procedure.

In this process, alginate is crosslinked in aqueous solutions ionotropically by a mechanism whereby pendant carboxylic acid moieties of G units chelate $Ca^{2+}$ or other divalent cations (e.g., $Sr^{2+}$, $Ba^{2+}$) to generate 3D networks that allow the incorporation of compounds (Tønnesen and Karlsen, 2002; Sosnik, 2014). This gelation is known as the "egg box model" and has been demonstrated to result from specific and strong interactions between calcium ions and blocks of guluronic acid residues (Braccini and Pérez, 2001). Biomolecules and other drugs can be loaded under mild conditions and retained in the 3D structure (Paques et al., 2014; Lopes et al., 2016). Ionotropic gelation can be divided into external and internal gelation. The main difference between these methods is the type of calcium salt used and consequently the gelling kinetics (Draget et al., 2005).

In the external gelation method, which is also referred to as the "diffusion method" particles are produced by dropping a drug-loaded alginate solution into the aqueous solution of a soluble salt of calcium, such as calcium chloride. The internal gelation method, also referred to as "internal setting," is characterized by the release of calcium ions in a controlled manner from an insoluble calcium source, such as calcium carbonate, within the alginate solution. Controlled release of calcium is usually obtained by a change in pH, by a limited solubility of the calcium salt source, and/or by the presence of chelating agents (Draget et al., 2005; Paques et al., 2014; Lopes et al., 2016).

Micro and nanoparticles of alginate are usually obtained using emulsification (W/O or O/W) followed by external or internal gelation (Hosseini et al., 2013; Paques et al., 2013; Song et al., 2013). Emulsions are basically obtained by dispersing a fluid into another immiscible fluid and are produced by fragmenting, through various processes, one phase into another, and leading to a dispersion of droplets in a continuous phase. The recombination of the freshly formed droplets may be partially suppressed by the addition of surfactants that locate at the droplet interface reducing the interfacial tension (Bibette and Leal-Calderon, 1996; Pillai et al., 1999).

## ALGINATE-BASED DELIVERY SYSTEMS FOR ANTIFUNGAL DRUGS

Several types of alginate-based delivery systems for antifungal agents have been studied in the last few years, such as nanoparticles and microparticles, beads, hydrogels, tablets, and films. In the next sections, alginate–based carriers for two classes of antifungal agents will be addressed: azoles and polyenes (**Table 1**).

### Azoles

Azoles inhibit the fungal cytochrome P450 (CYP) enzyme 14-α-sterol-demethylase, which is involved in ergosterol biosynthesis, a major sterol component of fungal cytoplasmic membranes (Kathiravan et al., 2012). Therapeutic use of azoles displays two main problems. The first one is their ability to interact with mammalian P450 isozymes, affecting the metabolism of other drugs that serve as substrates of these enzymes, which may result in significant drug interactions including reduced efficacy or increased incidence of adverse effects. The second drawback relates to the low aqueous solubility of several azoles: miconazole, ketoconazole, itraconazole, and posaconazole are all slightly water-soluble (<1 μg/ml) or insoluble at neutral pH (Yang et al., 2008). Low aqueous solubility is known to severely limit azole bioavailability after oral administration and its therapeutic effectiveness. The low concentration of the drug at the infection site may also induce antifungal resistance to some less susceptible species (Yang et al., 2008). The first limitation is more easily addressed by local drug delivery to the site of infection, which can be prolonged/controlled using alginate-based carriers. Systemic administration of alginate carriers can overcome the second, as they have been demonstrated to improve the bioavailability of antifungal imidazoles and triazoles in various studies, improving efficacy while potentially reducing the frequency of drug administration.

#### Imidazoles

Econazole and clotrimazole have been mainly used topically due to the low absorption after oral administration (Fromtling, 1988). To improve the oral bioavailability, Pandey et al. (2005) encapsulated these antifungals separately in alginate nanoparticles. When free drug was administered, it was detected in the plasma of animals for up to 3–4 h. In contrast, after administration of the alginate nanoparticles, econazole, and clotrimazole could be detected for longer periods of time (5–6 days). In addition, the drugs were detected in the lung, liver, and spleen up to 8 days following administration of the nanoparticles, while free antifungals were cleared within 12 h. Thus, reduced frequency of antifungal administration was proposed as a potential advantage of the alginate nanoparticles containing econazole or clotrimazole.

Ahmad et al. (2007) evaluated the chemotherapeutic potential of alginate nanoparticles encapsulating econazole and antitubercular drugs (ATDs) against murine tuberculosis. Azole drugs have proven their antimycobacterial potential under *in vitro*, *ex vivo*, and *in vivo* conditions against murine

**TABLE 1 | Alginate-based drug delivery systems for antifungal agents azoles and polyenes.**

| Antifungal | Carrier | Therapeutic goal | Experimental model | Reference |
|---|---|---|---|---|
| Clotrimazole | Alginate nanoparticles | Improve bioavailability of the drug | *In vivo* (mice) | Pandey et al., 2005 |
| | Films of sodium alginate, hydroxyl propylcellulose and propylene glycol | Treatment of vaginal candidiasis | *In vitro* | Mishra et al., 2016 |
| Econazole | Alginate nanoparticles | Improve bioavailability of the drug | *In vivo* (mice) | Pandey et al., 2005 |
| | Alginate nanoparticles | Chemotherapeutic potential against murine tuberculosis | *In vivo* (mice) | Ahmad et al., 2007 |
| Miconazole | Tablets of alginate | Evaluation of the buccal bioadhesive properties of slow-release tablets containing miconazole | *In vitro* and *in vivo* (human voluntary) | Mohammed and Khedr, 2003 |
| Fluconazole | Films of sodium alginate and polyvinyl alcohol | Overcome the problems of high drug dose requirement and toxicity | *In vitro* and *ex vivo* | Patel et al., 2015 |
| | Ethyl cellulose microspheres with internal phase of alginate | Antifungal activity against *Candida albicans* | *In vitro* | Maiti et al., 2009 |
| | Alginate mucoadhesive films and disks | Topical treatment of oral candidiasis | *In vitro* and *in vivo* (human voluntary) | Yehia et al., 2008, 2009 |
| Voriconazole | Pluronic and sodium alginate gels | Ocular drug delivery against *C. albicans* and *Aspergillus fumigatus* | *In vitro* | Pawar and Edgar, 2012 |
| Amphotericin B | Sodium alginate nanospheres | Treatment of systemic candidiasis | *In vitro* and *in vivo* (mice) | Sangeetha et al., 2007 |
| | Sodium alginate-glycol chitosan stearate nanoparticles | for better chemotherapy of visceral leishmaniasis | *In vitro* and *in vivo* (hamster) | Gupta et al., 2015 |
| | Alginate films with starch Pickering emulsions | Treatment of oral candidiasis | *In vitro* | Cossu et al., 2015 |
| | Alginate-capped amphotericin B lipid | Treatment of visceral leishmaniasis | *In vitro* | Singodia et al., 2011 |
| Nystatin | Alginate beads, micro- and nanoparticles incorporated in toothpaste | Increase the effectiveness of the nystatin in the treatment of oral candidiasis | *In vitro* | Reis et al., 2015 |
| | Alginate microspheres and alginate hydrogel | Treatment of oral candidiasis | *In vitro* and *in vivo* (pigs) | Martín et al., 2015 |
| | Alginate microparticles, chitosan and poloxamer 407 coated alginate microparticles | Treatment of *Candida* vaginitis | *In vitro* and *ex vivo* | Martín-Villena et al., 2013 |

tuberculosis caused by susceptible, resistant, and latent bacilli (Ahmad et al., 2006). They observed that co-encapsulation of these drugs in alginate nanoparticles reduced the dosing frequency of econazole and ATDs by 15-fold, suggesting the advantage of their encapsulation for sustained release of these drugs (Ahmad et al., 2007).

Other studies demonstrated the applicability of alginate to obtain mucoadhesive carriers for treatment of mucosal candidiasis. Mishra et al. (2016) investigated mucoadhesive films of clotrimazole for vaginal administration, a patient-convenient alternative for treatment of vaginal candidiasis. Conventional vaginal dosage forms, such as creams, foams, jellies have short residence time at the site of application, resulting in reduced therapeutic effect. Vaginal films possess several advantages including the ease of storage and handling, no need of an applicator, and better drug stability (Hussain and Ahsan, 2005; Mishra et al., 2016). The optimized film provided higher drug release than the marketed product Candid-V6® vaginal tablet (70% drug release in 1 h and 83% drug release in 6 h while marketed product showed 14% drug release in 1 h and 41% drug release in 6 h). In addition, the films maintained *in vitro* antifungal activity without inhibiting *Lactobacillus* growth (Mishra et al., 2016). Mohammed and Khedr (2003) obtained slow-release buccal bioadhesive alginate tablets of miconazole, and demonstrated that these tablets markedly prolonged the duration of antifungal activity of the drug in the saliva of human volunteers for more than 8 h compared with the commercial miconazole gel (Daktaren oral gel), improving patient convenience.

## Triazoles

Maiti et al. (2009) prepared ethyl cellulose microspheres with high entrapment levels of fluconazole by alginate facilitated water-in-oil-in-water (w/o/w) emulsion solvent evaporation technique. The drug entrapment efficiency (%) in ethyl cellulose microspheres, prepared by conventional w/o/w emulsion solvent evaporation technique, was found to be $10.93 \pm 1.23$, while the addition of 2% (w/v) sodium alginate in the internal aqueous phase of the multiple emulsion improved the efficiency of drug entrapment to 80% (Maiti et al., 2009), most likely due to an

increase in the viscosity of the internal phase (Gainza et al., 2013). In addition, *in vitro* antifungal activity of fluconazole incorporated in ethyl cellulose-alginate microspheres against *Candida albicans* (MIC ranges from 1.29 to 5.69 μg/ml) were comparable to the MIC values of free fluconazole (0.12 to >64 μg/ml) (Maiti et al., 2009). These studies suggested that the use of aqueous sodium alginate solution as an internal phase in conventional double emulsion solvent evaporation technique may be an alternative approach for the successful incorporation of slightly water soluble drugs in microspheres obtained with ethyl cellulose and other synthetic polymers (Maiti et al., 2009; Gainza et al., 2013).

Mucoadhesive disks and films (Yehia et al., 2008, 2009) containing a small dose of fluconazole were developed for topical treatment of oral candidiasis to ensure satisfactory drug levels in the mouth for prolonged time periods, reducing systemic adverse effects and the possibility of drug–drug interaction. Compared to other polymers (hydroxypropyl methyl cellulose, hydroxyethyl cellulose, chitosan, eudragit), the alginate-based disks containing fluconazole were considered the best formulation in terms of adhesion characteristics, residence times and release rates both in *in vitro* assays and *in vivo* using the oral mucosa of human volunteers (Yehia et al., 2009). The alginate disks containing fluconazole presented swelling and adhesion properties, increased *in vivo* residence time and prolonged drug release over approximately 5 h (Yehia et al., 2008). Recently, Patel et al. (2015) developed bioadhesive films of fluconazole to provide localized drug delivery exclusively at the site of infection, thereby reducing its total dose and hence, dose-related toxicity. The time necessary for complete erosion or detachment of the film was over 5 h in an *ex vivo* model of rat skin surface using a modified IP (Indian Pharmacopeia) disintegration apparatus; and the *in vitro* assays demonstrated a controlled release of the fluconazole up to 8 h using a diffusion cell method (Patel et al., 2015).

Pawar et al. (2013) evaluated the use of a pluronic/alginate-based gel for ophthalmic delivery of voriconazole. All batches of formulations were mucoadhesive and displayed a loading efficiency between 95 and 100%. Importantly, the antifungal efficiency of the formulation against *C. albicans* and *Aspergillus fumigatus in vitro* confirmed that the designed formulation has prolonged effect and retained its antifungal properties against fungal infection. The local voriconazole bioavailability obtained with alginate-based gel ranged from 19.74 to 30.82% in 4 h (Pawar et al., 2013) and it was considered an important advantage to conventional systems, such as eye drops, suspensions, and ointments that result in less than 5% of administered drug entering the eye (Gaudana et al., 2009).

## Polyenes

Polyene antibiotics form a complex with ergosterol and disrupt the fungal plasma membrane, increasing membrane permeability and leakage of the cytoplasmic contents, which results in the ultimate death of the fungal cell (Kathiravan et al., 2012). Polyene macrolides are rather toxic, causing serious side effects, such as renal failure, hypokalemia, and thrombophlebitis, especially upon intravenous administration. Besides that, these drugs are poorly soluble in water, and can easily form aggregates of micelles in aqueous media. This feature is apparently responsible for the difficulties encountered during administration of polyene macrolides including poor absorption after oral administration and poor distribution of the antibiotics in organs and tissues (Zotchev, 2003).

Amphotericin B alginate films containing starch Pickering emulsion were demonstrated to be a good alternative for treatment of mucosa candidiasis. *In vitro* results demonstrated efficacy of the emulsions dispersed in alginate films against *C. albicans* at concentrations above 5 μg/mL (Cossu et al., 2015). The inhibitory effect of amphotericin B in the microbiological assay showed that the addition of 100 U/mL α-amylase resulted in an enhanced effect on *C. albicans* due to the increased bioavailability of amphotericin B released from the emulsions. This result demonstrated that the release of amphotericin B from starch Pickering emulsions in alginate films could be controlled by α-amylase in the system, an interesting feature to provide release of hydrophobic antifungal, such as amphotericin B (Cossu et al., 2015).

Alginate nanospheres containing amphotericin B for treatment of systemic candidiasis in a murine model displayed higher antifungal efficacy in comparison to the conventional formulation of amphotericin B (Sangeetha et al., 2007). In the study, amphotericin B-containing nanospheres administered intravenously for 7 days led to a mice survival rate of 80% (compared to 60% for free drug) as well as 10-fold lower fungal load in the affected organs (liver and lungs) compared with the free drug (Sangeetha et al., 2007). The authors suggested that alginate nanospheres containing amphotericin B might improve biodistribution, enhancing drug localization in the liver and lungs while reducing it in the kidneys. As a result, a reduction in total dose as well as dose-related systemic adverse effects mainly in the kidneys was observed (Sangeetha et al., 2007). Gupta et al. (2015) produced amphotericin B-loaded alginate glycol chitosan stearate nanoparticles that presented efficacy in a visceral leishmaniasis hamster model after intraperitoneal administration. Drug encapsulation in the nanoparticles modified its tissue distribution, with higher drug concentrations being localized in *Leishmania* infected organs (i.e., spleen and liver) and lower concentrations in the kidneys, reducing toxicity compared to the free drug (Gupta et al., 2015).

Another study used amphotericin B in an alginate-capped lipid nanocarrier (Alg-Lip-nano) for leishmaniasis treatment (Singodia et al., 2011). *In vitro* results demonstrated that the percentage of parasite inhibition (intramacrophagic amastigotes) of Alg-Lip-nano (58%) was significantly higher compared to Lip-nano without alginate (48%) ($p \leq 0.05$). This supports the authors hypothesis that alginate coating over lipid particles activates macrophages to release pro-inflammatory cytokines, which synergistically act with amphotericin B and can potentially increase the cure rate in visceral leishmaniasis (Singodia et al., 2011).

Some work has also been carried out with the polyene agent nystatin. This compound is recommended only for topical administration due to its high toxicity. Martín-Villena et al. (2013) obtained alginate microparticles containing nystatin through the emulsification/internal gelation method with an

**TABLE 2 | Examples of alginate-based delivery systems for non-conventional antifungals.**

| Types of materials incorporated | | Carrier | Reference |
|---|---|---|---|
| Essential oils | Turmeric | chitosan-alginate nanocapsules | Lertsutthiwong and Rojsitthisak, 2011 |
| | Turmeric | Alginate nanocapsules | Lertsutthiwong et al., 2008 |
| | *Satureja hortensi* | Alginate microparticles | Hosseini et al., 2013 |
| | Elicriso italic, chamomile blue, cinnamon, lavender, tea tree, peppermint, eucalyptus, lemongrass, and lemon | Alginate films | Liakos et al., 2014 |
| | Clove, thyme, and cinnamon | Alginate microspheres | Soliman et al., 2013 |
| | Anise | Alginate gel | Gafiţanu et al., 2016 |
| Antiseptics | Chlorhexidine diacetate | Alginate and alginate/chitosan films | Juliano et al., 2008 |
| | Povidone iodine | Alginate beads and films | Liakos et al., 2013 |
| Pomegranate extract | | Alginate microparticles | Endo et al., 2012 |
| Lactoferrin | | Alginate tablets | Kuipers et al., 2002 |
| Silver | | Alginate as a stabilizer silver nanoparticles | Kubyshkin et al., 2016 |
| | | Cellulose/sodium alginate films | Shao et al., 2015 |

encapsulation efficiency of 80% for treatment of *Candida* vaginitis. After *ex vivo* permeation studies through porcine vaginal mucosa, determination of the amount of nystatin retained and antifungal activity assays, the authors inferred that the developed microparticulate system was efficacious against *C. albicans* without systemic absorption of toxic concentrations of the drug (Martín-Villena et al., 2013). More specifically, the formulation was able to adhere to the vaginal mucosa showing potential for safe treatment of localized infection. Nystatin release from microcapsules followed a concentration gradient pattern based on the first Fick's law (release rate constant: 1.60 $h^{-1}$) offering sustained release (Martín-Villena et al., 2013). Moreover, nystatin-loaded microparticles exhibited a clear inhibition effect on the *C. albicans* growth (Martín-Villena et al., 2013).

Alginate microspheres containing nystatin demonstrated ability to control *Candida* infection in the oral cavity of pigs without causing damage to the oral tissue and systemic nystatin absorption (Martín et al., 2015). Another study for treatment of oral candidiasis showed an improved nystatin effectiveness using beads, micro- and nanoparticles of alginate incorporated in toothpaste instead of free drug in suspension form (Reis et al., 2015). This study demonstrated that microparticles were the most suitable particulate system of nystatin showing the slowest release (complete release within 3 h for beads, 24 h for nanoparticles, and 48 h for microparticles), the highest inhibitory effect on *C. albicans* (MIC value of 13.5 μg/mL for beads, 38 μg/mL for nanoparticles, and 5.21 μg/mL for microparticles) and a high antifungal efficiency over time (1 year of evaluation) (Reis et al., 2015).

## ALGINATE-BASED DELIVERY SYSTEMS FOR NON-CONVENTIONAL ANTIFUNGALS

Alginate formulations have been used as delivery systems for other molecules with antifungal activity potential, such as essential oils, antiseptics, and others (**Table 2**).

Turmeric oil from the rhizome of *Curcuma longa* is an example of an essential oil encapsulated in alginate-based carriers. Turmeric oil is widely used as a food additive, condiment and household medicine in Southern Asia, and presents several pharmacological properties as an antibacterial, an antifungal, an antioxidant, an antimutagenic, and a repellent (Lertsutthiwong et al., 2008). Lertsutthiwong et al. (2008) encapsulated this oil in alginate nanocapsules, while Lertsutthiwong and Rojsitthisak (2011) produced chitosan-alginate nanocapsules containing turmeric oil. Chitosan-alginate nanocapsules increased the skin permeation of turmeric oil compared with an ethanolic solution (Lertsutthiwong and Rojsitthisak, 2011), representing a new approach for topical delivery and treatment of cutaneous infections (Lertsutthiwong and Rojsitthisak, 2011). These studies also demonstrated that alginate is an effective biopolymer for encapsulation of a volatile essential oil, producing nanocarriers with long-term physical stability (120 days) when stored at 4°C.

Hosseini et al. (2013) encapsulated *Satureja hortensis* essential oil (known for its antimicrobial and antioxidant activity) in alginate microparticles, and concluded that these microparticles could be used for antioxidant and antimicrobial purposes with controlled release properties in the food and nutraceuticals industries. Other essential oils, such as elicriso italic, chamomile

blue, cinnamon, lavender, tea tree, peppermint, eucalyptus, lemongrass, and lemon were dispersed in sodium alginate films and presented remarkable antibacterial and antifungal activities (Liakos et al., 2014). These alginate films enriched with essential oils should find multiple applications, including as disposable wound dressings, in food packaging, medical device protection and disinfection, and indoor air quality improvement materials (Liakos et al., 2014).

Soliman et al. (2013) encapsulated clove, thyme and cinnamon oils in alginate microspheres in order to achieve their optimal antifungal activity against two of mycotoxigenic fungi species, *Aspergillus niger* and *Fusarium verticillioides*, and prevent fungal contamination in stored grains. These microspheres showed antifungal activity in addition to increasing the storage time of oil with antifungal activity for up to 8 days, while the free oil lost activity within 2 days. Thus, the main advantage of encapsulation was to reduce the rate of evaporation of these essential oils prolonging antifungal activity (Soliman et al., 2013).

Plant extracts have also been incorporated in alginate-based nanocarriers. The anise crude extracts and active compounds manifest antimicrobial, antioxidant, insecticidal, analgesic, sedative, and convulsive activities (Wang et al., 2011). Anise-based bioadhesive alginate gels for vaginal application showed antibacterial activity, and no effect against *Candida* species was observed (Gafiţanu et al., 2016). Alginate microparticles containing pomegranate extract (*Punica granatum*) with encapsulation efficiency of 81.9% (Endo et al., 2012) displayed antifungal activity against *C. albicans* (minimum inhibitory concentration of 3.9 μg/ml), with the advantage of providing controlled extract release to achieve the desired therapeutic effect against oral fungal infection caused by *C. albicans* (Endo et al., 2012).

Sodium alginate tablets containing lactoferrin, a potential antifungal candidate for candidiasis treatment, displayed release-controlling and mucoadhesive properties (Kuipers et al., 2002). *In vitro* microbiological studies demonstrated that the formulation had the same antifungal properties as the free lactoferrin against several clinical isolates of *C. albicans* and *Candida glabrata* (Kuipers et al., 2002). The tablets (250 mg lactoferrin) on oral mucosa of human volunteers were able to keep the lactoferrin concentration in the saliva for at least 2 h, suggesting that they might improve the therapeutic efficacy of lactoferrin in oral candidiasis treatment (Kuipers et al., 2002).

Research showed that the use of sodium alginate as a stabilizer provided a highly stable solution of silver nanoparticles (nanosilver) that has significant antibacterial and antifungal activity. The nanosilver aqueous solution at concentrations of 0.0005–0.005% with sodium alginate completely inhibited *C. albicans* viability within 24 h (Kubyshkin et al., 2016). Shao et al. (2015) developed silver sulfadiazine-loaded cellulose/sodium alginate films and observed that these films had excellent antibacterial performances on *E. coli* and *S. aureus* and antifungal activity on *C. albicans*. They also showed good biocompatibility and accepted cytotoxicity (less than 20% using 0.1% of silver sulfadiazine). The authors suggested that these films containing silver sulfadiazine could be a potential antimicrobial for use in wound dressings.

Antiseptics have also been incorporated in alginate carriers for controlled release (Juliano et al., 2008; Liakos et al., 2013). Films of sodium alginate or sodium alginate/chitosan were well tolerated, and able to sustain the release of chlorhexidine diacetate, providing active concentrations against *C. albicans* for prolonged periods of time (approximately 3 h) on the buccal mucosa of human volunteers, which is in agreement with results showing *in vitro* mucoadhesion (Juliano et al., 2008). Another antiseptic incorporated in alginate beads and films was povidone iodine (PVPI) (Liakos et al., 2013). Controlled release of PVPI was possible when the composite films and beads were brought into direct contact with aqueous media, maintaining the bactericidal and fungicidal properties. This characteristic is highly desired in clinical applications to avoid toxic doses of PVPI (Liakos et al., 2013). A wide variety of applications of these systems are envisioned, such as wound dressings, hygienic and protective packaging films for medical devices, and polymer beads as water disinfectants (Liakos et al., 2013).

## CONCLUDING REMARKS

Alginate is a natural polymer widely used for obtainment of drug delivery systems due to its non-toxicity, biodegradability, biocompatibility, low cost, mucoadhesive, and non-immunogenic properties, in addition to the availability of simple protocols for production of these systems. In spite of the popularity of alginate-based carriers in the drug delivery field, few studies have been conducted with antifungals, mostly dealing with azoles and polyenes. Thus, there is a gap when it comes to the advantages and limitations of alginate-based carriers for other types of antifungal agents. To the best of our knowledge, this review is the first to directly focus on alginate carriers for antifungal drugs. Based on the studies discussed here, alginate-based antifungal delivery systems have shown great potential in the treatment of fungal infections, providing modified release, and decreasing administration frequency, toxicity and the dose necessary for antifungal efficacy. Therefore, the use of alginate-based carriers represents a promising approach for delivery of antifungal agents to improve the treatment protocols for cutaneous and systemic mycosis.

## AUTHOR CONTRIBUTIONS

CS did the literature review and wrote the manuscript. KI and LL designed and co-wrote the manuscript.

## ACKNOWLEDGMENT

This work was supported by the Fundação de Amparo a Pesquisa do Estado de São Paulo (FAPESP, 2015/07993-0 and 2013/16617-7) and Coordenação de Aperfeiçoamento de Pessoal de Nível Superior (CAPES).

## REFERENCES


Ahmad, Z., Sharma, S., and Khuller, G. K. (2006). The potential of azole antifungals against latent/persistent tuberculosis. *FEMS Microbiol. Lett.* 258, 200–203. doi: 10.1111/j.1574-6968.2006.00224.x

Ahmad, Z., Sharma, S., and Khuller, G. K. (2007). Chemotherapeutic evaluation of alginate nanoparticle-encapsulated azole antifungal and antitubercular drugs against murine tuberculosis. *Nanomedicine* 3, 239–243. doi: 10.1016/j.nano.2007.05.001

Al-Kassas, R., Wen, J., Cheng, A. E.-M., Kim, A. M.-J., Liu, S. S. M., and Yu, J. (2016). Transdermal delivery of propranolol hydrochloride through chitosan nanoparticles dispersed in mucoadhesive gel. *Carbohydr. Polym.* 153, 176–186. doi: 10.1016/j.carbpol.2016.06.096

Barrett, J. P., Vardulaki, K. A., Conlon, C., Cooke, J., Daza-Ramirez, P., Evans, E. G. V., et al. (2003). A systematic review of the antifungal effectiveness and tolerability of amphotericin B formulations. *Clin. Ther.* 25, 1295–1320. doi: 10.1016/S0149-2918(03)80125-X

Bibette, J., and Leal-Calderon, F. (1996). Surfactant-stabilized emulsions. *Curr. Opin. Colloid Interface Sci.* 1, 746–751. doi: 10.1016/S1359-0294(96)80076-8

Braccini, I., and Pérez, S. (2001). Molecular basis of $Ca^{2+}$-induced gelation in alginates and pectins: the egg-box model revisited. *Biomacromolecules* 2, 1089–1096. doi: 10.1021/bm010008g

Brown, G. D., Denning, D. W., Gow, N. A. R., Levitz, S. M., Netea, M. G., and White, T. C. (2012). Hidden killers: human fungal infections. *Sci. Transl. Med.* 4, 1–9. doi: 10.1126/scitranslmed.3004404

Cardoso, M. J., Costa, R. R., and Mano, J. F. (2016). Marine origin polysaccharides in drug delivery systems. *Mar. Drugs* 14, 34. doi: 10.3390/md14020034

Chen, S. C. A., Slavin, M. A., and Sorrell, T. C. (2011). Echinocandin antifungal drugs in fungal infections: a comparison. *Drugs* 71, 11–41. doi: 10.2165/11585270-000000000-00000

Cossu, A., Wang, M. S., Chaudhari, A., and Nitin, N. (2015). Antifungal activity against *Candida albicans* of starch Pickering emulsion with thymol or amphotericin B in suspension and calcium alginate films. *Int. J. Pharm.* 493, 233–242. doi: 10.1016/j.ijpharm.2015.07.065

Davoudi, S., Graviss, L. S., and Kontoyiannis, D. P. (2015). Healthcare-associated outbreaks due to Mucorales and other uncommon fungi. *Eur. J. Clin. Invest.* 45, 767–773. doi: 10.1111/eci.12467

Debele, T. A., Mekuria, S. L., and Tsai, H.-C. (2016). Polysaccharide based nanogels in the drug delivery system: application as the carrier of pharmaceutical agents. *Mater. Sci. Eng. C Mater. Biol. Appl.* 68, 964–981. doi: 10.1016/j.msec.2016.05.121

Denning, D. W., and Bromley, M. J. (2015). How to bolster the antifungal pipeline. *Science* 347, 1414–1416. doi: 10.1126/science.aaa6097

Draget, K., Smidsrød, O., and Skjåk-Bræk, G. (2005). Alginates from algae. *Biopolymers* 6, 1–30. doi: 10.1002/3527600035.bpol6008

Elsayed, M., Huang, J., and Edirisinghe, M. (2015). Bioinspired preparation of alginate nanoparticles using microbubble bursting. *Mater. Sci. Eng. C Mater. Biol. Appl.* 46, 132–139. doi: 10.1016/j.msec.2014.09.036

Endo, E. H., Ueda-Nakamura, T., Nakamura, C. V., and Dias-Filho, B. P. (2012). Activity of spray-dried microparticles containing pomegranate peel extract against *Candida albicans*. *Molecules* 17, 10094–10107. doi: 10.3390/molecules170910094

Falci, D. R., Da Rosa, F. B., and Pasqualotto, A. C. (2015). Comparison of nephrotoxicity associated to different lipid formulations of amphotericin B: a real-life study. *Mycoses* 58, 104–112. doi: 10.1111/myc.12283

Fromtling, R. A. (1988). Overview of medically important antifungal azole derivatives. *Clin. Microbiol. Rev.* 1, 187–217. doi: 10.1128/CMR.1.2.187. Updated

Gaffi – Global Action Fund for Fungal Infections (2016). *Gaffi – Global Action Fund for Fungal Infections*. Available at: http://www.gaffi.org/

Gafiţanu, C. A., Filip, D., Cernătescu, C., Ibănescu, C., Danu, M., Pâslaru, E., et al. (2016). Formulation and evaluation of anise-based bioadhesive vaginal gels. *Biomed. Pharmacother.* 83, 485–495. doi: 10.1016/j.biopha.2016.06.053

Gainza, G., Aguirre, J. J., Pedraz, J. L., Hernández, R. M., and Igartua, M. (2013). RhEGF-loaded PLGA-Alginate microspheres enhance the healing of full-thickness excisional wounds in diabetised Wistar rats. *Eur. J. Pharm. Sci.* 50, 243–252. doi: 10.1016/j.ejps.2013.07.003

Gallovic, M. D., Schully, K. L., Bell, M. G., Elberson, M. A., Palmer, J. R., Darko, C. A., et al. (2016). Acetalated dextran microparticulate vaccine formulated via coaxial electrospray preserves toxin neutralization and enhances murine survival following inhalational *Bacillus anthracis* exposure. *Adv. Healthc. Mater.* 5, 2617–2627. doi: 10.1002/adhm.201600642

Gaudana, R., Jwala, J., Boddu, S. H. S., and Mitra, A. K. (2009). Recent perspectives in ocular drug delivery. *Pharm. Res.* 26, 1197–1216. doi: 10.1007/s11095-008-9694-0

Goh, C. H., Heng, P. W. S., and Chan, L. W. (2012). Alginates as a useful natural polymer for microencapsulation and therapeutic applications. *Carbohydr. Polym.* 88, 1–12. doi: 10.1016/j.carbpol.2011.11.012

Gupta, P. K., Jaiswal, A. K., Asthana, S., Verma, A., Kumar, V., Shukla, P., et al. (2015). Self assembled ionically sodium alginate cross-linked amphotericin B encapsulated glycol chitosan stearate nanoparticles: applicability in better chemotherapy and non-toxic delivery in visceral leishmaniasis. *Pharm. Res.* 32, 1727–1740. doi: 10.1007/s11095-014-1571-4

Hamidi, M., Azadi, A., and Rafiei, P. (2008). Hydrogel nanoparticles in drug delivery. *Adv. Drug Deliv. Rev.* 60, 1638–1649. doi: 10.1016/j.addr.2008.08.002

Hamill, R. J. (2013). Amphotericin B formulations: a comparative review of efficacy and toxicity. *Drugs* 73, 919–934. doi: 10.1007/s40265-013-0069-4

Han, F. Y., Thurecht, K. J., Whittaker, A. K., and Smith, M. T. (2016). Bioerodable PLGA-based microparticles for producing sustained-release drug formulations and strategies for improving drug loading. *Front. Pharmacol.* 7:185. doi: 10.3389/fphar.2016.00185

Hosseini, S. M., Hosseini, H., Mohammadifar, M. A., Mortazavian, A. M., Mohammadi, A., Khosravi-Darani, K., et al. (2013). Incorporation of essential oil in alginate microparticles by multiple emulsion/ionic gelation process. *Int. J. Biol. Macromol.* 62, 582–588. doi: 10.1016/j.ijbiomac.2013.09.054

Hussain, A., and Ahsan, F. (2005). The vagina as a route for systemic drug delivery. *J. Control. Release* 103, 301–313. doi: 10.1016/j.jconrel.2004.11.034

Islam, N., and Ferro, V. (2016). Recent advances in chitosan-based nanoparticulate pulmonary drug delivery. *Nanoscale* 8, 14341–14358. doi: 10.1039/C6NR03256G

Jeevanandam, J., Chan, Y. S., and Danquah, M. K. (2016). Nano-formulations of drugs: recent developments, impact and challenges. *Biochimie* 128-129, 99–112. doi: 10.1016/j.biochi.2016.07.008

Juliano, C., Cossu, M., Pigozzi, P., Rassu, G., and Giunchedi, P. (2008). Preparation, in vitro characterization and preliminary in vivo evaluation of buccal polymeric films containing chlorhexidine. *AAPS PharmSciTech* 9, 1153–1158. doi: 10.1208/s12249-008-9153-6

Karkowska-Kuleta, J., Rapala-Kozik, M., and Kozik, A. (2009). Fungi pathogenic to humans: Molecular bases of virulence of *Candida albicans*, *Cryptococcus neoformans* and *Aspergillus fumigatus*. *Acta Biochim. Pol.* 56, 211–224.

Kathiravan, M. K., Salake, A. B., Chothe, A. S., Dudhe, P. B., Watode, R. P., Mukta, M. S., et al. (2012). The biology and chemistry of antifungal agents: a review. *Bioorg. Med. Chem.* 20, 5678–5698. doi: 10.1016/j.bmc.2012.04.045

Kubyshkin, A., Chegodar, D., Katsev, A., Petrosyan, A., Krivorutchenko, Y., and Postnikova, O. (2016). Antimicrobial effects of silver nanoparticles stabilized in solution by sodium alginate. *Biochem. Mol. Biol. J.* 2:13. doi10.21767/2471-8084.100022

Kuipers, M. E., Heegsma, J., Bakker, H. I., Meijer, D. K. F., Swart, P. J., Frijlink, E. W., et al. (2002). Design and fungicidal activity of mucoadhesive lactoferrin tablets for the treatment of oropharyngeal candidosis. *Drug Deliv.* 9, 31–38. doi: 10.1080/107175402753413154

Kumar, A., Chen, F., Mozhi, A., Zhang, X., Zhao, Y., Xue, X., et al. (2013). Innovative pharmaceutical development based on unique properties of nanoscale delivery formulation. *Nanoscale* 5, 8307–8325. doi: 10.1039/c3nr01525d

Lee, K. Y., and Mooney, D. J. (2012). Alginate: properties and biomedical applications. *Prog. Polym. Sci.* 37, 106–126. doi: 10.1016/j.progpolymsci.2011.06.003

Lertsutthiwong, P., Noomun, K., Jongaroonngamsang, N., Rojsitthisak, P., and Nimmannit, U. (2008). Preparation of alginate nanocapsules containing turmeric oil. *Carbohydr. Polym.* 74, 209–214. doi: 10.1016/j.carbpol.2008.02.009

Lertsutthiwong, P., and Rojsitthisak, P. (2011). Chitosan-alginate nanocapsules for encapsulation of turmeric oil. *Pharmazie* 66, 911–915. doi: 10.1691/ph.2011.1068

Liakos, I., Rizzello, L., Bayer, I. S., Pompa, P. P., Cingolani, R., and Athanassiou, A. (2013). Controlled antiseptic release by alginate polymer films and beads. *Carbohydr. Polym.* 92, 176–183. doi: 10.1016/j.carbpol.2012.09.034

Liakos, I., Rizzello, L., Scurr, D. J., Pompa, P. P., Bayer, I. S., and Athanassiou, A. (2014). All-natural composite wound dressing films of essential oils encapsulated in sodium alginate with antimicrobial properties. *Int. J. Pharm.* 463, 137–145. doi: 10.1016/j.ijpharm.2013.10.046

Lopes, M., Abrahim, B., Veiga, F., Seiça, R., Cabral, L. M., Arnaud, P., et al. (2016). Preparation methods and applications behind alginate-based particles. *Expert Opin. Drug Deliv.* 5247, 1–14. doi: 10.1080/17425247.2016.1214564

Mahor, A., Prajapati, S. K., Verma, A., Gupta, R., Iyer, A. K., and Kesharwani, P. (2016). Moxifloxacin loaded gelatin nanoparticles for ocular delivery: formulation and in-vitro, in-vivo evaluation. *J. Colloid Interface Sci.* 483, 132–138. doi: 10.1016/j.jcis.2016.08.018

Maiti, S., Dey, P., Kaity, S., Ray, S., Maji, S., and Sa, B. (2009). Investigation on processing variables for the preparation of fluconazole-loaded ethyl cellulose microspheres by modified multiple emulsion technique. *AAPS PharmSciTech* 10, 703–715. doi: 10.1208/s12249-009-9257-7

Martín, M. J., Calpena, A. C., Fernández, F., Mallandrich, M., Gálvez, P., and Clares, B. (2015). Development of alginate microspheres as nystatin carriers for oral mucosa drug delivery. *Carbohydr. Polym.* 117, 140–149. doi: 10.1016/j.carbpol.2014.09.032

Martinez, R. (2006). An update on the use of antifungal agents. *J. Bras. Pneumol.* 32, 449–460. doi: 10.1590/S1806-37132006000500013

Martín-Villena, M. J., Fernández-Campos, F., Calpena-Campmany, A. C., Bozal-De Febrer, N., Ruiz-Martínez, M. A., and Clares-Naveros, B. (2013). Novel microparticulate systems for the vaginal delivery of nystatin: development and characterization. *Carbohydr. Polym.* 94, 1–11. doi: 10.1016/j.carbpol.2013.01.005

Mishra, R., Joshi, P., and Mehta, T. (2016). Formulation, development and characterization of mucoadhesive film for treatment of vaginal candidiasis. *Int. J. Pharm. Investig.* 6, 47–55. doi: 10.4103/2230-973X.176487

Mohammed, F. A., and Khedr, H. (2003). Preparation and in vitro/in vivo evaluation of the buccal bioadhesive properties of slow-release tablets containing miconazole nitrate. *Drug Dev. Ind. Pharm.* 29, 321–337. doi: 10.1081/DDC-120018206

Ostrosky-Zeichner, L., Casadevall, A., Galgiani, J. N., Odds, F. C., and Rex, J. H. (2010). An insight into the antifungal pipeline: selected new molecules and beyond. *Nat. Rev. Drug Discov.* 9, 719–727. doi: 10.1038/nrd3074

Pandey, R., Ahmad, Z., Sharma, S., and Khuller, G. K. (2005). Nano-encapsulation of azole antifungals: potential applications to improve oral drug delivery. *Int. J. Pharm.* 301, 268–276. doi: 10.1016/j.ijpharm.2005.05.027

Paques, J. P., Van der Linden, E., Van Rijn, C. J. M., and Sagis, L. M. C. (2013). Alginate submicron beads prepared through w/o emulsification and gelation with CaCl2 nanoparticles. *Food Hydrocoll.* 31, 428–434. doi: 10.1016/j.foodhyd.2012.11.012

Paques, J. P., Van Der Linden, E., Van Rijn, C. J. M., and Sagis, L. M. C. (2014). Preparation methods of alginate nanoparticles. *Adv. Colloid Interface Sci.* 209, 163–171. doi: 10.1016/j.cis.2014.03.009

Patel, S. K., Shah, D. R., and Tiwari, S. (2015). Bioadhesive films containing fluconazole for mucocutaneous candidiasis. *Indian J. Pharm. Sci.* 77, 55–61. doi: 10.4103/0250-474X.151601

Pawar, P., Kashyap, H., Malhotra, S., and Sindhu, R. (2013). Hp-β-CD-voriconazole in situ gelling system for ocular drug delivery: in vitro, stability, and antifungal activities assessment. *Biomed Res. Int.* 2013:341218. doi: 10.1155/2013/341218

Pawar, S. N., and Edgar, K. J. (2012). Alginate derivatization: a review of chemistry, properties and applications. *Biomaterials* 33, 3279–3305. doi: 10.1016/j.biomaterials.2012.01.007

Peyton, L. R., Gallagher, S., and Hashemzadeh, M. (2015). Triazole antifungals: a review. *Drugs Today.* 51, 705–718. doi: 10.1358/dot.2015.51.12.2421058

Pfaller, M. A. (2012). Antifungal drug resistance: mechanisms, epidemiology, and consequences for treatment. *Am. J. Med.* 125, S3–S13. doi: 10.1016/j.amjmed.2011.11.001

Pillai, V., Kanicky, J., and Shah, D. (1999). "Application of microemulsions in enhanced oil recovery," in *Handbook of Microemulsion Science and Technology*, eds P. Kumar and K. L. Mittial (New York, NY: Marcel Dekker), 13–440.

Qin, Y. (2008). Alginate fibers: an overwiew of the production processes and applications in wound management. *Polym. Int.* 57, 171–180. doi: 10.1002/pi.2296

Reis, C. P., Roque, L. V., Baptista, M., and Rijo, P. (2015). Innovative formulation of nystatin particulate systems in toothpaste for candidiasis treatment. *Pharm. Dev. Technol.* 7450, 1–6. doi: 10.3109/10837450.2014.999783

Remminghorst, U., and Rehm, B. H. A. (2006). Bacterial alginates: from biosynthesis to applications. *Biotechnol. Lett.* 28, 1701–1712. doi: 10.1007/s10529-006-9156-x

Roilides, E. (2016). Emerging fungi causing human infection: new or better identified? *Clin. Microbiol. Infect.* 22, 660–661. doi: 10.1016/j.cmi.2016.07.023

Sangeetha, S., Venkatesh, D. N., Adhiyaman, R., Santhi, K., and Suresh, B. (2007). Formulation of sodium alginate nanospheres containing amphotericin B for the treatment of systemic candidiasis. *Trop. J. Pharm. Res.* 6, 653–659. doi: 10.4314/tjpr.v6i1.14643

Seneviratne, C. J., and Rosa, E. A. R. (2016). Editorial: antifungal drug discovery: new theories and new therapies. *Front. Microbiol.* 7:728. doi: 10.3389/fmicb.2016.00728

Shao, W., Liu, H., Liu, X., Wang, S., Wu, J., Zhang, R., et al. (2015). Development of silver sulfadiazine loaded bacterial cellulose/sodium alginate composite films with enhanced antibacterial property. *Carbohydr. Polym.* 132, 351–358. doi: 10.1016/j.carbpol.2015.06.057

Singodia, D., Khare, P., Dube, A., Talegaonkar, S., Khar, R. K., and Mishra, P. R. (2011). Development and performance evaluation of alginate-capped amphotericin B lipid nanoconstructs against visceral leishmaniasis. *J. Biomed. Nanotechnol.* 7, 123–124. doi: 10.1166/jbn.2011.1232

Soliman, E. A., El-Moghazy, A. Y., El-Din, M. S. M., and Massoud, M. A. (2013). Microencapsulation of essential oils within alginate: formulation and in vitro evaluation of antifungal activity. *J. Encapsulation Adsorpt. Sci.* 3, 48–55. doi: 10.4236/jeas.2013.31006

Song, H., Yu, W., Gao, M., Liu, X., and Ma, X. (2013). Microencapsulated probiotics using emulsification technique coupled with internal or external gelation process. *Carbohydr. Polym.* 96, 181–189. doi: 10.1016/j.carbpol.2013.03.068

Sosnik, A. (2014). Alginate particles as platform for drug delivery by the oral route: state-of-the-art. *ISRN Pharm.* 2014, 1–17. doi: 10.1155/2014/926157

Sundar, S., Kundu, J., and Kundu, S. C. (2010). Biopolymeric nanoparticles. *Sci. Technol. Adv. Mater.* 11:014104. doi: 10.1088/1468-6996/11/1/014104

Thomas, N., Thorn, C., Richter, K., Thierry, B., Prestidge, C., Bjarnsholt, T., et al. (2016). Efficacy of poly-lactic-co-glycolic acid micro- and nanoparticles of ciprofloxacin against bacterial biofilms. *J. Pharm. Sci.* 105, 3115–3122. doi: 10.1016/j.xphs.2016.06.022

Tiphine, M., Letscher-Bru, V., and Herbrecht, R. (1999). Amphotericin B and its new formulations: pharmacologic characteristics, clinical efficacy, and tolerability. *Transpl. Infect. Dis.* 1, 273–283. doi: 10.1034/j.1399-3062.1999.010406.x

Tønnesen, H. H., and Karlsen, J. (2002). Alginate in drug delivery systems. *Drug Dev. Ind. Pharm.* 28, 621–630. doi: 10.1081/DDC-120003853

Tyler, B., Gullotti, D., Mangraviti, A., Utsuki, T., and Brem, H. (2016). Polylactic acid (PLA) controlled delivery carriers for biomedical applications. *Adv. Drug Deliv. Rev.* 107, 163–175. doi: 10.1016/j.addr.2016.06.018

Van Vlerken, L. E., Vyas, T. K., and Amiji, M. M. (2007). Poly(ethylene glycol)-modified nanocarriers for tumor-targeted and intracellular delivery. *Pharm. Res.* 24, 1405–1414. doi: 10.1007/s11095-007-9284-6

Voltan, A. R., Quindós, G., Alarcón, K. P. M., Fusco-almeida, A. M., Mendes-Gianvini, M. J. S., and Fusco-almeida, A. M. (2016). Fungal diseases: could nanostructured drug delivery systems be a novel paradigm for therapy? *Int. J. Nanomedicine* 11, 3715–3730. doi: 10.2147/IJN.S93105

Wade, R. L., Chaudhari, P., Natoli, J. L., Taylor, R. J., Nathanson, B. H., and Horn, D. (2013). Comparison of adverse events and hospital length of stay associated with various amphotericin B formulations: sequential conventional amphotericin b/lipid versus lipid-only therapy for the treatment of invasive fungal infections in hospitalized patients. *P T* 38, 278–287.

Wang, G. W., Hu, W. T., Huang, B. K., and Qin, L. P. (2011). Illicium verum: a review on its botany, traditional use, chemistry and pharmacology. *J. Ethnopharmacol.* 136, 10–20. doi: 10.1016/j.jep.2011.04.051

Yang, W., Wiederhold, N. P., and Williams, R. O. (2008). Drug delivery strategies for improved azole antifungal action. *Expert Opin. Drug Deliv.* 5, 1199–1216. doi: 10.1517/17425240802457188

Yehia, S. A., El-Gazayerly, O. N., and Basalious, E. B. (2008). Design and in vitro/in vivo evaluation of novel mucoadhesive buccal discs of an antifungal drug: relationship between swelling, erosion, and drug release. *AAPS PharmSciTech* 9, 1207–1217. doi: 10.1208/s12249-008-9166-1

Yehia, S. A., El-Gazayerly, O. N., and Basalious, E. B. (2009). Fluconazole mucoadhesive buccal films: in vitro/in vivo performance. *Curr. Drug Deliv.* 6, 17–27. doi: 10.2174/156720109787048195

Zotchev, S. B. (2003). Polyene macrolide antibiotics and their applications in human therapy. *Curr. Med. Chem.* 10, 211–223. doi: 10.2174/0929867033368448

**Conflict of Interest Statement:** The authors declare that the research was conducted in the absence of any commercial or financial relationships that could be construed as a potential conflict of interest.

frontiers in Microbiology

ORIGINAL RESEARCH
published: 28 March 2017
doi: 10.3389/fmicb.2017.00535

# The Anti-helminthic Compound Mebendazole Has Multiple Antifungal Effects against *Cryptococcus neoformans*

*Luna S. Joffe[1], Rafael Schneider[2], William Lopes[2], Renata Azevedo[3], Charley C. Staats[2,4], Lívia Kmetzsch[2,4], Augusto Schrank[2,4], Maurizio Del Poeta[5,6], Marilene H. Vainstein[2,4] and Marcio L. Rodrigues[1,3]**

[1] Laboratório de Biologia Celular de Leveduras Patogênicas, Instituto de Microbiologia Paulo de Góes, Universidade Federal do Rio de Janeiro, Rio de Janeiro, Brazil, [2] Centro de Biotecnologia, Universidade Federal do Rio Grande do Sul, Porto Alegre, Brazil, [3] Fundação Oswaldo Cruz – Fiocruz, Centro de Desenvolvimento Tecnológico em Saúde, Rio de Janeiro, Brazil, [4] Departamento de Biologia Molecular e Biotecnologia, Universidade Federal do Rio Grande do Sul, Porto Alegre, Brazil, [5] Veterans Administration Medical Center, Northport, NY, USA, [6] Department of Molecular Genetics and Microbiology, Stony Brook University, Stony Brook, NY, USA

OPEN ACCESS

**Edited by:**
*Carlos Pelleschi Taborda, University of São Paulo, Brazil*

**Reviewed by:**
*Attila Gacser, University of Szeged, Hungary*
*João Nobrega De Almeida Júnior, Hospital das Clínicas da Faculdade de Medicina da Universidade de São Paulo, Brazil*

***Correspondence:**
*Marcio L. Rodrigues*
*marciolr@cdts.fiocruz.br*

**Specialty section:**
*This article was submitted to Fungi and Their Interactions, a section of the journal Frontiers in Microbiology*

**Received:** *05 November 2016*
**Accepted:** *14 March 2017*
**Published:** *28 March 2017*

**Citation:**
*Joffe LS, Schneider R, Lopes W, Azevedo R, Staats CC, Kmetzsch L, Schrank A, Del Poeta M, Vainstein MH and Rodrigues ML (2017) The Anti-helminthic Compound Mebendazole Has Multiple Antifungal Effects against Cryptococcus neoformans. Front. Microbiol. 8:535. doi: 10.3389/fmicb.2017.00535*

*Cryptococcus neoformans* is the most lethal pathogen of the central nervous system. The gold standard treatment of cryptococcosis, a combination of amphotericin B with 5-fluorocytosine, involves broad toxicity, high costs, low efficacy, and limited worldwide availability. Although the need for new antifungals is clear, drug research and development (R&D) is costly and time-consuming. Thus, drug repurposing is an alternative to R&D and to the currently available tools for treating fungal diseases. Here we screened a collection of compounds approved for use in humans seeking for those with anti-cryptococcal activity. We found that benzimidazoles consist of a broad class of chemicals inhibiting *C. neoformans* growth. Mebendazole and fenbendazole were the most efficient antifungals showing *in vitro* fungicidal activity. Since previous studies showed that mebendazole reaches the brain in biologically active concentrations, this compound was selected for further studies. Mebendazole showed antifungal activity against phagocytized *C. neoformans,* affected cryptococcal biofilms profoundly and caused marked morphological alterations in *C. neoformans*, including reduction of capsular dimensions. Amphotericin B and mebendazole had additive anti-cryptococcal effects. Mebendazole was also active against the *C. neoformans* sibling species, *C. gattii*. To further characterize the effects of the drug a random *C. gattii* mutant library was screened and indicated that the antifungal activity of mebendazole requires previously unknown cryptococcal targets. Our results indicate that mebendazole is as a promising prototype for the future development of anti-cryptococcal drugs.

**Keywords: *Cryptococcus neoformans*, benzimidazoles, mebendazole, antifungal, biofilm, antifungal targets, macrophages**

## INTRODUCTION

*Cryptococcus neoformans* is a yeast-like pathogen that causes expressive brain damage in immunosuppressed individuals (Colombo and Rodrigues, 2015). The fungus reaches the lungs of humans after inhalation of environmental cells. In the immunosuppressed host, *C. neoformans* efficiently disseminates to the brain and causes meningitis (Kwon-Chung et al., 2014). Cryptococcal meningitis is a global problem resulting in thousands of deaths annually (Park et al., 2009). Most cases occur among people with HIV/AIDS. Poor and late diagnosis, limited access to antifungals and drug resistance are directly associated to the high fatality rate of cryptococcosis, especially in developing countries (Rodrigues, 2016).

The standard antifungal regimen for cryptococcal meningitis is a combination of amphotericin B with 5-fluorocytosine (Krysan, 2015). Amphotericin B is nephrotoxic and is intravenously administered (Sloan et al., 2009; Micallef et al., 2015), which demands considerable medical infrastructure. A 15-day intravenous treatment with liposomal amphotericin B is estimated to cost from €10.000 to €20.000 in Europe (Ostermann et al., 2014) and 5-fluorocytosine is not widely available outside rich areas (Krysan, 2015). As an alternative, fluconazole is frequently used, although it is associated with poorer outcomes and relapses (Sloan et al., 2009). In South Africa, more than 60% of people with culture-positive relapsed disease had fluconazole resistance (Govender et al., 2011). Hence, the need for new anticryptococcal therapies is clear. In this context, a new class of antifungals targeting the synthesis of fungal sphingolipids has been recently described, but its efficacy in humans is still unknown (Mor et al., 2015).

Drug repurposing has emerged as an alternative to the costly and time-consuming processes of drug discovery and development (Nosengo, 2016). In the field of antifungal development, sertraline, an anti-depressive agent, has been reported to be an *in vitro* and *in vivo* fungicidal compound that, in combination with amphotericin B, improves the outcome of cryptococcosis (Zhai et al., 2012; Rhein et al., 2016). Sertraline is now under phase III trial to determine whether adjunctive therapy will lead to improved survival (ClinicalTrials.gov, 2016).

In this manuscript, we aimed at finding anti-cryptococcal activity in a collection of drugs previously approved for use in human diseases. Our results are in agreement with the notion that benzimidazole-like compounds are interesting prototypes for the future development of efficient anti-cryptococcal agents interfering with fungal morphology, biofilm formation, cellular proliferation and intracellular parasitism. This study also supports the hypothesis that the antifungal activity of mebendazole might involve previously unknown cellular targets.

## MATERIALS AND METHODS

### Strains and Growth Conditions

Strains H99 of *C. neoformans* (sorotype A) and R265 of *C. gattii* (sorotype B) were maintained in Sabouraud's agar. For capsule size determination and fluorescence microscopy, fungal cells were cultivated in a minimal medium composed of glucose (15 mM), $MgSO_4$ (10 mM), $KH_2PO_4$ (29.4 mM), glycine (13 mM), and thiamine-HCl (3 μM), pH5.5 for 48 h at 37°C with shaking. The *C. gattii* mutant library was maintained in 96-well plates containing yeast peptone-dextrose (YPD) broth with 30% glycerol at −20°C. The cell line J774.16 (murine macrophages) was maintained in Dulbecco's Modified Eagle Medium (DMEM) supplemented with 10% of Fetal Bovine Serum (FBS), and 1% of penicillin-streptomycin at 37°C in 5% $CO_2$ atmosphere. After four passages in culture medium, the macrophages were plated into 96 well plates for tests of mebendazole intracellular activity.

### Screening for Antifungal Activity in a Compound Collection

The National Institutes of Health (NIH) clinical collection (NCC) was screened for antifungal activity against *C. neoformans*. The NCC consists in a small molecule repository of 727 compounds arrayed in 96-well plates at 10 mM solution in DMSO. These compounds are part of screening library for the NIH Roadmap Molecular Libraries Screening Centers Network (MLSCN) and correspond to a collection of chemically diverse compounds that have been in phase I-III clinical trials. Each compound was first diluted to 1 mM in DMSO and stored at −20°C until use. For initial screening, all compounds were used at 10 μM in 100 μl of RPMI 1640 (two times concentrated) medium buffered with morpholinepropanesulfonic acid (MOPS) at pH 7 containing 2% of glucose, in 96-well plates. Final concentration of DMSO in all samples corresponded to 1%. *C. neoformans* cells ($10^4$) suspended in 100 μl of water were added to each well. The plates were incubated at 37°C with shaking for 48 h. The optical density at 540 nm ($OD_{540}$) was recorded using the FilterMax 5 microplate reader (Molecular Devices, Sunnyvale, CA, USA). Compounds producing values of $OD_{540}$ smaller than 0.05 after fungal growth were selected for further studies. As further detailed in the section "Results," mebendazole was the NCC compound selected for most of the analysis performed in this study.

### Analysis of Antifungal Activity of NCC Compounds

Values of minimum inhibitory concentrations (MICs) were determined using the methods proposed by the European Committee on Antimicrobial Susceptibility Testing (EUCAST) with minor modifications. NCC compounds showing antifungal activity were serially diluted (20 to 0.03 μM) in RPMI 1640 (two times concentrated, pH 7; 2% glucose) buffered with MOPS in 96-well plates. The inocula of *C. neoformans* (strain H99) and *C. gattii* (strain R265) were prepared following the EUCAST protocol (Subcommittee on Antifungal Susceptibility Testing of the EECfAST, 2008; Arendrup et al., 2012). The plates were incubated at 37°C with shaking for 48 h. MIC values corresponded to the lowest compound concentration producing inhibition of fungal growth. For determination of fungicidal activity, *C. neoformans* cells were grown overnight in YPD broth at 30°C, washed in PBS and suspended in RPMI 1640 buffered with MOPS, pH 7. The yeast suspension was adjusted to $2 \times 10^4$ cells per 10 ml of RPMI 1640 (pH

7; 2% glucose) buffered with MOPS and supplemented with 1.25, 0.3125, and 0.078 μM of antifungal compounds. Final concentration of DMSO corresponded to 0.6% in all samples. The samples were then incubated at 37°C in a rotary shaker at 200 rpm. Aliquots were taken at different time points and plated onto YPD agar plates that were incubated at 37°C for 48 h. The numbers of CFU were then counted and recorded. The minimum fungicidal concentration (MFC) was defined as the lowest drug concentration inhibiting CFU formation in at least 90% in comparison to systems containing no antifungals.

## Antifungal Activity of Mebendazole against Intracellular Cryptococci

To assess antifungal activity against intracellular *C. neoformans*, the fungus was first opsonized by incubation (20 min, 37°C, with shaking) in DMEM containing 10% FBS and 10 μg/ml of the 18B7 IgG1, an opsonic monoclonal antibody to GXM (Casadevall et al., 1998) kindly donated by Dr. Arturo Casadevall (Johns Hopkins University). The fungus was washed with fresh DMEM and incubated with J774.16 macrophages (1:1 ratio, $5 \times 10^5$ cells/well of 96 well-plates) for 2 h in DMEM containing 10% FBS, 0.3 μg/ml LPS and 0.005 μg/ml IFNγ (37°C, 5% $CO_2$). After interaction of *C. neoformans* with macrophages, the systems were washed with DMEM to remove extracellular fungal cells and fresh DMEM containing 10% FBS and variable concentrations of mebendazole (0.25, 0.5, and 1 μM, 200 μl/well) was added to each well. The plates were incubated at 37°C with 5% $CO_2$. After 8 or 24 h, supernatants were collected for inoculation of YPD agar plates and subsequent CFU counting. Alternatively, infected macrophages were lysed with cold, distillated water and the resulting lysates were plated onto YPD agar plates for CFU counting. To evaluate the toxicity of mebendazole for J774.16 macrophages, $5 \times 10^5$ macrophages suspended in DMEM containing 10% FBS were plated in each well of 96 wells plates and incubated overnight at 37°C with 5% $CO_2$. The medium was supplemented with fresh DMEM containing 10% FBS and mebendazole (0.25, 0.5, and 1 μM) or 0.5% DMSO. The plate was incubated at 37°C in a 5% $CO_2$ atmosphere. After 48 h, the systems were washed with DMEM and 50 μl of 3-(4,5-dimethylthiazol-2-yl)-2,5-diphenyltetrazolium bromide (MTT) at 5 mg/ml was added to each well, for further incubation for 4 h (37°C, 5% $CO_2$) under light protection (Mosmann, 1983). Supernatants were removed and 200 μl DMSO was added for dissolution of formazan crystals. Absorbances were recorded using the FilterMax 5 microplate reader (Molecular Devices, Sunnyvale, CA, USA) at 570 nm.

## Analysis of Synergistic Effects

Synergistic activity between mebendazole and standard antifungal drugs was determined on the basis of the calculation of the fractional inhibitory index (FIC) (Mor et al., 2015). Briefly, mebendazole (denominated drug A) was serially diluted (0.38–0.006 μg/ml, 8 dilutions) in 96-well plates. Standard antifungals (denominated drugs B) were serially diluted (11 dilutions) from 16 to 0.015 μg/ml (amphotericin B) or 64 to 0.06 μg/ml (fluconazole). The FIC was defined as:

$$\frac{MIC\ combined}{MIC\ drug\ A\ alone} + \frac{MIC\ combined}{MIC\ drug\ B\ alone}$$

Synergism was categorized as follows: strongly synergistic effect, FIC $< 0.5$; synergistic effect, FIC $< 1$; additive effect, FIC $= 1$; no effect, $1 <$ FIC $< 2$; antagonistic effect, FIC $> 2$ (Mor et al., 2015).

## Effects of Mebendazole on Glucuronoxylomannan (GXM) Release

*Cryptococcus neoformans* cells ($10^5$/well of 96-well plates, final volume of 200 μl, duplicates) were cultivated in RPMI 1640 buffered with MOPS, pH 7. The medium was supplemented with mebendazole (0.3125–0.001 μM). After 48 h of incubation at 37°C with shaking, the optical density of 540 nm ($OD_{540}$) was recorded using the FilterMax 5 microplate reader (Molecular Devices, Sunnyvale, CA, USA). The plate was centrifuged for 10 min and supernatants were used for GXM quantification by ELISA using the protocol described by Casadevall et al. (1992). *C. neoformans* viability was monitored by propidium iodide (PI) staining of fungal cells. For this analysis, fungal cells obtained after exposure to 0.3125, 0.15625, and 0.078 μM mebendazole as described above were stained with 1 mg/ml PI for 5 min on ice and analyzed by flow cytometry in a FACS Cabibur (BD Biosciences, CA, USA). The percentage of stained (non-viable) cells was obtained with the FlowJo 7 software.

## Analysis of Capsular Size and Morphology

*Cryptococcus neoformans* was grown overnight in YPD broth and washed twice with PBS. The fungus was then suspended in minimal medium containing sub-inhibitory concentrations of mebendazole and incubated for 48 h at 37°C with shaking. *C. neoformans* cells were collected by centrifugation, washed in PBS and analyzed by microscopic approaches. For capsule size determination, the suspension was counterstained with India ink and placed onto glass slides. The suspensions were covered with glass coverslips and analyzed with an Axioplan 2 (Zeiss, Germany) microscope. Capsule size, calculated with the ImageJ Software, was defined as the distance between the cell wall and the outer border of the capsule. Cell diameters were determined using the same software. For additional analysis of capsular morphology, cellular suspensions were processed for fluorescence microscopy. Staining reagents used in this analysis-included calcofluor white (cell wall chitin, blue fluorescence) and the monoclonal antibody 18B7 (Casadevall et al., 1998). *C. neoformans* cells were prepared for fluorescence microscopy following the protocols established by our laboratory for routinely analysis of surface architecture (Rodrigues et al., 2008).

## Effects of Mebendazole on *C. neoformans* Biofilms

*Cryptococcus neoformans* was grown in Sabouraud's dextrose broth for 24 h at 30°C with shaking. The cells were centrifuged at 3,000 *g* for 5 min, washed twice with PBS, suspended in

minimal medium and adjusted to a density of $10^7$ cells/ml. Cell suspensions (100 μl) were added into quadruplicate wells of polystyrene 96-well plates (Greiner Bio-One, Australia), following incubation at 37°C for 48 h. The wells containing biofilms were washed three times with PBS to remove non-adhered cryptococcal cells. Fungal cells that remained attached to the wells were considered mature biofilms. To evaluate the susceptibility of *C. neoformans* biofilms to mebendazole, 100 μl solutions (31.25, 15.63, 3.13, 1.56, 0.31, and 0.16 μM) were added to each well. Amphotericin B and fluconazole (2 and 8 μg/ml, respectively) were used as control systems of antifungal activity. Negative controls corresponded to wells containing only water and untreated biofilms. Mature biofilms and antifungal drugs were incubated at 37°C for 24 h, washed three times with PBS and the biofilm metabolic activity quantified by the 2,3-bis (2-methoxy-4-nitro-5-sulfophenyl)-5-[(phenylamino) carbonyl]-2H-tetrazolium hydroxide (XTT) reduction assay (Meshulam et al., 1995). Prior studies demonstrated that the XTT reduction assay measurements correlate with biofilm and fungal cell number (Martinez and Casadevall, 2007). In addition to testing the effects of mebendazole on established biofilms, we evaluated whether this compound would inhibit biofilm formation. Cryptococcal cells were suspended in minimal medium and adjusted to a density of $10^7$ cells/ml in the presence or absence of mebendazole (31.25, 15.63, 3.13, 1.56, 0.31, and 0.16 μM). These suspensions were added in quadruplicates to the wells of polystyrene 96-well plates, following incubation at 37°C for 48 h. Amphotericin B and fluconazole (2 and 8 μg/ml, respectively) were used as antifungal controls. In negative controls, wells contained only ultrapure water. The wells were washed three times with PBS and biofilm formation was quantified by the XTT assay.

## Analysis of the Antifungal Activity of Mebendazole against a Collection of *C. gattii* Mutants

A collection of randomly generated *C. gattii* mutants was screened for identification of possible cellular targets for antifungal activity. Mutants ($n$ = 7,569) were generated by insertional mutagenesis after incubation of *C. gattii* with *Agrobacterium tumefaciens* as previously described (Idnurm et al., 2004). All colonies that grew on YPD hygromycin plates were selected and maintained at −20°C in 96 wells plates containing 200 μl/well of YPD broth. Before exposure to mebendazole, mutant cells were first grown for 72 h (30°C) in 200 μl of YPD distributed into the wells of 96 wells plates. The antifungal activity of mebendazole against *C. neoformans* was reproduced in the *C. gattii* R265 strain. The mutants were tested for their ability to grow in the presence of RPMI 1640 supplemented with MOPS, 2% of glucose, 1% DMSO and 10 μM mebendazole. Resistance phenotypes ($A_{540}$ > 0.3) were selected for dose-response tests of antifungal activity as described above and potential target identification was performed as detailed below.

## Identification of Potential Cellular Targets Required for the Antifungal Activity of Mebendazole

Based on clear resistant phenotypes, two *C. gattii* mutant strains were selected for target identification by polymerase

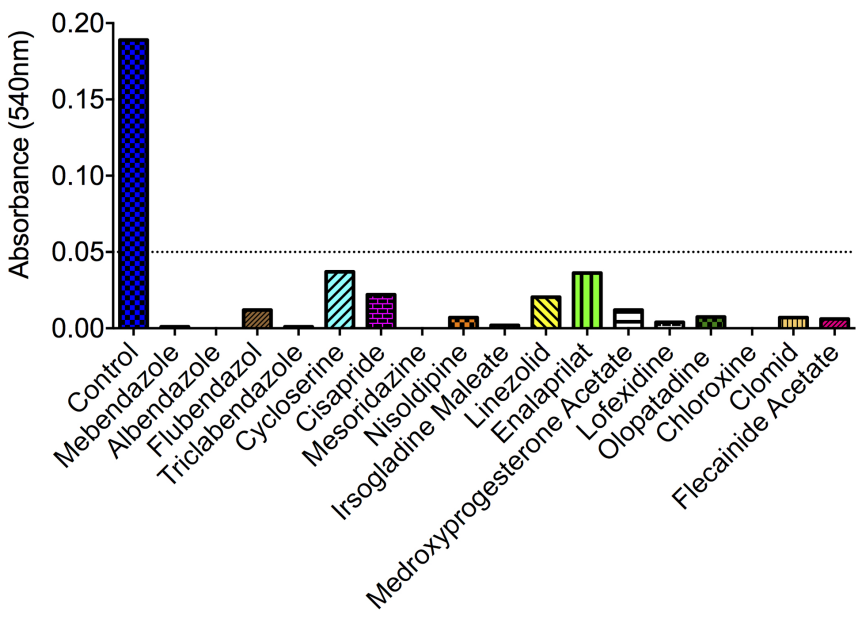


**FIGURE 1 | Identification of small-molecule inhibitors of *Cryptococcus neoformans* via drug-repurposing screening.** Out of 727 compounds tested, 17 molecules induced $A_{540}$ values smaller than 0.05 (dotted line). Compounds with no antifungal activity are not shown. For description of the primary activity of each molecule, see section "Results." Data illustrate a representative experiment of two independent screenings.

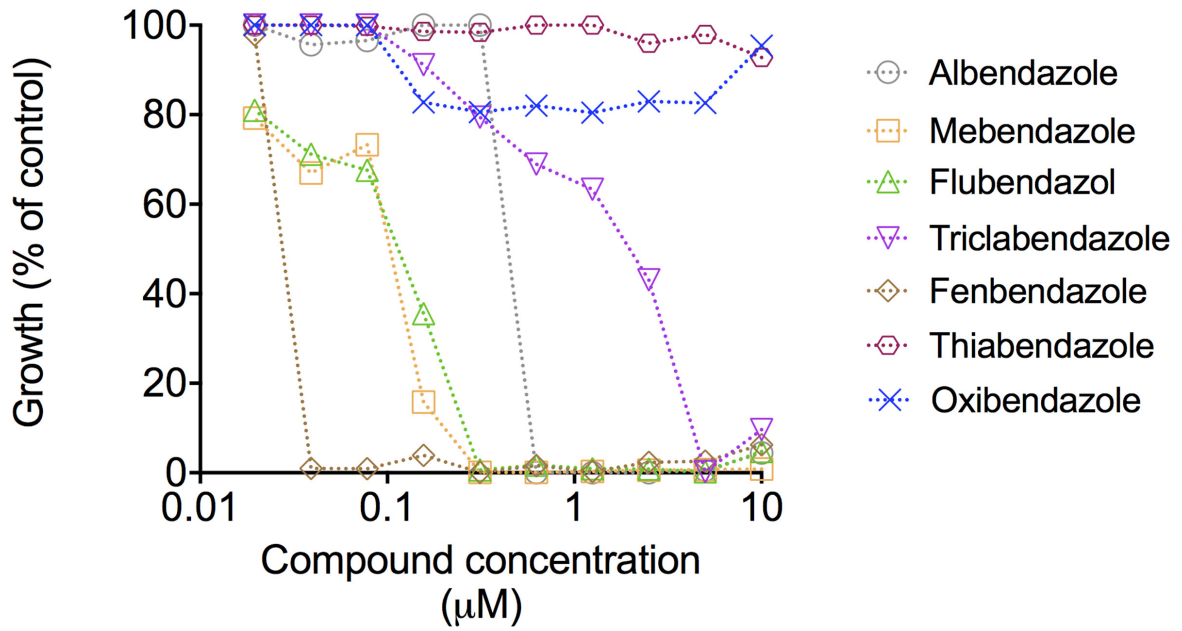


**FIGURE 2 | Dose-response curves of the antifungal effects of benzimidazoles against *C. neoformans*.** Curves represent *C. neoformans* growth in comparison with vehicle-treated cells (DMSO). Data illustrate a representative experiment of three independent replicates.

chain reaction (PCR). The fungus was cultivated overnight in 10 ml YPD at 30°C with constant rotation. Each culture (2 ml) was centrifuged for 2 min at 4,000 × *g* and cell pellets were washed twice with PBS and collected for DNA extraction (Bolano et al., 2001). The cells were suspended in 400 μl of lysis buffer (50 mM Tris-HCl 1 mM EDTA, 200 mM NaCl, 2% Triton X100, 0.5% SDS, pH 7.5), for further addition of 1 volume of a phenol-chloroform mixture (pH 8) and 100 μl of 2-μm, acid washed glass beads. Mechanical disruption was performed by alternate 1-min cycles of vortexing and ice incubation. Lysates were centrifuged 4,000 × *g* for 20 min at 4°C. Supernatants were collected and DNA was ethanol-precipitated overnight at −20°C for subsequent treatment with RNAse (Bolano et al., 2001). Identification of missing genes in the mutants was performed using inverse PCR (Pavlopoulos, 2011). DNA was quantified using the Qubit reagent (Invitrogen) and 1 μg of each sample was cleaved separately with BglII, SalI, or StuI (Promega) restriction enzymes. The cleavage product was submitted to T4 DNA ligase reaction (New England) followed by PCR using primers for inverse PCR. Amplicons were gel-purified with the QIAquick Gel Extraction Kit (Qiagen). For the DNA sequencing reaction, 50 ng of each sample and 5 pmol of each primer were used. Sequences were obtained in an ABI-Prism 3500 Genetic Analyzer (Applied Biosystems) and their qualities were determined by a electropherogram analysis based on phred[1]. The identification of genes interrupted by the T-DNA was performed by comparison of each sequenced DNA fragment, which correspond to the T-DNA flanks, with the genomic sequence of *C. neoformans* H99 strain, available in the *Cryptococcus* genome databases (Broad Institute[2]) using BLASTn. Orthologs distribution was evaluated using the OrthoMCL database (Chen et al., 2006).

Mutants showing resistance to mebendazole were analyzed for their ability to produce melanin and extracellular GXM as previously described by our group (Rodrigues et al., 2015).

## Statistical Analyses

Statistics were obtained with the GraphPad Prism 6.0 software. Unpaired *t* student test was used for mebendazole toxicity analysis. The variance two-way ANOVA was carried out using Tukey's and Bonferroni's comparisons test for fungicidal activity and intracellular activity of mebendazole in macrophages. For biofilm analyses, one-way ANOVA was performed using Dunnett's multiple comparisons.

# RESULTS

## Selection of Mebendazole as a Potential Anti-cryptococcal Agent

Of the 727 drugs tested at 10 μM, 17 compounds were active against *C. neoformans*, including antibacterials (chloroxine, cycloserine, and linezolid), a neuroleptic drug (mezoridazine), calcium channel blockers (nisoldipine and enalaprilat), antiarrhythmic agents (flecainide acetate), drugs for gastrointestinal malignances (irsogladine maleate and cisapride), gynecologic regulators (medroxyprogesterone acetate and clomid), an anti-histaminic (olopatadine) and the

[1]http://www.biomol.unb.br/phph/

[2]http://www.broadinstitute.org/scientific-community/science/projects/fungal-genome-initiative/cryptococcus-gattii-genome-project-0

anti-helminthic benzimidazoles (mebendazole, albendazole, flubendazole, and triclabendazole) (**Figure 1**). Noteworthy, none of the molecules showing antifungal activity were structurally related, except the benzimidazoles. Considering the currently observed efficacy in inhibiting the growth of *C. neoformans*, their structural similarity and previously described anti-cryptococcal activity (Cruz et al., 1994), we selected benzimidazoles for further investigation in our model.

We extended the results obtained with the compound collection to dose-response tests using the four benzimidazoles showing antifungal activity and other related molecules, including thiabendazole, oxibendazole, and fenbendazole. The most active compounds were mebendazole, fenbendazole, and flubendazole (**Figure 2**). Mebendazole and flubendazole produced the same MIC values (0.3125 μM). Fenbendazole was the most potent compound, with a MIC corresponding to 0.039 μM. Mebendazole, however, efficiently penetrates the brain in animal models (Bai et al., 2015) and is in clinical trial for the treatment of pediatric gliomas in humans (ClinicalTrials.gov, 2013). Considering that the worse clinical outcome of cryptococcosis includes colonization of the brain, we selected mebendazole as the molecular prototype for our subsequent analyses of fungicidal effects, ability to kill intracellular cryptococci, effects on fungal morphology, interference on fungal biofilms and identification of cellular targets.

## Mebendazole Is Fungicidal against *C. neoformans*

To test the fungicidal activity of mebendazole, *C. neoformans* was exposed to different drug concentrations for different periods of time. Mebendazole concentrations lower than 0.3125 μM had no effects on *C. neoformans* (**Figure 3**). At 0.3125 μM or higher, however, significant antifungal activity was observed after 6 to 12 h of exposure of *C. neoformans* to the drug. After 48 h, mebendazole killed 100% of *C. neoformans* cells.

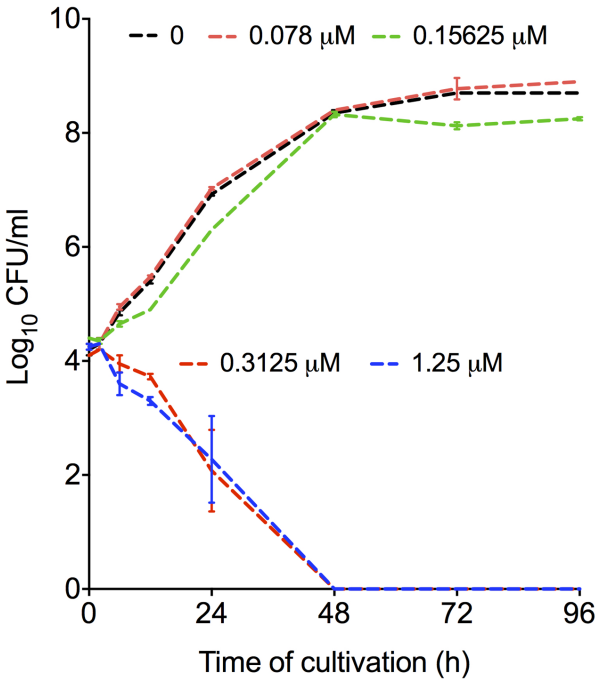


**FIGURE 3 | Fungicidal activity of mebendazole against *C. neoformans*. Fungal cells were exposed to mebendazole (0.078–1.25 μM) for periods varying from 0 to 96 h.** Fungicidal activity was evident after 48 h and required a minimum concentration of 0.3125 μM mebendazole. In comparison to control systems (no drug), mebendazole concentrations of 0.3125 and 1.25 μM significantly affected fungal growth in all incubation periods. All the other drug concentrations resulted in fungal growth that was similar to that observed in the absence of mebendazole. Data illustrate a representative experiment of three independent replicates.

## Activity of Mebendazole against Intracellular *C. neoformans*

*Cryptococcus neoformans* is a facultative intracellular pathogen and this characteristic likely has a negative impact on the anti-cryptococcal treatment (Feldmesser et al., 2000). We then evaluated the ability of mebendazole to kill intracellular fungi. J774.16 macrophages were first infected with *C. neoformans* and then the cultures were treated with mebendazole for different periods (8 and 24 h) at variable drug concentrations (1, 0.5, and 0.25 μM). Macrophage viability was monitored by treating non-infected J774.16 cells with mebendazole alone (**Figure 4A**). After 8 h, no differences were observed between the viability of untreated macrophages and mebendazole-treated cells ($P > 0.1$). After 24 h, macrophage viability was affected by higher mebendazole concentrations ($P = 0.0071$ for 1 μM mebendazole), but no differences were observed between untreated phagocytes and cells that were exposed to 0.25 μM mebendazole ($P = 0.3225$). In infected macrophages, all mebendazole concentrations showed antifungal activity against both extracellular and intracellular fungi (**Figure 4B**). The concentration showing the lowest impact on macrophage viability (0.25 μM) was efficient in killing both intracellular and extracellular *C. neoformans*.

## Analysis of Potential Synergism between Mebendazole and Standard Antifungals

To evaluate whether the association of mebendazole with amphotericin B or fluconazole results in improved anti-cryptococcal activity, checkerboard assays were performed for calculation of the FIC index (**Table 1**). We found that mebendazole had additive activity against *C. neoformans* when combined with amphotericin B. Fluconazole did not show any improved effect in combination with mebendazole.

## Mebendazole Affects Capsule Size and Fungal Morphology

To evaluate whether mebendazole affected key cellular structures of *C. neoformans* during regular growth, we cultivated the fungus for 48 h in the presence of a sub-inhibitory concentration (IC50; 0.22 μM) of the drug for further analysis of morphology and capsule size by a combination of fluorescence microscopy and India ink counterstaining. Fungal cells cultivated in the

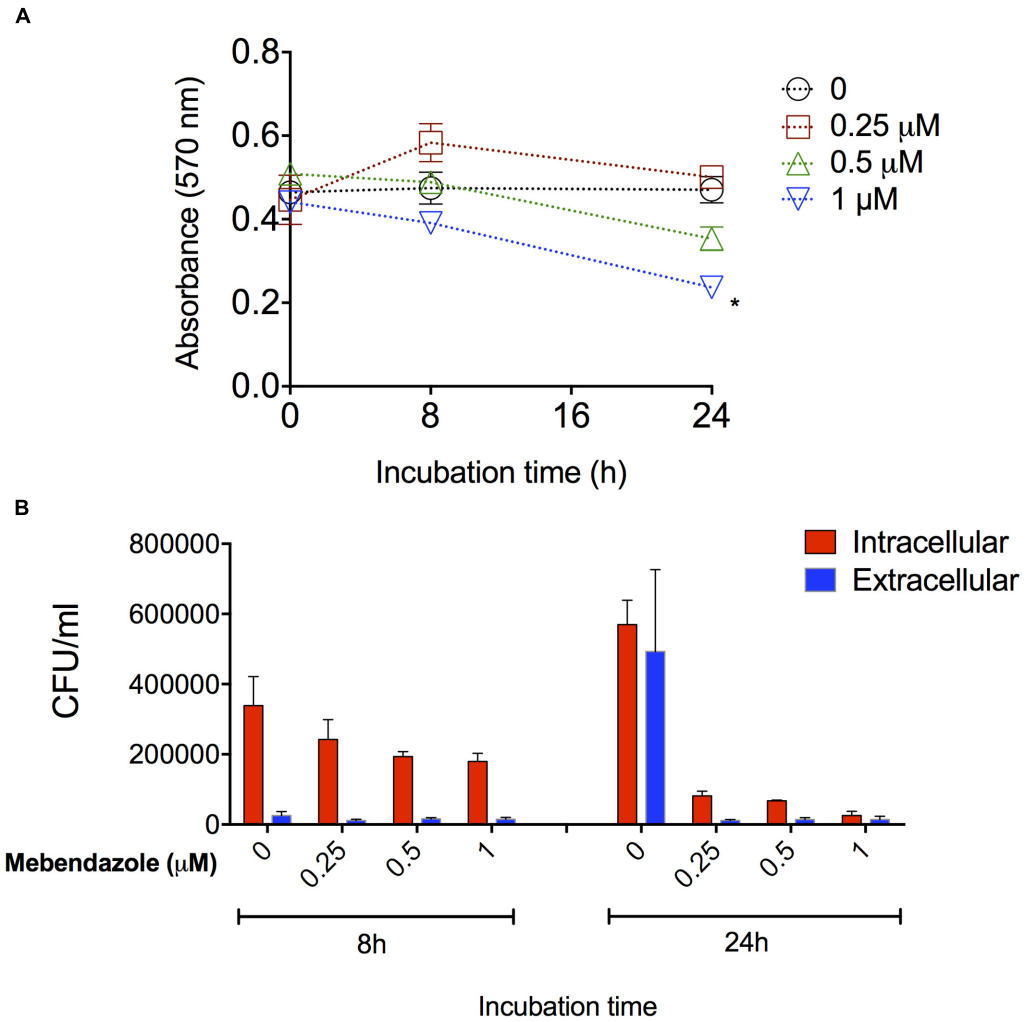


**FIGURE 4 | Activity of mebendazole against intracellular *C. neoformans*. (A)** Viability of drug-treated, non-infected macrophages. After 8 h, all systems had similar viability levels ($P > 0.1$). After 24 h, cell viability was only affected by 1 μM mebendazole concentration ($P = 0.0071$). **(B)** Activity of mebendazole against intracellular (red bars) or extracellular (blue bars) *C. neoformans*. In intracellular assays, statistical differences ($P < 0.05$) between no drug (0) and drug-treated systems were always observed, except when the 0.25 μM concentration of mebendazole was used in the 8 h incubation period. In extracellular assays, statistical differences ($P < 0.05$) between no drug (0) and drug-treated systems were observed for all mebendazole concentrations, but only after the 24 h incubation. Comparative analysis of fungal loads obtained from intracellular and extracellular assays revealed statistical differences ($P < 0.05$) only in the 8 h period of incubation, suggesting that mebendazole is initially more effective against extracellular fungi, but similarly active against both intracellular and extracellular cryptococci after prolonged (24 h) periods of exposure to infected macrophages. Data illustrate a representative experiment of three independent replicates.

**TABLE 1 | Impact of the association of mebendazole with amphotericin B (AmB) or fluconazole (FLC) on antifungal activity.**

| Drug A | | | Drug B | | | FIC* |
|---|---|---|---|---|---|---|
| | MIC Alone (μg/ml) | MIC Combined (μg/ml) | | MIC Alone (μg/ml) | MIC Combined (μg/ml) | |
| Mebendazole | 0.095 | 0.0475 | AmB | 0.25 | 0.125 | 1 |
| Mebendazole | 0.095 | 0.0475 | Fluconazole | 2 | 2 | 1.5 |

**Fractional inhibitory concentration index (FIC); Strongly synergistic: FIC < 0.5; Synergistic: FIC < 1; Additive: FIC = 1; No effect: 1 < FIC < 2; Antagonistic: FIC > 2.*

presence of mebendazole presented marked morphological alterations, including loss of spherical shape, intracellular furrows (**Figure 5A**) and reduced capsular dimensions (**Figure 5B**, $P < 0.05$).

## Effect of Mebendazole on GXM Release

Since mebendazole interfered with capsule size (**Figure 5B**), we asked whether GXM release was affected by exposure of *C. neoformans* to the drug. Supernatants of fungal cells

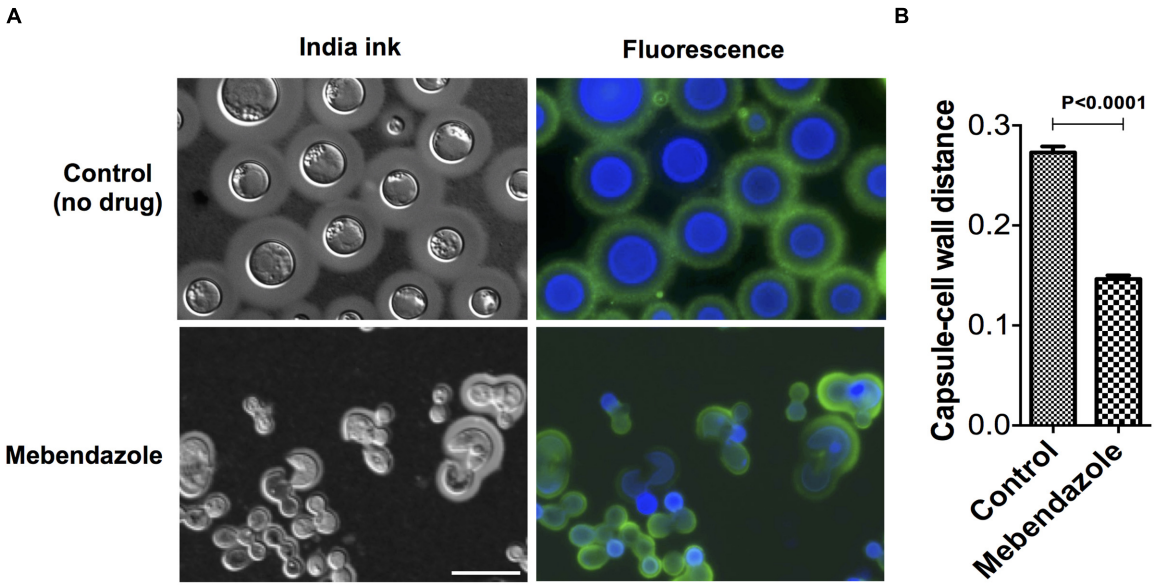


**FIGURE 5 | Morphological alterations of *C. neoformans* cells treated with mebendazole. (A)** India ink counterstaining (left panels) and fluorescence microscopy (right panels) showing GXM (green fluorescence) and chitin (blue fluorescence) detection. Scale bar represents 10 μm. **(B)** Capsule measurement of India ink counterstained cells showing reduction in capsular dimensions by mebendazole. Data illustrate a representative experiment of three independent replicates.

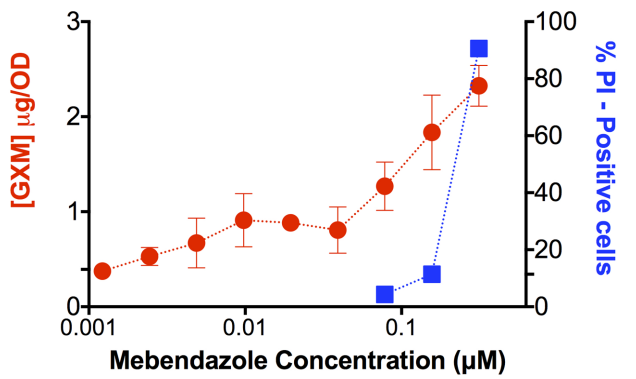


**FIGURE 6 | Extracellular release of GXM by *C. neoformans* cells treated with different concentrations of mebendazole.** GXM extracellular detection correlated with increasing mebendazole concentrations. Staining of fungal cells with PI after exposure to fungicidal doses of mebendazole revealed a similar profile, suggesting polysaccharide leakage. Data illustrate a representative experiment of three independent replicates.

cultivated in the presence of mebendazole were used for GXM quantification by ELISA (**Figure 6**). Unexpectedly, supernatants of mebendazole-treated cells had increased GXM concentration, mainly in the dose range required for fungal killing. Since the polysaccharide is synthesized intracellularly (Yoneda and Doering, 2006), we hypothesized that the increased GXM detection would result from leakage induced by membrane damage. To address this possibility, mebendazole-treated cells were stained with PI. Stained cells varied from 70 to 90% in the dose range generating cell death, which was compatible with membrane damage and polysaccharide leakage. Noteworthy, these results and those described in **Figure 5** are also compatible with the hypothesis of GXM release from the cell surface, so we cannot rule out the possibility that mebendazole promotes detachment of capsular structures in *C. neoformans*.

## Activity of Mebendazole against *C. neoformans* Biofilms

Biofilm formation causes well-known difficulties in the treatment of a number of infectious diseases, including cryptococcosis (Martinez and Casadevall, 2006; Borghi et al., 2016). Based on this observation, we evaluated whether co-incubation of mebendazole with yeast cells prevented *C. neoformans* biofilm formation or caused damage to mature biofilms. The metabolic activity was measured by XTT reduction assay (**Figure 7**). Fluconazole is known to have no effects on mature biofilms, in contrast to amphotericin B (Martinez and Casadevall, 2006). Therefore, these drugs were used as negative and positive controls, respectively. Mebendazole at MIC (0.3125 μM) affected biofilm formation (**Figure 7A**; $P < 0.0001$) and damaged mature biofilms (**Figure 7B**; $P < 0.0001$). Lower concentrations of mebendazole similarly affected *C. neoformans* mature biofilms (**Figure 7B**; $P < 0.0001$). As expected, higher concentrations of mebendazole had even clearer impacts on *C. neoformans* biofilms.

## Identification of Potential Cellular Targets for Mebendazole

Antifungal activities of benzimidazoles were described before (Cruz et al., 1994), but the mechanisms by which these drugs affected cryptococcal growth remained unknown. In order to identify potential targets for mebendazole in *Cryptococcus* spp.,

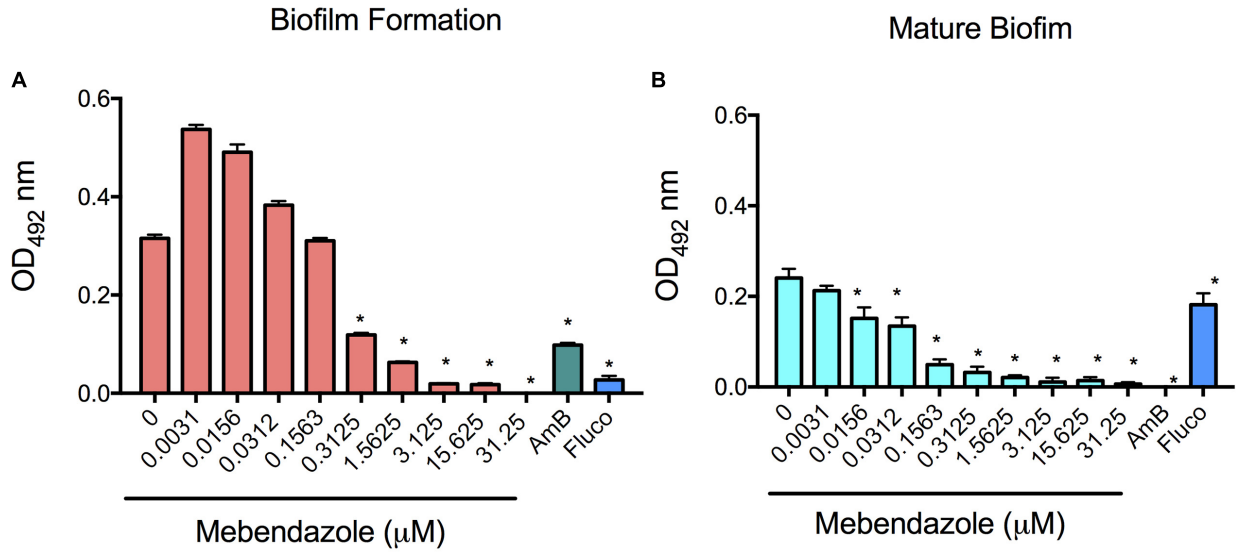


**FIGURE 7 | Effects of mebendazole on cryptococcal biofilms.** Biofilm formation and mature biofilm activity were measured indirectly by XTT reduction assay. **(A)** Incubation of *C. neformans* with mebendazole before biofilm formation. **(B)** Treatment of mature biofilms with mebendazole. AmB, amphotericin B (2 μg/ml); Fluco, fluconazole (8 μg/ml). Statistical significances after comparison with control systems are indicated by asterisks ($P < 0.0001$). Data illustrate a representative experiment of three independent replicates.

we first evaluated whether the drug affected the growth of *C. gattii* and *C. neoformans* in a similar fashion. In fact, growth inhibition curves were identical for both pathogens (**Figure 8A**).

A mutant collection generated by co-incubation of *C. gattii* and *A. tumefaciens* (Idnurm et al., 2004) was produced by our group for general purposes involving development of antifungals and pathogenic studies. In the present study, these mutants were screened for resistance phenotypes in the presence of 10 μM mebendazole, based on the assumption that, in the absence of a cellular target required for antifungal activity, the drug would lack anti-cryptococcal properties. Most of the mutants were sensitive to mebendazole and a number of strains were partially resistant to the drug (**Figure 8B**). However, two of the mutant strains clearly stood out from the entire collection, showing highest levels of resistance even in higher mebendazole concentrations (**Figure 8C**). Interrupted regions in these two mutants were identified by inverse PCR (**Figure 8D**). In the most mebendazole-resistant mutant, the protein codified by the interrupted gene contained a scramblase domain (PF03803 – CNBG_3981). In the second most resistant mutant, the gene coding for ribosome biogenesis protein Nop16 (PF09420 – CNBG_3695) was interrupted. These domains were found in diverse phylogenetic groups, according to the PFAM database (Finn et al., 2016). However, orthologs for these genes were found in a narrow group of organisms and absent in human cells (**Figure 8D**), according to OrthoMCL database (Chen et al., 2006). These results indicate that at least two novel cellular targets are involved in the antifungal activity of mebendazole.

Neutralizing cryptococcal virulence factors is also likely to be beneficial for the control of cryptococcosis. In this context, we evaluated whether the mutants lacking potential targets for activity of mebendazole had normal production of the most-well characterized cryptococcal virulence factors. The two mutants had normal urease activity (not shown). Analysis of extracellular GXM and pigmentation, however, showed important differences between WT and mutant cells (**Figure 9**). Mutants disrupted for expression of the putative scramblase and of nucleolar protein 16 had decreased contents of extracellular GXM, in comparison with WT cells ($P < 0.001$). The kinetics of melanin production was also negatively affected in the mutants.

## DISCUSSION

Processes of drug research and development are costly, time consuming and have questionable success (Kaitin, 2010; Kaitin and DiMasi, 2011). In this scenario, drug repurposing has provided a potential boost to the drug pipeline combating health emergencies and assisting neglected populations. Recent studies have provided evidence of successful drug repurposing to combat *Cryptococcus* (ClinicalTrials.gov, 2016; Rhein et al., 2016) and Zika virus (Veljkovic and Paessler, 2016; Xu et al., 2016; Sacramento et al., 2017) infections with promising results. The need for additional anti-infectious agents, however, is clear.

In this study, we identified small-molecule inhibitors of *C. neoformans* via a drug-repurposing screen. Our findings demonstrated antifungal activity in a group of anti-helminthic benzimidazoles and suggested potential targets for development of novel antifungals. Benzimidazoles are heterocyclic aromatic bis-nitrogen azoles that are considered promising anchors for development of new therapeutic agents (Bansal and Silakari, 2012). Benzimidazole derivatives have been associated to the control of infectious diseases

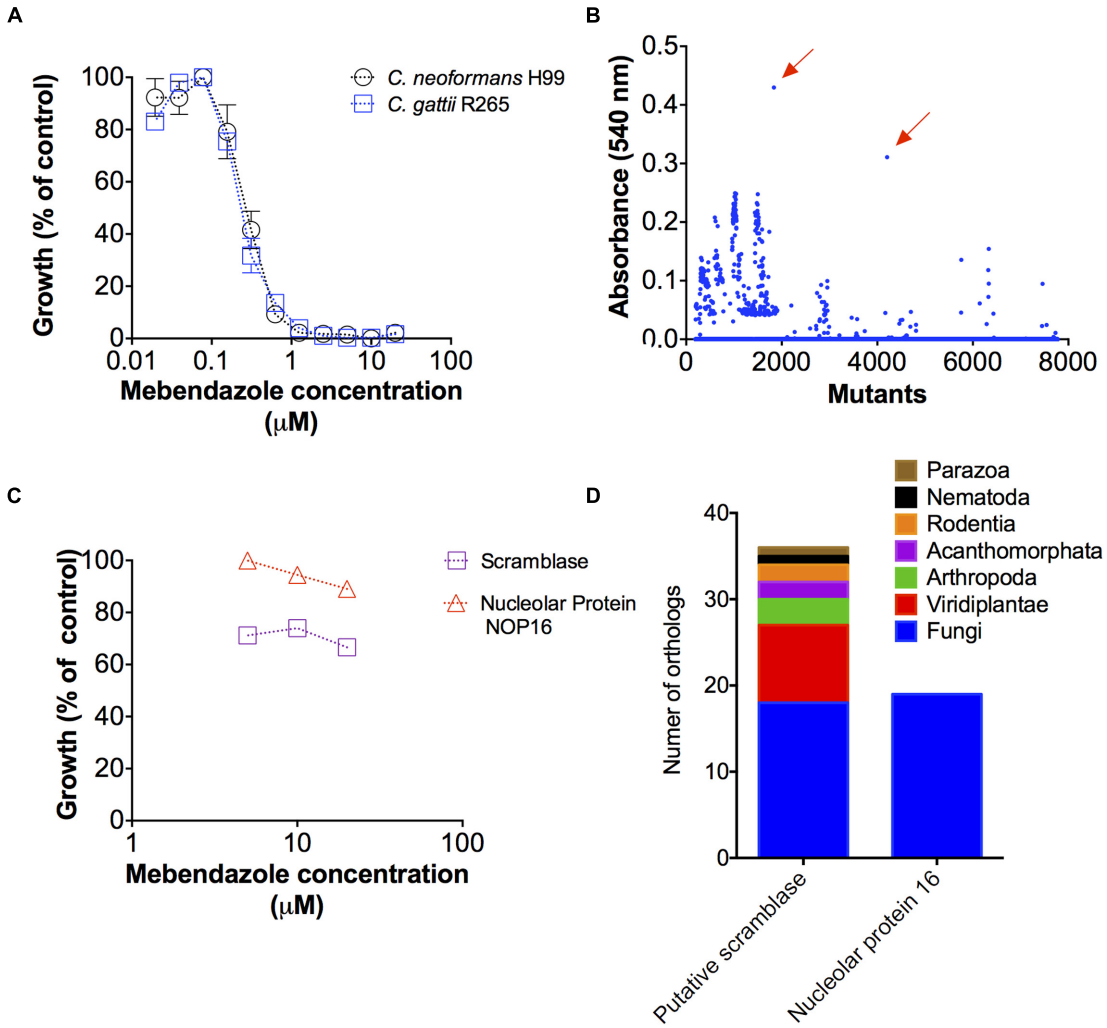


**FIGURE 8 | Potential cellular targets required for mebendazole activity. (A)** Comparative analysis showing that *C. neoformans* and *C. gattii* are similarly susceptible to mebendazole. **(B)** Screening of a *C. gattii* mutant library in the presence of 10 μM of mebendazole, revealing two highly resistant strains (arrows). **(C)** Growth of the two mutants selected in panel B in the presence of variable concentrations of mebendazole. **(D)** Sequence identification by PCR and distribution of cellular proteins required for mebendazole activity.

through antiviral, antifungal, antimicrobial, and antiprotozoal properties, but they also manifest antiinflammatory, anticancer, antioxidant, anticoagulant, antidiabetic and antihypertensive activities (Ates-Alagoz, 2016). The anti-cryptococcal activity of benzimidazoles was demonstrated two decades ago (Cruz et al., 1994), but the effects of these compounds on fungal morphology and biofilm formation were not explored. Similarly, their cellular targets and ability to kill intracellular fungi remained unknown. Mebendazole, one of the benzimidazoles showing antifungal activity, is in clinical trial for the treatment of human pediatric glioma (ClinicalTrials.gov, 2013). Since effective anti-cryptococcal agents obligatorily need to reach the central nervous system at biologically active concentrations, we selected mebendazole for our experiments of antifungal activity. This compound affected cryptococcal growth, morphology, biofilms and macrophage infection.

The pathogenic mechanisms used by *C. neoformans* during infection bring significant complexities in the management of cryptococcosis. Conditions favoring biofilm formation are thought to contribute to cryptococcal virulence (Benaducci et al., 2016). Like with other pathogens, *C. neoformans* biofilms are resistant to antimicrobial agents and host defense mechanisms, causing significant morbidity and mortality (Martinez and Casadevall, 2015). These characteristics are especially relevant in a scenario of increasing use of ventriculoperitoneal shunts to manage intracranial hypertension associated with cryptococcal meningoencephalitis (Martinez and Casadevall, 2015). In our model, mebendazole was an efficient antifungal agent against *C. neoformans* biofilms. The minimum mebendazole concentration required for antifungal activity against planktonic cells (0.325 μM) was much higher than the doses required for activity against mature biofilms (0.0156–0.0312 μM). The reason

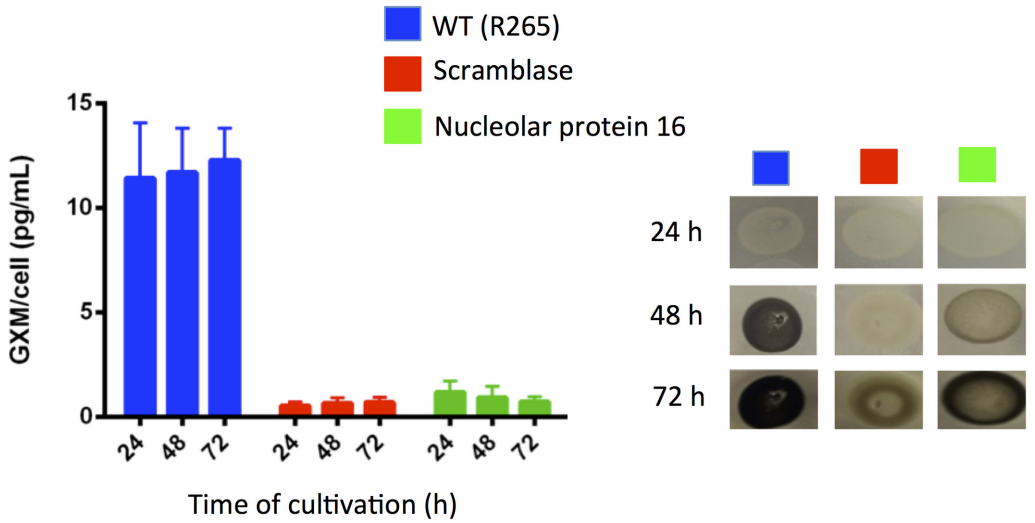


**FIGURE 9 | *Cryptococcus gattii* mutants lacking potential targets for mebendazole activity show defective capacity to produce well-known cryptococcal virulence factors.** GXM determination by ELISA (left panel) indicated that the putative scramblase and nucleolar protein 16 were required for polysaccharide export. Both proteins were apparently involved in the kinetics of pigmentation in *C. gattii* (right panel).

for this discrepancy is unclear. Since capsular polysaccharides have well described roles on the assembly of cryptococcal biofilms (Martinez and Casadevall, 2005), we hypothesize that the herein described impact of mebendazole on capsular architecture and GXM release may affect biofilm stability.

An additional complexity in the treatment of cryptococcosis is the ability of the fungus to reside inside phagocytes. In fact, persistent pulmonary infection is associated with the intracellular parasitism of *C. neoformans* (Goldman et al., 2000). In this context, targeting intracellular survival and growth and/or cryptococcal virulence factors expressed during intracellular parasitism might offer new strategies to improve anticryptococcal treatment, as reviewed by Voelz and May (2010). Mebendazole was effective against phagocytized fungi in our model. The fact that the anti-helminthic compound had an additive effect to AmB also suggests that benzimidazole-like compounds could be used in therapeutic protocols against cryptococcosis.

The primary mechanism of anthelmintic activity of mebendazole relies on binding the β-subunit of tubulin before dimerization with α-tubulin, with subsequent blocking of microtubule formation (Gardner and Hill, 2001). Tubulin may also be the target of mebendazole in *C. neoformans*, but our studies suggest the possibility that the antifungal effects of mebendazole may involve additional targets. Mebendazole induced membrane permeabilization, as concluded from increased levels of PI staining after exposure of *C. neoformans* to the drug. In addition, mutants lacking genes coding for a putative scramblase and the nucleolar protein Nop16 were highly resistant to mebendazole. Both mutants had defective formation of important virulence factors. Remarkably, sequences showing similarity to these two proteins were absent in human cells, suggesting a great potential for these two proteins as novel antifungal specific targets. Scramblases are ATP-independent enzymes that act to randomize lipid distribution by bidirectionally translocating lipids between leaflets (Hankins et al., 2015). Lipid-translocating enzymes, in fact, are fundamental for cryptococcal pathogenesis and GXM export (Hu and Kronstad, 2010; Rizzo et al., 2014). The functions of Nop16 in *C. neoformans* are unknown, but in *S. cerevisiae* this protein is a component of 66S pre-ribosomal particles required for 60S ribosomal subunit biogenesis (Harnpicharnchai et al., 2001; Horsey et al., 2004). Although there is no evidence in the literature linking tubulin polymerization, membrane permeability and cellular functions of these two potential targets, our studies suggest that a connection may exist and these proteins may be functionally integrated in fungi.

Cryptococcosis affects regions where health infrastructure resources are extremely limited. Considering the high mortality rates associated with this disease and the socio-economic scenario behind cryptococcosis, low-cost and efficient antifungal alternatives are urgent. Clinical use of novel drugs, however, depends on a number of properties of the molecular candidates. In this regard, the potential use of mebendazole against human cryptococcosis raises several concerns. For instance, the use of mebendazole at large doses may cause bone marrow suppression (Fernandez-Banares et al., 1986) and it is unclear if the compound is safe in pregnancy (Torp-Pedersen et al., 2012). Benzimidazoles have only limited water solubility, which impacts the rate and extent of their absorption and, consequently, systemic bioavailability, maximal plasma concentration, and tissue distribution (McKellar and Scott, 1990). Animal studies with mebendazole demonstrated drug distribution through all the organs, including the central nervous system (Lanusse and Prichard, 1993). However, the drug and its metabolites were

concentrated mainly in the liver, where they remain for at least 15 days post treatment (Lanusse and Prichard, 1993). Mebendazole is thought to be the active form of the drug rather than its metabolites (Gottschall et al., 1990). However, in the liver, benzimidazoles are mostly modified by the enzymatic system of hepatic microsomal oxidases, which are involved in sulfoxidation, demethylation, and hydroxylation (Short et al., 1988; Lanusse and Prichard, 1993). In fact, benzimidazoles are usually short lived and metabolic products predominate in plasma and all tissues and excreta of the host (Fetterer and Rew, 1984).

Although the difficulties associated with the clinical use of mebendazole are clear, our results combine a multiple antifungal activity with molecular targets that are absent in human cells, which encourages further development of benzimidazole-like molecules against *C. neoformans*. In fact, a number of reports have suggested that the benzimidazole core represents a promising scaffold for development of new therapeutic agents (Yadav and Ganguly, 2015). Montresor et al. (2010) estimated that the cost to procure one million doses of standard benzimidazoles (500 mg each) would be approximately US$ 20,000, including international transport. In this context, the ability of mebendazole to penetrate the brain (Bai et al., 2015) and to cause expressive damage in *C. neoformans* cells suggest great potential as a prototype for development of novel anti-cryptococcal agents.

## AUTHOR CONTRIBUTIONS

LJ, CS, LK, AS, MDP, MV, and MR prepared the experimental design. LJ, RS, WL, RA, and CS performed the experiments. LJ, CS, LK, AS, MDP, MV, and MR discussed the results, wrote and approved the final manuscript.

## ACKNOWLEDGMENTS

This work was supported by grants from Conselho Nacional de Desenvolvimento Científico e Tecnológico (CNPq) and Fundação de Amparo à Pesquisa do Estado do Rio de Janeiro (FAPERJ), by grants numbers 443586/2014-4, 300699/2013-1, E-26/102.835/2012 and 210.918/2015, and by NIH grant AI-116420 to MDP, MR is the recipient of a Pathfinder Award from the Wellcome Trust (United Kingdom; grant no. WT103212MF) and the author also acknowledges support from the Instituto Nacional de Ciência e Tecnologia de Inovação em Doenças Negligenciadas (INCT-IDN).

## REFERENCES

Arendrup, M. C., Cuenca-Estrella, M., Lass-Florl, C., Hope, W., and Eucast, A. (2012). EUCAST technical note on the EUCAST definitive document EDef 7.2: method for the determination of broth dilution minimum inhibitory concentrations of antifungal agents for yeasts EDef 7.2 (EUCAST-AFST). *Clin. Microbiol. Infect.* 18, E246–E247. doi: 10.1111/j.1469-0691.2012.03880.x

Ates-Alagoz, Z. (2016). Antimicrobial activities of 1-H-benzimidazole-based molecules. *Curr. Top. Med. Chem.* 16, 2953–2962. doi: 10.2174/1568026616666160506130226

Bai, R. Y., Staedtke, V., Wanjiku, T., Rudek, M. A., Joshi, A., Gallia, G. L., et al. (2015). Brain penetration and efficacy of different mebendazole polymorphs in a mouse brain tumor model. *Clin. Cancer Res.* 21, 3462–3470. doi: 10.1158/1078-0432.CCR-14-2681

Bansal, Y., and Silakari, O. (2012). The therapeutic journey of benzimidazoles: a review. *Bioorg. Med. Chem.* 20, 6208–6236. doi: 10.1016/j.bmc.2012.09.013

Benaducci, T., Sardi Jde, C., Lourencetti, N. M., Scorzoni, L., Gullo, F. P., Rossi, S. A., et al. (2016). Virulence of *Cryptococcus* sp. biofilms *in vitro* and *in vivo* using *Galleria mellonella* as an alternative model. *Front. Microbiol.* 7:290. doi: 10.3389/fmicb.2016.00290

Bolano, A., Stinchi, S., Preziosi, R., Bistoni, F., Allegrucci, M., Baldelli, F., et al. (2001). Rapid methods to extract DNA and RNA from *Cryptococcus neoformans*. *FEMS Yeast Res.* 1, 221–224.

Borghi, E., Borgo, F., and Morace, G. (2016). Fungal biofilms: update on resistance. *Adv. Exp. Med. Biol.* 931, 37–47. doi: 10.1007/5584_2016_7

Casadevall, A., Cleare, W., Feldmesser, M., Glatman-Freedman, A., Goldman, D. L., Kozel, T. R., et al. (1998). Characterization of a murine monoclonal antibody to *Cryptococcus neoformans* polysaccharide that is a candidate for human therapeutic studies. *Antimicrob. Agents Chemother.* 42, 1437–1446.

Casadevall, A., Mukherjee, J., and Scharff, M. D. (1992). Monoclonal antibody based ELISAs for cryptococcal polysaccharide. *J. Immunol. Methods* 154, 27–35. doi: 10.1016/0022-1759(92)90209-C

Chen, F., Mackey, A. J., Stoeckert, C. J. Jr., and Roos, D. S. (2006). OrthoMCL-DB: querying a comprehensive multi-species collection of ortholog groups. *Nucleic Acids Res.* 34, D363–D368. doi: 10.1093/nar/gkj123

ClinicalTrials.gov (2013). *Adjunctive Sertraline for the Treatment of HIV-Associated Cryptococcal Meningitis (ASTRO-CM)*. Available at: https://clinicaltrials.gov/ct2/show/NCT01802385

ClinicalTrials.gov (2016). *A Phase I Study of Mebendazole for the Treatment of Pediatric Gliomas*. Available at: https://clinicaltrials.gov/ct2/show/NCT01837862

Colombo, A. C., and Rodrigues, M. L. (2015). Fungal colonization of the brain: anatomopathological aspects of neurological cryptococcosis. *An. Acad. Bras. Cienc.* 87, 1293–1309. doi: 10.1590/0001-3765201520140704

Cruz, M. C., Bartlett, M. S., and Edlind, T. D. (1994). In vitro susceptibility of the opportunistic fungus *Cryptococcus neoformans* to anthelmintic benzimidazoles. *Antimicrob. Agents Chemother.* 38, 378–380. doi: 10.1128/AAC.38.2.378

Feldmesser, M., Kress, Y., Novikoff, P., and Casadevall, A. (2000). *Cryptococcus neoformans* is a facultative intracellular pathogen in murine pulmonary infection. *Infect. Immun.* 68, 4225–4237. doi: 10.1128/IAI.68.7.4225-4237.2000

Fernandez-Banares, F., Gonzalez-Huix, F., Xiol, X., Catala, I., Miro, J., Lopez, N., et al. (1986). Marrow aplasia during high dose mebendazole treatment. *Am. J. Trop. Med. Hyg.* 35, 350–351.

Fetterer, R. H., and Rew, R. S. (1984). Interaction of *Fasciola hepatica* with albendazole and its metabolites. *J. Vet. Pharmacol. Ther.* 7, 113–118. doi: 10.1111/j.1365-2885.1984.tb00886.x

Finn, R. D., Coggill, P., Eberhardt, R. Y., Eddy, S. R., Mistry, J., Mitchell, A. L., et al. (2016). The Pfam protein families database: towards a more sustainable future. *Nucleic Acids Res.* 44, D279–D285. doi: 10.1093/nar/gkv1344

Gardner, T. B., and Hill, D. R. (2001). Treatment of giardiasis. *Clin. Microbiol. Rev.* 14, 114–128. doi: 10.1128/CMR.14.1.114-128.2001

Goldman, D. L., Lee, S. C., Mednick, A. J., Montella, L., and Casadevall, A. (2000). Persistent *Cryptococcus neoformans* pulmonary infection in the rat is associated with intracellular parasitism, decreased inducible nitric oxide synthase expression, and altered antibody responsiveness to cryptococcal polysaccharide. *Infect. Immun.* 68, 832–838. doi: 10.1128/IAI.68.2.832-838.2000

Gottschall, D. W., Theodorides, V. J., and Wang, R. (1990). The metabolism of benzimidazole anthelmintics. *Parasitol. Today* 6, 115–124. doi: 10.1016/0169-4758(90)90228-V

Govender, N. P., Patel, J., van Wyk, M., Chiller, T. M., Lockhart, S. R., and Group for Enteric, Respiratory and Meningeal Disease Surveillance in South Africa (GERMS-SA) (2011). Trends in antifungal drug susceptibility of *Cryptococcus neoformans* isolates obtained through population-based surveillance in South Africa in 2002-2003 and 2007-2008. *Antimicrob. Agents Chemother.* 55, 2606–2611. doi: 10.1128/AAC.00048-11

Hankins, H. M., Baldridge, R. D., Xu, P., and Graham, T. R. (2015). Role of flippases, scramblases and transfer proteins in phosphatidylserine subcellular distribution. *Traffic* 16, 35–47. doi: 10.1111/tra.12233

Harnpicharnchai, P., Jakovljevic, J., Horsey, E., Miles, T., Roman, J., Rout, M., et al. (2001). Composition and functional characterization of yeast 66S ribosome assembly intermediates. *Mol. Cell* 8, 505–515. doi: 10.1016/S1097-2765(01)00344-6

Horsey, E. W., Jakovljevic, J., Miles, T. D., Harnpicharnchai, P., and Woolford, J. L. Jr. (2004). Role of the yeast Rrp1 protein in the dynamics of pre-ribosome maturation. *RNA* 10, 813–827. doi: 10.1261/rna.5255804

Hu, G., and Kronstad, J. W. (2010). A putative P-type ATPase, Apt1, is involved in stress tolerance and virulence in *Cryptococcus neoformans*. *Eukaryot. Cell* 9, 74–83. doi: 10.1128/EC.00289-09

Idnurm, A., Reedy, J. L., Nussbaum, J. C., and Heitman, J. (2004). *Cryptococcus neoformans* virulence gene discovery through insertional mutagenesis. *Eukaryot. Cell* 3, 420–429. doi: 10.1128/EC.3.2.420-429.2004

Kaitin, K. I. (2010). Deconstructing the drug development process: the new face of innovation. *Clin. Pharmacol. Ther.* 87, 356–361. doi: 10.1038/clpt.2009.293

Kaitin, K. I., and DiMasi, J. A. (2011). Pharmaceutical innovation in the 21st century: new drug approvals in the first decade, 2000-2009. *Clin. Pharmacol. Ther.* 89, 183–188. doi: 10.1038/clpt.2010.286

Krysan, D. J. (2015). Toward improved anti-cryptococcal drugs: novel molecules and repurposed drugs. *Fungal Genet. Biol.* 78, 93–98. doi: 10.1016/j.fgb.2014.12.001

Kwon-Chung, K. J., Fraser, J. A., Doering, T. L., Wang, Z., Janbon, G., Idnurm, A., et al. (2014). *Cryptococcus neoformans* and *Cryptococcus gattii*, the etiologic agents of cryptococcosis. *Cold Spring Harb. Perspect. Med.* 4:a019760. doi: 10.1101/cshperspect.a019760

Lanusse, C. E., and Prichard, R. K. (1993). Clinical pharmacokinetics and metabolism of benzimidazole anthelmintics in ruminants. *Drug Metab. Rev.* 25, 235–279. doi: 10.3109/03602539308993977

Martinez, L. R., and Casadevall, A. (2005). Specific antibody can prevent fungal biofilm formation and this effect correlates with protective efficacy. *Infect. Immun.* 73, 6350–6362. doi: 10.1128/IAI.73.10.6350-6362.2005

Martinez, L. R., and Casadevall, A. (2006). Susceptibility of *Cryptococcus neoformans* biofilms to antifungal agents in vitro. *Antimicrob. Agents Chemother.* 50, 1021–1033. doi: 10.1128/AAC.50.3.1021-1033.2006

Martinez, L. R., and Casadevall, A. (2007). *Cryptococcus neoformans* biofilm formation depends on surface support and carbon source and reduces fungal cell susceptibility to heat, cold, and UV light. *Appl. Environ. Microbiol.* 73, 4592–4601. doi: 10.1128/AEM.02506-06

Martinez, L. R., and Casadevall, A. (2015). Biofilm formation by *Cryptococcus neoformans*. *Microbiol. Spectr.* 3, doi: 10.1128/microbiolspec.MB-0006-2014

McKellar, Q. A., and Scott, E. W. (1990). The benzimidazole anthelmintic agents–a review. *J. Vet. Pharmacol. Ther.* 13, 223–247. doi: 10.1111/j.1365-2885.1990.tb00773.x

Meshulam, T., Levitz, S. M., Christin, L., and Diamond, R. D. (1995). A simplified new assay for assessment of fungal cell damage with the tetrazolium dye, (2,3)-bis-(2-methoxy-4-nitro-5-sulphenyl)-(2H)-tetrazolium-5-carboxanil ide (XTT). *J. Infect. Dis.* 172, 1153–1156. doi: 10.1093/infdis/172.4.1153

Micallef, C., Aliyu, S. H., Santos, R., Brown, N. M., Rosembert, D., and Enoch, D. A. (2015). Introduction of an antifungal stewardship programme targeting high-cost antifungals at a tertiary hospital in Cambridge, England. *J. Antimicrob. Chemother.* 70, 1908–1911. doi: 10.1093/jac/dkv040

Montresor, A., Gabrielli, A. F., Diarra, A., and Engels, D. (2010). Estimation of the cost of large-scale school deworming programmes with benzimidazoles. *Trans. R. Soc. Trop. Med. Hyg.* 104, 129–132. doi: 10.1016/j.trstmh.2009.10.007

Mor, V., Rella, A., Farnoud, A. M., Singh, A., Munshi, M., Bryan, A., et al. (2015). Identification of a new class of antifungals targeting the synthesis of fungal sphingolipids. *mBio* 6:e00647. doi: 10.1128/mBio.00647-15

Mosmann, T. (1983). Rapid colorimetric assay for cellular growth and survival: application to proliferation and cytotoxicity assays. *J. Immunol. Methods* 65, 55–63. doi: 10.1016/0022-1759(83)90303-4

Nosengo, N. (2016). Can you teach old drugs new tricks? *Nature* 534, 314–316. doi: 10.1038/534314a

Ostermann, H., Solano, C., Jarque, I., Garcia-Vidal, C., Gao, X., Barrueta, J. A., et al. (2014). Cost analysis of voriconazole versus liposomal amphotericin B for primary therapy of invasive aspergillosis among patients with haematological disorders in Germany and Spain. *BMC Pharmacol. Toxicol.* 15:52. doi: 10.1186/2050-6511-15-52

Park, B. J., Wannemuehler, K. A., Marston, B. J., Govender, N., Pappas, P. G., and Chiller, T. M. (2009). Estimation of the current global burden of cryptococcal meningitis among persons living with HIV/AIDS. *AIDS* 23, 525–530. doi: 10.1097/QAD.0b013e328322ffac

Pavlopoulos, A. (2011). Identification of DNA sequences that flank a known region by inverse PCR. *Methods Mol. Biol.* 772, 267–275. doi: 10.1007/978-1-61779-228-1_16

Rhein, J., Morawski, B. M., Hullsiek, K. H., Nabeta, H. W., Kiggundu, R., Tugume, L., et al. (2016). Efficacy of adjunctive sertraline for the treatment of HIV-associated cryptococcal meningitis: an open-label dose-ranging study. *Lancet Infect. Dis.* 16, 809–818. doi: 10.1016/S1473-3099(16)00074-8

Rizzo, J., Oliveira, D. L., Joffe, L. S., Hu, G., Gazos-Lopes, F., Fonseca, F. L., et al. (2014). Role of the Apt1 protein in polysaccharide secretion by *Cryptococcus neoformans*. *Eukaryot. Cell* 13, 715–726. doi: 10.1128/EC.00273-13

Rodrigues, J., Fonseca, F. L., Schneider, R. O., Godinho, R. M., Firacative, C., Maszewska, K., et al. (2015). Pathogenic diversity amongst serotype C VGIII and VGIV *Cryptococcus gattii* isolates. *Sci. Rep.* 5:11717. doi: 10.1038/srep11717

Rodrigues, M. L. (2016). Funding and innovation in diseases of neglected populations: the paradox of cryptococcal meningitis. *PLoS Negl. Trop. Dis.* 10:e0004429. doi: 10.1371/journal.pntd.0004429

Rodrigues, M. L., Alvarez, M., Fonseca, F. L., and Casadevall, A. (2008). Binding of the wheat germ lectin to *Cryptococcus neoformans* suggests an association of chitinlike structures with yeast budding and capsular glucuronoxylomannan. *Eukaryot. Cell* 7, 602–609. doi: 10.1128/EC.00307-07

Sacramento, C. Q., de Melo, G. R., de Freitas, C. S., Rocha, N., Hoelz, L. V., Miranda, M., et al. (2017). The clinically approved antiviral drug sofosbuvir inhibits Zika virus replication. *Sci Rep.* 7:40920. doi: 10.1038/srep40920

Short, C. R., Flory, W., Hsieh, L. C., and Barker, S. A. (1988). The oxidative metabolism of fenbendazole: a comparative study. *J. Vet. Pharmacol. Ther.* 11, 50–55. doi: 10.1111/j.1365-2885.1988.tb00120.x

Sloan, D. J., Dedicoat, M. J., and Lalloo, D. G. (2009). Treatment of cryptococcal meningitis in resource limited settings. *Curr. Opin. Infect. Dis.* 22, 455–463. doi: 10.1097/QCO.0b013e32832fa214

Subcommittee on Antifungal Susceptibility Testing of the EECfAST (2008). EUCAST definitive document EDef 7.1: method for the determination of broth dilution MICs of antifungal agents for fermentative yeasts. *Clin. Microbiol. Infect.* 14, 398–405. doi: 10.1111/j.1469-0691.2007.01935.x

Torp-Pedersen, A., Jimenez-Solem, E., Andersen, J. T., Broedbaek, K., Torp-Pedersen, C., and Poulsen, H. E. (2012). Exposure to mebendazole and pyrvinium during pregnancy: a Danish nationwide cohort study. *Infect. Dis. Obstet. Gynecol.* 2012:769851. doi: 10.1155/2012/769851

Veljkovic, V., and Paessler, S. (2016). Possible repurposing of seasonal influenza vaccine for prevention of Zika virus infection. *F1000Research* 5:190. doi: 10.12688/f1000research.8102.2

Voelz, K., and May, R. C. (2010). Cryptococcal interactions with the host immune system. *Eukaryot. Cell* 9, 835–846. doi: 10.1128/EC.00039-10

Xu, M., Lee, E. M., Wen, Z., Cheng, Y., Huang, W. K., Qian, X., et al. (2016). Identification of small-molecule inhibitors of Zika virus infection and induced neural cell death via a drug repurposing screen. *Nat. Med.* 22, 1101–1107. doi: 10.1038/nm.4184

Yadav, G., and Ganguly, S. (2015). Structure activity relationship (SAR) study of benzimidazole scaffold for different biological activities: a mini-review. *Eur. J. Med. Chem.* 97, 419–443. doi: 10.1016/j.ejmech.2014.11.053

Yoneda, A., and Doering, T. L. (2006). A eukaryotic capsular polysaccharide is synthesized intracellularly and secreted via exocytosis. *Mol. Biol. Cell* 17, 5131–5140. doi: 10.1091/mbc.E06-08-0701

Zhai, B., Wu, C., Wang, L., Sachs, M. S., and Lin, X. (2012). The antidepressant sertraline provides a promising therapeutic option for neurotropic cryptococcal infections. *Antimicrob. Agents Chemother.* 56, 3758–3766. doi: 10.1128/AAC.00212-12

**Conflict of Interest Statement:** The authors declare that the research was conducted in the absence of any commercial or financial relationships that could be construed as a potential conflict of interest.

Part of the data presented here is also the subject of a pending patent application (Ref.: BR1020170047300, National Institute of Industrial Property - INPI, Brazil).

The reviewer JNDAJ and handling Editor declared their shared affiliation, and the handling Editor states that the process nevertheless met the standards of a fair and objective review.

frontiers in Microbiology

ORIGINAL RESEARCH
published: 10 November 2016
doi: 10.3389/fmicb.2016.01798

# Hypovirulence of *Sclerotium rolfsii* Caused by Associated RNA Mycovirus

*Jie Zhong†, Dan Chen†, Hong J. Zhu, Bi D. Gao and Qian Zhou**

*Hunan Provincial Key Laboratory for Biology and Control of Plant Diseases and Insect Pests, Hunan Agricultural University, Changsha, China*

Mycoviruses associated with hypovirulence are potential biological control agents and could be useful to study the pathogenesis of fungal host pathogens. *Sclerotium rolfsii*, a pathogenic fungus, causes southern blight in a wide variety of crops. In this study, we isolated a series of dsRNAs from a debilitated *S. rolfsii* strain, BLH-1, which had pronounced phenotypic aberrations including reduced pathogenicity, mycelial growth and deficient sclerotia production. Virus-curing and horizontal transmission experiments that eliminated or transmitted, respectively, all dsRNA elements showed that the dsRNAs were involved in the hypovirulent traits of BLH-1. Ultrastructure examination also showed hyphae fracture and cytoplasm or organelle degeneration in BLH-1 hyphal cells compared to the virus-free strain. Three assembled cDNA contigs generated from the cDNA library cloned from the purified dsRNA indicated that strain BLH-1 was infected by at least three novel mycoviruses. One has similarity to the hypovirulence-associated Sclerotinia sclerotiorum hypovirus 2 (SsHV2) in the family *Hypoviridae*, and the other two are related to two different unclassified dsRNA mycovirus families. To our knowledge, this is the first report of *S. rolfsii* hypovirulence that was correlated with its associated dsRNA.

**Keywords: Mycovirus, hypovirulence, *Sclerotium rolfsii*, hypovirus, dsRNA**

OPEN ACCESS

***Edited by:***
*Joshua D. Nosanchuk, Albert Einstein College of Medicine, USA*

***Reviewed by:***
*Susana Rodriguez-Couto, Ikerbasque, Spain*
*Birinchi Kumar Sarma, Banaras Hindu University, India*

****Correspondence:***
*Qian Zhou*
*zhouqian2617@hunau.edu.cn*

*† These authors have contributed equally to this work.*

***Specialty section:***
*This article was submitted to Fungi and Their Interactions, a section of the journal Frontiers in Microbiology*

***Received:*** *01 August 2016*
***Accepted:*** *26 October 2016*
***Published:*** *10 November 2016*

***Citation:***
*Zhong J, Chen D, Zhu HJ, Gao BD and Zhou Q (2016) Hypovirulence of Sclerotium rolfsii Caused by Associated RNA Mycovirus. Front. Microbiol. 7:1798. doi: 10.3389/fmicb.2016.01798*

## INTRODUCTION

Mycoviruses (also denoted as fungal viruses) are widely described in major fungal groups, including most of the plant-pathogenic fungi (Ghabrial and Suzuki, 2009; Pearson et al., 2009; Xie and Jiang, 2014). All mycoviruses reported to date consist of double-stranded RNA (dsRNA), positive-sense single-stranded RNA (+ssRNA), the sole examples of negative-sense single-stranded RNA (-ssRNA), and single-stranded DNA (ssDNA) (Yu et al., 2010; Liu et al., 2014; Ghabrial et al., 2015). Generally, many mycoviruses are associated with latent infections in their fungal hosts. However, some mycoviruses can induce phenotypic aberrations or alterations, including hypovirulence and debilitation in their phytopathogenic fungal hosts. These mycoviruses are valuable for exploitation as biological agents to combat fungal diseases. In Europe, hypovirulent isolates of *Cryphonectria parasitica* infected by Cryphonectria hypovirus 1 (CHV1) have successfully been used to control chestnut blight caused by virulent strains of this pathogen (Nuss, 2005). Moreover, a hypovirulence-associated DNA virus, SsHADV1, also showed the ability to control Sclerotinia disease under field conditions (Yu et al., 2010, 2013), similar to Rosellinia necatrix megabirnavirus 1 (RnMBV1), which showed significant potential for

the biological control of apple white root rot disease (Chiba et al., 2009). Due to their potential use in biological control, studying the phenomenon of mycovirus-mediated hypovirulence is attractive for numerous researchers. In addition, the hypovirulence-associated mycoviruses, which have divergent molecular characteristics, will also enhance our understanding of virus diversity and evolution and contribute to the establishment of host-mycovirus systems (i.e., Cryphonectria parasitica-hypovirus, Helmintosporium victoriae-HvV190S, Sclerotinia sclerotiorum-mycovirus, Rosellinia necatrix-mycovirus, and Fusarium graminearum- mycovirus), which are beneficial for studying virus-host interactions including fungal and viral pathogenesis at the molecular level (Xie and Jiang, 2014; Wang et al., 2015).

*Sclerotium rolfsii* Sacc. [*Athelia rolfsii* (Curzi) Tu Kimbrough], a soil-borne fungus with a broad host range of more than 600 species (Rivard et al., 2010), is the causal agent of southern blight disease in a wide variety of crops. It forms brownish sclerotia that can survive in soil for long periods, making this disease difficult to control (Elad, 1995). Currently, the control of this serious plant disease is mainly based on the application of chemical pesticides; however, this strategy may give rise to fungicide resistance and environmental pollution. Consequently, screening for alternative environmentally friendly disease control measures, such as the use of mycoviruses possessing biological control potential, is attractive and significant. However, to date, no mycovirus has been reported for *S. rolfsii*.

In 2014, we isolated *S. rolfsii* strain BLH-1 from *Macleaya cordata*. When cultured on PDA and compared to other *S. rolfsii* strains isolated from other host plants, abnormal phenotypic traits in BLH-1, including slow growth, deficiency in sclerotia production and attenuation in pathogenicity, were occasionally found. In many cases, fungal phenotypic aberrations or alterations are attributed to mycovirus infection, by which we may explore novel biological control agents to combat the relevant plant pathogenic fungi. In addition, attenuated strains with abnormal phenotypic traits would be useful to study the pathogenesis of plant pathogens. In this study, we carried out experiments to (i) determine whether dsRNA mycoviruses were present in the attenuated *S. rolfsii* strain BLH-1, (ii) to determine the relationship between the dsRNAs and the discernible phenotypic changes of *S. rolfsii*, and (iii) to identify the molecular characteristics of partial dsRNA.

# MATERIALS AND METHODS

## Fungal Isolates and Culture Conditions

The *S. rolfsii* strain BLH-1 analyzed in this study was collected from a diseased *M. cordata* plant in the Hunan province of China and shared a series of dsRNA elements ranging from 1 to 15 kbp in size. Its identity was determined by rDNA-ITS sequencing, with the accession number KU885934. Derivative dsRNA-free isolates, represented by BLH-1-T1 and BLH-1-P1, were obtained from the paternal strain BLH-1 in hyphal tip culture and protoplast regeneration experiments, respectively. *S. rolfsii* strain LJ-01 was isolated from the roots of pepper plants infected by southern blight disease. All isolates and strains were cultured on potato dextrose agar (PDA) at 27°C.

## Curing of dsRNA

### Protoplast Regeneration

Spheroplasts were prepared by the method described in Moleleki et al. (2003) and Kanematsu et al. (2004), with minor modifications. Briefly, mycelial plugs from the actively growing PDA plate were transferred to potato dextrose (PD) broth with shaking (170 rpm) at 28°C for 7 days and then transferred to fresh PD with shaking culture for another 24 h. Mycelia were collected by filtering through four layers of gauze and washed once with osmoticum (0.7 M MgSO4). The mycelia were resuspended in a filter-sterilized enzyme-osmoticum mixture (containing 1% Snailase [Sigma], 1% Driselase [Sigma] and 0.1% Lysing Enzymes [Sigma]) and incubated at 28°C with gentle shaking for 4 h. Then, the cultures were filtered through a 120-μm pore size nylon mesh to remove debris. Protoplasts were precipitated by centrifugation at 3,000 × *g* for 10 min, washed twice with osmoticum, and resuspended in an appropriate volume of STC (1 M sorbitol, 50 mM Tris HCl [pH 8], 50 mM CaCl2). Final concentrations of the protoplast suspension were determined with a hemocytometer and maintained on ice. Finally, portions (200 μl) of the spheroplast preparation were gently mixed with 20 ml dissolved regeneration medium (1 g of casein hydrolysate per liter, 1 g of yeast extract per liter, 342 g of sucrose per liter, 16 g of agar per liter) in petri dishes and incubated at 27°C in the dark for 1–2 days. Blocks of agar from the edges of each single colony were collected and placed in fresh PDA plates.

### Hyphal Tip Isolation

Firstly, mycelial plugs were grown on PDA plates at 27°C for 2 days in the dark. Then, tips from single hyphae were removed from the colony margin with the aid of a dissecting microscope and transferred onto fresh PDA for four more cycles of hyphal tip isolation and culture. All regenerated isolates were randomly transferred to PD broth culture for mycelial collection and subjected to dsRNA extraction to detect mycovirus infection.

## Horizontal Transmission of Hypovirulence and the Associated dsRNAs

To determine if the hypovirulent trait of *S. rolfsii* BLH-1 was associated with dsRNA elements and was transmissible through hyphal anastomosis, pairing culture experiments for horizontal transmission were conducted (Wu et al., 2007, 2012). The dsRNA-containing hypovirulent strain BLH-1 was used as the donor, and virus-free virulent strains BLH-1-P1 and LJ-01 were recipients. Mycelial plugs of the two donor and recipient combinations (BLH-1/BLH-1-P1; BLH-1/LJ-01) were individually cultured 1 cm apart on a PDA dish. Mycelial agar plugs were taken from the edge of each colony of the two recipients (BLH-1-P1 and LJ-01) to obtain recipient derivative isolates.

To test if the dsRNAs could be transmitted horizontally to other fungal species, *Botrytis cinerea* strain HM-03 and

*Sclerotinia sclerotiorum* strain JH-05 were individually cultured using the pairing culture technique with BLH-1 on a PDA plate as described above. Each of the recipient derivative isolates was incubated in PDA and subjected to detection for the presence of dsRNA.

## Pathogenicity Assay

Pathogenicity tests were conducted on potato (*Solanum tuberosum*) and pepper (*Capsicum annuum*) to evaluate the virulence of the *S. rolfsii* strains. The stems of these seedling plants were needle-pricked in the center near the root and covered by mycelial plugs (0.5 mm in diameter) that were removed from the colony margin of PDA cultures of each strain. Control seedlings were mock-inoculated with sterile PDA plugs without mycelia growing in them. Alternatively, the plants were inoculated by diapiric injection of the stems near the root using toothpicks covered with mycelium produced by co-culture of autoclave-sterilized toothpicks and fungal strains on PDA plates. In the same way, diapiric injections with only autoclave-sterilized toothpicks were conducted as controls. All inoculations were individually sealed by wrapping them with absorbent cotton and kept in a greenhouse at 27°C and 80% relative humidity. Lesion length on each inoculated plant was measured after the disease symptoms developed 5–8 days post-inoculation. These tests were repeated once, with each having three replications. The fungal strains were re-isolated, and the presence of dsRNA was checked by dsRNA extraction and agar gel electrophoresis as described above.

## Comparisons of Mycelial Growth and Colony Morphology

Colony morphology and growth rates of the original virus-infected strain BLH-1 and the putatively virus-free derivative isolate BLH-1-P1 were compared by growing on PDA plates under the same culture conditions at 27°C. For these comparisons, mycelial agar plugs were picked from the colony margins of 2-day-old PDA cultures of each strain and transferred to the center of petri dishes containing 15 ml PDA. The colony diameter of each dish was measured daily, from 1 day after incubation until the mycelium had covered the entire plate. The colony morphology and formation of sclerotia were examined at approximately 5 and 14 days, respectively. The formula RGR $(\text{cm/day}) = (D3 - D2)/2$ was used to calculate the mycelial growth rate, where D2 and D3 represent the diameters of 2- and 3-day-old colonies in each dish, respectively. These tests were repeated once with each strain cultured for five dishes (replicates).

## Enzyme Activity Assays

Assays for laccase activity were conducted by adding 0.01% 2,2-Azino-bis 3-ethylbenzthiazoline-6-sulfonic acid (ABTS) to the PDA plate (Guetsky et al., 2005). Laccase activity was indicated by formation of green color after mycelial agar plugs had been transferred to the agar plate. Laccase activity was also assayed using mycelial culture filtrate dropped upon holes in an agar plate containing 0.01% ABTS. The culture filtrates were prepared by culturing the fungal strains in PDB (50 ml) on a shaker (180 rpm) at 27°C for 5 days and then filtered through a filter paper. The laccase activity was also indicated by formation of green color around the holes in agar plate where culture filtrates were dropped.

Colony surface hydrophobicity was tested using bromophenol blue as described by Yu J. et al. (2015). A 15-μl droplet of water containing bromophenol blue was added to fungal colonies of dsRNA-free and dsRNA-infected strains cultured on PDA agar.

For cellulase activity assays, mycelial agar plugs were cultured on PDA containing 20 g/l carboxymethyl cellulose sodium salt for 2 days and then stained with Congo red (Liao et al., 2012). We regard the diameter of a bright yellow color as an indicator of cellulase activity.

Acid-producing ability was tested by placing mycelial agar plugs on PDA containing 0.01% (wt/vol) bromophenol blue for 5 days (Xiao et al., 2014). The appearance of yellow in the culture medium was regarded as an indicator of acid production.

Quantitatively assay of the oxalic acid production was performed using the method described previously. Mycelial agar plugs of the two fungal strains were inoculated in PD with shaking at 150 rpm at 27°C for 5 days. Culture filtrates were retrieved from three flasks of each strain and subjected to pH assesse. The concentration of oxalic acid was determined using high-performance liquid chromatography (Xiao et al., 2014).

## Scanning Electron Microscopy (SEM) and Transmission Electron Microscopy (TEM)

Scanning electron microscopy was used for hyphal surface structure examination of the hypovirulent strain BLH-1 and virus-free virulent strain BLH-1-P1. The mycelia used for ultrathin sections of the two strains were collected from the 5-day cultured PDA petri dish. Samples were dehydrated with a graded series of acetone (30, 50, 70, 80, 90, and 100%; vol/vol), mounted on stubs, sputter coated as previously described (Li Y. et al., 2011), and then examined with a scanning electron microscope.

Subcellular characteristics of the two strains were also examined by TEM. Mycelia were collected from a sterilized coverslip inserted in a PDA petri dish and cultured with fungal strains for 5 days. The mycelial specimens were fixed and dehydrated using conventional procedures described previously (Wu et al., 2007). Ultrathin sections (50–60 nm in thickness) for the mycelial specimens were cut using a diamond knife, mounted on slotted, formvar-coated grids and stained with 5% aqueous lead citrate and 5% uranyl acetate. Finally, the ultrathin sections were examined under TEM.

## Extraction of dsRNA

The presence of dsRNA molecules can represent the genomes of dsRNA mycoviruses or the replicative forms of single-stranded RNA (ssRNA) mycoviruses. Extraction of dsRNAs from mycelia of each fungal strain was conducted using the cellulose chromatography method described by Morris and Dodds (1979). Mycelial mass was collected from PD broth culture in an orbital shaker at 110 rpm for 4 to 7 days at 27°C and by filtration through

four layers of cheesecloth, followed by washing with distilled water. Then, the dsRNAs were extracted and verified when sequentially treated with RNase-free DNaseI and S1 nuclease at 37°C for 30 min. The dsRNA size was estimated by 1% agarose electrophoresis and staining with 0.5 μg/ml ethidium bromide under UV.

## cDNA Synthesis, Cloning, and Sequence Analyses

We used cDNA library synthesis to partially characterize the dsRNAs from the hypovirulent strain BLH-1 based on the method described previously (Zhang et al., 2014). DsRNAs were purified from electrophoresed agarose gel and then served as a template to generate cDNA fragments with random hexanucleotide primers and reverse transcriptase. After the initial round of sequencing, sequence gaps that were not covered were filled by RT-PCR amplification using designed primers based on the obtained cDNA sequences flanking the gaps. All amplified cDNA products were cloned into the pMD18-T vector (TaKaRa) and sequenced at least three independent times for every base. Homology searches were conducted using the BLAST program against the National Center for Biotechnology Information (NCBI) databases[1]. Multiple sequence alignments were carried out using the ClustalX program (Larkin et al., 2007). A phylogenetic tree was made based on sequence alignment using the neighbor-joining (NJ) method, with a bootstrap test of 1,000 re-samplings in MEGA 6 (Tamura et al., 2013).

# RESULTS

## Strain BLH-1, Which Lost the Capacity to Produce Sclerotia, Carries dsRNA Elements

The *S. rolfsii* strain BLH-1 produced no sclerotia when cultured on PDA for more than 6 months, whereas the other *S. rolfsii* strain, LJ-01, contained no dsRNA element that can form sclerotia, an *S. rolfsii* trait. Some abnormal phenotypic traits in plant pathogenic fungus, such as deficiency in sclerotial production, were caused by mycovirus. Therefore, we tested for mycovirus infection in this abnormal strain BLH-1. By screening for the presence of dsRNAs using the cellulose chromatography method, strain BLH-1 was found to harbor 8–10 dsRNA segments ranging in size from 1 to 15 kbp (**Figure 1**). The dsRNA extractions were confirmed to be dsRNA due to their insusceptibility to enzyme digestion with S1 nuclease and Dnase I, as well as the extraction methods through CF11 cellulose column chromatography.

## Curing of dsRNA

To investigate the influence of these dsRNAs in their host fungus, we conducted protoplast regeneration and hyphal tip isolation experiments to eliminate the dsRNAs from host fungus. We obtained 30 protoplast-regenerated strains. Among these, some isolates showed similar colony morphology as their paternal strain BLH-1, whereas others showed different culture traits, such as having looser hyphae growing radially on PDA. The colony morphology and the dsRNA detection results (**Figures 2A,B**) displayed a correspondence between the colony morphology of loosely growing hyphae and negative results of dsRNA presence.

The hyphal tips cut from the colony margin were subjected to culture, and sequential hyphal tips were isolated up to six generations. Colony traits in PDA became looser after hyphal tip isolation had been conducted four times (**Figures 2C,D**). The dsRNA detection also showed the elimination of dsRNA from the four-generation culture.

Surprisingly, in the virus curing experiments, all dsRNAs were consistently eliminated, either from hyphal tip culture or protoplast regeneration, as no isolate contained only partial dsRNA segments. In this study, we selected strain BLH-1-P1, a derivative dsRNA-free isolate obtained by protoplast regeneration, for further analysis.

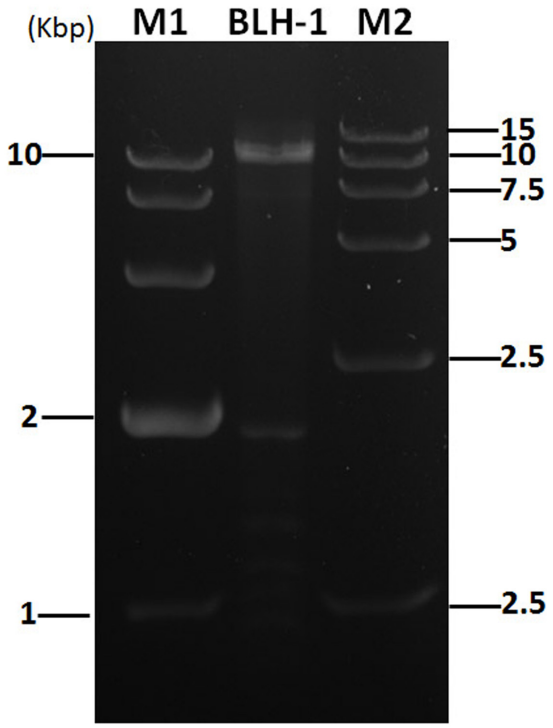


**FIGURE 1 | dsRNA segments extracted from strain BLH-1 using the cellulose chromatography method were agarose gel-electrophoresed on 1% agarose before being digested with S1 nuclease and Dnase I to eliminate contaminated ssDNA and ssRNA.** M1 and M2 represent the 10 and 15 kbp DNA markers, respectively.

## Presence of dsRNA Is Associated with Phenotypic Alterations

We compared the biological traits between the hypovirulent strain BLH-1 and the dsRNA-free derivative BLH-1-P1 in terms of colony morphology, growth rate, sclerotia formation and virulence (**Figure 3**).

[1]http://www.ncbi.nlm.nih.gov/genomes

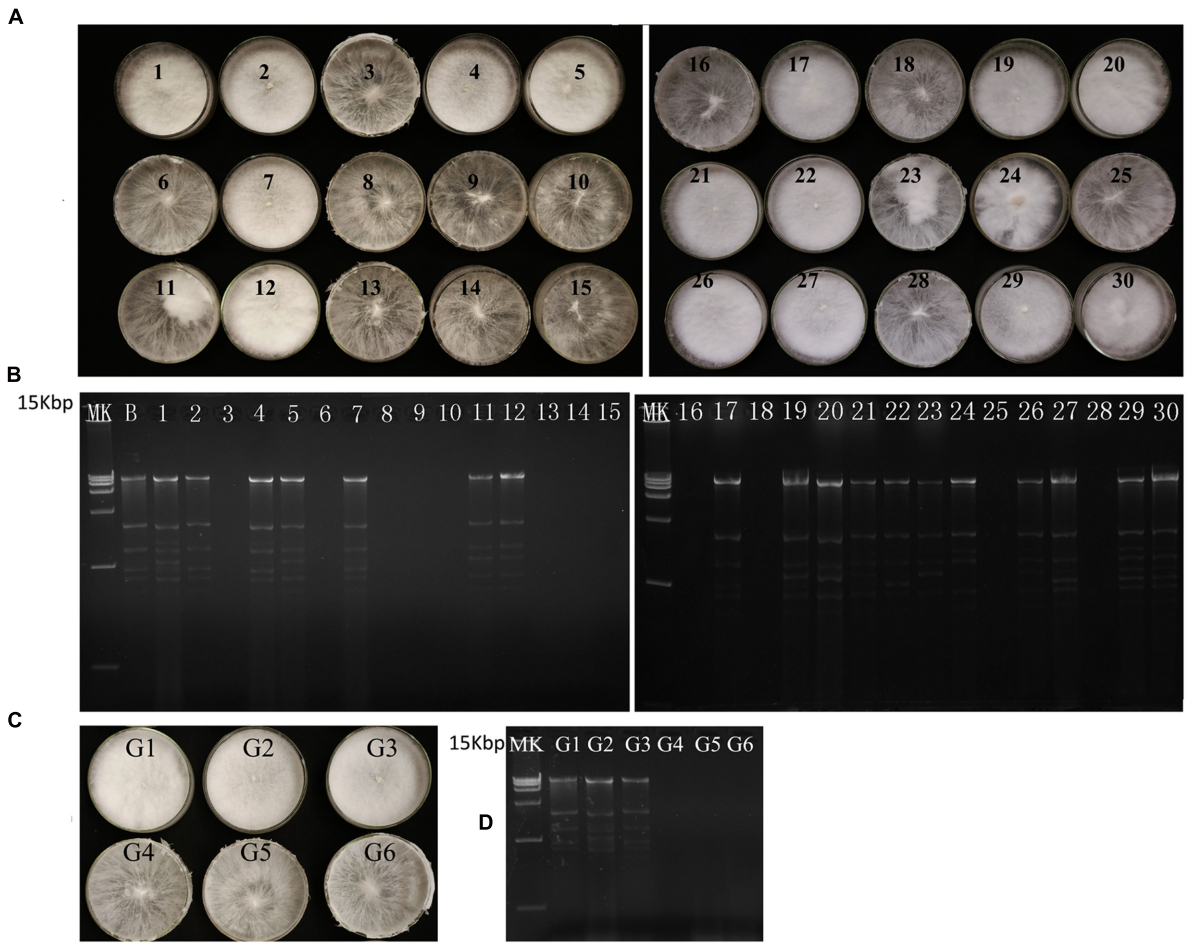


**FIGURE 2 | Colony morphology and dsRNA detection results of the BLH-1 derivative isolates generated during virus curing. (A)** Colony morphology of the BLH-1 derivative isolates obtained from protoplast regeneration. **(B)** dsRNA detection of these protoplast regenerating isolates. **(C)** Colony morphology of the BLH-1 derivative isolates obtained by hyphal tip isolation up to six consecutive generations represented by G1–G6. **(D)** dsRNA extraction from the G1 to G6 derivative isolates. No dsRNA can be extracted from the fourth generation of hyphal tip isolation.

Strain BLH-1, showing a much smaller colony size on PDA, was morphologically distinguishable from strain BLH-1-P1 (**Figure 3A**). In addition, when examined by light microscopy, the hyphal integrity of BLH-1-P1 was normal. However, the hyphae of BLH-1 were more contorted than those of BLH-1-P1 and were broken into small fragments (**Figure 3C**).

Significant differences in mycelial growth rates were detected. BLH-1 has a greater growth rate (29.83 mm/day) than BLH-1-P1 (19.12 mm/day) (**Figure 3E**).

BLH-1-P1 sclerotia initially formed after incubation for 3–4 days; brown sclerotia of 1–2 mm in diameter and with smooth surfaces were observed on each PDA plate containing almost eight grains when cultured for 8–12 days (**Figure 3B**). In contrast, no sclerotia could be found on the colonies of strain BLH-1, even when incubated for 6 months.

In the pathogenicity test, strain BLH-1-P1, within which detectable dsRNAs were lacking, caused extensive symptoms suggestive of southern blight (also called southern wilt, southern stem rot or white mold) on pepper (*Capsicum annuum*). When inoculated with BLH-1-P1, fungal threads (cobweb-like mats) expanded from the site of inoculation and rapidly covered the stem, resulting in an average lesion length of 33.00 cm. However, the dsRNA-containing strain BLH-1 merely caused small stem rot lesions confined to the inoculation site, with an average length of 7.17 cm (**Figures 3D,F**).

## Transmission of dsRNA and Hypovirulence Following Hyphal Anastomosis

We used the pairing culture technique to further confirm the effects of these dsRNA segments on the BLH-1 host and the transmissibility of the hypovirulent traits. The hyphae of the donor strain BLH-1 were fused with the recipients of BLH-1-P1, *S. rolfsii* strain LJ-01 isolated from pepper, *Botrytis cinerea* strain HM-03, and *S. sclerotiorum* strain JH-05.

The pairing culture experiments between *S. rolfsii* strains included five types of cultures, as shown in **Figure 4**: two

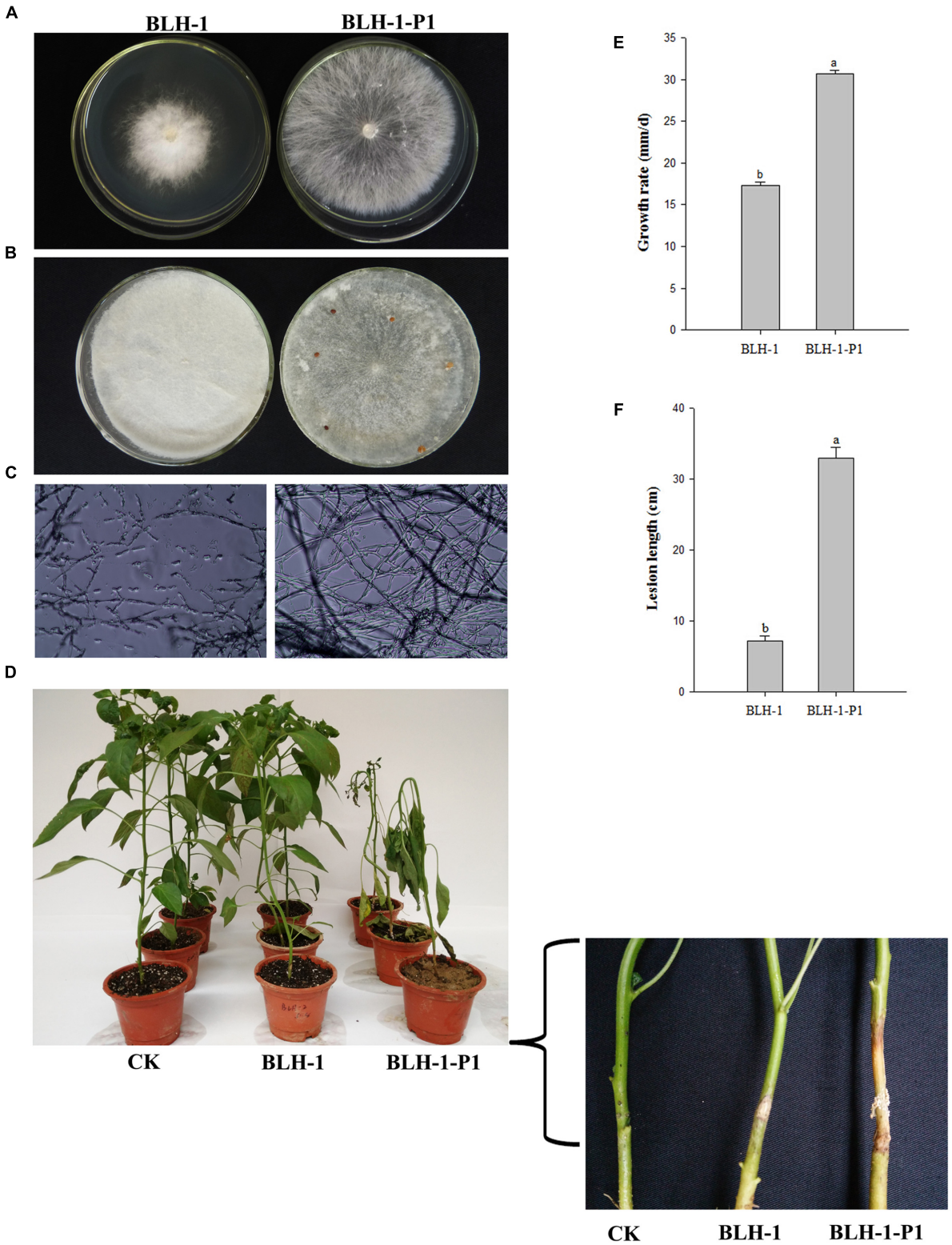


**FIGURE 3 | Biological properties of *Sclerotium rolfsii* strain BLH-1 and its dsRNA-free derivative strain BLH-1-P1. (A)** Colony morphology of strains BLH-1 and BLH-1-P1 grown on PDA for 5 days at 27°C. **(B)** Sclerotia were produced in strain BLH-1 instead of BLH-1-P1 when cultured for 14 days. **(C)** Microscopy morphology examination of the 5-day-old hyphae of strains BLH-1 and BLH-1-P1. The pictures are captured at 400× magnification **(D)** Virulence assay on pepper (*Capsicum annuum*). The stems near the roots of the pepper plant seedlings were needle-pricked and inoculated by mycelial plugs. The morbidity situation was photographed after inoculation at 27°C for 5–8 days. **(E)** Average mycelial growth rates of strains BLH-1 and BLH-1-P1 on PDA at 27°C. **(F)** Average lesion length caused by strains BLH-1 and BLH-1-P1 on pepper seedling stems.

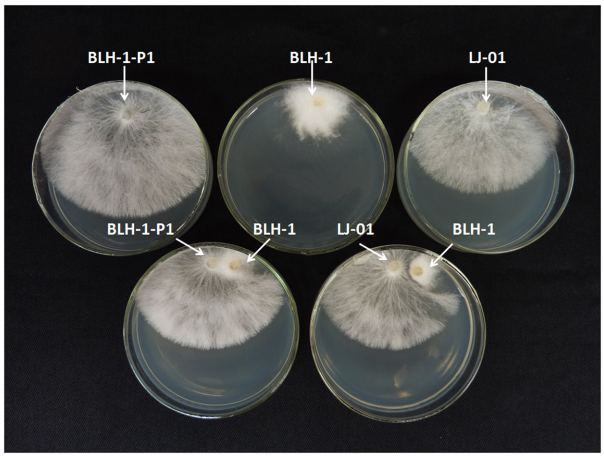


**FIGURE 4 | Transmission of dsRNA elements from the hypovirulent prototype strain BLH-1 (the donor) to dsRNA-curing strain BLH-1-P1 and other wild type dsRNA- free strain LJ-01 (the recipient) on PDA using contact culture.** Mycelial plugs from the BLH-1/BLH-1-P1 and BLH-1/LJ-01 combinations were individually cultured 1 cm apart on a PDA dish. Recipient derivative isolates were obtained by picking mycelial agar plugs from the edge of each colony of the two recipients.

double-strain contact cultures, BLH-1/BLH-1-P1 and BLH-1/LJ-01, and three single-strain cultures: BLH-1, BLH-1-P1, and LJ-01. The virulent strains BLH-1-P1 and LJ-01 grew rapidly on PDA in the single cultures, but the hypovirulent strain BLH-1 grew slowly and covered approximately one-quarter of the plate. In the contact cultures (BLH-1/BLH-1-P1 and BLH-1/LJ-01), the recipients BLH-1-P1 and LJ-01 still grew rapidly. However, a boundary formed between BLH-1 and LJ-01 in their contact culture plate, indicating a possible vegetative incompatibility reaction. Three mycelial derivative isolates of strain BLH-1-P1 and LJ-01 were obtained from the BLH-1-P1 and LJ-01 sides in each of the contact cultures. All of the dsRNA segments were detected in the derivative isolates from BLH-1-P1 but not from strain LJ-01. The dsRNAs in BLH-1 could be reintroduced to BLH-1-P1 but could not be transmitted to LJ-01 (**Figure 5B**). The representative BLH-1-P1 derivative isolate, named BLH-1-P1-R1, was similar to the hypovirulent strain BLH-1 and differed greatly from their parental strain BLH-1-P1 regarding the reduced virulence, which was tested by inoculation on potato (*S. tuberosum*) (**Figures 5C,D**), and deficient in sclerotia production (**Figure 5A**). In contrast, mycelial derivative isolates of strain LJ-01 were similar to their parental strain LJ-01, both in mycelial growth rate and colony morphology (date not shown), and can produce sclerotia (**Figure 5A**). The transmission experiments suggested that these dsRNA elements in BLH-1 could be horizontally re-introduced to BLH-1-P1 but could not be transmitted to LJ-01, and they are likely responsible for the hypovirulence phenotype of strain BLH-1.

In the pairing culture experiments between *S. rolfsii* strain BLH-1 and *B. cinerea* strain HM-03 or *S. sclerotiorum* strain JH-05, three mycelial derivative isolates of *B. cinerea* strain HM-03 and three mycelial derivative isolates of the *S. sclerotiorum* strain JH-05 were obtained from the recipient colonies of strain HM-03 and JH-05, respectively, in the contact cultures. All of the derivative isolates of HM-03 and JH-05, as well as their corresponding parental strains, showed similar colony morphology and contained no dsRNA when detected by dsRNA extraction (Supplementary Figure S1). Therefore, by hyphal contact, the dsRNAs in strain BLH cannot be horizontally transmitted to other fungal species, such as *B. cinerea* and *S. sclerotiorum*.

## Ultrastructure Examination

Scanning electron microscopy was used to examine the ultra-micro mycelial morphology of the dsRNA-containing BLH-1 and dsRNA-free BLH-1-P1 strains. Significant differences in the mycelial morphology between the two strains were observed. The hyphae of BLH-1 become shriveled and formed fractured fragments. In contrast, the hyphae of BLH-1-P1 had a glabrate surface, which appeared to be full and integrated, displaying few small fragments. Certainly, the phenomenon of hyphae fracture was also more clearly observed by the light microscope using microscopic sections from 5-day-cultured hyphae (**Figure 6**).

Ultrathin hyphal sections for each strain of BLH-1 and BLH-1-P1 were observed under TEM (**Figure 7**). Comparison of the ultrastructure of hyphal cells showed that the cytoplasm and mitochondria differed greatly between the two strains. The cytoplasm of BLH-1 was degenerated and formed vacuole-like membranous structures and small membranous vesicles, similar to the hypha of some mycovirus-infected fungi. Moreover, virus-like particles with a size under 100 nm were observed in the hyphal cells of BLH-1 (**Figure 7E**). In comparison, the virulent isolate BLH-1-P1 exhibited a relatively electronically dense and evenly distributed cytoplasm, with fewer membranous vacuoles or vesicles formed in hyphal cells (**Figures 7B,D,F**). Ultrastructure of mitochondria showed that BLH-1-P1 contained numerous mitochondria with normal oval or oblong shape (**Figure 7D**). The mitochondria in BLH-1 were significantly fewer and became swollen, exhibiting degradation syndrome (**Figure 7C**).

## Enzyme Activity Assays

Some reports suggested that laccase activity might be involved in fungal virulence (Ahn and Lee, 2001). We compared the laccase activities between strains BLH-1 and BLH-1-P1. The two strains growing on PDA plates containing ABTS produced a green color reaction, indicating the presence of laccase activity in each culture. However, the color reaction was more clearly observed in strain BLH-1-P1 than in the virus-infected strain BLH-1. When assayed using mycelial culture filtrate dropped upon holes on the ABTS containing PDA plates, the virus-cured strain BLH-1-P1 also showed higher laccase activity (**Figure 8A**). As the hydrophobicity of a fungal colony may reflect the cell wall integrity of fungal hyphae (Yu J. et al., 2015), we used a 15-μl droplet of water containing bromophenol blue to measure the hydrophobicity of the hyphal surfaces of the two strains. Unexpectedly, spherical droplets formed on both strains, and there was no significant difference in hydrophobicity between the two strains (**Figure 8B**). To examine cellulase activities, the

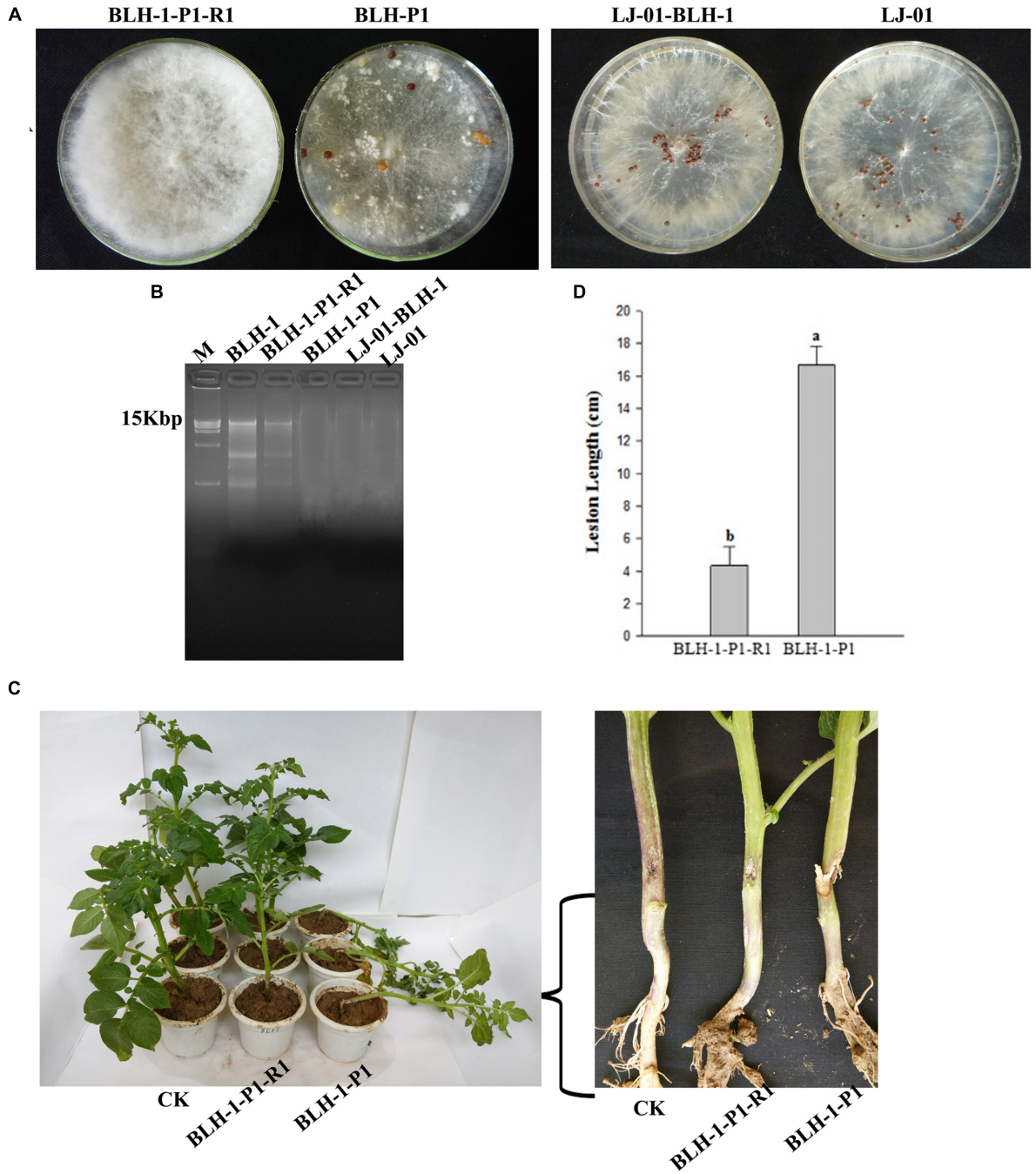


**FIGURE 5 | Comparison of the biological characteristics between the recipient derivative isolates and their parental strains. (A)** Fungal colony morphology and sclerotia formation of strains BLH-1-P1, LJ-01, BLH-1-P1-R1 and BLH-01-BLH-1, the latter of which were derived from the colony margins of the recipient strains BLH-1-P1 and LJ-01, respectively. These strains were grown on PDA at 27°C for 14 days. **(B)** The results of dsRNA detection of the four strains based on 1% agarose gel electrophoresis analysis. **(C)** Virulence tests of the dsRNA-reobtaining strain BLH-1-P1-R1 and the parental dsRNA-free strain BLH-1-P1 on potato (*Solanum tuberosum*). **(D)** Lesion diameters caused by strains BLH-1-P1-R1 and BLH-1-P1 were measured after inoculation for 5–8 days.

transparent circles around the fungal colonies, which indicate the capacity to degrade carboxymethyl cellulose, were obvious in BLH-1-P1 but not apparent in BLH-1 colonies (**Figure 8C**).

The PDA containing 0.01% (wt/vol) bromophenol blue became yellow during hyphal extension of the two strains after they had been cultured for 5 days. However, the degree of yellow in strain BLH-1-P1 was significant larger and obvious than that in strain BLH-1 (**Figure 8D**). Because the yellow would form if the pH decreased in the bromophenol blue-containing PDA, we can infer that both strains produced acid, with the virus-cured

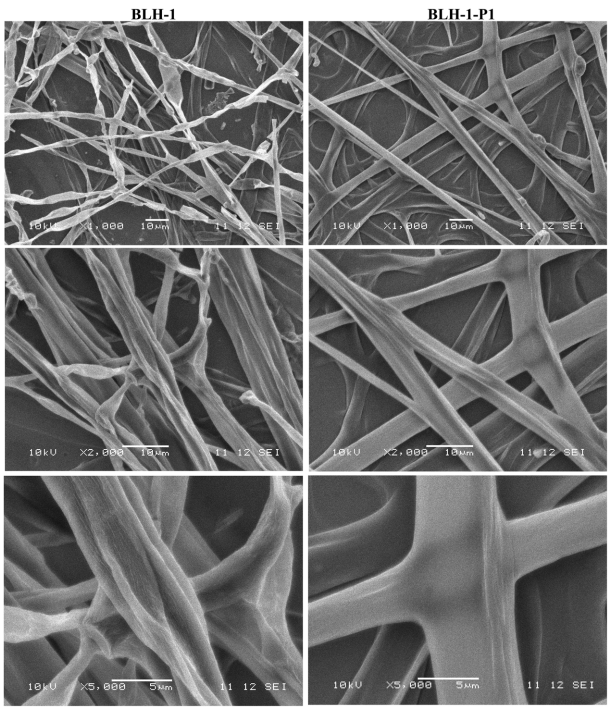


**FIGURE 6 | Electron micrographs of hyphal morphology of the dsRNA-containing strain BLH-1 and dsRNA-free strain BLH-1-P1.** The (top, middle, and lower panels) are photographs captured at 1000× (scale bar: 10 μm), 2000× (scale bar: 10 μm) and 5000× (scale bar: 5 μm) magnification. The images were taken from the ultrathin sections of hyphae collected from the actively growing margins of colonies cultured for 5 days on PDA at 27°C.

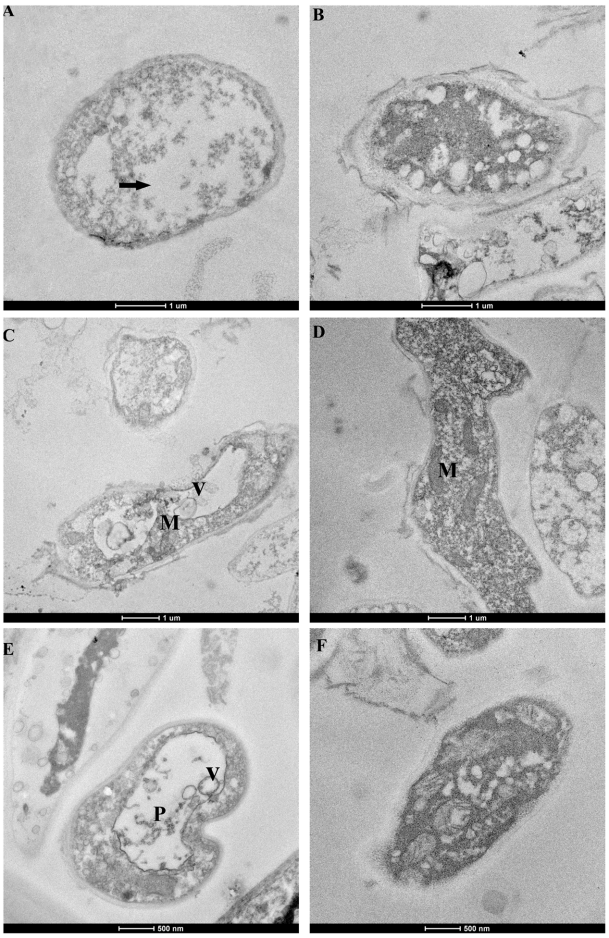


**FIGURE 7 | Cytoplasmic characteristics of the dsRNA-containing hypovirulent strain BLH-1 (A,C,E)** and the dsRNA-free virulent strain BLH-1-P1 **(B,D,F)** examined by TEM. **(A)** Hyphal cells of BLH-1 were degenerated, showing electron-sparse and unevenly distributed cytoplasm, indicated by arrow. **(C)** BLH-1 had significantly fewer mitochondria (indicated by M) with swollen shape, whereas BLH-1-P1 **(D)** contained numerous oval or oblong mitochondria. **(E)** Virus-like particles with sizes under 100 nm (indicated by P), and abundant vacuole-like membranous structures or small membranous vesicles (indicated by V) were observed in the hyphal cells of BLH-1. **(F)** Strain BLH-1-P1 shared dense and evenly distributed cytoplasm as that shown in **(B)**. Note: scale bars for pictures **(A–D)** were 1 μm and for **(E,F)** were 500 nm.

strain BLH-1-P1 producing more at this time point. However, the PDA of the two strains become yellow when cultured for a longer time (**Figure 8D**). The result indicated that both the two *S. rolfsii* strains of BLH-1 and BLH-1-P1 have the ability to produce acid, and the difference in acid-producing ability between the two strains in different culture time might be ascribed to difference in mycelial growth rate. The pH value of BLH-1 was slightly larger than that of BLH-1-P1(2.26 vs. 2.20) (**Figure 8E**), the oxalic acid yield of strain BLH-1 (649.76 mg/g of dry mycelia) quantitative assayed from the 5-day-old cultures grown in PD was significantly higher than that of strain BLH-1-P1 (212.74 mg/g) (**Figure 8F**).

## Partial Sequence Analysis of the dsRNAs Associated with BLH-1

A cDNA library was synthesized using dsRNAs from the hypovirulent strain BLH-1. After the first round of sequencing, sequence-specific primers were designed and used to fill the gaps between the cDNA clones. Consequently, three assembled cDNA contigs were obtained, named contig 1, contig 2, and contig 3. The nucleotide sequences of the contigs have been deposited in GenBank under the accession numbers KU885931, KU885932, and KU885933.

Contig 1 (3558 bp) was predicted to encode a protein with similarity to members of the family *Hypoviridae*. Significant hits included Sclerotinia sclerotiorum hypovirus 2 (SsHV2), Macrophomina phaseolina hypovirus 1 and Cryphonectria hypovirus 1; SsHV2 had the maximum amino acid similarity of 54% at query coverage of 99%. We suggested that contig 1 likely represented the partial genome sequences of a novel hypovirus related to SsHV2. Contig 2 (2781 bp) had sequence identities ranging from 32 to 33%, with query coverage of more than 90%, to the putative RNA-dependent RNA polymerase of Sclerotinia sclerotiorum dsRNA mycovirus-L (SsNsV-L) (Liu et al., 2012), Fusarium graminearum dsRNA

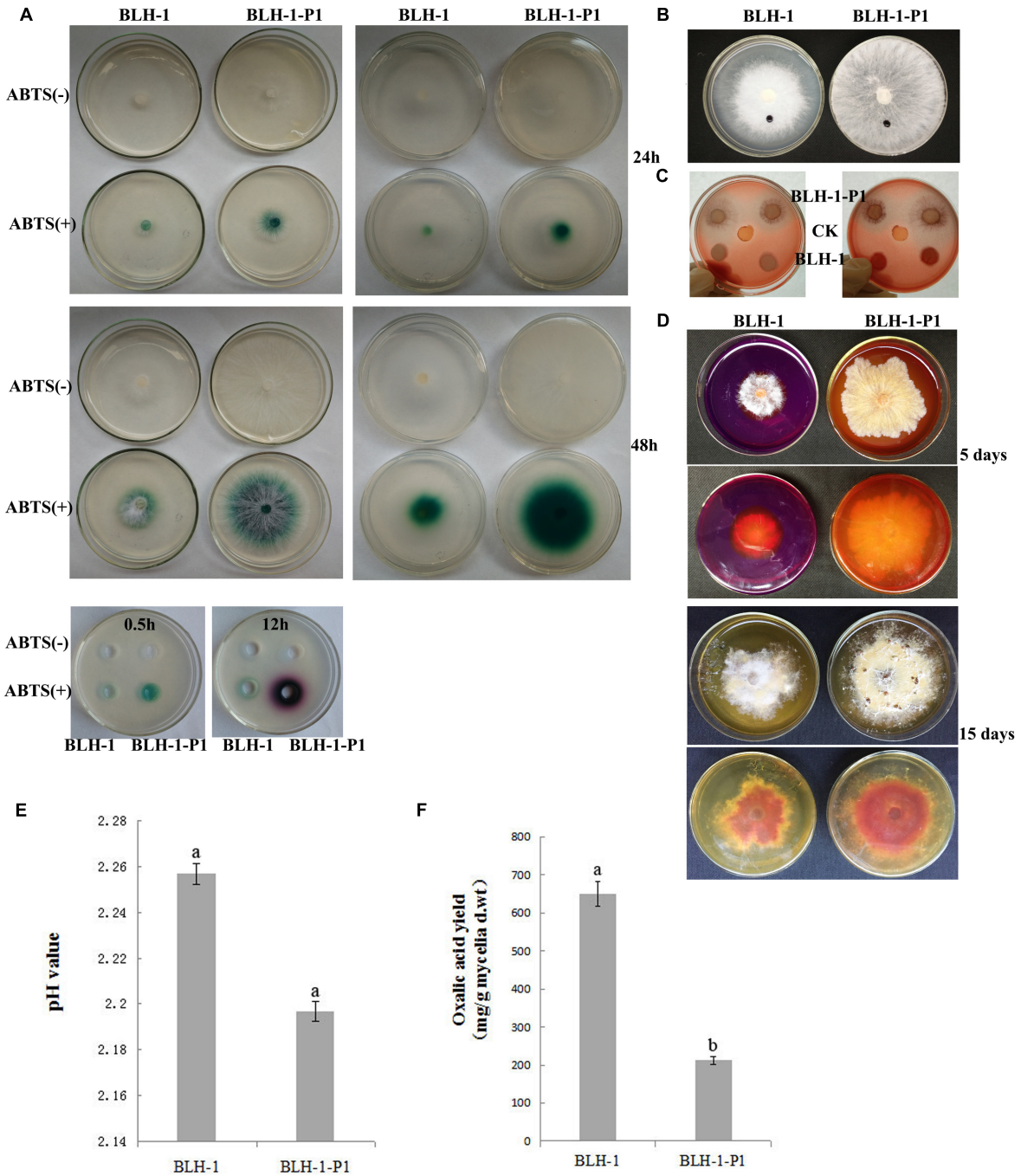


**FIGURE 8 | Assays for laccase activity, cellulase activity, acid-producing ability, ambient pH, yield of oxalic acid and the colony surface hydrophobicity. (A)** Laccase activity was tested after placing mycelial agar plugs on PDA containing ABTS for 24 and 48 h. It was also assayed using mycelial culture filtrate dropped upon holes on the same PDA agar. The images were collected after the culture filtrates were dropped for 0.5 and 12 h. **(B)** Colony surface hydrophobicity test using bromophenol blue. **(C)** Cellulase activity assays of the two strains by examination of the formation of bright yellow color around the fungal colonies. **(D)** Acid-producing ability was evaluated by culturing the mycelial agar plugs on PDA containing 0.01% bromophenol blue for 5 and 15 days, respectively; acid production was indicated by appearance of yellow in the culture medium. **(E)** pH values of cultures of strains BLH-1 and BLH-1-P1 that inoculated in PD for 5 days. **(F)** The amount of oxalic acid produced by the strains of BLH-1 and BLH-1-P1 were assessed by high-performance liquid chromatography.

mycovirus-3 (FgV3) (Yu et al., 2009) and Botrytis cinerea RNA virus 1(BcRV1) (Yu L. et al., 2015). Multiple protein sequence alignments and comparisons demonstrated that contig 2 encoded a protein with an RdRP_4 superfamily domain (cl19931) that contained conserved motifs characteristic of the RdRps of dsRNA mycoviruses (**Figure 9A**). Thus, we proposed

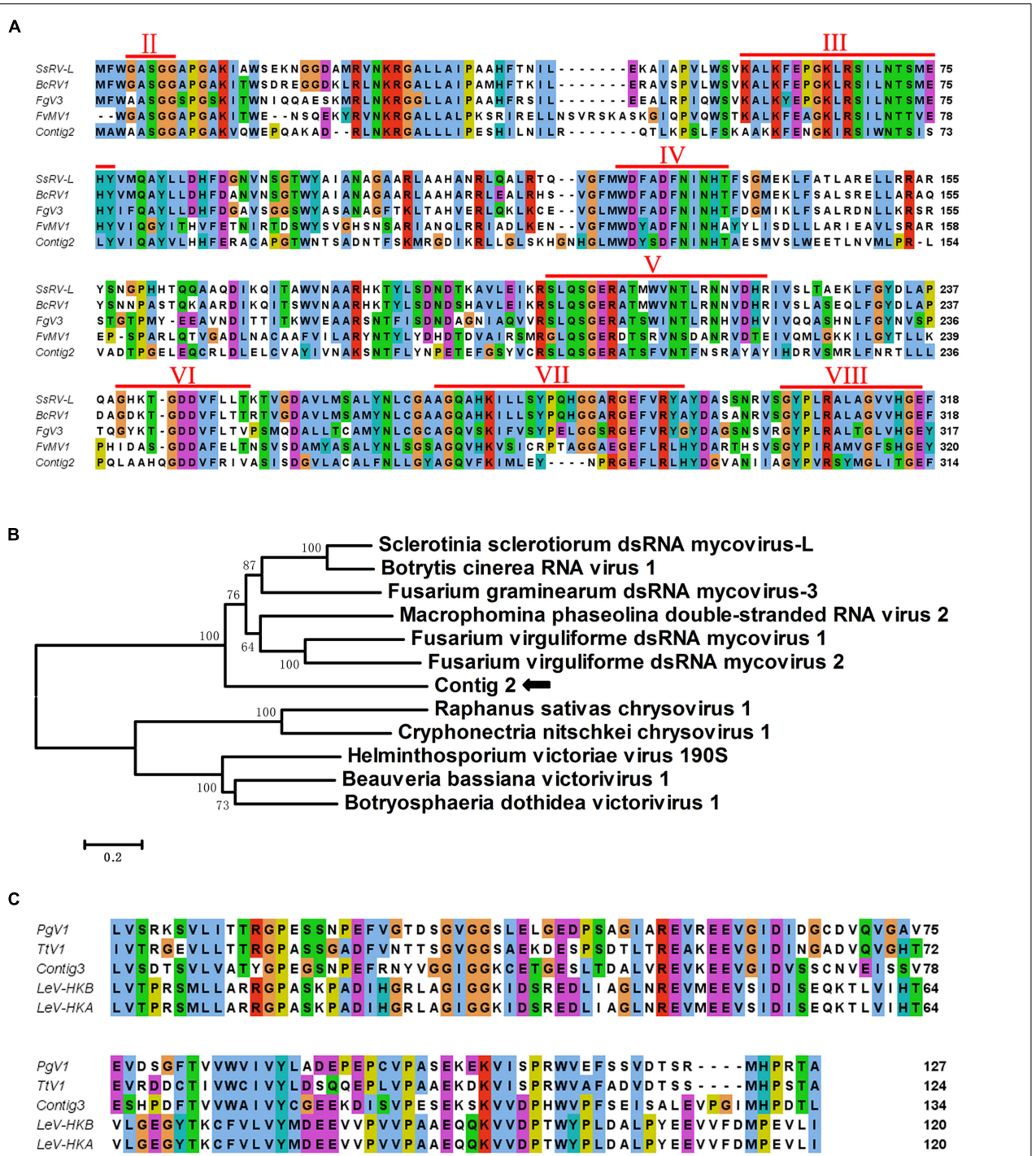


**FIGURE 9 | Multiple alignment of contig 2 and contig 3 translated amino acid sequences and phylogenetic analysis of the contig 2 encoded protein.** **(A)** Multiple alignment of the viral RNA-dependent RNA polymerases (RdRp) encoded by contig 2 and other similar dsRNA mycoviruses. Conserved sequence motifs (denoted by numbers II to VIII) characteristic of the RdRps of dsRNA mycoviruses are indicated. The alignment was prepared by the program CLUSTAL_X and viewed by Jalview. **(B)** A phylogenetic tree was constructed based on the alignment of the contig 2-encoded RdRp and selected viruses. The phylogenetic analysis was conducted with the neighbor-joining method using MEGA 6, with bootstrap of 1000 replicates. **(C)** The NUDIX domain was shown by multiple alignments of aa sequences of contig 3 and its related mycoviruses. The viral names and accession numbers for the above analysis are as follows: SsRV-L, Sclerotinia sclerotiorum dsRNA mycovirus-L (CEZ26307.1); BcRV1, Botrytis cinerea RNA virus 1(YP_009115498.1); FgV3, Fusarium graminearum dsRNA mycovirus-3 (YP_003288789.1); FvMV1, Fusarium virguliforme dsRNA mycovirus 1 (AEZ54148.1); FvMV2, Fusarium virguliforme dsRNA mycovirus 2 (AEZ54146.1); RsSCV1, Raphanus sativas chrysovirus 1 (AFE83590.1); CnCV1, Cryphonectria nitschkei chrysovirus 1 (ACT79256.1); HvV 190S, Helminthosporium victoriae virus 190S (NP_619670.2); BbV1, Beauveria bassiana victorivirus 1(CCC42235.1); BdV1, Botryosphaeria dothidea victorivirus 1 (YP_009072433.1); PgV1, Phlebiopsis gigantea mycovirus dsRNA 1 (YP_003541122.1); TtV1, Thelephora terrestris virus 1(YP_009209481.1); LeV-HKB, Lentinula edodes mycovirus HKB (BAG71789.2); LeV-HKA, Lentinula edodes mycovirus HKA (BAM34027.1).

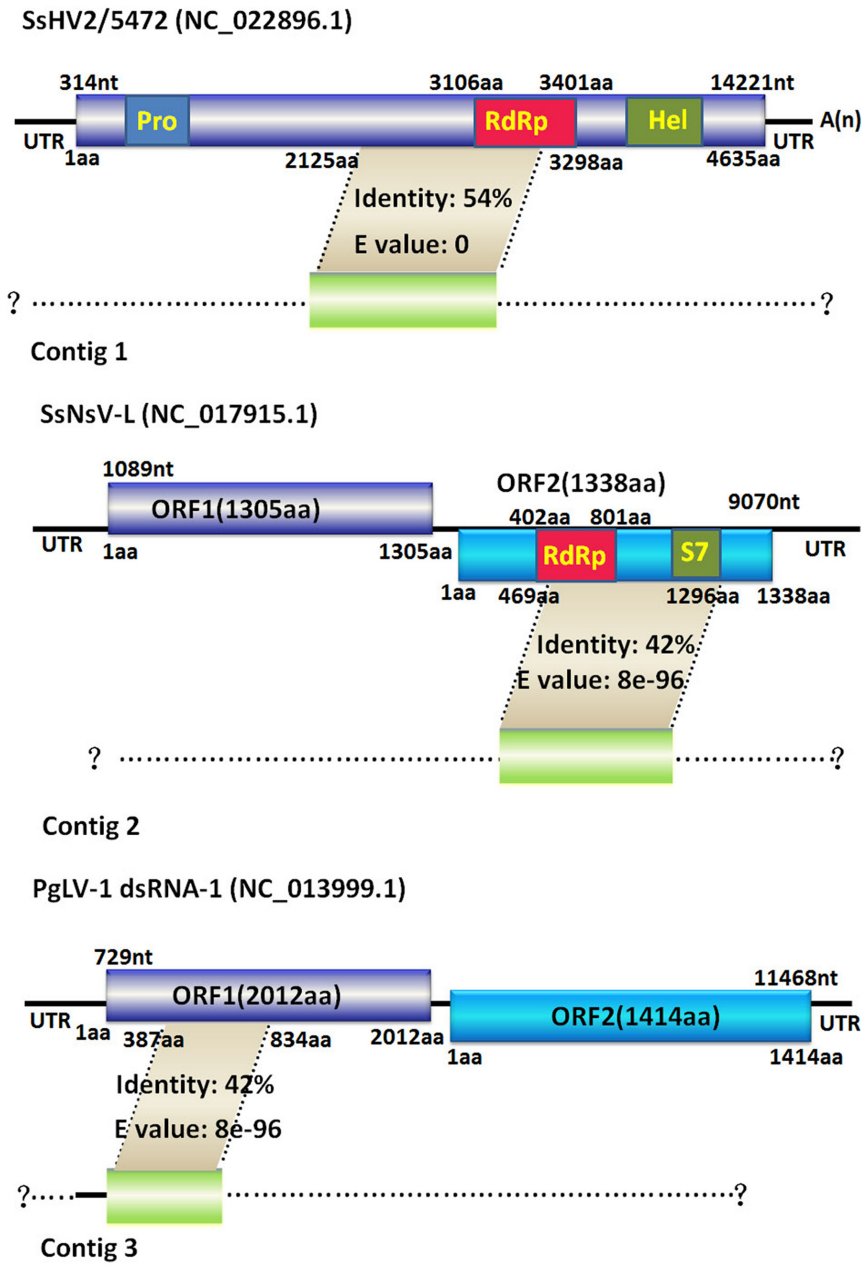


**FIGURE 10 | Genomic organization of the three contigs and their comparison with each similar reported mycovirus.** Contigs 1, 2, and 3 are schematically represented in the (top, middle, and lower panel), respectively. Contigs 1, 2, and 3 have maximum amino acid sequence similarities to SsHV2/5472, SsNsV-L and PgLV-1 dsRNA1, respectively. The dashed lines indicate the possible undetermined sequences of the three contigs' corresponding viruses. The colored boxes and lines represent ORFs and non-coding sequences (UTR), respectively. The smaller boxes in the SsHV2/5472 ORF and the SsNsV-L ORF2 showed conserved domains, such as Pro, RdRp, Hel and S7. The nt and aa numbers above the boxes indicate the map positions corresponding to their genomic structure. The gray areas between the three contigs and their respective most closely related mycoviruses denote the homologous regions with similarities to the translated amino acid sequences of the three contigs.

that contig 2 belongs to a novel mycovirus. Phylogenetic analysis showed that contig 2 clustered with SsNsV-L, FgV3, BcRV1 and other unassigned dsRNA mycoviruses, forming a clade distinct from the *Totiviridae* and *Chrysoviridae* clade (**Figure 9B**). Contig 3 (2449 bp) was identified with similarity to the hypothetical proteins of unclassified dsRNA mycoviruses, including Phlebiopsis gigantea mycovirus dsRNA 1 (PgV1) (Kozlakidis et al., 2009), Thelephora terrestris virus 1, Lentinula edodes mycovirus HKB (Lev-HKB) (Magae, 2012) and Lentinula edodes mycovirus HKA (LeV-HKA), displaying identities of 27–43% with query coverage of greater than 94%. LeV-HKB is a dsRNA mycovirus, with an 11-kbp monopartite genome

identified from *Lentinula edodes,* belonging to basidiomycetes. The genome of this virus contains two ORFs, with the 5′ proximal ORF (ORF1) encoding a hypothetical protein and the 3′ proximal ORF (ORF2) expressing a putative RdRp. Based on the similarities between the predicted protein of contig 3 and the ORF1-encoded hypothetical proteins of the Lev-HKB-like mycoviruses, together with the presence of the NUDIX domain (**Figure 9C**) (Parrish et al., 2007), which was conserved in Lev-HKB and the contig 3-encoded proteins, we suggest that contig 3 represents the 5′ half of a novel mycovirus closely related to the Lev-HKB-like mycoviruses. A comparison of the genomic organization between the three contigs and their respective most closely related viruses is shown in **Figure 10**.

## DISCUSSION

*Sclerotium rolfsii* Sacc. is a versatile soil-borne plant pathogen that causes Southern blight diseases on more than 600 plant species. This pathogen produces sclerotia, which can survive for a long time in the soil, as the primary inoculum source for disease development, making this disease a severe problem (Punja, 1985). Thus, either reducing the sclerotia population in the soil or preventing the infection of host plants is critical for Southern blight control. In this study, we provided the first evidence of hypovirulence caused by dsRNA elements in *S. rolfsii.* The presence of hypovirulence was demonstrated by hyphal tip isolation and transmission tests. The dsRNA-containing strain BHL-1 grew slowly and had debilitated virulence compared to dsRNA-free isogenic *S. rolfsii* isolates, which were obtained by hyphal tipping or protoplast regeneration. The dsRNA-free isolate exhibited a faster mycelial growth rate and became virulent on potato (*S. tuberosum*) and pepper (*C. annuum*). Moreover, the dsRNA acquisition of the dsRNA-free *S. rolfsii* isolate through hyphal anastomosis transmission restored the wild-type dsRNA-containing hypovirulent phenotype. These results provided clear evidence that the dsRNAs in the BHL-1 strain confer hypovirulence to *S. rolfsii* displayed mainly by reduced mycelial growth on PDA and pathogenicity on two tested plants, along with deficiency in sclerotia production.

In our study, based on virus curing and transmission tests, we confirmed that dsRNA elements have the ability to reduce the pathogenicity of *S. rolfsii.* Concurrently, several enzyme activities such as laccase and cellulose and oxalic acid production, which are all closely related with pathogenicity, were reduced in dsRNA-containing strain BLH-1 compared with virus-free strains. As reported previously, the production of laccase and cell wall degrading enzymes associated with fungal pathogenicity were reduced by mycovirus infection, such as the laccase activity decrease in *C. parasitica* caused by CHV1 infection. Castro et al. (2003) reported that the pathogenicity, conidiation and laccase production in the dsRNA-infected hypovirulent *Botrytis cinerea* strain were reduced to 50% compared to that in the virus-curing *B. cinerea* strain. During *S. rolfsii* infection, hyphae penetrate host tissue by formation of appressoria and with the aid of phytotoxins such as oxalic acid and cell wall degrading enzymes (pectinolytic and cellulolytic enzymes) (Bateman and Beer, 1965), which were the main pathogenic factor of *S. rolfsii.* Therefore, we can attribute the hypovirulence of *S. rolfsii* to the reduced production of pathogenic factors of *S. rolfsii* caused by the infected dsRNA elements. Nevertheless, the exact regulatory mechanism of the pathogenicity-related gene of *S. rolfsii* remains to be elucidated.

Compared to dsRNA-free BLH-1-P1, which showed an integrated hyphal structure, the hyphae of dsRNA-containing BLH-1 became shriveled, constricted and fractured into small fragments. We speculated that the damage to the hyphal structure consequently gave rise to the reduced infection ability of this pathogenic fungus. The ultrastructure of cellular cytoplasm in the hypovirulent strain was highly degenerated, as has been reported for other mycovirus-infected fungus, with the appearance of abundant vacuole-like membranous structures and disappearance of cellular organelles. In addition, mitochondria were rare and malformed. Moreover, some membrane-bound vesicles of less than 100 nm in diameter can also be found by TEM, which might represent the area formed by host membranes. Coincidently, the CHV1-infected fungal cells also contain pleomorphic lipid vesicles with diameters of 50–80 nm (Fahima et al., 1993; Suzuki and Nuss, 2002), and the virus has been confirmed to be packaged in membranous vesicles and the trans-Golgi network (TGN) for replication (Jacob-Wilk et al., 2006). Similar membrane structures were also examined in the *S. sclerotiorum* cytoplasm transfected with SsHV2L, a recombinant of SsHV2 (Marzano et al., 2015). These membranous vesicles in virus-infected fungal cells may have the ability to protect the viral nucleic acid from degradation by host nucleases (Mackenzie, 2005). Therefore, the membrane-bound vesicles in BLH-1 may possess the same function for virus replication and protection as in other hypovirus-infected fungi. Mitochondria are extremely important organelles for the energy generation used for cellular activities. Previous reports have shown that the fungal mitochondria were targeted by their infected mitoviruses and become ultrastructurally malformed, thus leading to the debilitation of plant pathogenic fungus (Park et al., 2006; Wu et al., 2010). Rogers et al. (1987) reported that the hypovirulence of *Ophiostoma novo-ulmi* resulted from a deficiency in cytochrome aa3 caused by mitoviruses that targeted the mitochondria of this plant pathogenic fungus. Although at present we cannot determine if there is any mitovirus infection in BLH-1, the mitochondrial malformations in *S. rolfsii* may contribute to the hypovirulence of this fungus.

Oxalic acid has been considered as a key pathogenicity factor utilized by some plant pathogenic fungi, such as the *S. sclerotiorum*, to rapidly kill host cells and tissues as well as to suppresses host oxygen burst, triggers ROS mediated programmed cell death (Dickman and Mitra, 1992; Criscitiello et al., 2013; Dickman and Fluhr, 2013). In *Botrytis cinerea*, an oxalate-deficient mutant strain also has reported to be non-pathogenic to plants (Kunz et al., 2006). However, in our study, the amount of oxalic acid produced by the hypovirulent dsRNA-containing strain BLH-1 was not inhibited, and was qualitative detected to be larger than that of the dsRNA-free BLH-1-P1. Therefore, we can hypothesis that the oxalic acid production might not be the decisive pathogenicity factor of *S. rolfsii.*

Actually, this complexity is not unusually, i.e., a T-DNA inserted secretory protein Ss-Caf1 mutant and a targeting silenced SSITL mutant of *S. sclerotiorum* were all reported to be less virulent, but produced significant amounts of oxalic acid (Zhu et al., 2013; Xiao et al., 2014); the oxalic acid production of a hypovirulent *B. cinerea* strain CanBc-1 that mediated by mycovirus was also reported to be higher than that for other virulent strains (Zhang et al., 2010). Thus, it seems plausible liking those have been proven in *S. sclerotiorum* that they have other factors involved in pathogenesis of *S. rolfsii.* However, to uncover the pathogenesis-related gene and the contributions of oxalic acid to pathogenicity in *S. rolfsii*, more studies remain needed.

In this study, culturing the dsRNA-containing hypovirulent *S. rolfsii* strain BLH-1 and the dsRNA-free strain BLH-1-P1 for 15 days on PDA containing 0.01% (wt/vol) bromophenol blue indicated that all the two strains produced acid and have the ability to reduce the ambient pH. This could be proven by detection of the pH of the two fungal cultures grown in PD broth for 5 days, within which BLH-1 and BLH-1-P1 strains showed the similar lower pH lever. In addition, the amount of oxalic acid (mg/g dry mycella) produced by the hypovirulent dsRNA-containing strain BLH-1 was qualitative detected to be three times larger than that of the dsRNA-free BLH-1-P1 when the two strains were cultured for 5 days in PD. Nevertheless, when the two strains were cultured for only 5 days on bromophenol blue contained PDA, the acid production of BLH-1 was lower than that of BLH-1-P1. This discrepancy was also reflected from the results of pH detection in PD broth clutures exhibiting that the pH of BLH-1 was slightly higher than that of BLH-1-P1 when cultured for 2 and 3 days, but slightly lower than that of BLH-1-P1 once cultured for exceeding time of more than 5 days (date not shown). This might be explained that the amount of oxalic acid production was correlated with the amount of mycelium mass. Although the amount of oxalic acid produced (mg/g dry mycella) by the hypovirulent BLH-1 was larger than that of BLH-1-P1, whereas the slower growth rate of BLH-1 at first few culture days resulted in a relatively less production of oxalic acid in total. With the extension of incubation time and the increasing of mycelia amount, the yield of oxalic acid in the PD cultures of BLH-1 will increase and exhibit a lower PH.

BLH-1 lost the capacity to produce sclerotia. The formation and development of sclerotia are associated with a series of signaling genes, such as reports in *S. sclerotiorum* that the microbial opsin homolog gene sop1 was involved in sclerotial development and virulence of this fungus (Lyu et al., 2015). Previous studies have shown that sclerotial development in some fungi was associated with and affected by a series of physical, chemical or nutritional factors, such as low temperatures, oxidative stress and low PH (Chet and Henis, 1975; Choi et al., 2002; Xing et al., 2013). In addition, the cAMP and the mitogen-activated protein kinase (MAPK) signal pathways are involved in sclerotial development of *S. sclerotiorum* (Rollins and Dickman, 1998; Chen et al., 2004), and this process also requires calcineurin in an oxalic-acid-independent manner (Harel et al., 2006). In *S. rolfsii*, sclerotial differentiation was proven to be closely related to a high degree of lipid peroxidation evoked by oxidative stress, and the sclerotial development could be inhibited by antioxidants such as β-carotene (Georgiou, 1997; Ellil, 1999; Georgiou et al., 2001). In *S. sclerotiorum,* oxalate production was previously assumed to be involved in sclerotial development (Dickman, 2007). Later, Xu et al. (2015) confirmed that it was the acidified conditions of low pH, which might be caused by oxalate production, not oxalic acid itself, that necessary for virulence and sclerotial development of *S. sclerotiorum*. Since the BLH-1 has the ability to produce an amount of oxalic acid and reduce the ambient pH, thus we can propose that other factors independent of oxalic acid and pH that were influenced by mycovirus infection in BLH-1 might involve in sclerotial production. Recently, oxalic acid was demonstrated to inhibit sclerotial formation of *P. umbellatus* (Xing et al., 2015). However, whether the sclerotia production deficiency of *S. rolfsii* was caused by the excessive production of oxalic acid that might inhibit sclerotial formation in this fungus or through blocking of other unknown pathways remains to be clarified. Besides, the molecular mechanism of sclerotial development of *S. rolfsii* is unclear. Therefore, it will be of interest and feasible to use the hypovirulent *S. rolfsii* strain as a model to investigate the sclerotial formation mechanism and its effect in pathogenesis. Moreover, because they are the primary inoculum source for disease epidemiology, this deficiency might be harmful for pathogen spread but favor the control of this pathogen. Interactions between some hypovirulence-associated viruses and their hosts have contributed to the establishment of some host-mycovirus systems, by which we can better understand the molecular basis of fungal biology, especially for fungal pathogenesis (Xie and Jiang, 2014; Wang et al., 2015). These host-mycovirus systems, including Cryphonectria parasitica-hypovirus (Nuss, 1996, 2011; Dawe and Nuss, 2001, 2013; Hillman and Suzuki, 2004; Milgroom and Cortesi, 2004; Nuss, 2005; Pearson et al., 2009), Helmintosporium victoriae-HvV190S (Li H. et al., 2011; Dunn et al., 2013; Ghabrial et al., 2013), Sclerotinia sclerotiorum-mycovirus (Li et al., 2008), Rosellinia necatrix-mycovirus (Salaipeth et al., 2013; Yaegashi et al., 2013), and Fusarium graminearum-mycovirus (Kwon et al., 2009; Cho et al., 2012), have been established and thoroughly elucidated, providing plenty of references to study fungal pathogenicity (Xie and Jiang, 2014). The isolation of the hypovirulent *S. rolfsii* strain displaying a series of abnormal phenotypic traits would be useful for further studying the biology of this plant pathogen, including the pathogenesis and mechanism of sclerotial formation, which we can target to reduce yield loss caused by this plant pathogenic fungus. To identify *S. rolfsii* host factors involved in abnormal host phenotypic traits or response to mycovirus infection, the interaction system at both the proteomic and transcriptional levels should be established.

Many mycoviruses in the families *Hypoviridae*, *Megabirnaviridae*, *Narnaviridae*, *Partitiviridae,* and *Reoviridae*, the unassigned ssRNA, and ssDNA mycoviruses that belong to the newly established family *Genomoviridae* have been reported to cause attenuated symptoms on the host fungi (Nuss, 2005; Chiba et al., 2009; Pearson et al., 2009; Yu et al., 2010; Liu et al., 2014; Krupovic et al., 2016). Moreover, there is a large number and diversity of mycoviruses showing divergent molecular characteristics in nature. Thus, it is difficult to

estimate the viral species by using electrophoretic profiles of dsRNA elements. In this study, we obtained three assembled sequence contigs, which might belong to the genome sequences of three different mycoviruses, through cDNA library synthesis using the total dsRNAs extracted from BLH-1 as templates. The results indicated that at least three mycoviruses co-infected the hypovirulent strain BLH-1. Although at present we could not definitely determine the numbers and species of mycoviruses infecting BLH-1, as well as which virus confers hypovirulence to the host fungus, some clues are provided in view of the possible effects imposed on the fungal host by these mycoviruses that are closely related to our obtained sequence contigs. Contig 1 was most closely related to a *S. sclerotiorum*-infecting hypovirus, SsHV2. Evidence was presented in three recent reports that SsHV2 and its recombinant strains are responsible for hypovirulence of *S. sclerotiorum* (Hu et al., 2014; Khalifa and Pearson, 2014; Marzano et al., 2015). In addition, Marzano et al. (2015) proposed that there was a symptom determinant associated with sclerotia production in the SsHV2 genome, according to genome structure comparison between the deleted SsHV2L, SsHV2/5472, and recombinant SsHV2L. We hypothesize that BLH-1 was infected by a putative novel hypovirus related to SsHV2. There was no example of contig 2-related Lev-HKB-like mycoviruses causing hypovirulence, and the phenotypic effects, especially for pathogenicity caused by contig 3-related SsNsV-L-like mycoviruses, were also diverse. Therefore, we hypothesized that the hypovirulence of BLH-1 was mainly ascribed to the infection of contig 1-associated hypovirus. Eventually, the attenuated phenotype of BLH-1 was similar to the SsHV2/SX247-infected *S. sclerotiorum* strain, which displayed a complete loss of sclerotia production and reduced pathogenicity (Hu et al., 2014). Nevertheless, whether the BLH-1 hypovirulence was caused directly by the contig 1-associated hypovirus or by combinations of multiple mycoviruses or satellite RNA is unclear and should be elucidated further, as other unknown mycoviruses that have not yet been cloned in cDNA library synthesis may exist in this fungus.

In our virus elimination and transmission experiments, all of the dsRNAs that belong to different mycovirus species were co-instantaneously eliminated or transmitted, demonstrating that the dsRNAs in BLH-1 harbor similar stability and equal transmission rates, resembling other mixed-infected viruses in *Epichloë festucae,* showing the consistent transmission rate to conidia (Romo et al., 2007). In addition, co-infection of multiple mycoviruses and satellite RNA or defective RNA, if any, in one fungal strain may give rise to potential interactions such as additive or synergistic effects between the mycoviruses. For example, a mutual interplay between mix-infected mycovirus has been reported for capsidless (+) ssRNA virus, yado-kari virus 1 (YkV1), which can hijack the capsid protein of a dsRNA virus, yado-nushi virus 1 (YnV1), for trans-encapsidation of not only its RNA but also the RdRp. The virus can replicate like a dsRNA virus and enhance YnV1 accumulation as well (Zhang et al., 2016). In addition, some mycoviruses rely on other co-infected mycoviruses or satellite RNA to cause host hypovirulence, such as Rosellinia necatrix megabirnavirus 2 (RnMBV2), which confers hypovirulence in *Rosellinia necatrix* only when another partitivirus was co-infected in the host fungus (Sasaki et al., 2016). Other mycoviruses including Sclerotinia sclerotiorum botybirnavirus 1 (SsBRV1) and Sclerotinia sclerotiorum hypovirus 1 (SsHV1/SZ-150) harbored satellite RNA as their requirements to cause hypovirulence (Xie et al., 2011; Liu et al., 2015). To fully determine the species and genomes of all of the mycoviruses infecting BLH-1, which could facilitate the construction of a full-length infectious cDNA clone of each viral genome that is necessary for the establishment of the cause-and-effect relationship between individual mycoviruses and their host, as well as clarify the possible interactions between these co-infected viruses, further sequencing study is needed and underway.

In summary, we confirmed in this study that BLH-1 was a hypovirulent strain and that the hypovirulence was positively correlated with its associated dsRNA elements. To our knowledge, this is the first report of hypovirulence caused by mycovirus in *S. rolfsii*, which may not only provide novel insights for the study of molecular mechanisms underlying the pathogenesis of this plant pathogenic fungus but also enrich virocontrol resources for southern blight disease.

## AUTHOR CONTRIBUTIONS

JZ and QZ conceived and designed the experiments; DC performed the experiments; HZ and BG analyzed the data; JZ wrote the paper.

## ACKNOWLEDGMENTS

This study is supported by Excellent Doctoral Dissertation Cultivating Fund of Hunan Agricultural University (YB2015002).

## SUPPLEMENTARY MATERIAL

The Supplementary Material for this article can be found online at: http://journal.frontiersin.org/article/10.3389/fmicb.2016.01798/full#supplementary-material

## REFERENCES

Ahn, I. P., and Lee, Y. H. (2001). A viral double-stranded RNA up regulates the fungal virulence of Nectria radicicola. *Mol. Plant Microbe Interact.* 14, 496–507. doi: 10.1094/MPMI.2001.14.4.496

Bateman, D. F., and Beer, S. V. (1965). Simultaneous production and synergistic action of oxalic acid and polygalacturonase during pathogenesis by *Sclerotium rolfsii*. *Phytopathology* 55, 204–211.

Castro, M., Kramer, K., Valdivia, L., Ortiz, S., and Castillo, A. (2003). A double-stranded RNA mycovirus confers hypovirulence-associated traits to

*Botrytis cinerea*. *FEMS Microbiol. Lett.* 228, 87–91. doi: 10.1016/S0378-1097(03)00755-9

Chen, C., Harel, A., Gorovoits, R., Yarden, O., and Dickman, M. B. (2004). MAPK regulation of sclerotial development in *Sclerotinia sclerotiorum* is linked with pH and cAMP sensing. *Mol. Plant Microbe Interact.* 17, 404–413. doi: 10.1094/MPMI.2004.17.4.404

Chet, I., and Henis, Y. (1975). Sclerotial morphogenesis in fungi. *Annu. Rev. Phytopathol.* 13, 169–192. doi: 10.1146/annurev.py.13.090175.001125

Chiba, S., Salaipeth, L., Lin, Y. H., Sasaki, A., Kanematsu, S., and Suzuki, N. (2009). A novel bipartite double-stranded RNA mycovirus from the white root rot fungus *Rosellinia necatrix*: molecular and biological characterization, taxonomic considerations, and potential for biological control. *J. Virol.* 83, 12801–12812. doi: 10.1128/JVI.01830-09

Cho, W. K., Yu, J., Lee, K. M., Son, M., Min, K., Lee, Y. W., et al. (2012). Genome-wide expression profiling shows transcriptional reprogramming in *Fusarium graminearum* by *Fusarium graminearum* virus 1-DK21 infection. *BMC Genomics* 13:173. doi: 10.1186/1471-2164-13-173

Choi, K. D., Kwon, J. K., Shim, J. O., Lee, S. S., Lee, T. S., and Lee, M. W. (2002). Sclerotial development of *Grifola umbellata*. *Mycobiology* 30, 65–69. doi: 10.4489/MYCO.2002.30.2.065

Criscitiello, M. F., Dickman, M. B., Samuel, J. E., and de Figueiredo, P. (2013). Tripping on acid: trans-kingdom perspectives on biological acids in immunity and pathogenesis. *PLoS Pathog.* 9:e1003402. doi: 10.1371/journal.ppat.1003402

Dawe, A. L., and Nuss, D. L. (2001). Hypoviruses and chestnut blight: exploiting viruses to understand and modulate fungal pathogenesis. *Annu. Rev. Genet.* 35, 1–29. doi: 10.1146/annurev.genet.35.102401.085929

Dawe, A. L., and Nuss, D. L. (2013). Hypovirus molecular biology: from Koch's postulates to host self-recognition genes that restrict virus transmission. *Adv. Virus Res.* 86, 109–147. doi: 10.1016/B978-0-12-394315-6.00005-2

Dickman, M. (2007). Approaches for improving crop resistance to soilborne fungal diseases through biotechnology using *Sclerotinia sclerotiorum* as a case study. *Australas. Plant Pathol.* 36, 116–123. doi: 10.1071/AP07010

Dickman, M. B., and Fluhr, R. (2013). Centrality of host cell death in plant-microbe interactions. *Annu. Rev. Phytopathol.* 51, 543–570. doi: 10.1146/annurev-phyto-081211-173027

Dickman, M. B., and Mitra, A. (1992). *Arabidopsis thaliana* as a model for studying *Sclerotinia sclerotiorum* pathogenesis. *Physiol. Mol. Plant Pathol.* 41, 255–263. doi: 10.1016/0885-5765(92)90025-Q

Dunn, S. E., Li, H., Cardone, G., Nibert, M. L., Ghabrial, S. A., and Baker, T. S. (2013). Three-dimensional structure of victorivirus HvV190S suggests coat proteins in most totiviruses share a conserved core. *PLoS Pathog.* 9:e1003225. doi: 10.1371/journal.ppat.1003225

Elad, Y. (1995). "Mycoparasitism," in *Pathogenesis and Host Specificity in Plant Diseases: Histopathological, Biochemical, Genetic and Molecular Bases: Eukaryotes*, Vol. II, eds K. Kohmoto, U. S. Singh, and R. P. Singh (Oxford: Pergamon Press), 285–307.

Ellil, A. H. A. (1999). Oxidative stress in relation to lipid peroxidation, sclerotial development and melanin production by *Sclerotium rolfsii*. *J. Phytopathol.* 147, 561–566. doi: 10.1046/j.1439-0434.1999.00431.x

Fahima, T., Kazmierczak, P., Hansen, D. R., Pfeiffer, P., and Vanalfen, N. K. (1993). Membrane associated replication of an unencapsidated double-strand RNA of the fungus, *Cryphonectria parasitica*. *Virology* 195, 81–89. doi: 10.1006/viro.1993.1348

Georgiou, C. D. (1997). Lipid peroxidation in *Sclerotium rolfsii*: a new look into the mechanism of sclerotial biogenesis in fungi. *Mycol. Res.* 101, 460–464. doi: 10.1017/S0953756296002882

Georgiou, C. D., Zervoudakis, G., Tairis, N., and Kornaros, M. (2001). β-Carotene production and its role in sclerotial differentiation of *Sclerotium rolfsii*. *Fungal Genet. Biol.* 34, 11–20. doi: 10.1006/fgbi.2001.1285

Ghabrial, S. A., Castón, J. R., Jiang, D., Nibert, M. L., and Suzuki, N. (2015). 50-plus years of fungal viruses. *Virology* 47, 356–368. doi: 10.1016/j.virol.2015.02.034

Ghabrial, S. A., Dunn, S. E., Li, H., Xie, J., and Baker, T. S. (2013). Viruses of *Helminthosporium* (Cochlioblus) victoriae. *Adv. Virus Res.* 86, 289–325. doi: 10.1016/B978-0-12-394315-6.00011-8

Ghabrial, S. A., and Suzuki, N. (2009). Viruses of plant pathogenic fungi. *Annu. Rev. Phytopathol.* 47, 353–384. doi: 10.1146/annurev-phyto-080508-081932

Guetsky, R., Kobiler, I., Wang, X., Perlman, N., Gollop, N., Avila-Quezada, G., et al. (2005). Metabolism of the flavonoid epicatechin by laccase of *Colletotrichum gloeosporioides* and its effect on pathogenicity on avocado fruits. *Phytopathology* 95, 1341–1348. doi: 10.1094/PHYTO-95-1341

Harel, A., Bercovich, S., and Yarden, O. (2006). Calcineurin is required for sclerotial development and pathogenicity of *Sclerotinia sclerotiorum* in an oxalic acid-independent manner. *Mol. Plant Microbe Interact.* 19, 682–693. doi: 10.1094/MPMI-19-0682

Hillman, B. I., and Suzuki, N. (2004). Viruses of the chestnut blight fungus, *Cryphonectria parasitica*. *Adv. Virus Res.* 63, 423–472. doi: 10.1016/S0065-3527(04)63007-7

Hu, Z., Wu, S., Cheng, J., Fu, Y., Jiang, D., and Xie, J. (2014). Molecular characterization of two positive-strand RNA viruses co-infecting a hypovirulent strain of *Sclerotinia sclerotiorum*. *Virology* 464, 450–459. doi: 10.1016/j.virol.2014.07.007

Jacob-Wilk, D., Turina, M., and Van Alfen, N. K. (2006). Mycovirus *Cryphonectria hypovirus* 1 elements cofractionate with trans-Golgi network membranes of the fungal host *Cryphonectria parasitica*. *J. Virol.* 80, 6588–6596. doi: 10.1128/JVI.02519-05

Kanematsu, S., Arakawa, M., Oikawa, Y., Onoue, M., Osaki, H., Nakamura, H., et al. (2004). A reovirus causes hypovirulence of *Rosellinia necatrix*. *Phytopathology* 94, 561–568. doi: 10.1094/PHYTO.2004.94.6.561

Khalifa, M. E., and Pearson, M. N. (2014). Characterisation of a novel hypovirus from *Sclerotinia sclerotiorum* potentially representing a new genus within the Hypoviridae. *Virology* 464, 441–449. doi: 10.1016/j.virol.2014.07.005

Kozlakidis, Z., Hacker, C. V., Bradley, D., Jamal, A., Phoon, X., Webber, J., et al. (2009). Molecular characterisation of two novel double-stranded RNA elements from Phlebiopsis gigantea. *Virus Genes* 39, 132–136. doi: 10.1007/s11262-009-0364-z

Krupovic, M., Ghabrial, S. A., Jiang, D., and Varsani, A. (2016). Genomoviridae: a new family of widespread single-stranded DNA viruses. *Arch. Virol.* 161, 2633–2643. doi: 10.1007/s00705-016-2943-3

Kunz, C., Vandelle, E., Rolland, S., Poinssot, B., Bruel, C., Cimerman, A., et al. (2006). Characterization of a new, nonpathogenic mutant of *Botrytis cinerea* with impaired plant colonization capacity. *N phytologist.* 170, 537–550. doi: 10.1111/j.1469-8137.2006.01682.x

Kwon, S. J., Cho, S. Y., Lee, K. M., Yu, J., Son, M., and Kim, K. H. (2009). Proteomic analysis of fungal host factors differentially expressed by *Fusarium graminearum* infected with *Fusarium graminearum* virus-DK21. *Virus Res.* 144, 96–106. doi: 10.1007/s00705-016-2943-3

Larkin, M. A., Blackshields, G., Brown, N. P., Chenna, R., McGettigan, P. A., McWilliam, H., et al. (2007). Clustal W and Clustal X version 2.0. *Bioinformatics* 23, 2947–2948. doi: 10.1093/bioinformatics/btm404

Li, H., Fu, Y., Jiang, D., Li, G., Ghabrial, S. A., and Yi, X. (2008). Down-regulation of *Sclerotinia sclerotiorum* gene expression in response to infectionwith *Sclerotinia sclerotiorum* debilitation-associated RNA virus. *Virus Res.* 135, 95–106. doi: 10.1016/j.virusres.2008.02.011

Li, H., Havens, W. M., Nibert, M. L., and Ghabrial, S. A. (2011). RNA sequence determinants of a coupled termination-reinitiation strategy for downstream open reading frame translation in *Helminthosporium victoriae* virus 190S and other victoriviruses (Family Totiviridae). *J. Virol.* 85, 7343–7352. doi: 10.1128/JVI.00364-11

Li, Y., Wang, C., Liu, W., Wang, G., Kang, Z., Kistler, H. C., et al. (2011). The HDF1 histone deacetylase gene is important for conidiation, sexual reproduction, and pathogenesis in *Fusarium graminearum*. *Mol. Plant Microbe Interact.* 24, 487–496. doi: 10.1094/MPMI-10-10-0233

Liao, C. Y., Chen, M. Y., Chen, Y. K., Wang, T. C., Sheu, Z. M., Kuo, K. C., et al. (2012). Characterization of three *Colletotrichum acutatum* isolates from *Capsicum* spp. *Eur. J. Plant Pathol.* 133, 599–608. doi: 10.1007/s10658-011-9935-7

Liu, H., Fu, Y., Xie, J., Cheng, J., Ghabrial, S. A., Li, G., et al. (2012). Evolutionary genomics of mycovirus-related dsRNA viruses reveals cross-family horizontal gene transfer and evolution of diverse viral lineages. *BMC Evol. Biol.* 12:1. doi: 10.1186/1471-2148-12-91

Liu, L., Wang, Q., Cheng, J., Fu, Y., Jiang, D., and Xie, J. (2015). Molecular characterization of a bipartite double-stranded RNA virus and its satellite-like RNA co-infecting the phytopathogenic fungus *Sclerotinia sclerotiorum*. *Front. Microbial.* 6:406. doi: 10.3389/fmicb.2015.00406

Liu, L., Xie, J., Cheng, J., Fu, Y., Li, G., Yi, X., et al. (2014). Fungal negative-stranded RNA virus that is related to bornaviruses and nyaviruses. *Proc. Natl. Acad. Sci. U.S.A.* 111, 12205–12210. doi: 10.1073/pnas.1401786111

Lyu, X., Shen, C., Fu, Y., Xie, J., Jiang, D., Li, G., et al. (2015). The microbial opsin homolog sop1 is involved in *Sclerotinia sclerotiorum* development and environmental stress response. *Front. Microbial.* 6:1504. doi: 10.3389/fmicb.2015.01504

Mackenzie, J. (2005). Wrapping things up about virus RNA replication. *Traffic* 6, 967–977. doi: 10.1111/j.1600-0854.2005.00339.x

Magae, Y. (2012). Molecular characterization of a novel mycovirus in the cultivated mushroom, *Lentinula edodes. Virol. J.* 9:60. doi: 10.1186/1743-422X-9-60

Marzano, S. Y. L., Hobbs, H. A., Nelson, B. D., Hartman, G. L., Eastburn, D. M., McCoppin, N. K., et al. (2015). Transfection of *Sclerotinia sclerotiorum* with in vitro transcripts of a naturally occurring interspecific recombinant of *Sclerotinia sclerotiorum* hypovirus 2 significantly reduces virulence of the fungus. *J. Virol.* 89, 5060–5071. doi: 10.1128/JVI.03199-14

Milgroom, M. G., and Cortesi, P. (2004). Biological control of chestnut blight with hypovirulence: a critical analysis. *Annu. Rev. Phytopathol.* 42, 311–338. doi: 10.1146/annurev.phyto.42.040803.140325

Moleleki, N., van Heerden, S. W., Wingfield, M. J., Wingfield, B. D., and Preisig, O. (2003). Transfection of *Diaporthe perjuncta* with diaporthe RNA virus. *Appl. Environ. Microbiol.* 69, 3952–3956. doi: 10.1128/AEM.69.7.3952-3956.2003

Morris, T. J., and Dodds, J. A. (1979). Isolation and analysis of double-stranded RNA from virus-infected plant and fungal tissue. *Phytopathology* 69, 854–858. doi: 10.1094/Phyto-69-854

Nuss, D. L. (1996). Using hypoviruses to probe and perturb signal transduction processes underlying fungal pathogenesis. *Plant Cell* 8, 1846–1853. doi: 10.1105/tpc.8.10.1845

Nuss, D. L. (2005). Hypovirulence: mycoviruses at the fungal-plant interface. *Nat. Rev. Microbiol.* 3, 632–642. doi: 10.1038/nrmicro1206

Nuss, D. L. (2011). Mycoviruses, RNA silencing, and viral RNA recombination. *Adv. Virus Res.* 80, 25–48. doi: 10.1016/B978-0-12-385987-7.00002-6

Park, Y., Chen, X., and Punja, Z. K. (2006). Molecular and biological characterization of a mitovirus in Chalara elegans (*Thielaviopsis basicola*). *Phytopathology* 96, 468–479. doi: 10.1094/PHYTO-96-0468

Parrish, S., Resch, W., and Moss, B. (2007). *Vaccinia virus* D10 protein has mRNA decapping activity, providing a mechanism for control of host and viral gene expression. *Proc. Natl. Acad. Sci. U.S.A.* 104, 2139–2144. doi: 10.1073/pnas.0611685104

Pearson, M. N., Beever, R. E., Boine, B., and Arthur, K. (2009). Mycoviruses of filamentous fungi and their relevance to plant pathology. *Mol. Plant Pathol.* 10, 115–128. doi: 10.1111/j.1364-3703.2008.00503.x

Punja, Z. K. (1985). The biology, ecology, and control of *Sclerotium rolfsii*. *Annu. Rev. Phytopathol.* 23, 97–127. doi: 10.1146/annurev.py.23.090185.000525

Rivard, C. L., O'Connell, S., Peet, M. M., and Louws, F. J. (2010). Grafting tomato with interspecific rootstock to manage diseases caused by *Sclerotium rolfsii* and southern root-knot nematode. *Plant Dis.* 94, 1015–1021. doi: 10.1094/PDIS-94-8-1015

Rogers, H. J., Buck, K. W., and Brasier, C. M. (1987). A mitochondrial target for double-stranded RNA in diseased isolates of the fungus that causes Dutch elm disease. *Nature* 329, 558–560. doi: 10.1038/329558a0

Rollins, J. A., and Dickman, M. B. (1998). Increase in endogenous and exogenous cyclic AMP levels inhibits sclerotial development in *Sclerotinia sclerotiorum*. *Appl. Environ. Microbiol.* 64, 2539–2544.

Romo, M., Leuchtmann, A., García, B., and Zabalgogeazcoa, I. (2007). A totivirus infecting the mutualistic fungal endophyte *Epichloë festucae*. *Virus Res.* 124, 38–43. doi: 10.1016/j.virusres.2006.09.008

Salaipeth, L., Chiba, S., Eusebio-Cope, A., Kanematsu, S., and Suzuki, N. (2013). Biological properties and expression strategy of *Rosellinia necatrix* megabirnavirus 1 analyzed in an experimental host, *Cryphonectria parasitica*. *J. Gen. Virol.* 95, 740–750. doi: 10.1099/vir.0.058164-0

Sasaki, A., Nakamura, H., Suzuki, N., and Kanematsu, S. (2016). Characterization of a new megabirnavirus that confers hypovirulence with the aid of a co-infecting partitivirus to the host fungus, *Rosellinia necatrix*. *Virus Res.* 219, 73–82. doi: 10.1016/j.virusres.2015.12.009

Suzuki, N., and Nuss, D. L. (2002). Contribution of protein p40 to hypovirus-mediated modulation of fungal host phenotype and viral RNA accumulation. *J. Virol.* 76, 7747–7759. doi: 10.1128/JVI.76.15.7747-7759.2002

Tamura, K., Stecher, G., Peterson, D., Filipski, A., and Kumar, S. (2013). MEGA6: molecular evolutionary genetics analysis version 6.0. *Mol. Biol. Evol.* 30, 2725–2729. doi: 10.1093/molbev/mst197

Wang, M., Wang, Y., Sun, X., Cheng, J., Fu, Y., Liu, H., et al. (2015). Characterization of a novel megabirnavirus from *Sclerotinia sclerotiorum* reveals horizontal gene transfer from ssRNA virus to dsRNA virus. *J. Virol.* 89, 8567–8579. doi: 10.1128/JVI.00243-15

Wu, M., Jin, F., Zhang, J., Yang, L., Jiang, D., and Li, G. (2012). Characterization of a novel bipartite double-stranded RNA mycovirus conferring hypovirulence in the phytopathogenic fungus *Botrytis porri*. *J. Virol.* 86, 6605–6619. doi: 10.1128/JVI.00292-12

Wu, M., Zhang, L., Li, G., Jiang, D., and Ghabrial, S. A. (2010). Genome characterization of a debilitation-associated mitovirus infecting the phytopathogenic fungus *Botrytis cinerea*. *Virology* 406, 117–126. doi: 10.1016/j.virol.2010.07.010

Wu, M. D., Zhang, L., Li, G. Q., Jiang, D. H., Hou, M. S., and Huang, H. C. (2007). Hypovirulence and double-stranded RNA in *Botrytis cinerea*. *Phytopathology* 97, 1590–1599. doi: 10.1094/PHYTO-97-12-1590

Xiao, X., Xie, J., Cheng, J., Li, G., Yi, X., Jiang, D., et al. (2014). Novel secretory protein Ss-Caf1 of the plant-pathogenic fungus *Sclerotinia sclerotiorum* is required for host penetration and normal sclerotial development. *Mol. Plant Microbe Interact.* 2, 40–55. doi: 10.1094/MPMI-05-13-0145-R

Xie, J., Xiao, X., Fu, Y., Liu, H., Cheng, J., Ghabrial, S. A., et al. (2011). A novel mycovirus closely related to hypoviruses that infects the plant pathogenic fungus *Sclerotinia sclerotiorum*. *Virology* 418, 49–56. doi: 10.1016/j.virol.2011.07.008

Xie, J. T., and Jiang, D. H. (2014). New Insights into mycoviruses and exploration for the biological control of crop fungal diseases. *Annu. Rev. Phytopathol.* 52, 45–68. doi: 10.1146/annurev-phyto-102313-050222

Xing, Y. M., Yin, W. Q., Liu, M. M., Wang, C. L., and Guo, S. X. (2015). Oxalic acid and sclerotial differentiation of *Polyporus umbellatus*. *Sci. Rep.* 5:10759. doi: 10.1038/srep10759

Xing, Y. M., Zhang, L. C., Liang, H. Q., Lv, J., Song, C., Guo, S. X., et al. (2013). Sclerotial formation of *Polyporus umbellatus* by low temperature treatment under artificial conditions. *PLoS ONE* 8:e56190. doi: 10.1371/journal.pone.0056190

Xu, L., Xiang, M., White, D., and Chen, W. (2015). pH dependency of sclerotial development and pathogenicity revealed by using genetically defined oxalate-minus mutants of *Sclerotinia sclerotiorum*. *Environ. Microbiol.* 17, 2896–2909. doi: 10.1111/1462-2920.12818

Yaegashi, H., Yoshikawa, N., Ito, T., and Kanematsu, S. (2013). A mycoreovirus suppresses RNA silencing in the white root rot fungus, *Rosellinia necatrix*. *Virology* 444, 409–416. doi: 10.1016/j.virol.2013.07.010

Yu, J., Kwon, S. J., Lee, K. M., Son, M., and Kim, K. H. (2009). Complete nucleotide sequence of double-stranded RNA viruses from *Fusarium graminearum* strain DK3. *Arch. Virol.* 154, 1855–1858. doi: 10.1007/s00705-009-0507-5

Yu, J., Lee, K. M., Son, M., and Kim, K. H. (2015). Effects of the deletion and over-expression of *Fusarium graminearum* gene FgHal2 on host response to mycovirus *Fusarium graminearum* virus 1. *Mol. Plant Pathol.* 16, 641–652. doi: 10.1111/mpp.12221

Yu, L., Sang, W., Wu, M. D., Zhang, J., Yang, L., Zhou, Y. J., et al. (2015). Novel hypovirulence-associated RNA mycovirus in the plant-pathogenic fungus *Botrytis cinerea*: molecular and biological characterization. *Appl. Environ. Microbiol.* 81, 2299–2310. doi: 10.1128/AEM.03992-14

Yu, X., Li, B., Fu, Y., Jiang, D., Ghabrial, S. A., Li, G., et al. (2010). A geminivirus-related DNA mycovirus that confers hypovirulence to a plant pathogenic fungus. *Proc. Natl. Acad. Sci. U.S.A.* 107, 8387–8392. doi: 10.1073/pnas.0913535107

Yu, X., Li, B., Fu, Y., Xie, J., Cheng, J., Ghabrial, S. A., et al. (2013). Extracellular transmission of a DNA mycovirus and its use as a natural fungicide. *Proc. Natl. Acad. Sci. U.S.A.* 110, 1452–1457. doi: 10.1073/pnas.1213755110

Zhang, L., De Wu, M., Li, G. Q., Jiang, D. H., and Huang, H. C. (2010). Effect of Mitovirus infection on formation of infection cushions and virulence of *Botrytis cinerea*. *Physiol. Mol. Plant Pathol.* 75, 71–80. doi: 10.1016/j.pmpp.2010.09.001

Zhang, R., Hisano, S., Tani, A., Kondo, H., Kanematsu, S., and Suzuki, N. (2016). A capsidless ssRNA virus hosted by an unrelated dsRNA virus. *Nat. Microbiol.* 1:15001. doi: 10.1038/nmicrobiol.2015.1

Zhang, R., Liu, S., Chiba, S., Kondo, H., Kanematsu, S., and Suzuki, N. (2014). A novel single-stranded RNA virus isolated from a phytopathogenic filamentous fungus, *Rosellinia necatrix*, with similarity to hypo-like viruses. *Front. Microbiol.* 5:360. doi: 10.3389/fmicb.2014.00360

Zhu, W., Wei, W., Fu, Y., Cheng, J., Xie, J., Li, G., et al. (2013). A secretory protein of necrotrophic fungus *Sclerotinia sclerotiorum* that suppresses host resistance. *PLoS ONE* 8:e53901. doi: 10.1371/journal.pone.0053901

**Conflict of Interest Statement:** The authors declare that the research was conducted in the absence of any commercial or financial relationships that could be construed as a potential conflict of interest.

frontiers in Microbiology

ORIGINAL RESEARCH
published: 31 January 2017
doi: 10.3389/fmicb.2017.00071

# Identification of a Novel *Alternaria alternata* Strain Able to Hyperparasitize *Puccinia striiformis* f. sp. *tritici*, the Causal Agent of Wheat Stripe Rust

*Li Zheng, Jie Zhao, Xiaofei Liang, Gangming Zhan, Shuchang Jiang and Zhensheng Kang**

*State Key Laboratory of Crop Stress Biology for Arid Areas and College of Plant Protection, Northwest A&F University, Yangling, China*

The obligate bitrophic fungus *Puccinia striiformis* f. sp. *tritici* (*Pst*) causes stripe (yellow) rust on wheat worldwide. Here, we report a novel fungal strain able to hyperparasitize *Pst*. The strain was isolated from gray-colored rust pustules, and was identified as *Alternaria alternata* (Fr.: Fr.) keissler based on a combination of morphological characteristics and multi-locus (ITS, GAPDH, and RPB2) phylogeny. Upon artificial inoculation, the hyperparasite reduced the production and viability of urediniospores, and produced a typical gray-colored rust pustule symptom. Scanning electron microscopy demonstrated that the strain could efficiently penetrate and colonize *Pst* urediniospores. This study first demonstrates that *A. alternata* could parasitize *Pst* and indicates its potential application in the biological control of wheat stripe rust disease.

**Keywords: wheat stripe rust, *Puccinia striiformis*, hyperparasite, *Alternaria alternata*, biological control**

OPEN ACCESS

***Edited by:***
*Joshua D. Nosanchuk, Albert Einstein College of Medicine, USA*

***Reviewed by:***
*Falk Hillmann, Leibniz Institute for Natural Product Research and Infection Biology e.V. - Hans-Knöll-Institute, Germany*
*Rachid Lahlali, Ecole Nationale d'Agriculture de Meknès, Morocco*

****Correspondence:***
*Zhensheng Kang*
*kangzs@nwsuaf.edu.cn*

***Specialty section:***
*This article was submitted to Fungi and Their Interactions, a section of the journal Frontiers in Microbiology*

***Received:*** *12 November 2016*
***Accepted:*** *11 January 2017*
***Published:*** *31 January 2017*

***Citation:***
*Zheng L, Zhao J, Liang X, Zhan G, Jiang S and Kang Z (2017) Identification of a Novel Alternaria alternata Strain Able to Hyperparasitize Puccinia striiformis f. sp. tritici, the Causal Agent of Wheat Stripe Rust. Front. Microbiol. 8:71. doi: 10.3389/fmicb.2017.00071*

## INTRODUCTION

Strip rust (yellow rust), caused by *Puccinia striiformis* Westend f. sp. *tritici* Erikss. (*Pst*), is one of the most important diseases of wheat in many regions of world (Saari and Prescott, 1985; Stubbs, 1985; Chen, 2005). Because the *Pst* urediniospores could be dispersed over long distances by the wind, the fungal pathogen is able to cause large-scale epidemics and severe yield losses under conducive environmental conditions (Brown and Hovmøller, 2002; Wan et al., 2007; Zhao et al., 2008). In China, the devastating epidemics occurring in 1950, 1964, 1990, and 2002, has caused up to $6.0 \times 10^9$, $3.0 \times 10^9$, $2.6 \times 10^9$, and $1.0 \times 10^9$ kg of yield losses, respectively (Wan et al., 2004; Chen et al., 2009; Gao et al., 2015). So far, cultivation of resistant varieties is the most effective way to control wheat stripe rust. Nevertheless, most resistant varieties were bred for major gene resistance and rapidly lost their resistance within 3–6 years after field cultivation (Cheng et al., 2014; Han et al., 2015). In addition, the constant and indiscriminate use of fungicides poses serious environmental problems and health hazards to animals and humans. Biological control strategy is thus attractive for the potential to achieve effective disease management with minimal environmental cost.

*Puccinia striiformis* f. sp. *tritici* (*Pst*) is an obligate biotrophic fungus, which normally forms yellow to orange urediniospores on leaf blade surfaces during disease progression

**TABLE 1 | Sources of *Alternaria* spp. strains with GenBank accession numbers.**

| Species name | Strain number | Gene and GenBank accession no. | | | Substrate/Host | Origin/Locality |
|---|---|---|---|---|---|---|
| | | ITS[a] | GAPDH[b] | RPB2[c] | | |
| *A. alternantherae* | CBS124392 | KC584179 | KC584096 | KC584374 | *Solanum melongena* | China |
| *A. iridiaustralis* | CBS118404 | KP124434 | KP124283 | KP124904 | *Iris* sp. | New Zealand |
| | CBS118486 | KP124435 | KP124284 | KP124905 | *Iris* sp. | Australia |
| | CBS118487 | KP124436 | KP124285 | KP124906 | *Iris* sp. | Australia |
| *A. betae-kenyensis* | CBS118810 | KP124419 | KP124270 | KP124888 | *Beta vulgaris* var. *cicla* | Kenya |
| *A. eichhorniae* | CBS489.92 | KC146356 | KP124276 | KP124895 | *Eichhornia crassipes* | India |
| *A. burnsii* | CBS107.38 | KP124420 | JQ646305 | KP124889 | *Cuminum cyminum* | India |
| | CBS110.50 | KP124421 | KP124271 | KP124890 | *Gossypium* sp. | Mozambique |
| | CBS118816 | KP124423 | KP124273 | KP124892 | *Rhizophora mucronata* | India |
| *A. tomato* | CBS103.30 | KP124445 | KP124294 | KP124915 | *Solanum lycopersicum* | Unknown |
| | CBS114.35 | KP124446 | KP124295 | KP124916 | *Solanum lycopersicum* | Unknown |
| *A. jacinthicola* | CBS878.95 | KP124437 | KP124286 | KP124907 | *Arachis hypogaea* | Mauritius |
| | CBS133751 | KP124438 | KP124287 | KP124908 | *Eichhornia crassipes* | Mali |
| | CPC25267 | KP124439 | KP124288 | KP124909 | *Cucumis melo* var. *indorus* | Unknown |
| *A. alternata* | CBS102599 | KP124330 | KP124185 | KP124798 | *Minneola tangelo* | Turkey |
| | CBS107.53 | KP124305 | KP124162 | KP124774 | *Pyrus pyrifolia* | Japan |
| | CBS115200 | KP124352 | KP124206 | KP124820 | *Minneola tangelo* | South Africa |
| | CBS115616 | AF347031 | AY278808 | KC584375 | *Arachis hypogaea* | India |
| | CBS117143 | KP124355 | KP124209 | KP124823 | *Capsicum annuum* | Italy |
| | CBS118812 | KC584193 | KC584112 | KC584393 | *Daucus carota* | USA |
| | CBS118814 | KP124357 | KP124211 | KP124825 | *Solanum lycopersicum* | USA |
| | CBS118815 | KP124358 | KP124212 | KP124826 | *Solanum lycopersicum* | USA |
| | CBS121348 | KP124367 | KP124219 | KP124836 | *Platycodon grandiflorus* | China |
| | CBS127671 | KP124381 | KP124233 | KP124851 | *Stanleya pinnata* | USA |
| | CBS127334 | KP124380 | KP124232 | KP124850 | soil | USA |
| | CBS121456 | KP124369 | KP124221 | KP124839 | *Sanguisorba officinalis* | China |
| | CBS126910 | KP124379 | KP124231 | KP124849 | *Stanleya pinnata* | USA |
| | CBS795.72 | KP124309 | KP124166 | KP125085 | *Plantago aristida* | USA |
| | CBS620.83 | KP124315 | KP124171 | KP124783 | *Nicotiana tabacum* | USA |
| *A. alternata* | CPA001[d] | KX976465 | KX976466 | KX976467 | *Puccinia striiformis* | China |
| | CBS102600 | KP124331 | KP124186 | KP124799 | *Citrus reticulata* | USA |
| | CBS115069 | KP124347 | KP124201 | KP124815 | *Malus domestica* | South Africa |
| | CBS119543 | KP124363 | KP124215 | KP124831 | *Citrus paradisi* | USA |
| *A. gaisen* | CBS632.93 | KC584197 | KC584116 | KC584399 | *Pyrus pyrifolia* | Japan |
| | CBS118488 | KP124427 | KP124278 | KP124897 | *Pyrus pyrifolia* | Japan |
| | CPC25268 | KP124428 | KP124279 | KP123976 | Unknown | Portugal |
| *A. arborescens SC* | CBS101.13 | KP124392 | KP124244 | KP124862 | Peat soil | Switzerland |
| | CBS105.24 | KP124393 | KP124245 | KP124863 | *Solanum tuberosum* | Unknown |
| | CBS116329 | KP124405 | KP124257 | KP124875 | *Malus domestica* | Germany |
| | CBS105.49 | KP124396 | KP124248 | KP124866 | Contaminant blood culture | Italy |
| | CBS126.60 | KP124397 | KP124249 | KP124867 | Wood | UK |
| | CBS109730 | KP124399 | KP124251 | KP124869 | *Solanum lycopersicum* | USA |
| | CBS112749 | KP124401 | KP124253 | KP124871 | *Malus domestica* | South Africa |
| | CBS112633 | KP124400 | KP124252 | KP124870 | *Malus domestica* | South Africa |
| *A. arborescens* SC | CBS117587 | KP124406 | KP124258 | KP124876 | *Brassica* sp. | Netherlands |
| | CBS118389 | KP124407 | KP124259 | KP124877 | *Pyrus pyrifolia* | Japan |
| | CBS123266 | KP124411 | KP124262 | KP124881 | Human toenail | Denmark |
| | CBS127263 | KP124417 | KP124268 | KP124886 | Human nasal infection | Mexico |
| | CBS115516 | KP124403 | KP124255 | KP124873 | *Malus domestica* | South Africa |

[a]*ITS complete rDNA-ITS region;* [b]*GAPDH glyceraldephyde-3-phosphate dehydrogenase;* [c]*RPB2 the second largest subunit of RNA polymerase II;* [d]*Sequences from isolates of A. alternatea from Puccinia striiformis.*

(Hovmøller et al., 2011). However, we have observed that the color appearance of uredinia (urediniospore mass) occasionally turn dark gray overtime during greenhouse propagation, especially under high humidity conditions. The color shift takes place gradually and becomes increasingly common in frequency, which finally causes the cessation of uredinia sporulation. Our previous study has demonstrated that such discoloration and sporulation cessation could be associated with hyperparasite infection (Zhan et al., 2014).

Hyperparasitism is common in filamentous fungi, and could be developed into a useful alternative to chemical fungicides for effective control of plant fungal diseases (Hijwegen and Buchenauer, 1984; Blakeman, 1992; McLaren et al., 1996; De Cal et al., 2008; Adhikari et al., 2014; Zhong et al., 2016). Previous studies showed that approximately 30 genera of fungi can hyperparasitize rust pathogens, which included *Tuberculina* spp. (Mijušković and Vučinić, 2001), *Darluca filum* (Yuan et al., 1999), *Fusarium* spp. (Kapooria and Sinha, 1969), *Scytalidium uredinicola* (Tsuneda et al., 2011), *Aphanocladium album* (Koç and Défago, 2008) and *Cladosporium* spp. (Moricca et al., 2001). However, so far only four species, *Cladosporium cladosporioides*, *Lecanicillium lecanii*, *Microdochium nivale,* and *Typhula idahoensis,* have been reported to infect uredinia and urediniospores of *Pst* (Littlefield, 1981; Zhan et al., 2014).

Here we describe the discovery of a novel *Pst* hyperparasite. Morphological observations and phylogenetic analysis demonstrated that the fungus belongs to the species of *Alternaria alternata* (Fr.: Fr.) keissler, which has never been reported to parasitize *Pst* or any other fungal organisms. Pathogenicity test and microscopic examination showed that the obtained *A. alternata* strain is able to reduce *Pst* urediniospore

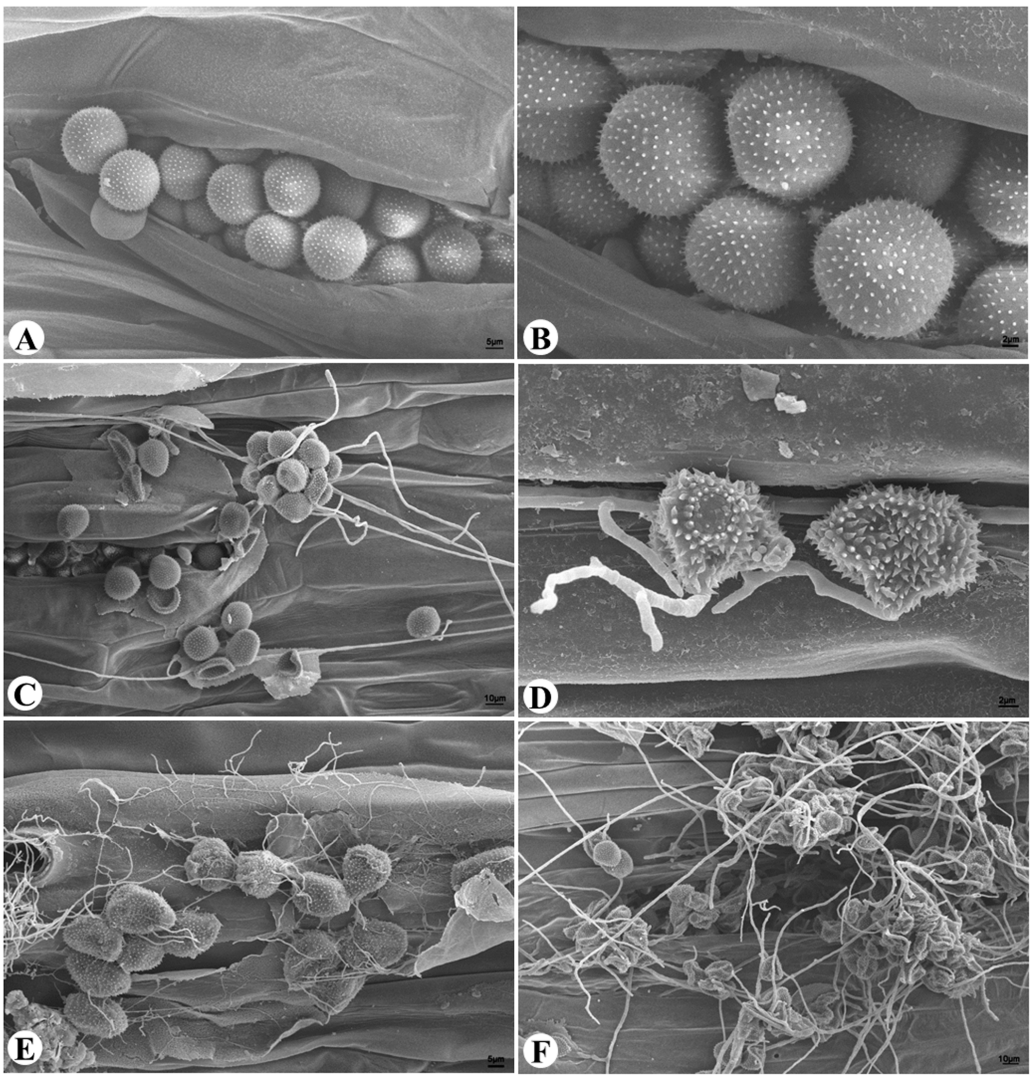


**FIGURE 1 | The hyperparasitic colonization of *Pst* uredinia and urediniospores. (A,B)** Uredinium and urediniospores in normal shape. **(C)** Early stage of hyperparasitic infection, note the shriveled urediniospores. **(D,E)** Mid infection stage. **(F)** Late infection stage.

production and viability, which indicates a biological control potential of this novel mycoparasite against wheat stripe rust disease.

## MATERIALS AND METHODS

### Isolation and Purification of the Mycoparasite

The hyperparasitic strain CPA001 was isolated from *Pst* urediniospores in Northwest A&F University, Yangling, Shaanxi, China. Firstly, urediniospores of *Pst* were propagated on the susceptible wheat cultivar Mingxian 169 as previously described (Cao et al., 2008). Wheat seedlings inoculated with urediniospores of *Pst* were kept in a growth chamber at about 16°C and 80–90% relative humidity (Lu et al., 2011). In total, 151 seedling plants were inoculated. Fourteen to twenty days after inoculation, more than half of the uredinia changed color from fresh yellow orange to gray or dark gray. Gray urediniospores were then transferred onto potato dextrose agar (PDA) medium with a sterilized needle. After incubation at 25° for 3 days, mycelia from the colony margins were transferred to fresh PDA plate and singe-spore purified to obtain a pure culture. The purified culture was stored on PDA slants at 4–8°C.

### Morphological Observation

For the morphological observation, mycelial disks of 5 mm in diameter were taken from the growing margins of 3-day old PDA culture, transferred to potato carrot agar (PCA) plates and incubated at 25°C in a 12-h photoperiod for 1 week to induce conidia production. In addition, microscope slide cultures were prepared by placing a small amount of mycelia on PDA medium blocks (5 mm diameter) overlaid by a cover slip (Wang et al., 2015). Examination of the morphological characteristics of hyphae, conidiophores and conidia were conducted using an Olympus BX51T-32P01 optical microscope.

To further observe the ultrastructure of the parasitic fungus, wheat leaves bearing uredinia with abnormal colors were cut into pieces approximately 0.5 cm × 0.5 cm in size for scanning electronic microscope (SEM). Samples were immersed in 4.0% glutaraldehyde (pH 6.8) and fixed at 4°C for 4 h. Then samples were washed four times with 0.1 M phosphate buffer for 15 min each. Subsequently, samples were dehydrated for 30 min each in 30, 50, 70, 80, and 90% ethanol series, and finally 3 repeats in 100% ethanol. Samples were dried in a $CO_2$ vacuum, and sputter coated with gold (E-1045, Hitachi, Japan) for SEM examination (S-4800, Hitachi, Japan).

### Pathogenicity Test to Confirm Hyperparasitism

The susceptible wheat cultivar Mingxian 169 was used for propagating *Pst* urediniospores. When the first leaf had successfully expanded after 10 days, seedlings were inoculated with CYR32, a predominant race of *Pst* in China. Approximately 14 days later, the diseased leaves bearing urediniospores were inoculated with the mycoparasite *A. alternata* strain CPA001. The pure culture of CPA001 was formulated into spore suspension ($1.0 \times 10^6$ spores/mL in concentration) for spray inoculation. Healthy wheat leaves receiving *A. alternata* inoculation represented control check1 (CK1). Wheat leaves infected by *Pst* but not treated with the *A. alternata* conidia suspension represented CK2. Each treatment was carried out with wheat seedlings growing in three independent pots, with each pot containing about 24 plants. All treatments were placed in the same growth chamber, and observation of the symptoms was performed at the same time.

Simultaneously, *Pst* urediniaspores were directly inoculated with the *A. alternata* strain CPA001. The *A. alternata* conidia suspension ($1.0 \times 10^6$ spores/mL in concentration) was mixed with the *Pst* urediniospores, the spore mixture was sprayed on PDA medium, and incubated at 25° for 24 h. During co-cultivation, samples were collected to observe the dynamic infection process with SEM. Ultrastructural sample treatments were the same as ones described above.

### Uredinia Quantification

The phenotype of disease was quantitively assessed by counting the number of uredinia pustules within a 5 $cm^2$ area at 9 days post CPA001 inoculation, using $I_{MAGE}$[1]. To avoid bias among leaf samples, 35 random leaves were selected for each treatment and the entire experiment was repeated for three times.

[1]http://rsb.info.nih.gov/ij

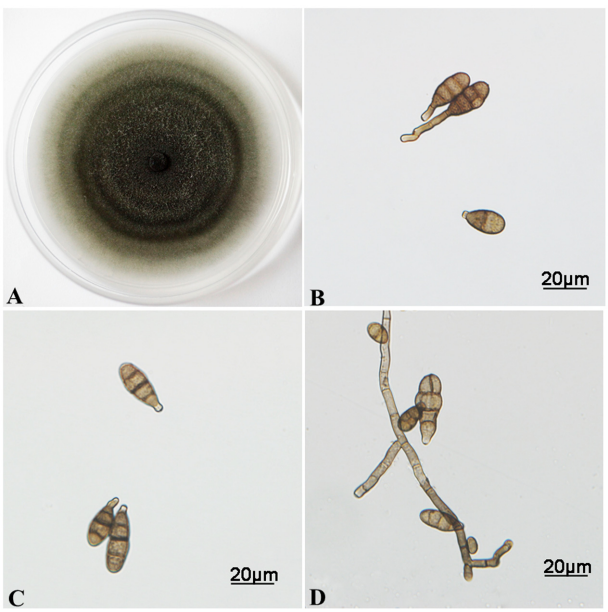


**FIGURE 2 | Morphological characterizations of *A. alternata* cultured on PCA medium. (A)** Colony morphology grown at 25°C for 7 days. **(B–D)** Conidia and vegetative hyphae morphology.

## Germination Rate of *Pst*

Freshly collected urediniospores were cultured on sterile water at 9°C for 6 h, then placed on slides to count the numbers of germinated urediniospores using an Olympus BX51T-32P01 optical microscope. A germ tube length up to the one-half spore diameter was defined as germination. The germination rate was expressed as a percentage based on 100 urediniospores. One hundred urediniospores were selected randomly, and all experiments were performed at least three times.

## Molecular Characterization

### DNA Extraction

The strain CPA001 was cultured on cellophane placed on top of PDA medium and incubated at 25°C for 7 days, the mycelia were then harvested for DNA extraction. Genomic DNA was extracted with CTAB method described by Wang et al. (2015). DNA concentration was measured with a spectrophotometry (Nanodrop 2000, Thermo Fisher Scientific, Wilmington, DE, USA). The DNA was stored at −20°C and diluted to 100 ng/μL as the working solution for polymerase chain reaction (PCR) amplification.

### PCR Amplification and Sequencing

Three representative genes [the complete rDNA-ITS (ITS) region, glyceraldephyde-3-phosphate dehydrogenase (GAPDH) and the second largest subunit of RNA polymerase II (RPB2)] of *A. alternata* were amplified using gene-specific PCR primers of the V9G (5′-TTACGTCCCTGCCCTTTGTA-3′) (Hoog and Gerrits van den Ende, 1998) and ITS4 (5′-TCCTCCGCTTATTGATATGC-3′) (White et al., 1990), gpd1 (5′-CAACGGCTTCGGTCGCATTG-3′) and gpd2 (5′-GCCAAGCAGTTGGTTGTGC-3′) (Berbee et al., 1999) and RPB2-5F2 (5′-GGGGWGAYCAGAAGAAGGC-3′) (Sung et al., 2007) and fRPB2-7cR (5′-CCCATRGCTTGTYYRCCCAT-3′)

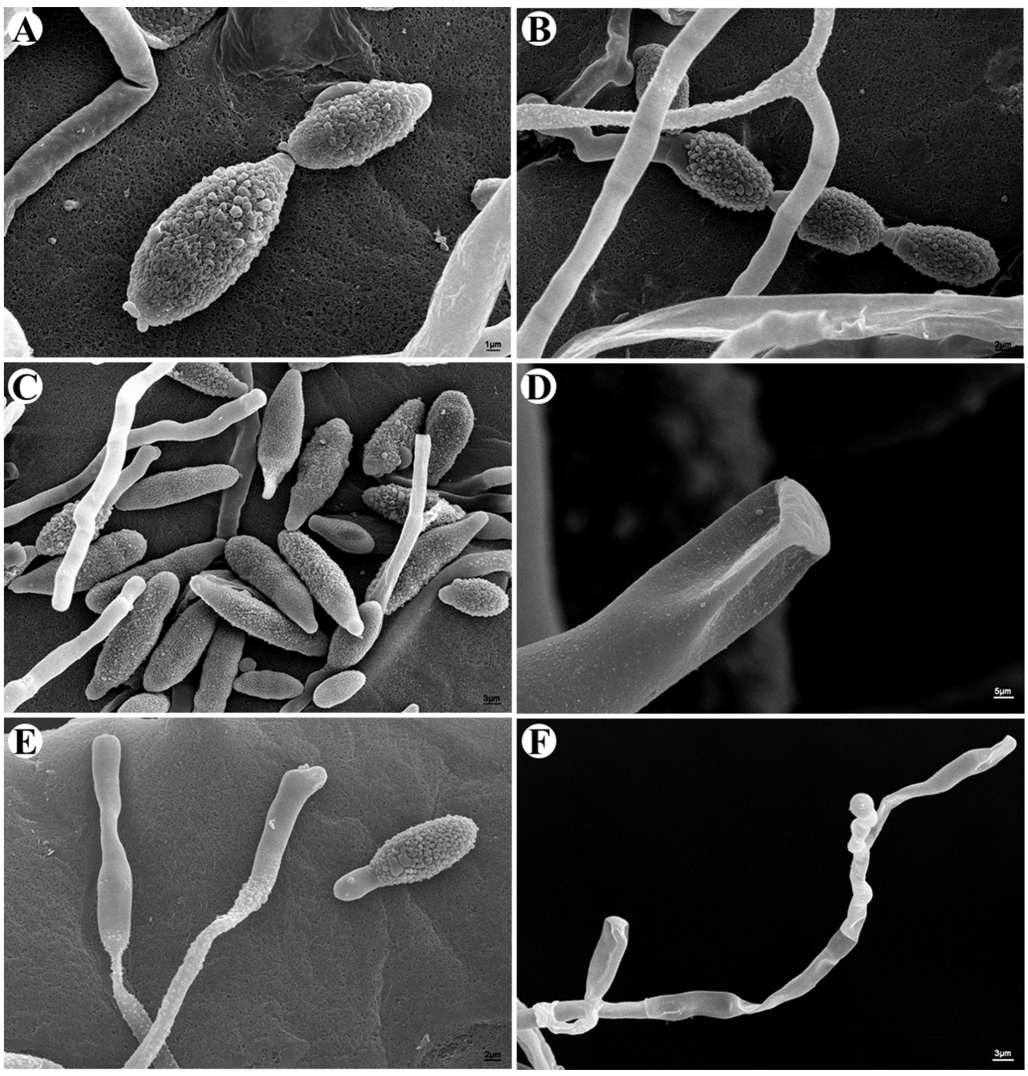


**FIGURE 3 | Morphological characterizations of *A. alternata* under SEM. (A–C)** Conidia. **(D)** Scars on a secondary conidium. **(E,F)** Conidiophores.

(Liu et al., 1999), respectively. Conditions for PCR amplification of the three genes were as follows: initial denaturing at 94°C for 5 min; 35 cycles of denaturing (each cycle at 94°C for 30 s), annealing at 55°C for 30 s, and extension at 72°C for 1 min; and then a final extension at 72°C for 10 min. PCR products were detected by 1.0% agarose gel electrophoresis, purified using a PCR Purification Kit (Bio-tek Co., Ltd, China) according to the manufacture's protocol. The amplified products were cloned into pMD20-T vector (Takara) for Sanger sequencing. All sequences were deposited in GenBank under accession numbers KX976465, KX976466, and KX976467, respectively.

## Phylogenetic Analysis

Reference sequences from other *Alternaria* spp. were retrieved from GenBank (**Table 1**). Sequences were aligned with Clustal X (Thompson et al., 1997), and the final alignment was inspected with BioEdit 5.0.9.1 (Saitou and Nei, 1987). On the basis of the aligned sequences, a phylogenetic tree was constructed with the Maximum Likelihood (ML) method in the Molecular Evolutionary Genetics Analysis (MEGA) software version 6.0 with 1000 bootstrap replicates (Efron et al., 1996; Tamura et al., 2013).

# RESULTS

## Isolation of an *Alternaria alternata* Strain from *Pst* Uredinia Showing Mycoparasitic Symptom

Wheat leaves bearing normal yellow-colored uredinia and leaves bearing gray-colored uredinia resembling hyperparasite infection were examined under SEM (**Figure 1**). Yellow-colored uredinia contained round-shaped urediniospores, and contained no mycelium or spore of other fungal organism (**Figures 1A,B**). On the other hand, gray-colored uredinia were made up of shriveled or ruptured urediniospores, these spores were intertwined by dense filamentous hyphae, which become increasingly prevalent over time (**Figures 1C–F**). The dramatic shape change of urediniospores indicated their loss of cell viability. The prevalence of intertwined hyphae strongly suggested hyperparasitic colonization events.

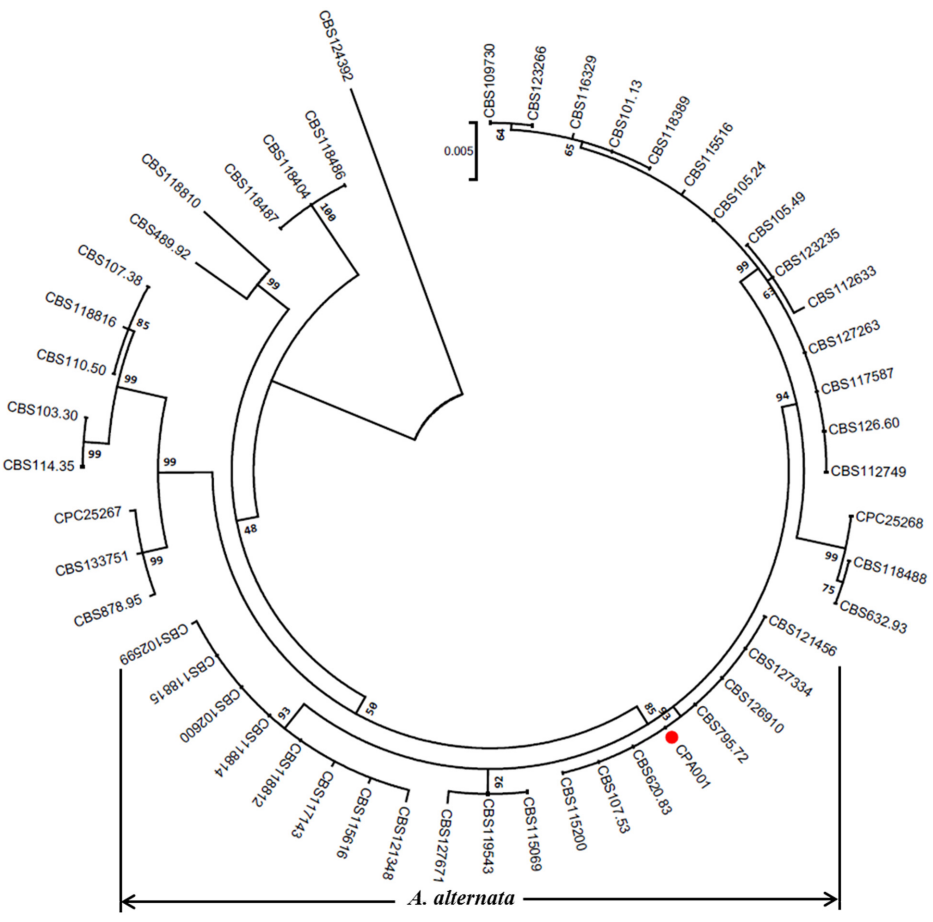


**FIGURE 4 | A phylogenetic tree constructed based on the three genes (ITS, GAPDH and RPB2) of the members in *Alternaria* genus using the maximum likelihood (ML) method with 1000 bootstrap replicates.** The red circle represents the *A. alternata* isolate characterized in the present study.

Through *in vitro* culture, several candidate mycoparasitic fungal strains were obtained. Most strains resembled the previously reported *C. cladosporioides* in morphological appearance (Zhan et al., 2014), which were not characterized further. One strain, named CPA001, was characterized further and reported here. On PCA medium, the CPA001 culture initially developed light-gray colony and the center turned dark gray after 7 days (**Figure 2A**). The vegetative hyphae were brown, branched, septate, and 4 μm in diameter (**Figure 2D**). Conidia were typically obpyriform, dark brown, 20.2 to 35.2 μm × 8.0 to 12.6 μm in size, with 1–3 transverse and 0–1 longitudinal septate. Most conidia also had a short beak with a dimension of 1.6 to 9.4 μm × 2.9 to 5.0 μm (**Figures 2B–D**). SEM observation obtained more detailed morphological characteristics of the conidia and conidiophores (**Figures 3A–F**). SEM observations indicated that the fungus produced abundant conidia in long chains on short conidiophores (**Figures 3A–C**). Conidiophores were single, straight or slightly curved, and ranged from 12.3 to

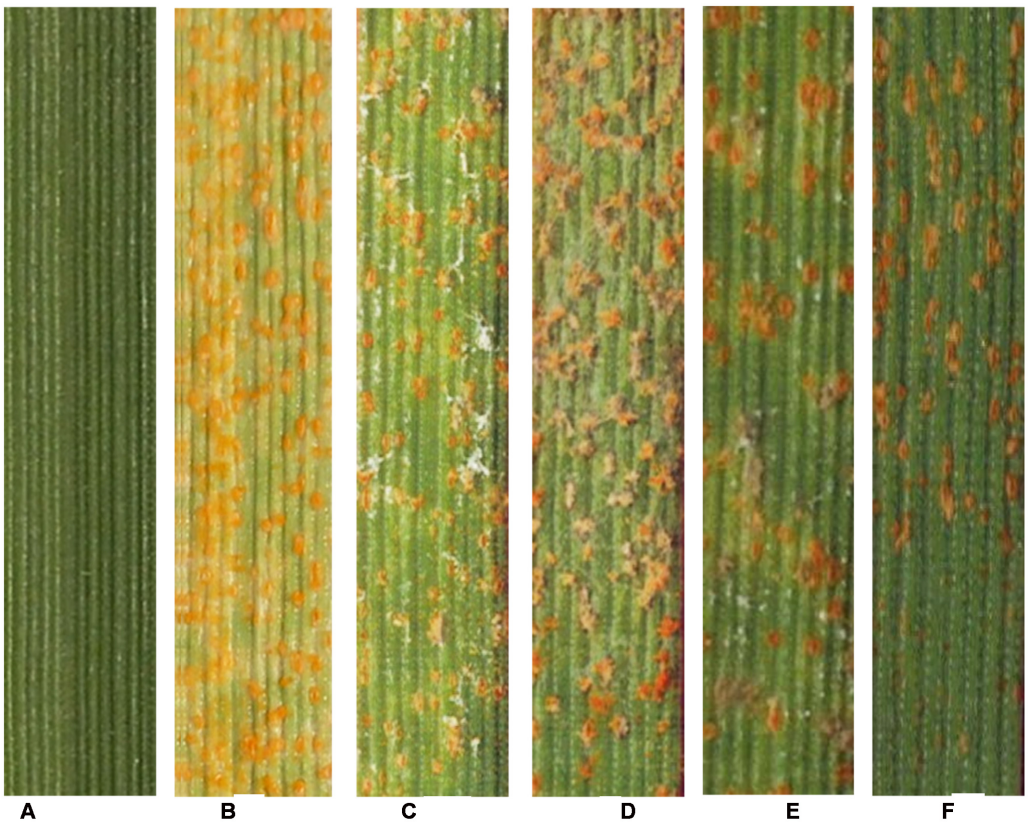


**FIGURE 5 | Pathogenicity test to confirm that *A. alternata* could hyperparasite *Pst*. (A)** CK1, wheat leaves inoculated with the spore suspension of *A. alternata*, 20 dpi, without any symptom; **(B)** CK2, wheat leaves only inoculated with CYR32, 20 dpi; **(C–F)** Wheat leaves inoculated with CYR32 for 14 days prior to inoculating with the spore suspension of *A. alternata*. **(C–F)** are symptoms at 3, 5, 7, and 9 d after *A. alternata* inoculation respectively.

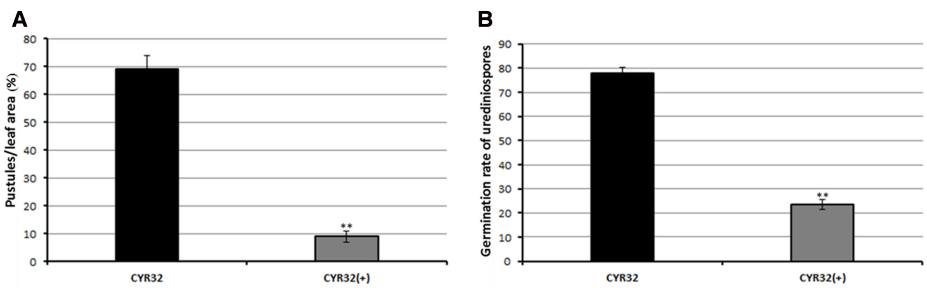


**FIGURE 6 | Quantification of the percentage of leaf area covered by *Pst* pustules (A)** and germination rate of *Pst* urediniospores **(B)**. CYR32 (+) means mycoparasite infected. Values represent mean ± standard errors of three independent assays, and the statistical analysis was assessed by using Student's *t*-tests. Double asterisks indicate $P < 0.01$.

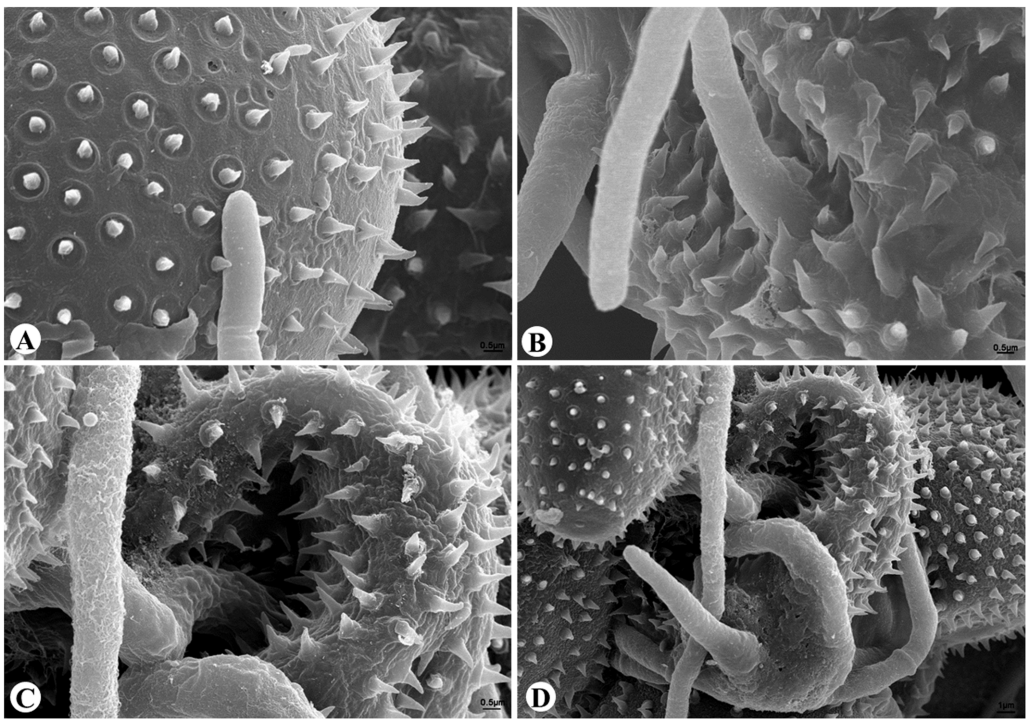


**FIGURE 7 | Scanning electronic microscope observations of *Pst* urediniospore infection by *A. alternata*. (A)** 24 h after inoculation, the *A. alternata* germ tube contacted with *Pst* urediniospore; **(B)** 36 h after inoculation, an *A. alternata* germ tube penetrated into a urediniospore; **(C,D)** 48 h after inoculation, the hyphae of *A. alternata* directly penetrated through the urediniospore.

60.6 μm × 2.2 to 4.0 μm (**Figures 3E,F**). These morphological features resembled *Alternaria* spp.

CPA001 was further identified to be *A. alternata* based on phylogenetic analysis with the ITS, GAPDH and RPB2 genetic markers (**Figure 4**). A range of *Alternaria* spp. reference isolates were selected for the phylogenetic tree construction. CPA001 was found to be most closely related to CBS121456, CBS127334, CBS126910,CBS795.72, CBS620.83, CBS107.53 and CBS115200, all belonging to the *A. alternata* species. The entire *A. alternata* clade was well-separated from other clades with a bootstrap value of 85%.

## Confirmation of Hyperparasitism

Pathogenicity testing showed that the obtained CPA001 strain could efficiently hyperparasitize *Pst* (**Figure 5**). Wheat leaves inoculated with *Pst* alone produced abundant orange-colored uredinia after 21 days post inoculation (**Figure 5B**). On the other hand, *Pst* pre-inoculated wheat leaves receiving subsequent *A. alternata* treatment showed a typical sign of mycoparasitic colonization, namely fewer rust pustule formation and abundant gray-colored hyphae covering the uredinia (**Figures 5C–F**). Such gray-colored hyphae were never observed with wheat leaves treated with *A. alternata* conidia suspension alone (CK1, **Figure 5A**). Reisolated strain from the parasitized uredinia showed the same morphological characteristics CPA001. At 9 days post CPA001 inoculation, the frequency of *Pst* pustule formation was merely 10% whereas that of the control treatment was 70% (**Figure 6A**). Urediniospores collected from CPA001-treated pustules also showed dramatically reduced viability (∼25% vs. 80%), indicated by germination rate (**Figure 6B**).

Scanning electronic microscope observations further confirmed that the *A. alternata* CPA001 strain could efficiently parasitize *Pst*. The *A. alternata* germ tube contacted with and penetrated into *Pst* urediniospores at 24 hpi, and caused complete urediniospore collapse at 36–48 hpi (**Figures 7A–D**).

# DISCUSSION

Characterization of newly isolated mycoparasites has contributed to a better understanding of the diversity of hyperparasites, and will lead to the discoveries of novel fungal species and the development of novel biocontrol agents (Vandermeer et al., 2009; Baiswar et al., 2014; Wang et al., 2015; Zhong et al., 2016). The present study revealed a novel mycoparasite infecting *Pst*, the causal agent of wheat stripe rust. In addition, the hyperparasite could reduce the production and viability of urediniospores, indicating its potential application in the biological control of *Pst*.

Conidial morphology and size used to be important features used in *Alternaria* taxonomy. However, these phenotypes are plastic, showing considerable variations under different environmental and culture conditions, making it difficult to identify species based on phenotype alone (Rotem, 1994). Although ITS region of nuclear ribosomal DNA (nrDNA)

is a universal marker used for the identification of fungal species (Seena et al., 2010; Schoch et al., 2012), it is ineffective in distinguishing closely related fungal species (Pryor and Gilbertson, 2002; Kiss, 2012). Currently, multiple gene-based phylogeny has been widely used in the classification of species in the genus *Alternaria* (Andrew and Pryor, 2008; Lawrence et al., 2013; Woudenberg et al., 2015). In the present study, a combination of three markers identified the obtained mycoparasite to be *A. alternata*. To our knowledge, this is the first report that *A. alternata* could hyperparasitize *Pst*, and also the first report of *A. alternata* as a hyperparasite.

Resistance breeding is critical for wheat rust disease control. Nevertheless, most resistant genes used for breeding are ones with major effect, which tend to lose their resistance rapidly upon field release (Line and Qayoum, 1992; Li and Zeng, 2000). So far, mycoparasitism has been reported as an effective measure for controlling several diseases (Zhong et al., 2016). For example, *Trichoderma* spp. has been successfully used to minimize the effect of *Fusarium oxysporum* pathogen on tomato plants (Adhikari et al., 2014). *Ampelomyces quisqualis* is in commercial use for biocontrol of powdery mildew on grapes and other crops (Sullivan and Maddock, 2000). However, there have been little known attempts to control *Pst* with hyperparasites.

The *A. alternata* strain CPA001 obtained in the present study can colonize *Pst* urediniospores in an aggressive manner. CPA001 treatment dramatically reduces uredinial pustule formation and the viability of ureniniospores. Moreover, our observation indicated that CPA001 can colonize a broad range of *Pst* isolates being different in virulence profile (physiological race) and geographic origin. These facts make CPA001 a good candidate for further characterization efforts to develop novel *Pst* biocontrol agent. But now, we are unclear about the mycoparasitism spectrum of CPA001 at a broader level (e.g., its hypoparasitic potential against other rust pathogens), and whether and how environmental factors affect the survival ability and hypoparasitic potential of CPA001. We also do not know by which strategies CPA001 kills and colonizes *Pst* urediniospores and whether these strategies are CPA001-unique or are general features of the *A. alternata* species. In the near future, it is important to study the hypoparasitic characteristics of CPA001 in more detail in the laboratory, so as to understand its parasitism spectrum, its hypoparasitic mechanisms, and the potential environmental and ecological impacts upon massive release. Key factors impacting mycoparasitism efficiency should be identified and controlled field test should be performed to determine the disease control effect.

Urediniospores are important inoculation materials for rust disease research. Based on our experience, mycoparasitic infection of *Pst* is common in the greenhouse, which could pose a great challenge to research activities such as spore propagation. In the near future, we are planning to further characterize the biological characteristics of the obtained mycoparasitic isolate, such as the experimental host range, the spore type specificity, and the effects of environmental conditions (e.g., humidity, moisture) on the final parasitic infection outcome. These efforts will offer important principle guidelines for the field application and greenhouse control of *Pst* mycoparasites.

## AUTHOR CONTRIBUTIONS

ZK designed experiments; LZ performed the experiments; JZ and XL analyzed the data; GZ and SJ joined the discussion and gave the original ideas; LZ wrote the paper.

## ACKNOWLEDGMENTS

This work was supported by the National Key Basic Research Program of China (2013CB127700), National 'Twelfth Five-Year' Plan for Science and Technology Support (2012BAD19B04-12), Modern Agro-industry Technology Research System in China (CARS-3-1-11) and the 111 Project of the Ministry of Education of China (No. B07049), and the China Postdoctoral Science Foundation (2016M592845).

## REFERENCES

Adhikari, A., Nandi, S., Dutta, S., Bhattacharya, I., and Mandal, T. (2014). Study of morphology and mycoparasitism of some antagonists of *Trichoderma* sp from West Bengal. India. *Int. J. Res.* 1, 593–605.

Andrew, M., and Pryor, B. M. (2008). An expanded multilocus phylogeny does not resolve morphological species within the small-spored *Alternaria* species complex. *Mycologia* 101, 95–109. doi: 10.3852/08-135

Baiswar, P., Ngachan, S., and Chandra, S. (2014). *Ramularia coleosporii*, a hyperparasite on *Coleosporium plumeriae*, in India. *J. Phytopathol.* 163, 407–410. doi: 10.1111/jph.12286

Berbee, M. L., Pirseyedi, M., and Hubbard, S. (1999). *Cochliobolus* phylogenetics and the origin of known, highly virulent pathogens, inferred from ITS and glyceraldehyde-3-phosphate dehydrogenase gene sequences. *Mycologia* 91, 964–977. doi: 10.2307/3761627

Blakeman, J. P. (1992). Potential for biological of plant diseases on the phyllosphere. *Annu. Rev. Phytopathol.* 20, 167–192. doi: 10.1146/annurev.py.20.090182.001123

Brown, J. K. M., and Hovmøller, M. S. (2002). Aerial dispersal of pathogens on the global and continental scales and its impact on plant disease. *Science* 297, 537–541. doi: 10.1126/science.1072678

Cao, L. H., Xu, S. C., Chen, W. Q., Liu, T. G., and Chen, W. Q. (2008). Early molecular diagnosis and detection of *Puccinia striiformis* f. sp. tritici in China. *Lett. Appl. Microbiol.* 46, 501–506. doi: 10.1111/j.1472-765X.2007.02313.x

Chen, W. Q., Wu, L. R., Liu, T. G., and Xu, S. C. (2009). Race dynamics, diversity, and virulence evolution in *Puccinia striiformis* f. sp. tritici, the causal agent of wheat stripe rust in China from 2003 to 2007. *Plant Dis.* 93, 1093–1101. doi: 10.1094/PDIS-93-11-1093

Chen, X. M. (2005). Epidemiology and control of stripe rust [*Puccinia striiformis* f. sp. tritici] on wheat. *Can. J. Plant Pathol.* 27, 314–337. doi: 10.1080/07060660509507230

Cheng, P., Xu, L. S., Wang, M. N., See, D. R., and Chen, X. M. (2014). Molecular mapping of genes Yr64 and Yr65 for stripe rust resistance in hexaploid derivatives of durum wheat accessions PI 331260 and PI 480016. *Theor. Appl. Genet.* 127, 2267–2277. doi: 10.1007/s00122-014-2378-8

De Cal, A., Redondo, C., Sztejnberg, A., and Melgarejo, P. (2008). Biocontrol of powdery mildew by *Penicillium oxalicum* in open-field nurseries of strawberries. *Biol. Control* 47, 103–107. doi: 10.1016/j.biocontrol.2008.07.010

Efron, B., Halloran, E., and Holmes, S. (1996). Bootstrap confidence levels for phylogenetic trees. *Proc. Natl. Acad. Sci. U.S.A.* 93, 13429–13434. doi: 10.1073/pnas.93.14.7085

Gao, L., Yu, H. X., Kang, X. H., Shen, H. M., Li, C., Liu, T. G., et al. (2015). Development of SCAR markers and an SYBR green assay to detect *Puccinia striiformis* f. sp. tritici in infected wheat leaves. *Plant Dis.* 100, 1840–1847. doi: 10.1094/PDIS-06-15-0693-RE

Han, D. J., Wang, Q. L., Chen, X. M., Zeng, Q. D., Wu, J. H., Xue, W. B., et al. (2015). Emerging Yr26 – virulent races of *Puccinia striiformis* f. tritici are threatening wheat production in the Sichuan basin. China. *Plant Dis.* 99, 754–760. doi: 10.1094/PDIS-08-14-0865-RE

Hijwegen, T., and Buchenauer, H. (1984). Isolation and identification of hyperparasitic fungi associated with erysiphaceae. *Neth. J. Plant Pathol.* 90, 79–83. doi: 10.1007/BF01999956

Hoog, G. S. D., and Gerrits van den Ende, A. H. G. (1998). Molecular diagnostics of clinical strains of filamentous basidiomycetes. *Mycoses* 41, 183–189. doi: 10.1111/j.1439-0507.1998.tb00321.x

Hovmøller, M. S., Sørensen, C. K., Walter, S., and Justesen, A. F. (2011). Diversity of *Puccinia striiformis* on cereals and grasses. *Annu. Rev. Phytopathol.* 49, 197–217. doi: 10.1146/annurev-phyto-072910-095230

Kapooria, R. G., and Sinha, S. (1969). Phylloplane mycoflora of pearl millet and its influence on the development of *Puccinia penniseti*. *Trans. Br. Mycol. Soc.* 53, 153–155. doi: 10.1016/S0007-1536(69)80024-0

Kiss, L. (2012). Limits of nuclear ribosomal DNA internal transcribed spacer (ITS) sequences as species barcodes for Fungi. *Proc. Natl. Acad. Sci. U.S.A.* 109, 10741–10742. doi: 10.1073/pnas.1207143109

Koç, N. K., and Défago, G. (2008). Studies on the host range of the hyperparasite *Aphanocladium album*. *J. Phytopathol.* 107, 214–218.

Lawrence, D. P., Gannibal, P. B., Peever, T. L., and Pryor, B. M. (2013). The sections of *Alternaria*: formalizing species-group concepts. *Mycologia* 105, 530–546. doi: 10.3852/12-249

Li, Z. Q., and Zeng, S. M. (2000). *Wheat Rust in China*. Beijing: China Agricultural Press.

Line, R. F., and Qayoum, A. (1992). Virulence, aggressiveness, evolution and distribution of races of *Puccinia striiformis* (the cause of stripe rust of wheat) in North America. *Tech. Bull.* 1968–1987.

Littlefield, L. J. (1981). *Biology of the Plant Rust: An Introduction*. Ames, IA: Iowa State University Press, 103.

Liu, Y. J., Whelen, S., and Hall, B. D. (1999). Phylogenetic relationships among ascomycetes: evidence from an RNA polymerse II subunit. *Mol. Biol. Evol.* 16, 1799–1808. doi: 10.1093/oxfordjournals.molbev.a026092

Lu, N. H., Wang, J. F., Chen, X. M., Zhan, G. M., Chen, C. Q., Huang, L. L., et al. (2011). Spatial genetic diversity and interregional spread of *Puccinia striiformis* f. sp. tritici in Northwest China. *Eur. J. Plant Pathol.* 131, 685–693. doi: 10.1007/s10658-011-9842-y

McLaren, D. L., Huang, H. C., and Rimmer, S. R. (1996). Control of apothecial production of *Sclerotinia sclerotiorum* by coniothyrium minitans and talaromyces flavus. *Plant Dis.* 80, 1373–1378. doi: 10.1094/PD-80-1373

Mijušković, M., and Vučinić, Z. (2001). *Hyperparasitic Fungi in Mycopopulation of Montenegro*. Podgorica: Montenegrien Mycological Center.

Moricca, S., Ragazzi, A., Mitchelson, K. R., and Assante, G. (2001). Antagonism of the two-needle pine stem rust fungi *Cronartium flaccidum* and *Peridermium pini* by *Cladosporium tenuissimum* in vitro and in planta. *Phytopathology* 91, 457–468. doi: 10.1094/PHYTO.2001.91.5.457

Pryor, B. M., and Gilbertson, R. L. (2002). Relationships and taxonomic status of alternaria radicina, A. carotiincultae, and A. petroselini based upon morphological, biochemical, and molecular characteristics. *Mycologia* 94, 49–61.

Rotem, J. (1994). *The Genus Alternaria: Biology, Epidemiology and Pathogenicity*. St Paul, MN: American Phytopathological Society Press.

Saari, E. E., and Prescott, J. M. (1985). World distribution in relation to economic losses. *Cereal Rusts* 2, 260–298.

Saitou, N., and Nei, M. (1987). The neighbor-joining method: a new method for reconstructing phylogenetic trees. *Mol. Biol. Evol.* 4, 406–425.

Schoch, C. L., Seifert, K. A., Huhndorf, S., Robert, V., Spouge, J. L., Levesque, C. A., et al. (2012). Nuclear ribosomal internal transcribed spacer (ITS) region as a universal DNA barcode marker for Fungi. *Proc. Natl. Acad. Sci. U.S.A.* 109, 6241–6246. doi: 10.1073/pnas.1117018109

Seena, S., Pascoal, C., Marvanová, L., Cássio, F., and Hyde, K. D. (2010). DNA barcoding of fungi: a case study using its sequences for identifying aquatic hyphomycete species. *Fungal Divers.* 44, 77–87. doi: 10.1007/s13225-010-0056-y

Stubbs, R. W. (1985). Stripe rust. *The Cereal Rusts* 2, 61–101.

Sullivan, S. M., and Maddock, J. R. (2000). Bacterial sporulation: pole-to-pole protein oscillation. *Curr. Biol.* 10, 159–161. doi: 10.1016/S0960-9822(00)00331-6

Sung, G. H., Sung, J. M., Hywel-Jones, N. L., and Spatafora, J. W. (2007). A multi-gene phylogeny of Clavicipitaceae (Ascomycota, Fungi): identification of localized incongruence using a combinational bootstrap approach. *Mol. Phylogenet. Evol.* 44, 1204–1223.

Tamura, K., Stecher, G., Peterson, D., Filipski, A., and Kumar, S. (2013). MEGA6: molecular evolutionary genetics analysis version 6.0. *Mol. Biol. Evol.* 30, 2725–2729. doi: 10.1093/molbev/mst197

Thompson, J. D., Gibson, T. J., Plewniak, F., and Higgins, D. G. (1997). The CLUSTAL_X windows interface: flexible strategies for multiple sequence alignment aided by quality analysis tools. *Nucleic Acids Res.* 25, 4876–4882. doi: 10.1093/nar/25.24.4876

Tsuneda, A., Hiratsuka, Y., and Maruyama, P. J. (2011). Hyperparasitism of *Scytalidium uredinicola* on western gall rust, *Endocronartium harknessii*. *Can. J. Bot.* 58, 1154–1159. doi: 10.1139/b80-143

Vandermeer, J., Perfecto, I., and Liere, H. (2009). Evidence for hyperparasitism of coffee rust ( *Hemileia vastatrix*) by the entomogenous fungus, *Lecanicillium lecanii*, through a complex ecological web. *Plant Pathol.* 58, 636–641.

Wan, A. M., Chen, X. M., and He, Z. H. (2007). Wheat stripe rust in China. *Aust. J. Agr. Res.* 58, 605–619. doi: 10.1071/AR06142

Wan, A. M., Zhao, Z. H., Chen, X. M., He, Z. H., Jin, S. L., Jia, Q. Z., et al. (2004). Wheat stripe rust 1139 epidemic and virulence of *Puccinia striiformis* f. sp. tritici in China in 2002. *Plant Dis.* 88, 896–904. doi: 10.1094/PDIS.2004.88.8.896

Wang, Y. B., Yu, H., Dai, Y. D., Wu, C. K., Zeng, W. B., Yuan, F., et al. (2015). *Polycephalomyces agaricus*, a new hyperparasite of *Ophiocordyceps*, sp. infecting melolonthid larvae in southwestern China. *Mycol. Prog.* 14, 1–9. doi: 10.1007/s11557-015-1090-7

White, T. J., Bruns, T., Lee, S., and Taylor, J. (1990). "Amplification and direct sequencing of fungal ribosomal RNA genes for phylogenetics," in *PCR Protocols: A Guide to Methods and Applications*, eds M. A. Innis, D. H. Gelfand, J. J. Sninsky, and T. J. White (San Diego, CA: Academic Press), 315–322.

Woudenberg, J. H. C., Seidl, M. F., Groenewald, J. Z., Vries, M. D., Stielow, J. B., Thomma, B. P. H. J., et al. (2015). *Alternaria* section *Alternaria*: species, formae speciales, or pathotypes? *Stud. Mycol.* 82, 1–21. doi: 10.1016/j.simyco.2015.07.001

Yuan, Z. M., Hunter, T., Ruiz, C., and Royle, D. J. (1999). Pathogenicity to willow rust, melampsora epitea, of the mycoparasite sphaerellopsis filum from different sources. *Mycol. Res.* 103, 509–512. doi: 10.1017/S0953756298007448

Zhan, G. M., Tian, Y., Wang, F. P., Chen, X. M., Guo, J., Jiao, M., et al. (2014). A novel fungal hyperparasite of *Puccinia striiformis* f. sp. tritici, the causal agent of wheat stripe rust. *PLoS ONE* 9:e111484. doi: 10.1371/journal.pone.0111484

Zhao, J., Wang, X. J., Chen, C. Q., Huang, L. L., and Kang, Z. S. (2008). A PCR-based assay for detection of *Puccinia striiformis* f. sp. tritici in wheat. *Plant Dis.* 91, 1669–1674. doi: 10.1094/PDIS-91-12-1669

Zhong, X., Li, S. S., Peng, Q. Y., Zhang, J. S., Kan, X. T., Zhang, G. R., et al. (2016). A polycephalomyces, hyperparasite of ophiocordyceps sinensis, leads to shortened duration of production and reduced numbers of host ascospores. *Fungal Ecol.* 21, 24–31. doi: 10.1016/j.funeco.2016.03.002

**Conflict of Interest Statement:** The authors declare that the research was conducted in the absence of any commercial or financial relationships that could be construed as a potential conflict of interest.

frontiers in Microbiology

ORIGINAL RESEARCH
published: 04 August 2016
doi: 10.3389/fmicb.2016.01236

# The L-type $Ca^{2+}$ Channel Blocker Nifedipine Inhibits Mycelial Growth, Sporulation, and Virulence of *Phytophthora capsici*

*Peiqing Liu, Jie Gong, Xueling Ding, Yue Jiang, Guoliang Chen, Benjin Li, Qiyong Weng* and Qinghe Chen**

*Fujian Key Laboratory for Monitoring and Integrated Management of Crop Pests, Institute of Plant Protection, Fujian Academy of Agricultural Sciences, Fuzhou, China*

The oomycete vegetable pathogen *Phytophthora capsici* causes significant losses of important vegetable crops worldwide. Calcium and other plant nutrients have been used in disease management of oomycete pathogens. Calcium homeostasis and signaling is essential for numerous biological processes, and $Ca^{2+}$ channel blockers prevent excessive $Ca^{2+}$ influx into the fungal cell. However, it is not known whether voltage-gated $Ca^{2+}$ channel blockers improve control over oomycete pathogens. In the present study, we compared the inhibitory effects of $CaCl_2$ and the extracellular $Ca^{2+}$ chelator EDTA on mycelial growth and found that calcium assimilation plays a key role in *P. capsici* mycelial growth. Next, we involved the voltage-gated $Ca^{2+}$ channel blockers verapamil (VP) and nifedipine (NFD) to analyze the effect of $Ca^{2+}$ channel blockers on mycelial growth and sporulation; the results suggested that NFD, but not VP, caused significant inhibition. Ion rescue in an NFD-induced inhibition assay suggested that NFD-induced inhibition is calcium-dependent. In addition, NFD increased *P. capsici* sensitivity to $H_2O_2$ in a calcium-dependent manner, and extracellular calcium rescued it. Furthermore, NFD inhibited the virulence and gene expression related to its pathogenicity. These results suggest that NFD inhibits mycelial growth, sporulation, and virulence of *P. capsici*.

**Keywords:** ***Phytophthora capsici*, nifedipine, calcium rescue, virulence, $H_2O_2$**

OPEN ACCESS

***Edited by:***
*Joshua D. Nosanchuk, Albert Einstein College of Medicine, USA*

***Reviewed by:***
*Gyöngyvér Mara, Sapientia Hungarian University of Transylvania, Romania*
*Huafeng Wang, University of Wisconsin–Madison, USA*

****Correspondence:***
*Qiyong Weng*
*wengqy@faas.cn*
*Qinghe Chen*
*chenqh@faas.cn*

***Specialty section:***
*This article was submitted to Fungi and Their Interactions, a section of the journal Frontiers in Microbiology*

***Received:*** *17 May 2016*
***Accepted:*** *25 July 2016*
***Published:*** *04 August 2016*

***Citation:***
*Liu P, Gong J, Ding X, Jiang Y, Chen G, Li B, Weng Q and Chen Q (2016) The L-type $Ca^{2+}$ Channel Blocker Nifedipine Inhibits Mycelial Growth, Sporulation, and Virulence of Phytophthora capsici. Front. Microbiol. 7:1236. doi: 10.3389/fmicb.2016.01236*

## INTRODUCTION

Calcium acts as a second messenger and plays a direct role in controlling the expression patterns of its signaling systems in fungi. It is essential for numerous intrinsic metabolic processes including spore germination, hypha tip growth and branching, sporulation, hypha infection structure differentiation, circadian clocks, and responses to various environmental stresses (Liu et al., 2015a). However, improper regulation of $Ca^{2+}$ in fungi can produce significant damages and even ultimately lead to cell death (Hu et al., 2013; Gonçalves et al., 2014; Liu et al., 2015b). Normally, calcium channels allow the passive flow of $Ca^{2+}$ across cell membranes into the cytosol. Two major calcium uptake pathways have been identified in *Saccharomyces* and other fungi: the high-affinity (HACS) and low-affinity (LACS) calcium uptake systems (Martin et al., 2011; Wang et al., 2012; Harren and Tudzynski, 2013). The Cch1 and Mid1 $Ca^{2+}$ channel complex constitutes the HACS (Cch1 functions as the pore, and Mid1 serves as a assistance) that mediates

the specific influx of $Ca^{2+}$ (Cavinder et al., 2011; Harren and Tudzynski, 2013). Mid1 and Cch1 have been identified in many filamentous fungi (Hallen and Trail, 2008; Yu et al., 2012), and deletion of Mid1 affects vegetative growth, cell wall synthesis, and virulence in *Claviceps purpurea* (Bormann and Tudzynski, 2009). In *Botrytis cinerea,* Cch1 and Mid1 are functionally required for vegetative growth under low-calcium conditions (Harren and Tudzynski, 2013). In *Gibberella zeae*, Mid1 affects the hypha growth, development processes, and even ascospore discharge significantly (Cavinder et al., 2011). In *Cryptococcus neoformans*, knock-out of Mid1 or Cch1 can caused significantly inhibition to oxidative stress (Vu et al., 2015).

In fact, voltage-gated $Ca^{2+}$ channel blockers function in various modes. VP, one of the important L-type calcium channel blocker, is widely used in the medical treatment and served as a miracle drug in the treatment of angina pectoris and even hypertension. It partially inhibits the function of HACS, resulting in decreased calcium influx under normal growth conditions in *S. cerevisiae* and *Candida albicans* (Breeuwer et al., 1995; Yu et al., 2014). Nifedipine (NFD), used as a dihydropyridine derivative commonly, forms a stable complex with the L-type calcium receptors' binding site, which is made up of six spatially separated amino acid residues while its conformation corresponds to the closed channel. NFD preferentially blocks $Ca^{2+}$ channels of various cell types and prevents $Ca^{2+}$ influx by reducing cytosolic $Ca^{2+}$ concentrations (Nguemo et al., 2013). Diltiazem, a benzothiazepine-type calcium channel blocker, blocks L-type calcium channel by way of their high-affinity binding (Hockerman et al., 2000). The voltage-gated $Ca^{2+}$ channel blockers can be used to treat the fungal pathogen *C. albicans* (Yu et al., 2014), and diltiazem and VP can block the opening of voltage-gated L-type $Ca^{2+}$ channels and prevent a severe $Ca^{2+}$ influx into the animal cells and *S. cerevisiae* (Teng et al., 2008). High concentrations of diltiazem also resulted in enhanced $Ca^{2+}$ accumulation in *S. cerevisiae* cells (Binder et al., 2010). In addition, chelating extracellular calcium modulates cytosolic calcium, which severely reduces the expression of several calcium transport proteins and influences the normal functions of fungi (Juvvadi et al., 2015; Puigpinós et al., 2015). The reduction of intracellular calcium is responsible for the inhibition of reactive oxygen species (ROS)-generating enzymes and formation of free radicals by the mitochondria respiratory chain (Gordeeva et al., 2003; Kraus and Heitman, 2003). The Cch1-Mid1 regulated HACS contributes to a virulence change in *C. neoformans* by mitigating oxidative stress (Vu et al., 2015), and VP has an inhibitory effect on the oxidative stress response in *C. albicans* (Yu et al., 2014), confirming the relationship between calcium signaling and oxidative stress.

The oomycete vegetable pathogen *P. capsici* is a virulent, hemibiotrophic pathogen of vegetable crops, which inflicts significant losses of important vegetable crops worldwide (Jackson et al., 2012). Although it was first described almost 90 years ago, no direct and effective managements have been developed (Lamour et al., 2012). *P. capsici* has shown remarkable adaptation to fungicides and new hosts. Cinnamaldehyde (CA) is a major constituent of cinnamon essential oils and has been used as a food antimicrobial agent for its inhibiting of bacteria, yeast, and filamentous fungus, which involves membrane action, cell wall synthesis, and specific cellular processes (Wang et al., 2005; Shreaz et al., 2010). Previous studies also have shown that calcium efflux is involved in CA-induced inhibition of *P. capsici* zoospores (Hu et al., 2013). In addition, treatment with the voltage-gated calcium channel blocker verapamil (VP) can lead to a higher level of CA-induced $Ca^{2+}$ efflux, suggesting that the $Ca^{2+}$ channel may be a target for controlling pathogens. Furthermore, plant nutrients, especially $Ca^{2+}$, can be applied to the disease management in *Phytophthora* spp. (Sugimoto et al., 2005), and more attention has focused on the suppressive effect of calcium on *Phytophthora* spp. (Sugimoto et al., 2010). In fact, $CaCl_2$ and $Ca(NO_3)_2$ can dramatically suppress disease incidence caused by *P. sojae* in black soybean and white soybean and affect plant resistance. Moreover, 4–30 mM $CaCl_2$ and $Ca(NO_3)_2$ can decrease the release of *P. sojae* zoospores (Sugimoto et al., 2005). Although voltage-gated $Ca^{2+}$ channel blockers have been used widely, it is not known whether they could be used to control oomycete pathogens, especially *P. capsici.* In the present study, we investigated the effects of voltage-gated $Ca^{2+}$ channel blockers on *P. capsici* mycelial growth, sporulation, and virulence.

## MATERIALS AND METHODS

### *Phytophthora capsici* Strains and Culture Conditions

The *P. capsici* genome-sequenced virulence strain LT1534 was provided by Prof. Lamour (University of Tennessee, Knoxville, TN, USA), which has been used as a model strain by more and more scientists (Stam et al., 2013; Iribarren et al., 2015; Liu et al., 2016). Strain LT1534 was grown on 10% V8 juice agar medium at 25°C in the dark (Lamour et al., 2012). Radial growth was measured at day 5, when the colony of the strain LT1534 had almost completely covered the surface of the media in the dishes. Radial growth was assessed by measuring the distance from the edge of the inoculum plug to the advancing margin of the colony.

### Effect of $CaCl_2$ and EDTA on Mycelial Growth of *P. capsici*

To test the inhibitory effect of $CaCl_2$ and the extracellular $Ca^{2+}$ chelator EDTA on *P. capsici* mycelial growth, strain LT1534 was grown on 10% V8 juice agar medium at 25°C, and then 1-week-old agar plugs (5 mm diameter) transferred onto the center of dish (10% V8 juice agar medium containing 0, 2.5, 5, 10, 25, and 50 mM $CaCl_2$, and 0, 0.5, 1.0, 2.5, 5, and 10 mM EDTA). Radial growth was measured at day 5. Stock solutions of $CaCl_2$ and EDTA were prepared as 1 M $CaCl_2$ in $H_2O$ (Sigma–Aldrich) and 1 M EDTA in $H_2O$ (Sigma–Aldrich).

### Effect of VP and NFD on Mycelial Growth and Sporulation

To analyze the growth inhibitory effect of VP and NFD on *P. capsici* strain LT1534, 0, 10, 40, 80, 160, and 320 μg/mL VP

and 0.1, 0.2, 0.5, 1, and 2 μM NFD were added to 10% V8 juice agar medium, and radial growth was measured at day 5. Stock solutions of VP and NFD were prepared as 320 mg/mL VP in $H_2O$ (Sigma–Aldrich) and 50 mM NFD in DMSO (Sigma–Aldrich).

To analyze zoosporangia density, the mycelia were washed three times with 30 mL of sterile distilled water and then an additional 20 mL of sterile distilled water was added to induce sporangia formation in the dark at 25°C for 24 h. The number of zoosporangia was counted and the mean of three duplications was used as the result of one replicate. Each experiment was repeated in triplicate wells at least three times.

To investigate whether calcium is associated with the inhibitory effect of NFD, strain LT1534 was grown on 10% V8 juice agar medium at 25°C, and then 1-week-old agar plugs (5 mm diameter) transferred onto the center of dish (10% V8 juice agar medium containing 0.5 μM NFD (Control), 0.5 μM NFD+20 mM $CaCl_2$, 0.5 μM NFD+50 mM $CaCl_2$, 0.5 μM NFD+20 mM KCl, and 0.5 μM NFD+20 mM NaCl). Radial growth was measured at day 5.

## Determination of Cytosolic Free $Ca^{2+}$ Levels by Using the Probe Fluo-3-AM

*P. capsici* strain LT1534 was cultured for 2–3 days on the 10% V8 juice agar medium containing 0.5 μM NFD. Fluo-3-AM was prepared from a 1 mM stock solution in DMSO (Sigma) and added to the small pieces (1 cm × 1 cm) of *P. capsici* to a final concentration of 150 μM. The cultures were incubated at 37°C for 1 h for dye loading. Images of calcium green fluorescence were observed under a Nikon microscope by using a 450- to 490-nm excitation filter and a 520-nm barrier filter.

## Sensitivity Test to Oxidative Stress during NFD Treatment

To test the sensitivity of mycelial growth to oxidative stress, strain LT1534 was grown on 10% V8 juice agar medium at 25°C, and then $H_2O_2$ was added onto 10% V8 juice agar medium at final concentrations of 0, 1.25, 2.5, 5, and 10 mM. To investigate the effect of NFD on *P. capsici* mycelial growth under $H_2O_2$, radial growth was measured at 25°C for 5 days in V8 medium containing 0.5 μM NFD, 5 mM $H_2O_2$, 20 mM $CaCl_2$, 0.5 μM NFD+1.25 mM $H_2O_2$, 0.5 μM NFD+2.5 mM $H_2O_2$, 0.5 μM NFD+5 mM $H_2O_2$, 0.5 μM NFD+10 mM $H_2O_2$, 0.5 μM NFD+10 mM $H_2O_2$ +20 mM $CaCl_2$, and 0.5 μM NFD+10 mM $H_2O_2$ +50 mM $CaCl_2$.

## Virulence Test

Zoospores were induced from 5-day-old sporangia by washing with sterile distilled water for 24 h at 25°C, and then harvested by centrifugation at 3000 × *g* for 5 min. The number of zoospores in 10 μL of zoospore suspension was counted using a blood cell counting chamber. Pepper cultivars (*Capsicum annuum* L. cv. yanshan01, CM334, and ECW) were collected from Yunnan province, China (Liu et al., 2015b) and grown in plastic pots containing vermiculite at 25°C for 4 days in the dark. The hypocotyls of etiolated seedlings were inoculated with 100 zoospores, and then etiolated seedlings were maintained in 80% humidity and darkness at 25°C. The pathogenicity results were investigated and photographs were taken 3 days post-inoculation (dpi).

## RNA Extraction and Quantitative Reverse Transcription Polymerase Chain Reaction (qRT-PCR)

Total RNA of mycelia was extracted using an RNA kit (Tiangen, China), and cDNA was generated according to the protocol of the PrimeScript RT reagent kit (TaKaRa). qRT-PCR assays were performed using the primers shown in **Table 1** and carried out in a BioRad CFX96 Real-Time PCR Detection instrument (Bio-Rad Laboratories) using standard PCR conditions. To confirm product specificity, we performed a melting curve analysis. Normally, a 20-μL reaction volume contained 2 μL of reverse transcription product, 10 μL of SYBR real-time PCR mix (2x), and 0.4 μL of each primer (10 μM). The *P. capsici* internal transcribed spacer (ITS) region was used as a constitutively expressed endogenous control, and the expression of each gene in **Table 1** was determined relative to the *P. capsici* ITS region using the $\Delta\Delta Ct$ method. qRT-PCR experiments were repeated in triplicate with independent RNA isolations.

## Statistical Analysis

All measurements were conducted at least three times. Data were analyzed by one-way analysis of variance (ANOVA) using SPSS software version 19.0 (IBM) and mean comparison was conducted by a Dunnett's test. Different letters above bars indicate statistical differences ($^{**}P < 0.01$ and $^{*}P < 0.05$).

# RESULTS

## Effect of Calcium on *P. capsici* Mycelial Growth

Plant nutrients are often used in disease management, and the application of $CaCl_2$ dramatically suppresses disease incidence caused by *P. sojae* in soybean under laboratory conditions and in field applications (Sugimoto et al., 2005). In the present study, we analyzed the effects of $CaCl_2$ (0, 2.5, 5.0, 10, 25, and 50 mM) and the extracellular $Ca^{2+}$ chelator EDTA (0, 0.5, 1.0, 2.5, 5.0, and 10 mM) on *P. capsici* virulence strain LT 1534 mycelial growth. In our results, 2.5 mM $CaCl_2$ increased mycelial growth; however,

**TABLE 1 | Sequences of primers used in the present study.**

| Gene | Primer sequence (5′–3′) |
|---|---|
| *P. capsici ITS region* | Forward: GTATAGCAGAGGTTTAGTGAA |
| | Reverse: GACGTTTTAGTTAGAGCACTG |
| *PcLAC2* | Forward: CTCATCAACTCAGTCACA |
| | Reverse: GGTTCTGCTTGGAATTAG |
| *PcPL16* | Forward: CCGACCTTGTCACTTATG |
| | Reverse: TGTTGTTGATTCCGAGAG |

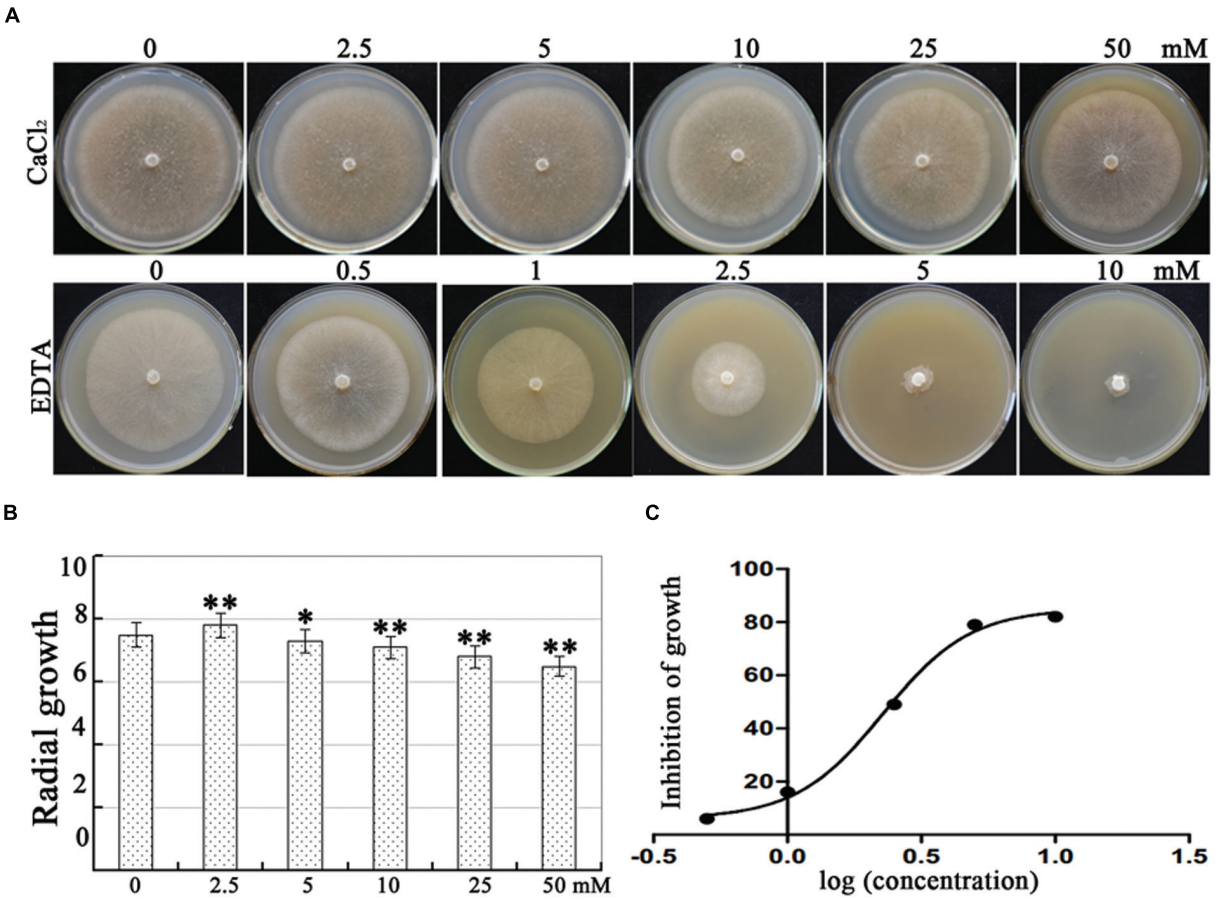


**FIGURE 1 | Effect of $CaCl_2$ and EDTA on mycelial growth of *Phytophthora capsici*.** **(A)** *P. capsici* cultures in Petri dishes illustrating the inhibition of mycelial radial growth with increasing $CaCl_2$ and EDTA concentrations. The mycelial colonies were 5 days old and radial growth (mm) was assessed by measuring the distance from the edge of the inoculum plug to the advancing margin of the colony. **(B)** Statistical analysis of the inhibition of *P. capsici* mycelial growth at various $CaCl_2$ concentrations. **(C)** Statistical analysis of the inhibition of *P. capsici* mycelial growth at various EDTA concentrations. The assays were repeated three times; $n = 5$ for each assay. EC50 is the concentration at which growth is inhibited by 50%. Trend-lines were fitted using a logarithmic function. Different letters above bars indicate statistical differences ($^{**}P < 0.01$ and $^{*}P < 0.05$, according to Dunnett's test).

growth was inhibited at 5 mM, reaching only 13% growth rate at 50 mM. In addition, EDTA reduced mycelial growth significantly and the half maximal effective concentration ($EC_{50}$) value for EDTA-induced inhibition of mycelial growth was 2.5 mM (**Figure 1**). These results showed that calcium is essential, but higher concentrations are destructive, suggesting that *P. capsici* mycelial growth is regulated by calcium assimilation significantly.

## Nfd, But Not Vp, Inhibits *P. capsici* Mycelial Growth and Sporulation Significantly

Disruption of the genes encoding calcium channels results in abnormal calcium uptake for homeostasis and signaling, and impacts vegetative growth, polarity, cell wall integrity, and virulence (Bormann and Tudzynski, 2009; Wang et al., 2012). We evaluated the inhibitory effect of VP and NFD on mycelial growth and sporulation in *P. capsici*. As shown in **Figure 2**, mycelial growth and sporulation were inhibited by VP and NFD compared with the non-treated control. The highest dose of NFD (2 μM) inhibited mycelial growth and sporulation by 53 and 100%, but the highest dose of VP (320 μg/mL) only inhibited by 21 and 28%, suggesting that NFD inhibits mycelial growth and sporulation of *P. capsici* significantly. In addition, NFD led to concentration-dependent inhibition of *P. capsici* mycelial growth and sporulation, which peaked at 2 μM. Furthermore, NFD showed 30–35% greater inhibition of mycelial growth and 55–60% greater inhibition of sporulation. The above results suggest that NFD, but not VP, inhibits *P. capsici* mycelial growth and sporulation significantly. Furthermore, we also evaluated the inhibitory effect of NFD on the intensity of fluorescence emission representing the relative amounts of free intracellular $Ca^{2+}$. As shown in **Figure 3**, strong green fluorescence was observed in the control. On the contrast, the fluorescence of NFD treated *P. capsici* decreased notably. These results suggest that NFD regulates the content of cytosolic free $Ca^{2+}$ levels.

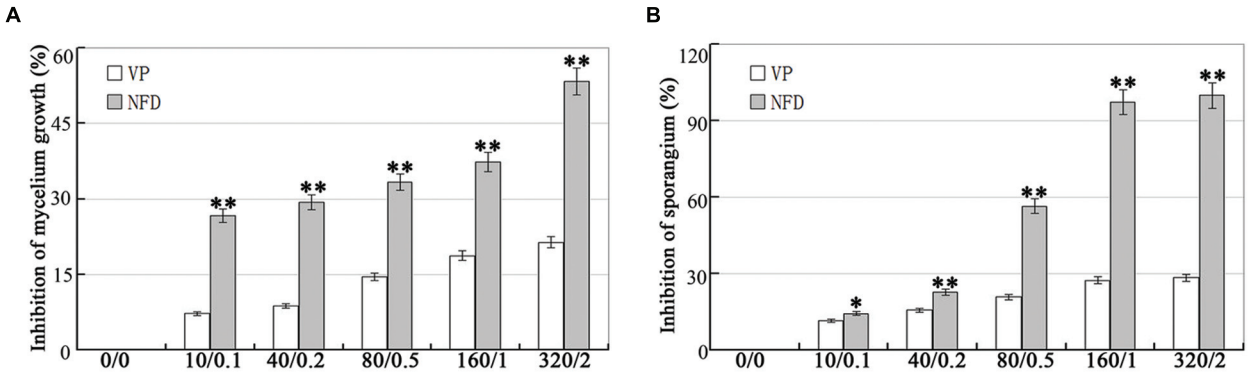


**FIGURE 2 | Effects of verapamil (VP) and nifedipine (NFD) on mycelial growth and sporulation of *P. capsici*. (A)** Analysis of the inhibition of *P. capsici* mycelium growth at various VP and NFD concentrations. The mycelial colonies were 5 days old and radial growth (mm) was assessed by measuring the distance from the edge of the inoculum plug to the advancing margin of the colony. **(B)** Analysis of the inhibition of *P. capsici* sporulation at various VP and NFD concentrations. The assays were repeated three times; $n = 5$ for each assay. Different letters above bars indicate statistical differences ($^{**}P < 0.01$ and $^{*}P < 0.05$, according to Dunnett's test).

## Rescue of NFD-Inhibited Mycelial Growth by Extracellular Calcium

Next, we investigated whether the inhibitory effect of NFD could be rescued by extracellular calcium levels. As shown in **Figure 4A**, NFD treated alone inhibited mycelial growth by 33.7% compared with the non-treated control, and NFD+20 mM $CaCl_2$ did not rescue NFD inhibited mycelial growth. However, the inhibition of mycelial growth in NFD+50 mM $CaCl_2$ was 19%, suggesting that 50 mM $CaCl_2$ can restrain NFD inhibited mycelial growth and rescue by 14.7%. To exclude non-specific (such as osmotic) effects of $CaCl_2$ due to its high concentrations, other salts (e.g., NaCl and KCl) was employed to investigate the effect of NFD-induced reduction of mycelial growth. Our results showed that 20 mM NaCl and KCl do not increase cell growth. These results suggest that NFD-induced inhibition of mycelial growth is calcium-dependent.

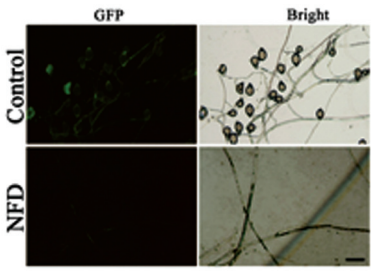


**FIGURE 3 | Cytosolic $Ca^{2+}$ images of *P. capsici* observed by light microscopy and fluorescence microscopy when NFD was added.** Fluo-3-AM (150 μM) was added to the small pieces (1 cm × 1 cm) of *P. capsici*. The intensities of green fluorescence represent the relative amounts of free cytosolic $Ca^{2+}$. Bar = 20 μm.

## NFD Increased *P. capsici* Sensitivity to $H_2O_2$ in a Calcium-Dependent Manner

Adaptation of pathogens to plant-derived ROS is important for their successful infection (Ermak and Davies, 2002; Sheng et al., 2015). In the present study, 0, 1.25, 2.5, 5, and 10 mM $H_2O_2$ was used to investigate the effect of oxidative stress on *P. capsici* mycelial growth. As shown in **Figure 4B**, the mycelial growth was significantly inhibited by 55–60%, when treated with 10 mM $H_2O_2$. The inhibitory effect of $H_2O_2$ on *P. capsici* mycelial growth was concentration dependent, suggesting that *P. capsici* is sensitive to oxidative stress in an $H_2O_2$ concentration-dependent manner. Furthermore, the effect of NFD on *P. capsici* oxidative stress and whether 0.5 μM NFD influenced the sensitivity of *P. capsici* to $H_2O_2$ were analyzed. As shown in **Figure 4C**, the inhibition of mycelial growth by NFD or 5 mM $H_2O_2$ treatment were 23.1 and 12.3% compared with the non-treated control, but NFD+5 mM $H_2O_2$ treatment inhibited mycelial growth by 41.5%. Furthermore, NFD+10 mM $H_2O_2$ treatment inhibited mycelial growth by 57%, suggesting that NFD increased the sensitivity of *P. capsici* to oxidative stress, which is dependent on the concentration of $H_2O_2$. However, NFD+$H_2O_2$ +50 mM $CaCl_2$ treatment restrained NFD+10 mM $H_2O_2$ inhibited mycelial growth and rescue by 49.2%, suggesting that 50 mM $CaCl_2$ can rescue the inhibitory effect of NFD+10 mM $H_2O_2$. Therefore, NFD increased *P. capsici* sensitivity to $H_2O_2$, and extracellular calcium rescued it.

## NFD Inhibition of *P. capsici* Virulence and Expression of Genes Involved in Pathogenicity

Zoospore suspensions were collected from strain LT1534 grown on 10% V8 juice agar medium containing NFD and inoculation assays were performed on etiolated *C. annuum* L. seedlings. As shown in **Figure 5A**, the hypocotyls of the etiolated seedlings inoculated with strain LT1534 zoospores showed typical disease symptoms and water-soaked lesions at 3 dpi. In contrast, NFD-treated strain LT1534 produced almost no lesions or very small lesions which did not expand beyond the inoculation site

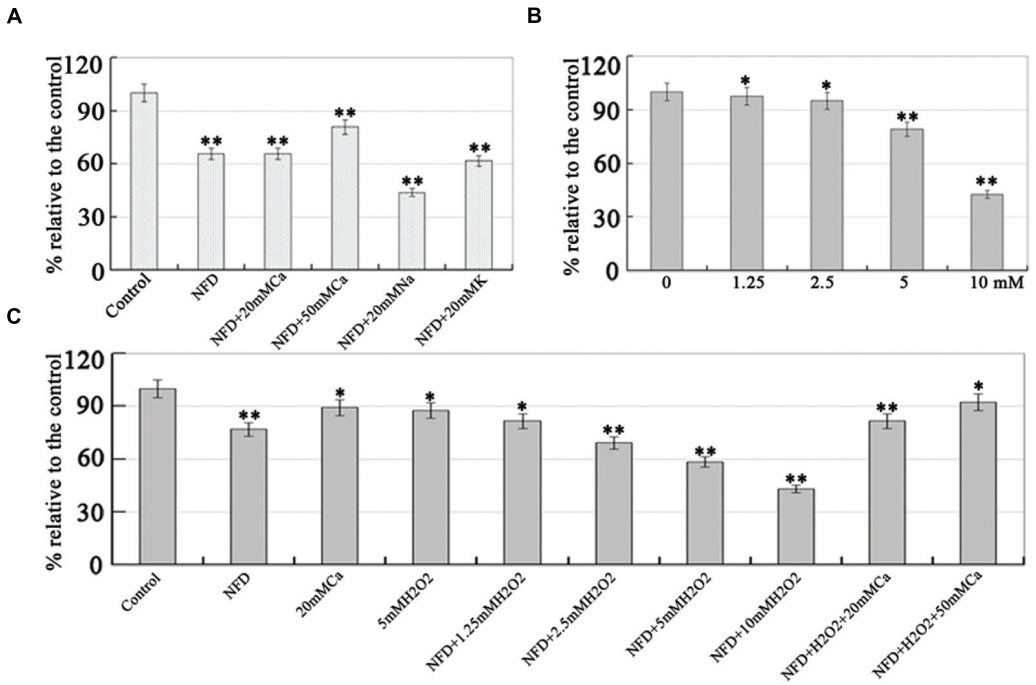


**FIGURE 4 | Effects of $CaCl_2$ and $H_2O_2$ on NFD-induced growth inhibition. (A)** Extracellular calcium rescued NFD-inhibited mycelial growth. Mycelial was grown on 10% V8 juice agar medium containing 0.5 μM NFD (Control), 0.5 μM NFD+20 mM $CaCl_2$, 0.5 μM NFD+50 mM $CaCl_2$, 0.5 μM NFD+20 mM NaCl, and 0.5 μM NFD+20 mM KCl. **(B)** Effect of $H_2O_2$ on *P. capsici* mycelial growth. Mycelial was grown on 10% V8 juice agar medium containing 0, 1.25, 2.5, 5, and 10 mM $H_2O_2$. **(C)** Effect of NFD on mycelial growth of *P. capsici* under various concentrations of $H_2O_2$. Mycelial was grown on 10% V8 juice agar medium containing 0.5 μM NFD, 20 mM $CaCl_2$, 5 mM $H_2O_2$, 0.5 μM NFD+1.25 mM $H_2O_2$, 0.5 μM NFD+2.5 mM $H_2O_2$, 0.5 μM NFD+5 mM $H_2O_2$, 0.5 μM NFD+10 mM $H_2O_2$, 0.5 μM NFD+10 mM $H_2O_2$+20 mM $CaCl_2$, and 0.5 μM NFD+10 mM $H_2O_2$+50 mM $CaCl_2$. The mycelial colonies were 5 days old and radial growth (mm) was assessed by measuring the distance from the edge of the inoculum plug to the advancing margin of the colony. The assays were repeated three times; $n = 5$ for each assay. Different letters above bars indicate statistical differences (**$P < 0.01$ and *$P < 0.05$, according to Dunnett's test).

(**Figure 5A**). To determine whether the pathogenicity defect was associated with the expression of pathogenicity-related genes during infection by *P. capsici*, we analyzed the relative expression ratios of the pectate lyase *PcPL16* and laccase *PcLAC2* genes. As shown in **Figures 5B,C**, the expression levels of *PcPL16* and *PcLAC2* were markedly higher in mycelia grown on V8 medium. In contrast, the expression levels of *PcPL16* and *PcLAC2* in the NFD-treated mycelia were significantly lower. Furthermore, the addition of calcium rescued the virulence and expression of *PcPL16* and *PcLAC2* to the levels observed in V8 medium. These results suggest that NFD inhibited the virulence and expression of pathogenicity-related genes in *P. capsici*.

## DISCUSSION

Calcium efflux is involved in the fungicide CA-induced inhibition of *P. capsici* (Hu et al., 2013). The antifungal protein PAF from *Penicillium chrysogenum* has been used to control disease by increasing cytosolic free $Ca^{2+}$, which is involved in hyphal tip growth, hyphal branching, sporulation, spore germination, different infection structure formation, circadian clocks, and responses to environment stimuli including osmotic stress, heat shock, mechanical stimulations, and oxidative stresses. Calcium channels allow the passive flow of $Ca^{2+}$ across cell membranes into the cytosol. Voltage-gated $Ca^{2+}$ channel blockers can inhibit the growth of fungal pathogens (Binder et al., 2010), but little is known about the effect of $Ca^{2+}$ homeostasis on mycelial growth, sporulation, and virulence of oomycetes. NFD is the prototype calcium channel blocker of the dihydropyridine class, and the half-life of capsule and tablet are 2 and 11 h for the management of hypertension and angina pectoris (Toal, 2004). Previous studies have shown that NFD can potentiate cardiopulmonary baroreflex control of sympathetic nerve activity (Ferguson and Hayes, 1989), inhibit contractions in the body of the human esophagus (Richter et al., 1985) and decrease lymphocyte blastogenesis, IL2 production and NK activity in healthy humans (Morgano et al., 1990). In the present study, we first explored the effects of two well-known calcium channel blockers, VP and NFD, on mycelial growth and sporulation. As shown in **Figure 2**, NFD, but not VP, inhibited mycelial growth and sporulation of *P. capsici* strain LT1534 significantly. Meanwhile, we also found that 2 μM NFD inhibited mycelial growth of Fujian and Jiangsu *P. capsici* strains significantly (**Supplementary Figure S1**), suggesting that NFD can inhibit mycelial growth of *P. capsici*. Lange and Peiter (2016) have shown that NFD drastically reduced colony growth in the filamentous fungal pathogen *Colletotrichum graminicola*, as observed before

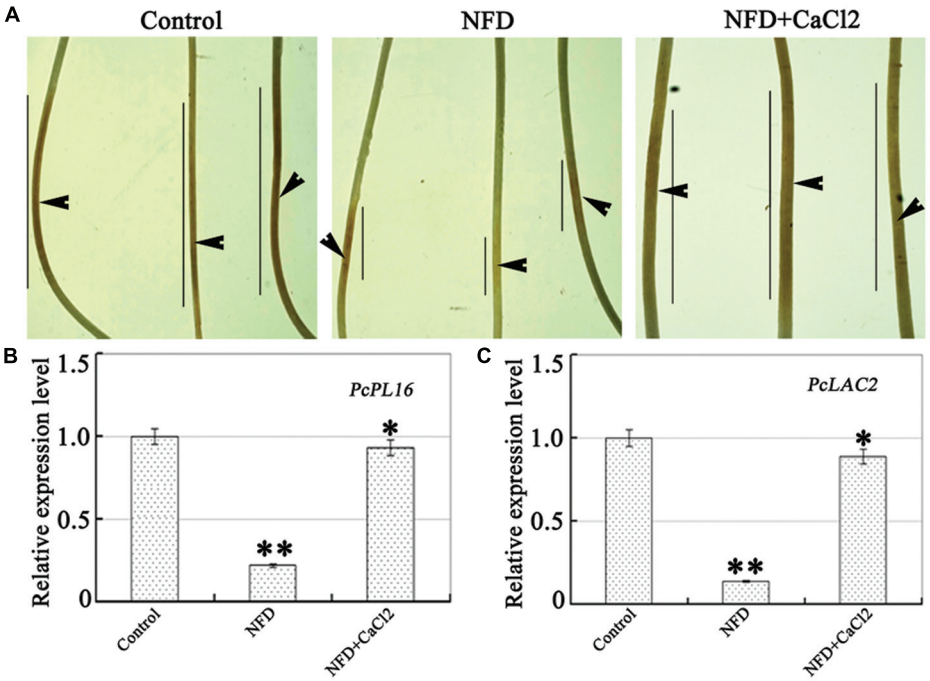


**FIGURE 5 | Effect of NFD on *P. capsici* virulence and expression of genes involved in pathogenicity. (A)** Pathogenicity assays were performed on etiolated pepper seedlings. Etiolated pepper seedlings (*C. annuum* L. cv. yanshan01, CM334, and ECW) were inoculated with freshly prepared zoospores (∼100 in 10 mL). Images were taken after 48 h, and the experiments were repeated at least three times. Arrows indicate the inoculation site and lines indicate the lesion size. **(B,C)** Relative transcription levels of defense-related genes *PcPL16* and *PcLAC2* in NFD-treated mycelia. Transcription of the *P. capsici* ITS region in mycelia was used as a reference, which was set to a value of 1. Error bars indicate the standard error. The experiments were repeated three times, together with at least three independent repetitions of the biological experiments. Values are means ± SE ($n = 6$). Different letters above bars indicate statistical differences (**$P < 0.01$ and *$P < 0.05$, according to Dunnett's test).

in *Fusarium graminearum*, and the affected growth to a much larger extent than external $Ca^{2+}$ chelation; meanwhile, Scherp et al. (2001) also have shown that NFD is capable of stimulating the callose deposition in cells undergoing cytokinesis in *Riella helicophylla* and *Arabidopsis thaliana*, suggesting that NFD can be used in the crop protection. Extracellular calcium rescued NFD-inhibited mycelial growth (**Figure 4A**), suggesting that NFD-regulated calcium uptake is significantly beneficial for hyphal growth in *P. capsici*. In addition, NFD increased *P. capsici* sensitivity to $H_2O_2$ in a calcium-dependent manner (**Figure 4C**). Furthermore, oxidative stress alters calcium signaling, and calcium homeostasis and signaling is linked to pathogenesis (Hallen and Trail, 2008; Liu et al., 2015a).

The $Ca^{2+}$ influx channels Cch1 and Mid1 in *S. cerevisiae* allow the passive flow of $Ca^{2+}$ across cell membranes into the cytosol (Harren and Tudzynski, 2013), and the Cch1-Mid1 complex in *Aspergillus fumigatus* mediates the specific influx of $Ca^{2+}$; calcium uptake impacts conidiation, vegetative growth, and polarity (Jiang et al., 2014). In the present study, we analyzed the effects of VP and NFD on mycelial growth and sporulation of *P. capsici*, and showed that VP functions in a mechanism that differs from that of NFD. In fact, NFD and VP use different binding sites in the cell wall (Nakayama and Kanaoka, 1996), and NFD and VP are members of the chemically unrelated classes of L-type blockers, dihydropyridines and phenylalkylamines, respectively. In addition, different inhibitory effects of three L-type calcium blockers (diltiazem, VP, and NFD) on ADP- and collagen-induced platelet aggregation of human and rabbit platelets have been reported (Toque et al., 2008). In fact, the bioavailabilities of diltiazem, NFD, and VP differ with ranges of 40–50%, 40–50%, and 10–30%, respectively (Echizen and Eichelbaum, 1986).

Previous studies have suggested that HACS is involved in the oxidative stress response, and the calcium channel blocker VP inhibits the oxidative stress response in *C. albicans* (Yu et al., 2014). In addition, deletion of three HACS regulator-encoding genes *Cch1*, *Mid1*, and *Ecm7* results in increased sensitivity to oxidative stress and decreased expression of several oxidative stress response genes (Ding et al., 2013). In the present study, NFD increased the sensitivity of *P. capsici* to $H_2O_2$ in a calcium-dependent manner, suggesting that *P. capsici* treated with $H_2O_2$ and NFD encounters more severe oxidative stress than with $H_2O_2$ treatment alone. However, 50 mM extracellular calcium rescued NFD-reduced mycelial growth under oxidative stress, suggesting that NFD inhibits mycelial growth under oxidative stress by disrupting calcium fluctuation.

In the present study, NFD-treated *P. capsici* produced very small lesions which showed no expansion beyond the inoculation site; in contrast, treatment with NFD and $CaCl_2$ showed typical disease symptoms (**Figure 5A**). In fungi, the changed

pathogenicity may be due to infection-related enzymes and effector-related protein secretion. During infection, diverse cell wall-degrading enzymes (e.g., pectinase) can be produced on the infection sites by *Phytophthora* spp. Pectinases degrade pectin, which is a major component of the primary cell wall and middle lamella of plants. Recent studies of the biological function of fungal laccases suggest that this enzyme plays an important role in fungal morphogenesis and fungal virulence (Li et al., 2013). In *P. capsici*, pectate lyase and laccase activities are important for successful infection during plant–pathogen interactions (Feng and Li, 2014; Fu et al., 2015). Laccases, which served as blue copper oxidases, catalyze the one-electron oxidation (e.g., aromatic amines and phenolics) and other electron-rich substrates; there also has a reduction of $O_2$ to $H_2O$ concomitantly. In the present study, the expression levels of laccase *PcLAC2*- and pectate lyase *PcPL16*-encoding genes were reduced significantly by 35–50% in NFD- and $H_2O_2$-treated *P. capsici*. In fact, *Bacillus subtilis* pectate lyase is in a complex with calcium (Pickersgill et al., 1994) and *Rhizoctonia solani* laccase activity is induced by $CaCl_2$ (Crowe and Olsson, 2001). The promoter regions of laccase genes have several putative *cis*-acting elements such as xenobiotic-responsive, metal-responsive, and stress-responsive elements. In addition, effector proteins function not only as toxins to induce plant cell death, but also to enable pathogens to suppress or evade plant defense responses. Necrosis-inducing NLP proteins have been reported to contribute strong virulence during infection by *P. capsici* (Feng et al., 2014). In our study, NFD treatment alone had no obvious effect on the expression of *PcLAC2* and *PcPL16*. Successful rescue by $CaCl_2$ suggested that NFD-inhibited $Ca^{2+}$ absorption is important for virulence. Therefore, plants can respond to pathogenic fungi or oomycete infection by rapidly producing ROS using membrane-bound NADPH oxidases or secreted peroxidases and amine oxidases, as part of the general pathogen-associated molecular pattern (PAMP)-triggered immunity or more specific effector-triggered immunity responses (Latijnhouwers et al., 2003).

In the present study, our results showed that the calcium channel blocker NFD has an inhibitory effect on *P. capsici* calcium fluctuation under oxidative stress and impacts the oxidative stress response, confirming a connection between calcium signaling and the oxidative stress response in this pathogen. Interestingly, Scherp et al. (2001) have shown that NFD is capable of stimulating the callose deposition in cells undergoing cytokinesis in *Riella helicophylla* and *Arabidopsis thaliana*, and Larkindale and Knight (2002) also have shown that NFD increases heat stress in *Arabidopsis thaliana*, suggesting that there has no phytotoxicity in NFD application. Therefore, calcium channels may be potential targets for therapy to enhance the efficacy of oxidative stress against *P. capsici*-related infections and NFD can be used to the crop protection safely.

## AUTHOR CONTRIBUTIONS

PL, QW, and QC designed the study. JG, XD, YJ, BL, and GC performed the experiments. All authors analyzed the data. PL, QW, and QC wrote the article. All authors contributed to the research and manuscript and read and approved the final version of the manuscript. All authors agree to be accountable for all aspects of the work.

## ACKNOWLEDGMENTS

This work was supported by the Provincial Public Project in Fujian Province (Grant No. 2014R1024-9); National Natural Science Foundation of China (Grant No. 31401701); Natural Science Foundation of Fujian Province (Grant No. 2014J05037 and 2014J01109); Hundred Young Talents of FAAS (Grant No. YC2015-3).

## SUPPLEMENTARY MATERIAL

The Supplementary Material for this article can be found online at: http://journal.frontiersin.org/article/10.3389/fmicb.2016.01236

**FIGURE S1 | Effects of nifedipine (NFD) on mycelial growth of Fujian and Jiangsu *P. capsici* strains.** Analysis of the inhibition of *P. capsici* strains PCZZ-10 and PCNJ9 mycelium growth at 2 μM NFD. The mycelial colonies were 5 days old and radial growth (mm) was assessed by measuring the distance from the edge of the inoculum plug to the advancing margin of the colony.

## REFERENCES

Binder, U., Chu, M., Read, N. D., and Marx, F. (2010). The antifungal activity of the *Penicillium chrysogenum* protein PAF disrupts calcium homeostasis in *Neurospora crassa*. *Eukaryot. Cell* 9, 1374–1382. doi: 10.1128/EC.00050-10

Bormann, J., and Tudzynski, P. (2009). Deletion of Mid1, a putative stretchactivated calcium channel in *Claviceps purpurea*, affects vegetative growth, cell wall synthesis and virulence. *Microbiology* 155, 3922–3933. doi: 10.1099/mic.0.030825-0

Breeuwer, P., Drocourt, J. L., Bunschoten, N., Zwietering, M. H., Rombouts, F. M., and Abee, T. (1995). Characterization of uptake and hydrolysis of fluorescein diacetate and carboxyfluorescein diacetate by intracellular esterases in *Saccharomyces cerevisiae*, which result in accumulation of fluorescent product. *Appl. Environ. Microbiol.* 61, 1614–1619.

Cavinder, B., Hamam, A., Lew, R. R., and Trail, F. (2011). Mid1, a mechanosensitive calcium ion channel, affects growth, development, and ascospore discharge in the filamentous fungus *Gibberella zeae*. *Eukaryot. Cell* 10, 832–841. doi: 10.1128/EC.00235-10

Crowe, J. D., and Olsson, S. (2001). Induction of laccase activity in *Rhizoctonia solani* by antagonistic *Pseudomonas fluorescens* strains and a range of chemical treatments. *Appl. Environ. Microbiol.* 67, 2088–2094. doi: 10.1128/AEM.67.5.2088-2094.2001

Ding, X., Yu, Q., Xu, N., Wang, Y., Cheng, X., Qian, K., et al. (2013). Ecm7, a regulator of HACS, functions in calcium homeostasis maintenance, oxidative stress response and hyphal development in *Candida albicans*. *Fungal Genet. Biol.* 57, 23–32. doi: 10.1016/j.fgb.2013.05.010

Echizen, H., and Eichelbaum, M. (1986). Clinical pharmacokinetics of verapamil, nifedipine and diltiazem. *Clin. Pharmacokinet.* 11, 425–449. doi: 10.2165/00003088-198611060-00002

Ermak, G., and Davies, K. J. (2002). Calcium and oxidative stress: from cell signaling to cell death. *Mol. Immunol.* 38, 713–721. doi: 10.1016/S0161-5890(01)00108-0

Feng, B. Z., and Li, P. (2014). Cloning, characterization and expression of a novel laccase gene Pclac2 from *Phytophthora capsici*. *Braz. J. Microbiol.* 45, 351–358. doi: 10.1590/S1517-83822014005000021

Feng, B. Z., Zhu, X. P., Fu, L., Lv, R.-F., Storey, D., Tooley, P., et al. (2014). Characterization of necrosis-inducing NLP proteins in *Phytophthora capsici*. *BMC Plant Biol.* 14:126. doi: 10.1186/1471-2229-14-126

Ferguson, D., and Hayes, D. (1989). Nifedipine potentiates cardiopulmonary baroreflex control of sympathetic nerve activity in healthy humans. Direct evidence from microneurographic studies. *Circulation* 80, 285–298. doi: 10.1161/01.CIR.80.2.285

Fu, L., Zhu, C., Ding, X., Yang, X., Morris, D., Tyler, B. M., et al. (2015). Characterization of cell death-inducing members of the pectate lyase gene family in *Phytophthora capsici* and their contributions to infection of pepper. *Mol. Plant-Microbe Interact.* 28, 766–775. doi: 10.1094/MPMI-11-14-0352-R

Gonçalves, A. P., Monteiro, J., Lucchi, C., Kowbel, D. J., Cordeiro, J. M., Correia-de-Sá, P., et al. (2014). Extracellular calcium triggers unique transcriptional programs and modulates staurosporine-induced cell death in *Neurospora crassa*. *Microbial. Cell* 1, 289–302. doi: 10.15698/mic2014.09.165

Gordeeva, A., Zvyagilskaya, R., and Labas, Y. A. (2003). Cross-talk between reactive oxygen species and calcium in living cells. *Biochemistry (Mosc).* 68, 1077–1080. doi: 10.1023/A:1026398310003

Hallen, H. E., and Trail, F. (2008). The L-type calcium ion channel cch1 affects ascospore discharge and mycelial growth in the filamentous fungus *Gibberella zeae* (anamorph *Fusarium graminearum*). *Eukaryot. cell* 7, 415–424. doi: 10.1128/EC.00248-07

Harren, K., and Tudzynski, B. (2013). Cch1 and Mid1 are functionally required for vegetative growth under low-calcium conditions in the phytopathogenic ascomycete *Botrytis cinerea*. *Eukaryot. cell* 12, 712–724. doi: 10.1128/EC.00338-12

Hockerman, G., Dilmac, N., Scheuer, T., and Catterall, W. (2000). Molecular determinants of diltiazem block in domains IIIS6 and IVS6 of L-type Ca(2+) channels. *Mol. Pharmacol.* 58, 1264–1270. doi: 10.1124/mol.58.6.1264

Hu, L., Wang, D., Liu, L., Chen, J., Xue, Y., and Shi, Z. (2013). Ca (2+) efflux is involved in cinnamaldehyde-induced growth inhibition of *Phytophthora capsici*. *PLoS ONE* 8:e76264. doi: 10.1371/journal.pone.0076264

Iribarren, M. J., Pascuan, C., Soto, G., and Ayub, N. D. (2015). Genetic analysis of environmental strains of the plant pathogen *Phytophthora capsici* reveals heterogeneous repertoire of effectors and possible effector evolution via genomic island. *FEMS Microbiol. Lett.* 362:fnv189. doi: 10.1093/femsle/fnv189

Jackson, K., Yin, J., and Ji, P. (2012). Sensitivity of *Phytophthora capsici* on vegetable crops in Georgia to mandipropamid, dimethomorph and cyazofamid. *Plant Dis.* 96, 1337–1342. doi: 10.1094/PDIS-12-11-1082-RE

Jiang, H., Shen, Y., Liu, W., and Lu, L. (2014). Deletion of the putative stretch-activated ion channel Mid1 is hypervirulent in *Aspergillus fumigatus*. *Fungal Genet. Biol.* 62, 62–70. doi: 10.1016/j.fgb.2013.11.003

Juvvadi, P. R., Muñoz, A., Lamoth, F., Soderblom, E. J., Moseley, M. A., Read, N. D., et al. (2015). Calcium-mediated induction of paradoxical growth following caspofungin treatment is associated with calcineurin activation and phosphorylation in *Aspergillus fumigatus*. *Antimicrob. Agents Chemother.* 59, 4946–4955. doi: 10.1128/AAC.00263-15

Kraus, P. R., and Heitman, J. (2003). Coping with stress: calmodulin and calcineurin in model and pathogenic fungi. *Biochem. Biophys. Res. Commun.* 311, 1151–1157. doi: 10.1016/S0006-291X(03)01528-6

Lamour, K. H., Mudge, J., Gobena, D., Hurtado-Gonzales, O. P., Schmutz, J., Kuo, A., et al. (2012). Genome sequencing and mapping reveal loss of heterozygosity as a mechanism for rapid adaptation in the vegetable pathogen *Phytophthora capsici*. *Mol. Plant-Microbe Interact.* 25, 1350–1360. doi: 10.1094/MPMI-02-12-0028-R

Lange, M., and Peiter, E. (2016). Cytosolic free calcium dynamics as related to hyphal and colony growth in the filamentous fungal pathogen *Colletotrichum graminicola*. *Fungal Genet. Biol.* 91, 55–65. doi: 10.1016/j.fgb.2016.04.001

Larkindale, J., and Knight, M. R. (2002). Protection against heat stress-induced oxidative damage in *Arabidopsis* involves calcium, abscisic acid, ethylene, and salicylic acid. *Plant Physiol.* 128, 682–695. doi: 10.1104/pp.010320

Latijnhouwers, M., de Wit, P. J., and Govers, F. (2003). Oomycetes and fungi: similar weaponry to attack plants. *Trends Microbiol.* 11, 462–469. doi: 10.1016/j.tim.2003.08.002

Li, D., Zhao, Z., Huang, Y., Lu, Z., Yao, M., Hao, Y., et al. (2013). PsVPS1, a dynamin-related protein, is involved in cyst germination and soybean infection of *Phytophthora sojae*. *PLoS ONE* 8:e58623. doi: 10.1371/journal.pone.0058623

Liu, P., Li, B., Lin, M., Chen, G., Ding, X., Weng, Q., et al. (2016). Phosphite-induced reactive oxygen species production and ethylene and ABA biosynthesis, mediate the control of *Phytophthora capsici* in pepper (*Capsicum annuum*). *Funct. Plant Biol.* 43, 563–574. doi: 10.1071/FP16006

Liu, S., Hou, Y., Liu, W., Lu, C., Wang, W., and Sun, S. (2015a). Components of the calcium-calcineurin signaling pathway in fungal cells and their potential as antifungal targets. *Eukaryot. cell* 14, 324–334. doi: 10.1128/EC.00271-14

Liu, Z. Q., Qiu, A. L., Shi, L. P., Cai, J. S., Huang, X. Y., Yang, S., et al. (2015b). SRC2-1 is required in PcINF1-induced pepper immunity by acting as an interacting partner of PcINF1. *J. Exp. Bot.* 66, 3683–3698. doi: 10.1093/jxb/erv161

Martin, D. C., Kim, H., Mackin, N., Maldonado-Báez, L., Evangelista, C., Beaudry, V., et al. (2011). New regulators of a high-affinity Ca2+ influx system revealed through a genome-wide screen in yeast. *J. Biol. Chem.* 286, 10744–10754. doi: 10.1074/jbc.m110.177451

Morgano, A., Pierri, I., Stagnaro, R., Setti, M., Puppo, F., and Indiveri, F. (1990). Decreased lymphocyte blastogenesis, IL2 production and NK activity following nifedipine administration to healthy humans. *Eur. J. Clin. Pharmacol.* 39, 545–550. doi: 10.1007/BF00316092

Nakayama, H., and Kanaoka, Y. (1996). Chemical identification of binding sites for calcium channel antagonists. *Heterocycles* 42, 901–909. doi: 10.3987/REV-95-SR4

Nguemo, F., Fleischmann, B. K., Gupta, M. K., Šarić, T., Malan, D., Liang, H., et al. (2013). The L-type Ca 2+ channels blocker nifedipine represses mesodermal fate determination in murine embryonic stem cells. *PLoS ONE* 8:e53407. doi: 10.1371/journal.pone.0053407

Pickersgill, R., Jenkins, J., Harris, G., Nasser, W., and Robert-Baudouy, J. (1994). The structure of *Bacillus subtilis* pectate lyase in complex with calcium. *Nat. Struct. Mol. Biol.* 1, 717–723. doi: 10.1038/nsb1094-717

Puigpinós, J., Casas, C., and Herrero, E. (2015). Altered intracellular calcium homeostasis and endoplasmic reticulum redox state in *Saccharomyces cerevisiae* cells lacking Grx6 glutaredoxin. *Mol. Biol. Cell.* 26, 104–116. doi: 10.1091/mbc.E14-06-1137

Richter, J. E., Dalton, C. B., Buice, R. G., and Castell, D. O. (1985). Nifedipine: a potent inhibitor of contractions in the body of the human esophagus: studies in healthy volunteers and patients with the nutcracker esophagus. *Gastroenterology* 89, 549–554. doi: 10.1016/0016-5085(85)90450-0

Scherp, P., Grotha, R., and Kutschera, U. (2001). Deposition of cytokinesis-related callose in *Riella helicophylla* and *Arabidopsis thaliana*. Effects of photolytically altered nifedipine. *Plant Biol.* 3, 311–318. doi: 10.1055/s-2001-16458

Sheng, Y., Wang, Y., Meijer, H. J., Yang, X., Hua, C., Ye, W., et al. (2015). The heat shock transcription factor PsHSF1 of Phytophthora sojae is required for oxidative stress tolerance and detoxifying the plant oxidative burst. *Environ. Microbiol.* 17, 1351–1364. doi: 10.1111/1462-2920.12609

Shreaz, S., Sheikh, R., Rimple, B., Hashmi, A., Nikhat, M., Khan, L. A., et al. (2010). Anticandidal activity of cinnamaldehyde, its ligand and Ni(II) complex: effect of increase in ring and side chain. *Microb. Pathog.* 49, 75–82. doi: 10.1016/j.micpath.2010.03.013

Stam, R., Motion, G., Boevink, P. C., and Huitema, E. (2013). A conserved oomycete CRN effector targets and modulates tomato TCP14-2 to enhance virulence. *BioRxiv* doi: 10.1101/001248

Sugimoto, T., Aino, M., Sugimoto, M., and Watanabe, K. (2005). Reduction of *Phytophthora* stem rot disease on soybeans by the application of CaCl2 and Ca (NO3) 2. *J. Phytopathol.* 153, 536–543. doi: 10.1111/j.1439-0434.2005.01016.x

Sugimoto, T., Watanabe, K., Yoshida, S., Aino, M., Furiki, M., Shiono, M., et al. (2010). Field application of calcium to reduce *Phytophthora* stem rot of soybean, and calcium distribution in plants. *Plant Dis.* 94, 812–819. doi: 10.1094/PDIS-94-7-0812

Teng, J., Goto, R., Iida, K., Kojima, I., and Iida, H. (2008). Ion-channel blocker sensitivity of voltage-gated calcium-channel homologue Cch1 in *Saccharomyces cerevisiae*. *Microbiology* 154 (Pt. 12), 3775–3781. doi: 10.1099/mic.0.2008/021089-0

Toal, C. B. (2004). Formulation dependent pharmacokinetics—does the dosage form matter for nifedipine? *J. Cardiovas. Pharmacol.* 44, 82–86. doi: 10.1097/00005344-200407000-00011

Toque, H., Teixeira, C., Priviero, F., Morganti, R., Antunes, E., and De Nucci, G. (2008). Vardenafil, but not sildenafil or tadalafil, has calcium-channel blocking activity in rabbit isolated pulmonary artery and human washed platelets. *Br. J. Pharmacol.* 154, 787–796. doi: 10.1038/bjp.2008.141

Vu, K., Bautos, J. M., and Gelli, A. (2015). The Cch1-Mid1 high-affinity calcium channel contributes to the virulence of *Cryptococcus neoformans* by mitigating oxidative stress. *Eukaryot. cell* 14, 1135–1143. doi: 10.1128/EC.00100-15

Wang, S., Cao, J., Liu, X., Hu, H., Shi, J., Zhang, S., et al. (2012). Putative calcium channels CchA and MidA play the important roles in conidiation, hyphal polarity and cell wall components in *Aspergillus nidulans*. *PLoS ONE* 7:e46564. doi: 10.1371/journal.pone.0046564

Wang, S., Chen, P., and Chang, S. (2005). Antifungal activities of essential oils and their constituents from indigenous cinnamon (*Cinnamomum osmophloeum*) leaves against wood decay fungi. *Bioresour. Technol.* 96, 813–818. doi: 10.1016/j.biortech.2004.07.010

Yu, Q., Wang,H., Cheng, X., Xu, N., Ding, X., Xing, L., et al. (2012). Roles of Cch1 and Mid1 in morphogenesis, oxidative stress response and virulence in *Candida albicans*. *Mycopathologia* 174, 359–369. doi: 10.1007/s11046-012-9569-0

Yu, Q., Xiao, C., Zhang, K., Jia, C., Ding, X., Zhang, B., et al. (2014). The calcium channel blocker verapamil inhibits oxidative stress response in *Candida albicans*. *Mycopathologia* 177, 167–177. doi: 10.1007/s11046-014-9735-7

**Conflict of Interest Statement:** The authors declare that the research was conducted in the absence of any commercial or financial relationships that could be construed as a potential conflict of interest.

frontiers in Microbiology

ORIGINAL RESEARCH
published: 05 January 2017
doi: 10.3389/fmicb.2016.02127

# The Regulatory Subunit of Protein Kinase A (Bcy1) in *Candida albicans* Plays Critical Roles in Filamentation and White-Opaque Switching but Is Not Essential for Cell Growth

*Xuefen Ding*[1,2], *Chengjun Cao*[1,2], *Qiushi Zheng*[1,2] *and Guanghua Huang*[1,2]*

[1] State Key Laboratory of Mycology, Institute of Microbiology, Chinese Academy of Sciences, Beijing, China, [2] College of Life Sciences, University of Chinese Academy of Sciences, Beijing, China

The conserved cAMP-dependent protein kinase (PKA) is composed of the regulatory and catalytic subunits and acts as the central component of the cAMP signaling pathway. In the human fungal pathogen *Candida albicans*, the PKA regulatory subunit Bcy1 plays a critical role in the regulation of cell differentiation and death. It has long been considered that Bcy1 is essential for cell viability in *C. albicans*. In the current study, surprisingly, we found that Bcy1 is not required for cell growth, and we successfully generated a *bcy1/bcy1* null mutant in *C. albicans*. Deletion of *BCY1* leads to multiple cellular morphologies and promotes the development of filaments. Filamentous and smooth colonies are two typical morphological types of the *bcy1/bcy1* mutant, which can undergo spontaneous switching between the two types. Cells of filamentous colonies grow better on a number of different culture media and have a higher survival rate than cells of smooth colonies. In addition, deletion of *BCY1* significantly increased the frequency of white-to-opaque switching on N-acetylglucosamine (GlcNAc)-containing medium. The *bcy1/bcy1* null mutant generated herein provides the field a new resource to study the biological functions of the cAMP signaling pathway in *C. albicans*.

**Keywords: *Candida albicans*, PKA regulatory subunit, *Bcy1*, filamentation, white-opaque switching, cAMP signaling pathway**

OPEN ACCESS

***Edited by:***
*Joshua D. Nosanchuk, Albert Einstein College of Medicine, USA*

***Reviewed by:***
*Yue Wang, Institute of Molecular and Cell Biology (A*STAR), Singapore*
*Aaron Hernday, University of California, Merced, USA*

***Correspondence:**
*Guanghua Huang*
*huanggh@im.ac.cn*

***Specialty section:***
*This article was submitted to Fungi and Their Interactions, a section of the journal Frontiers in Microbiology*

***Received:*** *11 November 2016*
***Accepted:*** *16 December 2016*
***Published:*** *05 January 2017*

***Citation:***
*Ding X, Cao C, Zheng Q and Huang G (2017) The Regulatory Subunit of Protein Kinase A (Bcy1) in Candida albicans Plays Critical Roles in Filamentation and White-Opaque Switching but Is Not Essential for Cell Growth. Front. Microbiol. 7:2127. doi: 10.3389/fmicb.2016.02127*

## INTRODUCTION

The cAMP signaling pathway regulates a plethora of biological processes in eukaryotic organisms (Wang and Heitman, 1999; Pan et al., 2000; Gancedo, 2001; Chin et al., 2002; Chiaradonna et al., 2008). In the human fungal pathogen *Candida albicans*, this pathway plays a central role in the regulation of morphological transitions, carbon source utilization, quorum sensing, cell death, and virulence (Leberer et al., 2001; Rocha et al., 2001; Phillips et al., 2006; Biswas et al., 2007; Huang et al., 2010; Huang, 2012; Du et al., 2015). In response to environmental stimulation [such as increased $CO_2$ levels, N-acetylglucosamine (GlcNAc), serum, and elevated temperatures], cells of *C. albicans* activate the cAMP signaling pathway and undergo morphological changes (Leberer et al., 2001; Phillips et al., 2006; Biswas et al., 2007; Huang et al., 2010; Huang, 2012).

Morphological plasticity is a striking feature of pathogenic *Candida* species and is tightly linked to virulence (Biswas et al., 2007; Whiteway and Bachewich, 2007; Huang, 2012). *C. albicans* can exist

in a number of morphological forms, such as the yeast form, filaments (hyphae and pseudohyphae), and white, gray, and opaque cell types (Biswas et al., 2007; Whiteway and Bachewich, 2007; Huang, 2012). Different cell types of *C. albicans* play distinct roles in its life cycle. For example, the yeast cell can be easily disseminated to different tissues through the host circulatory system, while filamentous cells are better at invading tissue and initiating infections (Gow et al., 2012). White cells are more virulent in systemic infections, while opaque and gray cells have an enhanced ability to colonize cutaneous tissues (Tao et al., 2014b). The cAMP-PKA pathway is the major pathway involved in the regulation of morphological transitions and virulence in *C. albicans* (Biswas et al., 2007; Huang, 2012). Ras1 is upstream of the cAMP signaling pathway and is required for serum-induced true hyphal formation, but it is not essential for cell growth and the development of pseudohyphae in *C. albicans* (Feng et al., 1999). In response to extracellular stimuli, the activated Ras protein (Ras1) signals the adenylyl cyclase Cyr1 (also named Cdc35) to increase the synthesis of cAMP in *C. albicans* (Feng et al., 1999; Rocha et al., 2001). Deletion of *CYR1* in *C. albicans* results in slow cell growth and serious defects in filamentation (Rocha et al., 2001). Cyr1 functions as a sensor for multiple extracellular signals including $CO_2$, quorum sensing molecules, GlcNAc, and bacterial peptidoglycan (Wang, 2013). The alterations of cAMP levels modulate the activity of the cAMP-dependent protein kinase (PKA).

The PKA kinase is composed of two catalytic and two regulatory subunits in *C. albicans* (Biswas et al., 2007). Tpk1 and Tpk2 are two isoforms of the PKA catalytic subunit, which physically interacts with and is regulated by Bcy1, the regulatory subunit in *C. albicans* (Bockmühl et al., 2001; Cassola et al., 2004; Giacometti et al., 2012; Schaekel et al., 2013). The binding of cAMP to the regulatory subunit leads to the release and activation of the catalytic subunits.Tpk1 and Tpk2 play distinct and redundant roles in the regulation of filamentation, the stress response, and glycogen storage (Bockmühl et al., 2001; Giacometti et al., 2009). Bockmühl et al. (2001) have shown that Tpk1 is required for the formation of filaments on solid media, while Tpk2 is required for filamentation in liquid media. The authors further conclude that the two isoforms of the catalytic subunit are essential for cell viability because they were unable to generate the *tpk1/tpk1 tpk2/tpk2* double mutant (Bockmühl et al., 2001; Giacometti et al., 2009). The PKA regulatory subunit Bcy1 plays a negative role in the regulation of the cAMP signaling pathway in fungal species (Cassola et al., 2004; Giacometti et al., 2006, 2012; Schaekel et al., 2013). Cassola et al. (2004) demonstrated that it is not possible to generate a *BCY1* null mutant in a WT strain of *C. albicans*, since inactivation of *BCY1* leads to constitutive activation of the cAMP/PKA pathway (Cassola et al., 2004). Alternatively, they generated a *bcy1/bcy1 tpk2/tpk2* double mutant by deletion of *BCY1* in a *tpk2/tpk2* background strain. This double mutant exhibits a defect in the development of filaments in response to GlcNAc and serum (Cassola et al., 2004). And deletion of BCY1 affects the nuclear localization of Tpk1, suggesting that Bcy1 may also regulate the activity of the catalytic subunit by controlling its subcellular localization.

In the present study, surprisingly, we found that Bcy1 is not essential for cell growth of *C. albicans*. We successfully deleted both alleles of *BCY1* and generated a *bcy1/bcy1* null mutant in a laboratory wild type strain of *C. albicans*. This mutant provides an opportunity to revisit the biological roles of the PKA regulatory subunit in this important fungal pathogen. Deletion of *BCY1* in *C. albicans* leads to multiple cellular morphologies and hyperfilamentation in certain media. We further show that Bcy1 plays an important role in the regulation of carbon source utilization and in white-opaque switching.

# MATERIALS AND METHODS

## Culture Conditions, Strains, and Plasmids

The strains used in this study are listed in **Table S1**. YPD medium (2% glucose, 2% peptone, 1% yeast extract) and modified Lee's glucose medium (Huang et al., 2010) were used for routine culture of *C. albicans*. The red dye phloxine B (5 μg/mL) was added to the solid medium for the filamentation and white-opaque switching assays. Media used for spot serial dilution growth assays: YPD, Lee's (Lee's medium without sugar) (Lee et al., 1975), Lee's media with different carbon sources (replacement of glucose with 1.25% fructose or 3% ethanol plus 2% glycerol), YNB media [yeast nitrogen base with 0.5% ammonium sulfate and 3 amino acids (0.13 g/L leucine, 0.03 g/L histidine, and 0.04 g/L arginine) and different carbon sources (2% glucose, 2% fructose, 2% mannitol, or 4% glycerol)].

*BCY1* were deleted in two WT strains (SN152 and SN152a) using the same strategy as described below. The two alleles of *BCY1* were deleted using the fusion PCR strategy (Noble and Johnson, 2005). The first allele of *BCY1* was replaced with the fusion PCR products of the *CdHIS1* marker amplified from plasmid pSN52. The second allele of *BCY1* was deleted with the fusion PCR products of the *CmLEU2* marker amplified from pSN40. The primers used for the PCR reactions are listed in **Table S2**. To construct the *BCY1*-reconstituted strain, the fusion PCR product of three fragments (the *CdARG4* marker amplified from plasmid pSN69, and fragments of *BCY1* 3′-UTR and *BCY1* ORF plus 5′-UTR) was used for transformation of the *bcy1/bcy1* mutant. The two *BCY1*-related fragments were amplified from genomic DNA of *C. albicans* (SC5314) with primer pairs (BCY1-5F-COM plus BCY1-5R-COM and BCY1-3R-COM plus BCY1-3R-COM, respectively).

Plasmid pACT1 was used to construct the *TPK1* and *TPK2*-overexpressing plasmids (Huang et al., 2010). The PCR products of *TPK1* were digested with *Eco*RV and *Hind*III and inserted into the *Eco*RV/*Hind*III site of pACT1 to generate plasmid pACT-TPK1. The PCR products of *TPK2* were digested with *Stu*I and *Hind*III and inserted into the *Eco*RI/*Hind*III site of pACT1, to generate plasmid pACT-TPK2. The AscI-linearized overexpressing plasmids were used for transformation of the WT and *bcy1/bcy1* mutant.

## White-Opaque Switching Assay

White-opaque switching assays were performed as described previously (Xie et al., 2013). Lee's glucose and Lee's GlcNAc media were used for the quantitative switching assays. The cells were

cultured on the plates at 25°C for 5 days. The cell identity was assessed by cellular morphology and verified by cell type-specific genes (data not shown).

## Filamentation Assays

Lee's glucose, Lee's GlcNAc, and YPD media were used for the filamentation assays. The cells were cultured at 25° and 37°C as indicated in the figure legends. For quantitative filamentous-smooth colony type switching assays (**Figure 4**), cells from a filamentous or smooth colony grown on Lee's glucose medium for 3 days were resuspended and cultured in liquid Lee's glucose for 24–96 h at 25°C. A small aliquot of cells was collected at the time point indicated and replated on YPD plates. After 5 days of growth at 30°C, colonies of the smooth and filamentous types were counted. The switching frequency = (number of colonies with alternative phenotype/total colony number) × 100%.

## PI and DAPI Staining Assays

The cells were grown in liquid Lee's glucose medium for 48 h at 25°C and collected for propidium iodide (PI) and 4′-6-diamidino-2-phenylindole (DAPI) staining assays as described previously (Du et al., 2015). The cells were washed with 1 × phosphate-buffered saline (PBS) and resuspended in 1 × PBS. PI was added to the cells at a concentration of 2 μg/mL. The cells were stained for 15 min at room temperature in the dark with slight shaking and used for microscopy assays. For the DAPI staining assays, cells collected from liquid Lee's glucose medium were first fixed in 70% ethanol for 20 min and then stained with 1 μg/mL of DAPI. The cells were then washed with 1 × PBS and used for microscopy assays.

## Quantitative Real-Time PCR (qRT-PCR) Assay

Cells were grown Lee's GlcNAc plates at 25°C for 3 days and collected for total RNA extraction. The qRT-PCR assay was performed as described in our previous report (Tao et al., 2014a). Total RNA was used to synthesize cDNA with RevertAid H Minus reverse transcriptase (Thermo Scientific). Quantification of transcripts was performed in Bio-Rad CFX96 real-time PCR detection system using SYBR green. The relative expression level of each gene was normalized to that of *C. albicans ACT1*.

# RESULTS

## Generation of the *bcy1*/*bcy1* Null Mutant in *C. albicans*

Although the PKA regulatory subunit plays critical roles in a variety of biological processes in fungal species, the gene encoding this subunit is not essential for cell growth in many fungi including the model organisms, *Saccharomyces cerevisiae* (Cannon and Tatchell, 1987; Toda et al., 1987), *Schizosaccharomyces pombe* (DeVoti et al., 1991), and *Neurospora crassa* (Bruno et al., 1996), and the human fungal pathogens, *Aspergillus fumigates* (Zhao et al., 2006) and *Cryptococcus neoformans* (D'Souza et al., 2001). However, it has been thought that *BCY1*, the sole gene encoding the PKA regulatory subunit in *C. albicans*, is an essential gene (Cassola et al., 2004). Considering the conserved feature of the cAMP signaling pathway, we suspected that *BCY1* might not be an essential gene in *C. albicans,* and thus the failure to obtain its null mutant in a previous report (Cassola et al., 2004) could be due to technical reasons. Using a fusion PCR deletion and prototrophic selection strategy (Noble and Johnson, 2005), we successfully deleted the two alleles of *BCY1* in a WT strain of *C. albicans* (SN152, **Figure 1**). Correct integration of the *CdHIS1* and *CmLEU2* markers into the *BCY1* locus was confirmed using PCR with two sets of flanking checking primers (**Figure 1B**, lanes 1–4). Moreover, one set of ORF primers was used to verify the absence of the *BCY1* ORF region in the genome (**Figure 1B**, lanes 5 and 6). These results indicate that the two alleles of *BCY1* were successfully deleted and replaced by the *CdHIS1* and *CmLEU2* markers, respectively. Therefore, as in other previously described fungi (Cannon and Tatchell, 1987; Toda et al., 1987; DeVoti et al., 1991; Bruno et al., 1996; D'Souza et al., 2001 and Zhao et al., 2006), the conserved PKA regulatory subunit Bcy1 is also not required for cell viability in *C. albicans*.

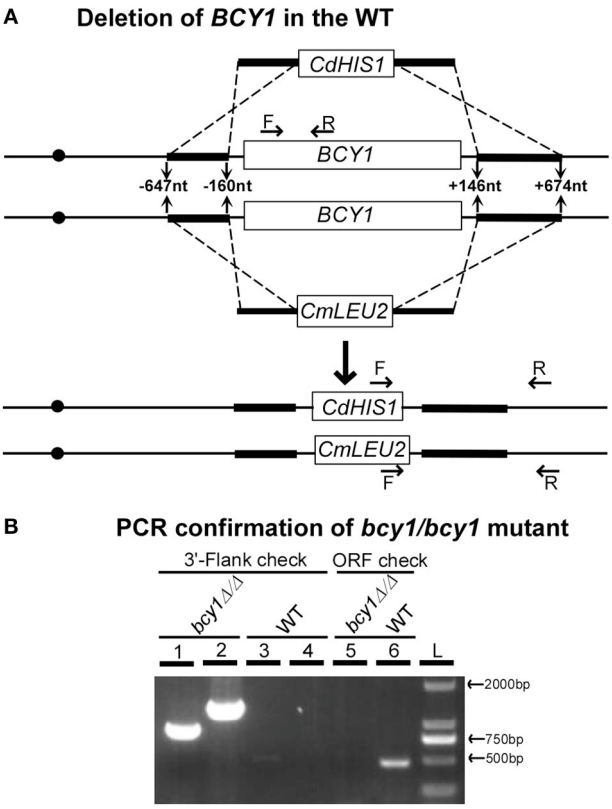


**FIGURE 1 | Deletion of both alleles of *BCY1* in *C. albicans*. (A)** Strategy for *BCY1* deletion. Fusion PCR deletion assays were used to delete the two alleles of *BCY1* as described in the Methods Section. *CdHIS1* and *CmLEU2* were used as selective markers for *BCY1* deletion. **(B)** PCR confirmation of *BCY1* deletion in the WT strain SN152. The primers used are indicated in **(A)**. Lanes 1 and 3: 3′-flanking checking primers for *CdHIS1* integration; lanes 2 and 4: 3′-flanking checking primers for *CmLUE2* integration; lanes 5 and 6: *BCY1* ORF checking primers. L, DNA ladder.

## Multiple Morphologies of the *bcy1/bcy1* Null Mutant

To evaluate the function of Bcy1 during filamentous development of *C. albicans*, we cultured the cells of WT, *BCY1/bcy1*, *bcy1/bcy1*, and BCY1-reconstituted strains on three different media (Lee's glucose, Lee's GlcNAc, and YPD) at two temperatures (25 and 37°C). These culture conditions were used because the three media exhibit different levels of filamentation induction in *C. albicans*. A high temperature (37°C) promotes filamentation, whereas a low temperature (25°C) favors yeast cell growth. Therefore, a combination of these conditions would facilitate the discrimination of the filamentation ability of different strains. At 25°C (**Figure 2**), deletion of one allele of *BCY1* had no obvious effect on filamentous growth. Consistently, the BCY1-reconstituted strain also exhibited a similar phenotype to that of the WT control. However, the *bcy1/bcy1* null mutant

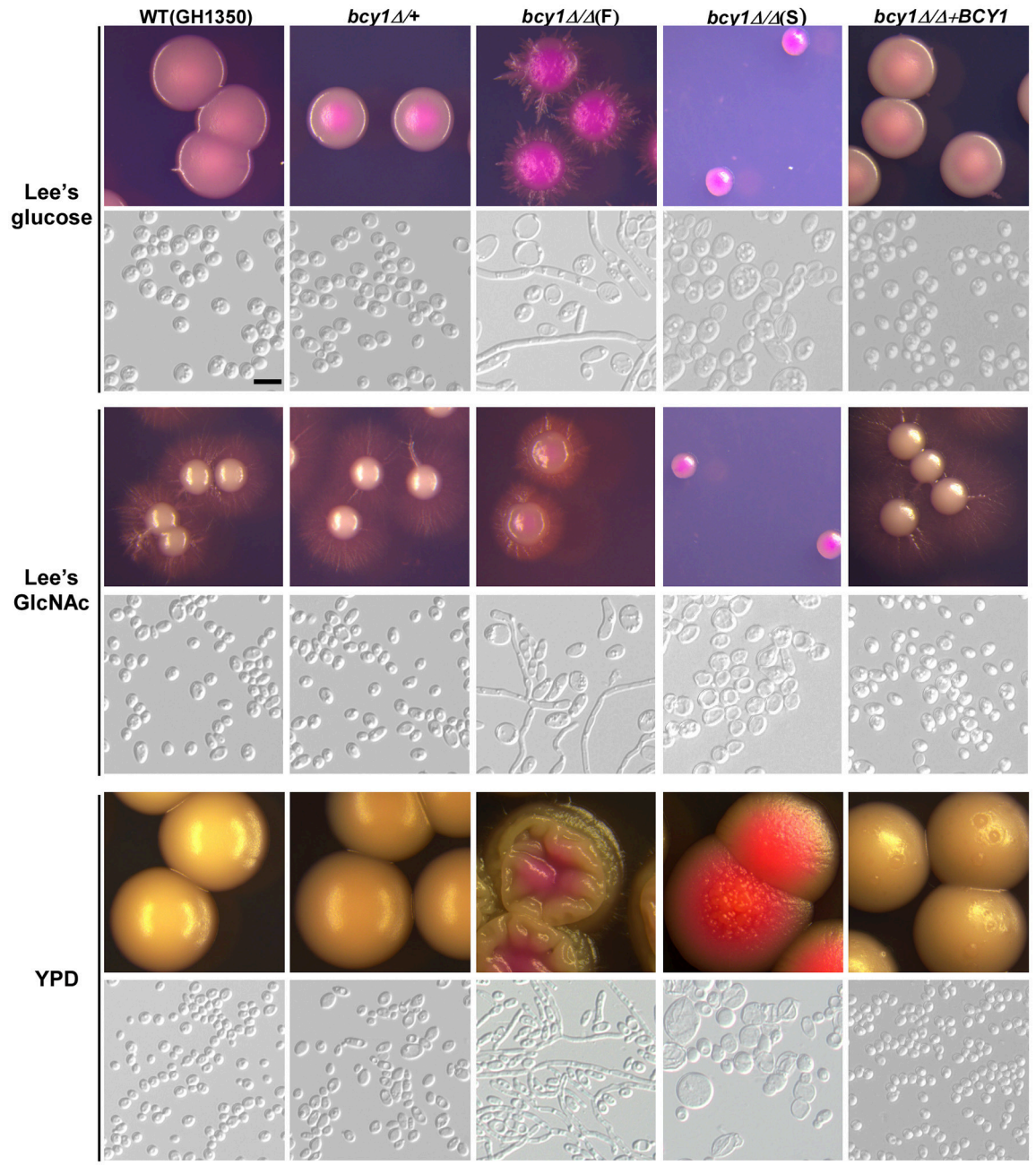


**FIGURE 2 | Cellular and colony morphologies of the WT, *BCY1/bcy1,* and *bcy1/bcy1* mutants, and the BCY1-reconstituted strain on Lee's glucose, Lee's GlcNAc, and YPD media at 25°C.** The cells were cultured on Lee's glucose and Lee's GlcNAc medium plates for 5 days or on YPD plates for 3 days. The *bcy1/bcy1* mutant consists of two colony phenotypes: smooth (S) and filamentous (F). Scale bar, 10 μm.

displayed a serious growth defect and had two distinct colony phenotypes (smooth and filamentous) on all three media. Cells of the smooth colonies were swollen and looked unhealthy, whereas filamentous cells had a much healthier appearance. On Lee's GlcNAc medium, a portion of the *bcy1/bcy1* mutant cells exhibited an opaque-like phenotype (**Figure 2**). At 37°C (**Figure 3**), two colony types of the *bcy1/bcy1* mutant were observed on three media. On Lee's glucose medium, filamentous colonies of the *bcy1/bcy1* mutant underwent more robust filamentation than the WT, *BCY1/bcy1*, and BCY1-reconstituted strains, whereas on Lee's GlcNAc medium, all four strains exhibited strong filamentation at 37°C. These results are consistent with previous reports showing that GlcNAc is a potent yeast-to-filamentous growth inducer (Simonetti et al., 1974).

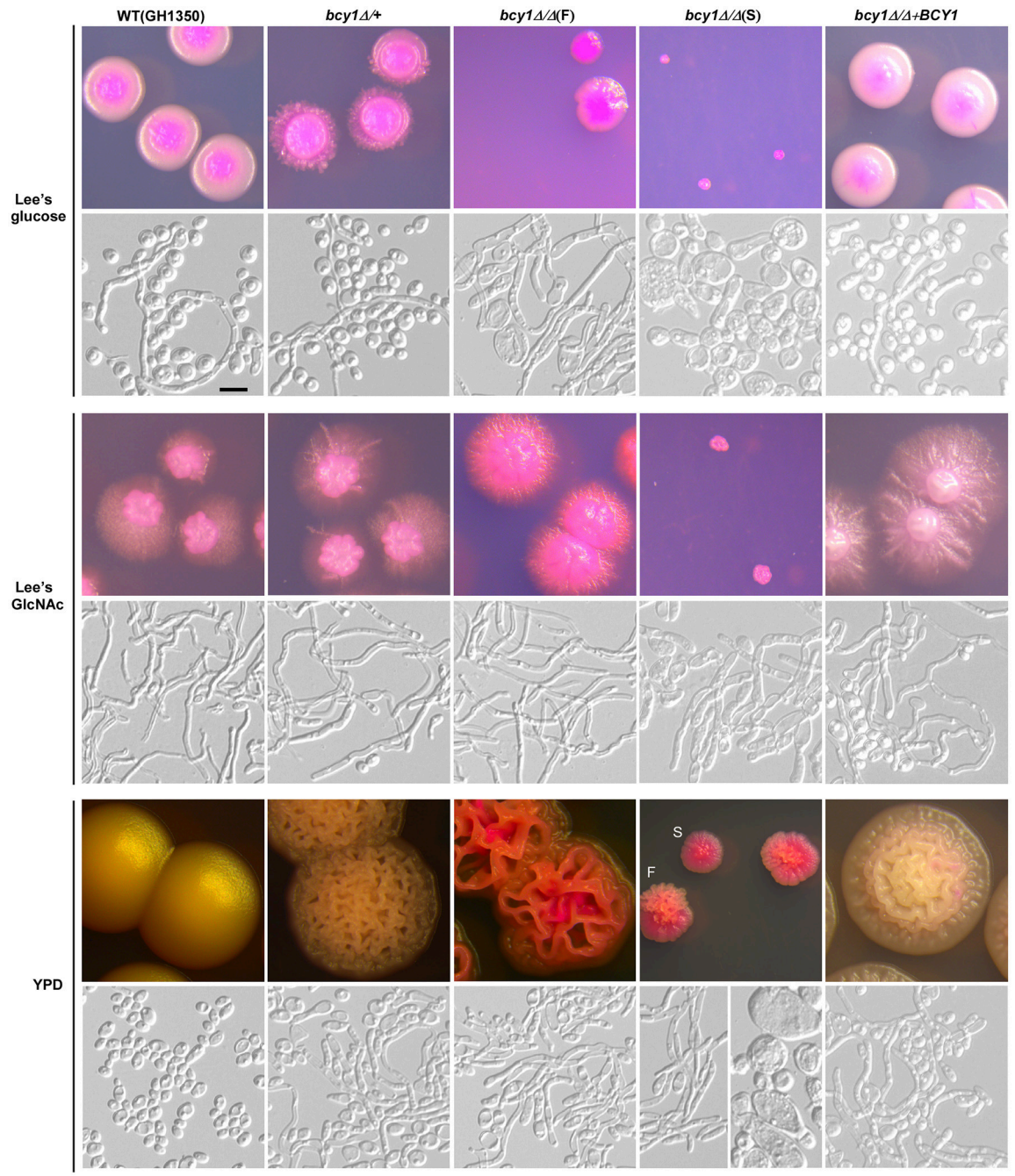


**FIGURE 3 | Cellular and colony morphologies of the WT, *BCY1/bcy1*, and *bcy1/bcy1* mutants, and BCY1-reconstituted strain on Lee's glucose, Lee's GlcNAc, and YPD media at 37°C.** The cells were cultured on Lee's glucose and Lee's GlcNAc medium plates for 5 days or on YPD plates for 3 days. At 37°C, all colonies of the *bcy1/bcy1* mutant underwent hyper-filamentation on Lee's GlcNAc medium. Scale bar, 10 μm.

The *bcy1/bcy1* mutant showed the most robust filametation on YPD medium, while the *BCY1/bcy1* and BCY1-reconstituted strains exhibited an intermediate level of filamentation at 37°C. The WT control maintained the yeast form on YPD medium at 37°C. These results suggest that Bcy1 plays a critical role in the regulation of filamentation and that the dosage of Bcy1 also affects this biological process.

## The *bcy1/bcy1* Null Mutant Can Switch between the Smooth and Filamentous Phenotypes

The *bcy1/bcy1* mutant has two colony phenotypes: smooth and filamentous (**Figures 2**, **3**, **4A**). To test whether the two phenotypes could switch between each other, we cultured the two cell types on YPD medium and calculated the switching frequencies of the original to alternative cell type after 3, 5, and 8 days at 30°C (**Figure 4B**). Extension of incubation on solid medium promoted the filamentous phenotype. To further characterize the switching feature of the *bcy1/bcy1* mutant, the smooth and filamentous colonies were cultured in liquid Lee's glucose medium for 0–96 h at 25°C (**Figure 4C**). The cells were then replated onto YPD medium and cultured at 30°C for 5 days. As shown in **Figure 4C**, the filamentous-to-smooth (F-to-S) switching frequencies at different time points were similar (20–40%), whereas the smooth-to-filamentous (S-to-F) switching frequencies increased dramatically with extension of the initial culture time.

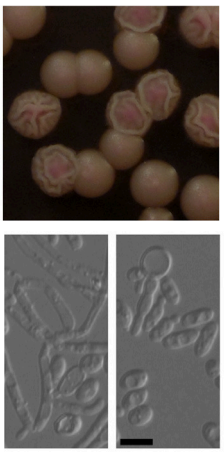


**B On YPD plates**

| Time (day) | Switching frequency F-to-S | S-to-F |
|---|---|---|
| 3 | 32.2±7.6 | 11.5±1.4 |
| 5 | 26.5±1.3 | 20.7±3.6 |
| 8 | 12.7±2.8 | 76.4±5.2 |

**C In liquid SD medium**

| Time (hour) | Switching frequency F-to-S | S-to-F |
|---|---|---|
| 0 | 21.1±12.7 | <0.4 |
| 24 | 23.5±8.4 | <0.5 |
| 48 | 24.5±5.9 | 51.7±6.1 |
| 72 | 38.3±2.1 | 100.0 |
| 96 | 26.5±3.9 | 100.0 |

**FIGURE 4 | Switching between smooth (S) and filamentous (F) forms of the *bcy1/bcy1* mutant at 30°C. (A)** Cellular and colony morphologies of the *bcy1/bcy1* mutant. The cells were cultured on YPD medium for 4 days. Scale bar, 10 μm. **(B)** Switching frequencies of S-to-F and F-to-S on YPD medium. Smooth and filamentous cells were plated on YPD medium and cultured for 3–8 days. **(C)** Switching frequencies of S-to-F and F-to-S in liquid SD medium. Cells were incubated in liquid SD medium for 0–96 h and then replated on YPD medium plates for 5 days.

## Effect of Overexpression of *TPK1* and *TPK2* in the *bcy1/bcy1* Null Mutant

Deletion of *BCY1* causes constitutive activation of the PKA kinase. We examined the effect of overexpression of *TPK1* and *TPK2*, which encode the two isoforms of the catalytic subunit, in the *bcy1/bcy1* null mutant. As shown in **Figure 5**, overexpression of *TPK1* in the *bcy1/bcy1* null mutant resulted in hyper-filamentation at 25°C, while overexpression of *TPK2* did not promote filamentation but led to the formation of two types of colonies: filamentous and opaque-like. On Lee's GlcNAc medium, one colony type was similar to the opaque phenotype, while the other underwent hyper filamentation. Of note, it was very difficult to obtain TPK2-overexpressing transformants in the *bcy1/bcy1* null mutant, suggesting that overexpression of *TPK2* may cause rapid cell death.

## Deletion of *BCY1* Promotes Cell Death

The cAMP signaling pathway regulates cell death in *C. albicans* (Phillips et al., 2006). Because the deletion of *BCY1* results in constitutive activation of this pathway, we next tested the viability of *bcy1/bcy1* mutant cells during incubation in Lee's glucose medium. Cells of the WT, smooth, and filamentous types of the *bcy1/bcy1* null mutant were grown in liquid Lee's glucose medium for 48 h at 25°C. The cells were then collected and stained with DAPI and PI. As shown in **Figure 6**, cells of the WT and filamentous form of the *bcy1/bcy1* mutant had intact DAPI-stained nuclei, while most cells of the smooth type of the *bcy1/bcy1* mutant had a fragmented nucleus or had no intact nuclei. PI staining verified that most cells of the smooth form of the *bcy1/bcy1* mutant underwent cell death. Quantitative assays demonstrated that more than 95% of the smooth cells and approximately 70% of filamentous cells of the *bcy1/bcy1* mutant were dead after 48 h of incubation in Lee's glucose medium at 25°C. Of note, more than 99% the WT control cells remained viable under the same culture conditions.

## Role of *Bcy1* in the Regulation of White-Opaque Switching

Huang et al. (2010) have demonstrated that activation of the cAMP signaling pathway promotes white-opaque switching in *C. albicans* (Huang et al., 2010). As shown in **Figure 2**, deletion of *BCY1* in the WT strain (*MTL*a/α) induced the formation of an opaque-like cell type on Lee's GlcNAc medium. Therefore, we deleted *BCY1* in a white-opaque switchable *MTL*a/Δ strain (SN152a Tao et al., 2014a) to generate the *BCY1/bcy1* and *bcy1/bcy1* mutants (*MTL*a/Δ). The colony and cellular morphologies of the WT, *BCY1/bcy1*, and *bcy1/bcy1* mutants (*MTL*a/Δ) are shown in **Figure 7A**. On both Lee's GlcNAc and Lee's glucose media, the *BCY1/bcy1* mutant exhibited similar colony and cellular phenotypes to those of the WT strain. Both the smooth and filamentous types of the *bcy1/bcy1* mutant could undergo white-opaque switching on Lee's glucose medium. However, both types underwent hyperfilamentation on Lee's GlcNAc medium. Replating and cell type-specific gene expression assays indicated that on Lee's GlcNAc medium, the filamentous

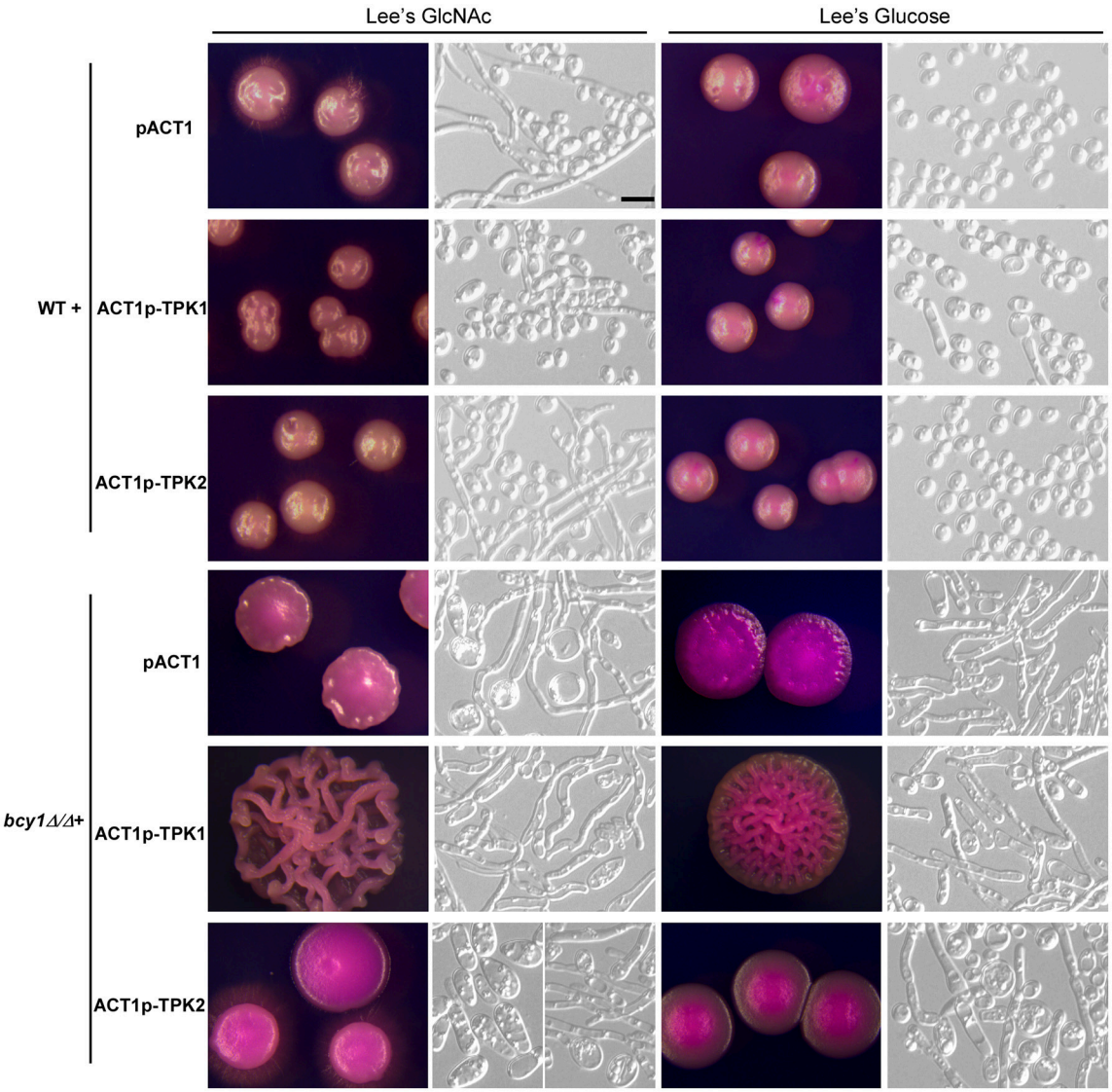


**FIGURE 5 | Overexpression of *TPK1* and *TPK2* in the WT and *bcy1/bcy1* mutant.** Cells were cultured on Lee's glucose and Lee's GlcNAc media at 25°C for 5 days. Scale bar, 10 μm.

cells had an opaque identity (**Figure S1**). Quantitative switching assays demonstrated that deletion of both alleles of *BCY1* caused a mass conversion to the opaque phenotype on Lee's GlcNAc medium (**Figure 7B**). These results suggest that Bcy1 plays a negative role in the regulation of the white-to-opaque transition under this culture condition.

## Role of *Bcy1* in the Regulation of Carbon Source Utilization

Next, we tested whether the regulatory subunit Bcy1 was involved in the regulation of carbon source utilization in *C. albicans*. As shown in **Figure 8**, nine media (including rich YPD medium, four Lee's media, and four YNB media containing different types of carbon sources) were used for this assay. The filamentous form of the *bcy1/bcy1* mutant grew well on all media, although its growth rate was slower than that of the WT. The smooth form of the *bcy1/bcy1* mutant grew well on YPD medium. However, the cells of this form showed a serious growth defect on both Lee's and YNB media. This defect did not appear to be related to the fermentative or non-fermentative features of the carbon sources.

# DISCUSSION

The cAMP/PKA pathway plays a critical role in the regulation of a number of features of the human fungal pathogen *C. albicans* (Hogan and Sundstrom, 2009; Huang, 2012). The regulatory subunit Bcy1 has been considered to be essential in this fungus (Cassola et al., 2004). In this study, we demonstrate that the two alleles of *BCY1* could be deleted in *C. albicans*. Given the

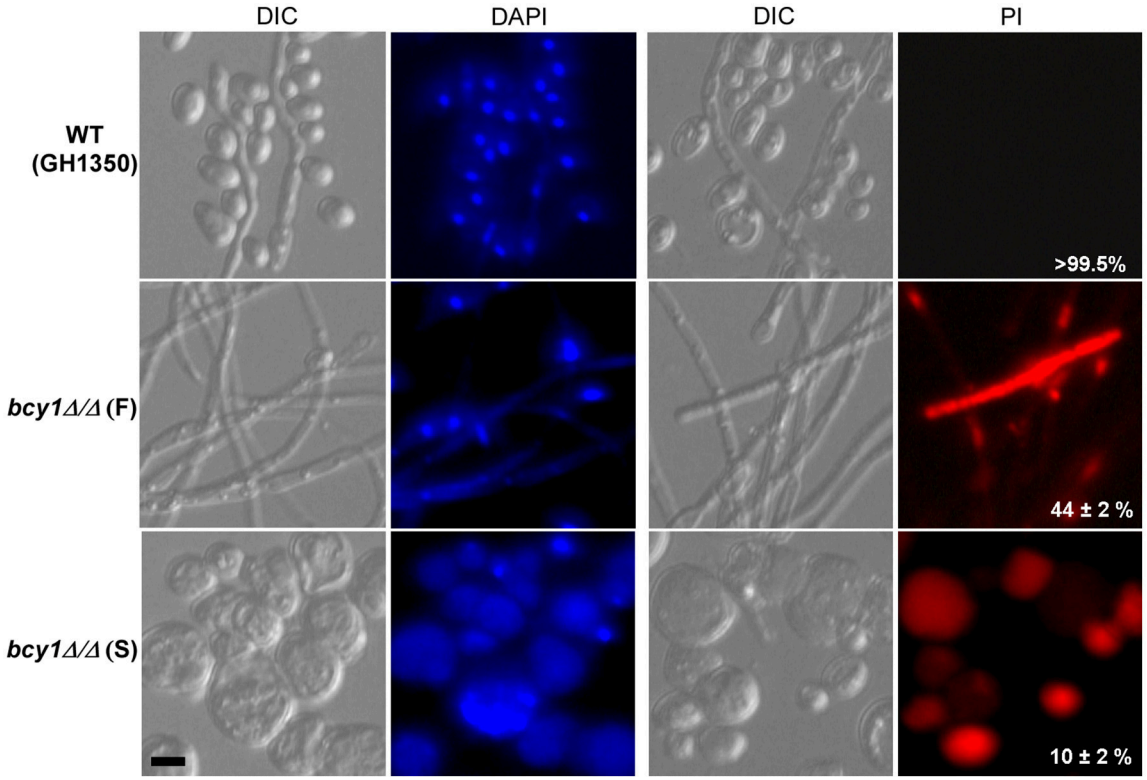


**FIGURE 6 | Deletion of *BCY1* in *C. albicans* promotes cell death, especially in the *bcy1/bcy1* smooth (S) form.** Cells of the WT, *bcy1/bcy1* filamentous (F), and *bcy1/bcy1* smooth (S) forms were incubated in Lee's glucose liquid medium for 48 h with shaking, and then used for DAPI and PI staining assays. The percentages (on PI-images) represent the survival rates using plating assays. DIC, differential interference contrast. Scale bar, 10 μm.

conserved feature of the cAMP signaling pathway in fungal species, our finding is reasonable because the orthologs of Bcy1 in several fungal species (such as Bcy1 in *S. cerevisiae*, Csg1 in *S. pombe*, and pkaR in *Aspergillus fumigatus* and *Cryptococcus neoformans*) are not essential for cell viability (Cannon and Tatchell, 1987; Toda et al., 1987; DeVoti et al., 1991; Bruno et al., 1996; D'Souza et al., 2001; Zhao et al., 2006). Based on the *bcy1/bcy1* null mutant generated in *C. albicans*, we re-evaluated the roles of Bcy1 in the regulation of filamentation, cell growth, and carbon source utilization. We also found that Bcy1 regulates white-opaque switching in *C. albicans*.

Deletion of *CYR1*, the sole gene encoding the adenylyl cyclase in *C. albicans*, completely blocked filamentation in response to several potent inducers including serum, $CO_2$, and bacterial peptidoglycan (Rocha et al., 2001; Klengel et al., 2005; Xu et al., 2008). Activation of the cAMP-PKA pathway by ectopic expression of the activating form of Ras1 (Ras1V13) or deletion of the high affinity cyclic nucleotide phosphodiesterase-encoding gene *PDE2* results in hyperfilamentation in *C. albicans* (Feng et al., 1999; Jung and Stateva, 2003). As expected, deletion of *BCY1* in *C. albicans* promotes filamentation under conditions favoring yeast cell growth (such as at low temperature and in rich media, **Figures 2**, **3**). Similar to the *pde2/pde2* mutant (Jung and Stateva, 2003), the PKA catalytic subunit could be constitutively activated in the *bcy1/bcy1* mutant. Moreover, the phenotypes of the *bcy1/bcy1* mutant are highly similar to the hyperactive *CYR1* mutant (Bai et al., 2011). The activated cAMP-PKA pathway then modulates downstream transcription factors (such as Efg1 and Flo8), which regulate filament-specific gene expression and promote filamentation (Bockmühl and Ernst, 2001; Cao et al., 2006).

Mutation of the PKA regulatory subunit in *S. cerevisiae* causes a variety of phenotypes (Cannon et al., 1990). In *C. albicans*, we found that deletion of *BCY1* also resulted in multiple colony and cellular phenotypes including yeast, filamentous, and opaque-like forms (**Figure 2**). Interestingly, different cell types of the *bcy1/bcy1* mutant exhibited different cell growth and carbon nutrient utilization abilities (**Figure 8**). Filamentous cells grew much better than cells of the smooth (yeast) form on all media, suggesting that both fermentative and non-fermentative carbon sources can be utilized by filamentous cells of the mutant. Switching between the filamentous and yeast cell forms can occur (**Figure 4**). Filamentous cells are healthier and display a better survival rate than cells of the smooth form when grown in regular media. Moreover, an extended culture time (which may represent a stressful condition) appeared to promote yeast-to-filamentous cell growth in the *bcy1/bcy1* mutant. These results suggest that deletion of *BCY1* in *C. albicans* promotes cell death, potentially due to constitutive activation of the

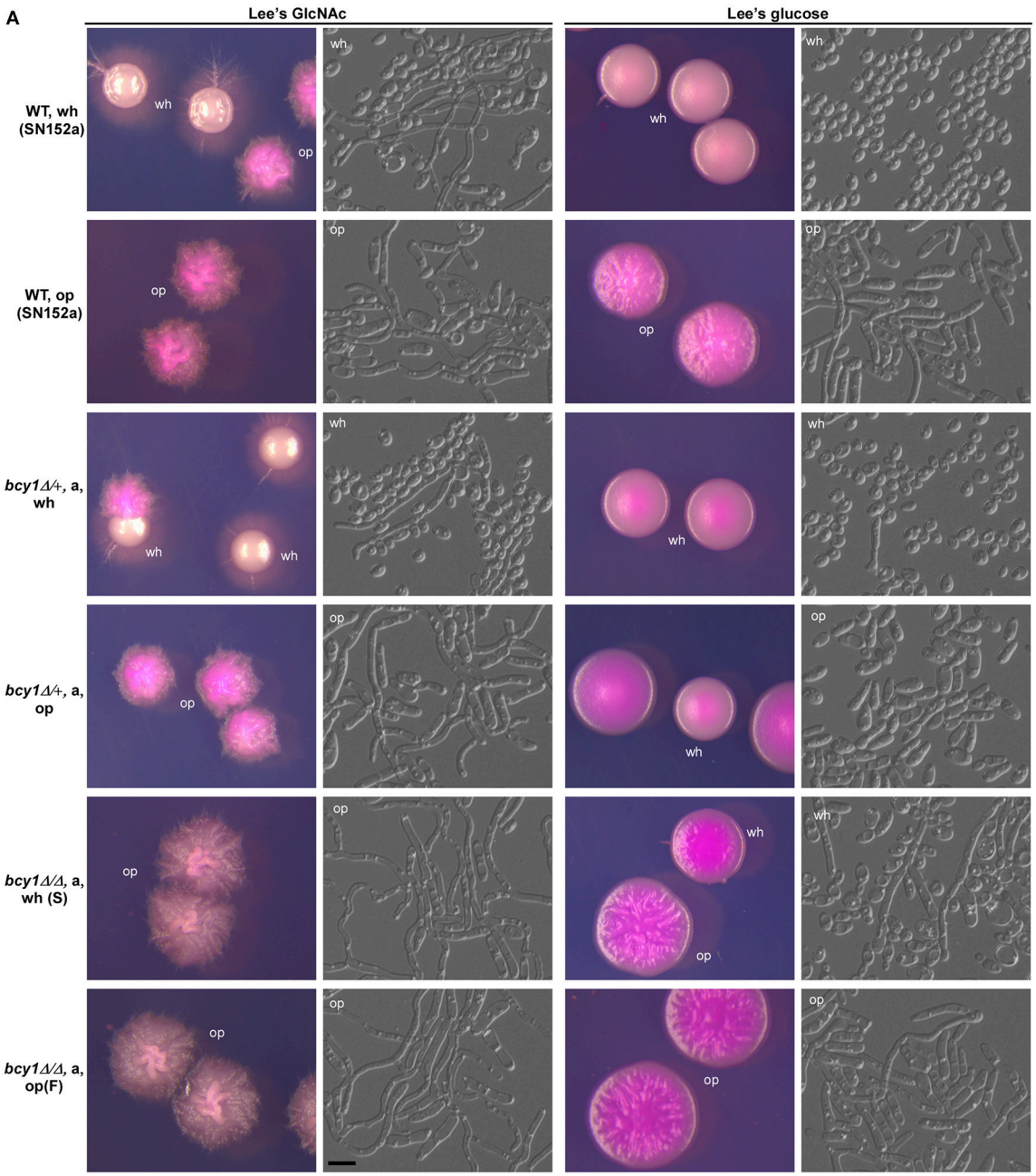


**B**

| | Lee's GlcNAc | | Lee's Glucose | |
|---|---|---|---|---|
| | wh-to-op | op-to-wh | wh-to-op | op-to-wh |
| WT **a** | 19.8±2.3 | <0.33 | <0.34 | 3.3±1.7 |
| *bcy1Δ/+* **a** | 23.5±3.3 | 12.4±2.4 | <0.51 | 23.3±5.9 |
| *bcy1Δ/Δ* **a** | 100.0 | 1.9±0.1 | <0.15 | 8.7±1.7 |

**FIGURE 7 | Deletion of *BCY1* affects white-opaque switching in *C. albicans*.** Cells were cultured on Lee's glucose and Lee's GlcNAc media at 25°C for 5 days. Scale bar, 10 μm. **(A)** Cellular and colony morphologies of the WT, *BCY1/bcy1*, and *bcy1/bcy1* mutants. On Lee's GlcNAc medium, no white colonies were observed since white cells switched to the opaque phenotype under this culture condition. Wh, white; op, opaque. **(B)** White-to-opaque and opaque-to-white switching frequencies of the WT, *BCY1/bcy1*, and *bcy1/bcy1* mutants.

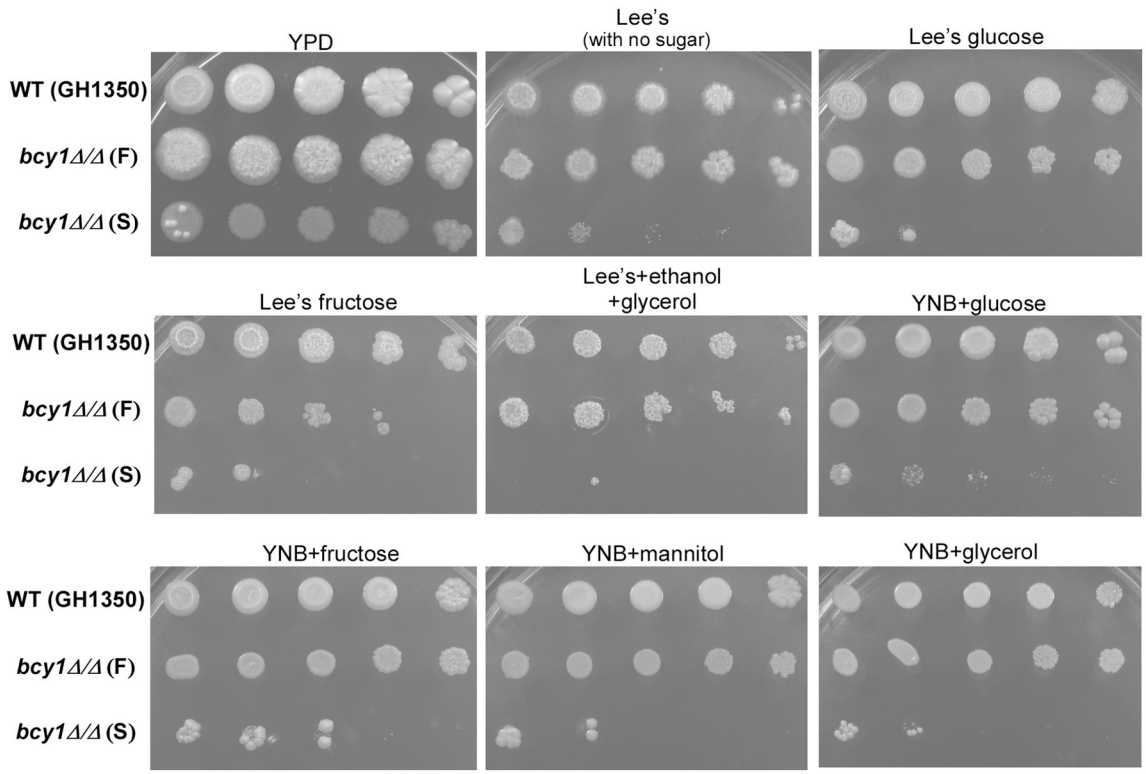


**FIGURE 8 | Bcy1 regulates carbon source utilization.** Cells of the WT, *bcy1/bcy1* filamentous (F), and *bcy1/bcy1* smooth (S) forms were adjusted to $5 \times 10^5$ cells/mL, and then spotted onto nine different medium plates at 10-fold serial dilutions. The plates were incubated at 37°C for 4 days. Media used: rich medium YPD; Lee's, Lee's medium containing no sugar; Lee's glucose, Lee's medium containing 1.25% glucose; Lee's fructose, Lee's medium containing 1.25% fructose; Lee's+ethanol+glycerol, Lee's medium containing 3% ethanol and 2% glycerol; YNB+glucose (fructose, mannitol, glycerol), YNB plus 2% glucose (2% fructose, 2% mannitol, or 4% glycerol).

cAMP-PKA pathway. Consistent with this idea, Phillips et al. (2006) demonstrated that the protein level of Bcy1 declined significantly during acetic acid-induced programmed cell death (Phillips et al., 2006). Filamentation in the *bcy1/bcy1* mutant could be a strategy of cells to avoid cell death or to improve their anti-stress abilities. Consistent with our study, Laprade et al. (2016) recently reported that filamentation of *C. albicans* provides protection against antifungal-induced programmed cell death (Laprade et al., 2016).

White-opaque switching is another important feature of *C. albicans* and is involved in the regulation of virulence, sexual mating, and stress responses (Slutsky et al., 1987; Lohse and Johnson, 2009; Soll, 2009). Inactivation of the cAMP signaling pathway by the deletion of *CYR1* suppresses GlcNAc and $CO_2$-induced white-to-opaque switching, whereas activation of this pathway by ectopic expression of the activating form of *RAS1*, *RAS1V13*, or deletion of *PDE2* promotes the opaque phenotype (Huang et al., 2009, 2010). Consistent with these observations, deletion of *BCY1* promotes white-to-opaque switching in *C. albicans* (**Figure 7**). This promoting effect is dosage-dependent because the deletion of one allele of *BCY1* leads to a moderate increase in this switch and deletion of both alleles causes a mass conversion on GlcNAc-containing media. GlcNAc is a potent inducer of the opaque phenotype. Consistent with the phenotype in the *bcy1/bcy1* mutant, Huang et al. (2010) reported that the deletion of *PDE2* also results in a mass white-to-opaque conversion on GlcNAc-containing media (Huang et al., 2010).

In summary, we successfully generated a *bcy1/bcy1* mutant in *C. albicans*, which clarifies the essential role of this PKA regulatory subunit and provides a new avenue to study the cAMP-PKA pathway in this medically important pathogen. Our study also provides new insights into the functional roles of Bcy1 in the regulation of filamentation, carbon source utilization, and white-opaque switching. The results reported herein further confirm the conserved features and central role of the cAMP-PKA pathway in the regulation of a variety of biological features of *C. albicans*.

## AUTHOR CONTRIBUTIONS

XD and GH designed the study. XD, CC, and QZ performed experiments. GH, XD, CC, and QZ analyzed data. GH, XD, CC, and QZ wrote the manuscript.

## ACKNOWLEDGMENTS

The authors thank Dr. Suzanne Noble for the generous gifts of plasmids and strains. This work was supported by grants from

the Chinese National Natural Science Foundation (31370175, 31170086, and 81322026) and the "100 Talent Program" grant from the Chinese Academy of Sciences (to GH).

## SUPPLEMENTARY MATERIAL

The Supplementary Material for this article can be found online at: http://journal.frontiersin.org/article/10.3389/fmicb.2016.02127/full#supplementary-material

**Figure S1 | Relative gene expression levels in white and opaque cells.** Cells collected from Lee's GlcNAc medium plates (three days, at 25°C) were used for qRT-PCR assays. The values of the expression level of each gene in white cells of the WT strain were set as "1." White and opaque cells of the WT served as controls. *bcy1/bcy1* op, opaque cells plated on Lee's GlcNAc medium; *bcy1/bcy1* original wh, white cells plated on Lee's GlcNAc medium. *ACT1* served as the reference gene for normalization.

**Table S1 | Strains used in this study.**

**Table S2 | Primers used in this study.**

## REFERENCES


Bai, C., Xu, X. L., Wang, H. S., Wang, Y. M., Chan, F. Y., and Wang, Y. (2011). Characterization of a hyperactive Cyr1 mutant reveals new regulatory mechanisms for cellular cAMP levels in *Candida albicans*. *Mol. Microbiol.* 82, 879–893. doi: 10.1111/j.1365-2958.2011.07859.x

Biswas, S., Van Dijck, P., and Datta, A. (2007). Environmental sensing and signal transduction pathways regulating morphopathogenic determinants of *Candida albicans*. *Microbiol. Mol. Biol. Rev.* 71, 348–376. doi: 10.1128/MMBR.00009-06

Bockmühl, D. P., and Ernst, J. F. (2001). A potential phosphorylation site for an A-type kinase in the Efg1 regulator protein contributes to hyphal morphogenesis of *Candida albicans*. *Genetics* 157, 1523–1530.

Bockmühl, D. P., Krishnamurthy, S., Gerads, M., Sonneborn, A., and Ernst, J. F. (2001). Distinct and redundant roles of the two protein kinase A isoforms Tpk1p and Tpk2p in morphogenesis and growth of *Candida albicans*. *Mol. Microbiol.* 42, 1243–1257. doi: 10.1046/j.1365-2958.2001.02688.x

Bruno, K. S., Aramayo, R., Minke, P. F., Metzenberg, R. L., and Plamann, M. (1996). Loss of growth polarity and mislocalization of septa in a Neurospora mutant altered in the regulatory subunit of cAMP-dependent protein kinase. *EMBO J.* 15, 5772–5782.

Cannon, J. F., Gitan, R., and Tatchell, K. (1990). Yeast cAMP-dependent protein kinase regulatory subunit mutations display a variety of phenotypes. *J. Biol. Chem.* 265, 11897–11904.

Cannon, J. F., and Tatchell, K. (1987). Characterization of *Saccharomyces cerevisiae* genes encoding subunits of cyclic AMP-dependent protein kinase. *Mol. Cell. Biol.* 7, 2653–2663. doi: 10.1128/MCB.7.8.2653

Cao, F., Lane, S., Raniga, P. P., Lu, Y., Zhou, Z., Ramon, K., et al. (2006). The Flo8 transcription factor is essential for hyphal development and virulence in *Candida albicans*. *Mol. Biol. Cell* 17, 295–307. doi: 10.1091/mbc.E05-06-0502

Cassola, A., Parrot, M., Silberstein, S., Magee, B. B., Passeron, S., Giasson, L., et al. (2004). *Candida albicans* lacking the gene encoding the regulatory subunit of protein kinase A displays a defect in hyphal formation and an altered localization of the catalytic subunit. *Eukaryot. Cell* 3, 190–199. doi: 10.1128/EC.3.1.190-199.2004

Chiaradonna, F., Balestrieri, C., Gaglio, D., and Vanoni, M. (2008). RAS and PKA pathways in cancer: new insight from transcriptional analysis. *Front. Biosci.* 13:5257–5278. doi: 10.2741/3079

Chin, K. V., Yang, W. L., Ravatn, R., Kita, T., Reitman, E., Vettori, D., et al. (2002). Reinventing the wheel of cyclic AMP: novel mechanisms of cAMP signaling. *Ann. N.Y. Acad. Sci.* 968, 49–64. doi: 10.1111/j.1749-6632.2002.tb04326.x

DeVoti, J., Seydoux, G., Beach, D., and McLeod, M. (1991). Interaction between ran1+ protein kinase and cAMP dependent protein kinase as negative regulators of fission yeast meiosis. *EMBO J.* 10, 3759–3768.

D'Souza, C. A., Alspaugh, J. A., Yue, C., Harashima, T., Cox, G. M., Perfect, J. R., et al. (2001). Cyclic AMP-dependent protein kinase controls virulence of the fungal pathogen *Cryptococcus neoformans*. *Mol. Cell. Biol.* 21, 3179–3191. doi: 10.1128/MCB.21.9.3179-3191.2001

Du, H., Guan, G., Li, X., Gulati, M., Tao, L., Cao, C., et al. (2015). N-acetylglucosamine-induced cell death in *Candida albicans* and its implications for adaptive mechanisms of nutrient sensing in yeasts. *MBio* 6, e01376–e01315. doi: 10.1128/mBio.01376-15

Feng, Q., Summers, E., Guo, B., and Fink, G. (1999). Ras signaling is required for serum-induced hyphal differentiation in *Candida albicans*. *J. Bacteriol.* 181, 6339–6346.

Gancedo, J. M. (2001). Control of pseudohyphae formation in *Saccharomyces cerevisiae*. *FEMS Microbiol. Rev.* 25, 107–123. doi: 10.1111/j.1574-6976.2001.tb00573.x

Giacometti, R., Kronberg, F., Biondi, R. M., Hernández, A. I., and Passeron, S. (2012). Cross regulation between *Candida albicans* catalytic and regulatory subunits of protein kinase A. *Fungal Genet. Biol.* 49, 74–85. doi: 10.1016/j.fgb.2011.12.001

Giacometti, R., Kronberg, F., Biondi, R. M., and Passeron, S. (2009). Catalytic isoforms Tpk1 and Tpk2 of *Candida albicans* PKA have non-redundant roles in stress response and glycogen storage. *Yeast* 26, 273–285. doi: 10.1002/yea.1665

Giacometti, R., Souto, G., Silberstein, S., Giasson, L., Cantore, M. L., and Passeron, S. (2006). Expression levels and subcellular localization of Bcy1p in *Candida albicans* mutant strains devoid of one BCY1 allele results in a defective morphogenetic behavior. *Biochim. Biophys. Acta* 1763, 64–72. doi: 10.1016/j.bbamcr.2005.11.016

Gow, N. A., van de Veerdonk, F. L., Brown, A. J., and Netea, M. G. (2012). *Candida albicans* morphogenesis and host defence: discriminating invasion from colonization. *Nat. Rev. Microbiol.* 10, 112–122. doi: 10.1038/nrmicro2711

Hogan, D. A., and Sundstrom, P. (2009). The Ras/cAMP/PKA signaling pathway and virulence in *Candida albicans*. *Future Microbiol.* 4, 1263–1270. doi: 10.2217/fmb.09.106

Huang, G. (2012). Regulation of phenotypic transitions in the fungal pathogen *Candida albicans*. *Virulence* 3, 251–261. doi: 10.4161/viru.20010

Huang, G., Srikantha, T., Sahni, N., Yi, S., and Soll, D. R. (2009). CO(2) regulates white-to-opaque switching in *Candida albicans*. *Curr. Biol.* 19, 330–334. doi: 10.1016/j.cub.2009.01.018

Huang, G., Yi, S., Sahni, N., Daniels, K. J., Srikantha, T., and Soll, D. R. (2010). N-acetylglucosamine induces white to opaque switching, a mating prerequisite in *Candida albicans*. *PLoS Pathog.* 6:e1000806. doi: 10.1371/journal.ppat.1000806

Jung, W. H., and Stateva, L. I. (2003). The cAMP phosphodiesterase encoded by CaPDE2 is required for hyphal development in *Candida albicans*. *Microbiology* 149, 2961–2976. doi: 10.1099/mic.0.26517-0

Klengel, T., Liang, W. J., Chaloupka, J., Ruoff, C., Schröppel, K., Naglik, J. R., et al. (2005). Fungal adenylyl cyclase integrates CO2 sensing with cAMP signaling and virulence. *Curr. Biol.* 15, 2021–2026. doi: 10.1016/j.cub.2005.10.040

Laprade, D. J., Brown, M. S., McCarthy, M. L., Ritch, J. J., and Austriaco, N. (2016). Filamentation protects *Candida albicans* from amphotericin B-induced programmed cell death via a mechanism involving the yeast metacaspase, MCA1. *Microb. Cell* 3, 285–292. doi: 10.15698/mic2016.07.512

Leberer, E., Harcus, D., Dignard, D., Johnson, L., Ushinsky, S., Thomas, D. Y., et al. (2001). Ras links cellular morphogenesis to virulence by regulation of the MAP kinase and cAMP signalling pathways in the pathogenic fungus *Candida albicans*. *Mol. Microbiol.* 42, 673–687. doi: 10.1046/j.1365-2958.2001.02672.x

Lee, K. L., Buckley, H. R., and Campbell, C. C. (1975). An amino acid liquid synthetic medium for the development of mycelial and yeast forms of *Candida albicans*. *Sabouraudia* 13, 148–153. doi: 10.1080/00362177585190271

Lohse, M. B., and Johnson, A. D. (2009). White-opaque switching in *Candida albicans*. *Curr. Opin. Microbiol.* 12, 650–654. doi: 10.1016/j.mib.2009.09.010

Noble, S. M., and Johnson, A. D. (2005). Strains and strategies for large-scale gene deletion studies of the diploid human fungal pathogen *Candida albicans*. *Eukaryot. Cell* 4, 298–309. doi: 10.1128/EC.4.2.298-309.2005

Pan, X., Harashima, T., and Heitman, J. (2000). Signal transduction cascades regulating pseudohyphal differentiation of *Saccharomyces cerevisiae*. *Curr. Opin. Microbiol.* 3, 567–572. doi: 10.1016/S1369-5274(00)00142-9

Phillips, A. J., Crowe, J. D., and Ramsdale, M. (2006). Ras pathway signaling accelerates programmed cell death in the pathogenic fungus *Candida albicans*. *Proc. Natl. Acad. Sci. U.S.A.* 103, 726–731. doi: 10.1073/pnas.0506405103

Rocha, C. R., Schröppel, K., Harcus, D., Marcil, A., Dignard, D., Taylor, B. N., et al. (2001). Signaling through adenylyl cyclase is essential for hyphal growth and virulence in the pathogenic fungus *Candida albicans*. *Mol. Biol. Cell* 12, 3631–3643. doi: 10.1091/mbc.12.11.3631

Schaekel, A., Desai, P. R., and Ernst, J. F. (2013). Morphogenesis-regulated localization of protein kinase A to genomic sites in *Candida albicans*. *BMC Genomics* 14:842. doi: 10.1186/1471-2164-14-842

Simonetti, N., Strippoli, V., and Cassone, A. (1974). Yeast-mycelial conversion induced by N-acetyl-D-glucosamine in *Candida albicans*. *Nature* 250, 344–346. doi: 10.1038/250344a0

Slutsky, B., Staebell, M., Anderson, J., Risen, L., Pfaller, M., and Soll, D. R. (1987). "White-opaque transition": a second high-frequency switching system in *Candida albicans*. *J. Bacteriol.* 169, 189–197. doi: 10.1128/jb.169.1.189-197.1987

Soll, D. R. (2009). Why does *Candida albicans* switch? *FEMS Yeast Res.* 9, 973–989. doi: 10.1111/j.1567-1364.2009.00562.x

Tao, L., Cao, C., Liang, W., Guan, G., Zhang, Q., Nobile, C. J., et al. (2014a). White cells facilitate opposite- and same-sex mating of opaque cells in *Candida albicans*. *PLoS Genet.* 10:e1004737. doi: 10.1371/journal.pgen.1004737

Tao, L., Du, H., Guan, G., Dai, Y., Nobile, C. J., Liang, W., et al. (2014b). Discovery of a "white-gray-opaque" tristable phenotypic switching system in candida albicans: roles of non-genetic diversity in host adaptation. *PLoS Biol.* 12:e1001830. doi: 10.1371/journal.pbio.1001830

Toda, T., Cameron, S., Sass, P., Zoller, M., Scott, J. D., McMullen, B., et al. (1987). Cloning and characterization of BCY1, a locus encoding a regulatory subunit of the cyclic AMP-dependent protein kinase in *Saccharomyces cerevisiae*. *Mol. Cell. Biol.* 7, 1371–1377. doi: 10.1128/MCB.7.4.1371

Wang, P., and Heitman, J. (1999). Signal transduction cascades regulating mating, filamentation, and virulence in *Cryptococcus neoformans*. *Curr. Opin. Microbiol.* 2, 358–362. doi: 10.1016/S1369-5274(99)80063-0

Wang, Y. (2013). Fungal adenylyl cyclase acts as a signal sensor and integrator and plays a central role in interaction with bacteria. *PLoS Pathog.* 9:e1003612. doi: 10.1371/journal.ppat.1003612

Whiteway, M., and Bachewich, C. (2007). Morphogenesis in *Candida albicans*. *Annu. Rev. Microbiol.* 61, 529–553. doi: 10.1146/annurev.micro.61.080706.093341

Xie, J., Tao, L., Nobile, C. J., Tong, Y., Guan, G., Sun, Y., et al. (2013). White-opaque switching in natural MTLa/alpha isolates of *Candida albicans*: evolutionary implications for roles in host adaptation, pathogenesis, and sex. *PLoS Biol.* 11:e1001525. doi: 10.1371/journal.pbio.1001525

Xu, X. L., Lee, R. T., Fang, H. M., Wang, Y. M., Li, R., Zou, H., et al. (2008). Bacterial peptidoglycan triggers *Candida albicans* hyphal growth by directly activating the adenylyl cyclase Cyr1p. *Cell Host Microbe* 4, 28–39. doi: 10.1016/j.chom.2008.05.014

Zhao, W., Panepinto, J. C., Fortwendel, J. R., Fox, L., Oliver, B. G., Askew, D. S., et al. (2006). Deletion of the regulatory subunit of protein kinase A in *Aspergillus fumigatus* alters morphology, sensitivity to oxidative damage, and virulence. *Infect. Immun.* 74, 4865–4874. doi: 10.1128/IAI.00565-06

**Conflict of Interest Statement:** The authors declare that the research was conducted in the absence of any commercial or financial relationships that could be construed as a potential conflict of interest.

# Advantages of publishing in Frontiers

**OPEN ACCESS**
Articles are free to read, for greatest visibility

**COLLABORATIVE PEER-REVIEW**
Designed to be rigorous – yet also collaborative, fair and constructive

**FAST PUBLICATION**
Average 85 days from submission to publication (across all journals)

**COPYRIGHT TO AUTHORS**
No limit to article distribution and re-use

**TRANSPARENT**
Editors and reviewers acknowledged by name on published articles

**SUPPORT**
By our Swiss-based editorial team

**IMPACT METRICS**
Advanced metrics track your article's impact

**GLOBAL SPREAD**
5'100'000+ monthly article views and downloads

**LOOP RESEARCH NETWORK**
Our network increases readership for your article

**Frontiers**
EPFL Innovation Park, Building I • 1015 Lausanne • Switzerland
Tel +41 21 510 17 00 • Fax +41 21 510 17 01 • info@frontiersin.org
**www.frontiersin.org**

**Find us on**